

Funded by the European Union within the
7th Framework Programme, Grant Agreement 603378.
Duration: February 1st, 2014 – January 31th, 2018



D4.1 Case study synthesis - Final Report

Lead-Authors: Teresa Ferreira (Universidade de Lisboa, Portugal), Yiannis Panagopoulos (Technical University of Athens, Greece), John Bloomfield (Natural Environment Research Council, UK), Raoul Marie Couture (Norwegian Institute for Water Research, Norway), Steve Ormerod (University of Cardiff, UK).

Authors and co-authors: Yiannis Panagopoulos, Kostas Stefanidis, Maria Mimikou (NTUA, Greece), Jenică Hanganu, Adrian Constantinescu (DDNI, Romania), Meryem Beklioğlu, Tuba Bucak, Şeyda Erdoğan, Ayşe İdil Çakıroğlu, Emel Çakmak, Jan Coppens (METU, Turkey), Carina Almeida, Paulo Branco, Ramiro Neves, Pedro Segurado (University of Lisbon, Portugal), Eugenio Molina-Navarro, Shenglan Lu, Dennis Trolle, and Hans Estrup Andersen (Aarhus University, Denmark), Lilith Kramer, Marijn Kuijper, Perry de Louw, Vince Kaandorp, Erwin Meijers, Ellis Penning and Dimmie Hendriks (Deltares, Netherlands), Ute Mischke, Judith Mahnkopf, Andreas Gericke and Markus Venohr (Leibniz Institute of Freshwater Ecology and Inland Fisheries, Germany), Christel Prudhomme, Mike Hutchins, John Bloomfield, Alex Elliott, Corinna Abesser, Olivia Hitt, Majdi Mansour and Mike Bowes (Natural Environment Research Council, U.K.), Alexander Gieswein (University of Duisberg-Essen, Germany), and Rafaela Schinegger, Christiane Aschauer and Stefan Schmutz (University of Natural Resources and Life Sciences, Austria), Raoul-Marie Couture, Richard F. Wright, Yan Lin, Øyvind Kaste, José-Luis Guerrero, Anne Christiansen, Jonas Persson, Petra Mutinova (Norwegian Institute for Water Research NIVA), Katri Rankinen, Ninni Liukko, Seppo Hellsten (Finnish Environment Institute SYKE), Fabien Cremona (Estonian University of Life Sciences), Paul G. Whitehead, Gianbattista Bussi (Water Resource Associates WRA), Cayetano Gutiérrez-Cánovas, Steve Ormerod (Cardiff University).

Due date of deliverable: **Month 30, July 2016**
Actual submission date: Month 32, September 2016

Dissemination Level	
PU	Public
PP	Restricted to other programme participants (including the Commission Services)
RE	Restricted to a group specified by the consortium (including the Commission Services)
CO	Confidential, only for members of the consortium (including the Commission Services)

TABLE OF CONTENTS

	<i>List of Figures</i>	<i>iv</i>
	<i>List of Tables</i>	<i>xvi</i>
1	INTRODUCTION	1
2	THE WORKPACKAGE 4 OF MARS	2
2.1	WP4 ORGANIZATION	3
2.2	WP4.1 CALENDAR AND OUTPUTS	5
3	THE MARS MODELLING PROCESS	6
3.1	CONCEPTUAL MARS MODELS	6
3.2	MODELLING STRATEGY	7
3.3	CLIMATE CHANGE SCENARIOS AND STORYLINES DEVELOPMENT.....	8
4	SOUTHERN BASINS	10
4.1	LOWER DANUBE	10
4.1.1	<i>Introduction</i>	10
4.1.2	<i>Study area and MARS concept development</i>	11
4.1.3	<i>Data and Methods</i>	13
4.1.4	<i>Results</i>	26
4.1.5	<i>Conclusions and discussion</i>	28
4.2	LAKE BEYSEHIR BASIN	29
4.2.1	<i>Introduction</i>	29
4.2.2	<i>Study area and MARS concept development</i>	30
4.2.3	<i>Data and Methods</i>	33
4.2.4	<i>Results</i>	43
4.2.5	<i>Discussion</i>	49
4.2.6	<i>Conclusions</i>	52
4.3	PINIOS	52
4.3.1	<i>Introduction</i>	52
4.3.2	<i>Study area and MARS concept development</i>	53
4.3.3	<i>Methods</i>	59
4.3.4	<i>Scenarios development</i>	69
4.3.5	<i>Results: Predicting responses to multiple stressors at the river basin scale</i>	73
4.3.6	<i>Conclusions and key outcomes</i>	82
4.4	SORRAIA	85
4.4.1	<i>Introduction</i>	85
4.4.2	<i>Study area (description of basin)</i>	87
4.4.3	<i>Methods</i>	92
4.4.4	<i>Scenarios development</i>	108
4.4.5	<i>Implementations of measures</i>	114
4.4.6	<i>Results</i>	115
4.4.7	<i>Ecosystem services</i>	135
4.4.8	<i>Implementation of measures</i>	144
4.4.9	<i>Discussion</i>	148
4.4.10	<i>Key outcomes</i>	150
5	CENTRAL BASINS	152
5.1	DRAVA.....	152
5.1.1	<i>Introduction</i>	152
5.1.2	<i>Context for modelling</i>	160
5.1.3	<i>Data and methods</i>	161
5.1.4	<i>Results</i>	169

5.1.5	<i>Discussion</i>	180
5.1.6	<i>Conclusions</i>	186
5.2	ELBE, HAVEL AND SAALE	187
5.2.1	<i>Introduction</i>	187
5.2.2	<i>Context for modelling and storylines</i>	189
5.2.3	<i>Data and methods</i>	192
5.2.4	<i>Results</i>	202
5.2.5	<i>Discussion</i>	218
5.2.6	<i>Conclusion</i>	220
5.2.7	<i>Acknowledgements</i>	220
5.3	ODENSE.....	221
5.3.1	<i>Introduction</i>	221
5.3.2	<i>Scenarios Definition</i>	225
5.3.3	<i>Development of empirical models for ecological indicators in Danish streams</i>	250
5.3.4	<i>Linking process-based and empirical models: assessing the impact of multiple stressors on stream water quality</i> 268	
5.3.5	<i>Conclusions</i>	277
5.4	REGGE AND DINKEL.....	278
5.4.1	<i>Introduction</i>	278
5.4.2	<i>Models</i>	282
5.4.3	<i>Data pre-processing</i>	290
5.4.4	<i>Methods</i>	294
5.4.5	<i>Results</i>	309
5.4.6	<i>Empirical models</i>	323
5.4.7	<i>Contribution of groundwater flow to stream ecology</i>	336
5.4.8	<i>Conclusions and recommendations</i>	340
5.5	RUHR	344
5.5.1	<i>Introduction</i>	344
5.5.2	<i>Context for modelling</i>	350
5.5.3	<i>Data and methods</i>	351
5.5.4	<i>Results</i>	358
5.5.5	<i>Discussion</i>	368
5.5.6	<i>Conclusion</i>	374
5.6	THAMES	375
5.6.1	<i>Introduction</i>	375
5.6.2	<i>Context for the modelling</i>	380
5.6.3	<i>Data and methods</i>	382
5.6.4	<i>Results</i>	395
5.6.5	<i>Discussion</i>	405
5.6.6	<i>Conclusion</i>	407
6	NORTHERN BASINS	408
6.1	VORSTJÄV, ESTONIA	408
6.1.1	<i>Introduction</i>	408
6.1.2	<i>Methods</i>	410
6.1.3	<i>Results</i>	417
6.1.4	<i>Discussion</i>	423
6.1.5	<i>Conclusion</i>	426
6.2	LEPSÄMÄNJOKI, FINLAND	427
6.2.1	<i>Area description</i>	427
6.2.2	<i>Conceptual Model</i>	430
6.2.3	<i>Data</i>	431
6.2.4	<i>Physical Models</i>	432

6.2.5	<i>Results of the physical model</i>	436
6.2.6	<i>Empirical Models</i>	439
6.2.7	<i>Results of the empirical models</i>	444
6.2.8	<i>Ecosystem services</i>	447
6.2.9	<i>Lessons Learned</i>	448
6.3	MUSTAJOKI/TEURONJOKI, FINLAND.....	450
6.3.1	<i>Area description</i>	450
6.3.2	<i>Conceptual model</i>	452
6.3.3	<i>Scenarios and storylines</i>	452
6.3.4	<i>Physical Models</i>	453
6.3.5	<i>Results of the physical models</i>	460
6.3.6	<i>Empirical Models</i>	462
6.3.7	<i>Ecosystem Services</i>	466
6.4	OTRA, NORWAY	467
6.4.1	<i>Introduction</i>	467
6.4.2	<i>Data and methods</i>	471
6.4.3	<i>Results</i>	483
6.4.4	<i>EM results</i>	489
6.4.5	<i>Discussion</i>	491
6.4.6	<i>Conclusion</i>	495
6.5	VANSJO, NORWAY	496
6.5.1	<i>Introduction</i>	496
6.5.2	<i>Data and Methods</i>	501
6.5.3	<i>Results</i>	512
6.5.4	<i>Discussion</i>	523
6.5.5	<i>Conclusion</i>	530
6.6	WALES	531
6.6.1	<i>Introduction</i>	531
6.6.2	<i>Data and Methods</i>	536
6.6.3	<i>Methods</i>	540
6.6.4	<i>Results</i>	545
6.6.5	<i>Discussion</i>	558
6.6.6	<i>Conclusion</i>	562
7	OVERALL	562
7.1	MULTIPLE STRESSORS AT THE BASIN SCALE	562
7.2	SCENARIOS OF CHANGE	564
7.3	LAST NOTES	567
8	REFERENCES	568

List of Figures

Figure 2.1. Map showing the locations of the MARS case study basins.....	3
Figure 3.1. MARS conceptual model (from Hering et al., 2015).....	6
Figure 3.2.. Future and baseline precipitation (mm)	9
Figure 3.3.. Future and baseline temperature (°C).....	9
Figure 4.1 Danube Delta Biosphere Reserve.....	11
Figure 4.2 Danube Delta flooding areas.....	12
Figure 4.3 Channels networks, left figure and right figure agriculture area (yellow) and fish polders (blue).	12
Figure 4.4 Danube Delta conceptual model	13
Figure 4.5 Months with low water discharge of the Danube River.....	14
Figure 4.6 Residence time gradient in the Danube Delta lakes.....	14
Figure 4.7 Summary of the models used	15
Figure 4.8 Schematic view of the Danube Delta hydraulic model.....	15
Figure 4.9 Water levels calibration of the Danube Delta hydraulic model at Isaccea station	16
Figure 4.10 Water discharges calibration of the Danube Delta hydraulic model at Isaccea station.....	16
Figure 4.11 Schematic figure of the AHP model	17
Figure 4.12 AHP – assessment of consistency ratio.....	17
Figure 4.13 Weight of each component after AHP processing	18
Figure 4.14 Equivalents of AHP final score and water quality classes	19
Figure 4.15 Schematic figure of the Aquatox ecological model (Park A. Richard et al., 2008).....	20
Figure 4.16 AQUATOX model calibration.....	20
Figure 4.17 Influence of BRT variables at low waters level of the Danube delta lakes on fish biomass.....	21
Figure 4.18 Influence of the nutrients stress and hydro-morphological pressure on fish biomass.....	22
Figure 4.19 Multiple regression results on selected lakes of the Danube delta for Fish	23
Figure 4.20 Multiannual mean changes (2011-2040 vs. 1916-1990) in air temperature.....	25
Figure 4.21 Multiannual mean changes (2011-2040 vs. 1916-1990) in precipitation (%).....	25
Figure 4.22 MARS climate changes scenarios.....	26
Figure 4.23 MARS storyline elements scenarios	26
Figure 4.24 Fish biomass of the on Danube delta lakes for MARS scenarios	27
Figure 4.25 a, b. Fish biomass gradient for MARS scenarios at the years 2030 (a) and 2060 (b)	28
Figure 4.26 Location of the study site and GIS layers that are used in SWAT model (a) Location of the study site; (b) digital elevation map of the Beyşehir catchment. Brown borders show the sub-catchment boundaries. Numbers indicate the inflows (local names of inflows are: Q1: Üstünler, Q2: Soğuksu, Q3: Hizar, Q4: Çeltek, Q5: Tolca-Ozan, Q6: Sarısu) used in the calibration and the black circle shows the outflow; (c) distribution of land use categories; (d) soil map.....	31
Figure 4.27 MARS conceptual model of Lake Beyşehir.....	32
Figure 4.28 Calibration and validation results. Daily simulated (grey, solid lines) and observed (black, dashed lines) flows after calibration of the SWAT model. Flow rates are given in m ³ sec ⁻¹ . (Q1: Üstünler, Q2: Soğuksu, Q3:Hizar, Q4: Çeltek, Q5: Tolca-Ozan, Q6: Sarısu). Taken from Bucak et al submitted.....	35
Figure 4.29 Calibration results of the lake models	40
Figure 4.30 Future and baseline precipitation (mm)	42
Figure 4.31 Future and baseline temperature(oC)	42
Figure 4.32 Minimum and maximum water levels (m) derived from all scenarios for 2030s and 2060s period	46
Figure 4.33 Ensemble run results derived from GLM-AED and PCLake for Chl-a and Cyanobacteria biomass	49
Figure 4.34 The Pinios river basin in Central Greece. Key data layers are shown including, among others, sub- basins as delineated in SWAT, irrigated areas and source of irrigation water as well as sample sites along the main river.....	54

Figure 4.35 Monthly average precipitation values over a 36 year period (1975-2010).	57
Figure 4.36 Conceptual model for Pinios catchment.....	58
Figure 4.37 Observed and simulated monthly flows in two gauging stations of Pinios river.	61
Figure 4.38 Simulated vs observed values for water concentrations of nitrate and total phosphorus.	62
Figure 4.39 Partial plots showing the response of the ASPT metric to each predictor.	66
Figure 4.40 Partial plots showing the response of the EPT metric to each predictor.	66
Figure 4.41 Partial responses of the ASPT to predictor variables included in the GLM	67
Figure 4.42 Combined response of ASPT to nitrate and dissolved oxygen (left graph) and to altitude and dissolved oxygen (right graph).....	68
Figure 4.43 Partial response of EPT to predictors included in the GLM.	68
Figure 4.44 Combined response of EPT to dissolved oxygen and water temperature (left graph) and to dissolved oxygen and nitrate (right graph).....	69
Figure 4.45 Average annual precipitation and simulated runoff, and temperature for the baseline period (1995-2005) and the future scenarios (2030 and 2060) in the Pinios basin.	75
Figure 4.46 Average annual sediment, TP and TN loads to rivers and streams for the baseline period (1995-2005) and the future scenarios (2030 and 2060) in the Pinios basin.	76
Figure 4.47 Average annual cotton and corn yields, and total irrigation water abstracted from the sources for the baseline period (1995-2005) and the future scenarios (2030 and 2060) in the Pinios basin.	78
Figure 4.48 Mean ASPT and 95% confidence levels calculated based on predicted values at each sub-basin for the baseline conditions and for each scenario run. Predictions were made with the use of GLMs.....	79
Figure 4.49 Mean EPT and 95% confidence levels calculated based on predicted values at each sub-basin for the baseline conditions and for each scenario run. Predictions were made with the use of GLMs.....	79
Figure 4.50 Mean ASPT and 95% confidence levels calculated based on predicted values at each sub-basin for the baseline conditions and for each scenario run. Predictions were made with the use of BRTs.....	80
Figure 4.51 -1. Sorraia watershed location; 2. Coordinates of the basin limits.....	87
Figure 4.52 Land use map (source: Mateus et al, 2009 – detailed Sorraia Valley – and Global Cover 2006).....	88
Figure 4.53 MARS-DPSIR Conceptual model for Sorraia Basin. DPSIR = Driver–Pressure–State–Impact–Response chain. Dashed lines represent.....	91
Figure 4.54 Spatial distribution of the inputs used in SWAT model: 1. Soil type; 2. Slope; 3. Precipitation station distribution; 4. Land use.	93
Figure 4.55 Comparison of monthly flow in “Moinho Novo” location: red line – observed; black line – modeled	94
Figure 4.56 Nitrate results in river- Local Moinho Novo (Line is the model results and dots are the observed); 2. Phosphorus results in river - Local Moinho Novo (Line is the model results and dots are the observed) .	95
Figure 4.57 -1. Nitrate in river - Local Samora Correia (Line is the model results and dots are the observed); 2. Phosphorus in river - Local Samora Correia (Line is the model results and dots are the observed).....	96
Figure 4.58 First plane of the Principal Component Analysis using a) variables describing natural environmental variability, b) stressor variables, c) fish-based indicators. Colours indicate the basin to which sites belong to (blue – Tagus basin; red – Sorraia basi	97
Figure 4.59 Location of sampling sites	98
Figure 4.60 Histograms of environmental, pressure and stressor variables before transformation.....	101
Figure 4.61 Comparison between meteorological data observed and climate modeled data for the period 2006-2015.....	109
Figure 4.62 Water balance in mm for each for each Storyline: precipitation, runoff, flow and actual evapotranspiration	117
Figure 4.63 Water balance in % for each scenario (IPSL climatic model and 2060 timeline example): Precipitation, runoff, percolation, flow and actual evapotranspiration	117
Figure 4.64 Sediments in ton/ha/year for each Storyline	118
Figure 4.65 First plane of the PCA using environmental, pressure and stressor variables (Tagus EFI+ dataset). Green rectangles indicate environmental variables; orange rectangles indicate abiotic stressors; yellow rectangles indicate predictors removed according to	119

Figure 4.66 Dendrogram of the hierarchical classification of fish based metrics using Euclidean distances and the unweighted pair-group average method. Highlighted metrics indicate the metrics that were used analyse the response to multiple stressors.....	121
Figure 4.67 Partial response of the predictor variables included in the GLM model for the % of potamodromous species.	128
Figure 4.68 Partial response of the predictor variables included in the GLM model for the % of tolerant species.	129
Figure 4.69 Partial response of the predictor variables included in the GLM model for the % of intolerant species.	130
Figure 4.70 Partial response of single (A) and combined effects (B) of the predictor variables included in the GLM model for the EQR of the Portuguese Diatoms biotic integrity index.....	132
Figure 4.71 Partial response of single (A) and combined effects (B) of the predictor variables included in the GLM model for the EQR of the Portuguese macrophytes biotic integrity index.....	133
Figure 4.72 Partial response of the predictor variables included in the GLM model for the EQR of the Portuguese Macroinvertebrates biotic integrity index.....	134
Figure 4.73 Partial response of single (A) and combined effects (B) of the predictor variables included in the GLM model for the EQR of the Portuguese fish biotic integrity inde	135
Figure 4.74 Annual water availability for each storyline (IPSL climatic model and 2060 timeline example), in mm.....	136
Figure 4.75 Distribution of Nutrient load (total nitrogen) in Sorraia basin for each storyline implemented (ton/ha/year)	137
Figure 4.76 Distribution of Nutrient load (total phosphorous) in Sorraia basin for each storyline implemented (ton/ha/year)	137
Figure 4.26 Partial response of single (A) and combined effects (B) of the predictor variables included in the GLM model for Ecological Status using 2011 data. The Y scale (A) and the blue-red gradient (B) represents the probability of Ecological Status to belong t	139
Figure 4.78 Partial response of single (A) and combined effects (B) of the predictor variables included in the GLM model for Ecological Status using 2011 data. The Y scale (A) and the blue-red gradient (B) represents the probability of Ecological Status to belong t	140
Figure 4.79 Partial response of single (A) and combined effects (B) of the predictor variables included in the GLMM model for Ecological Status. The Y scale (A) and the blue-red gradient (B) represents the probability of Ecological Status to belong to good/very good classes	141
Figure 4.80 Projections of the probability of sites to be classified into “good” or “very good” Ecological Status under the considered scenarios of future land use changes.	142
Figure 4.81 Partial response of single (A) and combined effects (B) of the predictor variables included in the GLM model for Fishery Quality Index.	144
Figure 4.82 Projections of fish–based EQR in the Sorraia River Basin under each story line and for each climatic model (a – IPSL model, b – GFDL model). In the X-axis labels, the baseline represents the current EQR values, str1 1-3 denotes each storyline and ipsl and gfdl denotes the climatic model	147
Figure 4.83 Projections of fish–based EQR in the Sorraia River Basin under different measures scenario, for each story line and for each climatic model (a – IPSL model, b – GFDL model). In the X-axis labels, the baseline represents the current EQR values, str1 1-3 denotes each storyline, ipsl and gfdl denotes the climatic model and m1-4 denotes each Program of Measures scenario.....	148
Figure 5.1 The river network of Austria with delineation of the Drava and Mura River Basins.	153
Figure 5.2 MARS empirical model for the Austrian Drava/Mura River Basins.	161
Figure 5.3 Fish zones and fish sampling sites in the Drava and Mura River Basins considered for further analyses.	162
Figure 5.4 Analytical design including the analysis of stressor distribution and patterns, the descriptive analysis of the relationship between variables ‘stressor category, ‘stressor quantity’ and selected indicators and the analysis to implement the MARS model for Drava and Mura River Basins.....	166
Figure 5.5 Frequency of water bodies with related fish sampling sites and the occurrence of single stressor intensities.....	169

Figure 5.6 Frequency of water bodies with related fish sampling sites and the occurrence of single stressor intensities).	170
Figure 5.7 Water bodies affected by different stressor categories in the Drava and Mura River Basins.	172
Figure 5.8 Water bodies affected by different stressor quantities in the Drava and Mura River Basins.	173
Figure 5.9 (a) and (b) Response of indicator ‘population age structure’ (AS) to variables ‘Stressor category’ and ‘Stressor quantity’	175
Figure 5.10 (a) and (b) Response of indicator ‘Fish Index Austria’ (FIA) to variables ‘Stressor category’ and ‘Stressor quantity’	175
Figure 5.11 (a) and (b) Response of indicator ‘ecological status’ (ES) to variables ‘Stressor combination’ and ‘Stressor quantity’	176
Figure 5.12 Proportion of variance explained by model 1 (stressor variables only) compared to model 2 (stressor variables and fish zone) for all fish based indicators as well as for the ecological status.	178
Figure 5.13 Distribution of the predictor importance based on the BRT models for the 16 indicators, separated by model (model 1 – stressors and model 2 – stressors and ‘fish zone’ (FIZ)).	179
Figure 5.14 DPSIR model for the Middle Elbe basin.	191
Figure 5.15 Landscape slope classes and observation stations with nearby gauges in the German Middle Elbe Basin with marker lines at main source station Schmilka at the Czech-German border and the basin outlet at dam Geesthacht.	193
Figure 5.16 Assumed population changes in dependence of population density for Storyline 1 (left), 2 (middle) and 3 (right) for the years 2025 and 2050 compared to the zensus data 2010 for German municipalities.	199
Figure 5.17 Share of municipalities and inhabitants in dependency of population density in Germany and the Elbe catchment according to zensus data 2010.	199
Figure 5.18 Observed and modelled monthly load of TP and TN at station near basin outlet (Neu Darchau)	203
Figure 5.19 Modelled and observed monthly loads for TN (left) and TP (right figure) different colored for the years at basin outlets of Middle Elbe in years of validation period. Hatched lines indicate the $\pm 30\%$ confidence interval.	203
Figure 5.20 Observed (hatched black line) and simulated chlorophyll a concentration as monthly means modeled with PhytoBasinRisk in river Spree at station Jannowitzbrücke	204
Figure 5.21 Observed and modelled chlorophyll a (chl _a) seasonal means in Elbe stations (left figure) and in tributaries (right figure)	204
Figure 5.22 Monthly simulated chlorophyll a concentrations in sub-basins Elde (Dömitz) and Spree (Baumschulenweg) under synthetically altered input data (see text) in comparison to simulation for currents means of the period 2006-2010.	205
Figure 5.23 Model performance of the empirical model derived from GLM model.	209
Figure 5.24 Residual for each of the terms used in the GLN model for Middle Elbe for response variable chlorophyll a-	210
Figure 5.25 Relative influence of each of the variables to the GLM.	210
Figure 5.26 Simulated emission of TN (upper graph) and TP (lower graph) at outlet of Middle Elbe basin by model MONERIS (vs. 3.0) for longterm monthly baseline simulation (71-01/2010) and for all three storylines (SL1 – 3) driven by ISI-MAP climate scenarios GFDL or IPSL for RCP 8.5 or 4.5 and as a long term mean for the periods 2025 (2020-2030) and 2050 (2045-2055). The emissions are separated for the pathways listed in	213
Figure 5.27 Comparison of simulated monthly values of cumulated discharge (Q), TN loads (L) and resulting TN concentration (C) for storyline 3 driven with climate GFDL and RCP 8.5 at basin outlet for the future period 2050.	213
Figure 5.28 Change of chlorophyll a concentration to baseline (zero) for each month at basin outlet (station Boizenburg) modeled by PhytoBasin Risk in the three MARS storyline driven by simulated nutrient concentrations (MONERIS), and discharges (SWIM) for two climate scenarios and two future periods (2025; 2050)	215
Figure 5.29 Proportion of calculated nutrient retentions (total P; upper graph; total N; lower graph) of total load in German area of Middle Elbe basin.	216

Figure 5.30 Location of the Odense River catchment, subbasin division and location of runoff and nutrients monitoring stations and climate change station.....	221
Figure 5.31 The DPSIR model for the Odense River basin. Outputs from a process-based hydrological catchment model are linked to empirical ecological models to assess biotic state and ecosystem services.	225
Figure 5.32 Land uses % coverage in the baseline and the three LUC scenarios (1=High-technology agriculture, 2=Agriculture for nature, 3=Market driven agriculture).....	228
Figure 5.33 Observed (black dots) and simulated (grey line) daily discharge (m ³ /s) at the four gauging stations in the Odense River catchment during calibration (2000-2005) and validation (2006-2009) periods.....	234
Figure 5.34 Daily nutrient loads (Kg) observed and predicted in sub-basin 14 during calibration (2000-2005) and validation (2006-2009) periods.....	235
Figure 5.35 Daily nutrient loads (Kg) observed and predicted in sub-basin 20 during calibration (2000-2005) and validation (2006-2009) periods.....	236
Figure 5.36 Daily nutrient loads (Kg) observed and predicted in sub-basin 21 during calibration (2000-2005) and validation (2006-2009) periods.....	237
Figure 5.37 Daily nutrient loads (Kg) observed and predicted in sub-basin 22 during calibration (2000-2005) and validation (2006-2009) periods.....	238
Figure 5.38 Changes expected in water balance components subject to be modified when analyzing the isolated effects of LUC scenarios under observed climate.....	241
Figure 5.39 Changes in flow components when analyzing the isolated effects of LUC scenarios under observed climate. a) Absolute changes in tile drain flow and groundwater flow with respect to baseline; b) % contribution of the different flow components in all the scenarios.	241
Figure 5.40 Changes in N and P applied in fertilizer for the different scenarios.	242
Figure 5.41 Changes expected in nutrient loads when analyzing the solely effects of LUC scenarios under observed climate.....	242
Figure 5.42 Changes predicted in the water balance components for the different scenarios.....	243
Figure 5.43 Absolute changes from baseline predicted in tile drainage flow and groundwater flow for the different scenarios. Total flow results are showed again to facilitate visualization.	244
Figure 5.44 depicts the expected changes in nutrient loads. While organic nutrients follow a similar trend, variations in predicted loads are different for the two mineral species modelled.	244
Figure 5.45 Changes predicted in nutrient loads for the different scenarios.	244
Figure 5.46 Predictions of BRT models with all pre-selected variables for each ecological indicator.....	253
Figure 5.47 Chang in predictive deviance by dropping variables	254
Figure 5.48 Partial interaction of all the variables against the fish index DFFV_EQR.....	255
Figure 5.49 Partial interaction of all variables in the plant index DVPI_EQR	256
Figure 5.50 Partial interaction of all variables in the macro-invertebrates index DVFI_EQR.....	257
Figure 5.51 Partial interactions of all variables in the MARS index BInd12 (Average score per taxon ASPT)	258
Figure 5.52 Histograms of the response variables (ecological indicators).....	259
Figure 5.53 Predictions verses input indicators from the previous models developed by EUREKA.	262
Figure 5.54 Predictions verses input indicators from the new GLM analysis.....	265
Figure 5.55 Predictions verses input indicators from the new GLM analysis for DVPI_EQR without pH variables.	266
Figure 5.56 DFFV_EQR, the Danish fish index, calculated for three combined climate change-land use change scenarios for 31 subbasins in the Odense catchment.....	272
Figure 5.57 DVPI_EQR, the Danish macrophyte index, calculated for three combined climate change-land use change scenarios for 31 subbasins in the Odense catchment.	273
Figure 5.58 DVFI_EQR, the Danish macroinvertebrate index, calculated for three combined climate change-land use change scenarios for 31 subbasins in the Odense catchment.	274
Figure 5.59 ASPT, average score per taxon, calculated for three combined climate change-land use change scenarios for 31 subbasins in the Odense catchment.....	275

Figure 5.60 DVFI_EQR, the Danish macroinvertebrate index, calculated for three combined climate change-land use change scenarios for 31 subbasins in the Odense catchment.	276
Figure 5.61 DVPI_EQR, the Danish macrophyte index, comparing baseline (DVFI_EQR_PLU_85) to MARS storyline 1 (high-tech agriculture, DVFI_EQR_HT_60, situation 2055-2064) for 31 subbasins in the Odense catchment.....	276
Figure 5.62 DVPI_EQR, the Danish macrophyte index, calculated for three combined climate change-land use change scenarios for 31 subbasins in the Odense catchment.	277
Figure 5.63 Maps of the case study area. Left: The Dinkel catchment in red, with the German part hatched and the Dutch part solid red, and the Regge catchment in grey. Right: The Dinkel catchment in yellow and the Dinkel river and its tributaries in the Netherlands in blue. The main cities and villages in the Dinkel catchment in the Netherlands are shown in red.....	280
Figure 5.64 River basins according to the RBMP in the Netherlands.....	280
Figure 5.65 Chemical status of surface water bodies in the Regge and Dinkel catchments (from Waterboard Vechtstromen, 2015). Left: Total Phosphate, Right: Total Nitrogen. Green: good, yellow: moderate, orange: poor and red: bad status. Blue: no WFD water body.....	282
Figure 5.66 MARS model of the Dinkel catchment. Boxes have been given a colour according to the model they belong to: red = input for the process models, green = output of the process models and input for the empirical models, purple = output of the empirical models. The solid lines indicate the relationships between the different elements of the MARS model: red = positive correlation, blue = a negative correlation. The capital letter C shows that the ‘capacity’ of the ecosystem service is modelled. The dashed arrows indicate on which MARS model element the response element has an e.....	284
Figure 5.67 Modelling chain for the Dinkel catchment. The elements in which the calculations take place are indicated by rectangular boxes. Blue boxes for the process model chain and green boxes for the empirical model (EM). The most important inputs for each calculation element have been displayed as thick arrows. The inputs that were used to make the EM are indicated by thick grey arrows. The most important outputs have been indicated by thin arrows. The inputs that were changed in the scenario runs are indicated by red arrows. The abbreviations stand for: GW = ground water, SW = surface water, EM = empirical model, P = phosphorus, N = Nitrogen, WWTP = waste water treatment plant.....	286
Figure 5.68 Overview of the LGSI areas (light brown), SOBEK/DELWAQ model schematization (coloured lines), calibration monitoring locations (red dots) and waste water treatment plants (black dots) in the process-based model. More than three calibration points were used for building the LGSI-model and the SOBEK model. The monitoring locations shown are used to calibrate the DELWAQ model.	297
Figure 5.69 LGSI areas (coloured areas) and inflow points (black dots) into the SOBEK/DELWAQ model. Red dots are the calibration points of the of the corresponding red-rimmed areas in the LGSI model. ..	298
Figure 5.70 Modelled and measured data for 2000-2012 for location 30-001. The modelled data are indicated by the solid black line and the measured data are indicated by the red dots. From top to bottom and from left to right: Chloride, chlorophyll-a, total nitrogen, total phosphorus, nitrate, phosphate, oxygen, water temperature and solid particulate matter.	311
Figure 5.71 Modelled and measured data for 2000-2012 for location 33-001. The modelled data are indicated by the solid black line and the measured data are indicated by the red dots. From top to bottom and from left to right: Chloride, chlorophyll-a, total nitrogen, total phosphorus, nitrate, phosphate, oxygen, water temperature and solid particulate matter.	312
Figure 5.72 Modelled and measured data for 2000-2012 for location 34-033. The modelled data are indicated by the solid black line and the measured data are indicated by the red dots. From top to bottom and from left to right: Chloride, chlorophyll-a, total nitrogen, total phosphorus, nitrate, phosphate, oxygen, water temperature and solid particulate matter.	313
Figure 5.73 Target diagram showing the normalized bias and signed, normalized, unbiased root-mean square deviance of the model results with respect to the observations. The results are shows for the locations 30-001, 33-001 and 34-033 for the winter and summer months between 2000 and 2012. The years are indicated by colour. From left to right: chloride, chlorophyll-a, total nitrogen, total phosphorus, nitrate, phosphate, oxygen, water temperature and suspended particulate matter. The x axis shows the root mean-squared-deviance (RMSD), which tells us whether the pattern of the model matches the pattern of the data, and the y axis shows us the bias, which tells us whether the mean of the model matches the mean of the data. Results	

within the drawn circle with overall score $RMSD = 1$ score at least ‘reasonable’, while results within the dashed circle $RMSD = 0.74$ score ‘good’ .	314
Figure 5.74 Yearly average rainfall and air temperature per climate model and climate scenario for the periods 2000, 2030 and 2060. T0-T12 (2000) = 2000-2012, T0-T12 (2030) = 2024-2036, T0-T12 (2060) = 2054-2066.	317
Figure 5.75 Cumulative frequency diagrams of the calculated discharge (for 13 years) at location 34-033 for the four different climate models (horizon 2060) and the baseline model (NO_O_2000).	318
Figure 5.76 Cumulative frequency diagrams of the calculated discharge (for 13 years) at location 34-033 for the three storylines (period 2000) and the baseline model (NO_O_2000).	321
Figure 5.77 Cumulative frequency diagrams of the calculated discharge (for 13 years) at monitoring location 34-033 for the different scenarios comprised of a combination of a climate model and a storyline (period 2060) and the baseline model (NO_O_2000).	323
Figure 5.78 Partial dependence plots showing the BRT-fitted functions for submerged macrophyte cover. Y axis are on the log scale and centred to have a zero mean over the data distribution. The X axis indicates the data range of (from left to right and from top to bottom) particulate matter (mg/l, summer decadal mean), water temperature ($^{\circ}C$, summer decadal mean), width-depth ratio, total phosphorus ($\mu g/L$, summer decadal mean), flow velocity (m/s, summer decadal mean), and total nitrogen (mg/l, summer decadal mean). The tick marks give an indication of the data distribution.	326
Figure 5.79 Partial responses of the BRT for flow velocity, for submerged (left) and emergent (right) macrophyte cover.	327
Figure 5.80 Partial dependence plots showing the BRT-fitted functions for emergent and floating macrophyte cover. The Y axis are on the log scale and centred to have a zero mean over the data distribution. The X axis indicates the data range of (from left to right and from top to bottom) emergent macrophytes for flow velocity (m/s, summer decadal mean) and water temperature ($^{\circ}C$, summer decadal mean) and for floating macrophytes for flow velocity (m/s, summer decadal mean), total phosphorus ($\mu g/L$, summer decadal mean), total nitrogen (mg/l, summer decadal mean), and water temperature ($^{\circ}C$, summer decadal mean). The tick marks give an indication of the data distribution.	327
Figure 5.81 From left to right and from top to bottom: Interaction effects for submerged macrophyte cover for flow velocity (m/s, summer decadal mean) * water temperature ($^{\circ}C$, summer decadal mean), particulate matter (mg/l, summer decadal mean) * water temperature ($^{\circ}C$, summer decadal mean) and width-depth ratio (-) * water temperature ($^{\circ}C$, summer decadal mean). Interaction effects for emergent macrophyte and floating macrophyte cover for flow velocity (m/s, summer decadal mean) * water temperature ($^{\circ}C$, summer decadal mean).	328
Figure 5.82 Partial responses of the BRT for the ASPT. From left to right and top to bottom: oxygen (mg/l, decadal summer mean), total nitrogen (mg/l, summer decadal mean), width-depth ratio, total phosphorus ($\mu g/L$, summer decadal mean), water temperature ($^{\circ}C$, summer decadal mean), flow velocity (m/s, summer decadal mean), and suspended particulate matter (mg/l, decadal summer mean).	331
Figure 5.83 Partial responses of the BRT for the function feeding group ratio (FFGr). From left to right and top to bottom: flow velocity (m/s, summer decadal mean), oxygen (mg/l, decadal summer mean), particulate matter (mg/l, decadal summer mean), width-depth ratio, total nitrogen (mg/l, summer decadal mean), and water temperature ($^{\circ}C$, summer decadal mean).	332
Figure 5.84 Visualisation of interaction effect of Ntot and flow for the ASPT.	333
Figure 5.85 Partial responses of the BRT for fish abundance. From left to right and top to bottom: water temperature ($^{\circ}C$, summer decadal mean), flow velocity (m/s, summer decadal mean), total phosphorus ($\mu g/L$, summer decadal mean), total nitrogen (mg/l, summer decadal mean), particulate matter (mg/l, decadal summer mean), oxygen (mg/l, decadal summer mean).	335
Figure 5.86 Result of the Travel Time modelling for the Springendalse Beek (left) and Roelinksbeek (right). Note the difference in scale of the y-axis.	338
Figure 5.87 Cumulative discharge versus Travel time (log-scale). Left: Springendalse beek. Right: Roelinksbeek.	339
Figure 5.88 Major urban areas within the Ruhr Basin (modified after MUNLV 2005).	345
Figure 5.89 Relative influence of natural and anthropogenic predictor groups on the metrics of the three organism groups	360

Figure 5.90 Relative influence (%) of the most important anthropogenic predictors on the three organism groups.....	362
Figure 5.91 Summary of the relative influence of predictor variables to the full BRT model.....	364
Figure 5.92 Partial Dependence Plots showing the fitted values for “Total biomass of brown trout” along selected predictor gradients.....	365
Figure 5.93 Scatter plot of observed vs predicted values of EQR.....	367
Figure 5.94 Map of Thames basin, showing location of some of the monitoring sites. Site 1 = Hannington Wick; Site 2 = Newbridge; Site 3 = Swinford; Site 4 = Wallingford; Site 5 = Reading; Site 6 = Sonning; Site 7 = Runnymede / Egham. Source: Bowes et al. (in press).....	376
Figure 5.95 DPSIR model for the Thames basin.....	381
Figure 5.96 Chemistry and chlorophyll sampling sites on the Thames basin (Thames Initiative data).....	383
Figure 5.97 Thames Basin Groundwater Models.....	386
Figure 5.98 PROTECH modelling performance: Comparison between observed and simulated total chlorophyll a in Farmoor Reservoir for 2014.....	389
Figure 5.99 Flow diagram of the modelling process for the MARS storylines simulations.....	392
Figure 5.100 Percentage changes associated with the MARS storylines for the Thames basin at site TC6, the Thames at Eynsham in the upper reaches (left) and at site TC18, the Thames at Wallingford in the middle reaches (right) for the growing seasonal chlorophyll-a concentration (days above 9°C) (BInd8) and a low flow indicator, the flow exceeded 90% of the time Q90.....	399
Figure 5.101 Percentage changes associated with the MARS storylines for the Thames basin at site TC6, the Thames at Eynsham in the upper reaches (left) and at site TC18, the Thames at Wallingford in the middle reaches, for the Total Phosphorus concentration during the growing seasonal (days above 9°C) (BInd9_TotalP), extreme temperature the water degree days above 9°C (DegreeDays_Above9) and a low Dissolved Oxygen indicator, the 10 th percentile DO (10 th %ile DO).....	400
Figure 5.102 Observed and modelled response of chlorophyll-a to left: nutrient and extreme temperature (AIC: 167.5); middle: extreme temperature and length of extreme low flow pulses (AIC: 166.5); right: extreme temperature and number of extreme high flow pulses (AIC: 170.5). Observations are shown as circle, radius being proportional to BInd8. Modelled response are shown as colour gradient shows (blue low to red high) and contour lines. Note difference in scale in the colour gradients.....	403
Figure 6.1 Location and surface are of Vörtsjärv and its tributary basins.....	409
Figure 6.2 Conceptual diagram of study design, with downscaling from basin to lake, from stressors to biotic indicators. Models and storylines are in ellipse-shaped boxes whereas variables are in polygon-shaped boxes. Solid and dashed arrows represent model inputs and outputs respectively.....	412
Figure 6.3 DPSIR model of Vörtsjärv basin, as designed in collaboration with Deltares.....	413
Figure 6.4 Calibration results for the Väike Emajõgi flow (left) and DIC concentrations (right) using respectively Persist and INCA models. Time-series of observed (blue solid line or dots) and predicted (red solid line) values comprise also statistical results of the model run.....	418
Figure 6.5 Annually-averaged time series of the Väike Emajõgi flow (m ³ s ⁻¹) as modelled by INCA-C for predictive scenarios using GFDL (left) and IPSL (right) climate models data as input values. Thicker double-headed arrow on the y axis corresponds to the flow range in reference conditions.....	419
Figure 6.6 Annually-averaged time series of the Väike Emajõgi DIC concentrations (mg L ⁻¹) as modelled by INCA-C for predictive scenarios using GFDL (left) and IPSL (right) climate models data as input values. Thicker double-headed arrow on the y axis corresponds to the DIC range in reference conditions.....	420
Figure 6.7 Annually-averaged time series of Lake Vörtsjärv Chl a (µg L ⁻¹) which was modelled by BRT for predictive scenarios using GFDL (left) and IPSL (right) climate models data as input values. Thicker, double-headed arrow on the y axis corresponds to the Chl a range in reference conditions.....	421
Figure 6.8 Annually-averaged time series of Lake Vörtsjärv cyanobacteria biomass (Bcyan mg ww L ⁻¹) which was modelled by BRT for predictive scenarios using GFDL (left) and IPSL (right) climate models data as input values. Thicker, double-headed arrow on the y axis corresponds to the range of Bcyan in reference conditions.....	422
Figure 6.9 Annually-averaged time series of Lake Vörtsjärv rotifer biomass (Broti µg ww L ⁻¹) which was modelled by BRT for predictive scenarios using GFDL (left) and IPSL (right) climate models data as input	

values. Thicker, double-headed arrow on the y axis corresponds to the range of Broti in reference conditions.	422
Figure 6.10 Location of the Lepsämänjoki catchment. Field areas are marked by gray color.....	429
Figure 6.11 Conceptual model of the Lepsämänjoki case.	430
Figure 6.12 Location of the river basins with Chl- α observations, and location of the weather stations.....	431
Figure 6.13 Change in peak flow according to the climate scenarios.	437
Figure 6.14 Mean duration of high and low pulses within each year.....	437
Figure 6.15 Suspended sediment and nutrient concentrations at the middle reaches on the river.	439
Figure 6.16 The single effects for Chl- α concentration; (a) TP, (b) T _w . Different colors represent different measurement points.	440
Figure 6.17 Residual of the GLMM model.	441
Figure 6.18 Partial responses of the parameters in GLMM model.....	442
Figure 6.19 Interactions between total P (TP) and water temperature (T _w) in the GLMM model.	442
Figure 6.20 Partial responses in BRT model.....	443
Figure 6.21 Interactions in the BRT model.	444
Figure 6.22 Shift in peak concentrations of Chl-a according to different story lines from current situation to years 2025-2034. (a) Härkälänjoki tributary, (b) middle reaches of the river Lepsämänjoki.	445
Figure 6.23 Shift in peak concentrations of Chl-a according to different story lines from current situation to years 2025-2034. (a) Härkälänjoki tributary, (b) middle reaches of the river Lepsämänjoki.	446
Figure 6.24 Catchment scale nutrient production/removal rate.....	447
Figure 6.25 Nutrient production/removal rate in agriculture.....	448
Figure 6.26 Location of the Mustajoki/Teuronjoki catchment with different monitoring sites.	451
Figure 6.27 Conceptual model of the Mustajoki case.	452
Figure 6.28 Temperature in model results and observations in Lake Pääjärvi during the calibration period 31.5.1995-27.11.2003.....	457
Figure 6.29 Temperature profiles in Lake Pääjärvi during the calibration period 31.5.1995-27.11.2003. ...	458
Figure 6.30 Temperature profiles in Lake Pääjärvi during the calibration period 31.5.1995-27.11.2003. ...	458
Figure 6.31 Dissolved organic carbon in surface water of Lake Pääjärvi during the calibration period 31.5.1995-27.11.2003. Observations are from depth layer 0-15m and model result is from depth layer 7-8m.....	459
Figure 6.32 Dissolved organic carbon in surface water of Lake Pääjärvi during the validation period 19.5.2005-29.12.2009. Observations are from depth layer 0-15m and model result is from depth layer 7-8m.	459
Figure 6.33 Monthly average flows of the river Mustajoki in different scenarios.	460
Figure 6.34 Changes in duration of high (over 75th percentile) and low (less 25th percentile) pulses.	461
Figure 6.35 Simulated DOC concentrations at the outlet of the river Mustajoki. The periods of interest are marked by black bars.....	461
Figure 6.36 Dissolved organic carbon in surface water of Lake Pääjärvi in present situation (31.5.1995-27.11.2003) and in four scenario situations.....	462
Figure 6.37 Observed and calculated max. growing depth of large isoetids in some humic reference lakes (n = 9).....	465
Figure 6.38 Maximum growing depth (m) of large isoetids according to different storylines.....	466
Figure 6.39 Map of the Otra River, southernmost Norway, showing the locations of the Brokke hydropower station, and the three points on the river (Ose, Evje, and Skråstad) for which the modelling simulations were made. Ose and Evje are habitat for the landlocked salmon (bleke) while Skråstad is located on the reach for anadromous salmon near the river mouth. The dashed line in the upper part of the catchment depicts the dams and tunnel used to conduct water from the high-lying areas to the power plant at Brokke. Insert: map of Norway showing location of the Otra River.	468
Figure 6.40 Ecological status as of 2013 of streams and lakes in the Otra River basin (Agder, 2014).....	469
Figure 6.41 Conceptual model for the modelling at Otra following the DPSIR approach.....	471
Figure 6.42 Difference between the observed discharge and the discharge scenarios.	476
Figure 6.43 Bias correction of the discharge scenarios.	477

Figure 6.44 Modelling scheme for the Otra River with the five sub-catchments (boxes) and Lake Byglandsfjord, and the three key points at Ose, Evje and Skråstad. The solid circles denote discharge stations.....	478
Figure 6.45 Linked model scheme used in this study. Drivers are combined with model outputs time-series to serve as inputs for the next model in the chain.	480
Figure 6.46 Deposition sequences used for non-marine SO ₄ (S*). Future scenarios are constant amounts at 2010 levels (CONST), agreed national and international legislation (NAT), and maximum feasible reduction (MFR). Factors are relative to amounts measured in 1995 (average for 1994-1996) at NILU stations, adjusted with SO ₄ factors (see text for details).....	482
Figure 6.47 Annual mean runoff (mm/yr) at Ose for four 10-year periods under five future climate scenarios. Periods are 2010 (2006-2015), 2030 (2025-2034), 2060 (2055-2064), and 2100 (2090-2099). Scenarios are base (no change in climate), G4 (global climate model GFDL with representative concentration pathway RCP4.5), G8 (GFDL with RCP8.5), I4 (global climate model IPSL with RCP4.5), and I8 (IPSL with RCP8.5).	484
Figure 6.48 Comparison of projected discharge for the different climate scenarios at Drivenes.....	484
Figure 6.49 Mean monthly pH at Ose, Evje and Skråstad in the Otra River, as simulated by MAGIC under five climate scenarios. Scenarios are base (no change in climate), G4 (global climate model GFDL with representative concentration pathway RCP4.5), G8 (GFDL with RCP8.5), I4 (global climate model IPSL with RCP4.5), and I8 (IPSL with RCP8.5).	485
Figure 6.50 Mean monthly pH at Ose, Evje and Skråstad in the Otra River, as simulated by MAGIC under three acid deposition scenarios. Scenarios are NAT (agreed legislation), CONST (constant at 2010 levels), and MFR (maximum feasible reduction). Climate was assumed not to change.	486
Figure 6.51 Simulated frequency of months with mean pH below the threshold for salmon for 10-year periods 2010 (2006-2015), 2030 (2025-2034), 2050 (2045-2054) and 2100 (2090-2099) at three stations on the Otra River. Left-hand panels: baseline (no climate change) and four climate change scenarios; right-hand panels: three acid deposition scenarios. The “base” scenario assumes no future change in climate, but with the NAT scenario of acid deposition.	488
Figure 6.52 Linear models for the salmon dataset (a) and b) Bleke dataset (b). The original data points (black dots), model predictions (solid lines) and the model prediction 95% confidence interval (dashed lines) is shown. See Table 5.4 for R ² and variable significance.....	490
Figure 6.53 Generalized additive models for the salmon dataset (a) and Bleke dataset (b). The original data points (black dots), model predictions (solid lines) and the model prediction 95% confidence interval (dashed lines) is shown. For the Bleke dataset an outlier datapoint was excluded from the analysis but it is shown as an empty point. See Table 5.4 for R ² and variable significance.	490
Figure 6.54 Conceptual DPSIR model for the MARS project at Vansjø-Hobøl.	500
Figure 6.55 Catchment land-use map and model chain schematics. Land-use distribution of the Vansjø-Hobøl catchment (right panel) and corresponding schematic representation of the catchment-lake model network (left panel) indicating river reaches (R) modelled with INCA-P and lake basins (L) modelled with MyLake. The hydrological model PERSiST provides input for the catchment model, and the climate models provide forcing for all models.	504
Figure 6.56 Structure of the Bayesian Network (BN) model for ecological status of Lake Vansjø, basin Vanemfjorden. The model consists of four modules: (1) Climate and management scenarios (2), output from the process-based lake model MyLake; (3) monitoring data from Lake Vansjø (1990-2012); (4) the national classification system for ecological status of lakes. The prior probability distribution for each node is displayed both as horizontal bars and by percentages (the first column in each node), across the states (the second column). The set of arrows pointing to one node represents the conditional probability table for this node. Status classes: HG = High-Good (required by the WFD), M = moderate, PB = Poor-Bad. From Moe et al. (2016).....	507
Figure 6.57 Calibration of the INCA-P model. Simulated (line) and measured (squares) runoff (top panel), total suspended solids (middle panel) and monthly TP loads (lower left panel) along with cumulative TP loads simulated (dashed line) and calculated from observations (solid line) using INCA-P at the Hobøl river during the calibration period.	512
Figure 6.58 MyLake calibration in basin L1 and L2. Calibration performance of MyLake at Storefjorden (L1, left panels) and Vanemfjorden (L2, right panels) for total phosphorus (TP), chlorophyll (Chl), particulate	

phosphorus (PP) and phosphate (PO₄) over the calibration period of 2005-2012. The results are reported as the median (solid line), daily quartile statistics sampled from the parameter sets of equal likelihood (continuous area) together with the observations (circles)..... 514

Figure 6.59 MyLake extension with Bayesian Network in basin L2. Observed (open black circles) and predicted (red curves) values of (a) temperature, (b) Secchi depth, (c) total P, (d) chl-a and (e) cyanobacteria. Predicted values are median values (with 25 and 75 percentiles) of 60 runs of the process model MyLake with different parameter combinations (see section 2.1.1). (Predicted values for cyanobacteria are not available from this model). Blue triangles represent seasonal mean values for Secchi depth, total P and chl-a, and seasonal maximum value for cyanobacteria (corresponding to the node CyanoMax). Horizontal lines indicate the boundaries between ecological status classes: High-Good (H-G), Moderate (M) and Poor-Bad (P-B). From Moe et al. (2016). 515

Figure 6.60 Boosted regression tree. Regression tree for effects of temperature on the variable CyanoMax (seasonal maximum of cyanobacteria biomass). The numbers on the branches (18.85 and 20.2) show the significant breakpoints along temperature gradient. The bar plots in each resulting node show the probability distribution of CyanoMax across the three status classes: 1: High-Good (<10.5 µg/L), 2: Moderate (10.5-20 µg/L), Poor-Bad (≥20 µg/L). n = number of observations in each node. From Moe et al. (2016). 516

Figure 6.61 Boosted Regression Tree results. Relative influence of the four predictor variables (Temperature, Colour, Secchi and TP) on (a) Chl-a, (b) Chl-a:TP, (c) Cyano and (d) Microcystin, estimated by Boosted Regression Tree..... 519

Figure 6.62 Partial responses estimated by BRT. Partial responses of Cyanobacteria to the four predictor variables (Temperature, Colour, Secchi and TP), estimated by Boosted Regression Tree..... 520

Figure 6.63 Interaction plot estimated by BRT. Interaction plot for combined effects of Temperature and Secchi on Cyano, estimated by Boosted Regression Tree..... 520

Figure 6.64 Random Forest results. Partial dependence plot for combined effects of Colour, Temperature and TP on Cyanobacteria, estimated by Random Forest..... 521

Figure 6.65 Random Forest results. Partial dependence plot for combined effects of Colour, Temperature and TP on Microcystin, estimated by Random Forest. 522

Figure 6.66 Simulated runoff. Simulated yearly runoff as a function of time loads at the outlet of the Hobøl river from 1995 to 2070 using the extended baseline climate (solid line), and the RCP8 climate scenario with either the IPSL (short dashed line) or the GFDL (long dashed line) model ensemble..... 524

Figure 6.67 Effect of climate scenario. Simulated annual TP loads (ton/yr) as a function of time at the outlet of the Hobøl river from 2030 to 2060 using the extended baseline climate (solid line), the RCP4 climate scenario (short dashed line) or the RCP8 climate scenario (long dashed line) by the IPSL model ensemble. 524

Figure 6.68 Effect of storylines. Simulated annual TP loads (ton/yr) as a function of time at the outlet of the Hobøl river from 2030 to 2060 during storylines M0 (extended, solid line), M4 (Techno, long dashed line), M5 (Consensus, short dashed line) and M6 (Fragmented, dotted line). Storylines are detailed on Tables 6.2 and 6.3. 525

Figure 6.69 Best vs Worst cases. Simulated annual TP loads (ton/yr) as a function of time at the outlet of the Hobøl river from 2030 to 2070 during storylines M1 (extended baseline, solid line), best-case scenario (i.e., Consensus with GFDL, short long dashed line) and worst-case (i.e., Techno with IPSL long dashed line) Storylines are detailed on Tables 6.17 and 6.18. 525

Figure 6.70 Effect of climate. Simulated annual average Chl (□g/L) at St river from 2030 to during from 2030 to 2060 using the extended baseline climate (solid line), the RCP4 climate scenario (short dashed line) or the RCP8 climate scenario (long dashed line) by the IPSL model ensemble..... 527

Figure 6.71 Effect of storylines. Simulated annual average Chl (□g/L) at St time river from 2030 to 2060 during storylines M0 (extended, solid line), M4 (Techno, long dashed line), M5 (Consensus, short dashed line) and M6 (Fragmented, dotted line). Storylines are detailed on Tables 6.2 and 6.3. 528

Figure 6.72 Best vs Worst cases. Simulated annual average Chl (□g/L) at St time river from 2030 to 2060 during storylines M1 (extended baseline, solid line), best-case scenario (i.e.,

Concensus with GFDL, short long dashed line) and worst-case (i.e., Techno with IPSL, long dashed line) Storylines are detailed on Tables 6.2 and 6.3.....	529
Figure 6.73 Monthly averages. Simulated monthly average Chl (□g/L) at St entire simulation period during storylines M1 (extended baseline, solid line), best-case scenario (i.e., Consensus with GFDL, short long dashed line) and worst-case (i.e., Techno with IPSL, long dashed line). The shaded area indicates the Good/Moderate WFD status threshold.....	530
Figure 6.74 Map of the sampling sites of upland Wales. Green dots represent locations included in the spatially spread dataset, while the red dots indicate those sites used for the long-term dataset. See Data section for more info.	532
Figure 6.75 Ecological status of surface water bodies in Western Wales in 2015.....	533
Figure 6.76 Reasons for not achieving a good ecological status in 2015 (acidification is not included).....	533
Figure 6.77 Percentage overall water body status and objectives for 2015, 2021 and 2027.....	533
Figure 6.78 Drivers – Pressures – States – Impact – Response (DPSIR) model for the Welsh catchments. See legend for more info.	536
Figure 6.79 Plots showing biological responses to multi-stress at acid forest river type. The interaction between pH and TON (a), TON and pH (b) and precipitation and pH (c) are shown. Lines represent fitted values at different levels of the interacting stressor non-showed in the abscise axis (red: minimum value, yellow: Q10, green: Q50, blue: Q90 and violet: maximum value). See Table 7.3 for more info.	551
Figure 6.80 Plots showing biological responses to multi-stress at acid moorland river type. The interaction between pH and TON (a), TON and pH (b) and precipitation and pH (c) are shown. Lines represent fitted values at different levels of the interacting stressor non-showed in the abscise axis (red: minimum value, yellow: Q10, green: Q50, blue: Q90 and violet: maximum value). See Table 7.4 for more info.	552
Figure 6.81 Plots showing biological responses to multi-stress at circumneutral moorland river type. The interaction between pH and TON (a), TON and pH (b) and minimum temperature and pH (c) are shown. Lines represent fitted values at different levels of the interacting stressor non-showed in the abscise axis (red: minimum value, yellow: Q10, green: Q50, blue: Q90 and violet: maximum value). See Table 7.5 for more info. We removed outlier data from year 1992.	553
Figure 6.82 Plots showing biological responses to multi-stress in the spatial dataset. The interaction between pH and TON (a), TON and pH (b) and pH and latitude (c) are shown. Lines represent fitted values at different levels of the interacting stressor non-showed in the abscise axis (red: minimum value, yellow: Q10, green: Q50, blue: Q90 and violet: maximum value). See Table 6 for more info.	554
Figure 6.83 Plots showing ecosystem services’ responses to multi-stress in the spatial dataset. The interaction between pH and TON (a, c) and TON and pH (b, d) are shown. Lines represent fitted values at different levels of the interacting stressor non-showed in the abscise axis (red: minimum value, yellow: Q10, green: Q50, blue: Q90 and violet: maximum value). See Table 7.7 for more info.	555
Figure 6.84 Projected changes for invertebrate abundance (abun) in the acid forest, acid moorland and circumneutral moorland river types (long-term dataset) for the baseline period (base), 2030 and 2060, and for each of the climatic models (GFDL, IPSL) and scenarios (cons: consensus world, tech: technoworld and frag: fragmented world).....	557
Figure 6.85 Projected changes for invertebrate response diversity (RD) in the upper, middle and low Wye catchment for the baseline period (base), 2030 and 2060, and for each of the climatic models (GFDL, IPSL) and scenarios (cons: consensus world, tech: technoworld and frag: fragmented world).	558

List of Tables

Table 3.1. Resume table of the Process-based (PM), Empirical (EM) and Ecosystem service models used of each of the study basins.	7
Table 4.1 Daily and monthly performance statistics for the main inflows. Calibration period = 2002-2011; validation period = 1995-2001. Mean values for the simulated and observed periods are in m ³ s ⁻¹ . Taken from Bucak et al submitted.	35
Table 4.2 Calibration statistics for daily Mineral P and Nitrate Loads. While calculating the statistics, a window function with a search timeframe of 7 days was used to sample the model outputs closest to observed values.	36
Table 4.3 Lake models calibration statistics. While calculating the statistics, a window function with a search timeframe of 7 days was used to sample the model outputs closest to observed values.	39
Table 4.4 % Changes in total flow, mineral P and nitrate load with future scenarios.	44
Table 4.5. Change in average water level (m) for 2030s and 2060s period. Default: No land use and no climate change scenario, G:GFDL, I:IPSL, C:Consensus, T:Techno, F:Fragmented, 4.5:RCP 4.5, 8.5:RCP 8.5.	45
Table 4.6 Baseline and future TP averages for both lake models and their mean. Default: No land use and no climate change scenario, G:GFDL, I:IPSL, C:Consensus, T:Techno, F:Fragmented, 4.5:RCP 4.5, 8.5:RCP 8.5.	46
Table 4.7 Baseline and future TN (mg L ⁻¹) averages for both lake models and their mean. Default: No land use and no climate change scenario, G:GFDL, I:IPSL, C:Consensus, T:Techno, F:Fragmented, 4.5:RCP 4.5, 8.5:RCP 8.5.	47
Table 4.8. Baseline and future chl-a, cyanobacteria averages and EQR for both lake models and their mean. Default: No land use and no climate change scenario, G:GFDL, I:IPSL, C:Consensus, T:Techno, F:Fragmented, 4.5:RCP 4.5, 8.5:RCP 8.5. Chl-a is given as µg L ⁻¹ an.	48
Table 4.9. Goodness of fit criteria in Ali Efenti and Amigdalia flow gauging stations (subbasins 17 and 33 in Figure 6.1).	60
Table 4.10. Descriptive statistics for the data used in our analysis.	63
Table 4.11. Boosted Regression Tree model details.	64
Table 4.12. General linear models details.	64
Table 4.13. Detailed presentation of scenario model runs performed for Pinios case study.	71
Table 4.14. Representative concentration pathways in the year 2100 (source van Vuuren et al., 2011).	71
Table 4.15. Numeric results from the implementation of scenarios with SWAT in the Pinios river basin.	74
Table 4.16. Program of measures to be implemented in the River Basin Management Plan that are relevant for the Sorraia basin.	89
Table 4.17. Required data and source of data for running SWAT model in the Sorraia basin.	93
Table 4.18. Calibrated parameters values used in the SWAT model.	94
Table 4.19. List of candidate predictor variables.	99
Table 4.20. Functional guilds.	103
Table 4.21. Monthly bias correction factors for temperature and precipitation.	110
Table 4.22. Sorraia basin stakeholders.	111
Table 4.23. Element change according to Storyline 1, 2 and 3.	111
Table 4.24. Evolution of land use area (in percentage) for the storylines defined (km ²).	113
Table 4.25. Adjustments made to the inputs of the SWAT model.	114
Table 4.26. Program of measures to be implemented in the River Basin Management Plan (RBMP) that are relevant for the Sorraia basin.	115
Table 4.27. Total annual of precipitation, flow and actual evapotranspiration (in mm) for each implemented scenario.	116
Table 4.28. Total amount of nutrients and sediments for each scenario (ton/ha/year).	118
Table 4.29. VIF values of the selected set of environmental, pressure and stressor predictors.	120
Table 4.30. Goodness-of-fit measures of BRT models for the selected fish-based metrics and ecological quality ratios for macroinvertebrates, diatoms, macrophytes and fish.	122
Table 4.31. Mean rank of variable importance estimates of BRT and RF models for each selected fish-based metrics (predictor variables are sorted by a decreasing order of mean variable importance as measured by the mean rank).	123
Table 4.32. Mean rank of variable importance estimates of BRT and RF models for each EQR of Portuguese biotic integrity indices (predictor variables are sorted by a decreasing order of mean variable importance as measured by the mean rank).	124
Table 4.33. Goodness-of-fit measures of GLM models for the selected fish-based metrics.	125
Table 4.34. Goodness-of-fit measures of GLMM models for the EQR indicators. R ² m – Marginal R-square; R ² c – Conditional R-square.	125

Table 4.35. Estimated regression standardized coefficients of the models for the selected biotic state indicators (p-value of the t test are shown between brackets).....	127
Table 4.36. Models' accuracy measures	138
Table 4.37. Mean rank of variable importance estimates of BRT and RF models for the binary reclassification of Ecological Status of surface waters.....	139
Table 4.38. Estimated coefficients, standard errors and z tests of GLM and GLMM models for Ecological Status.....	140
Table 4.39. Percentage of sites with Ecological Status classified as "good" or "very good"	142
Table 4.40. Summary table of the multiple linear model for the Fishery Quality Index, including model R-squared, adjusted R-squared, F test, standardized coefficients (effect size), standard errors and respective t-tests.	143
Table 4.41. Average of Annual evapotranspiration and flow according to different measures	145
Table 4.42. Nutrients and sediments according to different measures.....	146
Table 5.1. Stressor categories according to Mühlmann (2013) and translation into stressor classes.....	160
Table 5.2. Classification table for Austrian fish metrics.....	163
Table 5.3. Description of biotic indicators (FIA metrics and other indicator	164
Table 5.4. Description of stressor variable recoding and calculation of the new variables 'Stressor category and 'Stressor quantity'	165
Table 5.5. Number and percentage of water bodies affected by different stressor quantities for all water bodies of the total basin/water bodies with fish sampling sites and separated by sub-basins Mura and Drava, fish zone and drainage area. Values in bold mark categories occurring more than 20 times in total	174
Table 5.6. Number and percentage of water bodies affected by different stressor categories for all water bodies of the total basin/water bodies with fish sampling sites and separated by sub-basins Mura and Drava, fish zone and drainage area. Values in bold mark categories occurring more than 20 times in total.	174
Table 5.7. Results of the Random Forest model indicating goodness of fit, ranked variable importance (VIMP) and if indicator was selected for Boosted Regression Tree analysis.	177
Table 5.8. BRT results with percentage of explained variance, variable importance of the three most important predictors and interactions for model 1 (all stressors as predictors) and model 2 (all stressors plus fish zone as predictors). ..	178
Table 5.9. Number of rivers and lake water bodies (WB; 1st RBM-Plan (FGGE 2009)) and of observation stations for model fitting in the German coordination regions of Middle Elbe	192
Table 5.10. Variables used to build up the empirical model for Middle Elbe and minimum and maximum of not transformed value in the vegetation period (Apr –Oct) in the years 2006-2010	195
Table 5.11. Pathways separating the total emission in the model MONERIS	196
Table 5.12. Simulated discharge ($m^3 s^{-1}$; cum Q) and water temperature ($^{\circ}C$; WT) averaged for the vegetation period (Apr-Oct) at station Boitzenburg calculated as longterm means of each period, the baseline period and the two future periods and in two RCP-projections based on data provided by Potsdamer Climate Institute (Roers et al. 2016).....	198
Table 5.13. Final effluent of WWTP of different size classes for N and P assumed for the storylines (SL1 – SL3)	200
Table 5.14. Change of emission input data to run MONERIS model for validation (2006-2010) and for the 3 MARS storylines in the future time periods 2025 and 2050.	200
Table 5.15. Climate input data summarized as longterm mean of the periods: validation period (2006-2010), climate baseline (1971-2001 for GFDL and IPSL) and future MARS storylines in 2020-2030 (2025) and 2045-55 (2050).....	200
Table 5.16. Model summary for GLM for Middle Elbe with response variable chlorophyll a	209
Table 5.17. Key results of the scenario analysis as seasonal mean (Apr-Oct) for station Elbe, Boitzenburg near basin outlet for concentrations of chlorophyll a, total phosphorus (TP, mg/l) and total nitrogen (TN). Minima are in shaded fields and maxima are in bold values.....	217
Table 5.18. Characteristics of the Odense River catchment.	221
Table 5.19. Absolute area change of the different land use types for the three scenarios (and % of each change regarding total basin surface). In bold those changes involving more than a 5% of total basin area.	228
Table 5.20. Change in fertilizer application rates (%) for the different scenarios (1=High-technology agriculture, 2=Agriculture for nature, 3=Market driven agriculture). Absolute fertilization rates are shown for willow since it is a new land use in scenario 1.	229
Table 5.21. Crop management operation dates for current and long term (2060) scenario.	229
Table 5.22. Adaptation of pig farms in 2060 to include grain maize.....	230
Table 5.23. 20 scenarios run in SWAT to analyze the individual effect of land use (a) and the possible effects in MARS storylines (b).	231
Table 5.24. Initial range and calibrated values of the selected parameters (IV=Initial value of parameter before calibration).	232

Table 5.25. Calibration (2000-2005) and validation (2006-2009, in brackets) performance statistics values for daily runoff and nutrients at the six monitoring points (four for nutrients) in the Odense River catchment.	239
Table 5.26. Projected changes (annual averages) relative to the baseline period (2011-2020) for the climate variables forced in SWAT.	239
Table 5.27. Contribution (%) of the different flow components to total discharge across scenarios.	243
Table 5.28. Variables that have high correlation (R ²) with each ecological indicator.	251
Table 5.29. Ranking and relative influence of the pre-selected variables for each indicator calculated by the BRT.	252
Table 5.30. maximum correlation of the predictor variables and the correlation coefficient for each response variable (Indicator)	260
Table 5.31. Equations estimated by EUREKA and the interactions among variables.	260
Table 5.32. Result for the drop test on the EUREKA models to view the change in deviance when dropping each variable.	263
Table 5.33. Equations and interactions estimated with new variable ranking.	264
Table 5.34. The final recommended equations and the interactions among variables.	266
Table 5.35. Description of independent variables in the final recommended equations. All variables are based on a time series 2004-2011 from 131 stream water stations.	267
Table 5.36. Scenarios considered when assessing the impact of multiple stressors on stream water quality.	269
Table 5.37. The variables needed for the empirical models, average values for the 31 subbasins for each scenario.	270
Table 5.38. Ecologic quality indices, average values for the 31 subbasins for each scenario.	271
Table 5.39. Characteristics of the Water Framework Directive water bodies in the Dinkel catchment (Waterboard Vechtstromen, 2015b).	281
Table 5.40. Data availability of parameters at monitoring locations and at WWTP outfalls.	289
Table 5.41. Abiotic and biotic parameters used for the empirical model.	290
Table 5.42. Chlorophyll-a values from monitoring location 36-003.	291
Table 5.43. Storyline interpretation for the Dinkel case study.	304
Table 5.44. Model implementation of the storylines. The changes are relative according to the baseline situation.	306
Table 5.45. Overview of the scenario runs.	308
Table 5.46. Calculated abiotic state variables for monitoring location 34-033. The values are averaged for the 13-year period 2000-2013.	315
Table 5.47. Characteristics of the baseline climate (year 2000) and the four climate change scenarios for 2060 horizon (all characteristics are averaged over a period of 13 years).	317
Table 5.48. The calculated abiotic state variables for temperature and flow conditions (average values over period of 13 years), for the different scenarios (climate, storylines and combination of climate and storylines).	320
Table 5.49. The calculated change in abiotic state variables for temperature and flow conditions, for the different scenarios (climate, storylines and combination of climate and storylines): blue increase, red decrease, compared to the baseline.	320
Table 5.50. BRT results of macrophyte cover per macrophyte type. PM = particulate matter, T = Water temperature, WDR = Width-Depth ratio, TP = Total phosphorus, F = Flow velocity, TN = Total nitrogen. Based on summer decadal means of the abiotic variables.	324
Table 5.51. GLM results for macrophyte cover. Subm = submerged macrophytes, emer = emergent macrophytes, floa = floating macrophytes, SPM = suspended particulate matter, T = Water Temperature, WDR = Width-Depth ratio, TP = Total phosphorus, F = Flow velocity, TN = Total nitrogen, SF [n]= spatial filter and eigenvector value, Intc. = intercept at y-axis.	329
Table 5.52. BRT results for macroinvertebrates. O = oxygen, TN = total nitrogen, TP total phosphorus, WDR = width-depth ratio, T = water temperature, SPM = suspended particulate matter, F = flow velocity.	330
Table 5.53. GLM results for ASPT and FFGr. ASPT = ASPT, FFGr = functional feeding group ratio, SPM = suspended particulate matter, T = Water temperature, WDR = Width-Depth ratio, TP = Total phosphorus, F = Flow velocity, TN = Total nitrogen, O = Oxygen, SF [n]= spatial filter and eigenvector value, Intc. = intercept at y-axis, * = interaction.	333
Table 5.54. BRT results for fish abundance. O = oxygen, TN = total nitrogen, TP total phosphorus, T = water temperature, PM = particulate matter, F = flow velocity.	334
Table 5.55. GLM results for fish abundance. Fish = fish abundance, SPM = Suspended Particulate Matter, T = Water Temperature, WDR = Width-Depth ratio, TP = Total phosphorus, F = Flow velocity, TN = Total nitrogen, O = Oxygen, * = interaction.	335
Table 5.56. Characteristics of the three studied tributaries of the Dinkel.	337

Table 5.57.Land use categories, assigned vegetation types and total carbon stocks of above ground and belowground (modified after Cirjacks et al. 2010)	356
Table 5.58.Selected storyline elements to be implemented in the case study of the Ruhr and their qualitative change and quantification for a decrease (-) or increase (+) of naturally-forested land in the three different worlds.....	358
Table 5.59.Significant interaction terms, potential interaction types and directional classifications determined for the metrics of invertebrates and macrophytes	363
Table 5.60.Explained deviance derived from BRT and relative influence of predictor groups.....	364
Table 5.61.Percentage cover and total carbon stocks of different vegetation units in the riparian area of the Ruhr Basin	366
Table 5.62.Estimated benefits of C and CO ₂ and prices for additional sequestered CO ₂ for the four different reforested amounts of pasture land	367
Table 5.63.Predicted invertebrate mean EQR values for the storyline elements “Loss of riparian zones” and “Restoration of riparian zones” in the three different scenarios.....	368
Table 5.64.Permeability (%) of the Thames basin.....	376
Table 5.65.Causes for poor environment status of water bodies of the Thames basin. Source: Environment Agency, 2009a	378
Table 5.66.Main drivers and stressors identified in the Thames basin	379
Table 5.67.Variables modelled in the Thames basin	380
Table 5.68.Thames basin observational data network used for the analysis.....	382
Table 5.69.Thames basin sampling sites information.....	383
Table 5.70.Research question and stressor combinations considered for the Thames basin (BInd8 is always the response)	390
Table 5.71.GLMM analysis results for research questions of Table 6.....	391
Table 5.72.MARS story line scenarios and criteria applied to the Thames basin.....	394
Table 5.73.Modelled mean baseline conditions modelled (2009-12) for the MARS indicators for the Thames Basin..	396
Table 5.74.Percentage change associated with the MARS storylines for the Thames basin at site: TC6 (Thames at Eynsham, upper reach) and TC18 (Thames at Wallingford, middle reach). Cells are shaded in red for changes greater than 25%, white for changes between +/- 25%, and blue for changes lower than -25%.....	397
Table 5.75.Percentage change associated with the MARS storylines for the Farmoor reservoir for the mean total (total chl a) and cyanobacteria chlorophyll a (Cyanobacteria chl a) concentration during the growing season (days above 9°C). Cells are shaded in red for changes greater than 25%, white for changes between +/- 25%, and blue for changes lower than -25%	401
Table 5.76.Ecological and stressor indicators for the sampling sites of the Thames basin for the year 2009 and 2011. Sites on the main channel are marked with *	405
Table 6.1.Origin of the data.	432
Table 6.2.Goodness-of-fit values for calibration and validation periods.	434
Table 6.3.Implementation of the storylines.	436
Table 6.4.Finnish classification of the ecological status.....	438
Table 6.5.Goodness-of-fit values of the GLMM model	441
Table 6.6.Statistics from the GLM-model.	445
Table 6.7.Statistics from the BRT model.....	446
Table 6.8.Capacity of the ecosystem.	448
Table 6.9.Implementation of the storylines.	453
Table 6.10.Properties of the different DOC pools in Pääjärvi MyLake Application.	456
Table 6.11.Investigated lakes in Central-Finland (Kanninen et al. 2009).....	464
Table 6.12.Distribution of land cover types in each of the sub-catchments in the Otra River basin.	477
Table 6.13.Median values for prognoses of future changes in climate parameters for Norway. Annual values are given for the period 2071-2100 relative to the reference period 1971-2000. RCP: relative concentration pathway; ΔT: change in temperature; ΔP: change in precipitation; ΔQ: change in runoff. Source: Hanssen-Bauer et al. (2015)).	481
Table 6.14.Summary of scenarios run for the Otra River for the period 2014-2099. Present-day refers to the period 2008-2014.	482
Table 6.15.Summary table for the methods used for the empirical modelling of the Otra datasets. RF = Random forests, LM=Linear model, GAM=Generalized additive model.....	491
Table 6.16.Median values for prognoses of future changes in climate parameters for Norway. Annual values are given for the period 2071-2100 relative to the reference period 1971-2000. RCP: relative concentration pathway; ΔT: change in temperature; ΔP: change in precipitation; ΔQ: change in runoff. Source: Hanssen-Bauer et al. (2015)).	508

Table 6.17. Multiple stressor matrix and scenarios run for the Vansjø-Hobøl River basin under the three storylines for future development outlined in the MARS project. Control period: 1996-2012; scenario period: 2030-2060.	510
Table 6.18. Summary of possible measures within the agriculture and wastewater sectors that can be associated with the three storylines for future development outlined in the MARS project. Column 3 specifies how the measures are implemented in the model chain.	511
Table 6.19. Outcome of INCA-P calibration assessed against the coefficient of determination (R^2), the Nash-Sutcliffe metric (N-S), the normalized bias (B^*) and the normalized root-mean square deviation (RMSD*) targeting best performance against TP.	513
Table 6.20. Outcome of INCA-P calibration assessed against the coefficient of determination (R^2), the Nash-Sutcliffe metric (N-S), the normalized bias (B^*) and the normalized root-mean square deviation (RMSD*) targeting best performance against TP loads.	513
Table 6.21. Outcome of MyLake calibration targeting best performance against total phosphorus (TP), phosphates (PO_4), chlorophyll-a (Chl) and particulate P (PP).	514
Table 6.22. Paired interactions for Cyanobacteria, estimated by Random Forest.	518
Table 6.23. Paired interactions for Microcystin, estimated by Random Forest.	518
Table 6.24. CPT for Cyanobacteria conditional on Chl-a (observed) and water temperature (observed). Each column contains the probability distribution of a child node for a given combination of states of the parent nodes. The bottom row ("Experience") contains the total count of observations for each combination of parent nodes. From Moe et al. 2016.	518
Table 6.25. Biotic states used to characterise invertebrate biodiversity.	540
Table 6.26. Final set of predictors used in the global models. ¹ For the spatial dataset, these variables are the average of historical series of climatic data from worldclim.com. ² For the long-term dataset, we calculated the climatic features of the precedent 12 months from Met Office UK (Aberporth, latitude=52.139, longitude=-4.570).	541
Table 6.27. Results of the multi-model inference for acid forest long-term dataset, showing the averaged SES and significance of abiotic states. Goodness-of-fit (r^2) is also shown. See Tables 7.1 and 7.2 to see biotic and abiotic state descriptions. * $p < 0.05$, ** $p < 0.01$, *** $p < 0.001$. Abiotic states with $p < 0.05$ are in bold.	548
Table 6.28. Results of the multi-model inference for acid moorland long-term dataset, showing the averaged SES and significance of abiotic states. Goodness-of-fit (r^2) is also shown. See Table 7.1 and 7.2 to see biotic and abiotic state descriptions. * $p < 0.05$, ** $p < 0.01$, *** $p < 0.001$. Abiotic states with $p < 0.05$ are in bold.	548
Table 6.29. Results of the multi-model inference for circumneutral moorland long-term dataset, showing the averaged SES and significance of abiotic states. Goodness-of-fit (r^2) is also shown. See Table 7.1 and 7.2 to see biotic and abiotic state descriptions. * $p < 0.05$, ** $p < 0.01$, *** $p < 0.001$. Abiotic states with $p < 0.05$ are in bold. We removed outlier data from year 1992.	549
Table 6.30. Results of the multi-model inference for the spatial dataset (2012-13), showing the averaged SES and significance of abiotic states. Goodness-of-fit (r^2) is also shown. See Tables 7.1 and 7.2 to see biotic and abiotic state descriptions. * $p < 0.05$, ** $p < 0.01$, *** $p < 0.001$. Abiotic states with $p < 0.05$ are in bold.	549
Table 6.31. Results of the multi-model inference for the ecosystem service dataset, showing the averaged SES and significance of abiotic states. Goodness-of-fit of the fixed (r_m^2) and fixed and random (r_m^2) terms are also shown. See Tables 7.1 and 7.2 to see biotic and abiotic state descriptions. * $p < 0.05$, ** $p < 0.01$, *** $p < 0.001$. Abiotic states with $p < 0.05$ are in bold.	550

1 Introduction

The MARS project (Managing Aquatic ecosystems and water Resources under multiple Stress) is a project study funded by the European Union under the 7th Framework Programme, contract number 603378. Details of the project can be found on the project website (www.mars-project.eu) and an overview and introduction to the project is given by Hering et al. (2015).

The MARS project supports water managers and policy makers at the water body, river basin and European scales in the implementation of the Water Framework Directive (WFD). It aims to address how a complex mix of stressors, for example resulting from urban and agricultural land use, water power generation and climate change, impacts European rivers, lakes, groundwater and estuaries, and what implications these stressor combinations have for ecological services, such as water provision.

Three scales of investigation are used within the MARS project, as follows:

- Field experiments on lakes and rivers have been used to address the effect of extreme climate events, such as heavy rainfall, heatwaves and water scarcity and the effects of environmental flows on a range of ecological services (MARS Work Package 3, WP3).
- 16 river basins throughout Europe have been investigated to characterise relationships between multiple stressors and ecological responses, functions and services. These basins have been chosen to represent a wide range of catchment characteristics and multiple stress conditions and consist of five in Southern Europe, six basins across Central Europe, and five in Northern Europe. They include investigations of multiple stressor combinations such as water scarcity and flow alterations (Southern Europe); hydrology, morphology and nutrient stress (Central Europe); and, hydrology and temperature alterations (Northern Europe) (MARS Work Package 4, WP4).
- At the European scale, using Europe-wide data sets, the MARS project has identified relationships between stress intensity, status and service provision, with a focus on large transboundary rivers, lakes and fish as direct providers of ecosystem services (MARS Work Package 5, WP5).

Results of these studies are being synthesized and jointly analysed in the context of stressor combinations, scenarios and water and catchment management responses (Work Package 6, WP6); a series of easy-to-use tools to support water resource management is being developed by the MARS project (Work Package 7, WP7); and, in the context of the Water Framework Directive, the Floods Directive and the Blueprint to Safeguard Europe's Water Resources, a series of policy support initiatives and documents are being developed and produced (Work Package 8, WP8).

2 The Workpackage 4 of MARS

The overall objective of Workpackage 4 (WP4), set out in the Description of Work for the MARS project, is to develop and link a series of basin-scale surface water, groundwater and ecological models to systematically appraise how multiple stressors affect water quantity and quality, ecological status, ecological functions and ecosystem services under contrasting scenarios of water resource management (including restoration scenarios), land use and climate change.

WP4 deals with the basin scale under multi-stressor scenarios across Europe. WP4 aims to characterise relationships between pressures, water quantity and quality, ecological responses, ecological functioning and ecosystem services; to test and validate these relationships in case-study catchments in different hydro-ecological and geo-climatic settings; to assess complex multi-stressor scenarios by testing and improving existing modelling techniques including process-based models and empirical / statistical models; and to up-scale and generalize the results of the case studies, and contribute with these improved models to guide River Basin Management Plans (RBMP) and the best Programs of Measures (PoM) in order to achieve a good ecological status.

To achieve these WP4 aims, 16 basins were initially selected to undertake a broadly consistent programme of activities (Figure 2.1). All the basins proposed have extensive physical, chemical and biological data, in several cases spanning 2-3 decades (Table 1.C of the DOW from MARS). The river basins have been used extensively to support research including indicators of specific multistressors (e.g. climate and land use change) and new stress indicators (e.g. brownification and emerging contaminants), and all have figured in the development and calibration of biogeochemical models available to interface with ecological indicators and across ecological boundaries (e.g. rivers/lakes, inland/transitional waters, surface/groundwaters, channel/floodplains).

These basins have been chosen to represent a wide range of catchment characteristics and multiple stress conditions and consist of five in Southern Europe, six basins across Central Europe, and five in Northern Europe. They include investigations of multiple stressor combinations such as water scarcity and flow alterations (Southern Europe); hydrology, morphology and nutrient stress (Central Europe); and hydrology and temperature alterations (Northern Europe).

WP4 was identified as a crucial package in the MARS project, because single basins, groups of basins and all basins will provide the building blocks of the MARS conceptual models (described in Herring et al., 2015), feeding large part of the rest of MARS work program, notably WPs 6, 7 and 8. WP4 is complex because of the manifold actions required and people involved, and because of the different data treatments over varying spatial-temporal scales. WP4 also encompasses a challenging

combination of ideas, basin conditions and data specificities representing different approaches to river basin modeling and management across Europe.



Figure 2.1. Map showing the locations of the MARS case study basins.

2.1 WP4 organization

A total of 57 researchers were directly involved in the WP4 including coordinators and those that developed the MARS conceptual model and collected and screened the data, that developed the process-based models, that implemented and performed the empirical data treatment, that created the storylines for the climatic models, that reached out for end user's view. Furthermore because it was a sequential process, not all researchers were involved at the same time, nor had the same scientific background and skills, which included hydrology and hydraulics, biology, ecology, statistics, and others. Because of the variability displayed by teams and case-studies, and the many possibilities for data treatment, a conclusion was reached that MARS needed a permanent and interactive organization to maintain the research mainstreaming.

For the mainstreaming research coherence, a common workflow was developed:

- In partnership with basin stakeholders, key multiple-stressor combinations and change scenarios have been identified.
- Common and basin-specific research questions have been developed within the framework of the MARS conceptual model (a joint risk assessment, DPSIR scheme and ecosystem services cascade described in Herring et al., 2015)
- Based on the research questions and the basin-specific implementation of the MARS conceptual model, a programme of process-based modelling (PMs) and/or empirical modelling (EMs) has been designed, calibrated and validated using existing and new data.
- Using the calibrated models, interactions between common MARS stressors have been explored and quantified.
- Common MARS change scenarios have then been modelled and the sign and magnitude of changes in MARS benchmark indicators has been estimated.
- Finally, the models have also been run using MARS mitigation or restoration scenarios to predict the efficacy of these scenarios compared with on-going and alternative River Basin Management Plans (RBMPs) under various stressor combinations.

Basin leads were established with the following tasks: to insure the development of the MARS conceptual model and collection of data needed for modelling and empirical data treatment; to write a basin description and insure the application of the process-based models; to implement the empirical data treatments and the downscaling of the storylines; to present and discuss intra-region results whenever necessary and at plenary meetings; to do a quarterly update report to the regional leaders; to organize stakeholders meetings at basin scale and report back, keeping the a steady flux of information, back and forth.

Regional task leaders (see MARS DOW: Task 4.2 – Southern River Basins; Task 4.3- Central River Basins and Task 4.4 - Northern River Basins), had the crucial role of coordinating the regional array of basins, which were very diverse geo-climatically and physio-graphically, also to coordinate the various scientific expertise and maintain liaisons and communication. The regional leaders have collected the quarterly reports and pooled them into single reports accessible in the MARS intranet; they have collected basin and process-based model descriptions and insured direction and pace of empirical data treatment and MARS information and commonalities, and they maintain the reporting to the Steering Committee.

A Steering Committee was established composed of the two WP4 Leaders, the WP4 Task Regional Leaders (Southern, Central and Northern) and the Consortium Leader, mainstreaming ongoing modelling studies and the development of the MARS holistic approach, and to bridge among studies,

basins and groups of basins, from the same region or different regions, with the final aim at upscaling to the European level, also coordinating the various reports, minutes and manuscripts resulting from WP4. All this work is being fed to the MARS WPs for tools and communication, including policy briefs and the MARS net interfaces.

The common approaches had to be developed with the help of other WPs through several discussions both in meetings and remotely. Several documents arising from the MARS project have been used to elaborate a common modelling framework including the harmonization of terminology for the MARS model application, the methods for modeling, the indicators and services to be used, and empirical data treatment to be developed and the common future climatic scenarios and storylines, the latter to be densified and downscaled at each basin/region, according to its particular characteristics. These documents, that insured WP4 harmonious development, were the following:

- Task 2.3: Milestone 2: Selection of benchmark indicators (Sept 2014)
- Task 6.1: Guidance on analysing stressor-response relationship (Oct 2014)
- Task 2.6: Report Task 2.6 Definition of future scenarios (Dec 2014)
- Task 4.1: Conceptual models survey (Feb 2015, updated Feb 2016)
- Task 4.1 Cookbook on data analysis (July 2015)
- Task 2.2: Cook-book on Ecosystem service assessment and valuation (Nov. 2015)
- Task 4.1: Cook-Book on Scenarios Implementation for MARS (Nov. 2015)

2.2 WP4.1 calendar and outputs

A first WP4 meeting was held in Lisbon in October 2014 to create the common implementation structure and to start harmonising the MARS model conceptual for each basin and the process-based modelling.

Following a period of data collection, screening and template filling, and development of the empirically-based data treatment cookbooks and guidelines, a first data treatment workshop was held in Tulcea, Romania, in July 2015 to discuss the difficulties and results of the signals responses to stressors obtained, and move forward.

A 2nd Workshop was held in Lisbon in December 2015, to continue the discussions. Results were also presented and discussed, together with final harmonization of MARS conceptual models, at the mid-term MARS meeting in Fulda, on March 2016.

Finally, basin leads elaborated the basin reports, which were pooled together into three Regional Reports. These three important public documents, available in the MARS site, constitute the basis for the present report, which summarizes and discusses the overall results. This report is composed of the single basin reports (present herein) that constitute the building blocks of WP4, they are the raw material for the steps ahead.

3 The MARS modelling process

3.1 Conceptual MARS models

The modelling process follows the MARS conceptual modelling framework that is capable of providing a holistic approach to modelling multi-stressors across different scales. Every basin has populated the MARS conceptual model (Figure 3.1) to show the basin-specific stressors, indicators of state and indicators of ecosystem services. This approach manages to combine the use of a risk-assessment framework, a DPSIR scheme and the ecosystem service cascade in a joint modelling framework that enables to investigate the impacts of multiple stressors on biotic/abiotic state and on ecosystem services. These conceptual models are detailed in the individual Basin reports within section 4, 5 and 6 of this report.

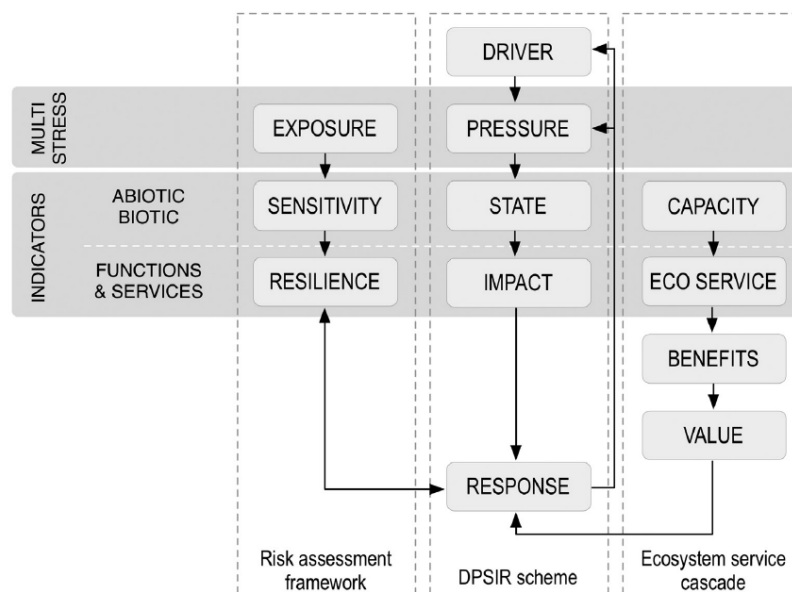


Figure 3.1. MARS conceptual model (from Hering et al., 2015)

Key elements in the modelling of the interactions between and impacts of multiple stressors have been identification of:

- the relevant basin-specific stressors;

- appropriate indicators of system status and environmental impact; and,
- key ecosystem services to be included in the modelling.

3.2 Modelling strategy

The modelling strategy followed by each basin varied slightly (Table 3.1) and was a result of the needs raised by each basin conceptual model. Fourteen different process-based models were employed, overall. Being Swat and PERSiST the most widespread, in terms of use among the several basins. The empirical modelling framework was more similar between basins and closely followed the deliverable “Cookbook on data analysis” (Task 4.1) and its translation into a scientific article “Analysing the impact of multiple stressors in aquatic biomonitoring data: A ‘cookbook’ with applications in R.” (Feld et al. 2016). Nonetheless, modelling strategies varied to some extent and input variables were different for each basin. Most of the ecosystem services modelling used the same PM and EM approach followed for each basin for the ecological status variables.

Detailed modelling approach followed in each basin is provided in section 4, 5 and 6 of this report.

Table 3.1. Resume table of the Process-based (PM), Empirical (EM) and Ecosystem service models used of each of the study basins.

Southern Basin	Process-based models	Empirical models	Ecosystem service modelling
Lower Danube	Sobek Rural 1D2D and AQUATOX	Analytic Hierarchy Process concept and Boosted Regression Tress (BRT)	Ecosystem services were simulated with the use of both PB and empirical models
Beyşehir	SWAT (Soil Water Assessment Tool), PCLake and GLM (General Lake Model) coupled through the Framework for Aquatic Biogeochemical Modeling (FABM) to the Aquatic EcoDynamics module library (AED)	No empirical model was applied.	Ecosystem services were simulated with the use the PB models
Pinios	SWAT	BRT and General Linear Models (GLM)	Ecosystem services were simulated with the use of SWAT
Sorraia	SWAT	BRT, Random Forests (RF), GLM and General linear mixed models (GLMM)	Ecosystem services were simulated with the use of both PB and empirical models
Central Basin	Process-based models	Empirical models	Ecosystem service modelling
Drava	No process-based models were developed for this basin	BRT and RF	No specific modelling was undertaken to investigate multi-stressor effects on ecosystem services.

Elbe, Havel, Saale	MONERIS and PhytoBasinRisk software.	MARS EM procedures and GLM	PM and EM
Odense	SWAT	BRT and GLM	No specific modelling was undertaken to investigate multi-stressor effects on ecosystem services.
Regge Dinkel/	A rainfall-runoff model, a 1D hydrodynamic model and a 1D water quality model including the modelling of water temperature and chlorophyll-a.	BRT and GLM	No specific modelling was undertaken to investigate multi-stressor effects on ecosystem services.
Ruhr	No process-based models were developed for this basin	BRT and GLM	BRT and GLM
Thames	BGS, QUESTOR and PROTECH	GLM	No specific modelling was undertaken to investigate multi-stressor effects on ecosystem services.
Northern Basin	Process-based models	Empirical models	Ecosystem service modelling
Lake Vörtsjärv	INCA-C (Integrated Catchment model for Carbon)	BRT and ANOVA	PCA and Spearman correlation – just to analyse the environmental factors affecting ecosystem services
Lepsämänjoki	INCA and PERSiST (Precipitation, Evapotranspiration and Runoff Simulator for Solute Transport)	GLMM and BRT	PM
Mustajoki-Pääjärvi	INCA and PERSiST	No EM, just a calculation of maximum growing depth and relation to measured maximum growing depth	PM
Otra	PRESiST and MAGIC	RF, GLM and GAM	No specific modelling was undertaken to investigate multi-stressor effects on ecosystem services.
Vansjø-Hobøl	PRESiST, INCA-P and MyLake	LM/GLM, GAM, Regression trees, BRT, RF, Baesian Network	No specific modelling was undertaken to investigate multi-stressor effects on ecosystem services.
Wye, Usk, Severn, Tywi, Dyfi, Teifi, Conwy	INCA	RF, GLM, GLMM	GLM

3.3 Climate change scenarios and storylines development

GFDL-ESM2M and IPSL-CMA-LR climate models were used for generating precipitation and temperature scenarios for two climate scenarios (RCP 4.5, RCP 8.5). Climate scenarios were available for period of 2006-2099. The period of 2006-2015 was used in general as the reference period and monthly linear correction was applied to observed climate data and scenarios outputs covering this period. Factors derived from linear correction were applied to projected temperature

and precipitation data series. Two distinct periods were considered (2025-2034, 2055-2064, hereafter will be mentioned as 2030s and 2060s respectively) were chosen for future scenario runs. For 2030s, predicted climate scenarios indicated a 0-26% increase in precipitation whereas for 2060s, precipitation change was predicted from 8% increase to 30% decrease (Fig. 3.2). Temperature outputs indicate 1-2 °C increase for 2030s and 2.5-4.5 °C increase for 2060s (Fig. 3.3).

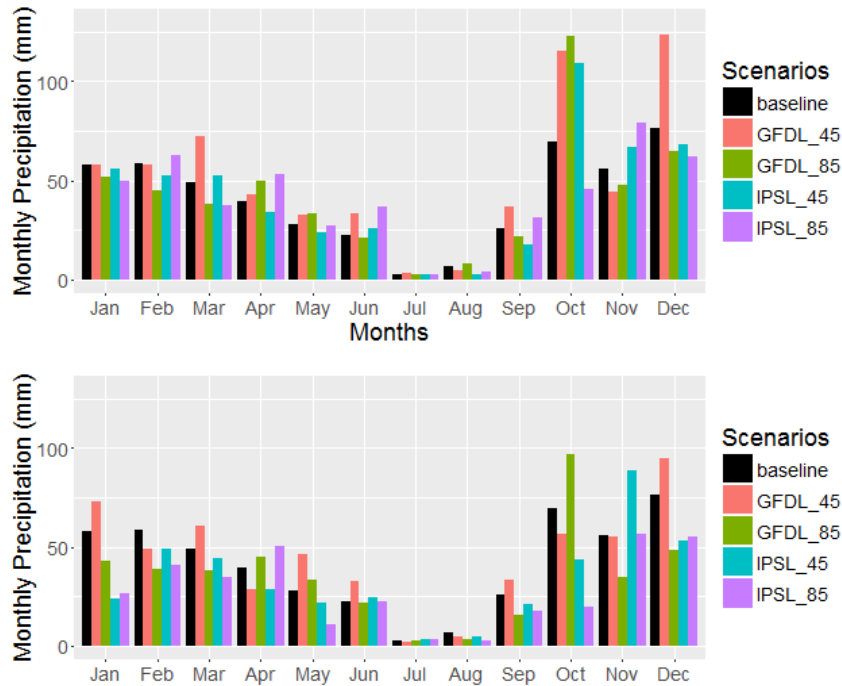


Figure 3.2. Future and baseline precipitation (mm)

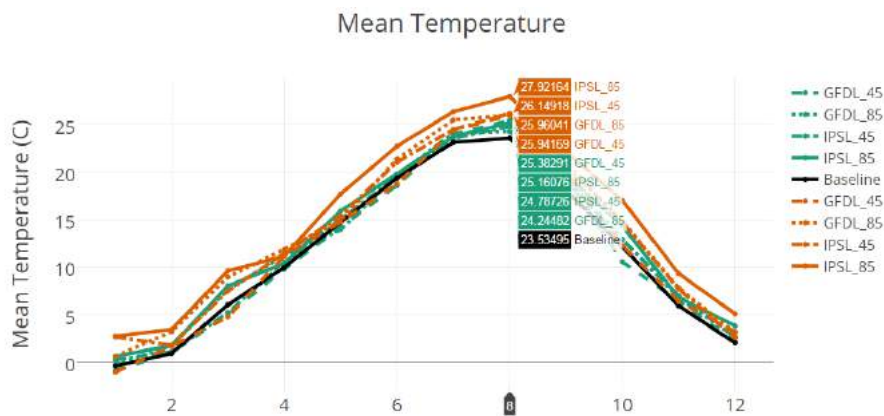


Figure 3.3. Future and baseline temperature (°C)

MARS land use scenarios

Three different storylines were developed for future land use scenarios. In each basin these storylines were downscaled according to specific characteristics of land use and programs of measures to be undertaken for the purpose of achieving a better ecological status (or downscaled at region level when consensus was reached).

Techno world (economic focus) : In Techno world scenario, economic growth is the main focus. Higher economic growth accompanied increase in energy demands and resources which brings agricultural expansion. However, environmental measures will be applied to mitigate human disturbance.

Consensus (green focus) : In Consensus world scenario, economic growth is as it is today. More efforts put in to promote sustainable use of sources. A lot of effort applied to promote conservation and to restore degraded ecosystems.

Fragmented world (Survival of the fittest) : In this scenario, there is an increase in economic development, in some cases also considering a big economic crisis (recession). There is no room almost for environmental issues.

4 Southern Basins

4.1 Lower Danube

4.1.1 Introduction

The Lower Danube River experienced substantial changes over the last decades and centuries. Navigation, land reclamation, intensive agriculture, flood control and damming together with an increase of temperature, evapotranspiration and a decrease of the amount of precipitation and consequently water inflow to flood plain lakes, as effect of climate changes, left their imprint on hydro-morphological and physico-chemical characteristics with corresponding effects on the aquatic biota. The main identified drivers of the region are agriculture, flood protection and climate changes. Here we address the impact of hydro-morphological alteration and physico-chemical pressures in the

flood plain lakes of the Danube delta based on time series data. The influence of waters scarcity and nutrients load to fish biomass in flood plain lakes was analyzed using the empirical models and processed based Aquatox software model. Based on Aquatox model we quantify the gradient of fish biomass for each MARS and climate change scenarios for the years 2030 and 2060.

4.1.2 Study area and MARS concept development

The Danube Delta refers to the area where the Danube River divides into three main branches near the city of Tulcea, into Chilia in the North, Sulina in the middle and Sfântu Gheorghe in the South (Fig. 4.1). The Danube Delta in Romania covers a total surface of 3,510 km². The Danube Delta area includes over 300 floodplain lakes with a size between 14 and 4530 ha with a water depth from 1.5 to 4 m.

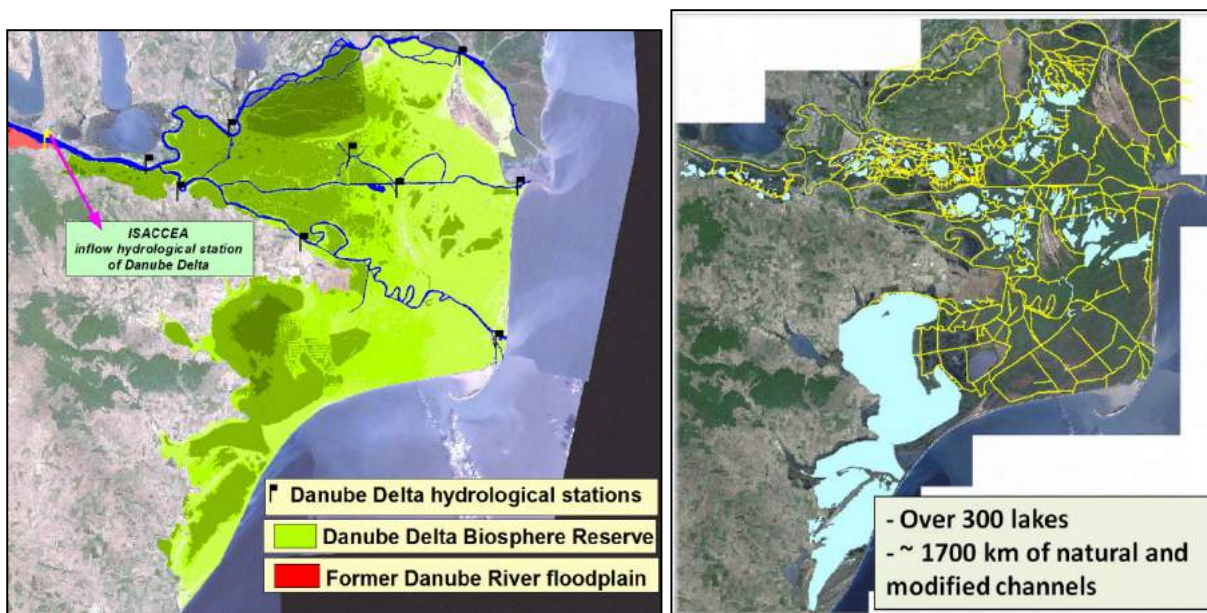


Figure 4.1 Danube Delta Biosphere Reserve

The lakes are supplied with fresh river water through a vast network of 2800 km natural and artificial canals. The water level in the lakes depends to the river pulse. Higher water level is recorded in spring (May-June) and low water levels in autumn (August-September-October). An overview of the flooding areas of the Danube Delta from maximum to minimum water level of the River Danube is given in Figure 4.2.

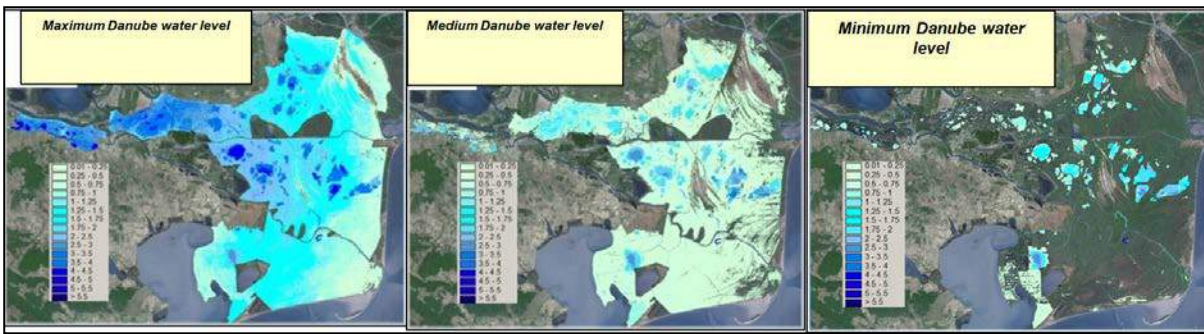


Figure 4.2 Danube Delta flooding areas

The main pressure on Danube Delta ecological system is the construction of agriculture and fish polders (Figure 4.3) and alteration of the hydrological regime due to upstream land reclamation, intensive agriculture, flood control and damming together with an increase of temperature, evapotranspiration and a decrease of the amount of precipitation conducting to seasonally water scarcity in the delta itself despite increasing river water inflow into remaining flood plain lakes due to channelization. The 2800 km networks of channels act also as a drainage system consequently reducing water residence time and keeping a longer period of time a low water depth in the lakes.

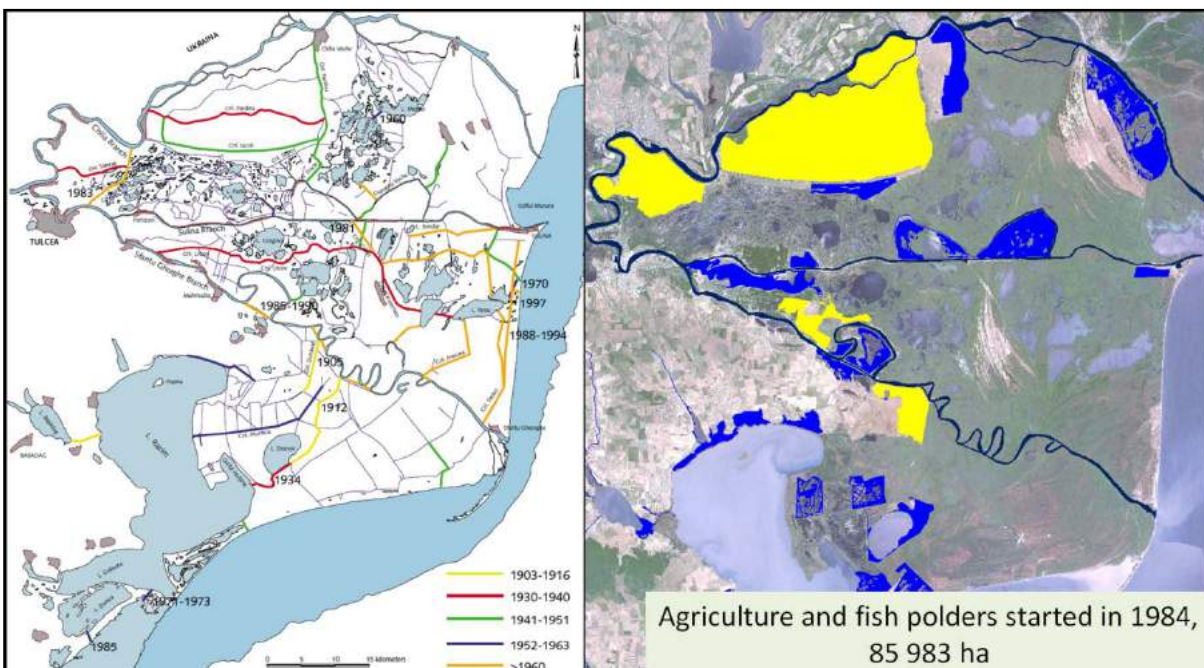


Figure 4.3 Channels networks, left figure and right figure agriculture area (yellow) and fish polders (blue).

For the lower Danube region we focused to quantify/analyze the impact of water scarcity in the lakes ecosystems of Danube Delta to fish biomass.

Low waters regime has direct impact on lakes ecosystems by:

- **Reducing water exchange between lakes and the Danube River branches;**
- **Bottom exposure of the very shallow lakes;**
- **Algae blooming;**
- **Oxygen depletion and local fish migration to favourable water bodies as deep channels or Danube River branches;**
- **Exposure of fishes to predators (birds).**

A synthetic view on relationship between drivers, pressures, biotic and abiotic indicators on state and impact and possible response actions is given in the conceptual model of the Danube delta (Figure 4.4).

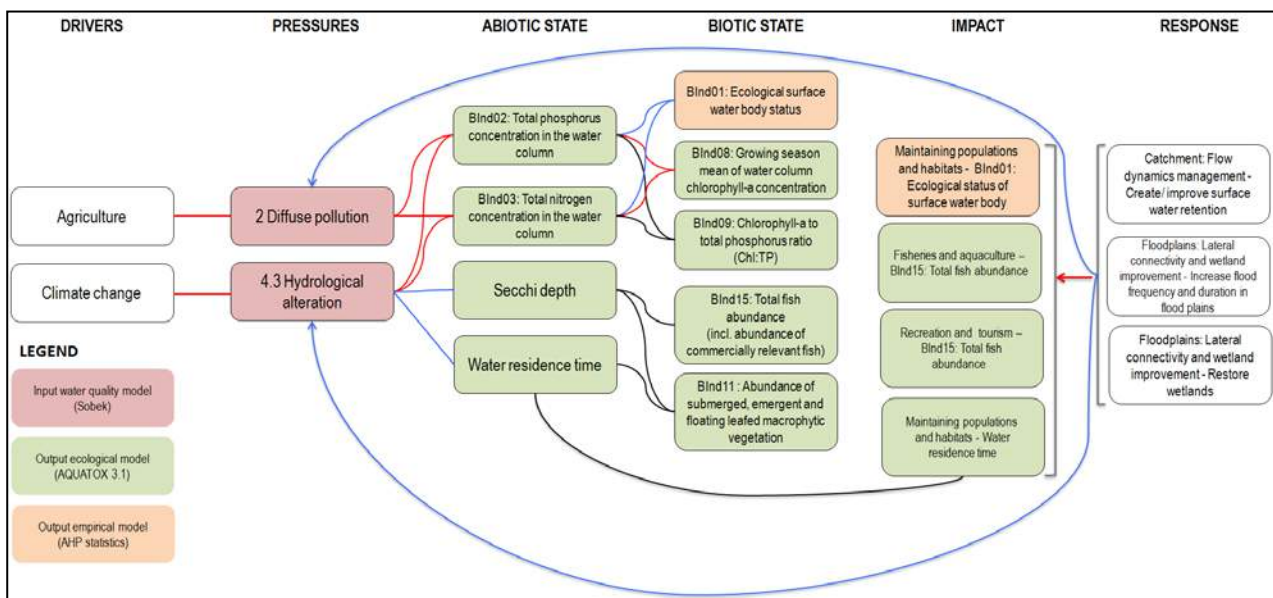


Figure 4.4 Danube Delta conceptual model

4.1.3 Data and Methods

4.1.3.1.1 PB modeling and calibration

In our models abiotic parameters represent independent variables and fish biomass dependent variable. For the ecological status of the Danube Delta lake the major impact is represented by water scarcity in August, September and October months due to low water level of the Danube River (Figure 4.5)

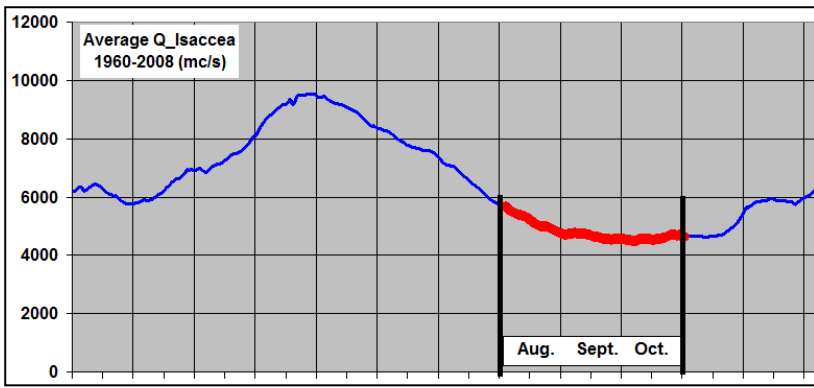


Figure 4.5 Months with low water discharge of the Danube River

Water residence time play an important role in balancing ecological status of the lakes and was treated as an important hydrological indicator in our models. The residence time reflects the local effects of different hydro-morphological changes as an indicator of water exchange between lakes and the Danube River branches.

Residence time can be computed as the water volume of a lake divided by the flow of the influx canals. Lake residence time differs from lake to lake and depending of their lateral connectivity (Figure 4.6).

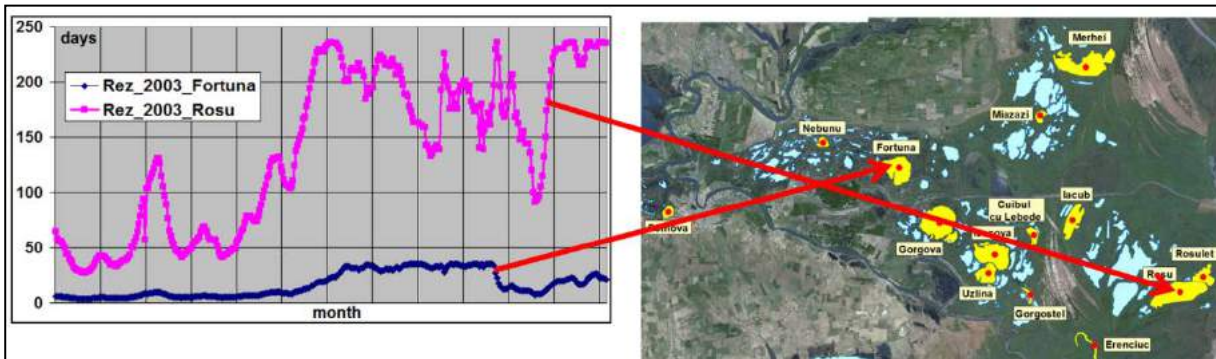


Figure 4.6 Residence time gradient in the Danube Delta lakes

The models used for analyses and processing are summarized in Figure 4.7. Hydrological parameters are the outputs of Sobek Rural 1D2D software model (Deltares Systems, 2014) calibrated for the Danube delta (Figure 4.8). The calibration of the model was done based on extreme water level recorded in Romania: 2003 for extreme low levels, 2006 for extreme high level and 2004 as an average water level year (Figures 4.9 and 4.10).

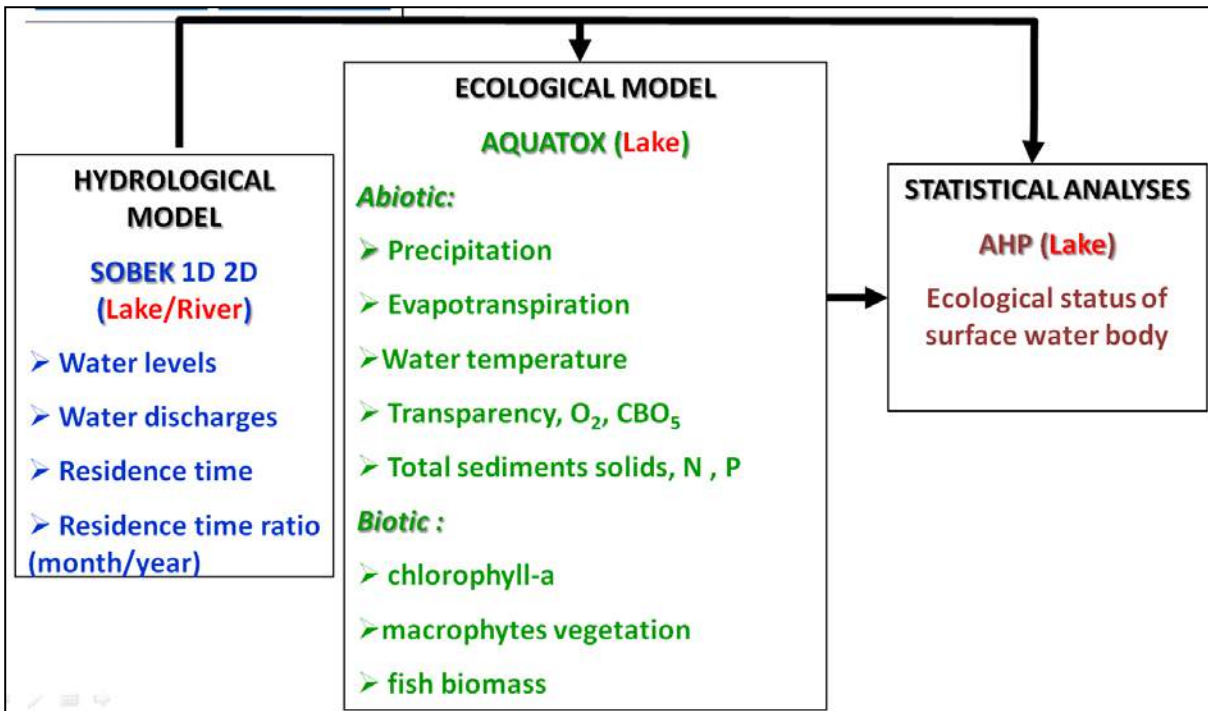


Figure 4.7 Summary of the models used

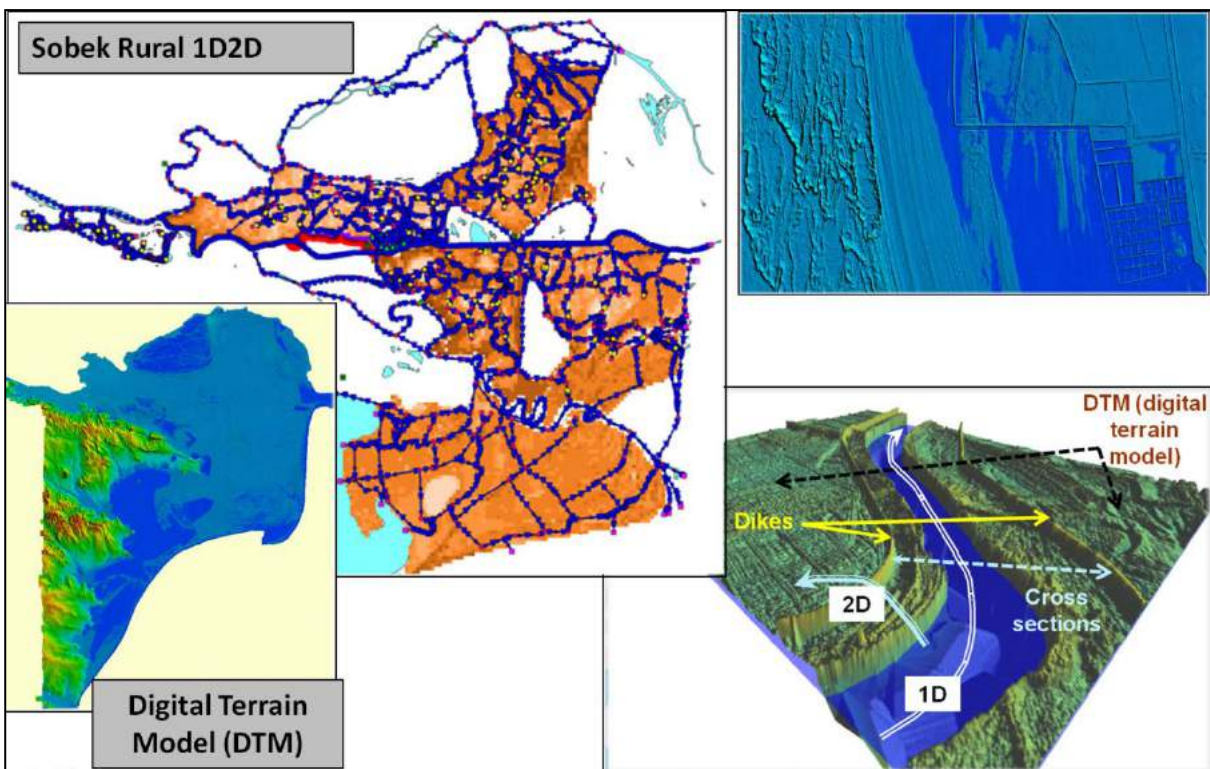


Figure 4.8 Schematic view of the Danube Delta hydraulic model

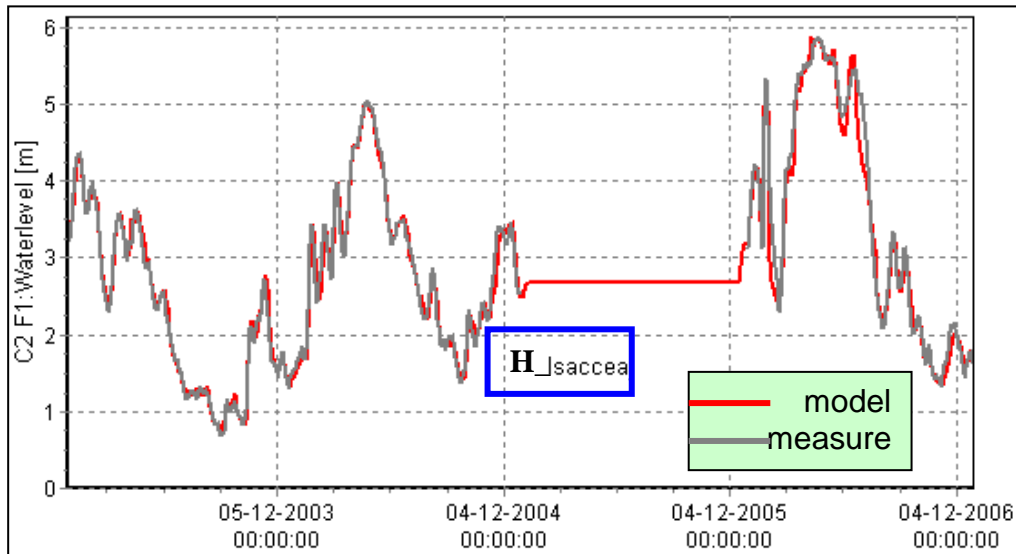


Figure 4.9 Water levels calibration of the Danube Delta hydraulic model at Isaccea station

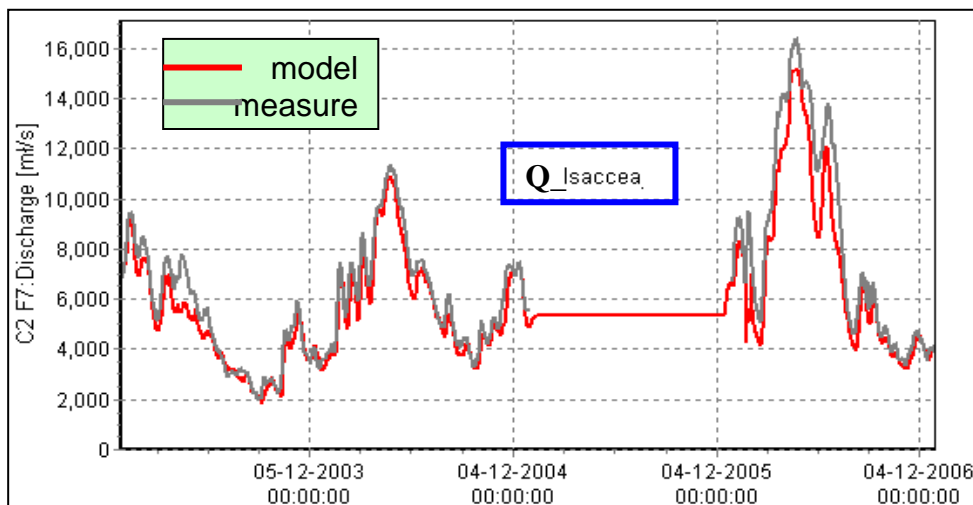


Figure 4.10 Water discharges calibration of the Danube Delta hydraulic model at Isaccea station

For the qualitative classification of ecological state of the lakes we use Analytical Hierarchy Process – AHP- concept (Saaty, T.L., 2008). Adaptation of the concept for deriving ecological statutes of the Danube delta lakes is shown in Figure 4.11.

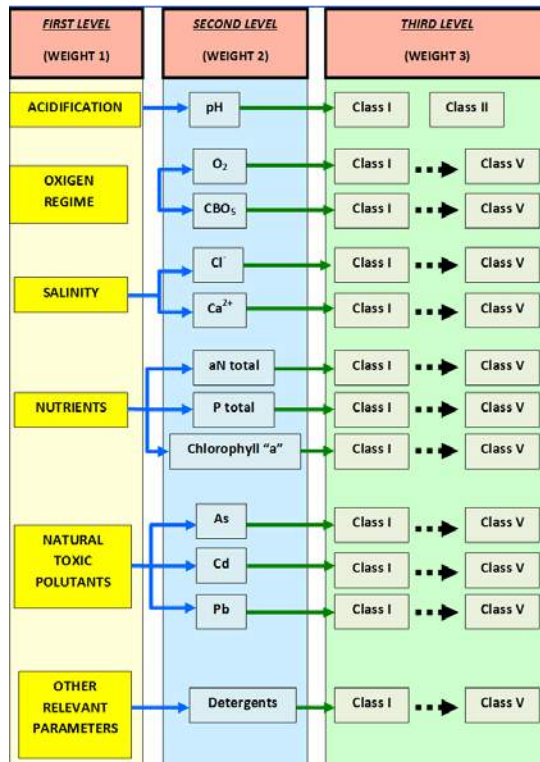


Figure 4.11 Schematic figure of the AHP model

The AHP processing will assign a weight to each component of each level according with its importance in the level hierarchy. The checking of the consistency of the judgment is made by consistency ratio factor (CR) which must be less than 0.1 (example in Figure 4.12).

OXIGEN REGIME						
	O2_I	O2_II	O2_III	O2_IV	O2_V	Weight
O2_I	1	2	3	5	7	0.42
O2_II	0.75	1	2	3	5	0.27
O2_III	0.5	0.75	1	2	3	0.17
O2_IV	0.25	0.5	0.75	1	2	0.10
O2_V	0.1	0.15	0.3	0.5	1	0.04
Lambda max =			6.58			
Consistency index (CI) =			0.12			
Consistency ratio (CR) =			0.09			
			CR must be < 0.1			

Figure 4.12 AHP – assessment of consistency ratio

The final results of the AHP analyses define the weight of each component from each level. The final score for a water quality area corresponding to a monitoring station is done by multiplying the weights of each level. If we want an analysis at level 2 then we have to multiply the weight from level 3 with the weight from level 2 or if we want a third level analyses than we have to multiply all the weights from all levels (example in Figure 4.13).

FIRST LEVEL		SECOND LEVEL		THIRD LEVEL		Limits
WEIGHT_1		WEIGHT_2		WEIGHT_3		
0.35	NATURAL TOXIC POLLUTANTS	0.33	As (ug/l)	0.42	As_I	10
				0.27	As_II	20
				0.17	As_III	50
				0.10	As_IV	100
				0.04	As_V	> 100
		0.33	Cd (ug/l)	0.42	Cd_I	0.5
				0.27	Cd_II	1
				0.17	Cd_III	2
				0.10	Cd_IV	5
				0.04	Cd_V	> 5
		0.33	Pb (ug/l)	0.42	Pb_I	5
				0.27	Pb_II	10
				0.17	Pb_III	25
				0.10	Pb_IV	50
				0.04	Pb_V	> 50

Figure 4.13 Weight of each component after AHP processing

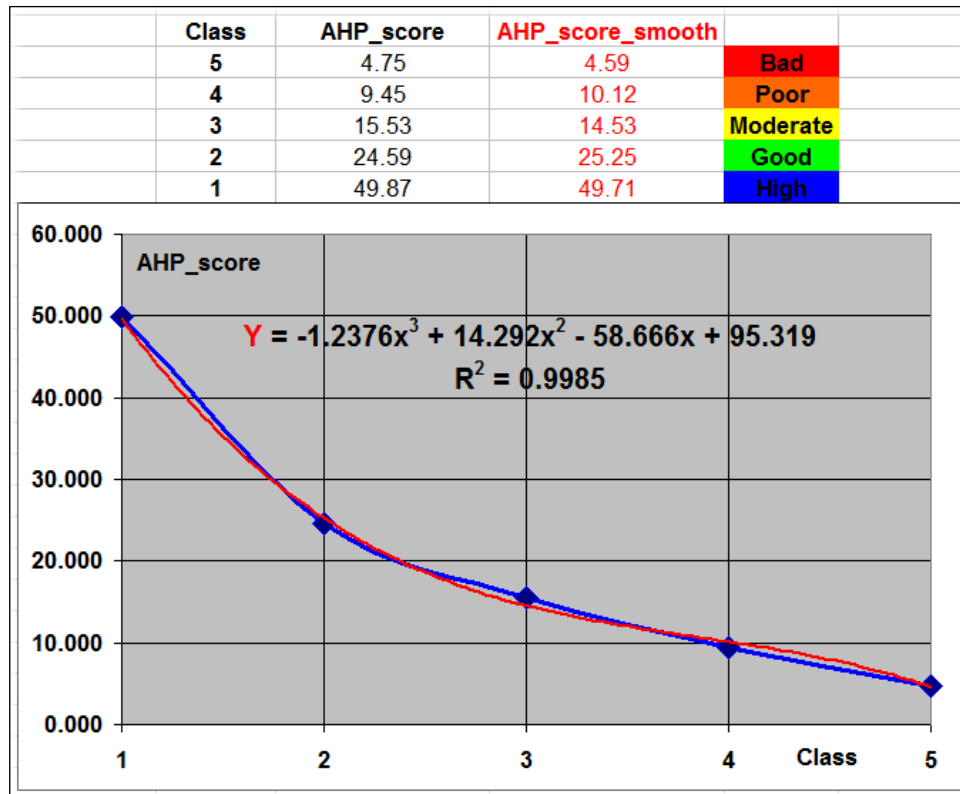
These procedures were applied for all parameters to all areas assigned to the water quality monitoring stations (the highest value means excellent water quality status and the lowest value means bad quality status).

In order to assign the equivalent water quality classes (High, Good, Moderate, Poor, Bad) to each final scores it was necessary to calculate the limits score of the AHP processing score (the highest, lowest and intermediary possible AHP score, Figure 4.14).

The highest value assumes that all the physico-chemical water parameters are in class 1 (High), the lowest that all the physicochemical water parameters are in class 5 (Bad) and the intermediary values correspond to the other classes 2 (Good), 3 (Moderate), 4 (Poor). In the end all the water quality areas within the Danube delta aquatic complexes will be described by a water quality class corresponding to each year.

Relationships between biotic and abiotic variables in lakes are assessed by AQUATOX software (Park A. Richard et al., 2008) which is an ecosystem simulation model that predicts the environmental

fate of various pollutants, such as excess nutrients and organic chemicals, and their effects on aquatic ecosystems, including fish, invertebrates, and aquatic plants (Figure 4.15).



Aquatic complex	Monitoring station	Code	Year	ACIDIFICATION	OXIGEN REGIME	SALINITY	NUTRIENTS	NATURAL TOXIC POLUTANTS	OTHER PARAMETERS	Final score	WQ_class
SOMOVA-PARCHES	Rotundu	L1	2006	7.20	6.18	1.61	8.92	2.53	1.25	27.69	2
SOMOVA-PARCHES	Somova	L2	2006	7.20	8.80	1.37	9.89	2.53	1.25	31.05	2
SOMOVA-PARCHES	Rotundu	L1	2007	0.80	5.49	1.97	7.85	4.78	1.25	22.14	3
SOMOVA-PARCHES	Somova	L2	2007	0.80	5.49	1.97	7.85	5.54	1.25	22.90	3
SOMOVA-PARCHES	Rotundu	L1	2008	7.20	6.18	1.61	6.87	8.42	1.25	31.54	2
SOMOVA-PARCHES	Somova	L2	2008	7.20	6.18	1.61	7.94	6.69	1.25	30.88	2
SOMOVA-PARCHES	Rotundu	L1	2009	0.80	6.18	1.97	10.87	6.69	1.25	27.76	2
SOMOVA-PARCHES	Somova	L2	2009	0.80	7.22	1.97	7.85	6.69	1.25	25.78	2
SOMOVA-PARCHES	Rotundu	L1	2010	7.20	5.49	1.97	9.25	5.54	1.25	30.71	2
SOMOVA-PARCHES	Somova	L2	2010	7.20	6.18	1.61	9.25	7.28	1.25	32.77	2
SOMOVA-PARCHES	Rotundu	L1	2011	7.20	3.92	1.61	9.25	7.38	1.25	30.61	2
SOMOVA-PARCHES	Somova	L2	2011	7.20	5.49	1.97	9.89	7.38	1.25	33.19	2

Figure 4.14 Equivalents of AHP final score and water quality classes

4.1.3.1.2 Empirical modeling and linkage between pressures and indicators

BRT analyses and other statistical analyses of the data have been done with “R” software. We use the following parameters: total phosphorus, total nitrogen, total suspended sediments, resident time ratio, water transparency, water depth, CBO₅, O₂, water temperature.

BRT analyses show that at a lower water level TP, TN, TSS and REZT_Ratio (Residence time ratio, monthly average / year average) are the most important independent variables affecting fish biomass (Figure 4.17).

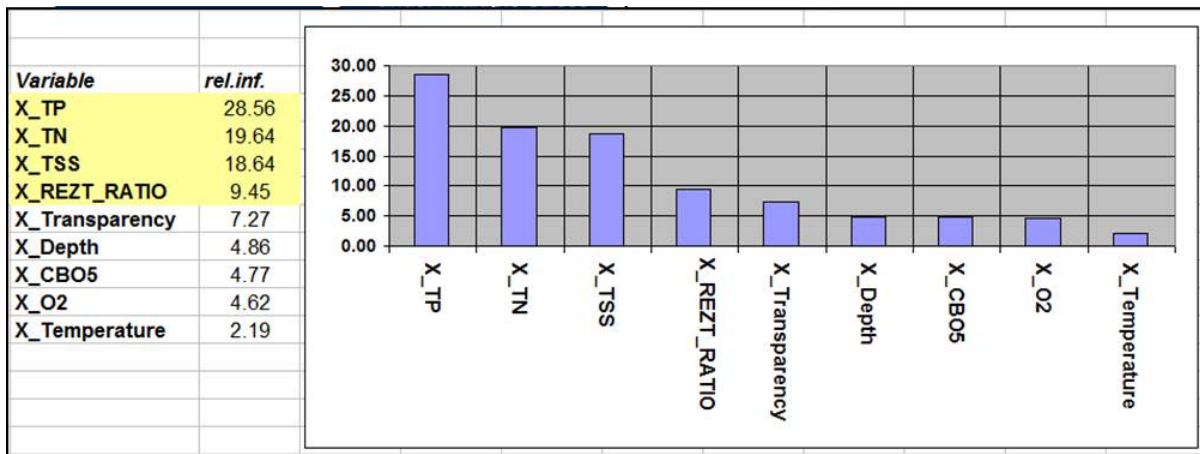


Figure 4.17 Influence of BRT variables at low waters level of the Danube delta lakes on fish biomass

Cumulated, the influence of the nutrients stress represents 54.9% and hydro-morphological pressure 45.1% (Figure 4.18).

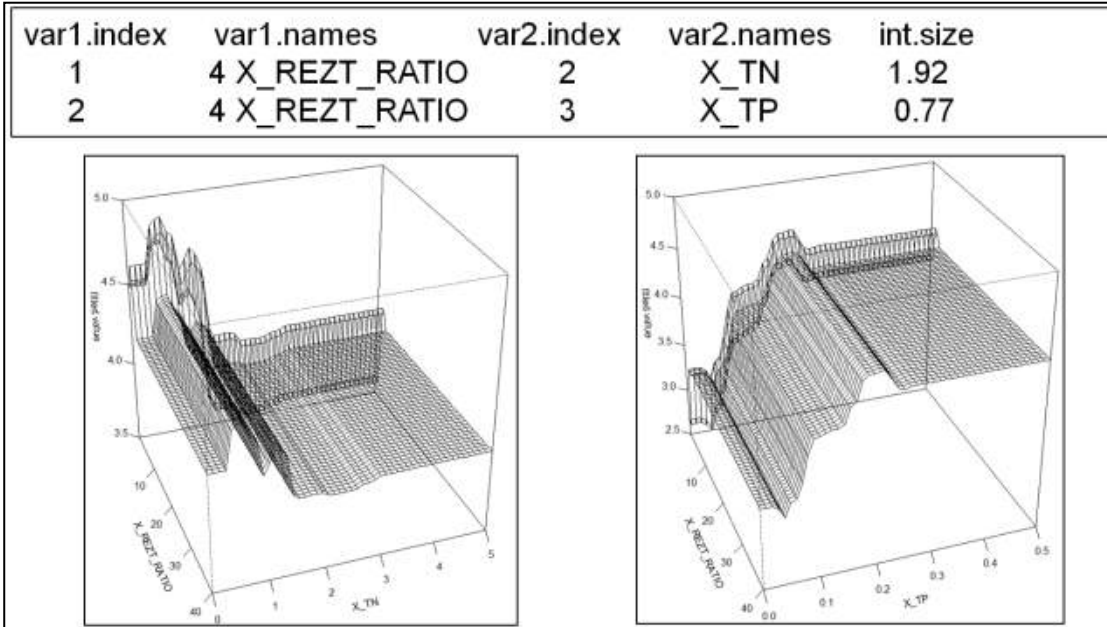
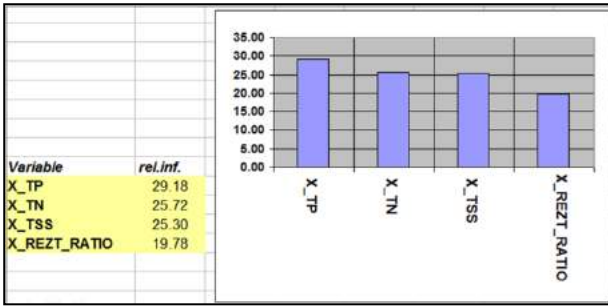


Figure 4.18 Influence of the nutrients stress and hydro-morphological pressure on fish biomass

Multiple regression results on selected lakes of the Danube delta for Fish biomass = f (TSS, TP, TN, REZT_RATIO) are shown in Figure 4.19.

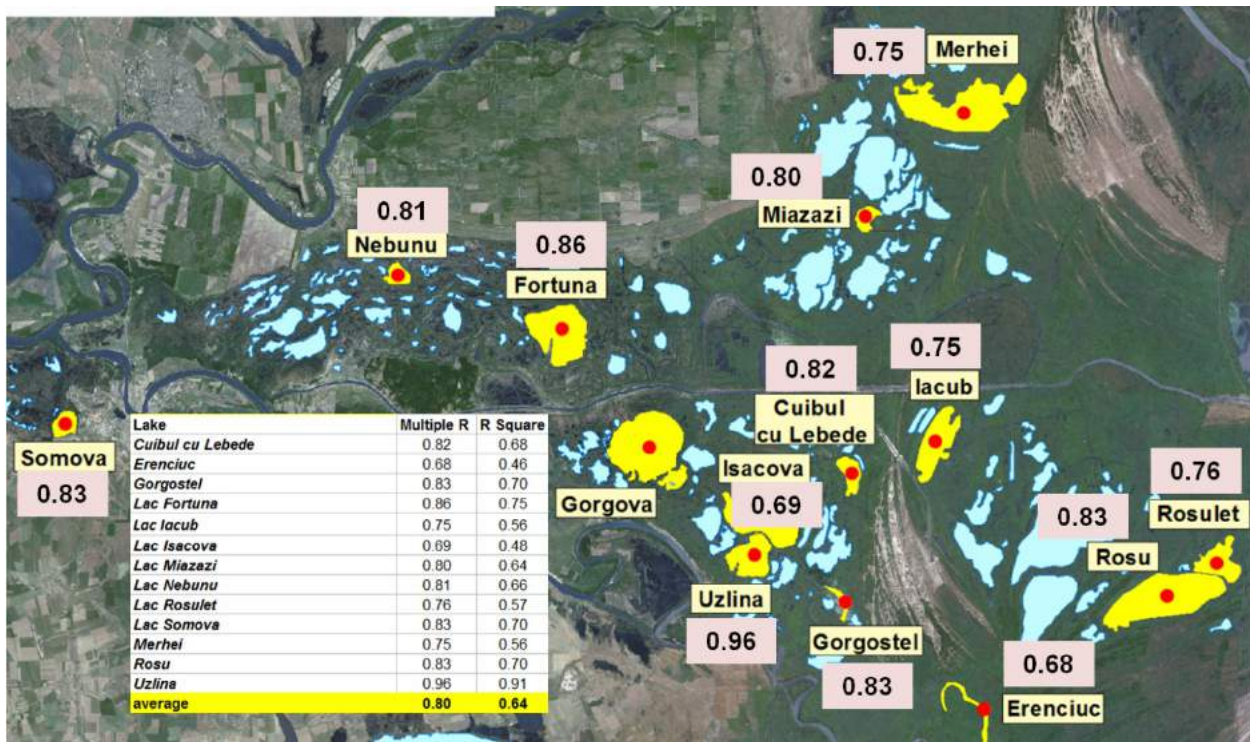


Figure 4.19 Multiple regression results on selected lakes of the Danube delta for Fish

4.1.3.1.3 Ecosystem services description and linkage with pressures

To structure the analysis of ecosystem services and select appropriate indicators, we used the conceptual framework proposed by (Grizzetti et al. 2016). For the lower Danube River basin selected Ecosystem Service indicator is fish flow. The main impact on the fisheries and aquaculture is represented by the total fish abundance. For the lower Danube River basin selected Ecosystem Service indicator is fish flow. The main impact on the fisheries and aquaculture is represented by the total fish abundance. The data series on commercially catch statistics starting from 1960 to 2008 reflected two major trends: firstly a constant decline of fish catches and secondly a shifting in the composition of the fish community from clear mesotrophic water to eutrophic algal turbid water fish species. The fish community dramatically changed due to habitat loss, hydro-morphological alteration and nutrient pollution. The climate change has also contributed influencing the hydrology. Furthermore, the construction of artificial canals introduces more sediments and nutrients into the lakes and changes their state in terms of eutrophication which in turn affects fish assemblage structure. Total fish catch in the Danube delta declined from 10-20.000 tons per year before and during the 1960s and to 5,000 - 6,000 tons after 1984. This development affected species differently. Especially for pike-perch (*Sander lucioperca*) and pike (*Esox lucious*) as phytophilic spawners

catches dropped in the late 1960s from 2,500 tons to about 500 tons in the 1970s and less after (for pike) and from up to 300 tons in the 1960s to 100 tons and less afterward.

4.1.3.1.4 Scenarios development

Scenarios analyzed are those proposed by MARS project, (MARS project, 2015):

- **MARS1 > Techno world / Economy rules / Economy first > *MARS ad hoc***
- **MARS2 > Consensus world / Compromise world / Autonomic Development world
*MARS world***
- **MARS3 > Fragmented world / Survival of the Fittest / Selfish world / Weak economy-
little environmental protection > *No MARS world***

In the context of global warming, changes in the climate regime of Romania are modulated by regional conditions. Regional modelling and dynamical downscaling provide supplementary policy-relevant information on detailed spatial features of climate change. The change in the near future, in temperature (Figure 4.20) is stronger over the Eastern and Southern regions (up to 1.3 °C) revealing the local influence of Carpathian mountains. As for precipitation (Figure 4.21), the most vulnerable areas from the standpoint of water scarcity are South Eastern and South Western regions of Romania (where the reduction in near future in annual precipitation is estimated to be up to around 10%).

Also, projections show that changes in mean temperature and precipitation occur along with changes in extreme meteorological events. Under climate change (Romania's Sixth National Communication on Climate Change and First Biennial Report, 2013) extremes related to temperature increase are spatially and temporally prevailing.

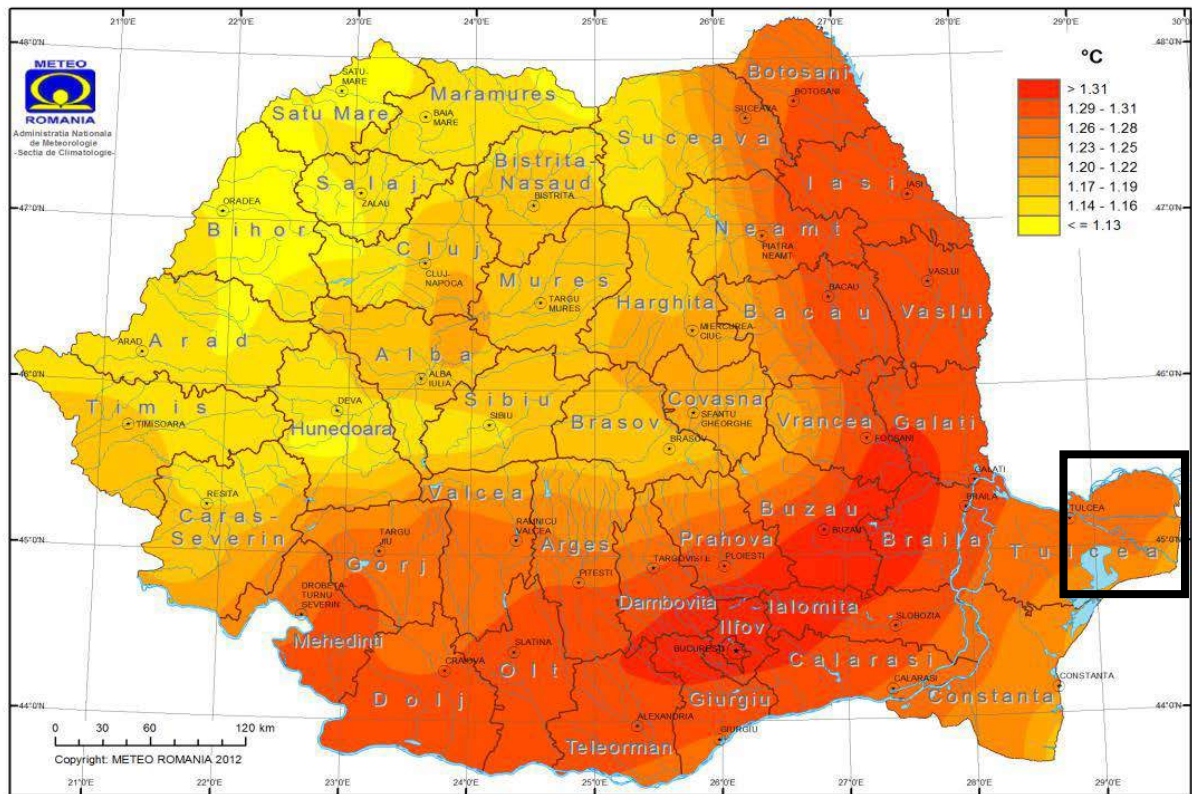


Figure 4.20 Multiannual mean changes (2011-2040 vs. 1916-1990) in air temperature

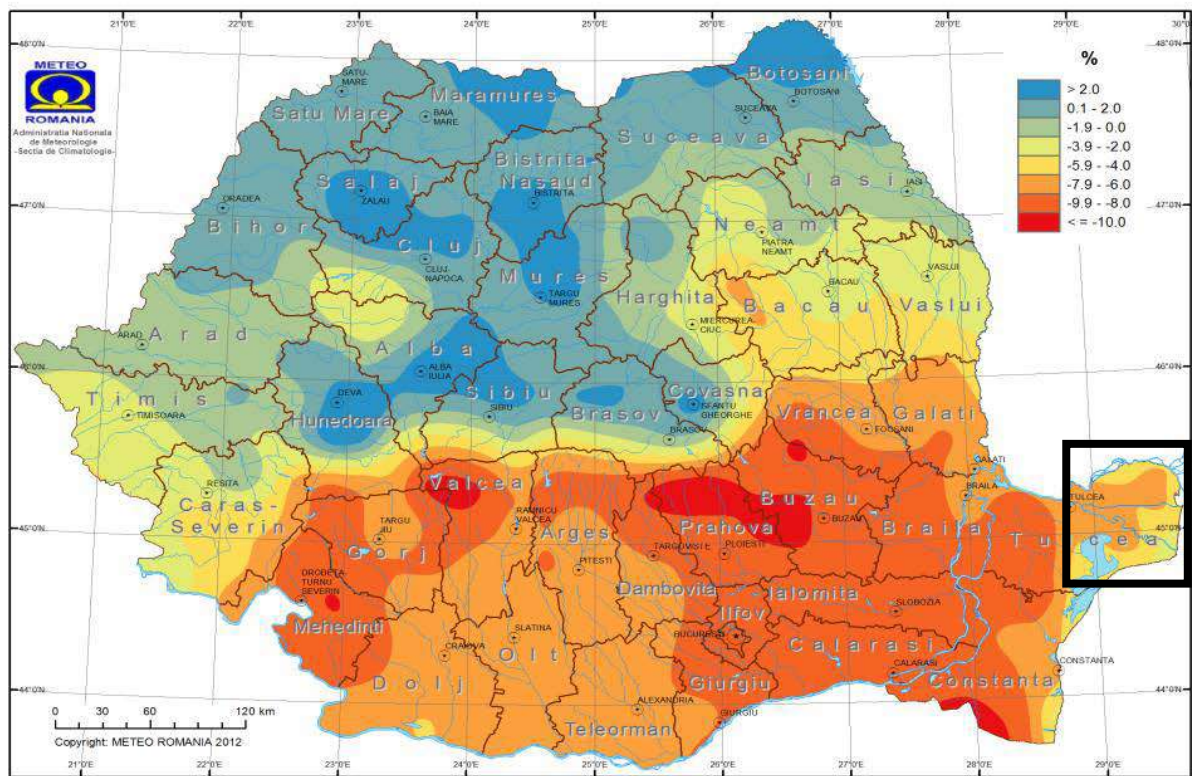


Figure 4.21 Multiannual mean changes (2011-2040 vs. 1916-1990) in precipitation (%)

For MARS climate changes scenarios (Figure 4.22) we used RPC85, RPC45 climate models and national forecast for each MARS storyline of two periods, 2030 and 2060. The climate variables considered in the model were temperature, precipitation and wind.

Climate variable	MARS1		MARS2		MARS3		Obs.
	RPC85		RPC45		RPC85		
	2030	2060	2030	2060	2030	2060	
Temperature	1.5 ⁰ C increase	4 ⁰ C increase	0.5 ⁰ C increase	2.5 ⁰ C increase	1.5 ⁰ C increase	4 ⁰ C increase	National forecast & RPC 85 / 45
Precipitation	6% (mm/day) decrease	15% (mm/day) decrease	2% (mm/day) decrease	5% (mm/day) decrease	6% (mm/day) decrease	15% (mm/day) decrease	National forecast & RPC 85 / 45
Wind	30% increase	25% increase	10% increase	20% decrease	30% increase	25% increase	RPC 85 / 45

Figure 4.22 MARS climate changes scenarios

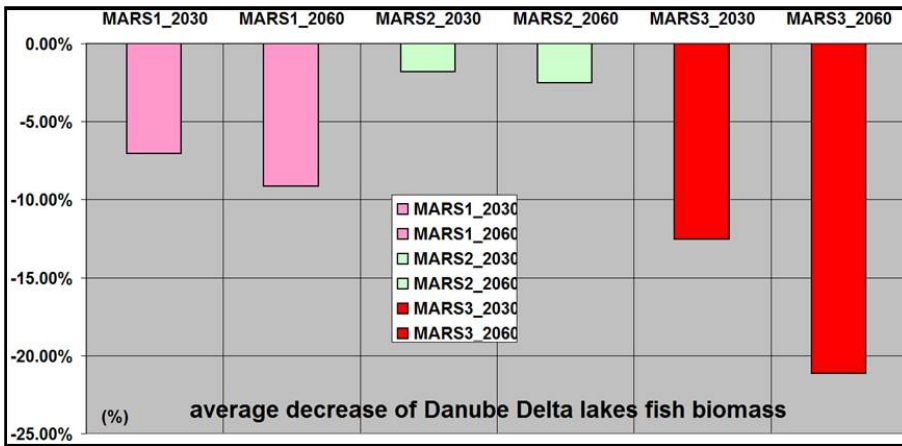
Quantification of MARS storyline elements (TN, TP, water levels) for each MARS storyline of the two periods, 2030 and 2060 is presented in Figure 4.23.

Criteria	Storylines Elements	MARS1		MARS2		MARS3				
		Qualitative change	Quantification		Qualitative change	Quantification		Qualitative change	Quantification	
			2030	2060		2030	2060		2030	2060
Nutrient loading	TN load	++	15% increase	30% increase	+	7% decrease	15% decrease	++	10% increase	25% increase
	TP load	++	15% increase	30% increase	+	7% decrease	15% decrease	++	10% increase	25% increase
Water levels	Natural flood retention	+			++			--	Q 10% decrease	Q 20% decrease

Figure 4.23 MARS storyline elements scenarios

4.1.4 Results

The climate change scenarios and MARS storyline elements inputs were loaded in the Aquatox models and run for actual, 2030 and 2060 periods. The gradient of the fish biomass for each lake and as average of all lakes for the MARS scenarios is presented in Figure 4.24.



Lake	MARS1		MARS2		MARS3	
	2030	2060	2030	2060	2030	2060
Fortuna	0.7%	-0.5%	2.2%	1.4%	-2.3%	-10.1%
Gorgova	-4.5%	-10.8%	0.1%	0.1%	-6.6%	-18.3%
Isac	-5.5%	-15.3%	-0.7%	-5.1%	-15.1%	-30.6%
Uzlina	-9.2%	-9.2%	-3.3%	-3.3%	-15.4%	-22.0%
Merhei	-10.8%	-11.0%	-4.5%	-4.3%	-17.1%	-23.4%
Miazazi	-11.2%	-8.4%	-2.6%	-2.7%	-14.9%	-21.6%
Rosu	-8.9%	-9.0%	-3.7%	-3.7%	-16.3%	-22.0%
	-7.1%	-9.2%	-1.8%	-2.5%	-12.5%	-21.1%

Figure 4.24 Fish biomass of the on Danube delta lakes for MARS scenarios

The gradient of fish biomass as average of all lakes for the MARS scenarios and 2030, 2060 periods are summarized in the Figure 4.25.

The results show that the MARS 3 scenario is the worst scenario for the years 2030 and 2060 followed by MARS1 scenario. MARS2 scenario seems to be the most desirable from all of the three. Nutrient stress is higher for the MARS1, 3 scenarios and moderate for MARS2. Regarding water stress some research forecast a decrease of the Danube River discharge up to 21.9% till 2100 (Daisuke, 2006) due to the climate changes. In our case predicted water level for MARS3 scenario is 20% for the year 2060, similar to above literature findings.

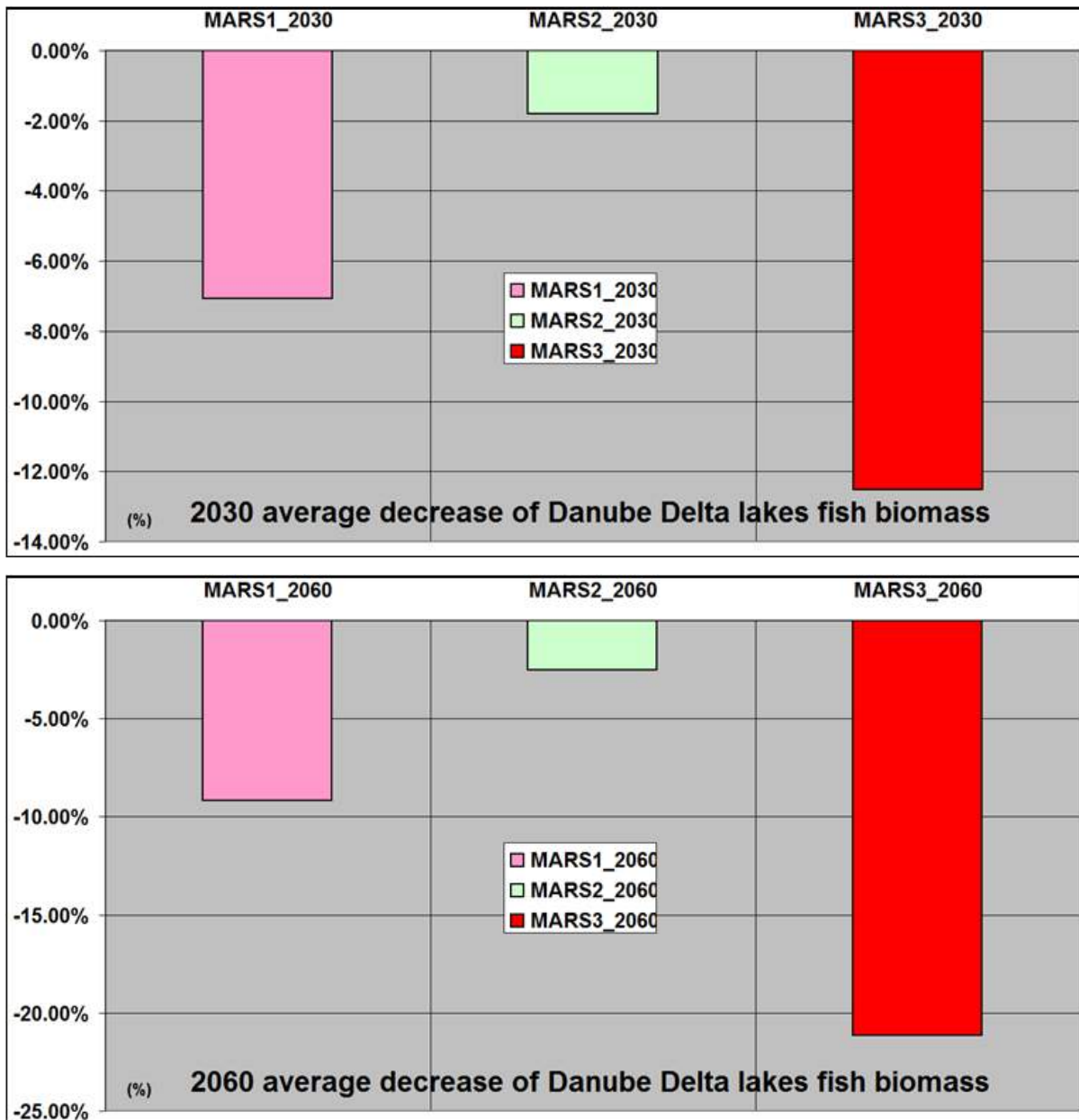


Figure 4.25 a, b. Fish biomass gradient for MARS scenarios at the years 2030 (a) and 2060 (b)

4.1.5 Conclusions and discussion

Influence of the main drivers to fish biomass in the Danube delta lakes was analyzed for the water scarcity scenarios corresponding to low waters regime of month August, September and October). For the analyses we use the hydrological and chemical database of 14 lakes of Danube delta within period 1996 - 2011. Empirical model results show that TP (total phosphorous), TN (total nitrogen), TSS (total suspended solids) and REZT_Ratio (Residence time ratio, monthly average / year average) are the most important independent variables affecting fish biomass. Nutrient stress is contributing with 54.9% and hydro-morphological pressures with 45.1%. Distribution map of multiple regression

results on selected lakes of the Danube delta give a good visual overview on relationship for each lake. For the lower Danube River basin selected Ecosystem Service indicator is fish flow. The climate change scenarios and MARS storyline elements inputs were loaded in the Aquatox lake models and run for actual, 2030 and 2060 periods. The results show a drastic decrease of lake fish biomass for MARS3 storyline (No MARS world) a significant decrease for MARS1 storyline (MARS ad hoc) and a realistic decrease for MARS2 storyline (MARS world). The main impact on the fisheries and aquaculture is represented by the total fish abundance and a shift in the composition of the fish community. The main pressures contributing to the decline of fish yield in Lower Danube are the Iron Gates I, II dams and embankment of the natural floodplain of the river and Danube Delta. The climate change has also contributed influencing the hydrology. Ecological reconstruction of flood plain areas may contribute to the revenue of fish stock and structure in the lakes of the Danube delta.

4.2 Lake Beysehir Basin

4.2.1 Introduction

Freshwater ecosystems serve various ecosystem services such as they supply water for different purposes and food as provisioning services; nitrogen retention, flood protection as regulating services and recreation as cultural services (Grizetti *et al.* 2015, Janssen *et al.* 2015). However, humans mostly put emphasis on provisional services like food production and water abstraction while the importance of regulatory and recreational services are ruled out which results in overexploitation of the services. Accordingly, freshwater ecosystems are one of the most altered ecosystems in the world and half of the wetlands were modified in worldwide (Mooney *et al.* 2009). These modifications such as dam construction, channelization, heavy water abstraction, and overfishing may have disrupting ecosystem functioning and resilience of the ecosystems. Climate change may further exacerbate a damage in ecosystem services of the freshwaters by changing the quantity and quality of them and all these may result in high ecological and economic lost (Erol and Randhir, 2012) since increased temperatures also known to enhance the eutrophication symptoms (Moss, 2011).

Climate change impact studies are at the core of the lake research due to necessity of understanding ecological consequences of climate change and developing adaptation strategies. According to climate projections, Mediterranean region is one of the most affected regions in world, and significant reductions in precipitation and increase in temperature is anticipated for future (Christensen *et al.*, 2013; Erol and Randhir, 2012). Climate change not only expected to decrease water availability and exacerbate water stress in Mediterranean (Calbó, 2010), it may also have significant impacts on lake

ecosystem structure and function (Beklioglu et al., 2007; Jeppesen et al., 2015). In semi-arid Mediterranean region, lower water availability in the catchment may decrease the external loading to the lakes; however internal loading and volume reduction due to increased evaporation may trigger nutrient increase (Bucak et al 2012, Özen et al 2010). In addition, increased temperature and retention may change the composition and duration of phytoplankton blooms which may trigger early spring bloom, increase in cyanobacteria (Reynolds, 1993; Carvalho et al., 2008; Paerl & Huisman, 2008) and longer duration of autumn bloom. Longer retention time and less mixing also gave advantage to cyanobacteria over green algae and diatoms (Visser 2015). Prolonged cyanobacteria blooms may limit the drinking water use. Apart from water quality, water quantity in Mediterranean region may also be at risk (Bucak *et al.* submitted) since it is expected that irrigation demand would increase with climate change, however less water availability would result in main conflict in Mediterranean freshwater ecosystems. However, due to site-specific characteristics and lake physical characteristics, responses of lake to climate change may show great diversity (Mooij 2005).

Land and water use management also important to mitigate the impacts of climate change. In Mediterranean region where there is higher variability between seasons in terms of water availability, water management and availability of water determines the socio-economic structure (García-Ruiz et al., 2011). Intensive irrigation needs in the least water available season (Moran Tejada et al 2014) trigger a main problem for freshwater ecosystems and may lead to significant water level reductions especially in shallow lakes which have a high surface area/depth ratio. Hence, efficient irrigation technologies and change in crop pattern (promoting drought-resistant crops) are some of the important mitigation measures to combat the negative consequences of climate change (Bucak *et al* submitted). Usage of chained models are essential to link climatic and management processes to lake dynamics and predict the future ecosystem dynamics, resilience and services of the lake ecosystems.

4.2.2 Study area and MARS concept development

Lake Beyşehir is located in the borders of Konya and Isparta (south-western Turkey, Fig 4.26a), is the largest freshwater lake in Turkey and Mediterranean basin. It is a shallow and mixing lake with having a surface area of approximately 650 km², and a mean and max depth of 5 and 9 m, respectively. The lake is located in borders of 2 National Parks (Beyşehir and Kızıldağ National Parks) and part of the catchment was also declared as 1st Degree Natural Sit Area. Lake supplies water for both drinking water for Beyşehir district and agricultural irrigation for Konya Basin with the canal built in 1914 (Oğuzkurt, 2001). The lake is also “Important Bird Area” (BirdLife International, 2015), “Important Plant Area” (PlantLife International, 2015) and host to the endemic fish species of *Chondrostoma*

beysehirensis Bogutskaya, 1997 and *Pseudophoxinus anatolicus* Hankó, 1925 as well as the recently extinct endemic species *Alburnus akili* Battalgil, 1942 (Yeğen et al., 2006).

Lake Beyşehir is primarily fed by waters from the Sultan and Anamas mountains and springs from cracks of mezozoik limestone. West part of the lake has a karstic structure, and groundwater-surface water interactions are important. The catchment area is approximately 4,704 km², consisting mostly of range land (brush, 48%), agriculture (30%) and forest (6%). The majority of agricultural land is cultivated with wheat, barley, chick peas or sugar beet. The catchment is located at relatively high elevation ranging 1050 - 3000 m.a.s.l. The trophic status of the lake itself is within an oligotrophic to mesotrophic range (Wetzel, 2001), in terms of low phytoplankton biomass and nutrient levels.

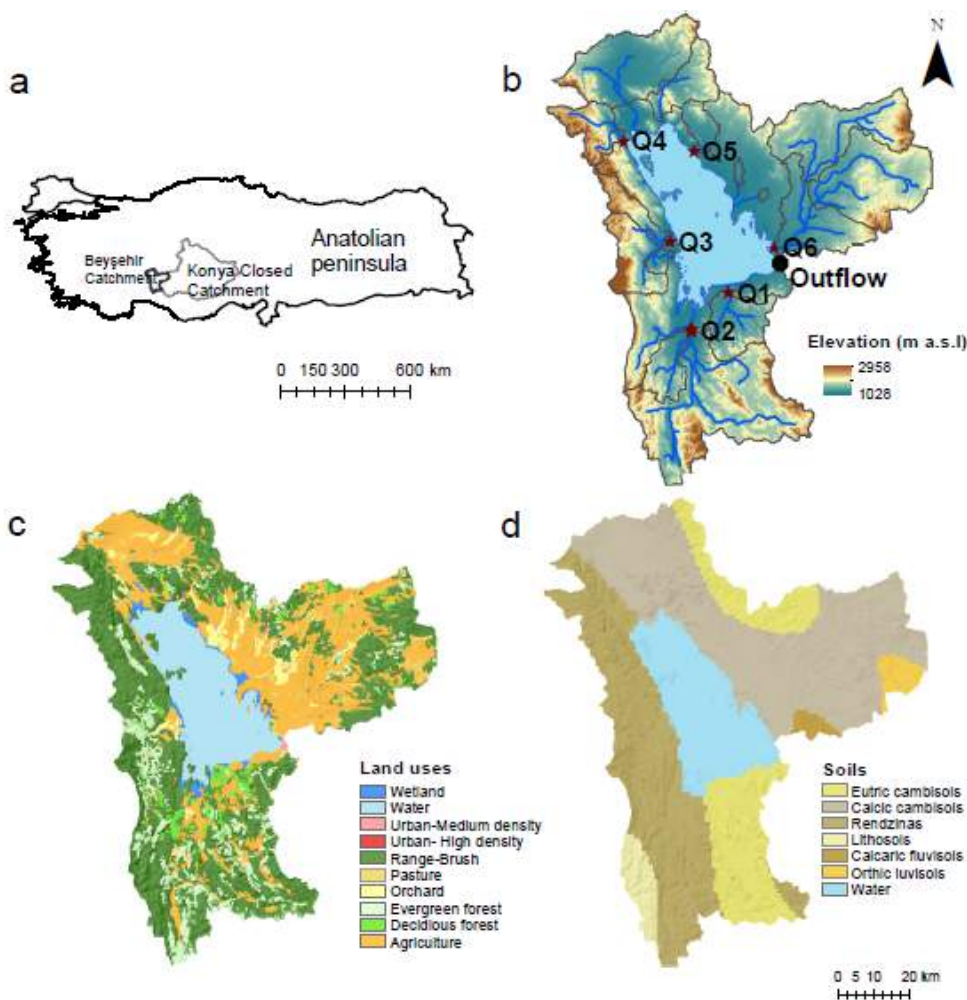


Figure 4.26 Location of the study site and GIS layers that are used in SWAT model (a) Location of the study site; (b) digital elevation map of the Beyşehir catchment. Brown borders show the sub-catchment boundaries. Numbers indicate the inflows (local names of inflows are: Q1: Üstünler, Q2: Soğuksu, Q3: Hizar, Q4: Çelttek, Q5: Tolca-Ozan, Q6: Sarısu) used in the calibration and the black circle shows the outflow; (c) distribution of land use categories; (d) soil map.

Regarding the objectives of MARS project, in this study we used ensemble approach by linking catchment model outputs to two different lake models (PCLake and GLM-AED) and applied to the largest freshwater lake of Turkey and Mediterranean, Lake Beyşehir. Within this study, we want to simulate the effects of multiple stressors on ecosystem services of Lake Beyşehir. Main stressors in Lake Beyşehir are defined as diffuse pollution, water abstraction and future climatic changes in temperature and precipitation. The most important ecosystem services of Lake Beyşehir include water for irrigation and drinking. As summarized in conceptual model (Fig 4.27.), we predicted the impacts of climate (temperature, precipitation) and land use stressors (change in land use and water abstraction) on the ecosystem service capacity of the lake (which are mainly drinking and irrigation water supply) by using proxies of chlorophyll *a*, water level, cyanobacteria biomass, TP, TN.

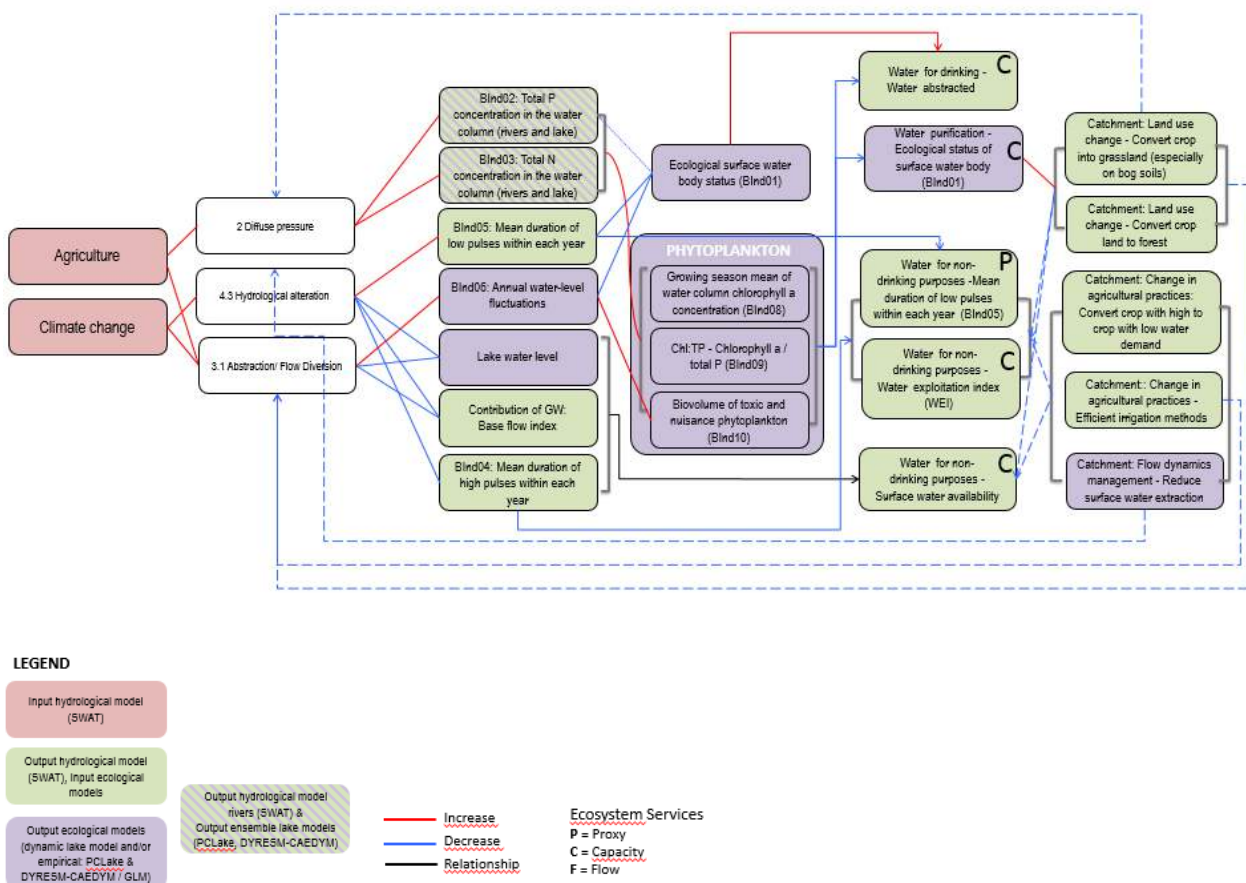


Figure 4.27 MARS conceptual model of Lake Beyşehir

4.2.3 Data and Methods

4.2.3.1.1 Processed based modelling and calibration

To describe the hydrological processes in the catchment and simulate the effects of future climate and land use changes on the hydrological state of Lake Beyşehir, the Soil and Water Assessment Tool (SWAT) model (SWAT 2012, Revision 622) (Arnold et al., 1998) was employed. SWAT is a catchment (river basin) model and was developed to quantify the impacts of land management practices on surface waters by simulating evapotranspiration, infiltration, percolation, runoff and nutrient loads (Neitsch et al., 2011). The model is a physically based, semi-distributed model, which has been tested (e.g. for agricultural water management purposes) and published extensively in peer-reviewed literature (Gassman et al., 2007).

Catchment processes in SWAT are modeled in two phases – the land phase covering; the loadings of water, sediment, nutrient and pesticides from every sub-basin to a main channel and the water routing phase covering; processes in the main channel to the catchment outlet (Neitsch et al., 2011).

SWAT model setup

The lake catchment was delineated using the ASTER (30 m resolution, <http://gdex.cr.usgs.gov/gdex/>) digital elevation model (DEM), which was smoothed to 90 m resolution, and a burn-in to a river network within the DEM based on the known locations of reaches and lake surface. The delineation resulted in 16 sub-catchments (Fig. 4.26b). Three slope intervals (less or equal to 5%, 5-20%, greater than 20%) were defined. Land use data were obtained from the Corine 2006 database (<http://www.eea.europa.eu/data-and-maps/data/corine-land-cover-2006-raster>) at 100 m resolution (Fig. 4.26c). For soil type definition, Harmonized World Soil Database with 1 km resolution was used (<http://webarchive.iiasa.ac.at/Research/LUC/External-World-soil-database/HTML>) (Fig. 4.26d). Soil hydrological and physical parameters were initially derived from soil texture data using the Hypres model (Wösten, 2000). Overlay of soil, slope and land use maps resulted in 714 hydrological response units (HRU), which are the key building blocks of the SWAT model.

Land use and agricultural management were described by splitting the generic (AGRL) areas into four dominant crop management systems (winter wheat: 41%, winter barley: 31%, chick peas: 24% and sugar beet: 4 %) based on data obtained from local authorities and the Turkish Statistical Institute (TÜİK, 2013). Agricultural management schedules were generated through consultation with local experts.

The Penman-Monteith method (Monteith, 1965) was used for estimating potential evapotranspiration, and surface runoff was calculated using the U.S. Soil Conservation Service curve number procedure (USDA Soil Conservation Service, 1972). The elevation range was divided into five elevation bands with an elevation fraction of 0.2 to account for the effects of the wide elevation gradient in the catchment.

Meteorological data on precipitation, minimum and maximum temperature, wind, solar radiation and relative humidity were compiled from the Turkish State Meteorological Service (www.mgm.gov.tr) for the period 1960-2012 for the Beyşehir (37° 41' N, 31° 44' E) and Seydisehir (37° 26'N, 31° 51'E) stations located in the south-eastern parts of the catchment.

Calibration results of SWAT

Hydrological calibration of the Lake Beyşehir catchment was explained in detail in Bucak *et al* submitted. The results of the calibration and validation of the flow rates for the main inflows of the lake are given in Fig. 4.28. Flow calibration was conducted for a daily time step and statistics were calculated on both a daily and monthly basis. Due to the characteristics of the climate and hydrological processes in the catchment, peak flow events were observed during spring after snowmelt events, and most of the inflows dried out during the summer. SWAT was able to capture most of the seasonal variation in the discharge values. According to the review by Moriasi *et al.* (2007), Nash–Sutcliffe model efficiency coefficients (NS values) over 0.5 are considered satisfactory for a monthly flow calibration, and the calibration results derived in our study were therefore satisfactory. Three of the inflows located close to the meteorology stations in the catchment exhibited NS values higher than 0.5, and for the remaining inflows, NS values were around 0.5. In addition, the rivers Üstünler (Q1) and Hizar (Q3) (Fig. 4.26, Fig. 4.28), located in the western part of the catchment, had lower NS values and generally lower discharge rates as well, and their contribution to the lake water budget was minor relative to that of the other rivers (Table 4.1).

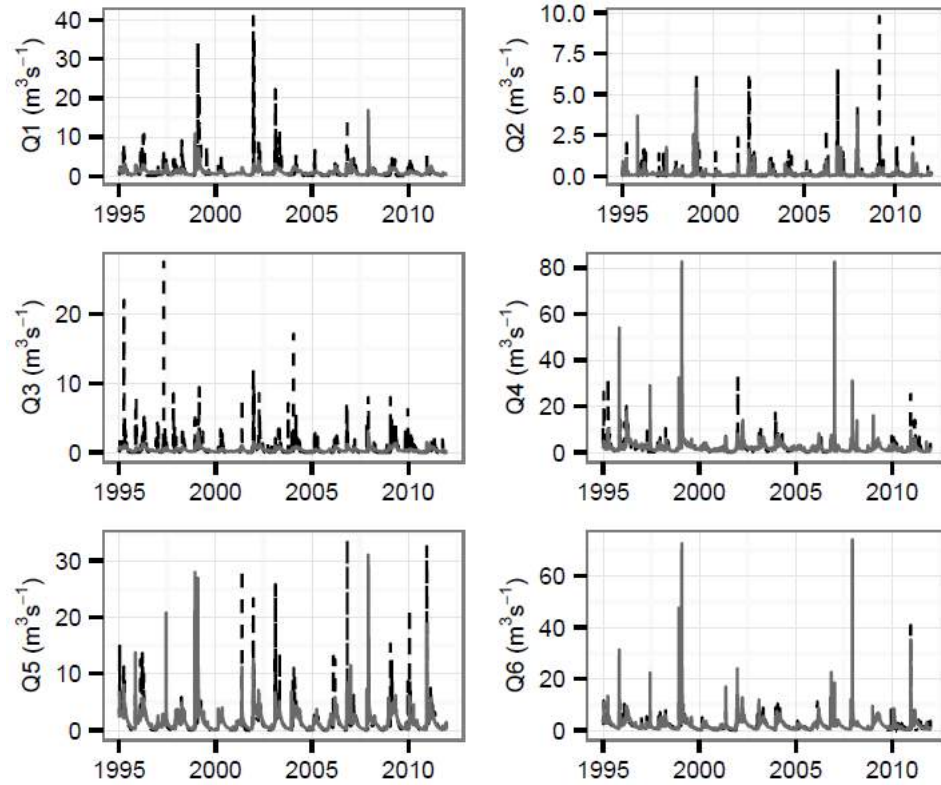


Figure 4.28 Calibration and validation results. Daily simulated (grey, solid lines) and observed (black, dashed lines) flows after calibration of the SWAT model. Flow rates are given in m³ sec⁻¹. (Q1: Üstünler, Q2: Soğuksu, Q3:Hizar, Q4: Çeltck, Q5: Tolca-Ozan, Q6: Sarısu). Taken from Bucak et al submitted.

Table 4.1 Daily and monthly performance statistics for the main inflows. Calibration period = 2002-2011; validation period = 1995-2001. Mean values for the simulated and observed periods are in m³ s⁻¹. Taken from Bucak et al submitted.

Station Name	Calibration				Validation							
	Monthly		Daily		Observed mean	Simulated mean	Monthly		Daily		Observed mean	Simulated mean
	NS	PBIAS	NS	PBIAS			NS	PBIAS	NS	PBIAS		
Q1	0.4	-11.7	0.28	-14.4	0.88	0.99	0.49	5.6	0.23	1.7	1.24	1.17
Q2	0.37	1.3	0.23	-2.2	0.12	0.12	0.54	-29.8	0.19	-36.1	0.1	0.13
Q3	0.48	8	0.27	4.3	0.42	0.39	0.25	26.9	0.10	27.8	0.54	0.4
Q4	0.51	2.6	0.44	-1.9	1.9	1.85	0.57	12.1	0.02	0.6	2.43	2.13
Q5	0.73	-0.9	0.53	-1.8	1.39	1.41	0.71	-7.6	0.48	-9.9	1.44	1.55
Q6	0.76	-2.4	0.61	8.1	2.1	2.15	0.65	-12.9	-0.29	-18.3	1.93	2.17

According to Moriasi et al (2007), for nutrient calibration percent bias (PBIAS) $< \pm 25$ can be regarded as *very good*, $< \pm 40$ as *good* and $< \pm 70$ as *satisfactory*. However, it should be noted that, these criterias for calibration statistics are for monthly calibration results; the results given here are for daily

calibration. Nutrient calibration results were both given in R^2 and Percent bias. As it is given in Table 4.2, for nitrate calibration, model results of the 4 out of 6 inflows are regarded as *very good* and two of them is *good*. For phosphorus calibration all inflow model calibration can be regarded as *very good*. Simulated nitrate values mostly followed the observed pattern with low bias. Phosphate concentrations in the inflows are mostly very low, sometimes under the detection limit which makes it harder to catch the observed trends in the simulation.

Table 4.2 Calibration statistics for daily Mineral P and Nitrate Loads. While calculating the statistics, a window function with a search timeframe of 7 days was used to sample the model outputs closest to observed values.

Inflows	Mineral P		Nitrate	
	PBIAS	R ²	PBIAS	R ²
Q1	5.4	0.3	23.8	0.09
Q4	0.5	0.01	-7.13	0.45
Q10	0.5	0.01	28.8	0.06
Q11	-3.0	0.19	-7.5	0.49
Q14	9.4	0.25	38.3	0.41
Q15	15.1	0.32	-19.2	0.47

Lake models

PCLake model

PCLake is initially developed to model the transition between alternative stable states, is zero dimensional model in which the lake body is represented as completely mixed water body and sediment top 10 cm. It is suitable for shallow lake bodies those are permanently mixed and having no vertical and horizontal variation. Interactions between water column and sediment top layer is modelled with detailed biogeochemical modules including processes like settling, resuspension, mineralization, diffusion and sorption. The nutrient cycles are dynamic and the mass balance per element is checked after every time step (Janse, 2005). Biological module comprises of three groups of phytoplankton, one zooplankton, one zoobenthos, planktivorous fish (adult and juveniles), piscivorous fish and submerged macrophytes. Phytoplankton biomass is calculated considering primary production, respiration, mortality, settling, resuspension, grazing and transport processes. All animal groups basically modelled as the product of feeding, egestion, respiration, mortality and predation. Zooplankton is set to feed on phytoplankton and detritus with grazing pressure depending on seston concentration, filtering rate and food preference parameters. Fish predation is modelled as

juvenile whitefish feeding on zooplankton, adult whitefish on zoobenthos and piscivorous fish on all whitefish (Janse, 1997; 2005). Though having advanced biogeochemical and biological module, it does not have hydrodynamics and thermodynamic module (Hu 2016).

GLM-FABM-AED model

General Lake Model (GLM v2.0.0), a one-dimensional (1D) hydrodynamic model which considers variation in vertical gradient is coupled through the Framework for Aquatic Biogeochemical Modeling (FABM) to the Aquatic EcoDynamics module library (AED) (Hipsey et al. 2013, 2014). GLM computes the temperature, salinity and density gradients in vertical profiles regarding inflow, outflow and meteorological forcings. GLM uses Lagrangian layer scheme (Imberger and Patterson, 1981) in which lake is represented as layers having equal thickness and the layers expand or contract considering density changes driven by surface heating, mixing and flows. Most of the hydrodynamics algorithms simulated in GLM adopted from widely used lake hydrodynamic model DYRESM (Han et al., 2000; Gal et al., 2003; Rinke et al., 2010; Trolle et al., 2011, Bruce et al. 2006, Gal et al. 2009, Trolle et al. 2011)

AED ecological module library enables to simulate various chemical processes including inorganic and organic nutrient cycles, oxygen dynamics and biological organisms as functional groups. Initial motivation of AED is developing a flexible aquatic ecosystem module which could be customized easily according to selected biogeochemical and ecological configurations. While customizing the modules, hierarchical dependences of the modules should be considered (Hipsey et al 2013). AED supports the oxygen, silica, phosphorus, nitrogen, organic matter, chlorophyll *a*, phytoplankton, zooplankton and pathogen modules. In nutrient modules, mineralization, decomposition, sediment fluxes, uptake by phytoplankton and excretion by organisms were simulated. For Nitrogen module, denitrification and nitrification processes were also included. Phytoplankton biomass was calculated considering nutrient uptake, excretion, mortality, respiration, vertical movement and grazing by zooplankton. For zooplankton module, processes of assimilation from grazing, respiration, excretion, faecal pellet production, mortality and predation by larger organisms were included.

Model setups

Since only two year field data is available, one year monthly data is used for calibration and other year used as validation period. PCLake does not have thermodynamic component, hence daily simulated temperature derived through GLM model was given as an input to PCLake. Monthly water chemistry values of inflows were linear interpolated to generate the daily data that is needed by lake

models. Residual flows were calculated from the simple water budget equations considering water level, precipitation, inflow, outflow and area information. Both of the models require the meteorological forcing of precipitation, wind speed, radiation, precipitation, however GLM requires additional cloud cover, relative humidity and air temperature. 3 Dominant functional phytoplankton groups were included as Cyanobacteria, Chlorophyte and Diatom since they constitute 85% of the total phytoplankton biomass. Zooplankton groups were pooled as 1 functional zooplankton group.

Sensitivity analysis

Since both models include high number of parameters, in order to reduce the efforts in the calibration, most sensitive parameters were determined. Sensitivity parameters were conducted using all parameters in GLM-AED and PCLake separately. Sensitivity index of the parameters were calculated using the equation given in Chen *et al.* (2002) and which was given below:

$$S_{ij} = \frac{\Delta F_i / \bar{F}_i}{\Delta Parameter_j / Parameter_j}$$

Where ΔF_i is the change in variable i corresponding to change in parameter j , F_i is the default value of the variable i , $\Delta Parameter_j$ is the change in value of parameter j , $Parameter_j$ is the default value of the parameter j .

Every parameter was adjusted $\pm 10\%$ except temperature multipliers which they are adjusted by ± 0.01 . Sensitivity index > 0.5 is regarded as sensitive parameters.

Calibration of the models

The most sensitive parameters (Sensitivity index > 0.5) was used in calibration of the lake models. Model calibration was conducted for temperature, oxygen, soluble reactive phosphorus, nitrate, ammonium, total chlorophyll a , Chlorophytes, Cyanophyta, Diatom. Firstly temperature and oxygen was calibrated, followed by nutrients and phytoplankton biomass. Calibration was conducted to find the best match between observed and simulated variables. Parameters were manually adjusted in literature ranges to find the best parameter set (given in Table 4.3) giving the minimum error between observed and simulated variables. In optimization algorithms Root Mean Square Deviation (RMSD) was used as an objective function. In addition to statistical measures, the results were also visually inspected to check the seasonal trends. In addition, for evaluating model performance, RMSD, Normalized bias and R^2 was calculated.

Table 4.3 Lake models calibration statistics. While calculating the statistics, a window function with a search timeframe of 7 days was used to sample the model outputs closest to observed values

	r^2		Normalized bias		RMSD	
	GLM	PCLake	GLM	PCLake	GLM	PCLake
Chl-<i>a</i>	0.02	0.31	-0.09	0.02	2.66	1.74
PO₄	0.17	0.14	0.34	0.41	2.01	2.4
NH₄	0.14	0.31	0.53	4.17	2.91	11.98
NO₃	0.13	0.03	0.86	8.39	16.39	83.71

The results of calibration of the lake models were given in Table 5.3 and Fig 5.4. Since PCLake does not have a thermodynamic module, water temperature simulated by GLM was given to PCLake. Simulated water temperatures fitted well with the observed temperatures ($R^2= 0.99$, Fig. 4.29). Chl-*a* and PO₄ visually match good with observed and simulated results, however goodness of fit is low regarding the low concentrations (lower than 10 $\mu\text{g L}^{-1}$ for both, sometimes even lower than detection limits) and not having strong seasonality. For NH₄ and NO₃, GLM matched better with observations. However, lower NH₄ levels (most of the time period =0), caused a low goodness of fit statistics.

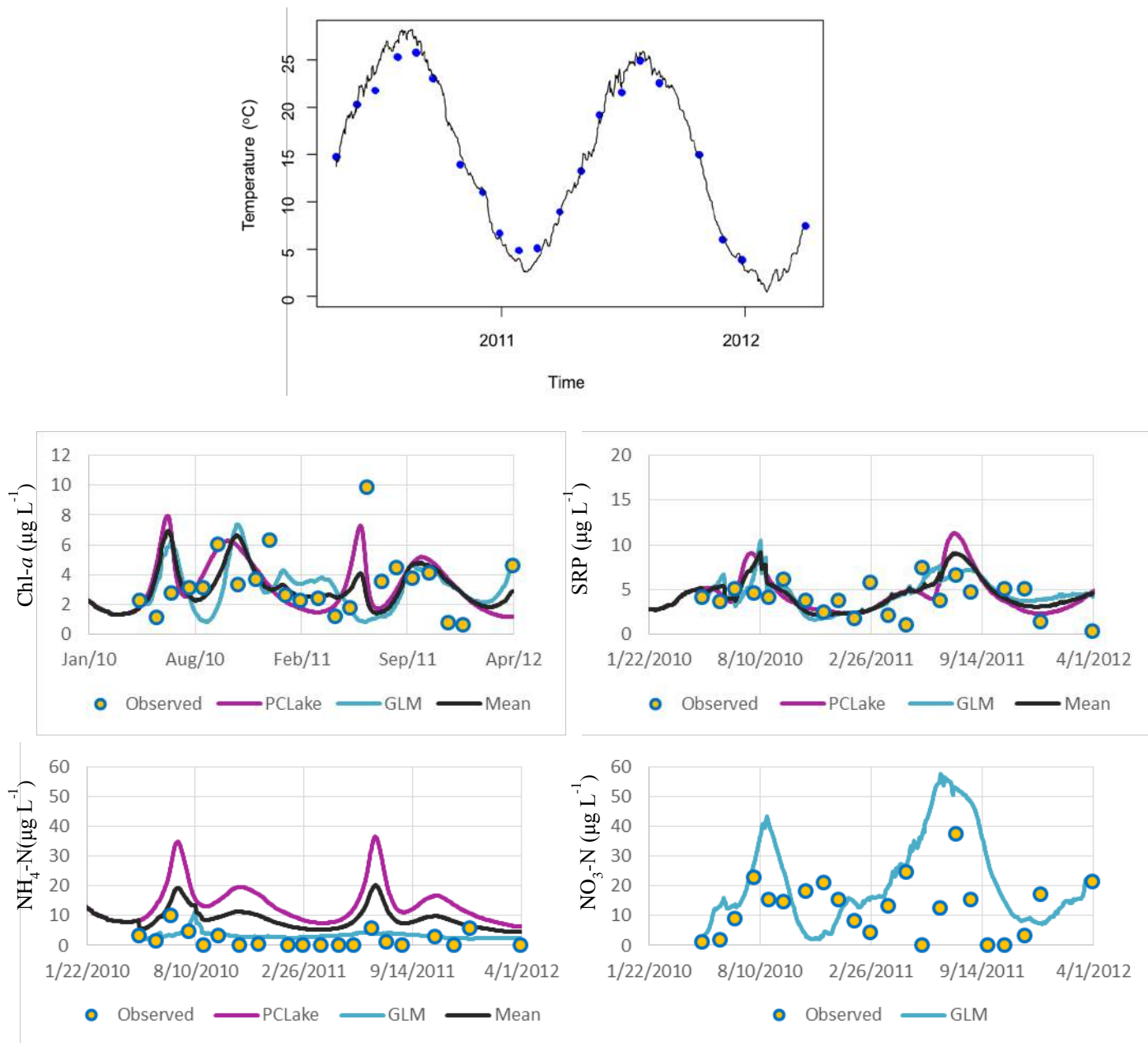


Figure 4.29 Calibration results of the lake models

Ecosystem services description and linkage with pressures (some accounting)

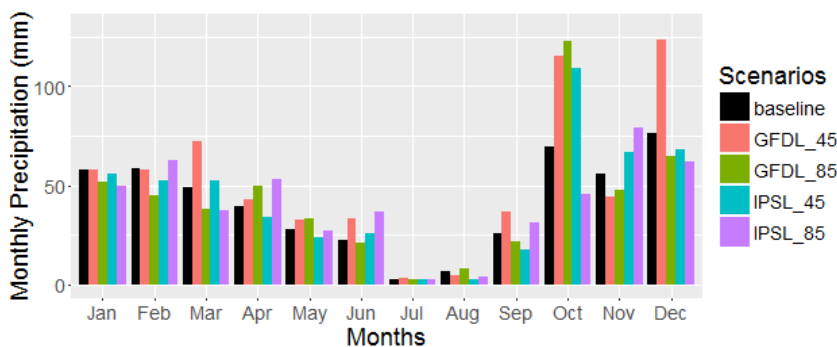
The most important ecosystem services of Lake Beyşehir include water for irrigation and drinking and fisheries. However, in this study, only drinking and irrigation value of Beyşehir is considered. Historical records of Lake Beyşehir shows, the lake is subjected heavy water abstractions which resulted in water level fluctuations. Based on the data collected from the State Hydraulic Works covering the period 1960-2012, the yearly average input of water (including precipitation, inflows and groundwater) to the lake varies between 550 hm³ and 1200 hm³, and evaporation from the lake surface constitutes 410-850 hm³. Moreover, average yearly water abstraction from the lake for

irrigation of the downstream basin is 325 hm³. Lake Beyşehir is also used as a major drinking water supply for the Beyşehir district, however the proportion of water used for drinking is of minor importance with 6 hm³ as the yearly average. Climate change projections may change the overall picture for Lake Beyşehir, since for Mediterranean region, increased drought periods with less precipitation and increased temperatures were expected. In this study, to evaluate the effects of climate change in addition to land use changes on ecosystem services of Lake Beyşehir, indicators of water level, TP, TN, Chlorophyll, cyanobacteria biomass is used. Water level is an indicator of irrigation water services while Chl-*a*, TP, TN, cyanobacteria percentage and are indicator for drinking water services. EQR values were also calculated from the chl-*a*, cyanobacteria and phytoplankton biomass based on the index developed from Turkish shallow lakes which the details were given in Erdoğan *et al* in preparation.

4.2.3.1.2 Scenarios development

Climate Change Scenarios

GFDL-ESM2M and IPSL-CMA-LR climate models, hereafter will be written as GFDL and IPSL were used for generating precipitation and temperature scenarios for two climate scenarios (RCP 4.5, RCP 8.5). Climate scenarios were available for period of 2006-2099. Period of 2006-2015 were used as a reference period and monthly linear correction was applied to observed climate data and scenarios outputs covering this period. Factors derived from linear correction were applied to projected temperature and precipitation data series. Two distinct periods (2025-2034, 2055-2064, hereafter will be mentioned as 2030s and 2060s respectively) were chosen for future scenario runs. For 2030s, predicted climate scenarios indicated a 0-26% increase in precipitation whereas for 2060s, precipitation change was predicted from 8% increase to 30% decrease (Fig. 4.30). Temperature outputs indicate 1-2 °C increase for 2030s and 2.5-4.5 °C increase for 2060s (Fig. 4.31).



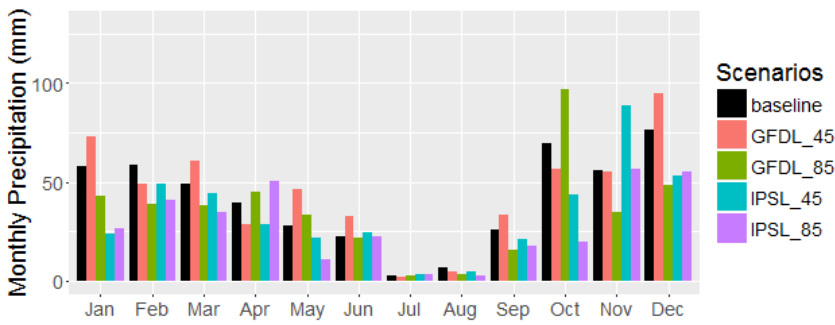


Figure 4.30 Future and baseline precipitation (mm)

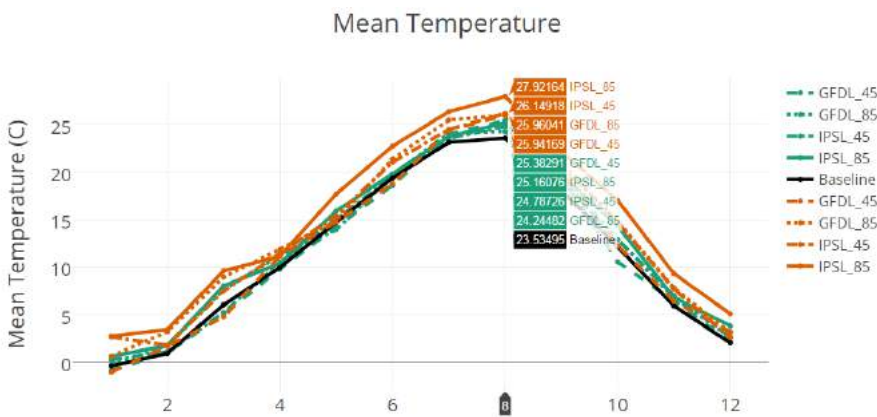


Figure 4.31 Future and baseline temperature(oC)

MARS land use scenarios

Three different storylines were developed for future land use scenarios.

Techno world (economic focus): In Techno world scenario, economic growth is the main focus. Higher economic growth accompanied increase in energy demands and resources which brings with agricultural expansion. In southern Europe, water consumption is expected to increase due to increased agriculture and tourism. In middle-south Turkey, there is also increased tendency towards irrigated farming. Hence, in this scenario, 20% of the forest areas and 10% of the grassland turned into cropland. Fertilizer amount and water abstraction increased as 10%. In Techno World Scenario, RCP 8.5 scenario is used.

Consensus (green focus): In Consensus world scenario, economic growth is as it is today. More efforts put in to promote sustainable use of sources. Water consumption would drop due to promoting drought resistant crops and increased irrigation efficiency. Due to increased temperature, 5% of forest

areas turned into shrubland. In addition, fertilizer amount and water abstraction decreased as 20% and 10% respectively. In Consensus World Scenario, RCP 4.5 scenario is used.

Fragmented world (Survival of the fittest) :In this scenario, there is no homogeneity across countries as there is an increase in economic development in some countries whereas some of them suffer from big economic crisis (recession). The southern Europe is expected to suffer from economical crisis since climate change is expected to decrease the agricultural productivity. Protection of environment is not a focus while the main focus is over-use of natural resources. In this scenario, 30% of forest and 30% cropland turned into shrubland. There is an 30% increase in fertilizer application and water abstraction. In Fragmented World scenario, RCP 8.5 scenario is used.

4.2.4 Results

4.2.4.1.1 Swat models outputs

Only Climate Change Scenarios

Two different Global Climate Models varied in their predictions for total flow generated in the catchment as for GFDL-4.5 model (GFDL-ESM2M with RCP 4.5 scenario), there was a pronounced increase in flow being 81.6% increase for 2030s and 21.4% increase for 2060s whereas IPSL 4.5 model predicted a 18.1% increase for 2030s and 44% decrease for 2060s. For RCP 8.5 scenarios, both models predicted a reduction in total flow, as there were slight change for 2030s from -8 to -9 % and for 2060s the change range in predictions were -36.6% to -59.9% (Table 4.4).

For future nitrate simulations, all climate scenario runs demonstrated a decrease in nitrate load. For the period of 2030s, 11.8% to 41.8% decrease in nitrate load was anticipated while it was -34.6% to -47.6% for 2060s period. For mineral phosphorus load, there is only an increase in GFDL- 4.5 scenario where 126.6% increase were projected for 2030s and %103 increase for 2060s. For other climate model and scenarios, there is an pronounced decrease in mineral P load up to 37.8% for 2030s and 77.6% for 2060s (Table 4.4).

Table 4.4% Changes in total flow, mineral P and nitrate load with future scenarios

Climate	Land use	Total flow		Nitrate		Mineral P	
		2030s	2060s	2030s	2060s	2030s	2060s
GFDL-4.5	Current	81.6	21.4	-11.8	-38.0	126.6	103
IPSL-4.5	Current	18.1	-44.0	-31.8	-34.6	-7.8	-49.7
GFDL-8.5	Current	-8.5	-36.6	-37.9	-41.9	-11.3	-40.8
IPSL-8.5	Current	-7.9	-59.9	-41.8	-47.6	-37.9	-77.6
GFDL-8.5	Techno	-3.5	-34.8	-31	-35.5	23.6	-20.8
GFDL-4.5	Consensus	85.8	25.6	-12.2	-43.6	132.9	102.1
GFDL-8.5	Fragmented	-2.7	-31.9	-50.4	-53.8	-6.7	-35.3
IPSL-8.5	Techno	-2.4	-60.5	-17.7	-44.4	4.9	-76.4
IPSL-4.5	Consensus	22	-41.0	-35.9	-31.7	3.5	-43.9
IPSL-85	Fragmented	-2.5	-56.9	-39.8	-59.6	-21.1	-80.7

Combined land use and climate scenarios

Techno world scenario: There is a slight decrease in total flow in Techno world storylines for both climate models in 2030s period whereas in 2060s there was a paramount drop in total flow (-34.8% to -60.5%). Nitrate load also reduced in both climate models and time periods as -31% to-17.7% change was predicted for 2030s and -35.5% to -44.4% for 2060s. For Mineral P load, two time periods differ since 4.9% to 23.6% increase was predicted for 2030s whereas significant drop (-20.8% to -74.6%) was found for 2060s.

Consensus world scenario: The outputs of consensus scenario runs differed in predictions for two time periods since there is a prominent increase in total flow for 2030s (22% to 85.8%) and for 2060s the change range was from -44% to 25.6%. There is also reduction in nitrate load from -12.2% to -31.7 % and -43.6% to -31.7% for 2030s and 2060s respectively. Combined runs with both climate change scenarios predicted an increase in mineral P load for 2030s (132.9-3.5%) whereas for 2060s IPSL model anticipated a decrease in mineral P loads (-43.9%).

Fragmented world scenario: Minor decrease in total flow was anticipated for 2030s while it was -31.9% to -56.9% for 2060s period. For nitrate load, results of both time periods indicates significant drop in nitrate load as for 2030s it was -39.8% to -50.4% and for 2060s it was -53.8% to -59.6%. Mineral P load scenario runs show that reduction in Mineral P was more prominent in 2060s within the range of -35.8% to -80.7% whereas it was -6.7% to -21.1% for 2030s time period.

4.2.4.1.2 Lake model outputs

Change in hydraulic loads, precipitation and temperature caused a water level changes, however magnitude and direction of the change differed among scenarios (Table 4.5). Highest water level observed in GFDL-4.5 scenarios with consensus land use due to higher runoff and precipitation predicted with this scenario for both 2030s and 2060 while the lowest water level was observed in IPSL-8.5 8.5 scenario with fragmented world scenario. According to the latest management policy, water level ranges of Lake Beyşehir should be between 7.4 and 9.6 m. According to scenario results of 2030s period, only GFDL-4.5 and GFDL-4.5 with consensus scenario exceeds the maximum management levels which means water abstraction for irrigation may increase for according to these scenario results. However, none of the scenarios resulted in water level below than minimum management level for 2030s period. For 2060s, only GFDL 4.5 with consensus scenario was above highest management water level, however six of the scenario results were below lowest management water level (which were mostly RCP 8.5 scenarios) indicating possible limitation in 2060s for water abstraction and lower water levels (Fig. 4.32).

Table 4.5. Change in average water level (m) for 2030s and 2060s period. Default: No land use and no climate change scenario, G:GFDL, I:IPSL, C:Consensus, T:Techno, F:Fragmented, 4.5:RCP 4.5, 8.5:RCP 8.5

	2030			2060		
	Min	Max	Average	Min	Max	Average
Default	7.71	8.59	8.30	7.71	8.59	8.30
Techno	7.56	8.42	8.14	7.56	8.42	8.14
Consensus	7.79	8.82	8.43	7.79	8.82	8.43
Fragmented	7.47	8.36	8.03	7.47	8.36	8.03
G_4.5	8.05	10.73	9.36	7.84	9.26	8.64
G_4.5_C	8.12	10.98	9.48	7.92	9.55	8.78
I_4.5	7.80	9.01	8.52	7.21	8.32	7.73
I_4.5_C	7.87	9.27	8.64	7.49	8.33	7.85
G_8.5	7.71	8.44	8.21	7.56	8.34	7.88
G_8.5_T	7.58	8.35	8.05	7.17	8.33	7.69
I_8.5	7.75	8.57	8.28	6.76	8.33	7.52
I_8.5_T	7.59	8.42	8.13	6.32	8.32	7.31
G_8.5_F	7.51	8.35	7.96	7.02	8.33	7.62

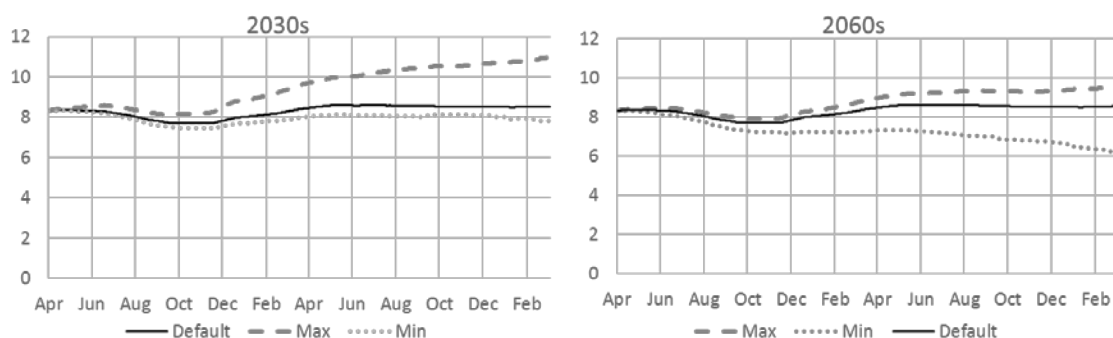


Figure 4.32 Minimum and maximum water levels (m) derived from all scenarios for 2030s and 2060s period

For all future scenarios, averages of the TP results for both lake models were higher than the average baseline TP concentrations (Table 4.6). For 2030s period, the highest TP was observed in GFDL-8.5 scenario while for 2060s, it was IPSL 4.5 scenario. TP concentrations increased in 2060s compared to 2030s and baseline period despite the decreased loads from the basement. For TN, scenario outputs for 2030s period exhibits slight changes and both lake models gave similar results, however for 2060s period, PCLake results indicated increased concentrations for future scenarios except GFDL-4.5 and GFDL-4.5 consensus scenario, while GLM results showed similar or less concentrations compared to baseline (Table 4.7).

Table 4.6 Baseline and future TP averages for both lake models and their mean. Default: No land use and no climate change scenario, G:GFDL, I:IPSL, C:Consensus, T:Techno, F:Fragmented, 4.5:RCP 4.5, 8.5:RCP 8.5

	TP ($\mu\text{g L}^{-1}$)					
	PCLake	GLM	Average	PCLake	GLM	Average
	2030			2060		
Default	23.82	32.44	28.13	23.82	32.44	28.13
Tec	24.81	33.11	28.96	24.81	33.11	28.96
Con	23.57	32.69	28.13	23.57	32.69	28.13
Frag	23.83	31.71	27.77	23.83	31.71	27.77
G_45	24.21	39.26	31.73	26.29	40.17	33.23
G_45_C	23.63	38.07	30.85	26.01	40.53	33.27

I_45	24.02	35.47	29.75	59.00	35.88	47.44
I_45_C	23.88	34.79	29.34	57.26	36.32	46.79
G_85	24.40	38.91	31.66	52.95	37.62	45.29
G_85_T	27.47	39.45	33.46	49.14	38.52	43.83
I_85	24.08	33.61	28.84	57.79	35.96	46.87
I_85_T	24.66	37.37	31.02	57.85	36.25	47.05
G_85_F	25.84	37.16	31.50	40.64	37.47	39.06
I_85_F	23.82	35.65	29.73	52.99	35.99	44.49

Table 4.7 Baseline and future TN (mg L⁻¹) averages for both lake models and their mean. Default: No land use and no climate change scenario, G:GFDL, I:IPSL, C:Consensus, T:Techno, F:Fragmented, 4.5:RCP 4.5, 8.5:RCP 8.5

	2030s			2060s		
	GLM	PCLake	Average	GLM	PCLake	Average
Default	0.17	0.22	0.20	0.17	0.22	0.20
Tec	0.18	0.28	0.23	0.18	0.28	0.23
Con	0.16	0.21	0.19	0.16	0.21	0.19
Frag	0.17	0.23	0.20	0.17	0.23	0.20
G_45	0.17	0.19	0.18	0.18	0.23	0.20
G_45_C	0.17	0.18	0.17	0.16	0.22	0.19
I_45	0.17	0.24	0.20	0.16	0.65	0.41
I_45_C	0.16	0.24	0.20	0.16	0.54	0.35
G_85	0.17	0.22	0.20	0.17	0.39	0.28
G_85_T	0.18	0.26	0.22	0.16	0.34	0.25
I_85	0.16	0.20	0.18	0.15	0.61	0.38
I_85_T	0.18	0.24	0.21	0.16	0.64	0.40
G_85_F	0.16	0.22	0.19	0.15	0.25	0.20
I_85_F	0.17	0.20	0.19	0.15	0.47	0.31

Ensemble run results for Chl-*a* and Cyanobacteria biomass was given in Fig 8.33. Although yearly averages for Chl-*a* (Table 4.8) show slight changes compared to baseline, ensemble mean Chl-*a* results given in Fig 7 indicated peak in growing season Chl-*a* values which were almost doubled in 2030s reach over to 17 $\mu\text{g L}^{-1}$ while for 2060s, it was over 20 $\mu\text{g L}^{-1}$. The lowest for Chl-*a* was

detected for GFDL-4.5 scenario with consensus land use scenario for both 2030s and 2060s while the highest chl-*a* was observed in GFDL-8.5 scenario for 2030s and GFDL-8.5 with fragmented land use scenario for 2060s. Cyanobacteria biomass increased in 2030s and 2060s in most scenarios. For 2030s, higher cyanobacteria biomass was observed in GFDL-8.5 fragmented scenario which is almost triple of the baseline scenario. For 2060s, highest cyanobacteria biomass was observed in IPSL-8.5 fragmented scenario which is almost 12 times of the baseline cyanobacteria biomass. Notwithstanding the increased cyanobacteria biovolume, due to slight changes in chlorophyll *a* concentrations, EQR values calculated from cyanobacteria, chl-*a* and total phytoplankton biovolume, are also between high-good status in the future as well.

Table 4.8. Baseline and future chl-a, cyanobacteria averages and EQR for both lake models and their mean. Default: No land use and no climate change scenario, G:GFDL, I:IPSL, C:Consensus, T:Techno, F:Fragmented, 4.5:RCP 4.5, 8.5:RCP 8.5. Chl-a is given as $\mu\text{g L}^{-1}\text{an}$

Scenarios	GLM		PCLake		Mean		EQR	GLM		PCLake		Mean Chla	Cyano	EQR
	2030	2030	2030	2030	2030	2030		2060	2060	2060	2060			
Default	3.15	3.67	3.41	0.03	Good	3.15	3.67	3.41	0.03	High				
Tec	3.45	3.14	3.29	0.03	High	3.45	3.14	3.29	0.03	High				
Con	2.72	3.06	2.89	0.02	High	2.72	3.06	2.89	0.02	High				
Frag	3.11	3.10	3.11	0.03	High	3.11	3.10	3.11	0.03	High				
G_45	3.59	2.00	2.79	0.01	High	2.80	3.24	3.02	0.02	High				
G_45_C	3.42	1.97	2.70	0.01	High	2.43	2.88	2.66	0.02	High				
I_45	3.31	3.05	3.18	0.02	Good	2.70	4.92	3.81	0.32	Good				
I_45_C	3.10	2.79	2.95	0.02	High	2.80	4.88	3.84	0.28	Good				
G_85	3.60	4.79	4.19	0.10	Good	2.99	6.03	4.51	0.26	Good				
G_85_T	3.88	3.84	3.86	0.12	High	2.99	7.28	5.14	0.38	High				
I_85	2.82	4.79	3.81	0.03	High	2.42	5.99	4.20	0.44	High				
I_85_T	3.03	3.75	3.39	0.04	High	2.58	5.76	4.17	0.46	High				
G_85_F	3.58	3.66	3.62	0.15	High	2.76	8.27	5.52	0.31	High				
I_85_F	2.69	3.75	3.22	0.05	High	2.65	3.84	3.25	0.50	High				

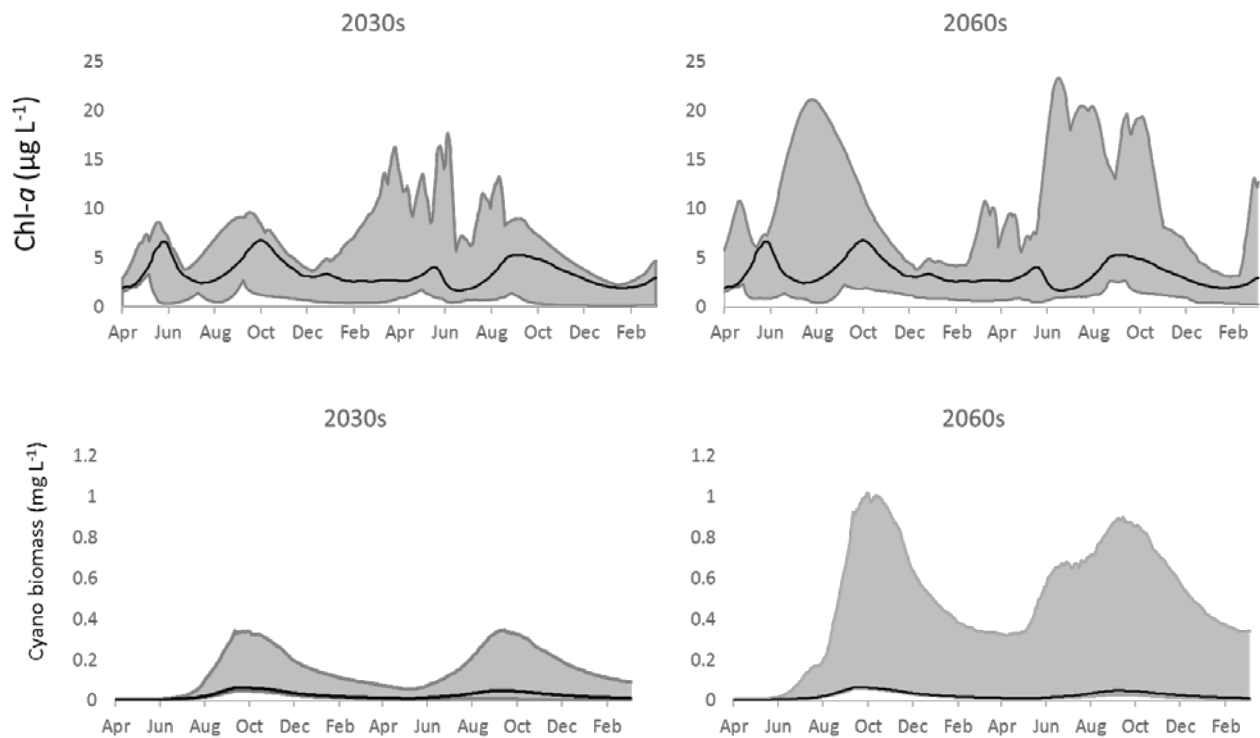


Figure 4.33 Ensemble run results derived from GLM-AED and PCLake for Chl-a and Cyanobacteria biomass

4.2.5 Discussion

In this study, to predict the future ecosystem services of Lake Beyşehir under the impacts of climate and land use changes, we used catchment model SWAT and linked the outputs of SWAT to 2 distinct lake models (GLM and PCLake). We used proxies of water level, TP, TN, chl-*a* and cyanobacteria biomass. We found decrease in hydraulic loads in most of the scenarios excluding GFDL-4.5 and IPSL-4.5 in which the total runoff increased due to higher precipitation. Overall, for 2060s period, magnitude of the decrease is found to be higher for both nitrate, mineral P and hydraulic loads compared to 2030s and baseline periods. Since nutrient load is associated with hydraulic loads, the most pronounced drop in runoff lead to most pronounced drop in nutrient loads as well.

Water level is highly regulated in Lake Beyşehir since it is the main water supply for irrigation in larger Konya Closed Basin. However, intense of water use for irrigation may also threaten and/or limit other ecosystem services of the lake such as drinking water supply and fisheries. Future water level decrease and outflow regulation could directly affect the agricultural production in the Konya Closed Basin where the dominant crop type is the water-thirsty sugarbeet. Climate scenarios showing increased evaporation and reduced precipitation may also increase the need for water for irrigation (Bunn and Arthington, 2002) and safe drinking water as well (Inglesias et al., 2007). In our study, most of the scenario results concur with studies from Mediterranean (Ertürk et al 2014, Molina-

Navarro et al. 2014) that decreased runoff leading a drop in water levels, however GFDL-4.5 results showed the opposite, especially in 2030s since it's predicted that there would be increase in precipitation which leads to increased runoff and water levels. The scenario results for 2060s period exhibit more dramatic change since for most of the scenarios, water level drop below the minimum management level which may also affect the downstream agriculture and lake ecosystem dynamics as well. Hence, the lake may lose its ecosystem services as irrigation water supply or managers may need to update management levels which may cause unpredicted ecological consequences.

Notwithstanding the decreased nutrient load, in-lake TP concentrations increased for both time periods, the magnitude of increase higher in 2060s period possibly due to increased evaporation driven lake volume loss and up-concentration of nutrients (Bucak et al 2012, Özen et al 2010). However lake model results differed in TN estimations as PCLake predicted increased TN concentrations in 2030s with increased temperature and more prominent water loss. The structure of both lake models differed since PCLake has a dynamic sediment-water interface module and sediment release of nutrients is dynamically modeled, however in sediment module of GLM, sediment release parameters are constant which may cause the different outcomes in TN predictions. It's well known that phytoplankton productivity increases with increasing temperatures, our results are also consistent with these findings since we found slight increase in chl-*a* concentrations despite prominent decrease in external nitrogen and phosphorus loads. Climate modeling studies from temperate lakes also showed that substantial reduction in external loads is needed up to 75% in TN and 40-50% in TP to prevent the phytoplankton blooms (Trolle 2008). Examples from New Zealand lakes also concur with these findings as 25-50% reduction is needed to sustain lakes current trophic status in the future (Trolle *et al* 2011). Although, change in chl-*a* concentrations are relatively minor, we found paramount increase in cyanobacteria biomass for both time periods and for 2060s, cyanobacteria biomass increases up to 17 fold in growing season. Similarly, Elliot *et al* 2012 also found minor changes at the chl-*a* level with marked changes in phytoplankton composition as a response to changes in flushing and temperature. Flushing has an important role in phytoplankton composition and increased flushing and mixing is known to favor green algae and diatoms over cyanobacteria regarding their higher growth rate and lower sedimentation losses (Visser *et al* 2015). Moreover, higher flushing also known to limit the bloom by flushing the nutrients out. However, during summer period with low flows and decreased external loads, carrying capacity of the system may decrease and competition increase among different phytoplankton groups (Jones et al 2007). Increased proportion of cyanobacteria in our results may have attributed to possible nitrogen limitation in water column with decreasing TN:TP ratios. There are studies reporting thresholds for

N limitation ratio (TN:TP) of 22 in which below the threshold, large N-fixing cyanobacteria favors (Gophen *et al.*, 1999, Smith *et al.*, 1995). In our scenario results, TN:TP ratio is always below this threshold which explains increased cyanobacteria dominance. As opposed to these results, in GFDL 4.5 climate scenario with consensus land use scenario, due to increased flushing rates, the lowest cyanobacteria is detected. For all scenarios, EQR calculated from the chl-*a*, phytoplankton and cyanobacteria biomass is also found to be in high-good boundary. However, these findings should be taken in caution since EQR calculation is based on the generalistic approach and species-level information is not used for calculation since lake models gave output on function group level. In most of the WFD phytoplankton indices (Philips *et al.* 2014), species level information is valuable and main determinant of the status of the lake. Hence, despite having EQR values of high-good boundary, increased temperatures may also favor toxic algae which may diminish the drinking value of the Lake Beyşehir in the future.

Calibration statistics of lake model variables mostly have small R^2 values which may indicate a lower fit between observed and simulated variables, however it should be noted that statistical good fit criteria should not be always the main criteria (Grimm, 1994), visual fit and following the general seasonal trend is vital as well (Elliot 2008) depends on the magnitude and range of the data (Elliott 2000). Moreover, low calibration fits can also be attributed to low concentrations since most of the time PO_4 and NH_4 concentrations were below detection limits ($5 \mu g L^{-1}$) In this kind of datasets, notwithstanding the low relative error measures, R^2 values could be low due to low variance and not having distinct seasonality (Trolle *et al.* 2011).

Our results mainly show that, Lake Beyşehir may have conserve its meso-oligotrophic status in the future which may result of current nutrient poor status with minor role of sediment as a source of nutrients and mainly decreased external loads. The current study and the earlier findings from warm lakes highlight the crucial role of nutrient control in maintaining the clear water state of lakes in future dry and warmer periods. However, notwithstanding the good-high EQR, most of the scenario results (especially 2060s) highlighted the continuous decrease of water level due to decreased runoff and increased evaporation which may have lead to extreme water level drops or complete dry-out of the lake in future. This may result loss of ecosystem services of lake as irrigation and drinking water supply and effects of decreasing water levels may affect whole ecosystem functioning. Our results also highlight the importance of land use management since consensus world scenario with efficient irrigation and lower water abstraction lead to higher water yield compared to other scenarios. Therefore, to overcome water scarcity problems in the future and wisely manage the limited water sources, adaptation measures such as promotion of drought-resistant crops and use of efficient irrigation technologies are crucial for Mediterranean basin.

Our results with different climate models and scenarios demonstrate the importance of model choice as well as scenario selection when anticipating future changes since there is high variation among climate models used in this study. Especially GFDL model with RCP 4.5 scenario predicted significant increase in precipitation which is contrary to the studies published from Mediterranean region. Hence results presented here should be interpreted with some caution considering the possible limitations as well as the uncertainties.

4.2.6 Conclusions

- Though there is high variation among scenarios, climate change may lead to decrease in water yield and further exacerbate the water stress of Lake Beyşehir especially for 2060s which may result in partly loss of its ecosystem service values as drinking and irrigation supply.
- The scenario results for 2060s period exhibit more dramatic change since for most of the scenarios, water level drop below the minimum management level.
- Since highest water yield is observed with consensus world scenario, we highlight the importance of promoting efficient irrigation technologies and water-stress tolerant crops to mitigate the impacts of climate change on water-limited Mediterranean.
- Although we observed significant temperature increases for future scenarios, slight increase in chl-*a* was found possibly due to decreased nutrient loading from catchment and nutrient limitation.
- Decreased flushing increased temperatures and N-limitation favoured cyanobacteria since paramount increase in cyanobacteria biomass was found for both 2030s and 2060s.

4.3 Pinios

4.3.1 Introduction

The objective of this document is to provide a detailed overview of the applied methods and the results derived by the MARS catchment-scale modeling (process-based and empirical), and scenario implementation in the Pinios case study. A description of the study area along with the implemented methodological approach is given followed by a presentation of the modelling findings. The results

are discussed with emphasis given on the effects of pressures on ecological and abiotic status and ecosystem services under the present climate and catchment management conditions, and different future scenarios.

In particular, the process-based (PB) SWAT (Soil and Water Assessment Tool) model was used for modeling hydrologic and water quality processes as well as crop productivity. The PB model has been fully calibrated based on historic monthly river flows and seasonal nutrient (NO₃-N and TP) observations. The model has estimated the water balance components of the hydrologic cycle and, by considering pressures in the basin, has linked them with ecosystem services, simulating appropriately water abstractions from groundwater and reservoirs and crop productivity. The linkage between pressures and biotic indicators was further achieved with the use of empirical modelling (EM) consisted of boosted regression trees (BRT) and general linear models (GLM). In our case, macroinvertebrate indicators (e.g ASPT, EPT) were selected as biotic response to abiotic indicators. The latter were mostly provided by the PB model.

4.3.2 Study area and MARS concept development

The Pinios basin covers almost entirely one of the Greek River Basin Districts (RBDs), the RBD of Thessaly in Central Greece (location shown in Figure 4.34). The basin has high relief in the western and northwestern part, and topography is smoother in the central, southern and southeastern part where the large agricultural valley is developed. The catchment (with an area of approximately 10,600 km²) is the most important agricultural producer in Greece, with fertile soils but a very dry climate during summer. Usually, the dry periods are accompanied with high temperatures, which lead to higher evapotranspiration rates and dry soils. These conditions inversely affect both the natural vegetation and the agriculture of the region resulting in irrigation cutbacks, overexploitation of groundwater and significant losses of crop yields (Vasiliades et al., 2011).

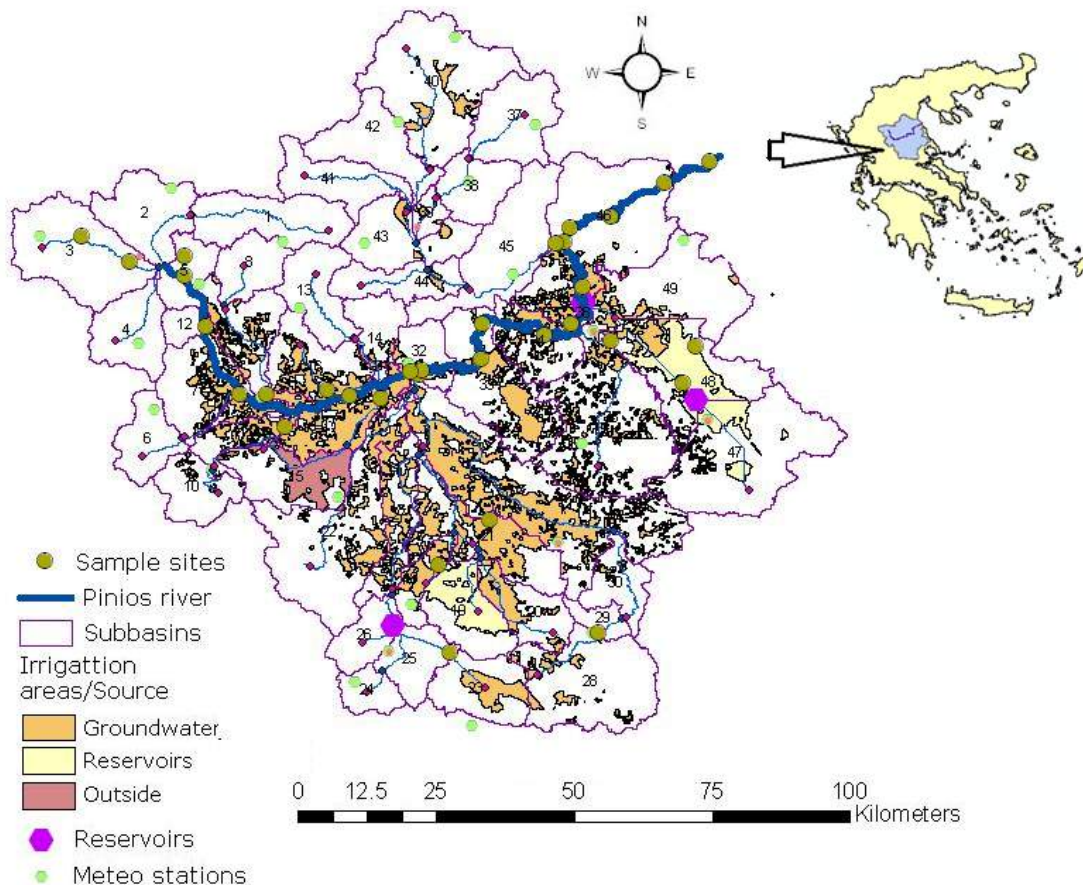


Figure 4.34 The Pinios river basin in Central Greece. Key data layers are shown including, among others, sub-basins as delineated in SWAT, irrigated areas and source of irrigation water as well as sample sites along the main river.

The irrigated crops are grown in the basin for feed (corn, alfalfa) and industrial (cotton) production. These crops occupy an area of almost 200,000 ha (20% of the catchment) and are irrigated in each dry period (May to September) with water extracted mostly from groundwater resources (Figure 4.34). The total water amount extracted annually has been estimated around $\sim 800 \text{ Mm}^3$ (Makropoulos and Mimikou, 2012), but it is neither adequate to cover entirely crop needs all across the basin, nor it is everywhere totally replaced from natural resources (precipitation, aquifers recharge). Moreover, there is still a great potential in the basin to increase in-field water use efficiency by upgrading the current inefficient irrigation methods and equipment in order to reduce water losses and thus exploit to a higher degree the extracted annual water amounts. Overall, high water needs and dry climate in combination with far from optimum water management have resulted in irrigation cutbacks and overexploitation of surface and groundwater resources with significant impacts on the Pinios basin's natural water cycle and water availability (Panagopoulos et al., 2013).

4.3.2.1.1 Current River basin management plan - Main drivers and pressures

There are various sources of information for Pinios basin such as previous projects (e.g. www.i-adapt.gr), published and unpublished studies as well as the RBMP of the Thessaly RBD, within which, Pinios basin is entirely located. The current RBMP reports the main characteristics of Pinios and has identified major pressures.

Water overexploitation in Pinios basin may lead to low river flows (negligible during summer), the drying up of small lakes/reservoirs and low groundwater levels, which make water more expensive to obtain (deep pumping) and enhance saline water intrusion in coastal areas in the eastern part. Therefore, the most important stressor in the Pinios basin is water abstraction for irrigation. Especially groundwater abstraction is the main issue in the area and there are large parts of the aquifers with very low groundwater tables. Another important environmental issue in the area is surface and groundwater nitrate pollution caused by intensive and sometimes excessive crop fertilization. Actually, due to this stressor Pinios has become a nitrate vulnerable zone. Climate change is also a possible future stressor due to the predicted lower precipitation and higher temperatures, especially within the dry period, when crops are growing.

Water movement in the study area is a complicated process due to the large number of water exploitation (and extraction) sites such as the existing dams and reservoirs, and the pumping wells, which alter the natural drainage of the basin. The abstracted water for irrigation from the reservoirs causes irrigation runoff losses to occur from land to the stream network contributing to downstream flow. On the other hand, river flow all across the basin is reduced due to groundwater abstractions for irrigation that result in low groundwater height decreasing groundwater contribution to streamflow, while direct water abstractions from rivers and streams further decrease river flows, in some cases in unacceptably low levels.

The main ecosystem services which are identified and highlighted in the RBM Plan are mostly related to water use services and specifically to provision of drinking and mostly of irrigation water. Other key service that is identified within the basin of Pinios is the agricultural land use and production. Secondary services are the industrial water use, aquacultures, recreational activity, mining and livestock activities.

The RBMP tries to classify all small rivers/streams and lakes into categories, therefore, there is not a single status characterizing the entire basin. Moreover, the classification system used is subjective and cannot represent a definite situation. However, from the experience gained so far with the study

area, it is clear that the quantitative status is bad in the southern and central part of the basin and the qualitative status is moderate in the greatest part of the basin's area.

The water abstraction needs for irrigation is the main cause of bad quantitative status of water bodies within Pinios, while the fertilization need is the main cause of nitrate pollution, which downgrades the quantitative status. There are several suggested measures, almost all related to agriculture, other already in practice, other just under negotiation or discussion. These are usually called 'Agricultural Best Management Practices - BMPs'. Some of these measures are: Fertilization reduction, placing fertilizers close to the crops, not fertilizing areas located close to ditches and streams, fencing grazing areas close to water bodies, avoid fertilization under rainy and/or windy conditions, reduce soil erosion, as well as, stop overexploitation of groundwater abstractions in sensitive areas, save water through the adoption of deficit irrigation techniques and the establishment of drip irrigation systems, build and operate new small reservoirs, transfer water from a neighboring catchment to Pinios (river diversion) or reduce the irrigated areas through changes in cropping systems.

Finally, it should be mentioned that the main stakeholders connected to the basin are: The General Water Agency of the Hellenic Ministry of Environment and Climate Change, the Region of Thessaly, many local water management organizations, agricultural institutes within the area (institute for cotton, soil institute etc.) and farmers. Their responsibilities and interests are mainly the efficient water exploitation and the guaranteed crop production.

4.3.2.1.2 Data availability in the Basin

Several data types exist for Pinios and have been collected from different sources. The most important information is the historic data on water quality parameters (observations) in water bodies, records of crop productivity data and water used. Regarding the latter however, it seems impossible for anyone to measure or estimate with accuracy the actual water volumes spent in agriculture given the existing illegal abstractions as well as other local exploitation rules, which are not under control. Therefore, for water abstractions, we have used our modeling estimations (Makropoulos and Mimikou, 2012; Panagopoulos et al., 2013; 2014). Precipitation, temperature and other meteorological variables are measured through point stations all across the Pinios basin from the Ministry of Environment and Climate Change & the Public Power Corporation. Precipitation is available to us from 1975. Annual precipitation in Pinios is between 390 mm and 1250 mm with an average annual depth of 760 mm and significant seasonal and monthly deviation as shown in Figure 4.35.

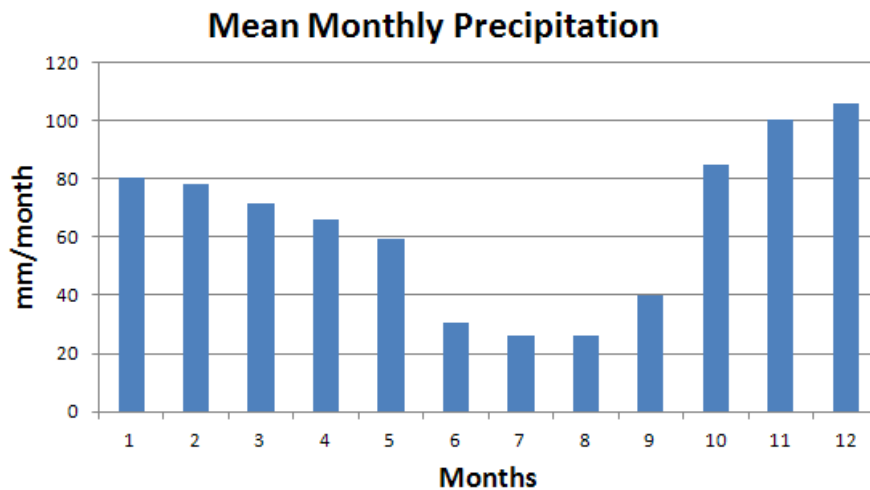


Figure 4.35 Monthly average precipitation values over a 36 year period (1975-2010).

The river station with reliable and adequate hydrologic time-series data along Pinios is named ‘Amigdalia’ from the name of the homonymous village nearby, and is located upstream the total outlet of the basin, draining a total area of 6,500 km² (subbasin 17 in Figure 4.34). Another station named ‘Ali-Efenti’ is further upstream in Pinios (subbasin 17 in Figure 4.34) and drains 2,800 km². Systematic measurements of nutrients were also used from two other stations with their locations almost coinciding with those of the hydrologic ones, while numerous other sites across the basin but mainly along Pinios have provided water quality and biotic data (see Figure 4.34). These mainly concern Macroinvertebrates (community data e.g taxa richness, abundance etc) fish, possibly some basic phytoplankton related data only for lakes and reservoirs within the basin.

Spatial data needed for modeling are: a) the Land use map: 100 m, b) the Soil map: 1 km and c) the DEM: 90 m. The DEM has been extracted from the NTUA’s Meteorological and Hydrological Database of Greece, the Land use layer from the Corine Land Cover 2000 layer and Farm Structure Survey (FSS) data and the soil layer from the Hydrolithological map of Greece after some editing based on more detailed information provided from soil layers of the Institute of Soil Mapping and Classification in Thessaly.

In summary both the RBMP and several previous projects and studies indicate that:

- a) The main stressors in Pinios are *irrigation water abstraction* and *nutrient deposition from fertilizers* and
- b) The most important Ecosystem Services (ES) are the *available water for irrigation* under the existing technical infrastructure and demands across the basin, the *Land uses* and *Crop yields*.

c) The question to be addressed by a combined PB and EM (in our case in MARS) is how the combined stress (first point above) both at present and under future conditions (MARS scenarios (storylines)) impacts on Pinios basin's water quantity and quality, its ecological status and the Ecosystem Services delivered.

A synthetic view on the relationships between drivers, pressures and indicators of state for the Pinios case study is depicted in Figure 4.36.

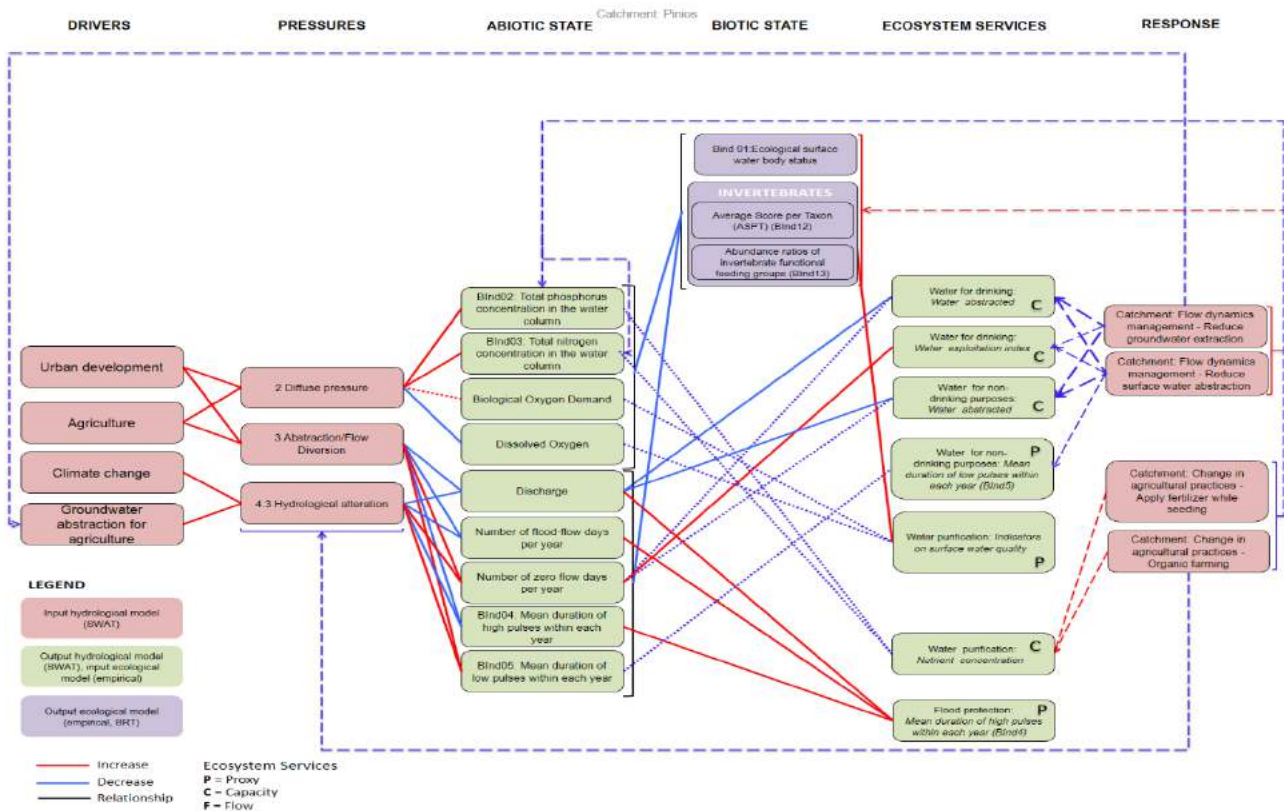


Figure 4.36 Conceptual model for Pinios catchment

4.3.3 Methods

4.3.3.1.1 Process based modelling

For the Pinios basin, the SWAT (Soil and Water Assessment Tool) model is used for simulating hydrologic and water quality processes as well as crop productivity. The Soil and Water Assessment Tool (SWAT) is a river basin model developed by the United States Department of Agriculture (USDA) for use in complex agricultural landscapes and is freely available via the website: <http://swatmodel.tamu.edu/>. SWAT includes mathematical descriptions of physical, biogeochemical and hydrochemical processes, and combines elements of a physical and conceptual semi-empirical nature (Neitsch et al., 2009). Today, it is considered a robust, interdisciplinary tool, extensively applied in Europe, USA and the rest of the world.

A catchment in the GIS-based SWAT environment is divided into subbasins and subsequently into Hydrologic Response Units (HRUs), which represent the different combinations of land use and soil types in each subbasin. The processes associated with water and sediment movement, crop growth and nutrient cycling are modeled at the HRU scale. Hydrology is based on the water balance equation in the soil profile, where the processes simulated include surface runoff/infiltration, evapotranspiration, lateral flow, percolation, and return flow. The model considers a shallow unconfined aquifer, which contributes to the return flow and a deep confined aquifer acting as a source or sink.

Agricultural management practices are defined in SWAT by specific management operations (Arabi et al., 2008). Planting, harvesting, tillage passes, irrigation, grazing and nutrient applications can be simulated for each cropping or livestock system with specific dates. Irrigation and fertilization can be additionally applied automatically according to crop nutrient stress. Management operations are more explicitly defined in each HRU by specific management parameters (e.g. tillage depth, N and P contents and amount of fertilizer and manure types, irrigation dates and amounts etc.). Thus, when alternative management practices are considered in a SWAT study, changes in the appropriate parameters are done. The crop growth component of SWAT is capable of simulating a wide range of crop rotation, grassland/pasture systems, and trees. In the SWAT model, potential crop growth and yield are usually not achieved as they are inhibited by temperature, water, nitrogen and phosphorus stress factors. There are two options for application of irrigation water and timing of fertilization: user specified and automatic. In the automatic option, an irrigation event is triggered based on a water-stress threshold, while fertilizer timing is based on a nitrogen stress factor.

The present study builds its development on the existing well-constructed Pinios basin model dividing the basin into 49 subbasins (Figure 4.34) and 361 Hydrologic Response Units (HRUs), which represent land pieces with unique combinations of land use, management, slope and soil characteristics. This has been done in the project i-adapt: <http://i-adapt.gr/>, a pilot project on development of prevention activities to halt desertification in Europe and has been reported in Makropoulos and Mimikou (2012) and published in Panagopoulos et al. (2013; 2014).

The model has been successfully calibrated and validated based on monthly river flows for a long period with available data (Figure 4.37). Several goodness of fit criteria were used for evaluating the model's performance including NS efficiency, PBIAS, RSR and R^2 (Moriassi et al., 2007), which are summarized in Table 4.9.

Table 4.9. Goodness of fit criteria in Ali Efenti and Amigdalia flow gauging stations (subbasins 17 and 33 in Figure 6.1).

River site	Variable (available data)	Statistics			
		NSE	RSR	PBIAS (%)	R^2
Ali Efenti	Calibration (1975-1984)	0.783	0.46	0.77	0.80
	Validation (1985-1994)	0.663	0.58	-7.14	0.67
Amigdalia	Calibration (1975-1984)	0.851	0.38	-0.12	0.89
	Validation (1985-1994)	0.705	0.54	-4.17	0.72

*NSE: Nash Sutcliffe Efficiency, RSR: Root mean square error to the Standard deviation of measured data Ratio, PBIAS: Percent BIAS, R^2 : Coefficient of Determination.

Crop yield predictions have also been compared with measured ones on a mean annual basis to ensure that SWAT produces reasonable estimates. As far as water quality calibration is concerned, simulated river loads have been compared with $\text{NO}_3\text{-N}$ (Nitrates-Nitrogen) and TP (Total Phosphorus) observations on a seasonal basis and the correlation was evaluated for two river sites within the basin based on R^2 values (Figure 4.38).

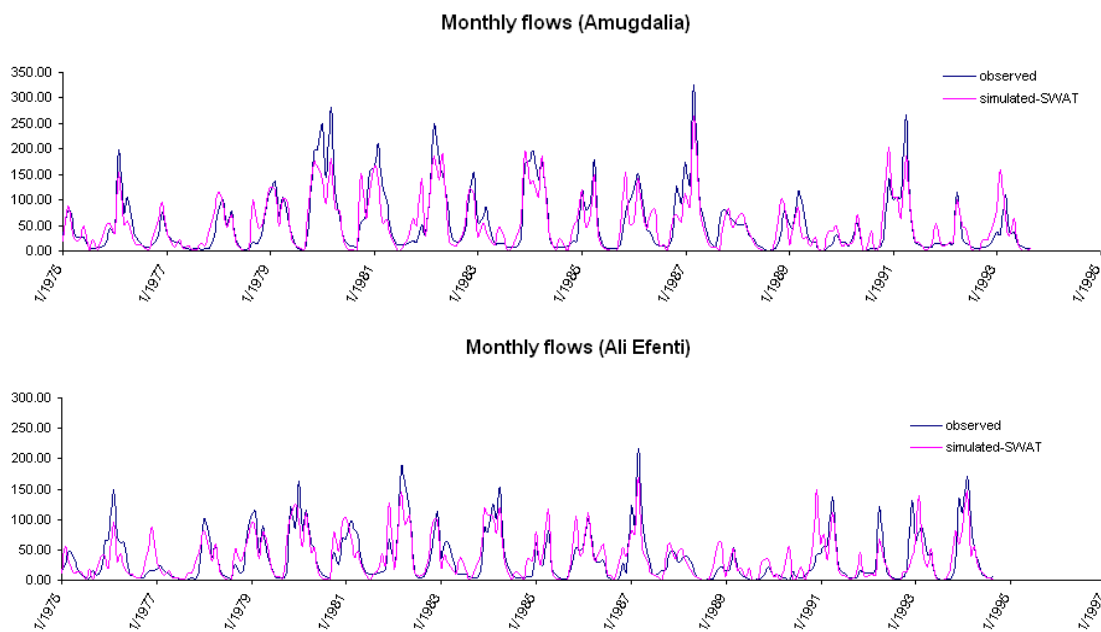


Figure 4.37 Observed and simulated monthly flows in two gauging stations of Pinios river.

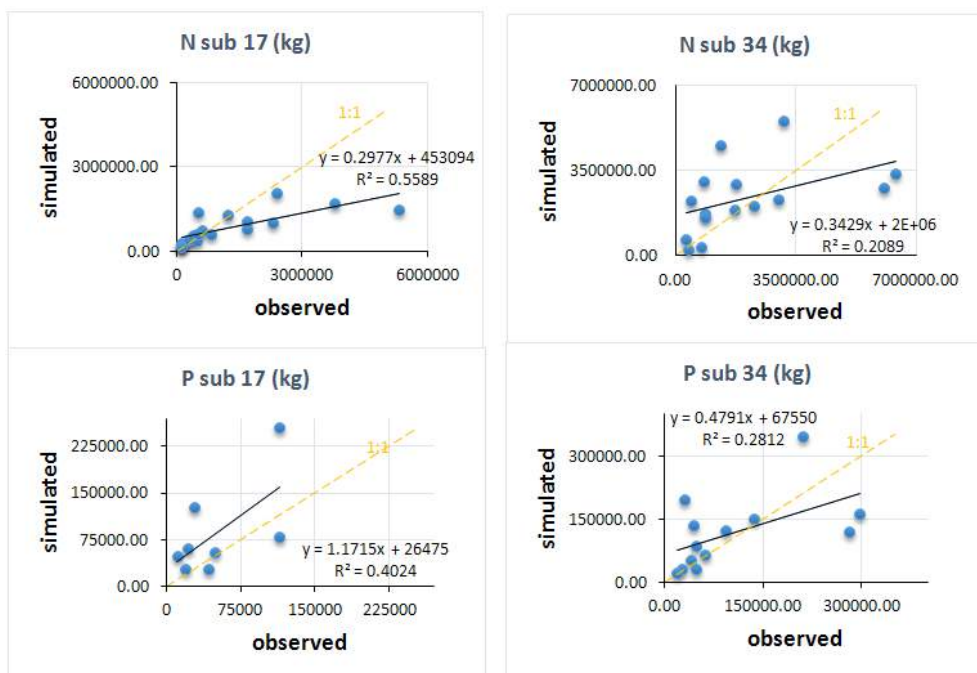


Figure 4.38 Simulated vs observed values for water concentrations of nitrate and total phosphorus.

4.3.3.1.2 Empirical modelling and linkage between pressures and indicators

For the empirical modelling and the linkage between biotic indicators and abiotic pressures we used a large dataset of macroinvertebrate community data comprised by data obtained from two different sources. The first source is based on previously published data collected from 80 sites along the stretch of river Pinios during autumn of 2002 (Chatzinikolaou, 2007; Chatzinikolaou et al., 2010). The second source is the Greek National Monitoring program which provided us with data collected from 30 sites in summer of 2012 and 32 sites in spring of 2013. The merged dataset contains semi-quantitative community information at family level from a total of 142 samples collected from 101 different sites across the catchment of river Pinios. Eleven sites were common among the three different sampling periods and 30 were common between 2012 and 2013. Based on the empirical data collected during the aforementioned samplings we calculated candidate metrics that we subsequently used as response variables to nutrient and hydrological parameters predicted by SWAT. Specifically, we calculated the BMWP (Biological Monitoring Working Party) and the ASPT (Average Score Per Taxon) score according to the BMWP system (Armitage et al., 1983). Most macroinvertebrate families have been assigned a score ranging from 1 to 10 depending to their perceived tolerance to organic pollution. The BMWP is the sum of the scores of the families present in the sample while ASPT is the average score. As such the BMWP score increases with sampling effort and is more susceptible to sampling efficiency whereas ASPT is independent of the sampling

effort. Depending on the data availability we calculated additional metrics such as the number of Ephemeroptera, Plecoptera and Trichoptera families (EPT), the relative abundance of Gastropoda, Oligochaeta and Diptera families subtracted from 1 (1-GOLD), the Log transformed abundance of selected families of Ephemeroptera, Plecoptera, Trichoptera and Diptera ($\text{Log}_{10}(\text{SelEPTD} + 1)$), the total number of taxa, the Shannon diversity index and the species evenness index. Summary statistics for the candidate metrics and the environmental parameters are presented in Table 4.10. This dataset also contains information for environmental data collected from the same sampling sites. These data include nutrient concentration in water (phosphate, nitrate, nitrite and ammonium) as well as BOD, surface dissolved oxygen (DO), saturation %, pH, conductivity, total suspended solids (TSS) and water discharge. These variables were used as stressor variables (predictors) when building the empirical models. In order to control for the effect of natural environmental gradients on the response of the biological metrics we used the altitude of the sampling sites as an additional “environmental” predictor.

Table 4.10. Descriptive statistics for the data used in our analysis

Variable	Mean	Std. error	Median	Min	Max	N
BMWP score	50.51	2.90	43.00	3	194	142
ASPT	4.65	0.10	4.53	1	7.44	142
EPT	3.84	0.27	3.00	0	11	142
1-GOLD	0.74	0.03	0.86	0.01	1	80
$\text{Log}_{10}(\text{SelEPTD}+1)$	0.39	0.07	0.00	0	2.03	80
Number of Taxa	10.39	0.47	9.00	1	35	142
Shannon diversity index	1.30	0.07	1.46	0	2.4	80
Evenness index	0.61	0.03	0.67	0	0.97	80
PO4-P (mg/L)	0.093	0.020	0.042	0	2412	142
NH4-N ($\mu\text{g/L}$)	69.98	9.99	29.71	0	793	120
NO2-N ($\mu\text{g/L}$)	36.29	4.46	19.06	0	350	128
NO3-N (mg/L)	1.728	0.195	1.158	0	17.082	140
DIN (mg/L)	1.76	0.194	1.157	0	17.167	140
BOD (mg/L)	2.427	0.207	1.85	0.11	6.79	80
DO (mg/L)	8.41	0.18	8.63	1.64	14.39	142
Saturation (%)	89.89	2.06	91.3	17.7	191	142
Water Temperature	18.68	0.38	18.5	8.3	34.2	142
pH	7.9	0.04	7.94	6.27	9.47	142
Conductivity (mS/cm)	0.53	0.03	0.48	0.22	5.01	142
TSS (mg/L)	268.93	18.16	239.67	110.00	2656.00	142
Discharge (m^3/s)	3.28	0.28	2.42	0.01	8.68	102

Based on data screening results we selected as best biological indicators the ASPT and EPT metrics. For the biotic/abiotic linkage, boosted regression trees (BRT) and general linear models (GLM) were applied in order to build models that best describe the response of the biotic indicators to abiotic descriptors. All the stressor variables were log transformed prior to the analysis and only the complete cases were considered. Collinearity between the variables was assessed with the use of the Variance Inflation Factor. All parameters exceeding a VIF value greater than 8 were excluded from the analysis

following a stepwise procedure. BRT modelling was performed with packages gbm and dismo (Elith et al., 2008; Hijmans et al., 2013) for R version 3.2.3 (R Core Team, 2015). The development of BRT was based on the guidelines from Elith et al. (2008). Tree complexity was set to 2 and the learning rate was adjusted to ensure that, approximately, from 1000 to 1500 trees were combined into the final model. For the next step, GLMs were developed using as predictors the most high ranking stressor variables. GLMs were run using the Gaussian family. In order to assess the goodness-of-fit for each model the Pseudo-R was computed. All the analyses were performed with the R version 3.2.3 (R Core Team, 2015).

Tables 4.11 and 4.12 provide information in regard to the final model characteristics. In regard to the BRTs, the best model for ASPT uses as predictors the dissolved oxygen, nitrate and phosphate concentration, discharge and altitude accounting for natural variability. For the EPT the model that was developed is based on dissolved oxygen, water temperature, phosphate and altitude (Table 6.3).

Table 4.11. Boosted Regression Tree model details.

ASPT		EPT	
<i>Predictor</i>	<i>Relative influence</i>	<i>Predictor</i>	<i>Relative influence</i>
Altitude	36.42	Altitude	39.92
Dissolved oxygen	18.79	Dissolved oxygen	22.53
Nitrate	11.80	Temp.	11.56
Phosphate	8.78	Phosphate	7.08
Discharge	8.42		
Mean total deviance	1.567	Mean total deviance	9.581
Mean residual deviance	0.708	Mean residual deviance	2.993
R ²	0.55	R ²	0.69
Training data correlation	0.766	Training data correlation	0.841
CV correlation	0.544	CV correlation	0.722

Table 4.12. General linear models details

ASPT			EPT		
<i>Predictor</i>	<i>Coefficient</i>	<i>Sig.</i>	<i>Predictor</i>	<i>Coefficient</i>	<i>Sig.</i>
<i>Dissolved oxygen</i>	3.62	p=0.012	<i>Altitude</i>	0.009	p<0.001
<i>Altitude</i>	0.002	p=0.015	<i>Dissolved oxygen</i>	15.663	p<0.001

<i>Temperature</i>	2.79	p=0.092	<i>Temperature</i>	7.834	p=0.019
<i>Nitrate</i>	-0.16	p=0.149	<i>Nitrate</i>	0.41	p=0.056
<i>Phosphate</i>	-0.27	p=0.154			
intercept	-1.85	p=0.49	<i>intercept</i>	-24.24	p<0.001
Null deviance	145.713		Null deviance	891.03	
Residual	89,54		Residual	411.69	
R ²	0.39		R ²	0.54	

Figures 4.39 and 4.40 show the partial responses of the ASPT and EPT metrics to the stressor predictors. The best GLM for ASPT uses as predictors nitrate and phosphate concentration, dissolved oxygen concentration and water temperature and altitude accounting for natural variability. The same variables, with the exception of phosphate, are used as predictors for the EPT. Figures 4.41 and 4.43 show the partial responses of ASPT and EPT to the predictors included in the analysis. ASPT presents a clear positive response to increased dissolved oxygen content and altitude gradient while it relates negatively with nitrate and phosphate concentration. These relationships clearly reflect the ability of ASPT to respond to organic pollution (e.g anoxic conditions). EPT relates positively with altitude, nitrate, water temperature and dissolved oxygen (Figure 4.43). The positive response to dissolved oxygen and altitude is related with the occurrence of these macroinvertebrate families in good water quality conditions, whereas the positive relation with temperature and nitrate possibly indicates a seasonal effect on the total species richness that affects the EPT number as well.

In regard to the interactions Figure 4.42 shows that dissolved oxygen and nitrate have an antagonistic effect where in low nitrate concentrations the positive effect of dissolved oxygen to ASPT is stronger in relation to higher nitrate concentrations. On the other hand, altitude and dissolved oxygen seem to have a synergistic effect where in high altitude environments and under higher oxygen conditions, ASPT shows higher positive response. Figure 4.44 indicates that water temperature and dissolved oxygen have a rather synergistic effect on EPT where in higher water temperatures the effect of dissolved oxygen is stronger.

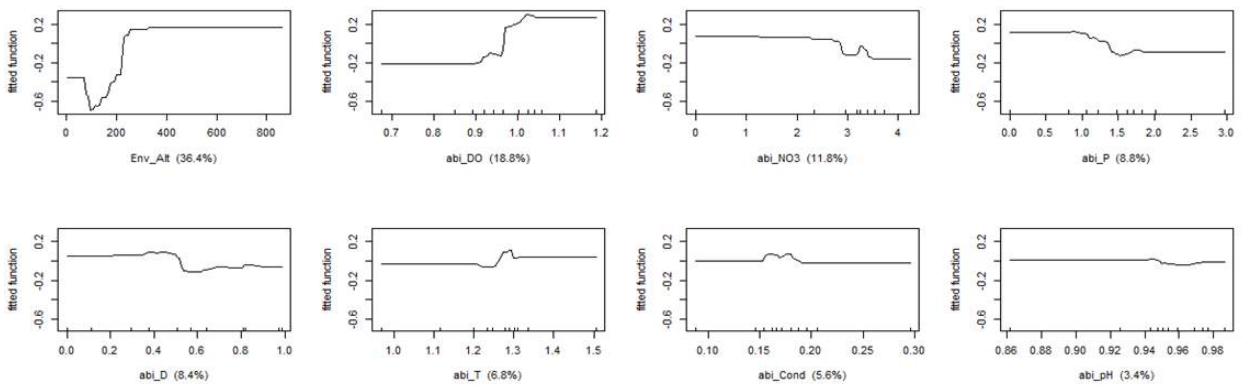


Figure 4.39 Partial plots showing the response of the ASPT metric to each predictor.

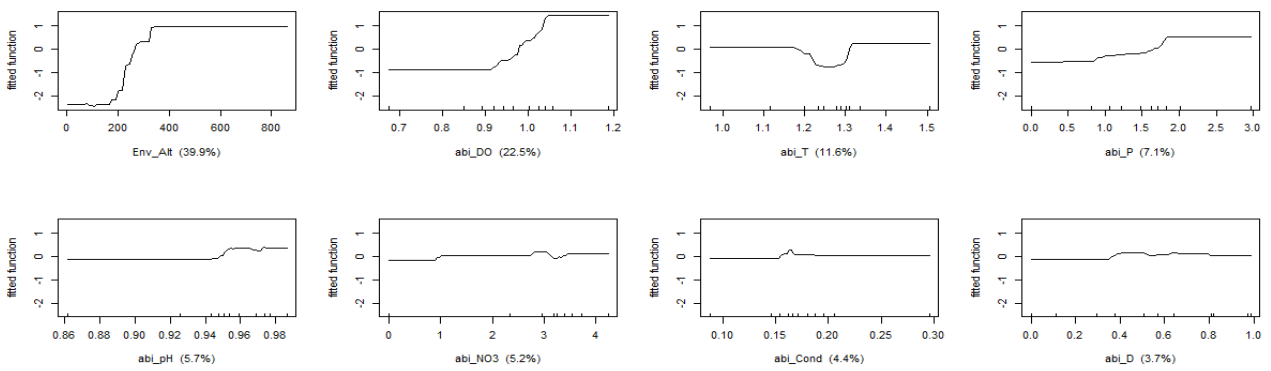


Figure 4.40 Partial plots showing the response of the EPT metric to each predictor.

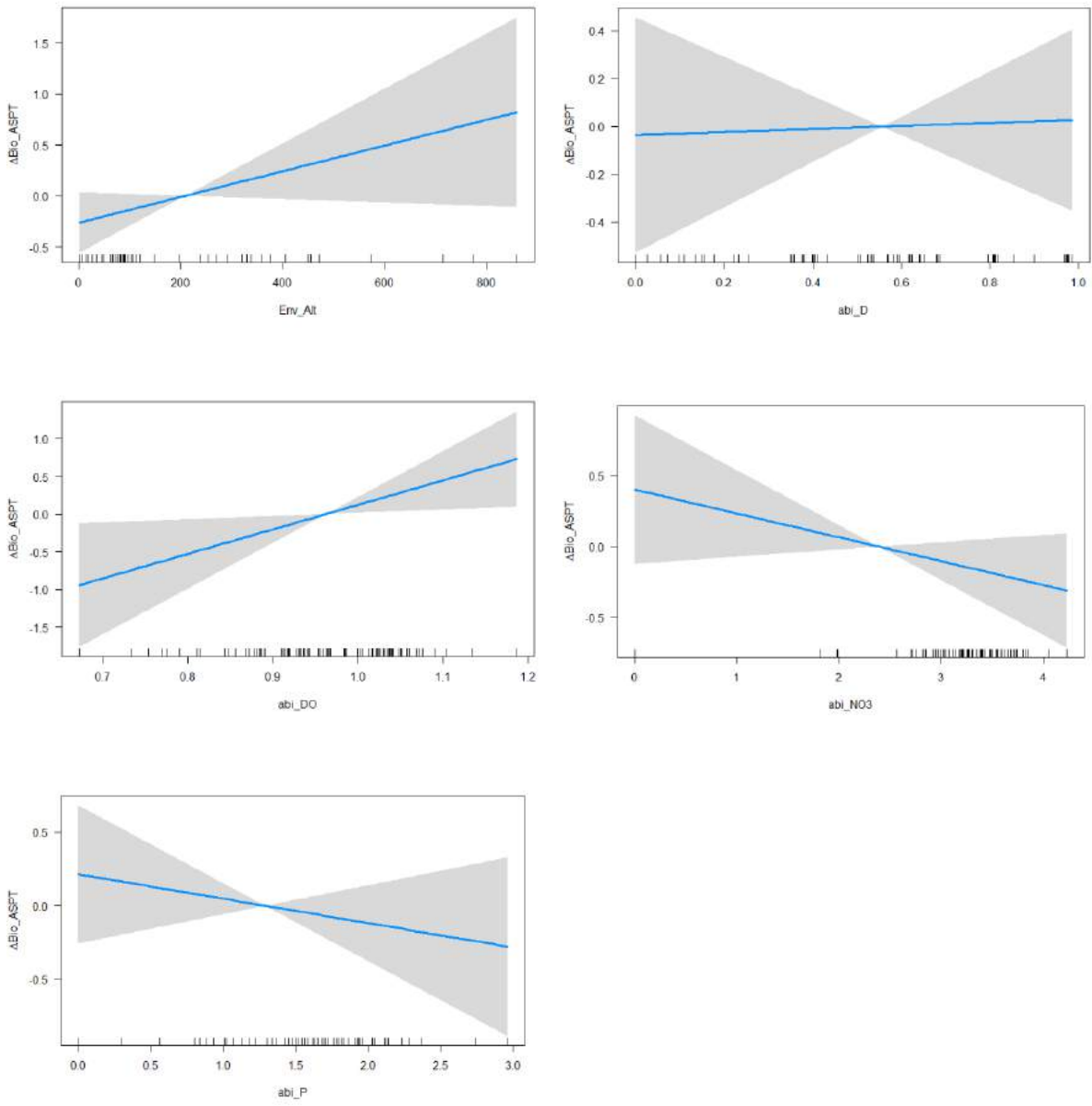


Figure 4.41 Partial responses of the ASPT to predictor variables included in the GLM

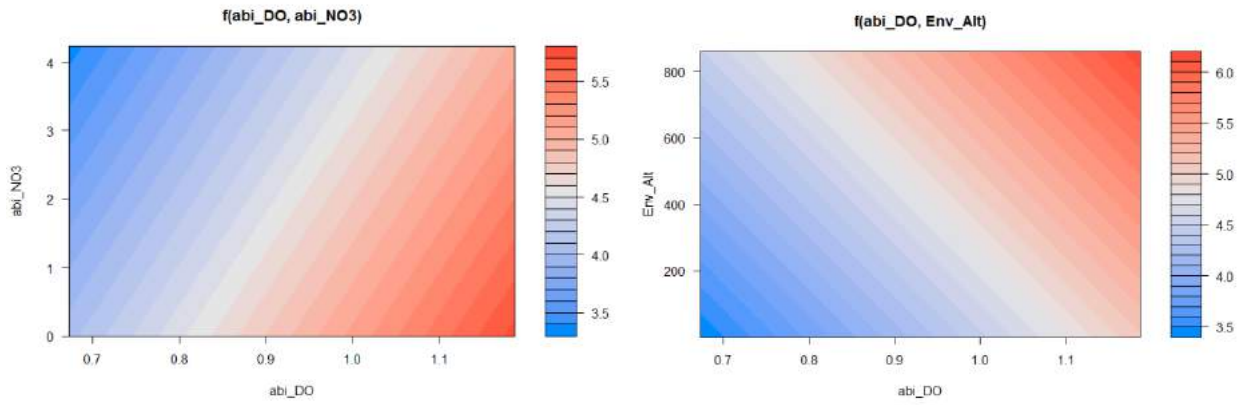


Figure 4.42 Combined response of ASPT to nitrate and dissolved oxygen (left graph) and to altitude and dissolved oxygen (right graph)

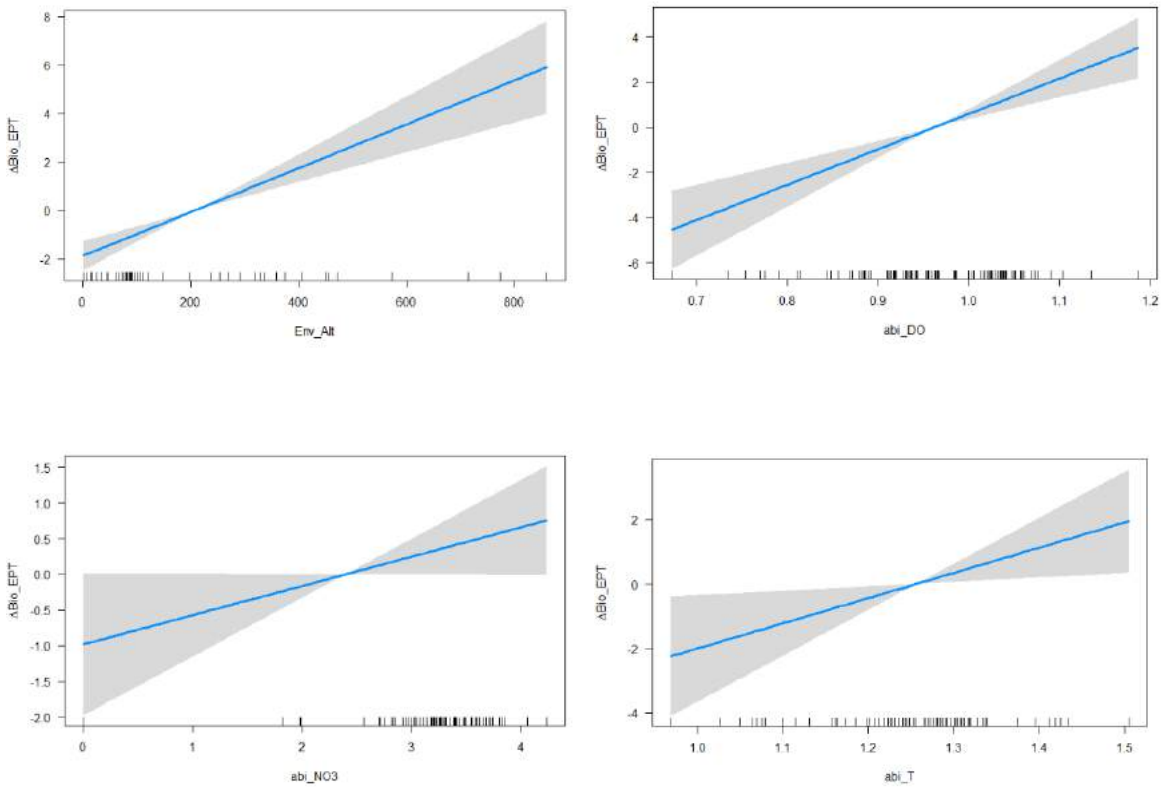


Figure 4.43 Partial response of EPT to predictors included in the GLM.

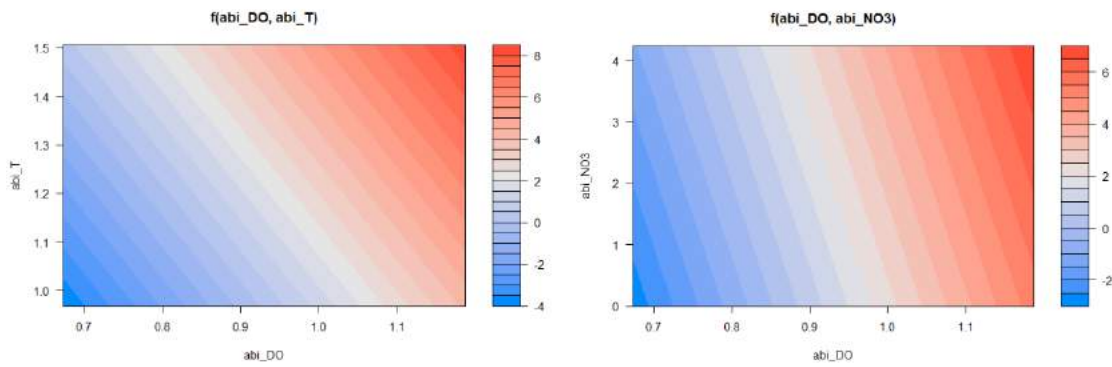


Figure 4.44 Combined response of EPT to dissolved oxygen and water temperature (left graph) and to dissolved oxygen and nitrate (right graph)

4.3.3.1.3 Ecosystems services description and linkage with pressures

The main ecosystem services in the Pinios basin are the provision of irrigation water and crop products. Secondary services are the industrial water use, aquacultures, recreational activity, mining and livestock activities but are not addressed in the study. Ecosystem services are quantified through the PB modeling, which, through a non-linear mathematical framework, considers the effect of pressures on them, while EM uses outputs of the PB model to derive biotic metrics.

4.3.4 Scenarios development

In MARS, two climate models (GFDL-ESM2M and IPSL-CMA-LR) are combined with three storylines ('worlds') (short description below) giving rise to multiple model runs. Each MARS storyline is associated to one specific climate scenario (RCP 4.5 or 8.5). The 'Techno world' is associated with climate scenario 8.5, the 'Consensus world' with 4.5 and the 'Fragmented world' with 8.5.

Storyline 1: ‘Techno world’ or ‘Economy rules’

This is a world driven by economy. A fast economic development increases the use of energy. Policies are not focused on the environment but on enhancing trade and benefitting the economic growth. Climate is changing rapidly. This world is based on a combination of SSP5 and climate scenario 8.5.

Storyline 2: ‘Consensus world’

Economy and population grow at the same pace as now. Policies to protect the environment are continued after 2020, and the preservation of nature is regulated by the government. This world is based on a combination of SSP2 and climate scenario 4.5.

Storyline 3: ‘Fragmented world’

This world is characterized by an unequal development of the different countries. International trade agreements are stopped and each country needs to fight for its own survival. Environment is just protected by rich countries at a local scale, but in general no attention is paid to the preservation of nature. This world is based on a combination of SSP3 and climate scenario 8.5.

There are three time periods to address, one centered around a historical 10-y period (e.g. 1995-2005), one centered around 2030 (2025-2035) and one around 2060 (2055-2065). The year 2030 is a WFD target-year, while 2060 a far future year of interest. As baseline period we selected the years 1995-2005 to maintain an equal (30-y) time distance between the three runs. Table 4.13 summarizes all runs.

For scenarios development we selected and then quantified storyline elements that are considered important and relevant to our case study and can be simulated within the modelling framework of SWAT. In this task, we took advantage of the past and present cooperation and communication with several stakeholders. These are: The General Water Agency of the Hellenic Ministry of Environment and Climate Change, the Region of Thessaly, many local water management organizations, agricultural institutes within the area (institute for cotton, soil institute etc..) and farmers. Their responsibilities and interests are mainly the efficient water exploitation and the guaranteed crop production.

Table 4.13. Detailed presentation of scenario model runs performed for Pinios case study.

Scenarios	Climate data	Climate model	Storylines	Period
Baseline	Recorded		Current	1995-2005
Techno World	RCP8.5	GFDL	Tech	2025-2035
				2055-2065
		IPSL		2025-2035
				2055-2065
Consensus World	RCP4.5	GFDL	Consensus	2025-2035
				2055-2065
		IPSL		2025-2035
				2055-2065
Fragmented	RCP8.5	GFDL	Fragmented	2025-2035
				2055-2065
		IPSL		2025-2035
				2055-2065

In order to assess the potential impacts of future scenarios on key hydrological components in our study area we applied three future scenarios that represent combinations of Representative Concentration Pathways (RCPs) and Shared Socioeconomic pathways (SSPs). The RCPs refer to radiative forcing pathways that describe an emission trajectory and concentration by the year 2100 (O'Neill et al., 2014). There are four radiative forcing scenarios and are defined depending on the total radiative forcing in year 2100 relative to 1750 (Table 4.14). Specifically, RCP 2.6 is a mitigation scenario the emissions of which peak and decline before 2100. RCPs 4.5 and 6.0 are stabilization scenarios and RCP 8.5 is a rising scenario with very high greenhouse gas emissions. These four RCPs are based on previous available in the literature scenarios, and they were built on specific socioeconomic assumptions. In our case, the two future scenarios are based on RCPs 4.5 and 8.5 respectively.

Table 4.14. Representative concentration pathways in the year 2100 (source van Vuuren et al., 2011).

	Radiative forcing	CO2 equivalent concentration	Rate of change of radiative forcing
RCP 8.5	8.5 W/m ²	1350ppm	Rising
RCP 6.0	6.0 W/m ²	850ppm	Stabilizing
RCP 4.5	4.5 W/m ²	650ppm	Stabilizing
RCP 2.6	2.6 W/m ²	450ppm	Declining

Regarding the SSPs, these were developed by O'Neill et al (2014) and are defined as 'reference pathways' describing plausible alternative trends in the evolution of society and ecosystems over a century timescale, in the absence of climate change or climate policies". SSPs are based on combinations of climate model projections and socio-economic conditions. Five SSPs (Kriegler et al., 2012; O' Neill et al., 2014) have been defined that provide a starting point for different narratives depending on the ability of the society to mitigate and adapt to the climate change. Therefore, these narratives contain qualitative information in regard to how the society responds under the correspondent SSP.

We applied future scenarios that are described by combinations of RCPs and SSPs. Climate model projections were obtained from the MARS project (MARS, 2014; <http://mars-project.eu/>). We used the projected surface air temperature and precipitation from GFDL-ESM2M and IPSL-CM5A-LR, after bias correction with linear scaling, as inputs to the SWAT model. Regarding SSPs, we used the SSP2 which refer to a techno world driven by a fast economic development, the SSP5 which refers to a consensus world, with economy and population growing in the same pace as now and the SSP3 for the fragmented world where each region fights for its own survival. For the detailed representation of each of the SSPs we chose management options that fit in their future socio-economic narratives.

Specifically, for the fast growing economy of the techno world, the representation in SWAT included a precision irrigation method for the irrigated crops assuming that methods and equipment are substantially upgraded and an extension of the irrigated areas by 40% (covering fallow areas) for growing more corn for biofuel production. This practically resulted to an increase of the irrigated area by 80,000 ha rising the total irrigated land to 280,000 ha to serve energy demands. Fallow areas in the baseline were located among the crop areas all across the catchment and such a severe corn increase is expected to result to a significant water abstraction increase in areas with high water availability but to a low or negligible exploitation increase in stressed areas with limited water resources. A third management change in the basin under the 'techno' world was the 20% fertilization increase to all crops, which serves as an additional practice towards the maximization of profit.

In the consensus world on the other hand, we decided not to change at all crop patterns and irrigation water amounts and scheduling in the basin, hence, the respective simulations are driven only from climate change (two models). Finally, the fragmented world was represented by a combined 20% increase in both the irrigation and fertilization amounts applied to the cropping systems of the baseline in an effort to 'mimic' Pinios farmers' efforts to fight for their survival without considering much the environment. The combination of the management options with the specific climate conditions as

derived by the climate scenarios resulted to 12 model runs (2 climate models \times 3 storylines \times 2 10-y periods). The total number of runs was 13 including the baseline (shown on Table 4.13).

Climate data bias correction has already been performed to some extent. Due to spatial-temporal patterns of climatic parameters additional regional bias correction was needed. In general it was tested whether the climate scenario data describe spatial distribution, seasonality and extreme events correctly. Therefore, climate scenario was compared with real data for the period over which they overlap (2006-2010) to ensure the robustness of each climate data set. For the Pinios case study a bias correction based on Linear Scaling method (LS) of precipitation and temperature data was applied. This method (LS) aims to match the monthly mean of corrected values with the observed ones. As a result it generates monthly correction factors based on the differences between observed and predicted data. Precipitation is corrected for each point station (30 in total) with a multiplier and temperature (8 stations) with an additive factor on monthly basis.

4.3.5 Results: Predicting responses to multiple stressors at the river basin scale

In the Techno world agriculture is intensified further in Pinios to increase productivity. There is an increase of corn areas for biofuel production, a general fertilization increase to enhance productivity of all crops as well as the transformation of irrigation systems to contemporary methods including closed pipe irrigation networks and sprinkler irrigation systems, which are appropriate for following a precision agriculture scheme. Precision agriculture practically refers to precision irrigation, which is the application of water to crops in optimum timings and doses based on their actual needs. SWAT has the capability to ‘mimic’ this practice with the auto-irrigation routine. For the Techno world, we assume that the investment on technological equipment is high and all cotton producers buy the necessary soil water and air temperature equipment to implement this novel irrigation schedule. Finally, in the consensus world, agricultural management remains as it is. The management scenarios for each world are combined with specific climate scenarios and refer to both the future periods of 2025-2035 and 2055-2065. Table 4.15 summarizes the baseline and scenario results on a mean annual basis (centered around 2000, 2030 and 2060). Finally, the following bar-graphs in Figures 4.45, 4.46 and 4.47 depict these numeric results in three groups:

- Hydrometeorologic (precipitation, runoff and temperature)
- Abiotic and biotic state (sediments, nutrients, macroinvertebrates) and
- Ecosystem services (productivity of crops or annual yield in the basin and irrigation water)

Table 4.15. Numeric results from the implementation of scenarios with SWAT in the Pinios river basin.

	Scenarios	PCP mm	IRR water hm ³	Runoff mm	Av T oC	Sed t/ha	TN kg/ha	TP kg/ha	COT t/ha	CORN t/ha	COT 1000 t/y	CORN 1000 t/y
	Baseline	692	547	235	15.2	1.31	9.2	0.29	2.38	11.38	390	261
Techno World	GFDL-rcp8p5_2030	746	739	249	15.9	0.65	11.5	0.17	2.39	10.71	392	1145
Techno World	IPSL-rcp8p5_2030	775	650	282	17.0	2.55	14.6	0.39	2.06	9.52	338	1018
Techno World	GFDL-rcp8p5_2060	633	729	175	16.9	0.60	7.9	0.13	2.15	10.21	352	1092
Techno World	IPSL-rcp8p5_2060	651	638	186	18.9	2.74	8.2	0.28	1.62	8.38	265	896
Consensus World	GFDL-rcp4p5_2030	824	639	334	15.8	1.47	13.3	0.24	2.69	11.74	441	269
Consensus World	IPSL-rcp4p5_2030	797	581	320	16.3	0.97	12.9	0.25	2.29	10.39	375	238
Consensus World	GFDL-rcp4p5_2060	780	634	275	15.7	1.02	9.7	0.22	2.61	11.51	428	264
Consensus World	IPSL-rcp4p5_2060	694	511	210	17.3	3.04	7.7	0.29	1.96	9.93	321	227
Fragmented World	GFDL-rcp8p5_2030	741	631	254	15.9	0.56	11.5	0.15	2.49	11.62	408	266
Fragmented World	IPSL-rcp8p5_2030	769	539	285	17.0	2.40	14.4	0.34	2.15	10.21	352	234
Fragmented World	GFDL-rcp8p5_2060	629	646	179	16.9	0.57	8.0	0.11	2.22	11.16	365	256
Fragmented World	IPSL-rcp8p5_2060	646	535	189	18.9	2.62	8.4	0.24	1.66	9.66	273	221

4.3.5.1.1 Change in precipitation, temperature and runoff

Figure 4.45 shows the predicted annual average precipitation and temperature and the simulated runoff for the baseline conditions and the climate projections made for climate models (GFDL-ESM2M and IPSL-CM5A-LR), centered around 2000, and 2030 and 2060 respectively. The results show an increase of total precipitation predicted by all the climate model runs in 2030 and a decrease following in 2060. The simulated runoff follows consistently the precipitation pattern. Temperatures increase under all scenarios with the differences from the baseline being higher for 2060, especially with the IPSL-rcp4.5 model (3°C).

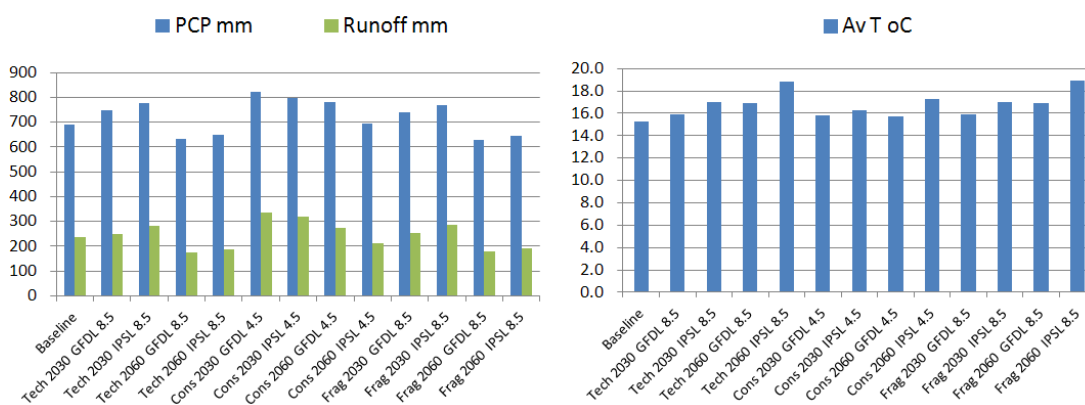


Figure 4.45 Average annual precipitation and simulated runoff, and temperature for the baseline period (1995-2005) and the future scenarios (2030 and 2060) in the Pinios basin.

The average annual precipitation simulated for the baseline period 1995-2005 is approximately 700 mm while the highest average annual precipitation is estimated for the GFDL-ESM2M RCP 4.5 scenario run (> 800 mm) in 2030 of the consensus world. The smallest precipitation is predicted by the GFDL-ESM2M RCP 8.5 close to 600 mm for the year 2060 of both the techno and the fragmented world. Generally, it appears that the most optimistic RCP 4.5 scenarios predict higher precipitations. In regards to the monthly variation of precipitation (not shown on a Figure), a sharp increase occurs in October for all the climate model runs. However, all the simulated runs predict lower precipitation during August in comparison to the baseline conditions. Overall, the climate scenarios predict an increase of annual precipitation, mostly during autumn, but very small changes (small increase or decrease) during the summer months.

4.3.5.1.2 Changes in abiotic state

Figure 4.46 shows the predicted annual average sediment and nutrient losses from land to waters of the Pinios catchment for the baseline conditions and the climate projections made for both climate models (GFDL-ESM2M and IPSL-CM5A-LR), centered around 2000, and 2030 and 2060 respectively. It should be mentioned first that in SWAT, sediments and P are mostly related to surface runoff while N to subsurface runoff (Neitsch et al., 2009). This means that under a climate with a large number of precipitation extremes, surface runoff and subsequently sediment and P losses are enhanced, while total runoff's magnitude mostly enhances loss of soluble forms of nutrients such as NO₃-N. The graphs in Figure 4.41 clearly show that climate is the major driver of pollutant losses. First, we observe that the IPSL climate model is this which increases annual sediment losses, obviously due to increased precipitation extremes, which are even more frequent farer in future (2060). The intensification of agricultural activities of both the techno and fragmented worlds does not seem as responsible as climate for the changes in sediment loads. Similarly, climate and specifically the projected increased total precipitation of both the GFDL and IPSL models for 2030 resulted to increased total runoff amounts causing higher N water pollution. Decreased precipitation and runoff in 2060 result to lower N losses accordingly. The role of agricultural management cannot be clearly indicated from the graph. Although N fertilization increases in the techno and fragmented worlds, N loss deviations from the baseline occur mostly due to the changes in climate. Moreover, under the same agricultural management of the consensus world N loss deviations occur from the baseline, indicating that climate alone is able to alter pollutant state in the basin.

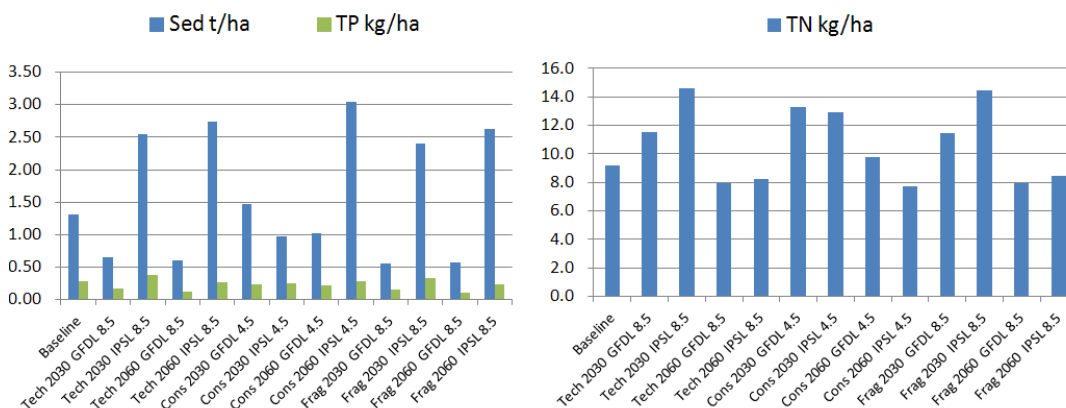


Figure 4.46 Average annual sediment, TP and TN loads to rivers and streams for the baseline period (1995-2005) and the future scenarios (2030 and 2060) in the Pinios basin.

4.3.5.1.3 Changes in ecosystem services

Figure 4.47 shows the predicted annual average cotton and corn yields in thousands tones per year and the actual water abstractions from the basin on a mean annual basis for the baseline conditions and the climate projections made for both climate models (GFDL-ESM2M and IPSL-CM5A-LR), centered around 2000, and 2030 and 2060 respectively. It should be noted here that water abstractions in our model are defined to occur under a number of restrictions related to groundwater and reservoir availability, which preserve water resources sustainability. For example, we have set very small initial depths of water in the shallow aquifers and reservoirs in order for the model to always need aquifer and reservoir water replenishment during the wet period of the hydrologic year (Oct-April) to be able to extract and apply water to crops during the dry period following. Also, minimum required flows downstream the reservoirs had to occur continuously in our model. Therefore, due to these plausible restrictions the amount of water abstracted for irrigation does not always meet the maximum theoretical doses set in the irrigation scheduling. In this way, sustainability of water bodies is ensured throughout the simulation as the irrigated water applied is the water that has naturally enriched water sources throughout the simulation period. In other words, only renewable water resources are used, thus, the irrigation water applied represents the guaranteed ecosystem service that the hydrologic system can deliver under each scenario. It should be finally mentioned that available but not used water resources (groundwater) always exist in the entire basin and this concerns the natural subbasins with small or negligible agricultural activities. However, it is not realistic to transfer these quantities in remote subbasins for use by crops. Therefore, in our model these water quantities are not practically considered as available ecosystem services. Finally, the total abstracted water depicted in the figure includes a fraction of water that is lost during its distribution to crops, thus, the water that is not used by the crop itself but which should be always considered in the calculations.

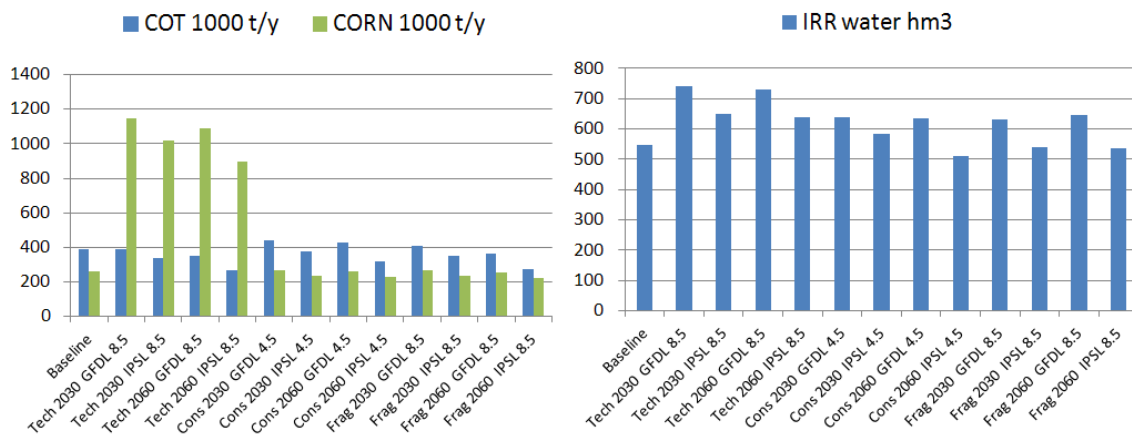


Figure 4.47 Average annual cotton and corn yields, and total irrigation water abstracted from the sources for the baseline period (1995-2005) and the future scenarios (2030 and 2060) in the Pinios basin.

The above graphs show clearly that the techno world increases substantially the production of corn due to the significant increase of corn areas for biofuel production (from ~20,000 ha to ~100,000 ha). Increased water availability of the climate models in 2030 has most of the times a positive effect on yields for both cotton and corn. However, IPSL always results in reduced yields and smaller water abstractions than the GFDL does. As was discussed previously, IPSL is characterized by a more intense temporal variability of rainfall with the enhancement of extreme events. This decreases water storage compared to the GFDL model, with less water availability and subsequent crop use. Compared to the baseline however, the total water abstracted under any world with the IPSL model is from significantly higher to only slightly lower. The reduced cotton and corn yields here are also attributed to the higher temperatures of this climate (see Figure 4.45), which leads to increased ET rates, thus higher water needs of the crops to reach the same productivity level.

4.3.5.1.4 Changes in biotic state

Based on the empirical models developed with the use of GLM and BRT techniques we predicted the response of ASPT and EPT metrics at each sub-basin using as predictors the mean annual values for the output variables simulated by SWAT. As a result we estimated the ASPT and EPT metrics at each sub-basin separately, under the baseline conditions and each scenario. Figures 4.48 and 4.49 show the mean values for ASPT and EPT metrics for

the whole basin calculated based on predictions made by the GLMs at subbasin level. Figure 4.50 shows the mean value for ASPT calculated based on predictions made by a BRT model.

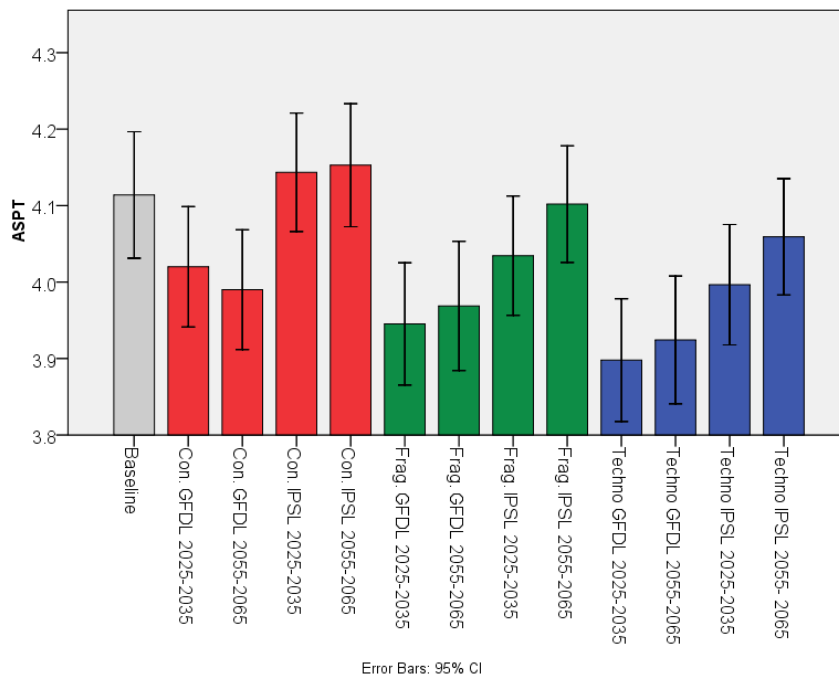


Figure 4.48 Mean ASPT and 95% confidence levels calculated based on predicted values at each sub-basin for the baseline conditions and for each scenario run. Predictions were made with the use of GLMs.

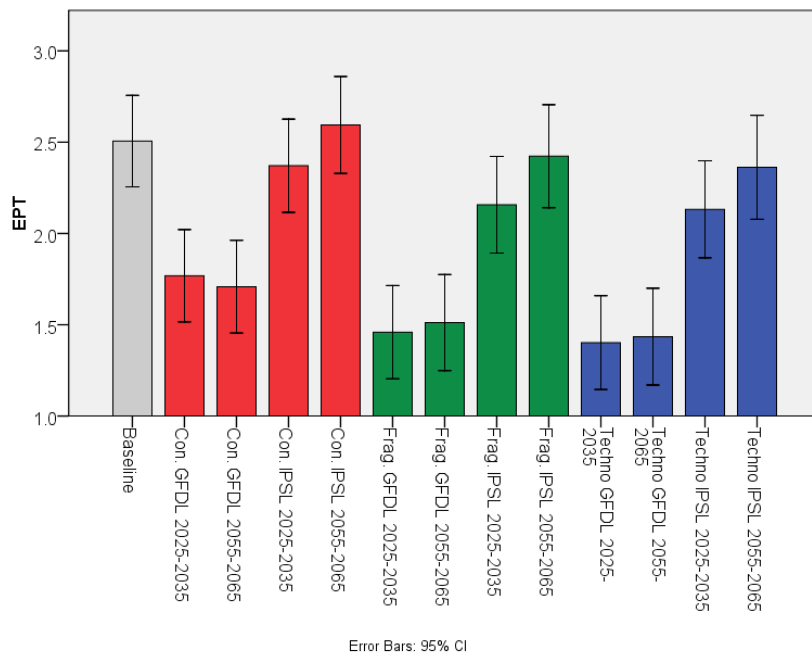


Figure 4.49 Mean EPT and 95% confidence levels calculated based on predicted values at each sub-basin for the baseline conditions and for each scenario run. Predictions were made with the use of GLMs.

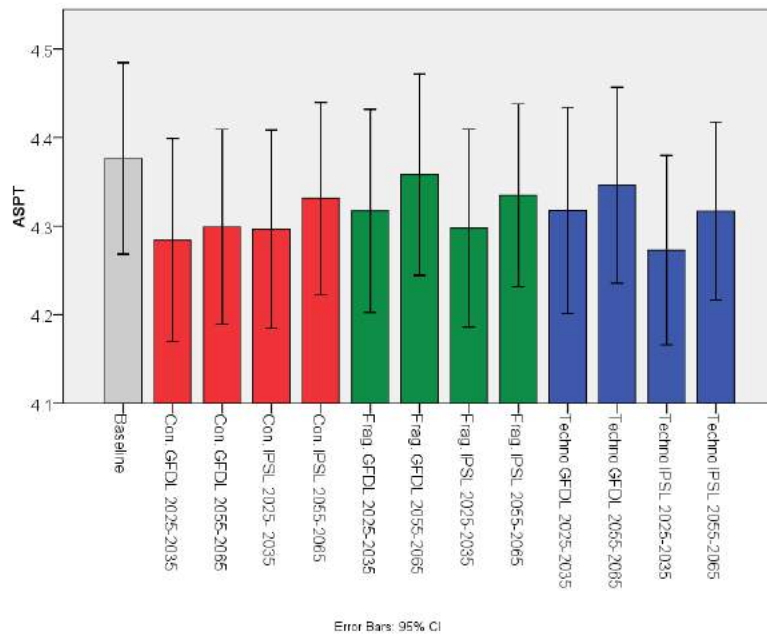


Figure 4.50 Mean ASPT and 95% confidence levels calculated based on predicted values at each sub-basin for the baseline conditions and for each scenario run. Predictions were made with the use of BRTs.

In regard to the ASPT predicted by the GLM for the baseline conditions we note that the overall mean for the whole basin is noticeably lower (4.11 vs 4.65) than the average ASPT calculated by real data collected by Chatzinikolaou (2007). The mean ASPT predicted by the BRT is 4.38, still lower than the average obtained by real data but slightly higher than the one predicted by the GLM. This small difference between simulated and measured values can be explained probably by the fact that Chatzinikolaou (2007) carried out samplings in sites with very low anthropogenic pressure that were characterized by high ASPT and EPT values, indicating a good ecological status. Nevertheless, under the baseline conditions our modelling approach resulted to realistic values that are representative of a wide range of nutrient concentrations, which also reflect the effect of agricultural activities in the area. Similar conclusions can be made for the predictions of the EPT compared to the measurements made by Chatzinikolaou (2007).

As far as the scenario results are concerned, the graphs clearly show that all the scenarios based on the GFDL climate model correspond to a decrease for both the ASPT and EPT predicted by the GLMs, with the sharpest decrease observed for the Techno World scenario results centered around 2030. Regarding the scenario runs based on the IPSL climate model we can note that the results are similar except the Consensus World future years (2030 and

2060). Similarly, we observed a slight increase for the EPT metric only for the 2055-2065 periods. For all the other cases there is a slight decrease in both ASPT and EPT metrics compared with the values for the baseline conditions.

These results can be related to the predictions made for the TN (Figure 4.46) as in some occasions it is obvious that the variability of the mean ASPT and EPT among the scenarios agrees with the variability of the nitrogen loads. The standard decrease of N in 2060 compared to 2030 of each scenario is consistent with a similar increase trend for ASPT as we move to the future. Moreover, the highest TN loads and the lowest ASPT average are both predicted for the Techno World IPSL scenario for the period centered around 2030 (Figures 4.46 and 4.48). However, we have found that in some cases the oxygen concentration is the key factor for the biotic response. In general, SWAT predicted for all scenarios a decrease of the average concentration of dissolved oxygen, due to the increase of the major associated parameter, the water temperature. The key role of the oxygen in determining the response of ASPT is more obvious in the cases where, although a decrease of nutrient (both N and P) loadings was predicted by SWAT, the biotic metrics did not respond accordingly. Specifically, the Techno and Fragmented World scenarios based on both GFDL and IPSL climate models predict a reduction of both nitrate and phosphate loads for the future period 2055-2065 that has a “positive” effect on the biotic response (increase of biotic indices). However, because of the oxygen reduction a decrease of ASPT is still observed under these scenarios. In other words, the oxygen factor is stronger. On the other hand, under the Consensus World scenario based on the IPSL climate model there is an increase of the ASPT metric because the predicted change in oxygen concentration is very small and is not able to “counteract” the “positive” effects of the nutrient loading reduction.

In regards to the ASPT predicted by the BRT the results appear slightly different compared to the ones already discussed under the GLM predictions. First, the predicted ASPT for all scenario runs is lower than the mean predicted for the baseline conditions, which agrees with the previous results. Moreover, a pattern where the means for the far future period are higher than the means for the 2025-2035 is still the case. This is possibly explained due to the higher run-offs and nitrogen loadings predicted during the period 2025-2035 that have a “negative” impact on the ASPT. What we don’t see however, is the consistently higher ASPT under the IPSL model runs for all worlds that was the case before. But overall, there are quite smaller numerical differences among the means of each scenario now. This

practically means that the existing variability does not allow us to clearly identify the effects of the scenarios on the ASPT with the BRT method.

4.3.6 Conclusions and key outcomes

In the MARS Pinios case study a combination of PB and EM has reproduced the two-stress (water abstraction and nutrient pressure) situation in waters both under the present conditions and future scenarios, with clear estimations of the two most important (provisional) ecosystem services (water for irrigation and crop productivity). The main outcomes of the study are:

- All scenarios show an increase of total precipitation in 2030 and a decrease following in 2060. The simulated runoff follows consistently the precipitation pattern.
- Temperatures increase under all scenarios with the differences from the baseline being higher for 2060.
- A sharp precipitation increase occurs in October for all the climate model runs. However, all the simulated runs predict lower precipitation during August in comparison to the baseline conditions. Overall, the climate scenarios predict an increase of annual precipitation, mostly during autumn, but very small changes (small increase or decrease) during the summer months.
- Climate is the major driver of pollutant losses, with agricultural management changes having a secondary role. When runoff increases, N losses also increase (2030) and the opposite (2060).
- Sediments and P annual losses follow the seasonal variation of hydrology, thus, they are getting clearly higher under scenarios with the IPSL climate model.
- Consistently, under all scenarios tested, the requirements for delivered Ecosystem Services to humans are satisfied or in the worst situation, they are very slightly disturbed from the baseline. In the techno world in particular, the production of corn is substantially increased due to the significant increase of corn areas for biofuel production.
- Increased water availability of the climate models in 2030 has most of the times a positive effect on yields for both cotton and corn. However, IPSL always results in

reduced yields and smaller water abstractions than the GFDL does due to: a) the more intense temporal climate variability that reduces water availability and b) the higher temperatures that lead to increased ET rates and crop water needs.

- Dissolved oxygen and nutrients are key predictors of both the biotic ASPT and EPT indexes. Oxygen seems to be stronger though, as even under scenarios where nutrients decrease, the biotic metrics still decline due to reduction of oxygen concentration mostly caused by the rise of water temperature
- The scenarios based on IPSL climate models are more optimistic in regard to their effects on the biotic indicators resulting in smaller reductions of the biotic indices than the GFDL models do. The biggest negative impact (reduction) on both ASPT and EPT is predicted under the Techno World scenario and for the future period 2025-2035.

It should be noted that the scenario results and subsequent conclusions presented herein are subject to uncertainty that mainly arises from the climate model data provided to MARS. Local topography and special climate conditions might have not been accurately considered by the GCMs. Thus, projections for small scale study areas (catchments) and the associated water quantity and quality results should be treated with caution.

The climate models used in this work predicted an increase of annual precipitation in Pinios for the reporting period 2025-2035 resulting to a consequent increase in annual runoff compared to the baseline. This result at first appears as a paradox as there are several studies that have shown a general trend of intensification of aridity in the Mediterranean region due to decrease of precipitation and rise of temperature. For example Papadaki et al. (2016) showed that A1B (2021-2050, 2071-2100), A2 (2071-2100) climate scenarios predicted a decrease of rainfall that along with an increment in temperature were responsible for decreased stream flows in two mountainous Mediterranean catchments. Indeed, studies that have employed CMIP3 models (Coupled Model Intercomparison Project Phase 3), such as A1B and A2, have shown a remarkable decrease of precipitation in some areas of Greece by the end of the century, up to 60% (Paparrizos et al. 2016; Tolika et al. 2012).

However, there are few studies based on the more recent CMIP5 models that predict intensification of heavy rainfall events during winter and in some cases an increase of the annual precipitation. For example in an article of Scoccimarro et al. (2016) it was shown that under RCP 8.5 scenario, CMIP5 models project an increase of heavy precipitation

during winter in South Europe (including regions of Mediterranean) by the end of 21st century, while during summer the duration and the intensity of rainfall events is expected to decrease. Other studies that use CMIP5 models have also predicted an increase of annual precipitation even in arid areas like Sudan (Basheer et al., 2016).

This increase occurs in our study area mainly during the winter months. During summer, precipitation remains in low levels similar to the baseline conditions. This finding seemingly agrees with the remarks made by Scoccimarro et al. (2016). Nevertheless, the presented results imply that although annual precipitation increases, the water availability during the dry period will not increase. On the other hand, during the winter months the intensity of flood events is expected to increase.

However, the situation is different for the period 2055-2065 where scenarios mostly predict a decrease in the river discharge. Regardless the scenario, the scenario runs suggest that hydrology and nutrient pollution in the catchment are expected to change significantly. This has been shown from the changes in monthly flows that imply a severe modification of the hydrologic regime in relation to the natural flow, although annual changes are as significant. An important modeling result was also the 57% TN annual load increase of the Fragmented World scenario (2025-2035) compared to the baseline.

Consequently, such important possible changes may have significant effects on the aquatic habitats and the river ecology. An increase of flood frequency and magnitude could have both beneficial and detrimental effects depending on the channel morphology, type of substrate, depth and other hydromorphological characteristics. High flows are considered important for maintaining a certain aquatic community structure (Bunn and Arthington, 2002) and can induce mobilization of sediments and modify the shape of the channel, playing a vital role to habitat formation (Poff *et al.*, 1997; Bunn and Arthington, 2002).

Based on our results it seems that the climate effect prevail over any other effect generated by the management options that could have an impact on the flow regime of the catchment. This of course depends largely on the hydrologic characteristics of the catchment but also on the type of water use services provided. In Pinios, irrigation is the most important water use, with the total amount of water abstracted, mostly by groundwater sources, to be estimated approximately as $900 \times 10^6 \text{ m}^3$ per year. Management options, such as deficit irrigation and precision agriculture, although they can reduce significantly the abstracted water, they had a small impact on changing the surface runoff and the river flows. For

example, a deficit irrigation by 30% led to very small and non-significant increase of the mean annual flow by 0.38 m³/s (Stefanidis et al. 2016). Based on this information we can assume that the hydrologic and nutrient load changes identified in this study are attributed mostly to climate and that the management options had only a small effect (actually in the consensus world no management changes were defined to our model). We consider this finding important for future research.

4.4 Sorraia

4.4.1 Introduction

Water resources and ecosystems of Europe are impacted by several stressors (Herring et al. 2010) that affect ecological and chemical quality, water availability and ecosystem functions. Additionally, the increase in human population numbers linked with future climate changes will predictably increase the impact of stressors acting upon river ecosystems. When more than one stressor affect a system, interactions may occur, these interactions can vary on their impact on the ecological and chemical quality of rivers. Interactions can be: additive when the impact of isolated pressures is summed; synergistic when the combined impact is larger than the sum of the individual impacts; or even antagonistic when the combined impacts are lower than the sum of the isolated impacts (Underwood 1989). There are still few studies that deal with the combination of several impacts (Vinebrooke et al. 2004), which creates a lack of mechanistic understanding of the interaction of stressors. This diminishes our ability to predict responses to changing environments, risk assessment, management, impact mitigation and ecosystem restoration (Fauth et al. 1996).

The Sorraia floodplain is one of the largest areas of irrigated crops in Portugal. Therefore, in this basin the major anthropogenic impacts are mainly related with hydrological (e.g. irrigation, flow regulation, damming) and nutrient stressors. In this report we investigate the single and combined effects of hydrological and nutrient stressors on several biotic state variables and ecosystem services. This is accomplished through empirical models using land use data, and data derived from process-based hydrological models and biomonitoring records of several biotic quality elements (BQE) and measured services.

This report will closely follow the DPSIR terminology (DPSIR = Driver–Pressure–State–Impact–Response chain).

Main research questions

The research questions addressed in this report will not only contribute to the knowledge of multiple stressors at the basin scale (WP4), but also will be an important contribution to the synthesis of multiple stressor effects (WP6, task 6.1) and the multiple stressor tools planned in WP7, namely the MARS Information System (Task 7.1) and diagnostic tools (task 7.2). In a greater or lesser extent, the following research questions are addressed in this report:

- Q1. Which multi-stressor combinations are the most prominent in the Sorraia basin?
- Q2. How stressors (i.e. pressure and state) interact in their effects on the biotic state?
- Q3. Which benchmark indicators or other state variables show strong effects of multiple stressors?
- Q4. Do multiple stressors affect ecological quality differently when they interact and what is the impact of the interaction? Can we derive management guidance there from?
- Q5. Do multiple stressors affect ecosystem functions and/or services? Are results different when the stressors interact? Can we derive management guidance there from?
- Q6. What is the ecological response to conditions of extreme low flow and nutrient stress? What are the consequences for eFlows and recreation (including angling)?
- Q7. What is the ecological response to conditions of extreme high flow and nutrient stress? What are the consequences for water supply?
- Q8. Which biological quality elements (BQE) reveal strong effects of multiple stressors and their interactions?
- Q9. Are thresholds identifiable at which multiple stressors cause abrupt changes of an indicator (change/tipping points)?

Questions Q6 and Q7 will be especially helpful to implement the synthesis that is planned in WP6, while Q8 and Q9 will also inform WP7 with response patterns of aquatic biota to multiple stressors.

This study will facilitate an accurate definition of the ecological state of river sites, but following a basin/wide approach that will allow for an overall understanding of the processes acting on the basin making it possible to implement effective management and restoration policies.

4.4.2 Study area (description of basin)

The Sorraia basin (Fig 4.51) has an area of 7730 Km² and a length of 155km. It flows towards the Tagus river estuary (outlet - latitude 38.83 and longitude -8.99) and it is the Tagus tributary with the largest basin area.

Over the years the Sorraia River had a vital role for the region. According to historical records, Romans and Arabs had settlements in the Sorraia Valley, due to its fertile soils and as a communication way to export their agricultural products. Here, they were responsible for developing ingenious irrigation systems that are still present. In the second half of the twentieth century the Sorraia Valley Irrigation Plan was put into practice, through the construction of Montargil and Maranhão reservoirs. Together with the Sorraia Channel, the aim was to enhance agriculture income in the region.



Figure 4.51 -1. Sorraia watershed location; 2. Coordinates of the basin limits

The Sorraia river is on average 1.70 m in depth and its source is located near Couço by the confluence of the streams Sor and Raia (latitude 38.994; longitude -8.27; 50 m). The Sor stream source is located at an altitude of 330m, on the other hand Raia stream is the junction of another two streams rising at 370m and 355m of altitude. About one half of the Sorraia watershed is covered by cork-oak forest while the other half is covered by

the biggest irrigated area in Portugal (about 15 500 ha) (Fig 4.52). According to the Global Cover 2006 and to the work developed by Mateus et al. (2009), about 41% of the area is forest, 28% range-grasses, 17% agriculture, 9% pine, 2% orchard, 2% urban and industrial and 1% pasture.

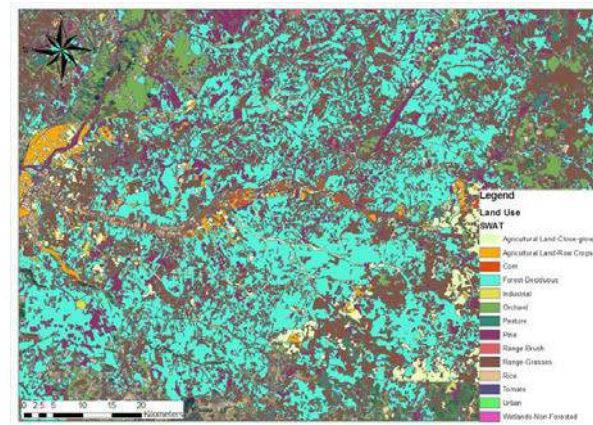


Figure 4.52 Land use map (source: Mateus et al, 2009 – detailed Sorraia Valley – and Global Cover 2006)

In terms of human population, the Sorraia watershed has a total of 153 099 habitants with a density of 20 hab/km². According to “Censos 2011” from National Institute of Statistics (INE, 2011), the human population is mainly concentrated in three core areas: (Figure 2.3): Ponte de Sôr (16 722 hab), Samora Correia (17 123 hab) and Coruche (19 944 hab). Sorraia watershed is characterized by a Mediterranean climate, with high temperature and dry summers, and low temperature wet winters. Considering a period of 31 years (between the hydrological years 1981 and 2011) and 14 precipitation stations, the average annual precipitation is about 600 mm, from 400 mm in the dry years to up to 900 mm in the wet years. The average monthly precipitation is 50 mm, ranging from 25 mm in hot months (between April and September) to 70 mm in cold months (between October and March). Because of the presence of the two reservoirs in the basin, runoff at the gauging stations is affected. Natural flow is affected by the use of water for agriculture purposes. Flow is especially reduced by water abstraction for irrigation.

According to the River Basin Management Plan (RBMP), the main pressures on the basin are: 1. Hydromorphological changes, 2. Diffuse pollution, 3. Municipal discharges, 4. Flow regulation, 5. Extraction of water. And key ecosystem services identified by the RBMP are: 1. Water for irrigation, 2. recreation services and 3. Waste water treatment. The Water Framework Directive (WFD) status of 122 water bodies is: 54 good (44%), 15

moderate (12%), 12 poor (10%), 2 bad (2%) and 39 (32%) unclassified. The causes of poor or failing status have been identified as: Urban and agro-livestock residual water treatment systems are either inefficient, inappropriate or absent. The main activities in the catchment: livestock (cattle and pig), poultry, olive oil mills, small cheese factories and wine cellars. The water need for agricultural purposes in the Sorraia basin is the highest within the Tagus river basin region (26% of the total need).

The Program of Measures for the Sorraia basin (Table 4.16) aiming at attaining the good quality status is essentially related to the improvement of the efficiency and sustainability of the use of water resources.

Table 4.16. Program of measures to be implemented in the River Basin Management Plan that are relevant for the Sorraia basin

Measure code	Aim of the measures
SUP_P347_AT1	Increase the efficiency of Water treatment plants and/or renewal of the distribution net to overcome the failure to attain quality parameters.
SUP_P36_AT1	Efficient solutions for the drainage and wastewater treatment of small urban areas.
SUP_P2_AT1	Implementation of good agricultural practices (rational fertilization, handling and storage of chemical fertilizers; handling and storage of cattle effluents; soil management and use considering the nitrogen dynamics; irrigation management and pollution prevention by nitrates).
SUP_P9_AT2	Irrigation management (improvement of irrigation practices, namely the decrease of losses of irrigation systems).
SUP_P39_AT1	Construction of new livestock effluents treatment plants.

4.4.2.1.1 MARS-DPSIR conceptual model

A basin wide theoretical model based on the DPSIR framework was developed for the Sorraia Basin (Fig. 4.53). Here we identify the main drivers and pressures acting upon the Sorraia Basin. In this case “Ecosystems Services” was used as a proxy for the DPSIR “Impact”. This conceptual model was used to frame the process and empirical based modeling in a way that these modeling approaches inform the conceptual model. This link between both modeling approaches and the basin-model allow biotic and abiotic state predictions under climate and land-use changes. This working basin-model will also allow testing a set of responses (measures) and seeing how the combinations of such

measures will alter the future status of water bodies, acting as an efficient management tool.

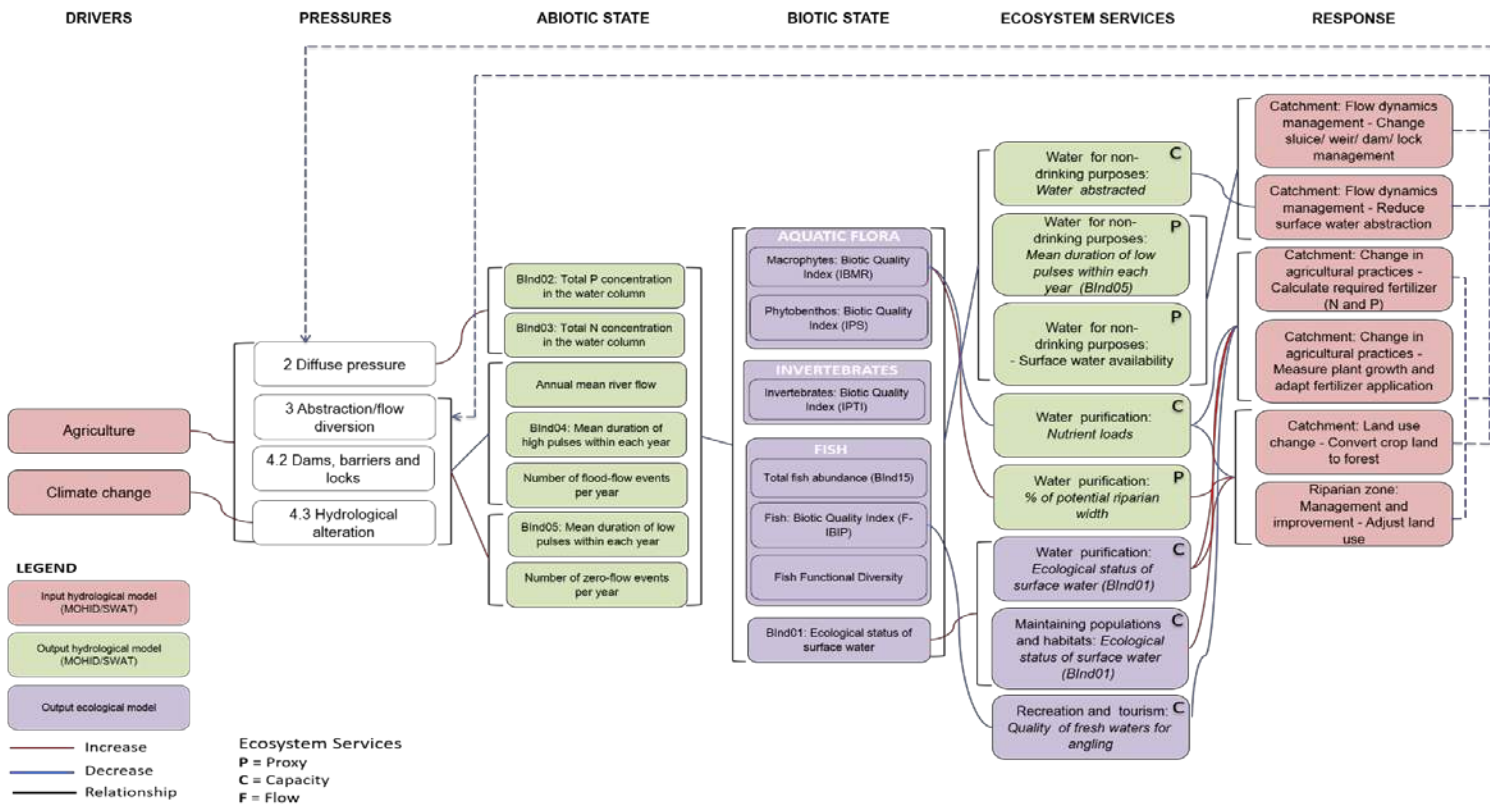


Figure 4.53 MARS-DPSIR Conceptual model for Sorraia Basin. DPSIR = Driver–Pressure–State–Impact–Response chain. Dashed lines represent changes that would only occur with response implementat

4.4.3 Methods

4.4.3.1.1 Process-based modelling

Model description

The model used in this work is the SWAT model (Neitsch et al., 2005), a semi-distributed watershed model focused on land management at reach or basin scale in which a big effort and knowledge was put into the crop database (with growth parameters of around 100 species) and vegetation growth model; both developed under the knowledge of the Grassland laboratory in USDA. SWAT model divides the watershed into subareas that are assumed to be homogeneous in their hydrologic response units (HRU), uses a daily time step, and infiltration or groundwater flow is computed based on empiric or semi-empiric formulations (as the SCS rainfall-runoff curves or soil-shallow aquifer-river transfer times). The hydrology of the model is based on the water balance equation which includes runoff, precipitation, evaporation, infiltration and lateral flow in the soil profile.

The potential evapotranspiration can be calculated by the Hargreaves method (Hargreaves *et al.*, 1985), Priestley-Taylor method (Priestley and Taylor, 1972) or by the Penman-Monteith method (Monteith, 1965). The actual evapotranspiration is estimated by the sum of three components: plant canopy evaporation, plant transpiration and soil evaporation. For the calculation of transpiration is necessary Leaf Area Index (LAI). This parameter is estimated for each HRU through a model plant growth. The relative straightforward formulation allows the model to produce in reasonable time (minutes or hours) simulations of decades in large watersheds (up to 10 000 Km² – e.g. Jayakrishnan et al. 2005). In this case, SWAT allowed running the entire Sorraia watershed on a daily time step.

The SWAT model was applied to the Sorraia basin using the ArcSWAT interface, which is an ArcGIS extension from ESRI. Available GIS maps for topography, land use from EO data (Earth Observation data) adapt to the SWAT classification, and soils of the study area were used. Table 4.17 gives an overview of the input data and Figure 4.54 shows the spatial distribution in the Sorraia basin.

parameters that can influence the behaviour of the flow results were tested. To determine which parameters should be adjusted in the model, flows modelled and observed in the same location and during the same period are compared and deviations interpreted. Table 4.18 shows the parameters changed.

Table 4.18. Calibrated parameters values used in the SWAT model.

Parameter	Description	Default	Calibrated Value
Mgt1_CN2	SCS runoff curve number for moisture condition II	20 to 70	80 to 90
SOL_ZMX	Maximum rooting depth of soil profile. (mm)	-	1000 to 3000
SOL_Z	Depth from soil surface to bottom of layer (mm)	300 to 800	1000 to 3000

Model results were compared with data available in three locations: one upstream of each reservoir (*Moinho Novo* and *Ponte Vila Formosa*) and one downstream of both reservoirs (*Samora Correia*) (p.ex. Fig4.55). Both flow and nutrient data were considered at these locations.

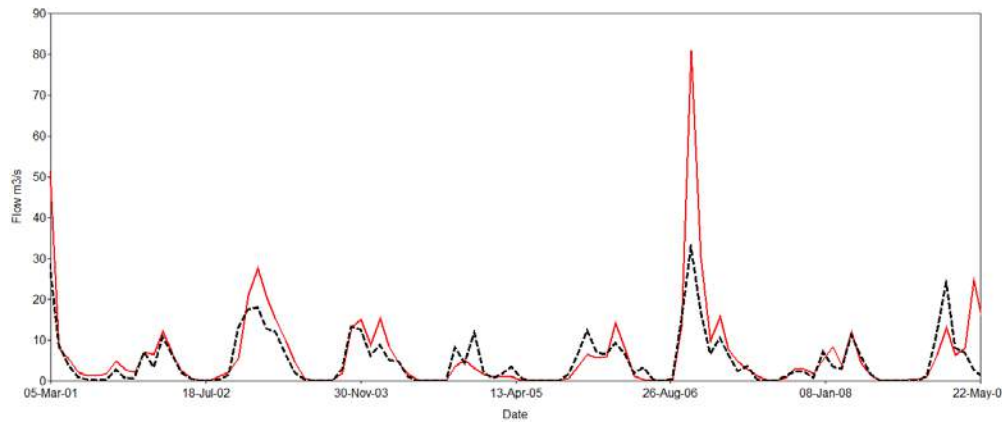


Figure 4.55 Comparison of monthly flow in “Moinho Novo” location: red line – observed; black line – modeled

The period considered for the calibration and validation analyses was between 1996 and 2015. The linear correlation between the monthly flow modeled and observed is statistically significant ($R^2=0.77$). Monthly observed flows average is $6.97 \text{ m}^3/\text{s}$ and flows modeled present an average of

6.22 m³/s, a Bias of -0.75, a Root Mean Square Error of 6.3 m³/s and a model efficiency of 0.73 m³/s (Nash–Sutcliffe coefficient). Figures 4.56 and 4.57 show the comparison between modeled results for water quality and measured values at two sites

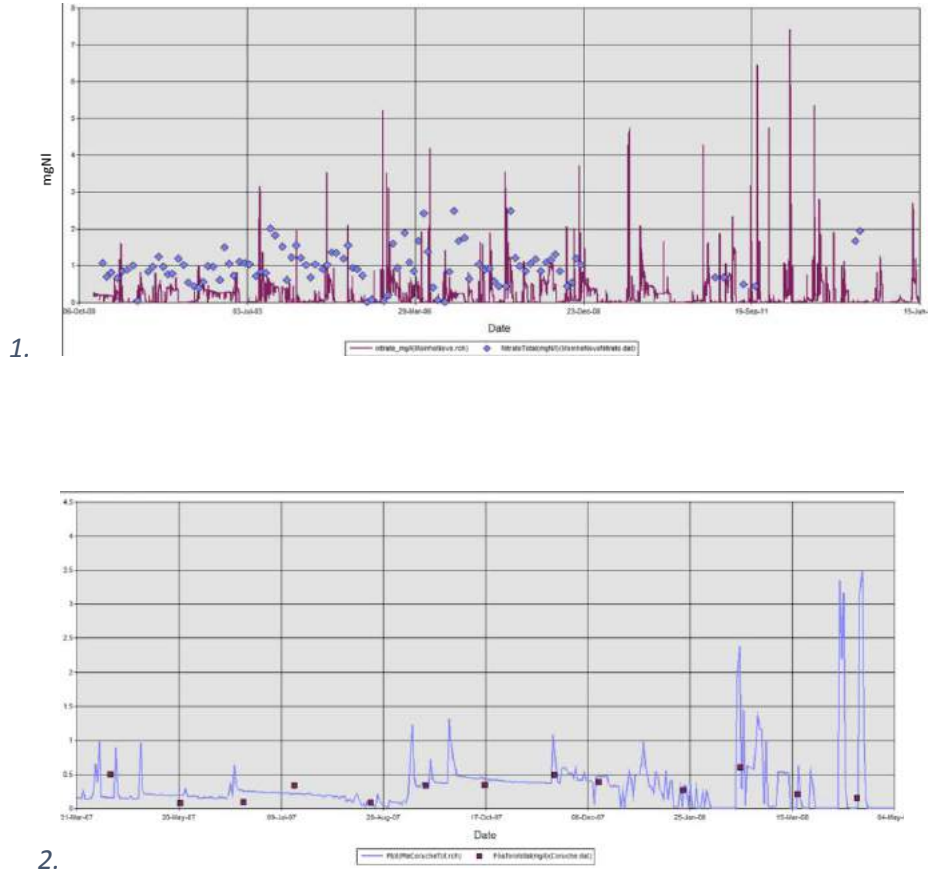


Figure 4.56 Nitrate results in river- Local Moinho Novo (Line is the model results and dots are the observed);2. Phosphorus results in river - Local Moinho Novo (Line is the model results and dots are the observed)

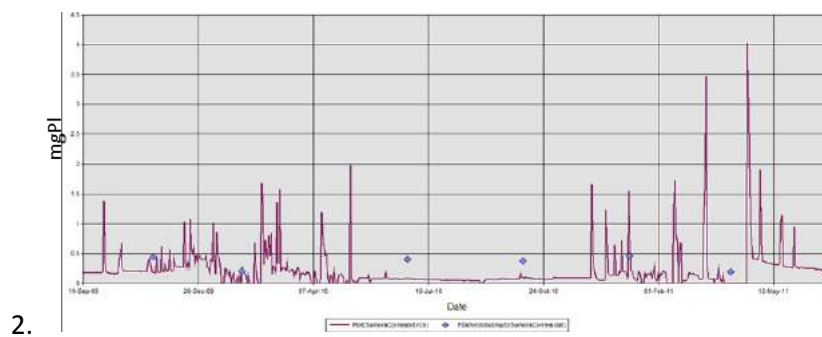
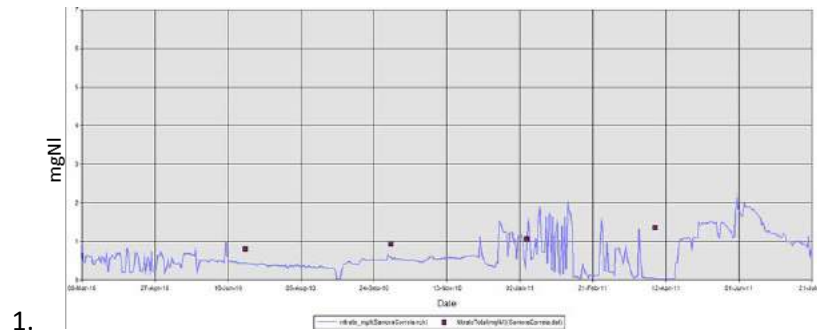


Figure 4.57 -1. Nitrate in river - Local Samora Correia (Line is the model results and dots are the observed); 2. Phosphorus in river - Local Samora Correia (Line is the model results and dots are the observed)

4.4.3.1.2 Empirical modelling

Data

The database used to fit empirical models was mainly compiled from two independent datasets (APA and EFI+ - Segurado et al. 2015). Due to data limitations, and also to encompass a wider environmental and stressor gradient, we used data from the whole Tagus river basin to fit empirical models. This was possible because the environmental conditions of Sorraia and Tagus basins widely overlapped (Fig. 4.58). The first dataset comprised 205 sites with fish data from the EU-funded project EFI+ (<http://efi-plus.boku.ac.at>), sampled between 1995 and 2005 in the context of several biomonitoring programs (Fig. 4.59). The dataset comprises site/fishing occasion descriptors, including climatic, geomorphological, land use and pressure variables. Fish data includes species presence and abundance and a list of 118 metrics based on 19 guilds. Sites were sampled by electrofishing during low flow periods employing standard European methods (CEN, 2003). The

second dataset comprised 141 sites from the Water Frame Directive biomonitoring program (Portuguese Environmental Agency, APA), with two sampling occasions (2010-11) (Fig. 4.58). The dataset included information on the overall ecological status and also National EQR values for four biotic quality elements: fish, macroinvertebrates, macrophytes and phytobenthos. The two datasets were used to perform two independent analyses: the EFI+ dataset was used to assess the response of fish-based functional indicators to multiple stressors while the APA dataset was used to assess the response of ecological status indicators.

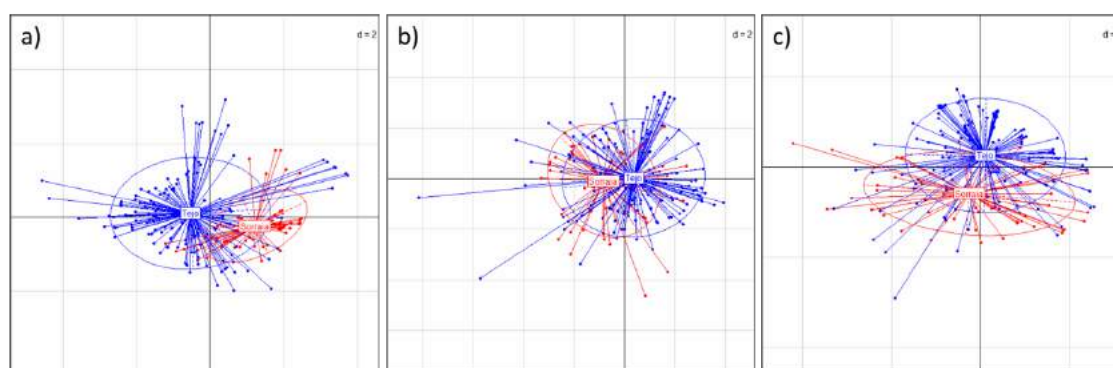


Figure 4.58 First plane of the Principal Component Analysis using a) variables describing natural environmental variability, b) stressor variables, c) fish-based indicators. Colours indicate the basin to which sites belong to (blue – Tagus basin; red – Sorraia basi

The two datasets comprised 23 predictor variables, including 8 land use pressure variables, 2 nutrient stressors, 7 hydrological stressors and 6 variables describing natural environmental variability (Table 4.19). Land use and environmental variables were available for the EFI+ sites but were compiled from the CCM2 river network database (Vogt et al. 2007) for the remaining sites. All hydrological and nutrient stressor variables were derived from process-based hydrological models. These stressors consisted in annual average values for the respective sampling year (which, in the case of the EFI+ dataset, it could be different from site to site).

The land use pressures were based on the percentage of area derived from two very different spatial scales: a wide spatial scale corresponding to the whole upstream catchment and a local spatial scale corresponding to the area that drains laterally to the river segment (segment between two tributaries) of the site (primary catchment). These pressure variables are in fact proxy of

different environmental stressors (e.g. nutrient enrichment, water abstraction, sediment pollution, damming, flow regulation) rather than a stressor in itself. We considered to be important to include these variables as predictors to control for the effects of other sources of variability that were not measured or modelled. Due to the smaller size of the APA dataset, we did not include local scale land use variables in order to reduce the set of candidate variables. The percentage of area in the upstream catchment was computed with the RivTool software v1.0.0.1 (Duarte et al. 2016).

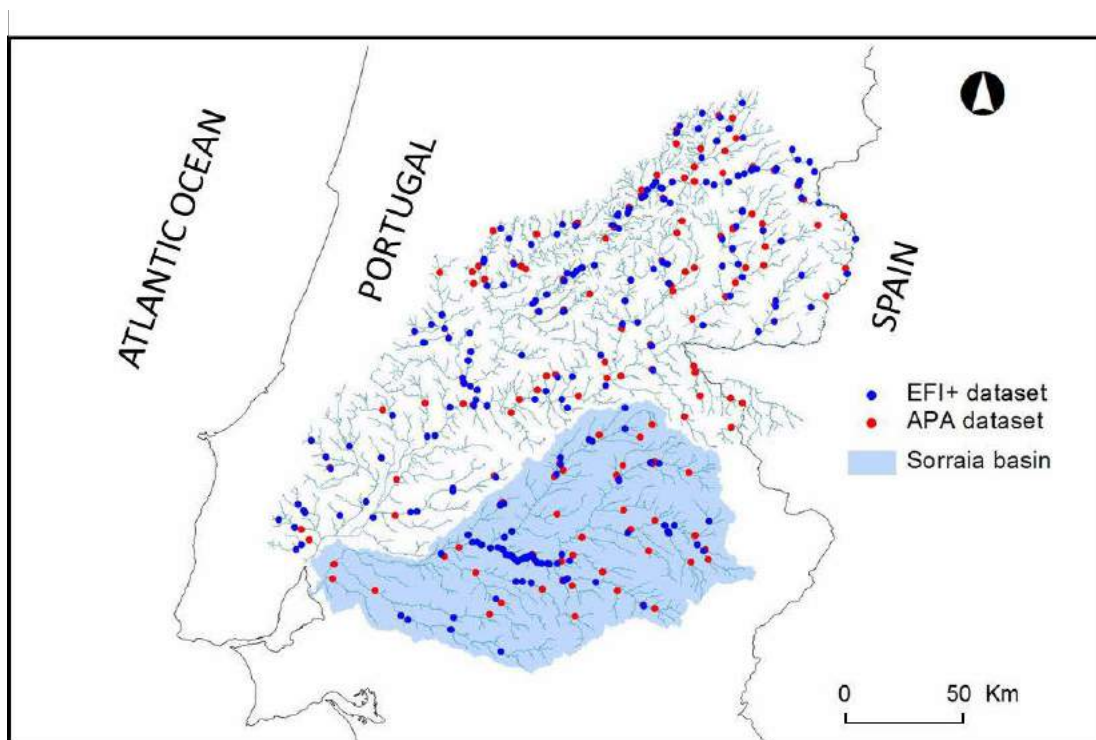


Figure 4.59 Location of sampling sites

Because biotic indicators are affected by natural environmental gradients, it is crucial to control this effect when testing relationships with stressor variables. For the Tagus basin we considered two main natural environmental gradients as the most relevant: a climatic gradient and a river longitudinal gradient. These gradients, expressed in our datasets by 6 environmental variables (Table 4.19), were included as candidate predictors in the empirical modelling framework to control as much as possible for the effect of natural environmental variability.

Table 4.19. List of candidate predictor variables

Predictor variables	Units	Range
<i>Land use pressures</i>		
Agriculture in the primary catchment	%	0-100
Irrigated croplands in the primary catchment	%	0-75
Forest in the primary catchment	%	0-95
Urban in the primary catchment	%	0-42
Agriculture in the upstream catchment	%	0-96
Irrigated croplands in the upstream catchment	%	0-19
Forest in the upstream catchment	%	0-83
Urban in the upstream catchment	%	0-12
<i>Nutrient stressors</i>		
Total P annual mean	mg/l	0.003-1.457
Total N annual mean	mg/l	0.333-5.687
<i>Hydrological stressors</i>		
Annual Mean Flow	m ³ /s	0.13-129.01
High flow pulse – Number of events	.	1-25
High flow pulse – mean duration (days)	Number of days	2.24-101.00
Low flow pulse – Number of events	.	0-40
Low flow pulse – mean duration (days)	Number of days	0.00-106.00
Zero flow pulse – Number of events	.	0-11
Zero flow pulse – mean duration (days)	Number of days	0.00-16.50
<i>Natural environmental variability</i>		
Distance from source	km	2-981
River slope	%	0.01-75.01
Size of the upstream catchment	km ³	8-67051
Altitude	m	5-1090
Mean annual temperature	°C	9.9-17.2
Mean total annual precipitation	mm	628-1552

Overall modelling strategy

We used a stepwise analytical procedure, closely following the steps proposed in Feld et al. (In press) to analyse the impacts of multiple stressors in aquatic biomonitoring data. After checking data quality and consistency, we performed a first exploratory analysis by running two machine learning techniques, Boosted Regression Trees (Elith et al. 2008) and Random Forests (Breiman 2001). These techniques were mainly used to rank the importance of both multiple stressors and potential pairwise interaction among predictor variables for each selected biological indicator. After selecting the most relevant stressor candidates, we quantified and tested both individual and multiple stressor effects through Generalised Linear Models (McCullagh & Nelder 1989), when only one sample occasion was carried out per site, or Generalised Linear Mixed Models (Zuur et al. 2009), when more than one sampling occasion was available for each site. The response of indicators and interactions among stressors were visually assessed through partial dependent plots and coplots. BRT, RF and GLM/GLMM models were evaluated using a crossvalidation procedure to estimate their explanatory and predictive performance. We then used the calibrated models with the best predictive power to make future projections of the most responsive biological indicators and ecosystem services under the climate change and land use scenarios selected and developed within the MARS project. All the analyses were performed with R version 3.2.3 (R Core Team, 2015).

Data validation and preparation

Because we had dispersed missing data throughout the dataset, the first step on data preparation was to select only the table rows with complete cases. We then checked for outliers, variable distribution and skewness. We found left skewness problems in almost all predictors (Fig. 4.60) and therefore opted to apply a data transformation to the whole set of predictors, except for mean annual temperature. We applied a logit transformation to land use values (proportion values) and a log transformation to the remaining variables (continuous values). After the transformation procedure, all variables were centred to mean=0 and standardized to SD=1, to enable the direct comparison of the effect sizes.

We explored the relationships among predictor variables (environmental, pressure and stressor variables) using Principal Component Analyses (PCA) to assess the importance of controlling for the natural environmental gradients and detect problems of collinearity. PCA was computed using the correlation matrix.

The Variance Inflation Factor (VIF) was used to quantify collinearity (Zuur et al. 2007). This method has the advantage of accounting for non-linear relationships, which may remain undetected using correlation analysis. A VIFs >8 indicates variance-inflated variables (Zuur et al. 2007). We used this criteria to exclude predictors in a stepwise fashion, by starting to remove the predictor with the highest VIF and repeating the VIF computation until all variable's VIFs were <8. We used the function vifstep of the package usdm that automatically performs the stepwise deletion based on a VIF threshold defined by the user (Naimi 2015).

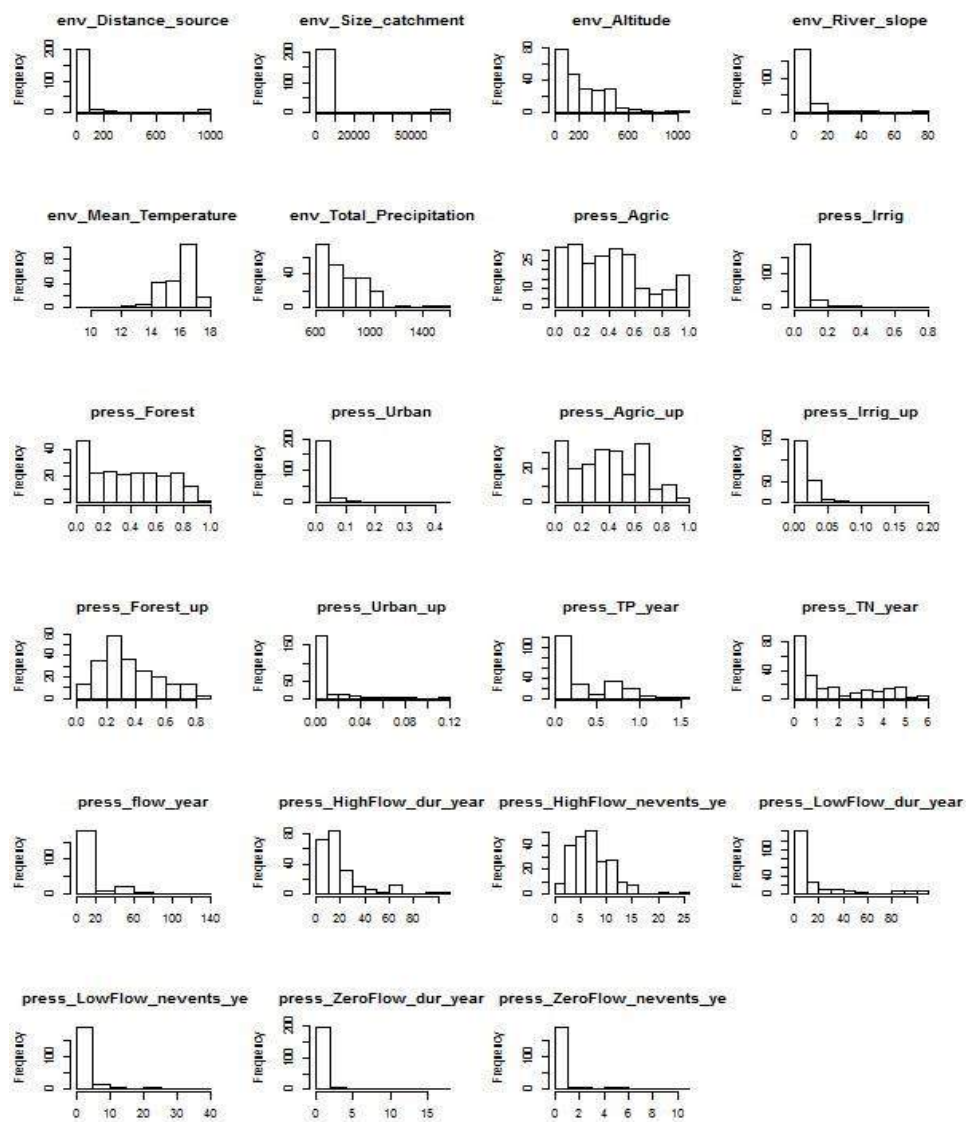


Figure 4.60 Histograms of environmental, pressure and stressor variables before transformation.

Selection of fish-based metrics

For the analyses carried out with the EFI+ dataset, we retained 55 of the available 118 fish-based metrics. These were based on 3 tolerance classifications and 9 functional; we did not consider the density-based metrics since only one sampling occasion was available for each site, carried out in different seasons. This led to a high variability among sites that do not necessarily reflect exclusively site characteristics. Only metrics based on species counts were therefore used as candidate indicators. These metrics were either based on number of species or % of species and were included in three main types: (1) taxon and functional diversity (3 metrics: number of native species and functional dispersion), (2) functional trait guilds (11 functional traits, Table 4.20) and (3) tolerance guilds (3 types, Table 4.20). To classify the metrics into homogeneous groups, we used a hierarchical classification of metrics using Euclidean distances and the unweighted pair-group average method. To investigate the response of biotic state variables to stressors we then selected a set of fish-based indicators that was as much as possible representative of the resulting metrics groups.

Exploratory analysis of pressure/stressor importance and potential interactions

A first analysis was performed to explore the strength of the relationship between biotic indicators and stressors using two machine learning techniques: Boosted Regression Trees (BRT) and Random Forests (RF). Because these techniques have almost no data assumptions and can handle non-linear effects, while lacking more formal statistical inference procedures, they are very adequate for exploratory purposes. They were used to select sets of more responsive biotic indicators as well as more influential predictors. These methods also allowed to assess the most potential pairwise interactions among predictor variables.

BRT is an ensemble methodology that combines two modelling techniques, (i) regression trees - that use binary splits to adjust the response to the predictors; and (ii) boosting - a method that combines multiple models to increase predictor ability. BRT adjusts trees that increasingly explain bits of the data that are not explained by previous trees. This method has the advantage of handling any kind of predictor variables in the same analysis, to deal with collinear predictors, handling non-linear responses and dealing automatically with interactions among predictor variables (Elith et al., 2008).

Table 4.20 Functional guilds

Trait	Class/Guild	abbreviation
Habitat degradation tolerance	Intermediate	HTOL_HIM
	Intolerant	HTOL_HINTOL
	tolerant	HTOL_HTOL
General water quality tolerance	Intermediate	WQgen_IM
	Intolerant	WQgen_INTOL
	tolerant	WQgen_TOL
Cluster based on tolerance guilds - 3 groups	Intermediate	CLU5_3_Intermediate
	Intolerant	CLU5_3_Intolerant
	tolerant	CLU5_3_Tolerant
Adult trophic guild	Detritivorous	Atroph_DETR
	Insectivorous	Atroph_INSV
	Omnivorous	Atroph_OMNI
Feeding habitat	Benthic	FeHab_B
	Water column	FeHab_WC
Habitat	Eurytopic	Hab_EURY
	Limnophilic	Hab_LIMNO
	Rheophilic	Hab_RH
Habitat spawning preferences	Eurytopic	HabSp_EUPAR
	Limnophilic	HabSp_LIPAR
	Rheophilic	HabSp_RHPAR
Migration guild	Long catadromous	Mig_LONG_LMC
	Potamodromous	Mig_POTAD
	Resident	Mig_RESID
Parental care	No protection	PC_NOP
	Protection (eggs and/or larvae)	PC_PROT
Reproductive guild	Lithophilic	Repro_LITH
	Pelagic	Repro_PELA
	Phyto-lithophilic	Repro_PHLI
	Phytophilic	Repro_PHYT
	Polyphilic	Repro_POLY
	psammophilic	Repro_PSAM
Reproductive behaviour	Fractional spawners	ReproB_FR
	Single spawners	ReproB_SIN

To fit BRT models, we followed the procedures proposed by Elith et al. (2008). To optimize the number of trees of each model, a stepwise procedure based on 10-fold cross validation. The number of trees needed for correct predictions are determined by the learning rate, which sets the contribution of each tree to the model, and by the tree complexity, that defines the maximum interaction order that the model will consider (e.g. $tc=2$ allows to-way interactions to be considered). Tree complexity was set to 2 and for each species the learning rate was adjusted to ensure that, approximately, from 1000 to 1500 trees were combined into the final model (Elith et al., 2008).

The importance of each environmental variable in the model (variable importance) was estimated by averaging the number of times a variable is selected for splitting a tree in the BRT model and the squared improvement resulting from these splits (Friedman, 2001). BRT modelling was performed with packages `gbm` (Ridgeway, 2007) and `dismo` (Elith et al., 2008; Hijmans et al., 2013) for R version 3.2.3 (R Core Team, 2015). In the `dismo` package, an algorithm is also available to identify the most potential pairwise interactions and rank their importance.

We used BRT to model all 55 fish-based metrics retained from the EFI+ Tagus dataset based on the predictor variable set resulting from the stepwise VIF selection procedure to select the most responsive metrics of each group. We specified the Poisson family in BRT for metrics based on species counts and the Gaussian family for metrics based on proportions and EQR.

Along with the BRT, RF is a machine learning technique based on classification and regression trees (Breiman 2001). In opposition to BRT, that sequentially adjust trees to the residuals of previous ones, RF produces a number of concurring trees and the model estimates are obtained using the mode or mean predictions of the individual trees. RF has the same flexibility as BR in handling different kinds of variables, response shapes and interactions. The number of metrics randomly selected at each tree node and the minimum number of unique observations in a terminal node were both fixed at 5. The percentage of variance explained by the model (i.e. goodness-of-fit) was estimated based on the out-of-bag observations.

The importance of each predictor variable in the Random Forest models, were computed using an approach based on Breiman-Cutler permutations. For each tree, the prediction error in the out-of-bag data is recorded and then for each predictor the cases are randomly permuted and the prediction error is recorded. The variable importance (VIMP) is then defined as the difference between the perturbed and unperturbed error rate averaged over all trees in the Forest (Ishwaran, 2007). A measure of relative importance (%) expressing the proportion of each VIMP to the sum of VIMP of all stressors was then computed in order to compare the variable importance among different fish metrics. The same permutations also allow to test the paired importance of variables and to rank the most potential pairwise interactions. Random forests and VIMP were computed with the R package `randomForestSRC` (Ishwaran and Kogalur 2016).

The mean rank variable importance according to BRT and RF was computed for each predictor variable and used to guide the selection of candidate variables to be included in the subsequent analyses based regression-based analytical tools.

Quantitative analysis of pressure/stressor effects and interactions

After assessing the stressors and interactions that most likely are affecting the biotic indicators with BRT and RF, it is important to demonstrate the strength of these effects using a more formal statistical approach. We therefore followed a second analytical step based on regression-based analytical tools, including Generalized Linear Models (GLM; McCullagh and Nelder, 1989) and Generalized Linear Mixed Models (GLMM; Zuur et al. 2009).

In the case of fish based-metrics based on proportions of species, we used GLM of the binomial family with the logit link function following the R codes described in Crawley (2007). To model the metric based on number of species we used a GLM of the Poisson family with a log link function. In the case of the National EQR indices, because we had two sample occasions available, we used a GLMM using site as the random factor. Since it only had two classes, the variable Year could not be included as a random factor. Hence, we included year as a candidate variable in the models to account for its potential effect.

To select GLM and GLMM models we used a Multi-model inference based on the information theoretic approach (ITA) (Burnham & Anderson, 2002), using the Akaike information criterion (AIC) as a measure of information loss of each candidate model, with the best fitting models having the lowest AIC and consequently the highest Akaike weight (w_i). We first used the $\Delta AIC \leq 2$ criteria to select the top models that potentially best describe multiple-stressor patterns. We then inspected the z-test results for each averaged variable coefficient to select variables for the final best approximating models. Candidate models were selected using all combinations of a maximum of four predictor variables. Multi-model inference was performed with the MuMIn package for R (Bartoń 2016).

A Moran's test was performed to check for spatial autocorrelation in the residuals of the best approximating model. In the case Moran's I was > 0.1 and the p-value < 0.001 , we used an eigenvector-based spatial filtering approach (Griffith & Peres-Neto 2006) to cancel the bias introduced by the spatial autocorrelation of the residuals. Both Moran's I test and spatial filtering

were computed with the `spdep` package for R (Bivand 2011) using, respectively, “Moran.test” and “ME” functions.

We computed pseudo R-squared to assess models’ goodness-of-fit. For GLM we used a coefficient of determination derived from the likelihood-ratio test, based on an improvement from null (intercept only) model to the fitted model. For GLMM we computed the conditional and marginal coefficient of determination (Nakagawa & Schielzeth, 2013). The marginal pseudo R-squared represents the variance explained by fixed factors, while the conditional pseudo R-squared represents the variance explained by both fixed and random factors. All pseudo R-squared for GLM and GLMM were computed with the functions `squaredLR` and `r.squaredGLMM` of the `MuMIn` package for R (Bartoń 2016).

Models that showed pseudo R-squared values > 0.2 and had no significant problems of autocorrelation in the residuals, after applying the eigenvector-based spatial filtering, were retained for further interpretation and/or prediction purposes.

Ecosystem services description and modelling

Taking into account the main pressures that are perceived to occur in the future on the Sorraia the ecosystem services considered, were:

- Water for non-drinking purposes:
 - Water abstracted (for irrigation)
 - Surface water availability
- Water purification:
 - Nutrients loads
 - Ecological status of surface water
- Recreation and tourism
- Quality of fresh waters for angling

Process-based modelling allows to quantify and analyze the increase and decrease of the indicators of the ecosystem services under different future scenarios. We considered the simulations

developed in the “Process-based modelling” chapter, including the scenarios developed, as explained above.

The water abstracted is one of the indicators for the ecosystem service “water for non-drinking purposes”. It gives the water quantity that is used to irrigate in millimeters per year, and is obtained directly by the SWAT process-based model, per sub-basin. The surface water availability shows the amount of water available to be used and is obtained by the model with the sum of the flow, baseflow and runoff water, by year and per sub basin, in millimeters. The water purification ecosystem service is related with the influence of the ecosystem has in the nutrients cycling (retention, filtration, loading, decomposition, etc). In the case study of the Sorraia basin, nutrients loads indicator was selected. In the process-base model this is obtained summing the nitrogen lost in runoff and percolation, and the phosphorous lost by runoff, per sub basin in tons/ha/year.

Ecological status of surface waters

The ecological status of surface waters was used as an indicator of the capacity of ecosystems to provide pure water and maintain populations and habitats. We used the final classification of the Ecological Status from the Water Frame Directive biomonitoring program (Portuguese Environmental Agency, APA), computed separately for 2010 and 2011, at 240 sites in the Tagus and Sorraia river basins. The Ecological Status is classified in 5 quality classes: bad, poor, moderate, good, very good. To model the response of Ecological Status to stressors we followed the same empirical modelling framework used with biotic indicators. We used the adequate methods to deal with ordinal scale responses, including Random Forests and Cumulative Link Mixed Models (CLMM) implemented in the “ordinal” package for R (Christensen 2015). We also reclassified Ecological Status into 2 classes using the moderate-good boundary, i.e., aggregating the bad, poor and moderate classes into one class and the good and very good classes into a second class. In this case we used appropriate methods that deal with binary outcomes (Boosted Regression Trees from the Bernoulli family; Random Forests and GLMM from the binomial family). We used only data from 2011 (n=141) to run Boosted regression trees and Random Forests. To run CLMM and GLMM we used all the data and defined site as the random effect. In the case of BRT, we followed a model simplification procedure by eliminating

sequentially the least contributing variables to model fit, performing a k-fold cross validation at each step to help deciding when to stop the selection process (Elith et al. 2008).

Quality of freshwaters for angling

Angling is amongst the most relevant recreational ecosystem services provided by water courses (Oliveira et al. 2009). Angling is a multifaceted outdoor activity centered not only in catching fish but also with a strong component of relaxation, escape and outdoor enjoyment, among other things (Arlinghaus 2006). To quantify the capacity of a site to provide this service in the Sorraia basin and investigate its response to stressors, we used the Fishery Quality Index (FQI) for Portuguese streams, developed by Oliveira et al. (2009). The index is based in the primary game species sought by Portuguese anglers, including the native brown trout *Salmo trutta*, the cyprinid *Luciobarbus bocagei*, the chubs *Squalius carolitertii* and *S. pyrenaicus*, and the nases *Pseudochondrostoma duriense* and *P. polylepis*, plus the nonnative common carp *Cyprinus carpio*, pumpkinseed *Lepomis gibbosus*, and largemouth bass *Micropterus salmoides*. For each species a Species Quality Index (SQI) is first computed. SQIs are based on the average of four biological metrics commonly related to the performance and fishery quality of a species: recruitment, abundance of legally catchable specimens, a measure of large specimens (maximum individual total length of a species at a site), and an estimate of overall abundance (species total CPUE). SQIs are then weighted according to the preferences of anglers and summed up to give the final FQI score.

To investigate the response of FQI to stressors we followed the same empirical modelling framework used with biotic indicators. Because we had only 63 sites with data required to compute FQI, we used only Random Forest as the exploratory analysis. A linear regression model was then used to quantify the responses to stressors and test interactions.

4.4.4 Scenarios development

To assess the impact of the climate scenarios on the aquatic ecosystems, WP2.6 advised the use of the climate scenarios produced by the project ISIMIP, and proposed especially the application of the outcomes of model GFDL-ESM2M and model IPSL-CMA-LR for each climate scenario,

to all case studies. For each model the RCPs 4.5 and 8.5 runs (Moss et al. 2010) were considered for each Storyline defined in MARS project (Panagopoulos, et al 2015). Storylines are described below.

- GFDL-ESM2M

orcp4p5 is for MARS Storyline 2 (used in this text as GFDL2)

orcp8p5 is for MARS Storyline 1 and for MARS Storyline 3 (used in this text as GFDL13)

- IPSL-CM5A-LR

orcp4p5 is for MARS Storyline 2 (used in this text as IPSL2)

orcp8p5 is for MARS Storyline 1 and for MARS Storyline 3 (used in this text as IPSL13)

Meteorological data available in the Sorraia river basin was analyzed and compared with the data available corresponding to each climate model. This is the first step to develop the Bias correction. Only after the Bias Correction, climate data, from the IPSL and GFDL models, can be applied to the process-based model SWAT. It was observed (Figure 4.61) that in average wind is overestimated by 0.5 to 1.5 m/s, temperature is also overestimated ca. 3 to 4°C, precipitation is more realistic during the summer period and overestimated during winter, and solar radiation does not fit at all.

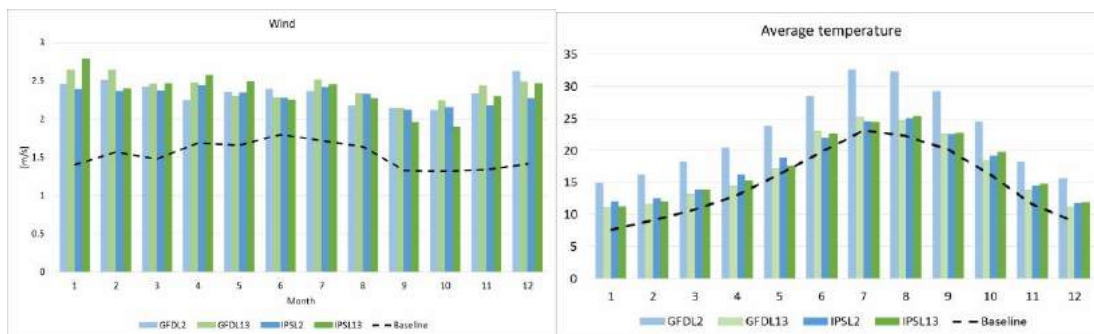


Figure 4.61 Comparison between meteorological data observed and climate modeled data for the period 2006-2015.

In this work only precipitation and temperature were corrected and implemented in the process-based model SWAT. The temperature and precipitation data series were bias corrected (Table 4.21) according to the methods developed by Shrestha M. (2015) using the excel spreadsheet made available by Shrestha M. Monthly factors of temperature (maximum and minimum) and precipitation were obtained and applied to the climate data from the models available.

Storylines were defined to the Sorraia case study according with the feedback obtained with the stakeholders during the MARS project (Table 4.22). MARS project set 3 storylines (Panagopoulos, et al 2015):

- 1)'Techno World' represents a rapid global economic growth, enabling technological development but with high energy demands and no real drive to specifically enhance or ignore natural ecosystem health. This world is based on a combination of SSP5 and climate scenario 8.5.
- 2)'Consensus world' represents a world where current policies continue after 2020, economy growing at the same pace as now, with awareness for environment preservation. This world is based on a combination of SSP2 and climate scenario 4.5.
- 3)'Survival of the fittest' represents a fragmented world driven by countries own interests, with fast economic growth in NW Europe but decrease in other regions, with minimal or no investment and effort in environmental protection, conservation and restoration. This world is based on a combination of SSP3 and climate scenario 8.5.

Table 4.21. Monthly bias correction factors for temperature and precipitation

Month	Temperature factor				Precipitation factor			
	GFDL2	IPSL2	GFDL13	IPSL13	GFDL	IPSL2	GFDL13	IPSL13
1	-12.498	-7.220	-9.192	-8.475	0.746	0.711	0.524	0.769
2	-11.982	-7.313	-8.488	-8.447	0.722	0.770	0.724	0.643
3	-10.972	-6.019	-6.855	-6.273	0.635	0.829	0.516	0.738
4	-9.728	-5.608	-5.639	-5.950	0.682	0.673	0.646	0.708
5	-7.226	-4.604	-4.055	-4.190	0.274	0.234	0.281	0.258
6	-5.084	-0.415	-1.265	-1.366	0.133	0.123	0.145	0.131
7	-0.894	3.495	3.214	3.567	0.006	0.007	0.007	0.007
8	-1.304	3.261	3.386	3.673	0.024	0.025	0.022	0.020
9	-2.367	2.368	1.975	1.992	0.203	0.235	0.206	0.217
10	-4.888	-0.963	-1.334	-0.704	1.138	0.838	1.252	0.824
11	-9.117	-6.111	-5.042	-5.554	0.822	1.061	0.852	1.084
12	-11.543	-6.980	-7.612	-8.068	0.818	1.175	0.772	1.172

Table 4.22.Sorraia basin stakeholders

Stakeholder	Responsibilities / interests
ARBVS www.arbvs.pt	Land management, water managements, reservoirs
FENAREG www.fenareg.pt	Land management, water managements
EDP www.edp.pt	Energy
ICNF www.icnf.pt	Forest conservation
APA www.apambiente.pt	Land planning and management, regulatory responsibilities
ALTRI	Forest plantations
Tomasor - Sociedade de Produtores Agrícolas de Tomate do Vale do Sorraia e Sul, Lda	Tomato Industry
ORIVÁRZEA - Orizicultores da Várzea de Samora e Benavente, SA http://www.orivarzea.pt/	Rice Industry
Verdeleite - Sociedade de Exploração Agro-Pecuaria de Leite e Gado Lda	Stock raising Industry
Municipality of Coruche www.cm-coruche.pt	Municipalities
Municipality of Ponte de Sôr http://www.cmpontedesor.pt/	Municipalities
Municipality of Avis http://www.cmavis.pt/	Municipalities
Municipality of Arraiolos http://www.cm-arraiolos.pt/	Municipalities
Municipality of Montemor-o-novo http://www.cm-montemornovo.pt/	Municipalities

Sorraia is a typical agriculture basin and all economy and growth is associated with it. The three tables below (Table 4.23, 4.24 and 4.25) show the change that can happen on each storyline.

Table 4.23.Element change according to Storyline 1, 2 and 3

Criteria	Element	Techno World		Consensus World		Survival World	
		Storyline 1		Storyline 2		Storyline 3	
		2030	2060	2030	2060	2030	2060
Environ ment and Ecosyst ems	<i>Desertificat ion</i>	Decreasing 20% natural forest areas and shrubland	Decreasing 25% natural forest areas and shrubland	Decreasing 10% natural forest areas and shrubland	Decreasing 15% natural forest areas and shrubland	Decreasing 30% natural forest areas and shrubland	Decreasing 35% natural forest areas and shrubland
	<i>Growth of non-native plantations</i>	10% increase in eucalyptus	15% increase in eucalyptus	10% increase in eucalyptus	15% increase in eucalyptus	30% increase in eucalyptus	35% increase in eucalyptus

Criteria	Element	Techno World		Consensus World		Survival World	
		Storyline 1		Storyline 2		Storyline 3	
		2030	2060	2030	2060	2030	2060
Land use change	<i>Urbanization</i>	Increasing 5% urban areas – Slow population increase	Increasing 10% urban areas – Slow population increase	No change	No change	Increasing 15% urban areas – Rapid population growth	Increasing 20% urban areas – Rapid population growth
	<i>deforestation</i>	Decreasing 20% forest areas	Decreasing 25% forest areas	Decreasing 10% forest areas	Decreasing 15% forest areas	Decreasing 30% forest areas	Decreasing 35% forest areas
Agriculture	<i>Nutrient load</i>	Increasing 10% of fertilizers due to biofuel crops	Increasing 15% of fertilizers due to biofuel crops	Decreasing 10% of fertilizers	Decreasing 15% of fertilizers	Increasing 30% of fertilizers	Increasing 35% of fertilizers
	<i>Efficient use of resources</i>	Decreasing 30% of water for irrigation	Decreasing 35% of water for irrigation	Decreasing 20% of water for irrigation	Decreasing 20% of water for irrigation	Increasing 30% of water for irrigation	Increasing 30% of water for irrigation
	<i>Agricultural areas for crops</i>	Increasing 5% agricultural areas for crops	Increasing 10% agricultural areas for crops	No change	No change	Increasing 15% agricultural areas for crops (With no trade agreements, each country will have to try to be self-sufficient)	Increasing 20% agricultural areas for crops (With no trade agreements, each country will have to try to be self-sufficient)
	<i>Efficient irrigation</i>	Increasing 30% of efficiency	Increasing 35% of efficiency	Increasing 20% of efficiency	Increasing 25% of efficiency	Decreasing 30% of efficiency	Decreasing 35% of efficiency
	<i>Industrialization</i>	Increasing 15% industry areas	Increasing 20% industry areas	No increase of industry areas	No increase of industry areas	Increasing 10% industry areas	Increasing 10% industry areas
	<i>Use of fertilizers</i>	Increasing 10% fertilizers	Increasing 15% fertilizers	Decreasing 10% fertilizers	Decreasing 15% fertilizers	Increasing 30% fertilizers	Increasing 35% fertilizers
	<i>Water pollution</i>	5% events of faecal coliforms	5% events of faecal coliforms	10% decrease of events in faecal coliforms	10% decrease of events in faecal coliforms	30% increase in events of faecal coliforms	30% increase in events of faecal coliforms
	<i>Local agriculture</i>	Biofuel crops	Biofuel crops	No change	No change	Increasing 30% agriculture	Increasing 35% agriculture
Water levels	<i>Environmental flow needs covered</i>	10% flow retained for environmental needs	15% flow retained for environmental needs	35% flow retained for environmental needs	40% flow retained for environmental needs	No flow retention for environmental needs	No flow retention for environmental needs
	<i>Natural flood retention</i>	Hydropower will increase	Hydropower will increase	Environmental policies will persist past 2020 but climate change	Environmental policies will persist past 2020 but climate change	Hydropower will increase	Hydropower will increase

Criteria	Element	Techno World		Consensus World		Survival World	
		Storyline 1		Storyline 2		Storyline 3	
		2030	2060	2030	2060	2030	2060
				will force dams and weirs to be built	will force dams and weirs to be built		
	<i>Increase water reservoirs and weirs</i>	Increasing 20%	Increasing 25%	Increasing 10%	Increasing 15%	Increasing 30%	Increasing 35%
	<i>Overexploitation of water resources</i>	Increasing 20%	Increasing 25%	Increasing 10%	Increasing 15%	Increasing 30%	Increasing 35%
	<i>Water use efficiency</i>	Increasing 30%	Increasing 35%	Increasing 10%	Increasing 15%	Decreasing 30%	Decreasing 35%
	<i>Restoration of riparian zones</i>	No change	No change	10% increase in riparian width	10% increase in riparian width	30% decrease in riparian width	30% decrease in riparian width

These changes were introduced into SWAT model by altering inputs that can be adjusted to run future scenarios with the climate models. Table 4.28 shows the adjustments done to represent each storyline. The Mediterranean climate will impose additional stresses on agriculture in the basin, so all the changes were focused on management practices, such as fertilizer application amount and precipitation. The MARS project defined two-time period to run the models: 2030 and 2060. These two periods are defined as an average of the 10 years for the period between 2025 and 2035, and 2055 and 2065. For each storyline and timeline, the land use evolution area is presented in the table below.

Table 4.24. Evolution of land use area (in percentage) for the storylines defined (km²).

Land Use	Area (km ²)						
	Baseline	STL1_2030	STL1_2060	STL2_2030	STL2_2060	STL3_2030	STL3_2060
Agriculture	1606.7	1687.5	1765.6	1606.7	1606.7	2088.3	2175.4
Forest	3458.2	2763.6	2589.0	3114.1	2828.3	2417.7	2214.9
Industrial	2.03	2.40	2.60	2.03	2.03	2.19	2.38
Water bodies	18.9	18.9	18.9	18.88	18.88	18.88	18.88
Eucalyptus	-	0.10	0.15	0.10	0.15	0.32	0.32
Urban	-	0.07	0.10	-	-	0.11	0.28
Others	2485.1	3098.3	3194.5	2829.1	3114.9	3043.4	3158.8

Table 4.25. Adjustments made to the inputs of the SWAT model

Storyline	Time	Management Practices	Variation (%)	Baseline	Scenario
STL1	2030	Fertilization (kgN/ha)	10+	492	541
	2060		15+		566
	2030	Irrigation (mm)	30-	430	301
	2060		35-		280
STL2	2030	Fertilization (kgN/ha)	10-	492	443
	2060		15-		418
	2030	Irrigation (mm)	20-	430	344
	2060		25-		323
STL3	2030	Fertilization (kgN/ha)	30+	492	640
	2060		35+		664
	2030	Irrigation (mm)	30+	430	559
	2060		35+		581

4.4.5 Implementations of measures

The Program of Measures for the Sorraia Basin (Table 4.26) aiming at attaining the good quality status is essentially related to the improvement of the efficiency and sustainability of the use of water resources. In the Sorraia River basin the main focus is on water quality affected by agriculture, livestock and river regulation.

In this work the measures presented on the RBMP were adapted, taken into account the capabilities of the process-based model SWAT. It was tested 4 measures:

1. No regulation – in this measure SWAT model was implemented without reservoirs, and all agriculture areas are using the nearest river to irrigate the crops;
2. Change Agriculture practices – in this measure SWAT model was implemented considering the automatic irrigation/fertilization option. In this option, we assumed that farmers are irrigating and applying the fertilizers optimally.
3. Application of the measures 1. and 2. – in this measure we assume the absence of reservoirs and optimum agriculture.

4. Land use changes – in this measure we assume that all Sorraia Basin changed to forest, with no reservoirs and no agriculture.

Table 4.26. Program of measures to be implemented in the River Basin Management Plan (RBMP) that are relevant for the Sorraia basin

Measure code	Aim of the measures
SUP_P347_AT1	Increase the efficiency of Water treatment plants and/or renewal of the distribution net to overcome the failure to attain quality parameters.
SUP_P36_AT1	Efficient solutions for the drainage and wastewater treatment of small urban areas.
SUP_P2_AT1	Implementation of good agricultural practices (rational fertilization, handling and storage of chemical fertilizers; handling and storage of cattle effluents; soil management and use considering the nitrogen dynamics; irrigation management and pollution prevention by nitrates).
SUP_P9_AT2	Irrigation management (improvement of irrigation practices, namely the decrease of losses of irrigation systems).
SUP_P39_AT1	Construction of new livestock effluents treatment plants.

4.4.6 Results

4.4.6.1.1 Process-based modelling

After the model calibration and validation to the baseline presented on chapter 7.1, SWAT model was implemented considering the scenarios developed on chapter 4.4. Hydrological modelling has the advantage of estimate water balance and nutrients in watersheds for different scenarios. Table 4.27 shows the precipitation, flow and actual evapotranspiration for each storyline modelled in Sorraia basin. For the future scenarios, the water available in the Sorraia basin will decrease (precipitation), having a significant impact on river flow and as a consequence the actual evapotranspiration will increase in percentage because of the evaporation from soil water and the transpiration by plants. Figure 4.27 shows the weights of each variable for the baseline and for the scenarios. It is observed that even in the most aggressive scenario (in terms of amount of precipitation and temperature) the water balance in the Sorraia basin is similar, where about of 20% of the available water is evapotranspired and about 20% flows to the river. Figure

4.63 shows the water balance, in percentage, with precipitation, runoff, percolation, flow and actual

evapotranspiration for each storyline and timeline. The scenarios developed with the climate model IPSL to the storyline 1 and 3 shows a similar amount of water in river and evapotranspired. When comparing climate model impact, the water flow in river decreases when considered the climate model GFDL, having a considerable impact on the basin dynamics.

Table 4.28 shows the loads of nutrients (nitrogen and phosphorous in ton/ha/year) and sediments (ton/ha/year) in Sorraia River. These model results can show the reflection of the management practices, land use and climatic changes. The increase of the agriculture in area (Storylines 1 and 3) or the increase of the fertilizer (Storylines 1 and 3) and water amount (Storyline 3) can lead to an increase in nutrient loads to the river. Of course the increase in precipitation will influence the concentration of these nutrients. Figure 4.64 shows the variation of the amount of sediments in the river for each storyline considered. Sediments loads can be seen as proxies for the erosion occurring in the basin and of the potential capacity to transport phosphorus adsorbed on it.

Table 4.27. Total annual of precipitation, flow and actual evapotranspiration (in mm) for each implemented scenario

Scenario		Precipitation (mm)	Flow (mm)	Evapotranspiration(mm)
Baseline		611	325	267
Storyline 1	GFDL_2030	245	66	159
	GFDL_2060	232	42	168
	IPSL_2030	333	147	162
	IPSL_2060	326	131	166
Storyline 2	GFDL_2030	253	67	164
	GFDL_2060	230	44	161
	IPSL_2030	226	73	142
	IPSL_2060	272	103	164
Storyline 3	GFDL_2030	246	58	168
	GFDL_2060	232	42	168
	IPSL_2030	333	136	173
	IPSL_2060	326	132	165

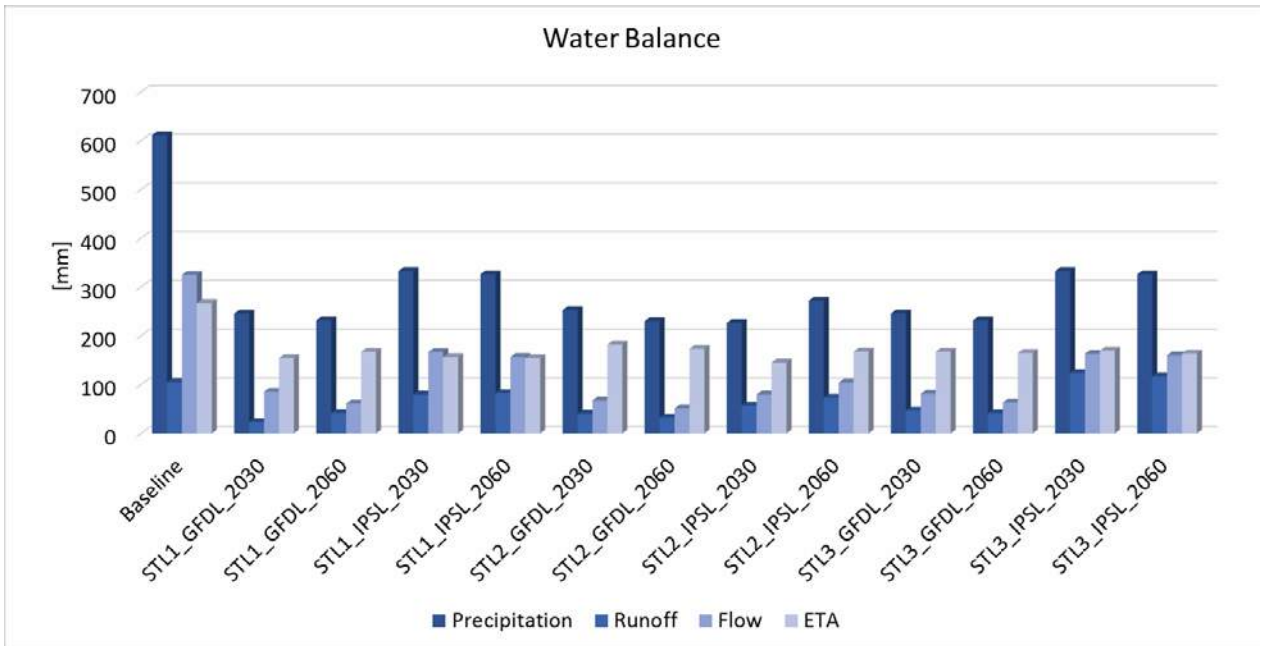


Figure 4.62 Water balance in mm for each for each Storyline: precipitation, runoff, flow and actual evapotranspiration

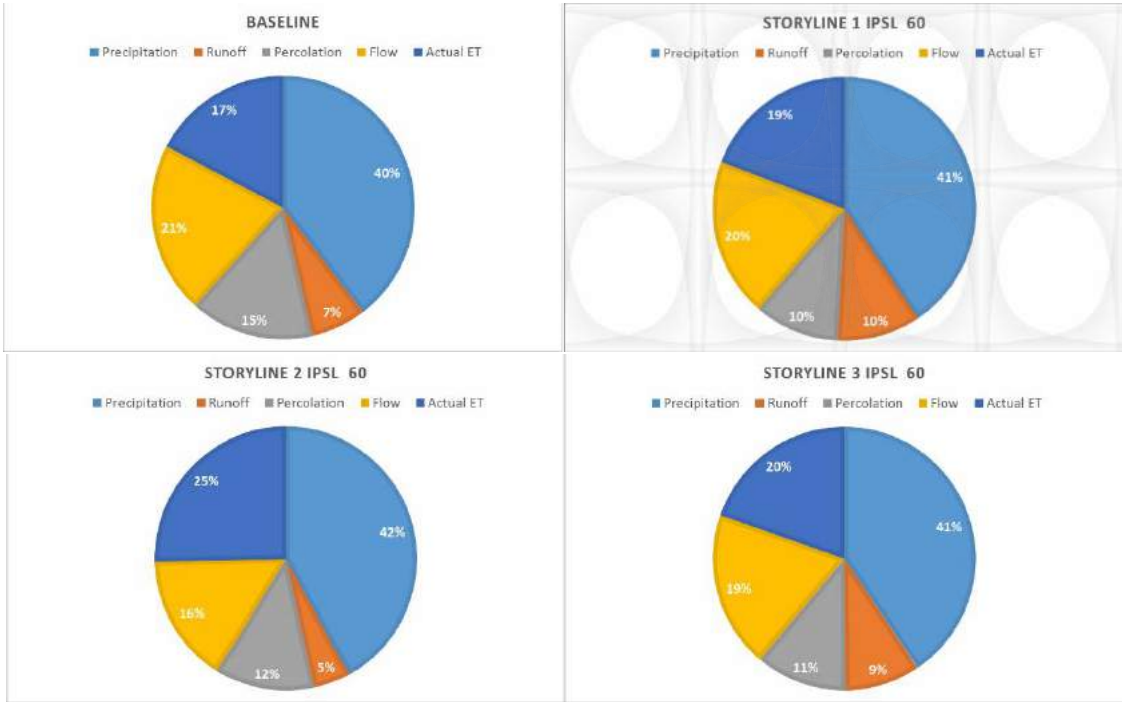


Figure 4.63 Water balance in % for each scenario (IPSL climatic model and 2060 timeline example): Precipitation, runoff, percolation, flow and actual evapotranspiration

Table 4.28. Total amount of nutrients and sediments for each scenario (ton/ha/year)

Scenario		Tot P	Tot N	Sediments
Baseline		1.8	16.5	3.7
Storyline 1	GFDL_2030	0.9	15.3	0.7
	GFDL_2060	1.2	14.4	0.8
	IPSL_2030	2.9	22.7	4.2
	IPSL_2060	3.2	23.7	3.7
Storyline 2	GFDL_2030	0.5	9.7	0.8
	GFDL_2060	0.3	8.3	0.5
	IPSL_2030	0.9	13.0	1.3
	IPSL_2060	1.2	13.0	2.2
Storyline 3	GFDL_2030	1.0	17.9	0.8
	GFDL_2060	1.1	22.3	0.9
	IPSL_2030	3.8	29.2	5.1
	IPSL_2060	3.8	36.6	4.6

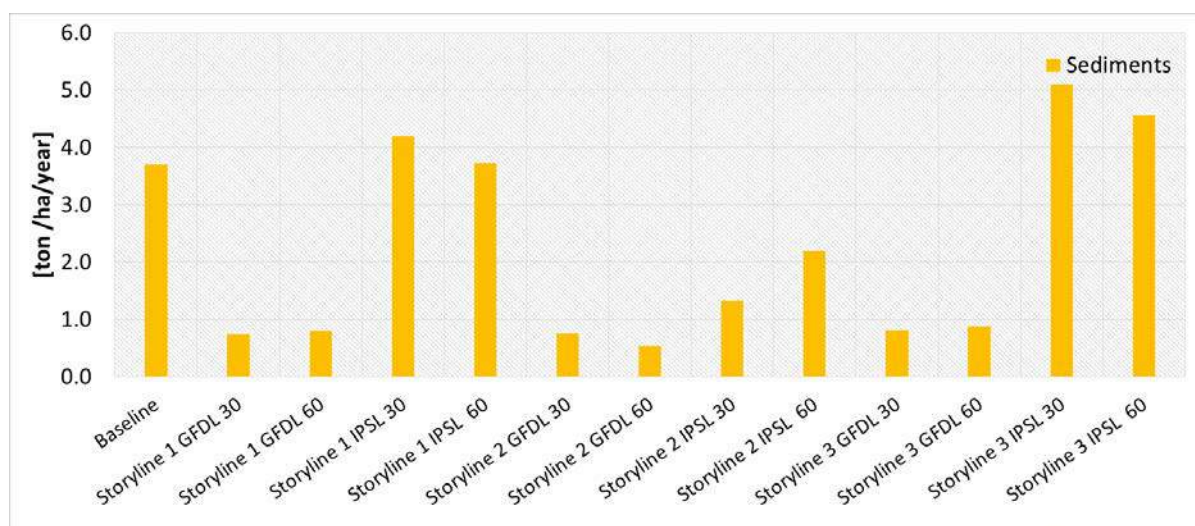


Figure 4.64 Sediments in ton/ha/year for each Storyline

4.4.6.1.2 Empirical modelling and linkage between pressures and biotic indicators

Data validation and preparation for empirical modelling

For the EFI+ Tagus dataset, the first two axis of the PCA based on the environmental, pressure and stressor variables explained 43% of the variation (see Fig. 7.15). A covariability between stressor variables and natural environmental gradients was found (Fig. 4.65). For example, the % of agriculture, irrigation and urban areas (both in the upstream and primary catchments) were positively related with the distance to source and temperature, while the % of forest in the

upstream catchment was positively related with river slope, altitude and total precipitation. These relationships reflect a gradient of increasing pressures from inland towards the coast and confirm the need to consider natural environmental gradients when testing the effects of multiple stressors on biotic indicators.

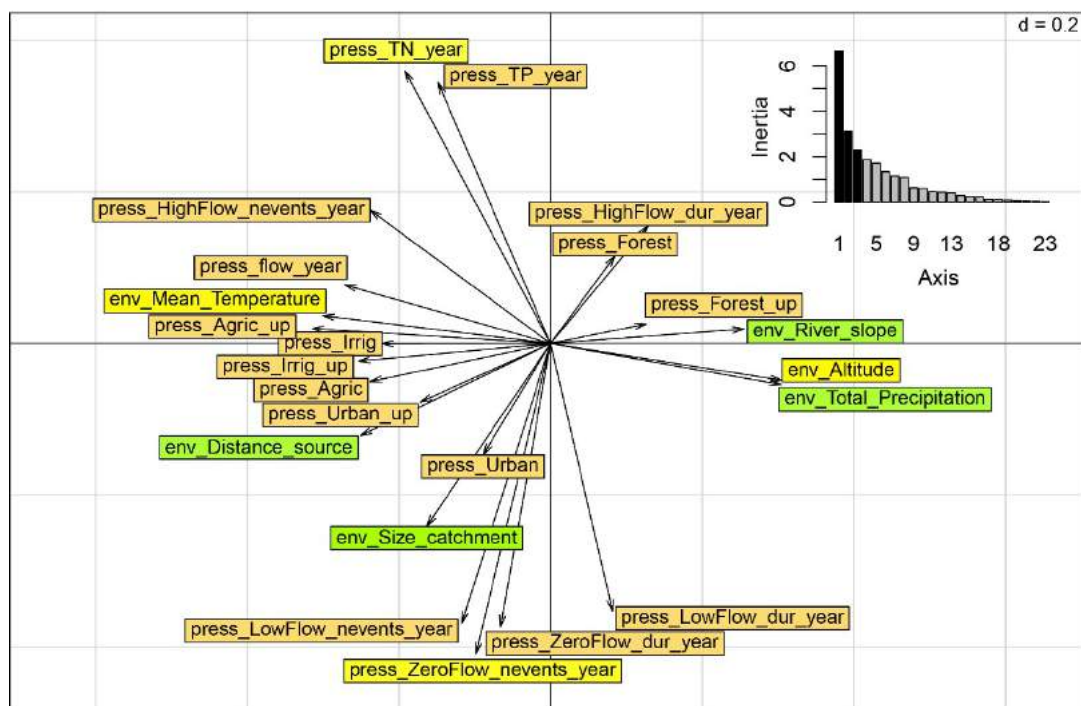


Figure 4.65 First plane of the PCA using environmental, pressure and stressor variables (Tagus EFI+ dataset). Green rectangles indicate environmental variables; orange rectangles indicate abiotic stressors; yellow rectangles indicate predictors removed according to

In the Tagus EFI+ dataset, one environmental variable (mean annual temperature) and two stressor variables (total Nitrogen and number of zero flow events per year) were removed from subsequent analyses based on this procedure (Table 4.29; Fig. 4.65). Because Altitude was highly correlated with total precipitation and a higher VIF we also decided to remove also this variable from subsequent analyses.

Selection of fish-based metrics

The cluster analysis of the fish-based metrics originated five major groups of metrics (Fig. 4.66). We considered 3 sub-groups within one metric group (Group 3, Fig. 7.5.5), since it resulted very heterogeneous. For each group, the most responsive metrics according to BRT was selected: % of potamodromous species (Group 1), % of tolerant species (Group 2), % of intolerant species (Group 3A), number of potamodromous species (Group 3B), % of detritivorous species (Group 3C), % of invertivorous species (Group 4) and % of native species (Group 5).

Table 4.29. VIF values of the selected set of environmental, pressure and stressor predictors.

Variables	VIF	VIF
	(EFI+ Dataset)	(APA dataset)
Distance to source	7.08	-
Size of the upstream catchment	2.44	2.21
Altitude	6.01	2.19
River slope	2.03	1.44
Total Precipitation	5.82	-
% Agriculture in the primary catchment	3.90	-
% Irrigated croplands in the primary catchment	2.32	-
% Forest in the primary catchment	2.98	-
% Urban in the primary catchment	1.53	-
% Agriculture in the upstream catchment	6.17	2.61
% Irrigated croplands in the upstream catchment	2.63	1.27
% Forest in the upstream catchment	2.87	2.11
% Urban in the upstream catchment	1.94	1.42
Total P annual mean	1.84	3.64
Total N annual mean	-	2.68
Annual Mean Flow	6.64	2.51
High flow pulse - mean duration (days)	6.12	1.36
High flow pulse - Number of events/year	7.52	2.85
Low flow pulse - mean duration (days)	2.82	1.37
Low flow pulse - Number of events/year	2.24	1.66
Zero flow pulse - mean duration (days)	1.41	2.54
Zero flow pulse - Number of events/year	-	2.56

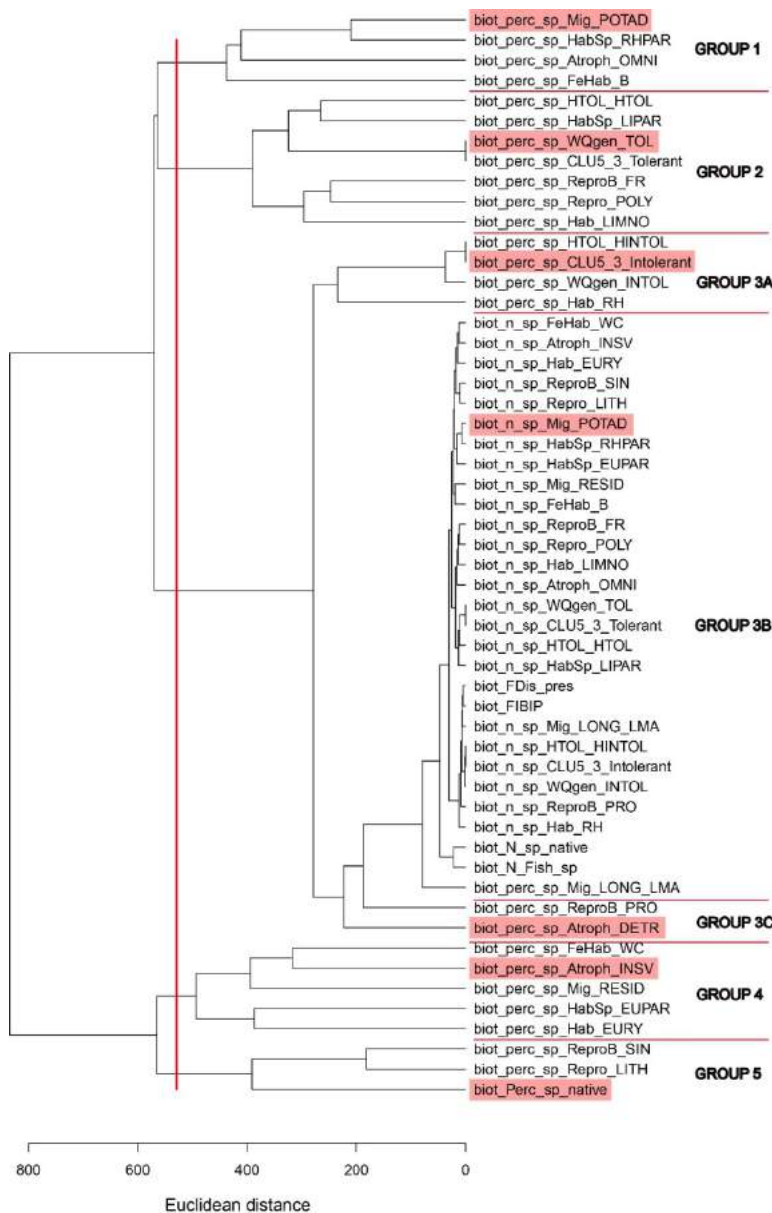


Figure 4.66 Dendrogram of the hierarchical classification of fish based metrics using Euclidean distances and the unweighted pair-group average method. Highlighted metrics indicate the metrics that were used analyse the response to multiple stressors.

Explanatory analysis of pressure/stressor importance and potential interactions/Strength of the response

According to the correlation of fitted values with the metrics in the training dataset, the fish-based metric with the stronger link with stressor variables was the % of Intolerant species (Table 4.30). The % of tolerant species was the fish-based metric that yielded BRT models with the highest

predictive ability, according to the cross-validation results. Among the national EQR indicators, the EQR of diatoms, macroinvertebrates and fish yielded the best models according to the resulting correlations in the training dataset. The model for the national EQR of the fish biotic integrity index showed the strongest predictive power among all the analysed indicators.

Table 4.30. Goodness-of-fit measures of BRT models for the selected fish-based metrics and ecological quality ratios for macroinvertebrates, diatoms, macrophytes and fish.

Fish-based metrics	mean total deviance	mean residual deviance	Correlation - training	Correlation - Cross- validation	SE cross validation
% potamodromous sp.	542.277	173.941	0.840	0.563	0.067
% tolerant sp.	887.504	370.34	0.787	0.637	0.053
% intolerant sp.	264.459	41.39	0.926	0.575	0.013
N potamodromous sp.	0.861	0.285	0.899	0.606	0.030
% detritivorous sp.	130.636	45.364	0.828	0.555	0.045
% invertivorous sp.	525.215	237.079	0.841	0.442	0.074
% native sp.	706.43	363.530	0.732	0.562	0.047
EQR diatoms	0.027	0.007	0.884	0.468	0.085
EQR macrophytes	0.009	0.005	0.780	0.376	0.083
EQR macroinvertebrates	0.065	0.014	0.900	0.591	0.046
EQR fish	0.111	0.024	0.897	0.770	0.029

Variable importance

Different kinds of predictor variables tended to show different abilities to explain biotic indicators. In general, for fish-based metrics and national EQR indicators, the variables describing the natural environmental variability showed the strongest relationship with biotic indicators, followed by land use variables (pressures/stressor proxies) and then by nutrient and hydrological abiotic state variables (stressors) (Table 4.31 and 4.32).

Table 4.31. Mean rank of variable importance estimates of BRT and RF models for each selected fish-based metrics (predictor variables are sorted by a decreasing order of mean variable importance as measured by the mean rank).

Predictor variables	Mean	% potamodromous sp.	% tolerant sp.	% intolerant sp.	N potamodromous sp.	% detritivorous sp.	% invertivorous sp.	% native sp.
Total_Precipitation	2.6	1.5	2.5	1	5.5	1	4	2.5
Agric_up	4.4	5	2	2	5	8	6.5	2.5
Altitude	5.4	1.5	4.5	4.5	4.5	7	4	11.5
Distance_source	6.4	4	11	7	1	3.5	12.5	6
Mean_Temperature	7.3	5	1.5	8.5	11.5	11	12.5	1
flow_year	7.4	6	7.5	12.5	2	6.5	1	16
River_slope	7.9	9	11	8.5	9.5	5.5	3	9
Size_catchment	8.1	10	8.5	12	7	4.5	5.5	9.5
Urban_up	10.2	16	4.5	7.5	9.5	6.5	13.5	14
Forest_up	10.6	5.5	14.5	4	12.5	12.5	16	9.5
Irrig_up	13.1	16	12	15	14	9.5	13	12
TN_year	13.6	19	8.5	13.5	14	13.5	8	19
HighFlow_nevents_year	13.7	12.5	19	17.5	9.5	9.5	9	19
TP_year	13.9	15.5	20.5	10.5	7	15	9.5	19
Agric	13.9	11.5	21	11.5	14	15	7	17.5
Forest	14.2	12	19.5	7.5	19.5	13	13	15
HighFlow_dur_year	14.8	18.5	8	13	17.5	19.5	20	7
Urban	14.8	8	15.5	22	10.5	17.5	19.5	10.5
LowFlow_dur_year	15.7	16	16.5	17	18.5	18	16	8
ZeroFlow_dur_year	18.9	23.5	13	22	21	20.5	22	10
Irrig	19.1	20.5	14	20	22	17	18.5	21.5
LowFlow_nevents_year	20.9	20.5	20	23	19	20.5	23	20.5
ZeroFlow_nevents_year	21.2	22	21	23	23.5	22.5	20.5	16
Habit_alt	21.9	21	24	17	22	23	22.5	23.5

Table 4.32. Mean rank of variable importance estimates of BRT and RF models for each EQR of Portuguese biotic integrity indices (predictor variables are sorted by a decreasing order of mean variable importance as measured by the mean rank).

Predictor variables	Mean	EQR Invert	EQR Diatoms	EQR Macrophytes	EQR Fish
Agric	5.5	1.5	1.0	15.0	4.5
Urban	6.3	8.0	2.5	4.5	10.0
Altitude	6.4	2.5	13.0	7.5	2.5
Forest	7.9	7.5	14.0	3.5	6.5
flow_year	8.5	11.0	6.5	1.0	15.5
Total_Precipitation	9.3	8.0	10.5	17.5	1.0
TP_year	9.5	11.0	11.5	9.0	6.5
Mean_Temperature	9.6	9.0	11.5	15.5	2.5
TN_year	10.6	16.5	10.0	9.5	6.5
River_slope	10.8	14.5	13.0	2.0	13.5
Agric_up	11.9	10.0	10.0	16.5	11.0
HighFlow_dur_year	12.4	7.5	17.5	7.5	17.0
LowFlow_dur_year	12.4	11.0	4.0	14.5	20.0
Distance_source	14.1	16.0	8.5	18.0	14.0
LowFlow_nevents_year	14.1	17.5	13.0	12.5	13.5
Forest_up	14.3	15.5	15.5	11.5	14.5
Urban_up	14.4	15.5	12.5	13.5	16.0
Size_catchment	14.8	15.0	17.0	17.0	10.0
HighFlow_nevents_year	15.3	18.5	13.0	13.0	16.5
Irrig_up	15.9	12.0	17.0	18.5	16.0
ZeroFlow_dur_year	20.1	20.5	22.0	16.5	21.5
ZeroFlow_nevents_year	21.1	22.5	22.0	17.5	22.5

Quantitative analysis of pressure/stressor effects and interactions

Among the seven representative fish-based metrics, only three showed to be conveniently modelled with GLM: % of potamodromous species, % of tolerance species and intolerant species (Table 4.33). The remaining metrics either yielded poor models or showed spatial autocorrelation problems that were not solved with the spatial eigenvector filtering approach (% native species). The % of tolerant species yielded the model with the best goodness-of-fit measure

($R.LR_{2adj} = 0.42$), followed by the % of intolerant species ($R.LR_{2adj} = 0.38$) and then by % of potamodromous species ($R.LR_{2adj} = 0.24$).

Table 4.33. Goodness-of-fit measures of GLM models for the selected fish-based metrics.

Biotic state variables	GLM	Original models		With spatial filters	
	family	R.LR ²	R.LR ² _{adj}	R.LR ²	R.LR ² _{adj}
% potamodromous species*	Binomial	0.22	0.24	0.26	0.28
% tolerant species*	Binomial	0.40	0.42	0.44	0.46
% intolerant species*	Binomial	0.27	0.38	0.29	0.40
Number of potamodromous species	Poisson	0.11	0.12	0.13	0.13
% detritivorous species	Binomial	0.13	0.17	-	-
% invertivorous species	Binomial	0.10	0.11	-	-
% native species	Binomial	0.40	0.44	**	**

* - Variables retained; ** - spatial filters did not solve the problem of spatial autocorrelation

All GLMM models using national EQR indicators showed R-squared values above 0.2 (Table 4.34). The EQR Fish yielded the model with the best goodness-of-fit measure ($R^2_m = 0.56$), followed by EQR macroinvertebrates ($R^2_m = 0.39$), then by EQR macrophytes ($R^2_m = 0.36$) and finally by EQR Diatoms ($R^2_m = 0.29$).

Table 4.34. Goodness-of-fit measures of GLMM models for the EQR indicators. R²_m – Marginal R-square; R²_c – Conditional R-square.

Biotic state variables	R ² _m	R ² _c
EQR diatoms	0.29	0.65
EQR macrophytes	0.36	0.79
EQR macroinvertebrates	0.39	0.82
EQR fish	0.56	0.94

Among the selected models, land use predictor variables were the most frequently selected for inclusion in the models and were only absent from one model (EQR Fish) (Table 4.35). Variables describing natural environmental variability were also included in all models except

one (EQR Diatoms). Hydrological stressors were absent from two models (EQR Diatoms and EQR Fish) and nutrient stressors were only selected in one model (EQR Fish).

The % of agriculture upstream was the most frequent predictor variable in the selected models (4 out of 7), showing a consistent negative effect on the biotic indicators (Table 4.35). However, its effect size was relatively low in comparison with the other variables include in the models (Table 4.35). Total annual precipitation was included in the models of the three fish-based biotic indicators, with varying effect directions (positive for % potamodromous species and % of intolerant species; negative for % tolerant species), always showing the highest effect sizes. Mean annual flow was included in three models and was the most common selected hydrological variable. Altitude, % forest upstream and % urban upstream were selected for inclusion in two models.

Four models included pairwise interaction terms, one interaction between a stressor and an environmental variable (Altitude x Total N) and three between stressors (Mean annual flow x % Forest upstream ; % Agriculture upstream x % Forest upstream; % Agriculture upstream x % Urban upstream).

Percentage of potamodromous species

In the Sorraia basin, this indicator includes the following species: *Luciobarbus bocagei*, *Luciobarbus comizo*, *Pseudochondrostoma polylepis*, *Iberochondrostoma lemmingii* and *Liza ramada*. The model for this biotic indicator included four variables, one environmental covariate (Total annual precipitation) with the highest effect size (Table 4.35), and three stressor variables with similar effect sizes: two land use pressures (% Forest and % Urban areas in the primary catchment) and one hydrological variable (Mean annual flow). According to the partial response plots (Fig 4.67), the indicator relates positively with the total annual precipitation and the mean annual flow and negatively with the % of forested and urban areas in the primary catchment. Stressor variables show large 95% confidence bands, but this is especially the case for the extremes of the sampled gradient.

Table 4.35. Estimated regression standardized coefficients of the models for the selected biotic state indicators (p-value of the t test are shown between brackets).

Variable	% potamodromous species	% tolerant species	% intolerant species	EQR diatoms	EQR macrophytes	EQR macroinvertebrates	EQR fish
(Intercept)	-0.62 (<0.001)	-0.52 (<0.001)	-3.15 (<0.001)	0.78 (<0.001)	0.89 (<0.001)	-311.52 (<0.001)	0.48 (<0.001)
Year						0.16 (<0.001)	
Altitude						0.10 (<0.001)	0.22 (<0.001)
River slope					0.03 (0.020)		
Total_Precipitation	0.54 (<0.001)	-0.64 (<0.001)	0.89 (<0.001)				
Forest	-0.19 (0.011)						
Urban	-0.19 (0.008)						
Agric_up			-0.33 (0.174)	-0.04 (0.014)		-0.09 (0.000)	
Irrig_up				-0.03 (0.056)			
Forest_up			0.51 (0.094)		0.04 (0.005)		
Urban_up		0.21 (0.006)		-0.06 (0.001)			
TN_year							-0.09 (0.003)
Mean_flow	0.21 (0.009)	0.17 (0.024)			-0.03 (0.011)		
HighFlow_dur		0.13 (0.068)					
LowFlow_nevents						0.03 (0.034)	
Altitude: TN_year							-0.14 (<0.001)
Mean_flow_year: Forest_up					0.04 (0.005)		
Agric_up: Forest_up			0.63 (0.010)				
Agric_up:Urban_up				0.03 (0.008)			

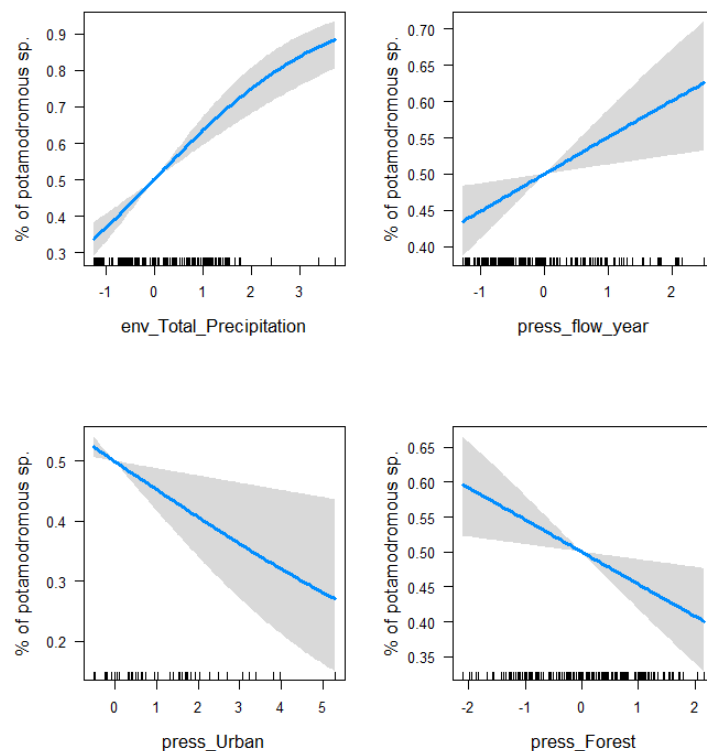


Figure 4.67 Partial response of the predictor variables included in the GLM model for the % of potamodromous species.

Percentage of tolerant species

This indicator is composed of several generalists native (e.g. *Anguilla anguilla*, *Luciobarbus bocagei* and *Liza ramada*) and introduced species (e.g. *Gambusia holbrooki*, *Lepomis gibbosus*, *Micropterus salmoides*). The model for this biotic indicator included four variables: one environmental covariate (Total annual precipitation) with the highest effect size (Table 4.35), one land use pressure (% of Urban areas in the upstream catchment) and two hydrological variable (Mean annual flow and mean annual duration of high flow events). The partial response plots show a neat negative response of the indicator to total annual precipitation and a positive relationship with the remaining three stressor variables (Fig. 4.68).

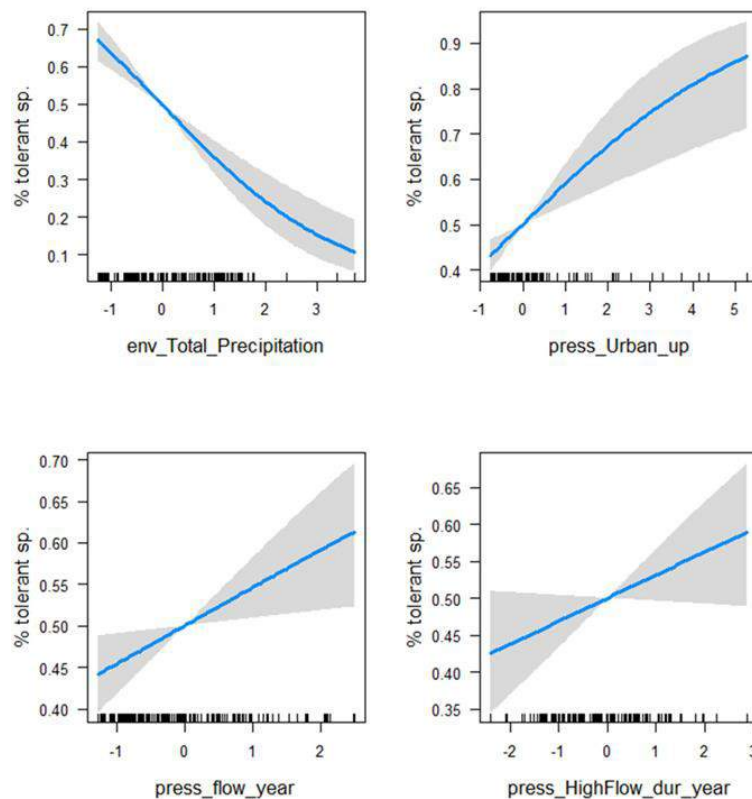


Figure 4.68 Partial response of the predictor variables included in the GLM model for the % of tolerant species.

Percentage of intolerant species

This indicator is composed of several specialist native species occurring in the Tagus basin: (e.g. *Lampetra fluviatilis*, *Lampetra planeri*, *Petromyzon marinus*, *Salmo trutta fario*). The model for this biotic indicator included three variables: one environmental covariate (Total annual precipitation) with the highest effect size (Table 4.35) and two interacting land use pressure (% of agriculture and % of forest areas in the upstream catchment). The partial response plots show a positive response of the indicator to total annual precipitation, a negative single effect of % of agriculture in the upstream catchment (estimated effect for mean values of % of forest area in the upstream catchment) and a positive single effect of % of forest area in the upstream catchment (estimated effect for mean values of % of agriculture area in the upstream catchment). The single partial responses of the two land use pressures show very large 95% confidence bands (Fig. 4.69a), as the consequence of the interactive effect with each other.

The interaction plot shows that the two variables show an opposing interaction (Fig. 4.69b): when the % of forested areas in the upstream catchment is low, the effect of the % of agriculture areas in the upstream catchment is negative; when the % of forested areas in the upstream catchment is high, the effect of the % of agriculture areas in the upstream catchment is positive, although in this case this is not supported by the data because there is a limit beyond which it is not possible to have higher % of area simultaneously for the two land use classes (see limits of data plotted in the graph of Fig. 4.69b).

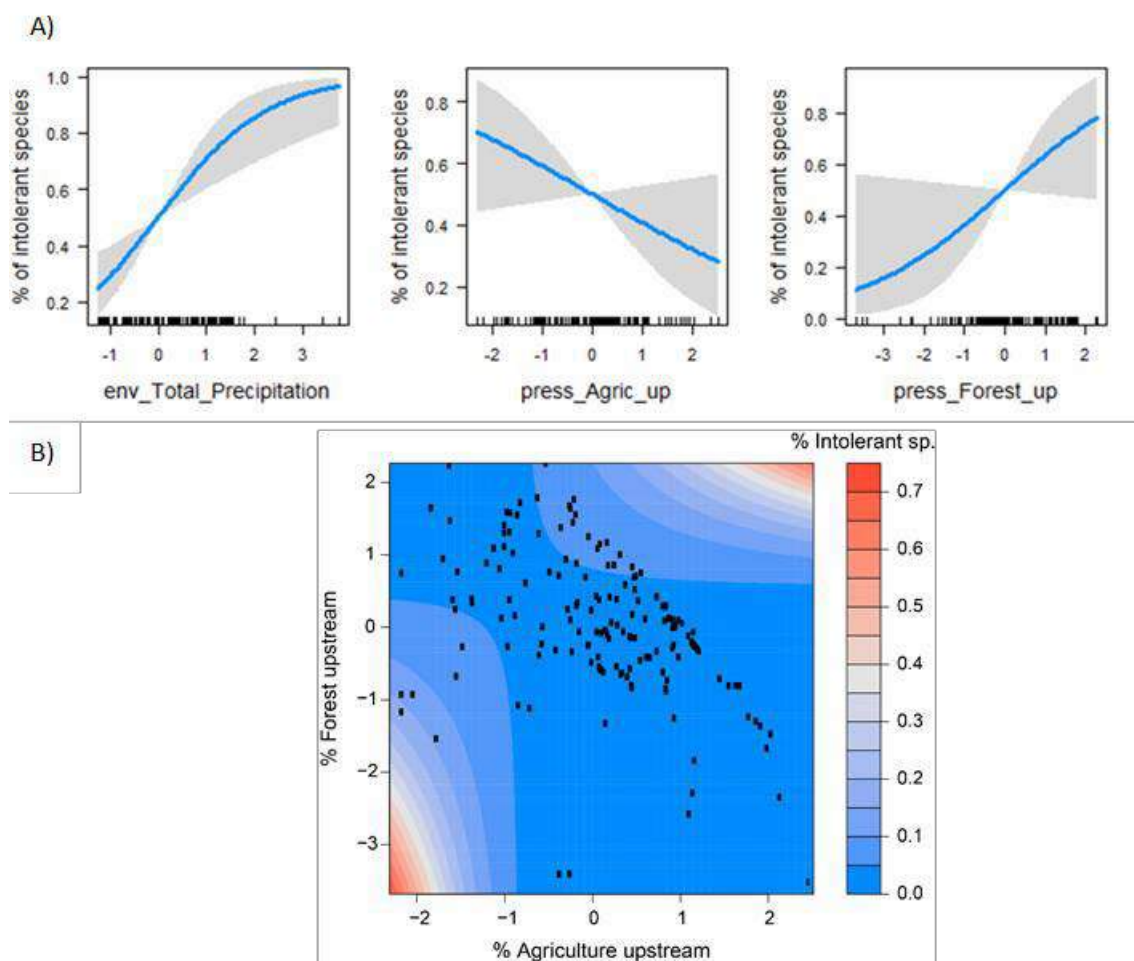


Figure 4.69 Partial response of the predictor variables included in the GLM model for the % of intolerant species.

National EQR - Diatoms

The model for this biotic indicator included only three land use variables (% of agriculture, irrigated crops and urban areas in the upstream catchment) and an interaction term between % of agriculture and % of urban areas in the upstream catchment. According to the partial response plots, the indicator relates negatively with the three land use variables. The large 95% confidence bands of the interacting land use variables (Fig. 4.70a) are the consequence of the interactive effect with each other.

The interaction plot shows an antagonistic, slightly opposing, interaction between % of agriculture and % of urban areas in the upstream catchment (Fig. 4.70b): when the % of urban areas in the upstream catchment is low, the effect of the % of agriculture areas in the upstream catchment is slightly positive; when the % of urban areas in the upstream catchment is high, the effect of the % of agriculture areas in the upstream catchment is markedly positive (Fig. 4.70b).

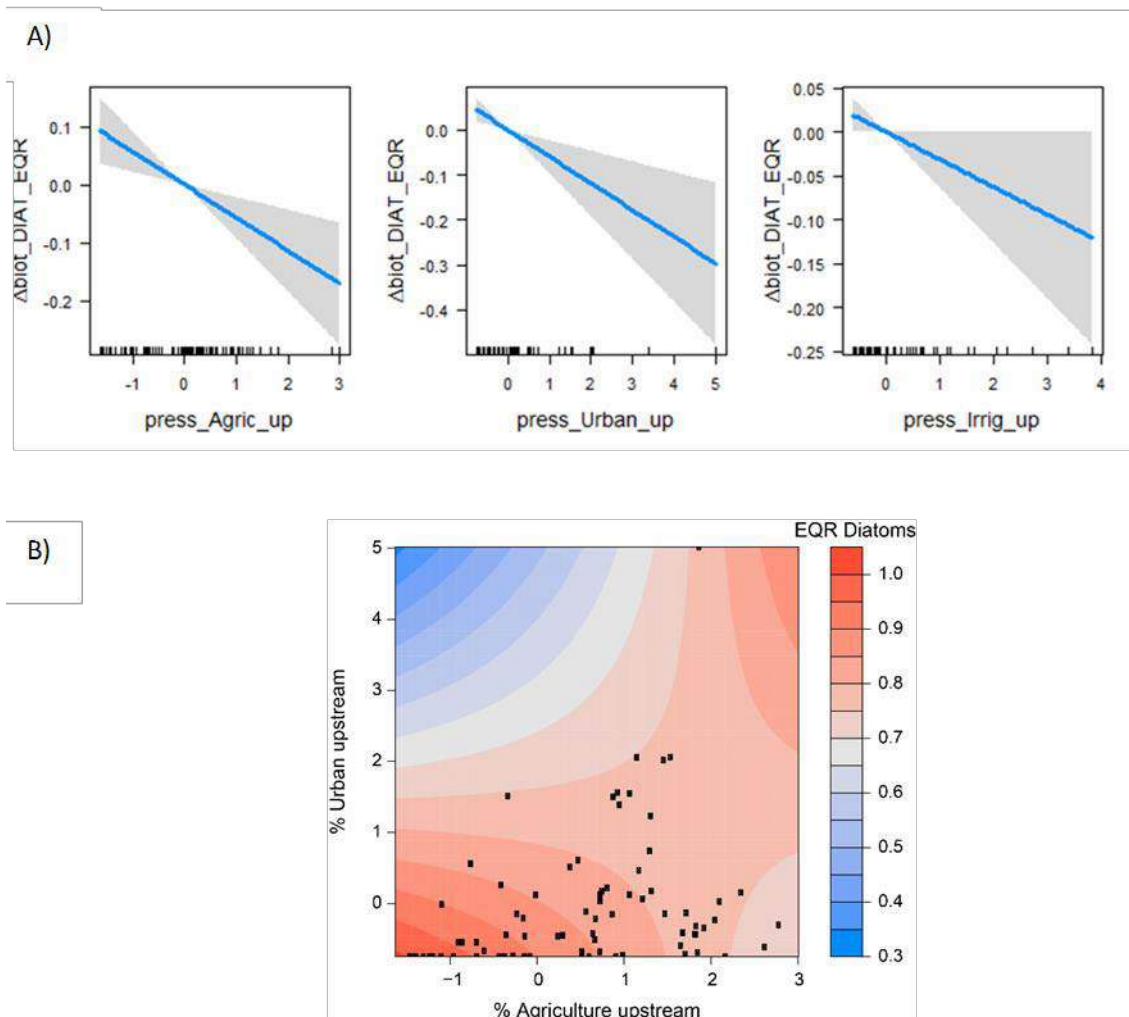


Figure 4.70 Partial response of single (A) and combined effects (B) of the predictor variables included in the GLM model for the EQR of the Portuguese Diatoms biotic integrity index.

National EQR - Macrophytes

The model for this biotic indicator included one environmental covariate (River slope), one land use pressure (% of forested areas in the upstream catchment), one hydrological stressor (mean annual flow) and an interaction term between % of forested areas in the upstream catchment and mean annual flow. According to the partial response plots (Fig. 4.71a), the indicator relates positively with river slope and the % of forested areas in the upstream catchment and negatively with the mean annual flow. The interaction plot (Fig. 4.71b) shows a slightly opposing interaction between mean annual flow and the % of forested areas in the upstream catchment: when the mean annual flow is low, the effect of the % of forested areas in the upstream

catchment is very weak and slightly negative; when the mean annual flow is high, the effect of the % of forested areas in the upstream catchment is markedly positive (Fig. 4.71b).

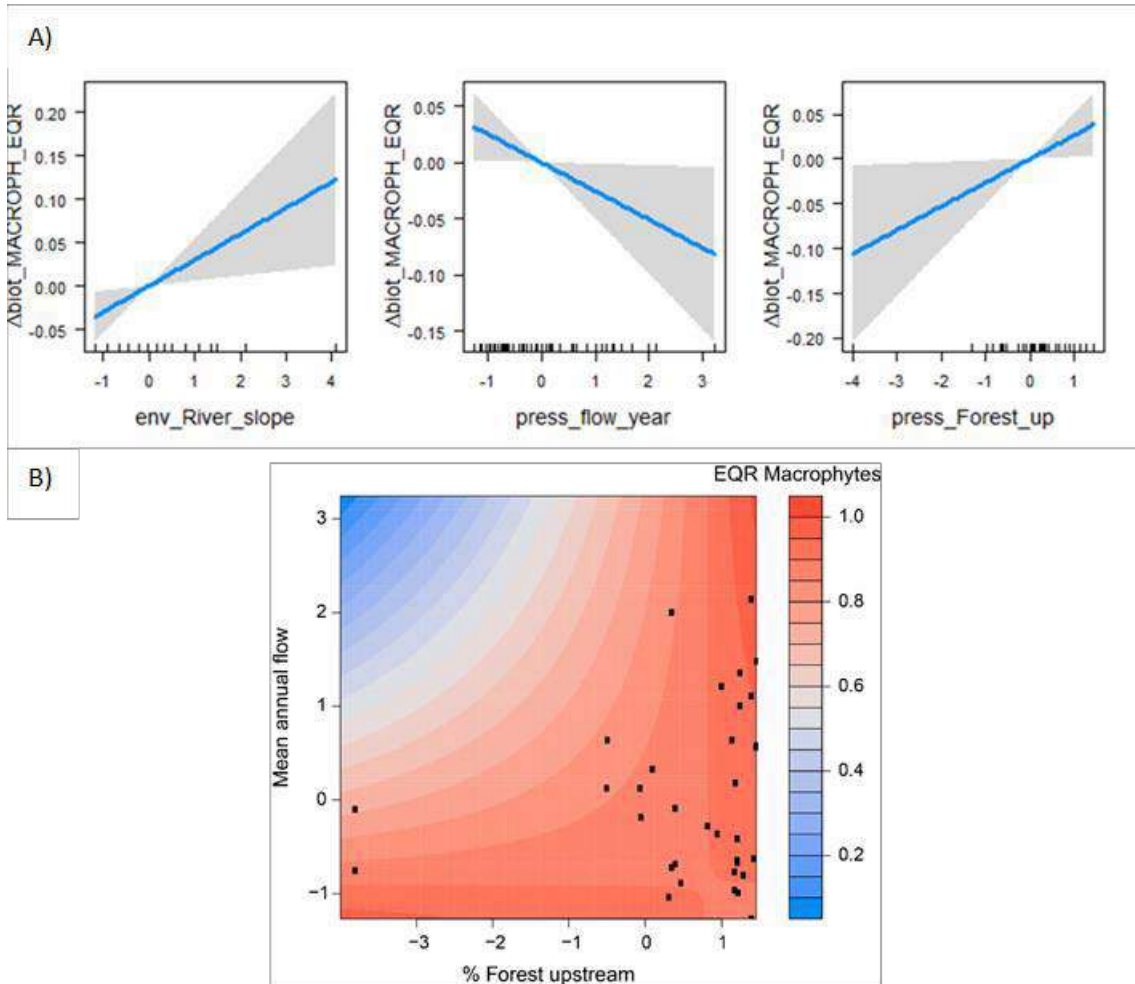


Figure 4.71 Partial response of single (A) and combined effects (B) of the predictor variables included in the GLM model for the EQR of the Portuguese macrophytes biotic integrity index.

National EQR - Macroinvertebrates

The model for this biotic indicator included four variables: one environmental covariate (Altitude), one land use pressure (% of agriculture areas in the upstream catchment), one hydrological stressor (number of annual low flow events) and the variable Year. According to the partial response plots (Fig. 4.72), the indicator relates positively with altitude and the

number of annual low flow events and negatively with the % of agriculture areas in the upstream catchment.

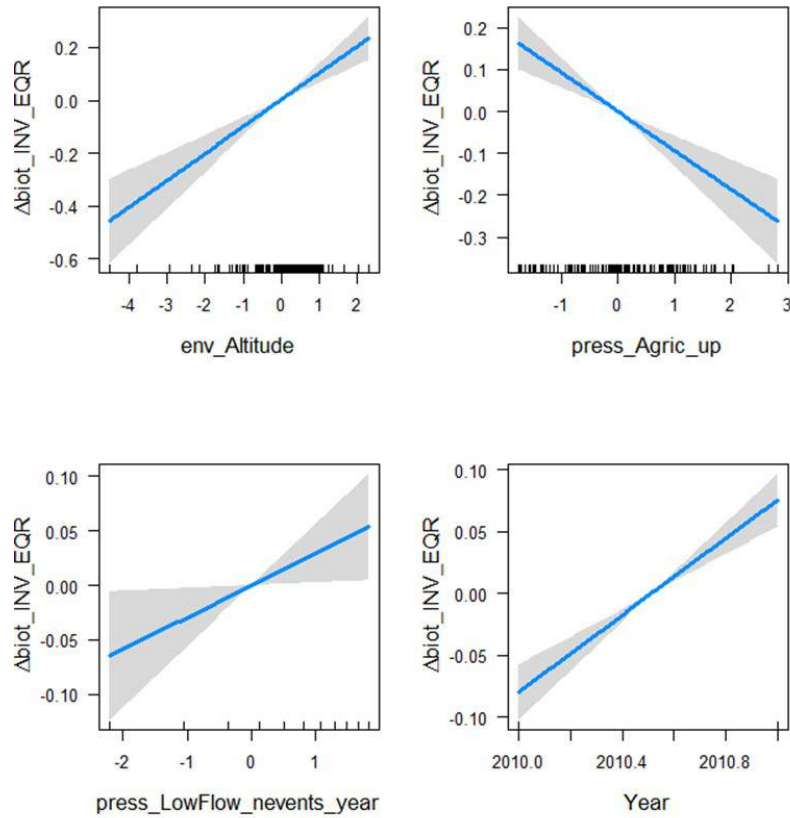


Figure 4.72 Partial response of the predictor variables included in the GLM model for the EQR of the Portuguese Macroinvertebrates biotic integrity index.

National EQR - Fish

The model for this biotic indicator included only two interacting variables: one environmental covariate (Altitude) and one nutrient stressor (Total N). According to the single partial response plots (Fig. 4.71a), the indicator relates positively with altitude and negatively with total N.

The interaction plot (Fig. 4.73b) shows a clear opposing interaction between altitude and total N: for low altitudes the effect of total N is positive, while for higher altitudes the effect of total N is negative (Fig. 4.73b). However, the positive effect of total N in the indicator is supported by much fewer data than the negative effect (see data plotted in the interaction plot of Fig. 4.73b).

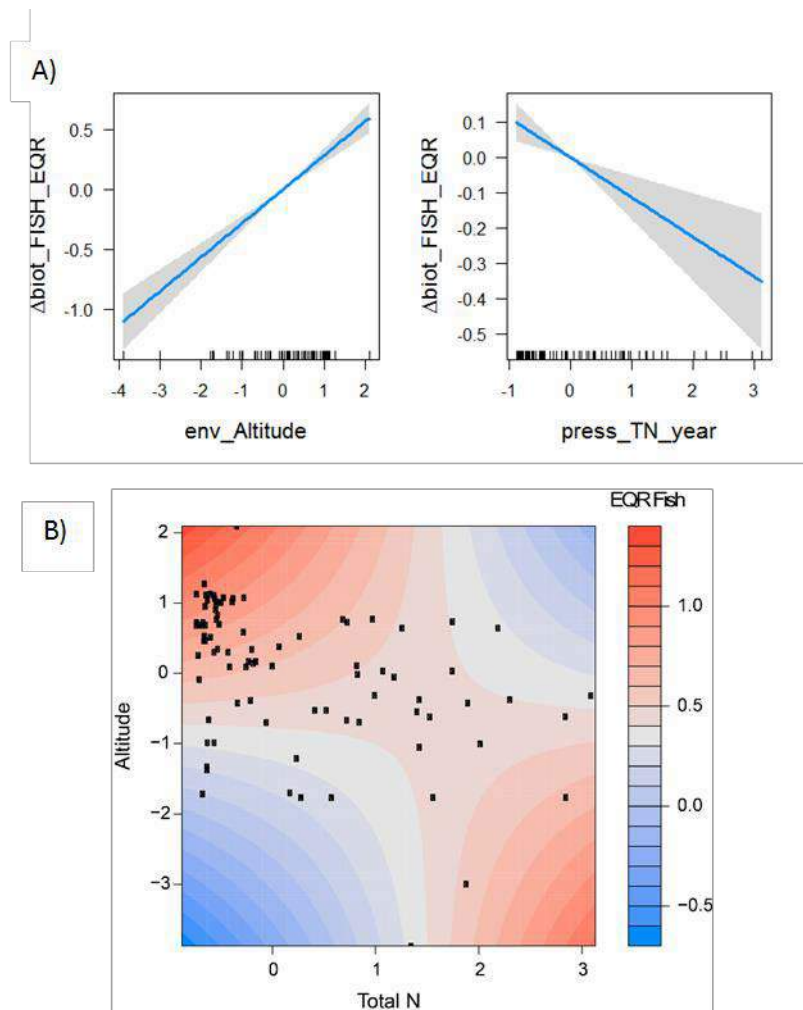


Figure 4.73 Partial response of single (A) and combined effects (B) of the predictor variables included in the GLM model for the EQR of the Portuguese fish biotic integrity index

4.4.7 Ecosystem services

The spatial indicators for ecosystem services that are presented in this report represent only a first spatially explicit baseline for assessing the state of ecosystem services in Sorraia basin. The main goal is to evaluate the scenarios studied related to land use and detect areas where ecosystem services increase or decrease.

Water availability

We selected the modelling results from the climatic model IPSL and the timeline 2060 to be depicted because this is the most aggressive scenario for Sorraia. Figure 4.74 shows the annual average water provision based on surface water flow for each storyline for the scenario considered. The proposed “water availability” is inserted on the ecosystem service category “water for non-drinking purpose”, and in this context is mainly for irrigation. The decrease in available water in the Sorraia River basin is visible, having a bigger impact in the Storyline 1.

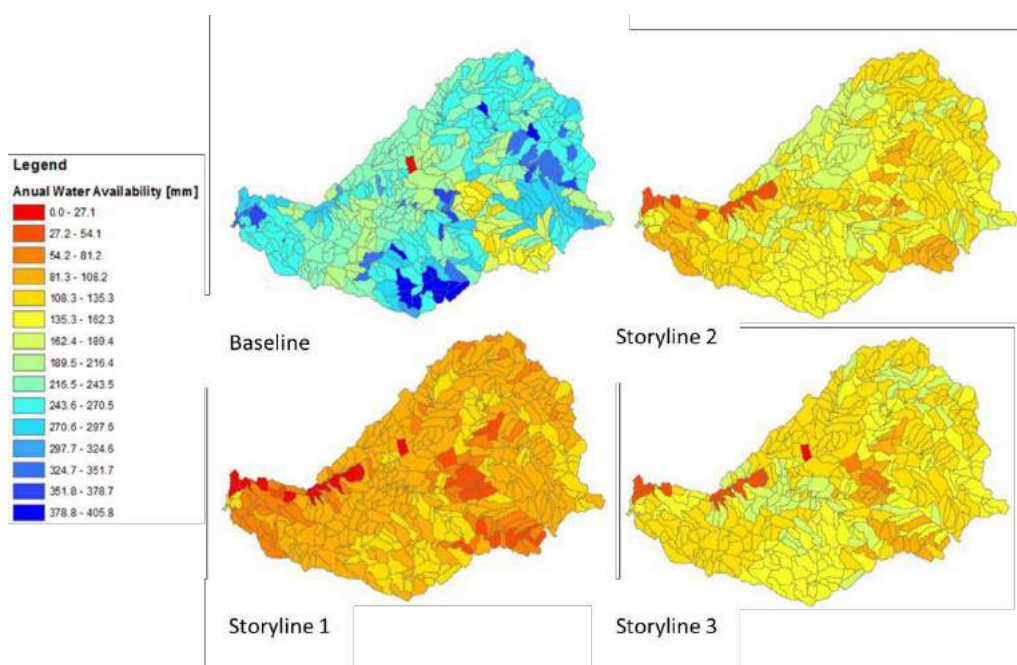


Figure 4.74 Annual water availability for each storyline (IPSL climatic model and 2060 timeline example), in mm

Nutrient Purification

Figure 4.75 and Figure 4.76 show, as an example, the “Nutrient Purification” ecosystem service category, and the indicators considered were the nutrient loads: total nitrogen and phosphorous. Although we can see a general increase in nutrient loads to the river, Storyline 2 evidences almost no increase of Total Nitrogen, and an overall reduction of Total Phosphorus.

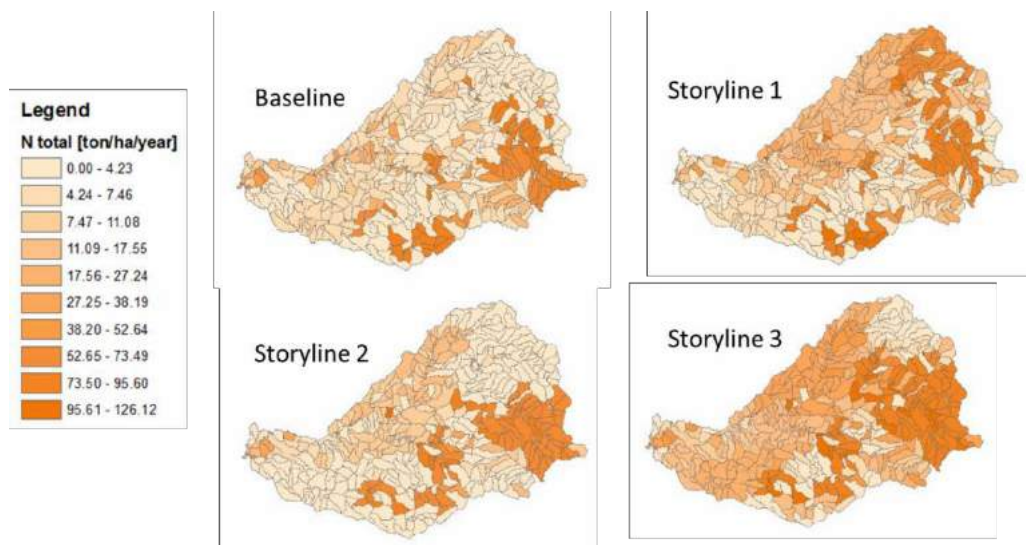


Figure 4.75 Distribution of Nutrient load (total nitrogen) in Sorraia basin for each storyline implemented (ton/ha/year)

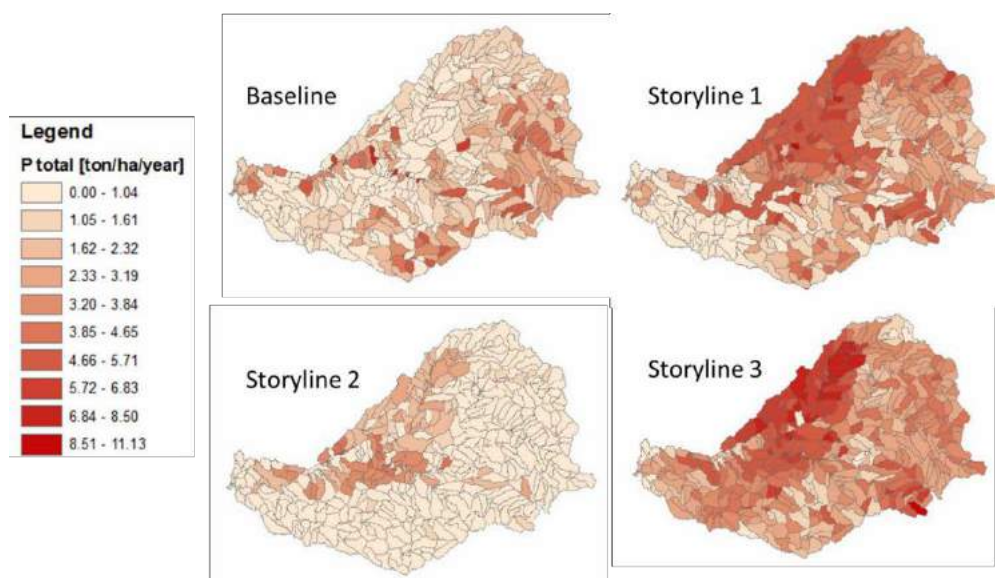


Figure 4.76 Distribution of Nutrient load (total phosphorous) in Sorraia basin for each storyline implemented (ton/ha/year)

Ecological status of surface waters

Both RF and GLMM using the five class outcome of Ecological Status yielded models with percentages of accurate classification below 50% (47% for RF and 50.0% for CLMM). Therefore, we only present the results of models that used the binary aggregation (defined by the moderate-good boundary) of Ecological Status as the response ecosystem service indicator.

The resulting models showed overall good classification accuracies, as given by the area under the ROC, True Skill Statistics and the misclassification rate (Table 4.36). The RF model showed the highest classification accuracy, although we did not follow any procedure to avoid overfitting as with the stepwise procedure used for BRT. The simplified version of the BRT model, which included 4 variables (altitude, % of agriculture area in the upstream catchment, % of agriculture area in the primary catchment and % of urban area in the upstream catchment) performed only slightly worse than the full model. Regression-based techniques showed lower classification accuracy according to all three measures, in comparison to the two learning machine techniques (Table 4.36).

Table 4.36. Models' accuracy measures

Accuracy measures	RF	BRT	BRT simplified	GLM	GLMM
Area Under the ROC	0.99	0.90	0.89	0.80	0.82
True Skill Statistics	0.95	0.65	0.63	0.51	0.49
Misclassification rate	0.03	0.21	0.19	0.24	0.27

The mean rank of variable importance according to RF and BRT (Table 4.37) shows that an environmental covariate (Altitude) is the most important variable according both to RF and BRT analyses, followed by three land use variables (% of agriculture area in the upstream catchment, % of agriculture area in the primary catchment and % of urban area in the upstream). Nutrient stressors tend to be also important in explaining the variation in the Ecological Status, while variables related to low flow events tend to have low importance (Table 4.37).

Table 4.37. Mean rank of variable importance estimates of BRT and RF models for the binary reclassification of Ecological Status of surface waters

	Mean rank	Rank	Rank
Altitude	1.0	1.0	1.0
Agric_up	2.0	2.0	2.0
Agric	3.0	3.0	3.0
Urban_up	4.0	4.0	4.0
Size_catchment	5.0	5.0	5.0
TP_year	7.0	6.0	8.0
TN_year	9.0	7.0	11.0
Forest	9.5	10.0	9.0
Forest_up	9.5	13.0	6.0
HighFlow_dur_year	10.5	14.0	7.0
flow_year	11.0	8.0	14.0
Irrig	12.5	15.0	10.0
HighFlow_nevents_year	13.0	9.0	17.0
Urban	13.5	11.0	16.0
LowFlow_nevents_year	15.0	17.0	13.0
LowFlow_dur_year	15.5	19.0	12.0
ZeroFlow_dur_year	15.5	12.0	19.0
Irrig_up	17.5	20.0	15.0
River_slope	18.0	18.0	18.0
ZeroFlow_nevents_year	18.0	16.0	20.0

According to the standardized coefficient estimates (effect sizes) (Table 4.38) and the partial response plots (Fig. 4.77 and 4.78) of the variables included in GLM and GLMM models, Ecological Status is affected positively by altitude, which have the highest effect size, and negatively by the % of urban areas and % of agriculture areas in the upstream catchment. A significant opposing interaction between altitude and % of urban areas in the upstream catchment (Table 4.37) was found. At low altitudes the % of urban areas in the upstream catchment has a negative effect while at high altitudes it shows a positively effect on Ecological Status (Fig. 4.77 b and 4.78b).

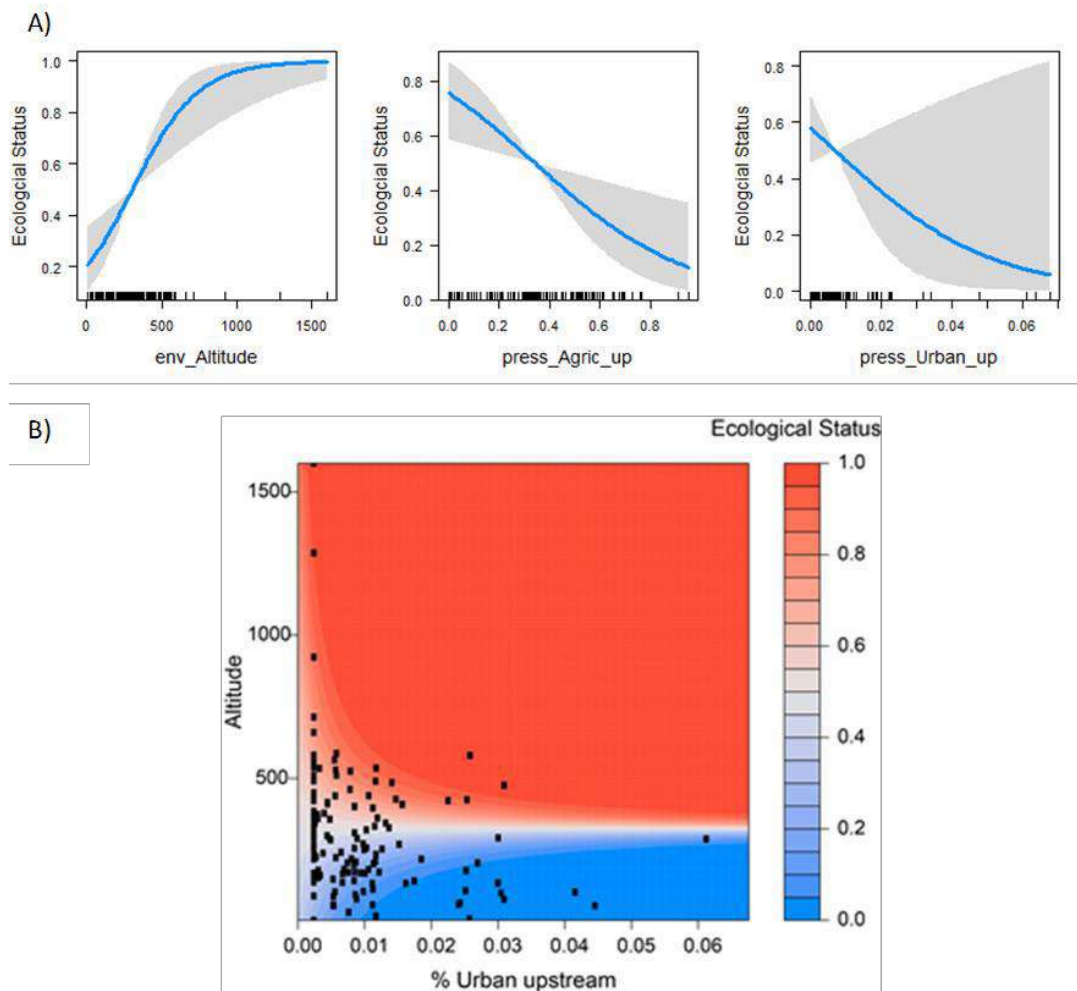


Figure 4.78 Partial response of single (A) and combined effects (B) of the predictor variables included in the GLM model for Ecological Status using 2011 data. The Y scale (A) and the blue-red gradient (B) represents the probability of Ecological Status to belong to t

Table 4.38. Estimated coefficients, standard errors and z tests of GLM and GLMM models for Ecological Status

Variables selected	Estimate	Std. Error	z value	P-value
GLM (2011)				
(Intercept)	-0.09	0.22	-0.42	0.674
Altitude	1.39	0.39	3.52	0.000
Agric_up	-0.86	0.27	-3.18	0.001
Urban_up	-0.19	0.32	-0.57	0.566
Altitude: Urban_up	1.67	0.58	2.87	0.004
GLMM (2010-11)				
(Intercept)	-1.14	0.20	-5.62	0.000
Altitude	1.35	0.30	4.55	0.000
Urban_up	-0.65	0.29	-2.21	0.027
Year	1.05	0.19	5.41	0.000
Altitude: Urban_up	1.30	0.40	3.28	0.001

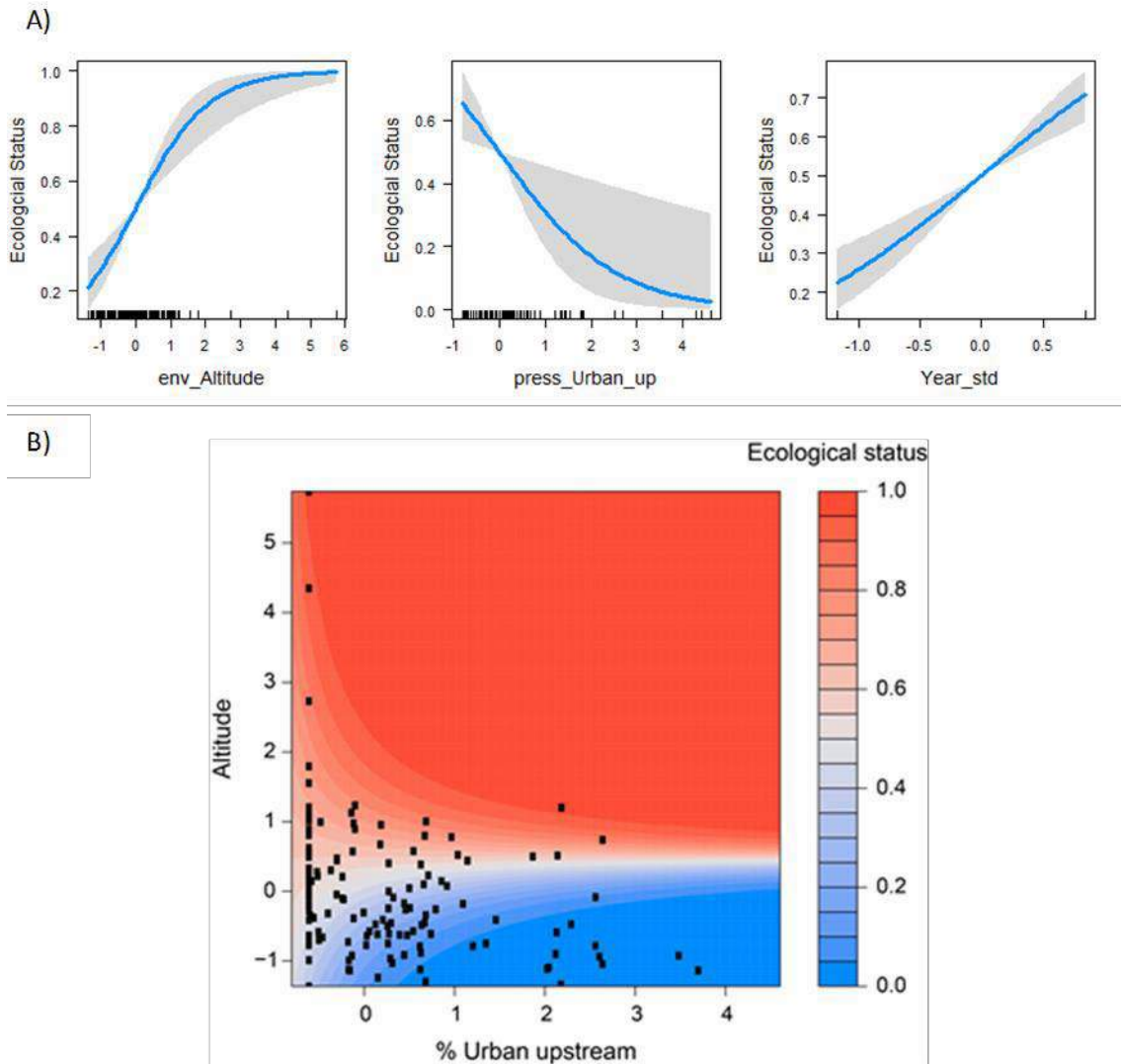


Figure 4.79 Partial response of single (A) and combined effects (B) of the predictor variables included in the GLMM model for Ecological Status. The Y scale (A) and the blue-red gradient (B) represents the probability of Ecological Status to belong to good/very good classes

Projections for the future

When applying the future scenarios according to the storylines defined by the MARS project and downscaled to the Sorraia basin we can see that for the Ecological status of surface waters the projected impacts are mild (Figure 4.79 and Table 4.39). There is a slight reduction of the overall good and very good ecological status sites for Storylines 1 and 3, for both timelines, and no future alterations, for either timeline, when considering storyline 2.

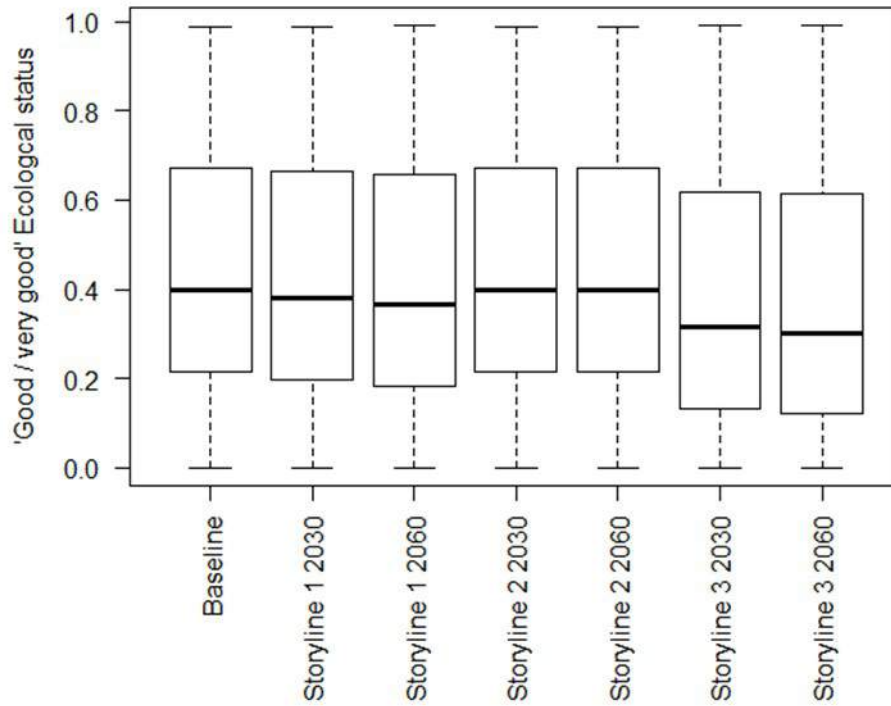


Figure 4.80 Projections of the probability of sites to be classified into “good” or “very good” Ecological Status under the considered scenarios of future land use changes.

Table 4.39. Percentage of sites with Ecological Status classified as “good” or “very good”

Scenario	% of sites with "good" or "very good" Ecological Status
Baseline	39.29
Storyline 1 2030	38.57
Storyline 1 2060	38.57
Storyline 2 2030	39.29
Storyline 2 2060	39.29
Storyline 3 2030	35.71
Storyline 3 2060	34.29

Quality of freshwaters for angling

The resulting best approximating regression model of FQI against predictor variables showed a relatively weak goodness-of-fit ($R^2 = 0.33$; Table 4.40). Three variables were selected, with very similar effect sizes: one environmental covariate (distance to source), one land use pressure (% of agriculture area in the upstream catchment) and a hydrological stressor (mean yearly duration of high flow events). A significant interaction term between distance to source and (% of agriculture area in the upstream catchment) was also included in the model. All variables showed a positive single effect on FQI (Fig. 4.80), although the effect of the % of agriculture area in the upstream catchment is dependent of the distance to source: the effect of % of agriculture upstream in FQI is slightly negative at sites that are more distant from the river source (although this is supported by few data – see data plotted in Fig. 4.80), while it becomes markedly positive for sites closer to the river source (Fig. 4.80).

Table 4.40. Summary table of the multiple linear model for the Fishery Quality Index, including model R-squared, adjusted R-squared, F test, standardized coefficients (effect size), standard errors and respective t-tests.

Selected variables	Estimate	Std. Error	t value	p-value
$R^2 = 0.33$; $R^2_{adj} = 0.28$; $F = 7.125$ (4 and 58 DF), p -value: $9.763e-05$				
(Intercept)	0.750	0.058	12.921	0.000
Distance_source	0.123	0.059	2.086	0.041
Agric_up	0.148	0.065	2.294	0.025
HighFlow_dur_year	0.118	0.059	1.987	0.052
Distance_source: Agric_up	0.232	0.076	3.060	0.003

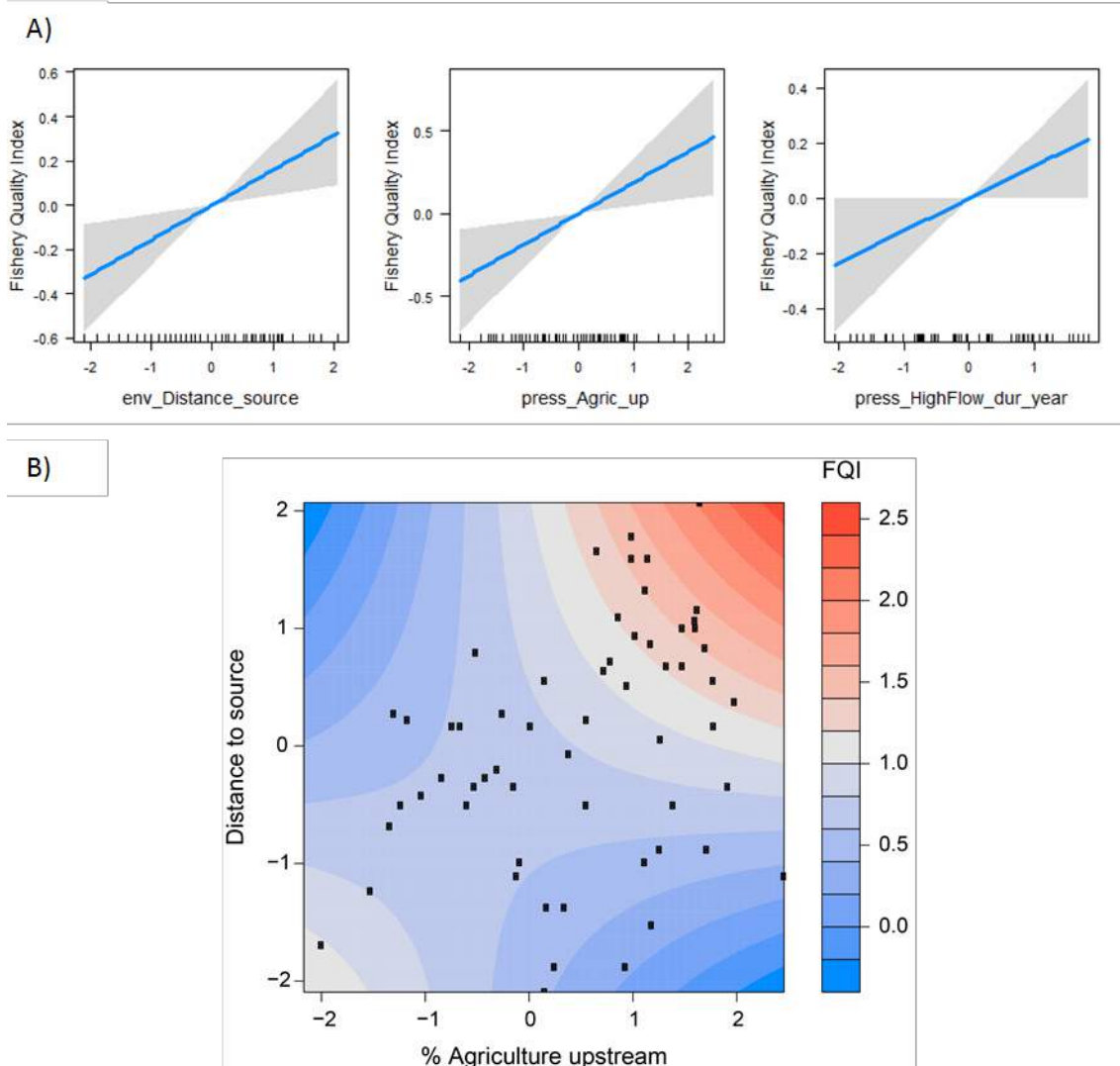


Figure 4.81 Partial response of single (A) and combined effects (B) of the predictor variables included in the GLM model for Fishery Quality Index.

4.4.8 Implementation of measures

Projections of abiotic state variables

Tables 4.41 and 4.42 show the model results to each measure implementation in all Storylines and both climate models. For Storyline 3 measure 4 was not implemented because it considered the same climate model than the storyline 1. We can observe that in terms of river flows, measure 1

has practically no impact on the water availability in the rivers, mainly because the water is still used for irrigation. With a detailed analysis we can observed a significant change on behaviour of river flows, especially for baseflows. The biggest improvement in the flow behavior is the flow maintenance throughout the year. Measures 2 and 3 have positive results, with an increase of water flow in the river. Measure 2 shows that agriculture can be sustainable if practices (irrigation and fertilization) are implemented correctly and with no water and nutrient excess. Measure 4 shows that forest can increase considerably the evapotranspiration, decreasing the water flow in river when compared with the baseflow scenario.

Table 4.41. Average of Annual evapotranspiration and flow according to different measures

Scenario	Measure	Flow	ETA
Storyline1_GFDL_2060	1	41.6	167.9
	2	54.7	168.1
	3	54.7	168.1
	4	11.6	204.4
Storyline1_IPSL_2060	1	131.1	165.6
	2	143.5	165.7
	3	143.5	165.7
	4	70.1	226.1
Storyline2_GFDL_2060	1	44.4	161.0
	2	61.4	183.3
	3	58.4	161.4
	4	49.9	171.0
Storyline2_IPSL_2060	1	87.9	164.7
	2	103.6	193.5
	3	102.0	165.1
	4	102.5	164.1
Storyline3_GFDL_2060	1	41.8	167.6
	2	55.0	167.8
	3	55.0	167.8
Storyline3_IPSL_2060	1	131.4	165.2
	2	143.7	165.4
	3	143.7	165.4

In terms of nutrients in river, only measures 2, 3 and 4 produced a significant improvement. Measure 2 - because the amount of nutrients applied was reduced and those would be consumed by plants. Measure 4 - because with forest there are no fertilization practices. Measure 3 – It shows a reduction of the nutrient concentration in the river basin, but it is only influenced by measure 2.

Table 4.42. Nutrients and sediments according to different measures

Scenario	Measure	Tot P	Tot N	Sediments
		(ton/ha/year)	(ton/ha/year)	(ton/ha/year)
Storyline1_GFDL_2060	1	0.4	10.0	0.3
	2	0.57	1.90	0.35
	3	1.90	0.35	0.57
	4	0.33	0.001	0.004
Storyline2_GFDL_2060	1	0.6	8.4	0.4
	2	0.52	3.01	0.35
	3	2.40	0.34	0.56
	4	7.49	0.23	0.41
Storyline3_GFDL_2060	1	0.56	15.30	0.46
	2	0.61	2.22	0.39
	3	2.22	0.39	0.61
Storyline1_IPSL_2060	1	4.0	21.8	2.4
	2	4.28	8.78	2.05
	3	8.78	2.05	4.28
	4	1.06	0.15	0.38
Storyline2_IPSL_2060	1	2.27	13.05	1.24
	2	2.05	6.19	1.17
	3	6.36	1.22	2.28
	4	9.74	0.66	1.43
Storyline3_IPSL_2060	1	4.13	28.12	2.74
	2	4.49	10.17	2.28
	3	10.17	2.28	4.49

Projections of biotic state variables

To illustrate how the program of measures for the Sorraia Basin will impact the ecological status in terms of the biotic component, we used the empirical models to project changes in the fish-based EQR under different measures scenarios, for each story line and for each climatic model. For Storyline 3 measure 4 was not implemented because it considered the same climate model than the storyline 1.

The overall differences in the fish EQR values between the baseline and the three storylines for both climatic models were not very marked (Fig. 4.81). However for the IPSL model a near significant difference was found for storylines 1 (Wilcoxon signed rank test, $p=0.068$) and 2

(Wilcoxon signed rank test, $p=0.051$), suggesting an overall increase of EQR values under these scenarios.

Overall, for both climatic models, measure 1 was the less efficient measure, consistently among the 3 storylines and 2 climatic models (Fig. 4.82). The pairwise comparison between EQR values of the scenarios before and after considering the implementation of this measure (measure efficiency) was never significant (Wilcoxon signed rank test, $p>0.05$). Measure 4 was efficient for storyline 1, for both IPSL (Wilcoxon signed rank test, $p<0.05$) and GFDL (Wilcoxon signed rank test, $p<0.01$) models. The efficiency of measure 2 and 3 was similar, showing a significant efficiency for the three storylines of the IPSL model (Wilcoxon signed rank test, $p<0.025$, except for storyline 2 where $p<0.05$) and for storylines 1 and 3 of the GFDL model (Wilcoxon signed rank test, $p<0.025$).

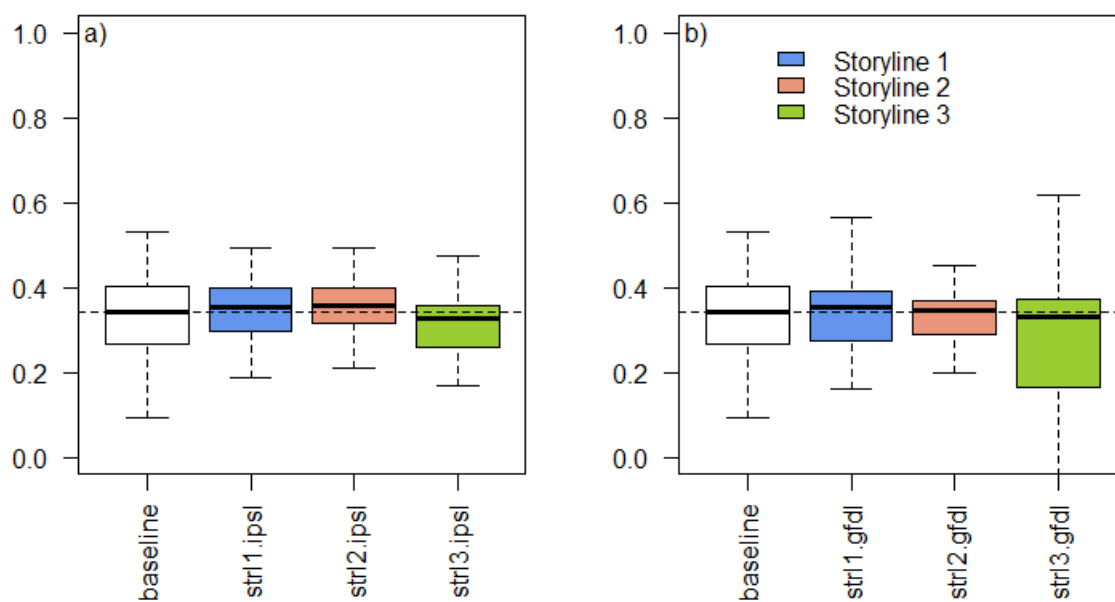


Figure 4.82 Projections of fish-based EQR in the Sorraia River Basin under each story line and for each climatic model (a – IPSL model, b – GFDL model). In the X-axis labels, the baseline represents the current EQR values, str1 1-3 denotes each storyline and ipsl and gfdl denotes the climatic model

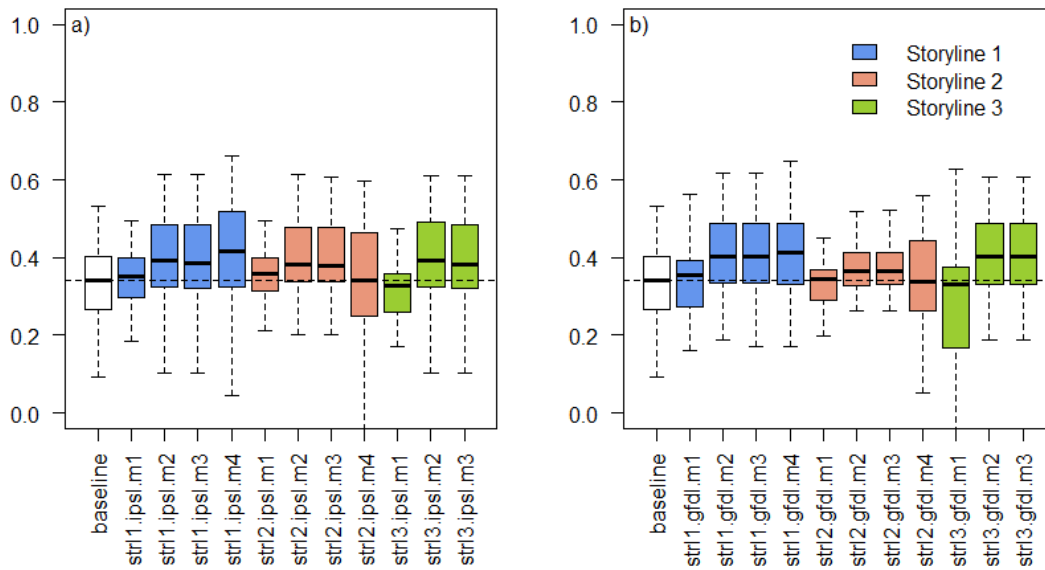


Figure 4.83 Projections of fish-based EQR in the Sorraia River Basin under different measures scenario, for each storyline and for each climatic model (a – IPSL model, b – GFDL model). In the X-axis labels, the baseline represents the current EQR values, str1-3 denotes each storyline, ipsl and gfdl denotes the climatic model and m1-4 denotes each Program of Measures scenario

4.4.9 Discussion

The approach of using process-based models to estimate abiotic indicators can have an important role on environmental studies. Process-based models require a significant effort on the implementation and especially on the calibration and validation process. SWAT model is a widely known process-based model that allows manager to work with accurate predictions. In the Sorraia case study, SWAT model was applied and a high accuracy was obtained during the calibration and validation process (with a linear correlation about 0.77) using the period between 1996 and 2015. Process based models by including climate models have the ability to estimate indicators for future scenarios, as well as to study the ecosystems services of aquatic ecosystems. This approach, allowed future scenarios to be implemented for the estimation of abiotic indicators. These were then linked to empirical models.

After calibration and validation of the SWAT model in Sorraia River Basin, climate models and land use scenarios were implemented. The scenarios were implemented based on Storylines developed on MARS project, and in Sorraia basin the main focus on this storylines approach

was the management practices and land use changes. These changes were associated with climate change models IPSL and GFDL developed for this purpose.

Future scenarios applied in Sorraia show a significant decrease of water flow, related to the significant decrease of precipitation. The available river water is a reflex of precipitation, irrigation practices on the basin, evapotranspiration, soil water content and temperature. The decrease of water in the basin has a significant influence on sediments that are lost to the river bed, when the decrease of soil erosion is significant. There was also projected an important impact on nutrient loads to the basin, particularly for storyline 3 in combination with the IPSL climate model. Here the irrigated areas were enlarged (and the fertilizers/irrigation application augmented), due to the severe climate change, nutrients loads had an intensification of about 100%.

The study of the implementation of the measures in the storyline during the strictest climate scenario shows that only adopting optimum farming practices, with the application of the right amount of fertilizer and water to irrigate, can the agriculture in the Sorraia basin be sustainable.

The application of empirical modelling has an important part to play in order to reply to the project's main goal - to understand how interacting stressors affect the response, being it biotic elements or abiotic indicators of environmental quality. For this, at the basin scale, we evaluated the effects of the isolated impacts to see if the interactions, when existed (meaning when selected to be part of the best model for each biotic-based variable), had an effect and if that effect was bigger smaller or equal to sum of the individual effects. Overall, stressors, had a lower relationship with biotic elements than environmental variables. But land use related stressors had a stronger relationship with the biotic elements than the single stressors (Nutrients and Hydrology). This may have occurred because land use variables can be seen as proxies for multiple stressors on their own, thus explaining the stronger effect noticed. Nonetheless we cannot fully exclude the existence of other important single stressors that were not considered in this analysis (either by lack of data or by difficulty of integration them into the modelling strategy followed herein), such as, Channelization, Impoundment, Embankment, Transverse barriers, Industrial pollution, etc. Additionally, land use stressors being proxies for multiple pressures may exert such an effect on the biotic elements that an otherwise significant effect stressor is overridden by the land use and its effect is not noticeable at the scale of the response variable.

Only three models included interaction terms between stressors (Mean annual flow x % Forest upstream

– EQR Macrophytes; % Agriculture upstream x % Forest upstream – Percentage of intolerant species; % Agriculture upstream x % Urban upstream – EQR Diatoms). In all cases the interactions show that the two variables have an opposing interaction. The combined effect seems even to be lower than the sum of the isolated effects. There was also one model that included an interaction term between an environmental variable and a stressor (National EQR Fish - *interaction term* (altitude X total N)) also showing an opposing effect.

4.4.10 Key outcomes

- Although having future reduction in available water due to precipitation reduction, the water balance within the basin will be similar (%) for future scenarios;
- GFDL climate model is more stringent when modelling water flowing in the river, having consequences in the basin dynamics;
- IPSL climate model, on the other hand, had a stronger impact by increasing future nutrient loads to the river;
- Percentage of tolerant fish species was the fish-based metric that yielded BRT models with the highest predictive ability;
- EQR of the fish biotic integrity index showed the strongest predictive power among all the analysed indicators;
- For fish-based metrics and national EQR indicators had higher relationship with natural environmental variability followed by land use variables and then by nutrient and hydrological abiotic state variables;
- Four out of the seven GLM models for the biotic indicators included interaction terms:
 - **% intolerant species** – *interaction term* (% forest upstream X % agriculture upstream) opposing interaction;

- **National EQR Diatoms** - *interaction term* (% urban upstream X % agriculture upstream) antagonistic, slightly opposing interaction;
 - **National EQR Macrophytes** - *interaction term* (% mean annual flow X % forest upstream) slightly opposing interaction;
 - **National EQR Fish** - *interaction term* (altitude X total N) opposing interaction.
- Ecosystems services:

- **Water availability** – This service will suffer in the future. Projections for all storylines show a general decrease of available water in the Sorraia basin;
- **Nutrient purification** – Although there is a future general increase of Nutrients in the systems, Storyline 2 shows almost no increase of Total Nitrogen, and an overall reduction of Total Phosphorus;
- **Ecological status of surface waters** – Altitude followed by land use variables were the most important variables. Nutrient stressors tend to be also important while variables related to low flow events tend to have low importance. *Interaction term* (altitude X % urban upstream) opposing interaction. *Projections for storylines* – Only mild future reduction of the number of Good and very good sites for both timelines of storylines 1 and 3;
- **Quality of freshwaters for angling** - *Interaction term* (distance to source X % agriculture upstream) effect of the % of agriculture area in the upstream catchment is dependent of the distance to source.

- Measure implementation:

- Only adopting optimum farming practices, with the application of the right amount of fertilizer and water to irrigate, can the agriculture in the Sorraia basin be sustainable;
- Measure 1 was, overall, the least effective for both biotic and abiotic elements;
- The remaining measures (2, 3 and 4) improved water availability and reduced nutrient concentration;

- Measure 2 and 3 effectively increase the National Fish EQR for all storylines under both climatic models (excluding Storyline 2 – GFDL).

5 Central Basins

5.1 Drava

5.1.1 Introduction

5.1.1.1 Basin overview

The Austrian Drava and Mura River Basins are part of the Danube River Basin and comprise about 23.000 km² of size (12.800 km² and 10.300 km² each) (Figure 5.1). The Mura River drains into the Drava River at the Croatian-Hungarian border. Both basins are located in the ecoregions Alps and Dinaric Western Balkan (Illies, 1978) and are representing the characteristics of Central European River Basins in MARS. The runoff of both river basins is mainly determined by nival, and glacial regimes in the Alps and by pluvial and pluvio-nival regimes in the Dinaric western Balkan regions (Fink et al., 2000).

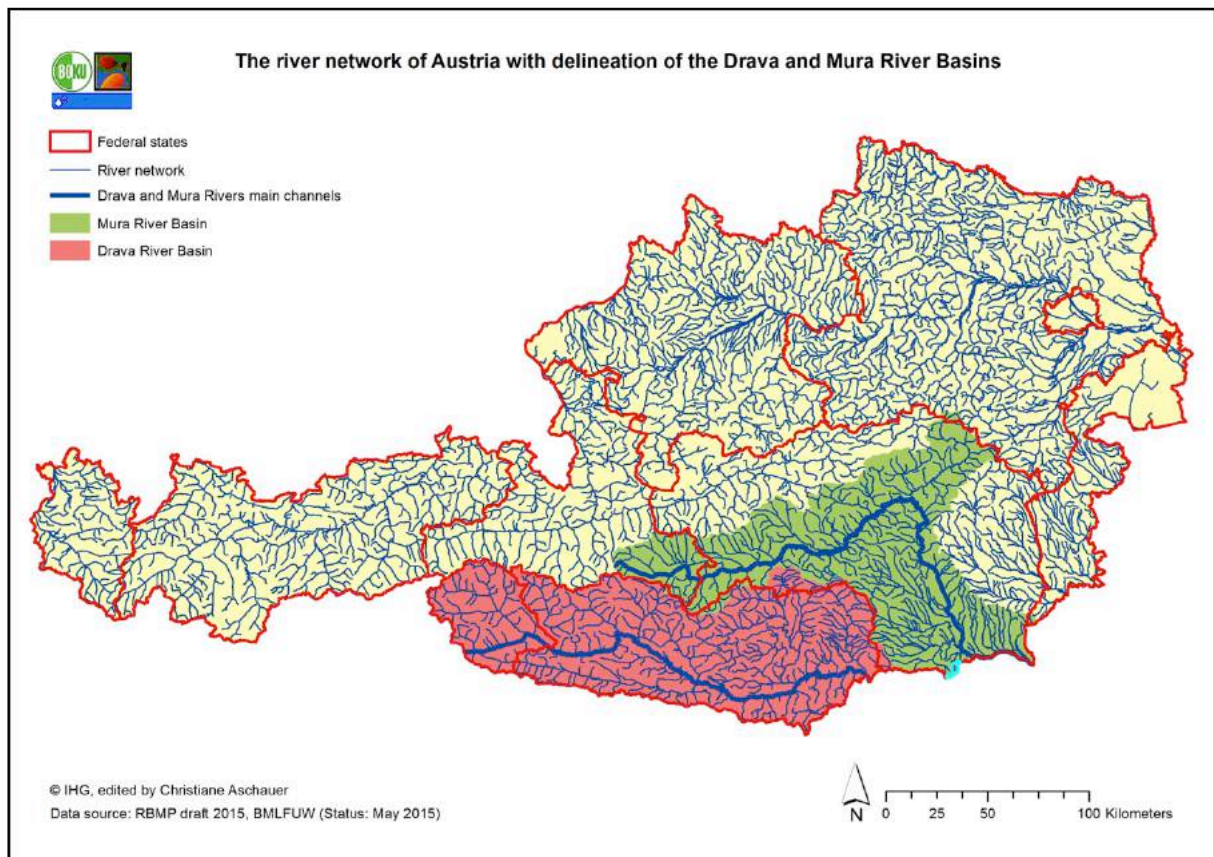


Figure 5.1 The river network of Austria with delineation of the Drava and Mura River Basins.

5.1.1.1.2 Description of current RBMP: Stressor situation in Austria and in the Drava and Mura River Basins

In Austria, the last inventory assessment executed within the WFD implementation was carried out in 2013 (BMLFUW, 2013) and supported the most recent River Basin Management Plan (RBMP), which was published in 2015 (BMLFUW, 2015). The inventory assessment aims at assessing the risk for each water body to fail the objective of the good ecological status in the years 2015, 2021 and 2027. This risk is defined by the results of a pressure assessment (compilation of pressures, here referred to as stressors), an impact assessment (evaluation of risk criteria by defining the impact of a stressor according to certain criteria) and by a risk assessment (verification of the impacts through a measured actual status of biota) (BMLFUW, 2013). The stressors assessed include physicochemical pollution (point source or diffuse source), hydromorphological alteration and other stressors, including invasive neobiota, predation, fishery and aquaculture, alterations of the sediment regime and climate change (BMLFUW, 2015).

In Austria, the inventory and status assessment revealed that for the RBMP 2015, 49,4% of the Austrian surface water bodies river length fail the good ecological status and another 9,9% fail the good ecological potential (objective for water bodies designated as heavily modified and artificial according to the WFD) (BMLFUW, 2015). Sources of risk are manifold– the risk for Austrian water bodies for 2021 is present as following: 21% due to residual flow, 8% due to impoundments, 2,8% due to hydropeaking, 32% due to morphological alterations, 46% due to connectivity disruption, 17% due to chemical point stressors and 25% due to chemical diffuse stressors. For Austria and especially the Drava and Mura River Basins, water quality issues are not priority (Schmutz et al., 2008), as multi-stress situations mainly occur due to hydromorphological alterations (BMLFUW, 2015). Thus, hydromorphological stressors are the main focal issue here. They include hydrological alterations as hydropeaking, impoundment and residual flow (due to water abstraction). Further, morphological alterations and connectivity disruption due to migration barriers are considered.

There is a long and huge interest in river restoration in various parts of Austria (summed up by Humpel, 2011; Kogler, 2008; Zitek et al., 2008) to improve ecological conditions. Especially in the Upper Drava River in the province of Carinthia (between Oberdrauburg and Spittal/Drau), multiple surveys and projects were conducted. These include the implementation of first river management concepts and multiple restoration measures, which are summarized in Appendix 12.1. For example, within the most recent project ‘SEE River’, relevant outputs generated include a detailed concept of measures to be implemented at the Upper Drava River corridor (‘Gewässerentwicklungskonzept’) (Amt der Kärnter Landesregierung, 2014). However, within the scope of these projects and measures, specific knowledge on the effects of multiple stressors is lacking and thus has not been addressed in previous water management concepts.

Most recent studies which quantified the relationship between stressors and fish using national data revealed divergent responses of fish assemblages: In a first stressor-specific and multi-stressor analysis, Schmutz et al. (2008) identified land use, connectivity disruption, impoundment length and mean discharge among best predictors to describe the impact on fish assemblages. A strong response of fishes is visible for impoundments (Schmutz et al., 2010). Mielach, (2010) confirms the reactivity of fish metrics to different nationally identified stressors. Moreover, the development of the Fish Index Austria (FIA, Haunschmid et al., 2006) is based on the evaluation of a set of hydromorphological stressor variables. It therefore is interesting to see whether the actual data of the inventory assessment reaffirm these results for the FIA and its single metrics,

as knowledge on most important influential variables is specifically important to identify priority of measures for hydromorphological restoration (Schmutz et al., 2010).

5.1.1.1.3 Main drivers / stressors in the basin

The Drava and Mura River Basins include 2.419 water bodies out of the RBMP database, which are located within the natural or potential fish occurrence area as defined by the Quality Objective Ordinance Ecology (QZV Ökologie, 2010) and the RBMP database (RBMP-DB, 2015). Water bodies are the smallest units of the federal water management level and thus the scale of investigation of MARS. After the general WFD classification (European Commission, 2000), water bodies are divided into inland waters (surface- and groundwater bodies) and transitional and coastal waters. Surface water bodies are distinguished according to the WFD and the national RBMP (BMLFUW, 2015) in terms of their water body category (rivers versus lakes), physical and other distinctive features, state (based on the impact and risk evaluation), and whether they are highly modified or artificial water bodies.

For each water body, five hydromorphological stressors, i.e. ‘residual flow’ (R), ‘morphological alteration’ (M), ‘connectivity disruption’ (B), ‘impoundment’ (I) and ‘hydropeaking’ (H) were available in the Austrian RBMP database (RBMP-DB, 2015). These stressors were derived during the impact assessment (‘Auswirkungsanalyse’) carried out as part of the Federal Inventory Assessment 2013 (‘Istbestandsanalyse 2013’) for the 2nd Austrian RBMP. The stressors were coded in stressor intensity classes from A to D based on specific criteria (see Table 5.1 and BMLFUW, 2013). Additionally, the stressor ‘chemical status’ (C) was derived from the Federal Inventory Assessment and the RBMP-database and coded in stressor intensity classes 1 to 3 (see Table 5.1 and BMLFUW, 2013).

5.1.1.1.4 Research questions

Based on the facts stated in the previous sections, this work aims to apply the MARS model and to identify the distribution and patterns of human stressors at the river basin scale. The focus is set on the Austrian Drava and Mura River Basins as an example for Alpine river catchments.

The following research questions are of interest:

- Which distribution and patterns of stressors can be identified within the Austrian Drava and Mura River Basins?
 - Which stressor categories (single and multiple stressors) occur and which stressor quantities (no, single, multiple numbers of stressors) can be detected on a water body?
 - Where do stressors occur in terms of fish zone?
- How do these stressors affect fish based indicators and the ecological status?
- How does the factor ‘fish zone’ influence the response of fish based indicators and the ecological status?
- How do multiple stressors interact and is this reflected by the response of fish based indicators and the ecological status?

5.1.1.1.5 Recreational fishing as an ecosystem services in the Drava and Mure River Basins – a theoretical discussion for future analyses (with input from Susanne Prinz and Kurt Pinter)

Ecosystem Services are the contributions of ecosystems to human well-being, these services are final in the sense that they are ecosystem outputs that most directly affecting the well-being. (Millenium Ecosystem Assessment, 2005). Freshwater recreational fishing (FRF) is a prominent example of Cultural Ecosystem Services (CES) (Haines- Young & Potschin, 2013), as it is important to many people and generates income, jobs, and funding for conservation. Dating back to the mMiddle sStone age, angling and fishing for pleasure is an ancient practice in the acquisition of natural resources (Henshilwood et al, 2011; Hughes, 2015). In Austria, a large angling community was analysed in a survey by (Kohl (, 2000) with around 410.000 active

fishermen (about 21 % of Austria's population). This survey showed that anglers in Austria spent almost 182 Million Euros for angling holidays, fisheries licenses and angling equipment. The main motives for angling are clearly recovery and relaxation, followed by experiencing and enjoying nature. "Fish hunting" itself makes just one third of angler's motivation for their sport (Kohl, 2000). This shows that anglers have a direct economic impact and represent a strong lobby, due to their straight dedication on protection of rivers and lakes or indirectly with their license fees (Kohl 2000).

In terms of ecosystem service valuation, one can assume that the quality of water bodies can be affiliated with a value - . This value is the sum of various different values for different consumers of its Ecosystem services (ESS). The special case of recreational fishing In this context, the special case of recreational fishing as a CES is that its ESS demands comprise both non-material benefits such as enjoying beautiful river landscape and the appearance of fish as well as consumptive services as catching fish, which is also high connected to healthy fish stocks.

A recent global-level study has provided empirical evidence that human dependence on CES increases in the course of a country's economic development, while dependence on substitutable provisioning ecosystem services decreases. Recognition and observation of CES dynamics is, therefore, vital for assessing the impacts of ecosystem degradation on human well-being (Hernández-Morcillo et al, 2013). This among other factors causes difficulties in monetizing its values. Therefore, also recreational fishing is a challenge in finding indicators and appropriate valuation methods. Furthermore, there is also a big lack in research and literature sources dealing with investigations on potential connection between fishing licenses' price level and the river condition of a fishing beat. As a consequence, no publications could be found explaining the driving factors of fishing beat prices yet. However, some scientific publications could be consulted as support for the setup of athis new approach of fishing license price indicators in order to receive the monetary value of recreational fishing services for enhanced applications on sustainable conservation strategies. The most frequent indicator for cultural services (CES) is the number of visitors of a lake, river or wetland (Haines-Young & Potschin, 2013).

In the case study of Amy M. Villamagna et al. (2014), the number of fishing licenses and the number of licenced anglers within a specific distance to the next fishable water bodies were consulted as indicators in parts of the United Sstates. They were used for the calculation of

capacity and demand for detection of areas with potential overuse of freshwater recreational fishing as the flow of benefits from the FRF experience is driven by demand and often constrained by capacity (Villamagna et al., 2014). Villamagna et al 2014 also transferred the results of Hunt and Hutt (2010) into their methods, by including the distances in kilometres of the fishing beat to the next highway and state capitals as potential additional drivers of the fishing license price levels. Furthermore, a calculation with the indicator “number of days spent with angling” was considered. This approach is difficult to apply in the case of Austria, where there are two groups of anglers were identified, spending time for tone spending heir hobby. One group spends around 5 days per year and the other one more than 30 days angling, which makes a total of about 23,3 fishing days within 12 months in the year 2000 (Kohl, 2000).

Villamagna et al (2014) transferred the results of the study of Hunt and Hunt, 2010, in their methods that licensed anglers most likely go fishing within a distance of 16.09 km from their home to fishable waterbodies.

Consequently this study adopted also this approach and includes the distances in kilometres of the fishing beat to the next highway and state capitals as potential additional drivers of the fishing license price levels.

For future regional approaches in the Drava and Mura River basins, a more specific indicator (as quality of fresh waters for fishing) could be the morphological status of a river. This quality element has not been used so far for a valuation approach for recreational fishing even though morphological status is an important factor for fish due to its habitat requirements. TThere has been considerable scientific effort to define appropriate fish metrics and fish indices for the assessment of the ecological status of different types of running waters in the United States. In Europe even, the EU Water Framework Directive (WFD, European Commission, 2000) has been a major driver in the development of standardised fish based assessment methods and metrics to determine the ecological status of European rivers and the classification of human degradation (Schinegger et al, 2013). Subsequent, EU-funded projects such as FAME (FAME Consortium, 2004) and “European Fish Index Plus (EFI+)” (EFI+ Consortium, 2009), have developed multi-metric indices based on fish assemblages and analysed relationships between fishes and human pressures (Schinegger et al, 2013).

In the last decades the morphological status of Austrian rivers decreased constantly in the last decades and in . In total, 82 % of Austria’s bigger river stretches arewere strongly affected by

anthropogenic influences. (Muhar, 2013 et al). Due to some measure the morphological status could be enhanced. Nevertheless after 'Ist- Bestandsanalyse 2013' almost 60% of Austria's water bodies are at risk of failing good ecological status caused by hydromorphological pressures by 2015 according the EU Water Framework Directive. Main Chief causes are extensive flood protection measures and the intensive usage of water powerplants as renewable energy source (BMLFUW, 20154).

This might also resulted into a decline of ecosystem service capacity and value. Therefore an approach of detecting the connection between morphological status and the ecosystem service value is to take the fishing beat prices into account.

Furthermore, head water streams (HWS) are very sensitive to hydromorphological pressures (Schinegger et al, 2013) which is the reason why in this study focuses on the upper and low trout region.

Due to the fact that many of potential indicators of recreational fishing are difficult to monetize as mentioned before, fisheries license prizes could be a good starting point for the valuation approach. However, a big challenge is data research on fishing license prices, leases of beat etc. in Austria, as no joint database exists yet. In the near future, about 50 stretches with data for fishing license prices might be available for rivers with a catchment size larger than 100km² in the upper and lower trout zone of Austria. As a consequence, the achievement of detecting value of high morphological status and recreational fishing with its strong angling lobby could lead further to the direction of conservation of natural river stretches instead of alter them severely for small inefficient hydropower plants or impoundments.

Table 5.1. Stressor categories according to Mühlmann (2013) and translation into stressor classes

Stressor intensity classes of the national impact assessment used in MARS model	Stressor classification used in stressor analysis	Stressors							
		Impoundment (I)		Hydropeaking (H)		Residual flow (R)	Connectivity disruption (B)	Morphological alteration (M)	Chemical state (C)*****
		River basin district <1.000km ²	River basin district >1.000km ²	Small & medium surface water bodies	Type "large rivers"		Within fish habitat		
A (0) No or very low impact	0 Less impacted	No I		No H		No abstraction or abstraction according to QOO Ecology** §12 heel 2	No B or passable without fish migration facility (e.g. ramp)	All 500m-sections within SWB = class 1*****	1
B (1) Low impact	0 Less impacted	No I >500m & sum I <10% of surface water body (SWB)		<1:3 or designated as "no significant H-impact**"	Very slight H or designated as "no significant H-impact**"	Abstraction with dotation order during full year or with dotation order during authorized abstraction period; according to QOO Ecology** §13 heel 2 values are met or abstraction at facilities authorized 1990-2010 according to specifications of ecological functioning/good status	Limited passability of B or B**** passable due to fish migration facility & no additional non-passable length elements	<30% class 3-5*****	2
C (2) Possible significant impact	1 More impacted	Single I 500-1.000m or sum of multiple I cover 10-30% of SWB	Single I 500-2.000m or sum of multiple I cover 10-30% of SWB	1:3-1:5 or H amplitude unknown or designated as "significant H-present risk**"	Designated as "significant H-present risk**"	Abstraction with regulated dotation during the whole year or with regulated dotation within authorized period; values according to QOO Ecology** §13 heel 2 are not met*** or abstracted dotation unknown	>=1 non-passable B	30-70% class 3-5 & <30% class 4-5*****	3
D (3) Strong significant impact	1 More impacted	Single I >1000m or sum of multiple I cover >30% of SWB	Single I >2000m or sum of multiple I cover >30% of SWB	>1:5 or designated as "significant H-present risk**"	>each distinct flush or designated as "significant H-present risk**"	No or no dotation order during full year or no continuous dotation order during authorized abstraction period or water body sections, which fall dry due to insufficient dotation during the whole year or during certain periods.	-	>70% class 3-5 or >30% class 4-5*****	-

* According to 'BOKU Hydropeaking-study' by Schmutz et. al (2013)

** Quality objective ordinance ecology

*** abstractions with MQRW < MJNQTnat or NQTRW < NQTnat

**** Barriers with functioning fish migration facilities and barriers with (possibly) limited passability

***** Classes according to 'Guidance on hydromorphological state assessment' by Mühlmann (2013)

***** Chemical status expressed in intensity classes 1-3 was selected instead of values proposed by impact assessment chemistry

5.1.2 Context for modelling

Overall MARS model and DPSIR model for the Drava/Mura Basins

The MARS conceptual model is implemented by the river basin case studies within MARS for the Austrian Drava and Mura River Basins (Figure 5.2). The main idea is that drivers (D) (e.g. energy – hydropower production) cause pressures (P) (equivalent to stressors; e.g. dams, barriers and locks) and consequently affect water body state (e.g. connectivity loss, changes in the hydraulic regime – abiotic state), which impacts the ecosystem functioning (e.g. by reduction of fish biomass – biotic state). Consequently, ecosystem services are reduced and may demand for response through policies or management actions (R) (e.g. restoration). Within the MARS empirical models for the river basin approach, the focus of interest is on drivers, pressures (here stressors) as well as abiotic- and biotic states.

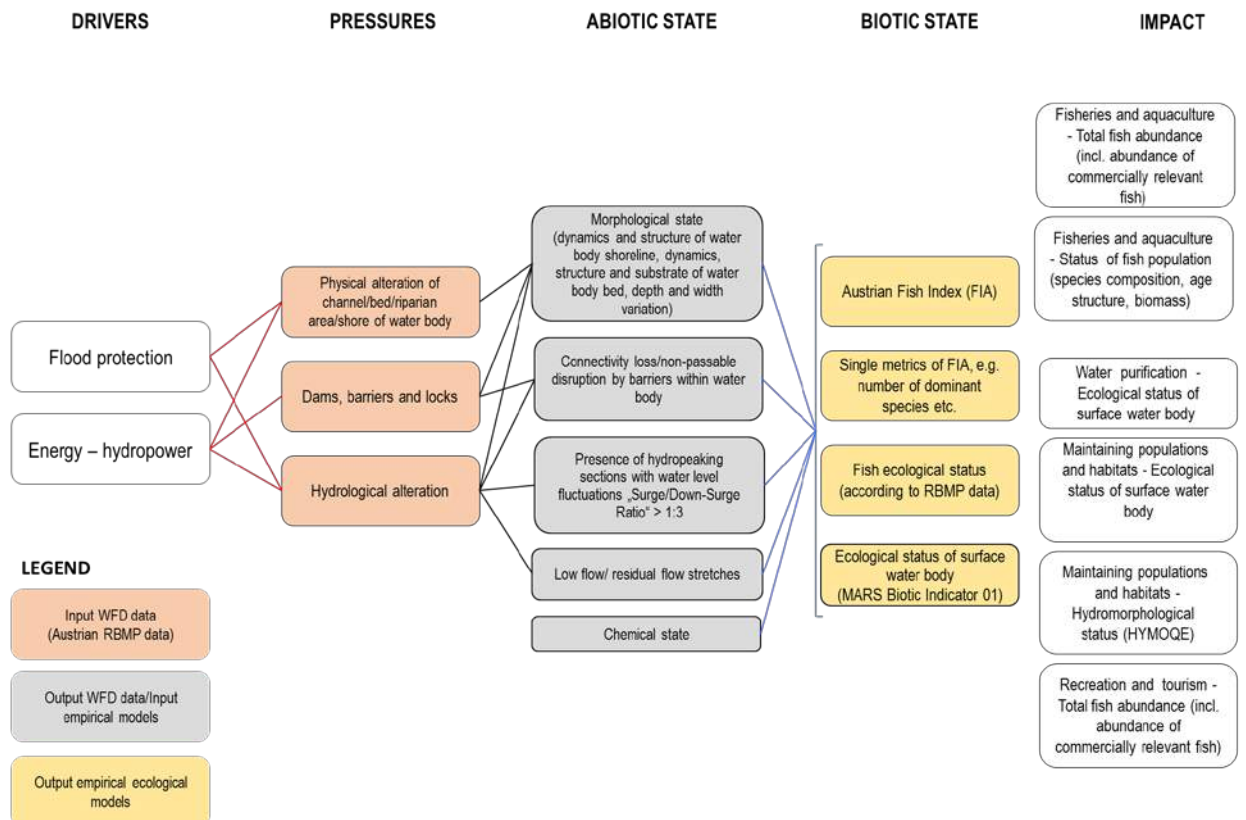


Figure 5.2 MARS empirical model for the Austrian Drava/Mura River Basins.

5.1.3 Data and methods

5.1.3.1.1 Data

Data overview: Fish data

Fish sampling sites were available from the biocoenetic regions Epirhithral to Epipotamal (sensu Huet, 1959) (Figure 5.3). Fish data were obtained from the ‘Fish Database Austria’ (FDBA) (FDBA, 2015), which is managed by the Institute for water ecology, fish biology and lake ecology (IGF)¹ of the Federal Office of Water management (BAW)². It contains fish samples surveyed according to the decree on water body state survey (Gewässerzustandsüberwachungsverordnung, GZÜV). Fish sampling was conducted based on a standard sampling protocol (Haunschmid et al.,

¹ Institut für Gewässerökologie, Fischereibiologie und Seenkunde; <http://www.baw.at/index.php/igf-home.html>

² Bundesamt für Wasserwirtschaft; <http://www.baw.at/>

2010). Samples were available from years 2006 to 2014, which fit well to the stressor data, derived from Austrian RBMPs 2009 and 2015.

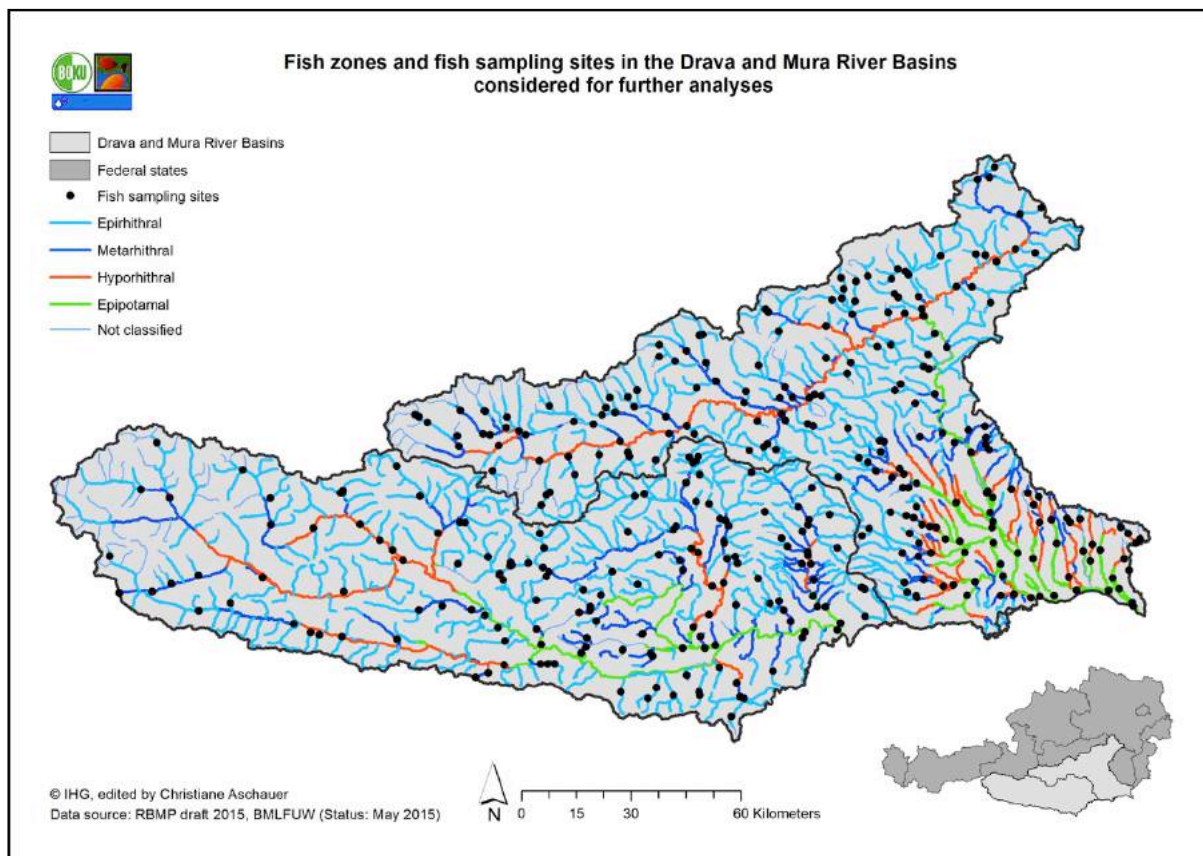


Figure 5.3 Fish zones and fish sampling sites in the Drava and Mura River Basins considered for further analyses.

The fish based indicators available here include the Fish Index Austria (FIA) and its single metrics, an IBI that was developed for the assessment of the fish-ecological status in Austria according to the WFD’s needs. The FIA is composed of a number of core metrics. They include number of dominant species, number of subdominant species, number of rare species, number of habitat guilds (rheophil, limnophil, indifferent), number of reproductive guilds (lithophil, phytophil, psammophil), fish zonation index and population age structure of dominant and subdominant species (Table 5.2). The assessment evaluation is based on the deviation between a predefined expected reference condition (‘Leitbildkatalog’ BAW IGF, 2015a) and the actual values observed (Haunschmid et al., 2006). Moreover, the fish biomass serves as ‘knock-out’ criterion, whereby sampling sites with less than 50 of 25 kg/ha are assigned to ‘poor’ or ‘bad’ ecological status, independent from the scores of the other metrics. The final FIA is calculated as

weighted mean of grouped metrics (see Table 5.2) ranging from WFD-class one (high status) to class five (bad status). A tool to calculate the FIA is provided by the IGF³.

In addition to the FIA and related metrics described above, the final database here contains information on the number of occurring species (calculated as sum of actually caught dominant, subdominant and rare species) and the ecological state (derived from RBMP-DB) (see Table 5.3 for a complete list of indicators). These variables were analysed in terms of their response to stressors and will later on be referred to as biotic indicators or fish based indicators and the ecological status.

Table 5.2. Classification table for Austrian fish metrics.

Metric name	Metric ID	Evaluation class				
		1	2	3	4	5
Dominant species	%DS	100%	90-99 %	70-89 %	50-69 %	<50 %
Subdominant species	%SDS	100-75%	74-50%	49-25%	<25%	0
Rare species	%RS	>49%	49-20%	19-10%	<10%	0
Habitat guilds	DEV_HG	none missing	1 missing	2 missing	> 2 missing	all missing
Reproductive guilds	DEV_RG	none missing	1 missing	2 missing	> 2 missing	all missing
Deviation Fish Zonation Index (FIZI)	DEV_FIZI	0-0,3	≥0,3-0,6	≥0,6-0,9	≥0,9-0,1,2	1,2
Age structure dominant species	AS_DS	1	2	3	4	5
Age structure subdominant species	AS_SDS	1	2	3	4	5

The FDDBA for Drava and Mura River Basins originally contained 525 fish samples at 465 sampling sites. The data had to undergo a filtering process, as multiple fish samples per water body and fish sampling site (of different years) occurred. This was performed in a stepwise procedure and selection was chosen as following:

- 1) A data extract from the RBMP-DB in January 2016 gave information on the fish samples, which were selected for the evaluation of the hydromorphological status evaluation (GZÜV- ID in field 'ZUST_BIOLOGIE_HYDROM_2015_MESSUNG' of table 'Monstertabelle'). The respective sample was selected as final sample for the associated water body (160 samples).
- 2) For remaining water bodies and fish samples, the samples with most recent date were selected (186 samples and unique sampling sites per water body).
- 3) A random selection function in R was used for selecting unique fish samples for the remaining water bodies (26 out of 58 samples).

Finally, 372 fish samples associated with a unique sampling site and linked to a unique water body remained for further analysis.

Table 5.3. Description of biotic indicators (FIA metrics and other indicator)

Trait category	Indicator abbreviation	Description	Measurable indicator reaction with increasing stressor	N	Median (Range)
FIA metrics					
Biocoenosis	%DS	Percentage dominant species - fish species must occur in particular bioregion/biocoenetic region in high relative frequency	decrease	372	100 (0-100)
Biocoenosis	%SDS	Percentage subdominant species - fish species must occur in particular bioregion/biocoenetic region in medium relative frequency	decrease	372	0 (0-100)
Biocoenosis	%RS	Percentage rare species - fish species can occur in particular bioregion/biocoenetic region in low relative frequency	decrease	372	0 (0-100)
Biocoenosis	EVAL_DS	Evaluation of dominant species	increase	372	1 (1-5)
Biocoenosis	EVAL_SDS	Evaluation of subdominant species	increase	372	1 (0-5)
Biocoenosis	EVAL_RS	Evaluation of rare species	increase	372	3 (0-5)
Reproductive guild	DEV_RG	Deviation of actual present number of reproductive guilds from reference	increase	372	1 (0-5)
Reproductive guild	EVAL_RG	Evaluation of the reproductive guilds	increase	372	2 (1-5)
Trophic guild	BM	Biomass in kg/ha of native species and rainbow trout	decrease	372	69.1 (0-1664,0)
Habitat guild	DEV_HG	Deviation of actual present number of habitat guilds from reference	increase	372	0 (0-4)
Habitat guild	EVAL_HG	Evaluation of habitat guilds	increase	372	1 (1-5)
Biocoenetic region	DEV_FIZI	Deviation of actual fish zonation index from reference	increase	372	0,1 (0-5.7)
Age structure	AS_DS	Evaluation of length-frequency diagram of actual present dominant species	increase	372	1 (0-10)
Age structure	AS_SDS	Evaluation of length-frequency diagram of actual present subdominant species	increase	372	0 (0-9)
Age structure	EVAL_AS_DS	Evaluation of length-frequency diagram of actual present dominant species	increase	372	2,3 (1-5)
Age structure	EVAL_AS_SDS	Evaluation of length-frequency diagram of actual present subdominant species	increase	372	3,5 (1-5)
Age structure	AS	Total evaluation of population age structure of dominant and subdominant species	increase	372	3 (1-5)
Guilds	GUILDS	Total evaluation of habitat guilds and reproductive guilds	increase	372	1,5 (1-5)
Dominance	DOMIN	Total evaluation of dominance expressed by FIZI	increase	372	1 (1-5)
Species	SPEC	Total evaluation of percent of dominant, subdominant and rare species	increase	372	3 (1-5)
Species composition	SPCOM	Total evaluation of species composition evaluated by SP and GUILDS	increase	372	1,9 (1-5)
Other indicators					
	ES	Ecological status of water body	increase	329	3 (1-5)
	FIA	Fish Index Austria	increase	372	2,5 (1-5)
	NSP	Total number of species caught at site	increase, decrease	372	2 (0-26)

Description of and pre-processing of data: Distribution and patterns of single and multiple stressors in water bodies

To perform an analysis on distribution and patterns of single and multiple stressors, original stressor intensity classes from the national impact assessment were recoded according to the following scheme:

- Intensity classes A and B were associated with value 0 (less impacted)
- Intensity classes C and D were associated with value 1 (more impacted)

In a second step, stressors classified as ‘1/more impacted’ were summed up and combined into two new variables for each water body - these are ‘Stressor category’ and ‘Stressor quantity’ (for an example see Table 5.4). Stressor category shows the occurrence of single and multiple stressors. Stressor quantity informs whether no, single, or multiple (double, triple, fourfold, fivefold) stressors occur at a water body. The analysis on stressor distribution and patterns was performed for all water bodies of the Drava and Mura River Basins (2.419 water bodies) and separately for those water bodies where fish sampling sites were available (372 water bodies). From here on, the Drava and Mura River Basins are referred to as ‘total basin’.

The variable recoding and calculation process was performed with statistical software R version 3.1.3 (R Development Core Team, 2015), graphs were plotted using the ‘ggplot2’ package (Wickham, 2009), and the geospatial analysis was executed using ESRI’s ArcGIS 10.2.2 software (ESRI, 2011).

Table 5.4 Description of stressor variable recoding and calculation of the new variables ‘Stressor category and ‘Stressor quantity’.

Water body ID	Stressors												Stressor category	Stressor quantity
	M		I		R		H		B		C			
	IA	01	IA	01	IA	01	IA	01	IA	01	IA	01		
902340003	C	1	B	0	C	1	A	0	C	1	A	0	MxRxB	3

M... Morphological alterations; I... Impoundment; R... Residual flow; H... Hydropeaking;

B... Connectivity disruptions; C... Chemical status

IA... Stressor intensity class of the national impact assessment

01... Classification as less (0) and more (1) impacted

5.1.3.1.2 Methods

EM approach: Response of fish assemblages to multiple stressors

The selected modelling approach is based on the MARS cookbook, which was developed to give guidance for MARS analysis of multiple stressors and to guarantee a common strategy for reaching the MARS objectives. It proposes a stepwise procedure by applying Boosted Regression Trees (BRTs), Random Forest (RF) and Generalized Linear Models (GLMs) for quantifications of the stressor-response relationships.

Thus, the analytical approach to investigate the relationship between human stressors and fish assemblages (as biotic indicators) was divided into two parts (see Figure 5.4).

First, a descriptive analysis of the relationship between the variables ‘Stressor category, ‘Stressor quantity’ and selected indicators was conducted with the use of boxplots.

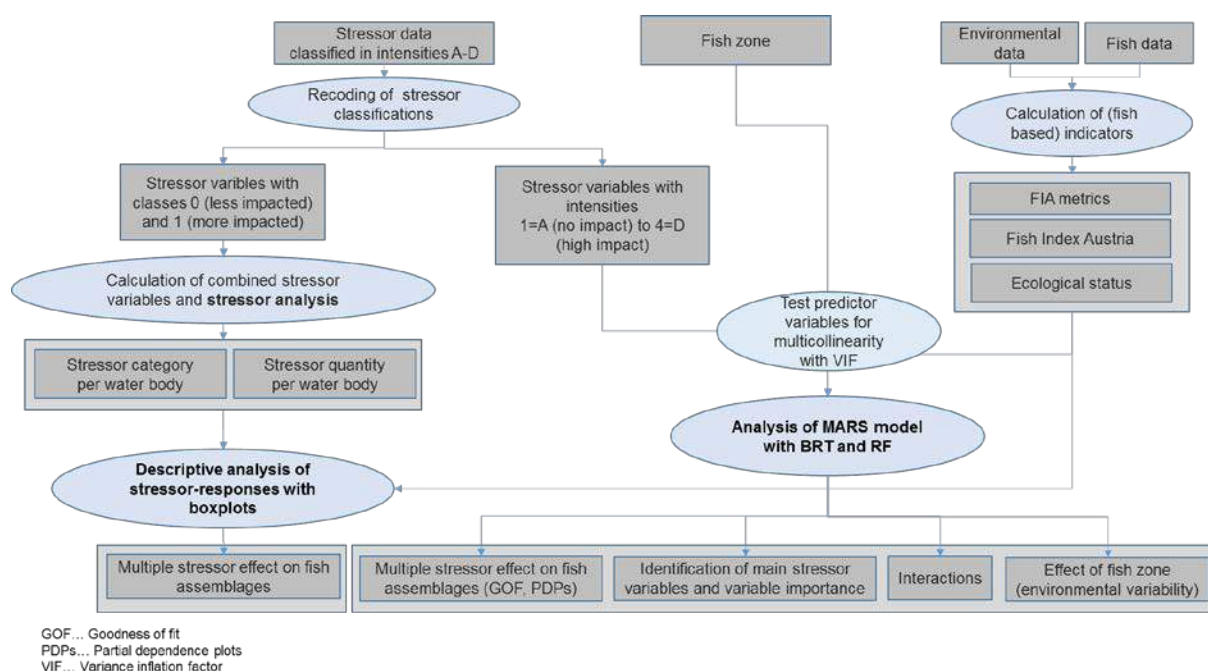


Figure 5.4 Analytical design including the analysis of stressor distribution and patterns, the descriptive analysis of the relationship between variables ‘stressor category, ‘stressor quantity’ and selected indicators and the analysis to implement the MARS model for Drava and Mura River Basins.

Statistical methods for modelling stressor-indicator relationships are manifold and include among others rather descriptive explanations without quantifications of multiple impacts (Cunjak et al.,

2013; Schinegger et al., 2013). Machine learning approaches such as BRTs (Clapcott et al., 2012), conditional tree forest models (Nelson et al., 2009), Bayesian belief networks (Mantyka-Pringle et al., 2014; Roberts et al., 2013) and linear models are frequently applied. They include general linear models (De Zwart et al., 2006; Lange et al., 2014; Van Looy et al., 2014) and linear and logistic regressions (e.g. Johnson et al. 2009; Ayllón et al. 2009; Wenger et al. 2011; Walters et al. 2013). An advantage of machine learning methods such as BRTs and RF (Breiman, 2001) is that they can handle mixed normal, categorical and continuous predictor variables. Further, they allow missing values in the data, no transformations are required (parametric data), outliers are accepted, interaction effects between predictors are handled, and non-linear relationships are also allowed (Elith et al., 2008; Mercier et al., 2011). However, ecological hypothesis testing in order to relate empirically and observed phenomena to explanatory variables (such as stressor effects on biota) is supposed to be more suitable with regression-based analytical tools, such as GLMs (Argillier et al., 2014).

Further in MARS, BRTs aim to identify the stressor's hierarchy in the dataset as well as interactions of stressors. The variable hierarchy (in terms of ranking and contribution to the overall variance explained) is important, as it later on affects the ranking and selection of stressor variables to be included in the GLM.

In contrast, the benefit of running RF is that it may further contribute understanding the hierarchy of stressors. The outputs of BRTs and RF measure the contribution of multiple predictor variables to one single output variable and the goodness of fit (GOF) (% variance explained). Additionally, interaction terms and plots of the fitted function (partial dependence) are derived from the BRT model. Partial dependence plots (PDPs) show the fitted response of indicators to predictors. They give guidance on shape of fitted surface and are available as boxplots, as predictors here are categorical and ordinal data. They are showing the values of response variables that have been predicted by models and were fitted to the dataset. This enables to identify patterns of metric responses and can therefore help to set potential thresholds at which the metric value sharply changes (Feld et al., 2016; Hering et al., 2013).

Before running BRTs and RF, the variance inflation factor (VIF) as a descriptor of collinearity among predictor variables was calculated for further variable selection. This index measures the extent of increase in variance of an estimated regression coefficient due to collinearity. To be on

the safe side, the threshold was set at >8 , as collinearity imposes serious flaw upon a regression model if the descriptors show a VIF >10 (Zuur et al., 2007).

For BRT, two models were then run:

- Model 1 examined the response of indicators to all six stressor variables (H, M, C, B, I, R see Table 4.1) giving information on the suitability to indicate ecosystem integrity (Karr, 1991).
- Model 2 adds the variable fish zone (FIZ) to the set of stressor variables as predictor to explore the effect of natural variability.

For BRT analysis, model parameters were set as follows:

- Tree complexity was fixed at level 2, as it sets the order of interactions.
- The learning rate determines the weight applied to individual trees and was tuned for each model assuring that at least 1000 trees were fitted.
- The bag fraction is the proportion of observations, which are used for the model when selecting variables. It was set to level 0.5.
- The response variable's family type was selected according to their nature as 'Gaussian' for continuous and as 'Poisson' for count data.

For RF analysis, model parameters were set as following:

- A forest of 2000 trees was built according to the cumulative out-of-bag (OOB) error rate.
- The maximum depth allowed for a tree was set at 5 (node depth).
- The number of variables per level was set at 3 (mtry).

Analyses were performed in R version 3.1.3 (R Core Team, 2015) using the 'gbm' package of Ridgeway (2013) for BRTs and RF was carried out using the 'randomForestSRC' package of Ishwaran and Kogalur (2014). The MARS empirical modelling approach includes a quantification of multiple stressor effects on biotic indicators by running GLMs. This study accounts for a preliminary and exploratory analysis to quantify stressor-response relationships with the most recent Austrian RBMP-data with BRTs and RF. Running GLMs is thus not part of this investigation, as complexity would surmount the scope of this present work. However GLMs will be included in a following step in the implementation of the MARS model.

5.1.4 Results

EM results: Distribution and patterns of single and multiple stressors in water bodies

Occurrence of single stressors

The RBMP-DB includes data on single stressor intensities (Figure 5.5) that were aggregated to categories ‘less impacted’ (class 0) and ‘more impacted’ (class 1) (Figure 5.6). In the total basin, water bodies were mostly affected by connectivity disruptions (B) in 293 water bodies. Morphological alterations (M) were detected in 153 water bodies and water abstractions (leading to residual flow sections, R) in 127 water bodies. In only a few cases, category ‘more impacted’ was present in water bodies with fish sampling sites: For hydropeaking (H) 11 water bodies, for impoundment (I) 22 water bodies and for the chemical status (C) 4 water bodies.

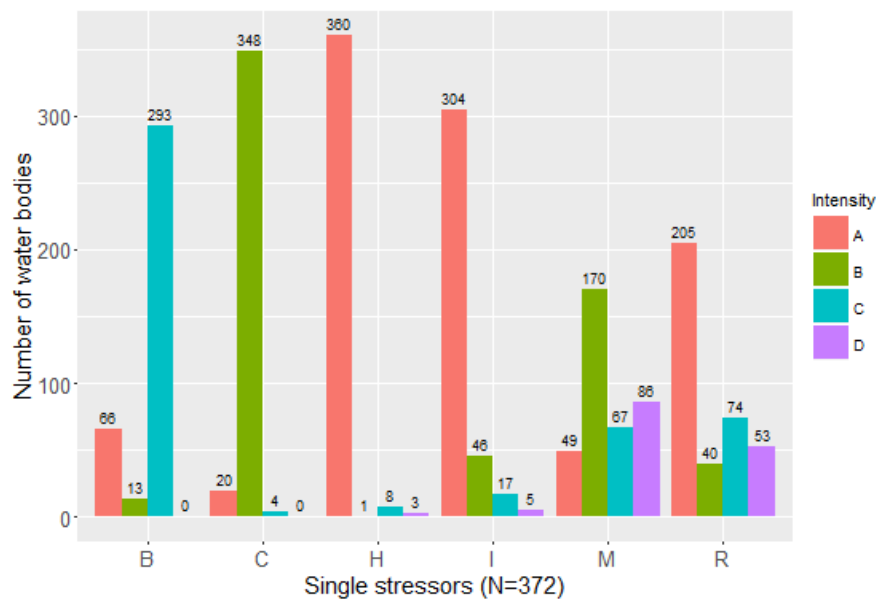


Figure 5.5 Frequency of water bodies with related fish sampling sites and the occurrence of single stressor intensities.

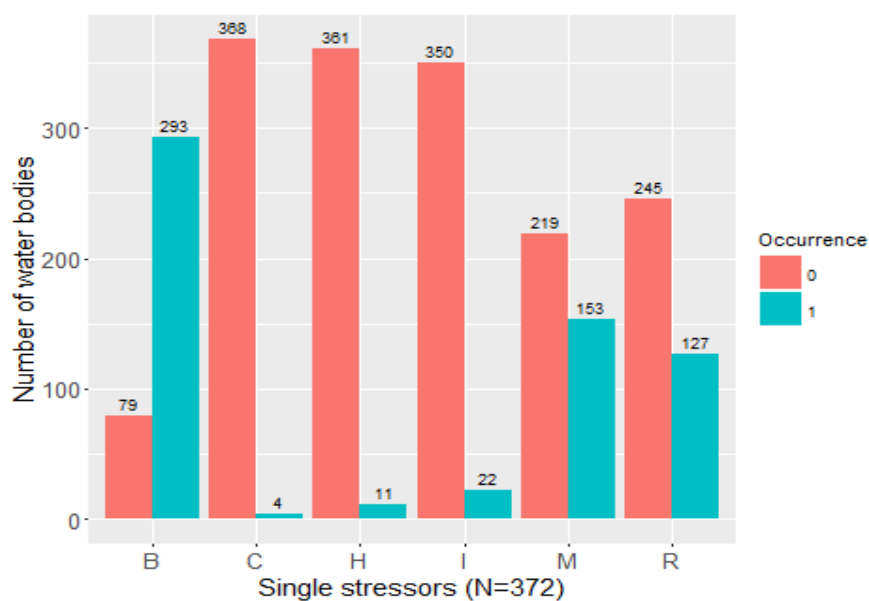


Figure 5.6 Frequency of water bodies with related fish sampling sites and the occurrence of single stressor intensities).

Distribution and patterns of variable ‘Stressor category’

The conducted descriptive analysis revealed that 28% of water bodies in the Drava and Mura River Basins are impacted by single, 27% by multiple stressors and only 44% face no or lower human stress (noS) (Table 5.5). Among the water bodies where fish were sampled, only 9% are under low or no stress and 91% are significantly or highly impacted (according to the stressor intensity classes of the national impact assessment, see also Table 5.1). In both river basins, 28 stressor categories (single and multiple stressors) are observed, whereas in water bodies with fish sampling sites, 26 stressor categories are present. There are however only five categories of single and multiple stressors which occur in at least 20 water bodies (without and with related fish sampling sites). These include the single stressors connectivity disruption (B), morphological alterations (M) and the multiple stressor categories morphological alteration combined with connectivity disruption (MB), connectivity disruption combined with residual flow (BR) as well as morphological alteration combined with connectivity disruption and residual flow (MBR).

In the following description of results, the focus is set on the distribution and patterns of stressors within water bodies of the total basin, presenting the stressor situation (first value). The second value after the slash informs on results for water bodies where fish sampling sites were available.

In terms of fish zone, a large majority of water bodies are situated in zone Epirhithral 1.815/195. The fish zone Metarhithral represents 380/88 water bodies, the Hyporhithral 155/44 and the

Epirhithral 95/43 water bodies. For the five most frequently occurring categories of single and multiple stressors, the following patterns were found: In Epirhithral, connectivity disruption (B) as single stressor is dominating with an occurrence of 23%/35% of the water bodies. This is followed by a combination of connectivity disruption and residual flow (BR) with 10%/15% occurrence and connectivity disruption combined with morphological alteration (MB) in 11%/25% of water bodies. In Metarhithral, also connectivity disruption (B) dominates with 18%/23% of water bodies affected, combined morphological alteration and connectivity disruption (MB) occur in 16%/24% and connectivity disruption combined with residual flow (BR) in 9%/20% of water bodies. For Hyporhithral, the patterns change with 17%/23% of water bodies affected by morphological alterations combined with connectivity disruption (MB), only 15%/9% by connectivity disruption (B), 14%/18% by morphological alteration (M) and 8%/11% by connectivity disruption combined with residual flow (BR). In Epipotamal, 24%/26% of water bodies are affected by morphological alteration combined with connectivity disruption (MB), 17%/14% by single morphological alteration (M) and 11%/12% by connectivity disruption (B) only.

Water bodies affected by connectivity disruption (B) and connectivity disruption combined with residual flow (BR) decrease from Epirhithral to Epipotamal. Numbers of water bodies impacted by morphological alteration (M) only or combined with connectivity disruption (MB) increase. An overall combination of connectivity disruption together with morphological alteration and residual flow (MBR) are most present in Metarhithral (7%/13%) and Hyporhithral (5%/7%). Water bodies with no or low stress can be found to 48%/12% in the Epirhithral, in 36%/2% of Metarhithral, in 35%/2 of Hyporhithral and in 28%/19% of Epipotamal. Thus, more water bodies are classified as less impacted upstream than downstream. Figure 5.7 shows the spatial location of the most frequently occurring stressor categories in water bodies where fish were sampled.

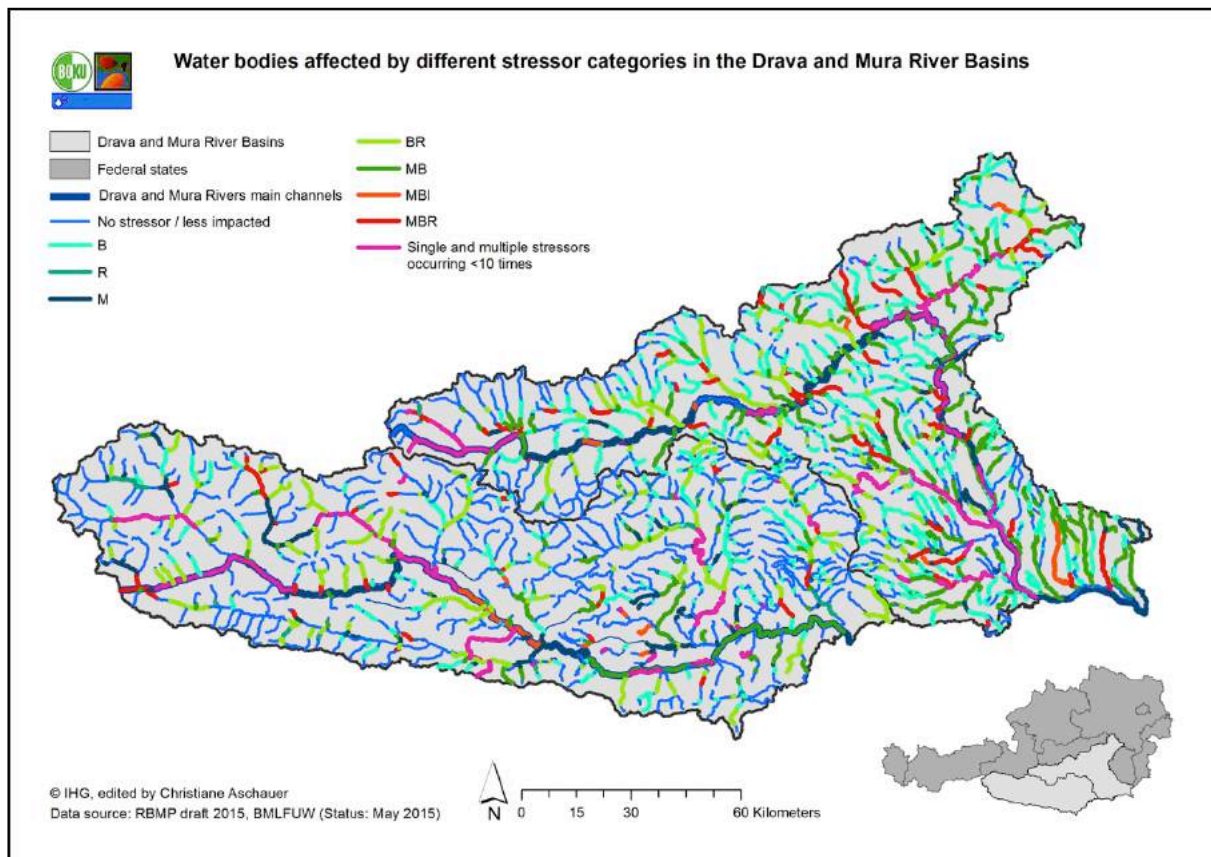


Figure 5.7 Water bodies affected by different stressor categories in the Drava and Mura River Basins.

Distribution and patterns of variable ‘Stressor quantity’

In the total basin, up to 5 stressors co-occur at a water body. When analysing the stressor quantity, clear patterns could be observed for all water bodies of the total basin/water bodies with fish sampling sites available: One or two stressors per water body are most frequently present and account together for 51%/76% of the cases. Three to five stressors per water body account for only 6/14% percent. The analysis of the total basins’ water bodies showed the following distribution and patterns: The proportion of less impacted sites (i.e. low number of stressor quantity) decreases from Epirhithral to Epipotamal (from 48% to 28%). In water bodies where fish sampling sites are located, less impacted water bodies are most present in Epirhithral and Epipotamal (31% together) and only few less impacted water bodies are present in Meta- and Hyporhithral (4%). The proportion of water bodies affected by single and double stressors account for the largest amount and approximately remain the same between fish zones (22-32%/30-34%). The occurrence of threefold stressors was most frequently observed in Metarhithral, mostly due to the stressor category MBR. Four- and fivefold stressors are very rare, only 16/10 water bodies

are affected by this stressor quantity. Figure 5.8 shows the spatial location of the most frequently occurring stressor quantities in water bodies where fish were sampled.

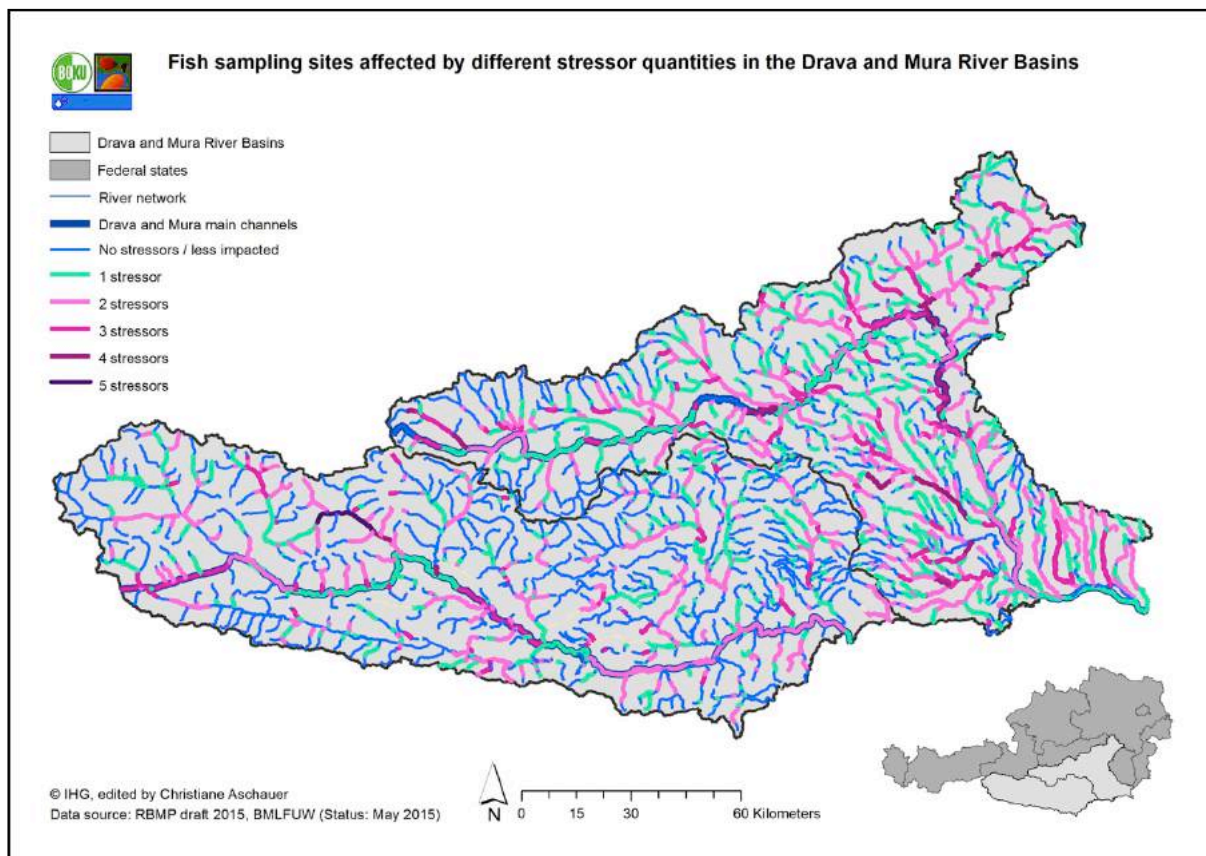


Figure 5.8 Water bodies affected by different stressor quantities in the Drava and Mura River Basins.

Tables 5.5 and 5.6 show the results of the stressor analysis. They give information on the number and percentage of water bodies of the total basin/water bodies with fish sampling sites affected by different stressor categories and quantities. Results were separated by sub-basin, fish zone and drainage area.

Table 5.5. Number and percentage of water bodies affected by different stressor quantities for all water bodies of the total basin/water bodies with fish sampling sites and separated by sub-basins Mura and Drava, fish zone and drainage area. Values in bold mark categories occurring more than 20 times in total

Stressor quantity	Total catchment														Sampling sites																						
	Total		Mura		Drava		EpiR		MetaR		HypoR		EpiP		<10 km ²	10-100 km ²	101-1000 km ²	1001-10000 km ²	no assignm	ent	Total	Mura		Drava		EpiR		MetaR		HypoR		EpiP		<10 km ²	10-100 km ²	101-1000 km ²	1001-10000 km ²
	N	%	N	%	N	%	N	%	N	%	N	%	N	%	N	%	N	%	N	%	N	%	N	%	N	%	N	%	N	%	N	%	N	%	N	%	
0	1065	44	377	688	822	48	135	36	39	25	27	28	2	24	5	2	0	34	9	9	25	23	12	2	2	1	2	8	19	2	24	5	2				
1	655	27	370	285	452	26	101	27	50	32	30	32	15	86	22	8	6	131	35	70	61	74	38	27	31	15	34	13	30	15	86	22	8				
2	551	23	303	248	371	22	102	27	46	30	28	29	7	105	33	8	16	153	41	99	54	78	40	41	47	19	43	15	35	7	107	32	8				
3	132	5	77	55	68	4	39	10	12	8	7	7	2	25	16	1	24	44	12	30	14	19	10	16	18	4	9	5	12	2	24	17	1				
4	15	1	10	5	2	0	3	1	7	5	3	3	0	1	5	3	16	9	2	7	2	1	1	2	2	4	9	2	5	0	1	5	3				
5	1	0	0	1	0	0	0	1	1	0	0	0	0	0	1	0	5	1	0	0	1	0	0	0	0	1	2	0	0	0	1	0					
Sum	2419	100	1137	1282	1715	100	380	100	155	100	95	100	26	241	82	22	67	372	100	215	157	195	100	88	100	44	100	43	100	26	242	82	22				

N...Total number of sites, %...Percentage of total sites, MUR...Mura, DRA...Drava, EpiR...Epihithral, MetaR...Metahithral, HypoR...Hypohithral, EpiP...Epiopotamal

Table 5.6. Number and percentage of water bodies affected by different stressor categories for all water bodies of the total basin/water bodies with fish sampling sites and separated by sub-basins Mura and Drava, fish zone and drainage area. Values in bold mark categories occurring more than 20 times in total.

Stressor category	Total catchment														Sampling sites																						
	Total		Mura		Drava		EpiR		MetaR		HypoR		EpiP		<10 km ²	10-100 km ²	101-1000 km ²	1001-10000 km ²	no assignm	ent	Total	Mura		Drava		EpiR		MetaR		HypoR		EpiP		<10 km ²	10-100 km ²	101-1000 km ²	1001-10000 km ²
	N	%	N	%	N	%	N	%	N	%	N	%	N	%	N	%	N	%	N	%	N	%	N	%	N	%	N	%	N	%	N	%	N	%	N	%	
noS	1065	44	377	688	822	48	135	36	39	25	27	28	2	24	5	2	0	34	9	9	25	23	12	2	2	1	2	8	19	2	24	5	2				
B	507	21	318	189	387	23	70	18	24	15	10	11	11	76	11	1	1	99	27	55	44	69	35	20	23	4	9	5	12	11	76	11	1				
M	116	5	43	73	50	3	26	7	21	14	16	17	2	8	9	4	1	23	6	14	9	2	1	7	8	8	18	6	14	2	8	9	4				
R	17	1	3	14	11	1	1	0	1	1	2	2	2	2	2	0	1	6	2	1	5	3	2	0	0	0	0	2	5	2	2	2	0				
H	5	0	4	1	0	0	2	1	1	1	1	1	0	0	0	1	1	1	0	0	1	0	0	0	0	0	1	2	0	0	0	0	0	1			
I	5	0	2	3	1	0	1	0	2	1	1	1	0	0	0	1	1	1	0	0	1	0	0	0	0	0	1	2	0	0	0	0	0	1			
C	5	0	0	5	3	0	1	0	1	1	0	0	0	0	0	1	1	1	0	0	1	0	0	0	0	0	1	2	0	0	0	0	0	1			
MB	283	12	196	87	171	10	59	16	27	17	23	24	3	60	8	1	2	72	19	58	14	30	15	21	24	10	23	11	26	3	60	8	1				
BR	241	10	97	144	190	11	36	9	12	8	2	2	4	45	21	2	2	72	19	35	37	48	25	18	20	5	11	1	2	4	46	21	2				
MI	7	0	6	1	2	0	0	0	2	1	3	3	0	0	1	3	2	4	1	4	0	0	0	0	1	2	3	7	0	0	1	3					
MR	7	0	0	7	3	0	3	1	1	1	0	0	0	0	1	1	2	2	1	0	2	0	0	1	1	1	2	0	0	0	1	1					
BI	6	0	2	4	2	0	4	1	0	0	0	0	0	0	1	0	2	1	0	1	0	0	1	1	0	0	0	0	0	1	0	0					
MH	4	0	2	2	0	0	0	0	4	3	0	0	0	0	1	1	2	2	1	1	1	0	0	0	0	2	5	0	0	0	1	1					
MC	2	0	0	2	0	0	0	0	0	0	0	0	0	0	0	0	2	0	0	0	0	0	0	0	0	0	0	0	0	0	0	0	0				
RC	1	0	0	1	1	0	0	0	0	0	0	0	0	0	0	0	2	0	0	0	0	0	0	0	0	0	0	0	0	0	0	0	0				
MBR	97	4	60	37	57	3	26	7	8	5	3	3	0	19	11	0	3	30	8	23	7	15	8	11	13	3	7	1	2	0	19	11	0				
MBI	14	1	7	2	0	0	8	2	2	1	2	2	2	2	2	0	0	3	4	1	3	1	1	2	2	0	0	1	2	2	2	0	0				
MIR	4	0	4	0	0	0	0	0	0	1	1	0	0	0	2	1	3	3	1	3	0	0	0	0	0	1	2	2	5	0	0	2	1				
BRC	8	0	0	8	7	0	1	0	0	0	0	0	0	1	1	0	3	2	1	0	2	1	1	1	1	1	0	0	0	0	1	1	0				
MBH	3	0	2	1	1	0	2	1	0	0	0	0	0	0	1	1	0	3	2	1	1	1	1	1	1	1	0	0	0	0	1	1	0				
BIR	3	0	1	2	1	0	1	0	1	1	0	0	0	1	0	0	3	1	0	1	0	1	0	0	0	0	0	0	0	0	1	0	0				
BHR	2	0	2	0	0	0	1	0	1	1	0	0	0	1	0	0	3	1	0	0	1	0	0	1	1	0	0	0	0	0	0	1	0				
MHI	1	0	1	0	0	0	0	0	0	0	1	1	0	0	1	0	3	1	0	1	0	0	0	0	0	0	0	1	2	0	0	1	0				
MBIR	9	0	8	1	1	0	1	0	5	3	2	2	0	1	2	2	4	5	1	5	0	1	1	0	0	2	5	2	5	0	1	2	2				
MBRC	3	0	0	3	1	0	1	0	1	1	0	0	0	0	1	0	4	1	0	1	0	0	1	1	0	0	0	0	0	0	0	1	0				
MBHR	2	0	2	0	0	0	1	0	0	0	1	1	0	0	2	0	4	2	1	2	0	0	0	1	1	1	2	0	0	0	0	2	0				
MHR	1	0	0	1	0	0	0	0	1	1	0	0	0	0	0	1	4	1	0	0	1	0	0	0	0	1	2	0	0	0	0	0	1				
MBIHR	1	0	0	1	0	0	0	0	1	1	0	0	0	0	1	0	5	1	0	0	1	0	0	0	0	1	2	0	0	0	0	1	0				
Sum	2419	100	1137	1282	1715	100	380	100	155	100	95	100	26	241	82	22	67	372	100	215	157	195	100	88	100	44	100	43	100	26	242	82	22				

N...Total number of sites, %...Percentage of total sites, MUR...Mura, DRA...Drava, EpiR...Epihithral, MetaR...Metahithral, HypoR...Hypohithral, EpiP...Epiopotamal
noS...no flow stressor, B...Connectivity disruption, M...Morphology, R...Residual flow, H...Hydropeaking, I...Impoundment, C...Chemical status
Combined capital letters...multi-stressor situation e.g. MI...impact by morphological alterations and impoundment occur at water body

Response of fish assemblages to multiple stressors: Descriptive analysis of the relationship between human stressors and fish assemblages

In terms of fish assemblage response to stressors, Figures 5.9 to 5.11 show the response of three selected fish based indicators ‘population age structure’ (EVAL_AS), ‘Fish Index Austria’ (FIA), ‘ecological status’ (ES) to the aggregated stressor variables ‘Stressor category’ and ‘Stressor quantity’ representing the occurrence of single and multiple stressors. The indicators respond in a similar way to ‘Stressor category’ and ‘Stressor quantity’. For single stressors, strongest results can be observed for residual flow (R) followed by morphological alteration (M) and for morphological alteration combined with connectivity disruption, impoundment and residual flow (MBIR). Here, most values are associated with evaluation classes 3 and 4. Connectivity disruption

(B) alone doesn't seem to change the indicator value compared to category less impacted (noS) with a median between evaluation class 2 and 3. Water bodies affected by stressor categories connectivity disruption combined with residual flow (BR), morphological alteration combined with connectivity disruption (MB) as well as morphological alteration combined with connectivity disruption and residual flow (MBR) have a wide value range from the 1st to 3rd quartile of the box for these indicators.

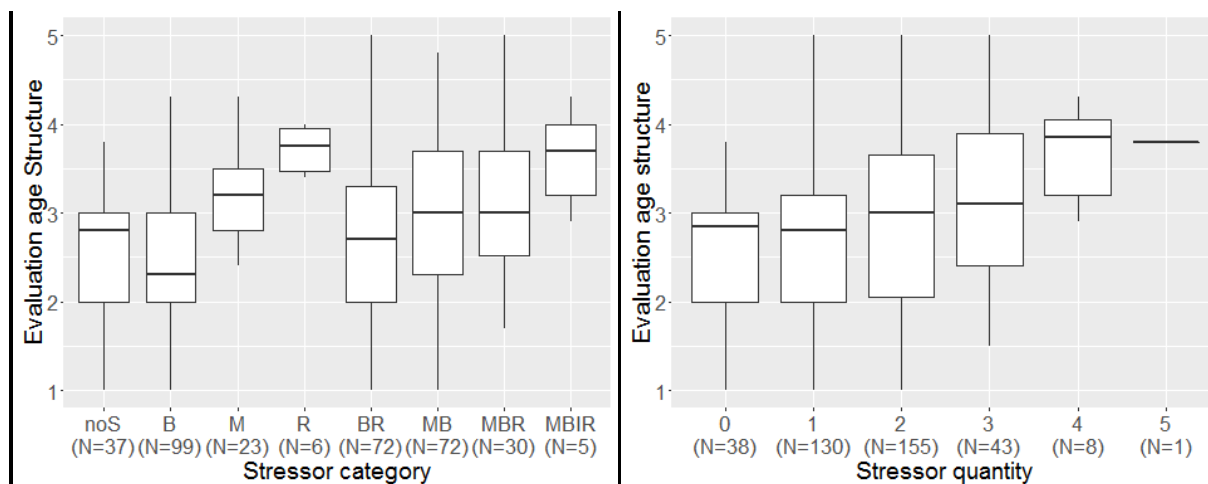


Figure 5.9 (a) and (b) Response of indicator 'population age structure' (AS) to variables 'Stressor category' and 'Stressor quantity'.

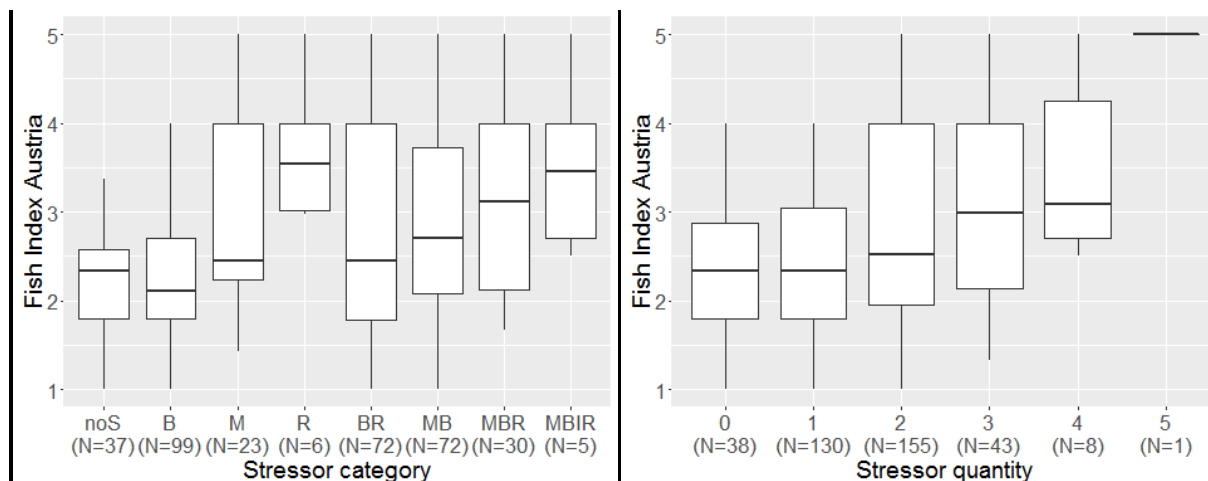


Figure 5.10 (a) and (b) Response of indicator 'Fish Index Austria' (FIA) to variables 'Stressor category' and 'Stressor quantity'.

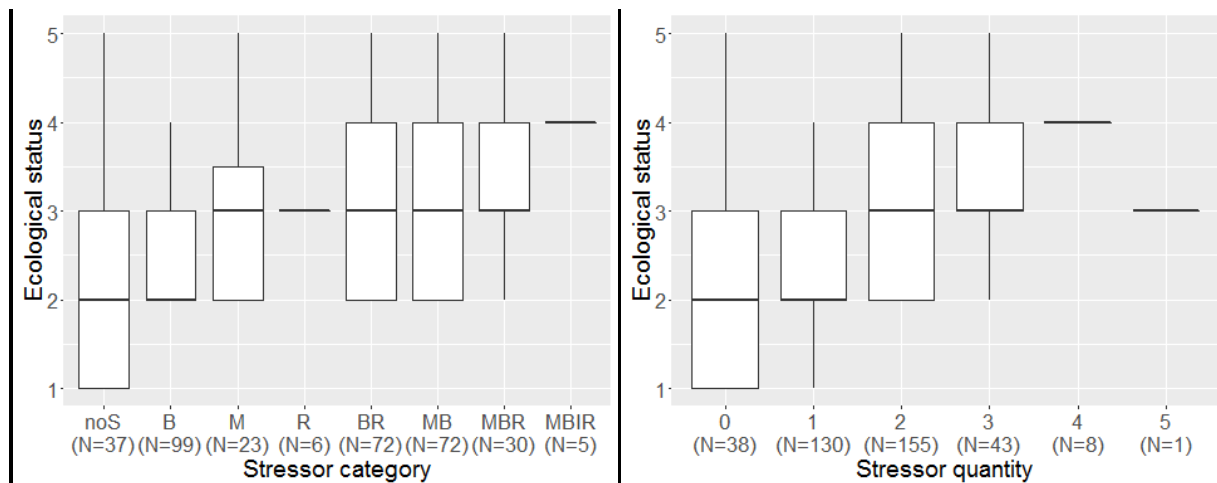


Figure 5.11 (a) and (b) Response of indicator ‘ecological status’ (ES) to variables ‘Stressor combination’ and ‘Stressor quantity’.

Analysis of the relationship between multiple human stressors and fish assemblages following the MARS modelling approach

The outputs of the Random Forest (RF) analysis (Table 5.7) include the goodness of fit and the ranked variable importance. These criteria were used to select indicators to be further investigated by Boosted Regression Trees (BRTs) in the next step. RF and BRT ranked variable importance (VIMP) of ‘ecological status’ (ES) ‘Fish Index Austria’ (FIA) and ‘age structure of dominant and subdominant species’ (AS_DS, AS_SDS) were in compliance for the three most important variables. In ‘age structure’ (AS) this was the case the first and second important predictors. The comparison of Goodness of Fit (GOF) between the two methods revealed, that BRTs always exceeded the results of RF. This observation was also made among the other MARS river basins (as discussed during a modelling workshop in Lisbon in December 2015). This is why a common agreement on focusing on the results of BRTs arose.

Table 5.7. Results of the Random Forest model indicating goodness of fit, ranked variable importance (VIMP) and if indicator was selected for Boosted Regression Tree analysis.

Indicator	Goodness of fit	Ranked VIMP	In BRT models	Indicator	Goodness of fit	Ranked VIMP	In BRT models
BM	-1,4	I,R,C,H,C,M		AS_DS	20,4	B,I,M,R,C,H	x
%DS	-1,0	R,M,C,B,H,I		AS_SDS	26,0	B,I,M,R,C,H	x
EVAL_DS	2,8	R,M,H,B,C,I	x	EVAL_AS_DS	5,7	M,R,C,B,I,H	x
%SDS	0,5	M,I,C,B,H,R		EVAL_AS_SDS	13,0	M,I,C,H,B,R	x
EVAL_SDS	5,6	M,C,I,H,R,B	x	SP	-0,4	R,M,H,I,B,C	
%_RS	-4,1	C,B,H,M,R,I		GUILDS	4,1	R,B,M,I,H,C	x
EVAL_RS	-3,0	I,H,B,C,R,M		SPCOM	3,9	R,M,H,I,B,C	x
DEV_HG	4,5	M,H,B,C,I,R	x	DOM	0,9	R,B,M,H,I,C	
EVAL_HG	-0,1	M,R,B,C,H,I	x	AS	10,9	M,R,C,B,I,H	x
DEV_RG	13,7	I,B,H,M,R,C	x	FIA	5,4	M,R,C,B,I,H	x
EVAL_RG	8,0	I,B,R,H,M,C	x	ES	22,2	R,C,M,I,B,H	x
DEV_FIZI	-2,8	R,M,B,C,I,H	x				

M...Morphological alteration, B...Connectivity disruption, R...Residual flow, I...Impoundment, H...Hydropeaking, C...Chemical status

In total, 16 biotic indicators were analysed in two BRT models (Table 5.8). The variance explained by predictors ranged from 9,2% to 34,8% in model 1 (without variable fish zone), and from 13,7% to 76,9% in model 2 (including variable fish zone). The inclusion of variable fish zone increased the percentage of variance explained for almost all indicators (model 2 versus model 1) (Figure 5.12 and Table 5.8).

Table 5.8. BRT results with percentage of explained variance, variable importance of the three most important predictors and interactions for model 1 (all stressors as predictors) and model 2 (all stressors plus fish zone as predictors).

Indicator	Direction of reaction	Model 1			Model 2		
		%	VIMP	Interactions	%	VIMP	Interactions
EVAL_SDS	increase	9,4	M(65), R(18), I(11)		13,7	FIZ(46), M(35), R(12)	
DEV_RG	increase	15,1	I(55), B(17), M(15)		34,5	FIZ(67), I(13), R(10)	
EVAL_RG	increase	16,1	I(43), R(21), B(21)		32,4	FIZ(68), R(12), I(10)	
DEV_HG	increase	9,2	M(63), B(13), I(12)		69,8	FIZ(90), M(3), I(3)	
EVAL_HG	increase	10,1	M(48), R(31), B(9)		53,5	FIZ(83), R(9), M(5)	
GUILDS	increase	14,0	M(30), R(27), I(23)		38,6	FIZ(78), R(11), M(6)	
DEV_FIZI	increase	10,0	R(47), M(34), I(13)		15,3	FIZ(75), R(14), M(7)	
AS_DS	increase	34,8	M(37), B(27), I(24)	BxM	76,9	FIZ(82), M(9), B(5)	
AS_SDS	increase	29,6	I(45), B(33), M(18)	BxM	62,4	FIZ(81), B(8), I(7)	
EVAL_AS_DS	increase	12,9	M(39), R(33), I(12)		16,1	FIZ(54), R(19), M(18)	
EVAL_AS_SDS	increase	17,4	M(63), I(16), R(10)		32,2	FIZ(67), M(20), R(6)	FIZxM
AS	increase	20,3	M(41), R(30), I(11)	RxM	21,9	FIZ(51), M(22), R(19)	
SPCOMP	increase	14,2	M(35), R(33), I(19)		27,4	FIZ(71), R(15), M(9)	
FIA	increase	10,9	M(40), R(26), C(13)		18,1	FIZ(61), R(17), M(14)	
ES	increase	30,0	R(39), M(34), C(19)		34,9	R(31), FIZ(22), M(22)	

M...Morphological alteration, B...Connectivity disruption, R...Residual flow, I...Impoundment, H...Hydropeaking, C...Chemical status, FIZ...Fish zone

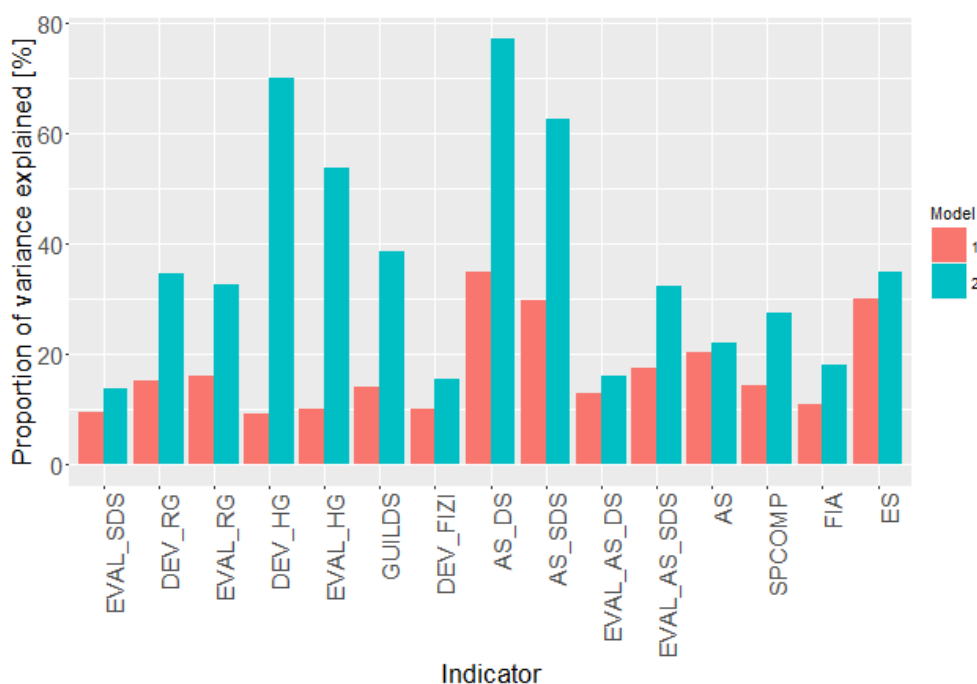


Figure 5.12 Proportion of variance explained by model 1 (stressor variables only) compared to model 2 (stressor variables and fish zone) for all fish based indicators as well as for the ecological status.

Five out of 6 stressors were selected as most important predictors with different rankings (VIMP) for explaining the response of biotic indicators in model 1 (Table 5.8 and Figure 5.13). The highest share of explained variance was observed for morphological alteration (M) followed by residual flow (R), impoundment (I), connectivity disruption (B), and chemical status (C). Hydropeaking was never among the three most important variables contributing to the models. In model 2, the

fish zone (FIZ) was the predictor with the highest VIMP in almost all biotic indicator models, accounting for most of the variation with a mean and median of about 50% for all indicators (Figure 5.13). The only exception is the ‘ecological status’ (ES) (Table 5.7). Besides ‘fish zone’ (FIZ), stressors morphological alteration (M) and residual flow (R) are the selected variables contributing to the models’ explanatory power. Figure 5.13 shows boxplots of the distribution of variable importance of the predictors for all indicators, separated by model (1 and 2).

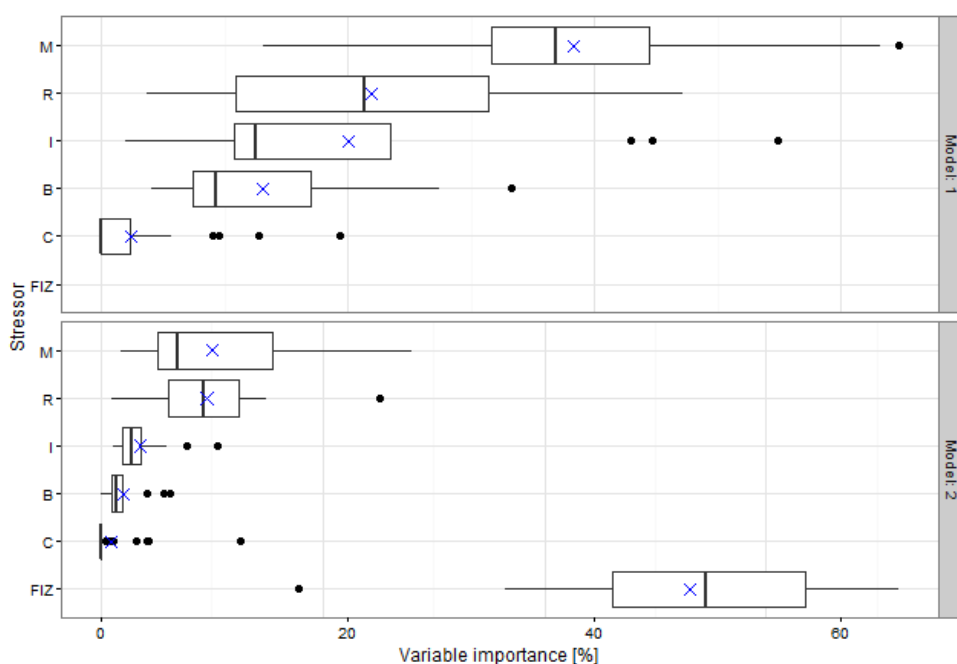


Figure 5.13 Distribution of the predictor importance based on the BRT models for the 16 indicators, separated by model (model 1 – stressors and model 2 – stressors and ‘fish zone’ (FIZ)).

Relevant pairwise stressor interactions include connectivity disruption (B) with morphological alteration (M) for AS_DS, AS_SDS as well as residual flow (R) with morphological alteration (M) in model 1. Fish zonation (FIZ) with morphological alteration (M) was most relevant for AS_SDS in model 2 (Table 5.8).

5.1.5 Discussion

5.1.5.1.1 Discussion of modelling process: Relationship between human stressors and fish assemblages

The boxplots of the descriptive analysis of multi-stressor-response patterns showed divergent results. The indicators ‘Fish Index Austria’ (FIA) and ‘ecological status’ (ES) resulted in very similar patterns in their responses to the variable ‘stressor category’. This may be explained by the fact that the FIA contributes to the Austrian national assessment of ecological status as one important Biological Quality Element (others are benthic macroinvertebrates, phytobenthos and macrophytes). The metric ‘evaluation age structure’ (AS) showed a response to the same stressor patterns as FIA and ES, which confirms that this indicator is firm and highly relevant for the evaluation of the FIA and ES. In water bodies affected by residual flow (R), we expected a ‘rithralization-effect’ and thus, a decrease of fish zonation index value (DEV_FIZI), accompanied by a shift in community structure. However, our results are unclear. It has to be kept in mind that this result builds on only five observations. Other categories combined with residual flow occur in less than 5 water bodies. Still, the indicator DEV_FIZI showed a slight increase when stressor R was present.

Due to the required step of aggregating stressor data to derive variable ‘stressor category’, the response of biota may be similar in strength and characteristics for multiple stressors with low intensities as to few stressors with high intensities. Other studies tried to reflect this issue by creating ‘pressure indices’ (Schinegger et al., 2013; Unterberger, 2014), however this is not addressed by our analysis. Nonetheless, a general trend of decreasing ecosystem integrity with increasing number of stressors (‘Stressor quantity’) was visually observed here for all metrics, implying the necessity to remove impacts due to occurring single and multiple stressors from water bodies. Random Forest (RF) models served as indicator-pre-selector for Boosted Regression Trees (BRTs) and as an additional comparative modelling approach to BRTs according to the MARS cookbook. We assumed high confidence of the methods and models, when patterns in terms of variable importance (VIMP) of the most important predictors and goodness of fit (GOF) between RF and BRT were equal. This is the case for all indicators in focus (AS, FIA, ES) and those with overall highest GOF (AS_DS, AS_SDS, ES). In general, most biotic indicators reflect lower ecosystem integrity when single and multiple stressors were present. As shown in the results section, the variance explained by stressors ranged from 9 to 35 %. This may

seem very low, however, literature on fish models for lotic systems confirm similar values and stress the lack of explanation in stressor-indicator relationships (Nõges et al., 2015).

In model one, indicators that responded strongest to the selected stressors were ‘age structure of dominant and subdominant species’ (AS_DS, AS_SDS) and ‘ecological status’ (ES). In model 2, AS_DS, ‘deviation of habitat guilds’ (DEV_HG) and AS_SDS showed strongest responses. Even though goodness of fit diverged between model 1 and 2, three out of four selected indicators with highest GOF were the same in both models, thus overlap. This implies strong relationships and high explanatory potential.

5.1.5.1.2 Basin-specific discussion of results: Role of stressors contributing to the models

Our findings show that only five single and multiple stressor categories occur at least 20 times in the investigated total basin. A pattern frequently identified the number of water bodies impacted by connectivity disruption (B) and by connectivity disruption combined with residual flow (BR), decreasing from Epirhithral to Epipotamal. In contrary, the number of water bodies where the stressor morphological alteration (M) or morphological alteration combined with connectivity disruption (MB) occurs do increase from Epirhithral to Epipotamal. This can be explained with the fact that in higher elevated areas of the total basin, multiple barriers were constructed for flood protection, torrent control and hydropower production. Headwater streams are often naturally straightened, therefore morphological alterations are not as significant in contrast to medium gradient streams and lowland rivers (Hyporhithral and Epipotamal), which naturally were braided or meandering, but were regulated by humans for agricultural and urban land use.

Morphological alteration was found to be the main stressor shaping the response of biotic indicators in most BRT models. For the development of the FIA, river straightening as one feature of morphological change showed medium suitability to characterize indicator response, as shown by Haunschmid et al. (2006). The same author shows that metrics ‘deviation of habitat guilds’ (DEV_HG) and ‘subdominant species age structure’ (AS_SDS) responded to this stressor. Our work (based on the same metrics) confirms these results: Stressor morphological alteration (M) was selected as the most important variable and the visually observed PDPs showed a shift in fitted values with increasing stressor intensity (Appendix, 12.1). Thus, this stressor was well

identified by the above-mentioned indicators. In general, various parameters determine morphological alterations. The four-level evaluation of morphological alterations (M) here builds on underlying features of the River Basin Management Plan database (RBMP-DB, 2015). These include the assessment of channel geometry-, riverbed and flow characteristics, the water-land transition zone, the condition of river bank and riparian zone as well as the vegetation of the adjacent area. In previous studies, different characteristics of morphological alterations, such as channelization, cross section alteration, embankment (Schinegger et al., 2013) or surrogates, such as human land use in the riparian corridor (Marzin et al., 2013; Schmutz et al., 2008; Trautwein et al., 2011) were investigated and have shown significant responses of metrics to this stressor. We therefore suppose that a set of stressor variables with a larger range of intensity values may contribute to better explaining mechanistic functions in ecological relationships. Moreover, instead of using an aggregated evaluation for morphology, the fundamental variables assessed within the national inventory assessment may increase the power of the models and improve interpretability.

Beside this, multi-stressor responses may identify interactions, which were discovered here between stressors morphological alteration (M) and connectivity disruption (C) for AS_DS and AS_SDS. In literature, we found no evidence for these interactions. Further, we would expect interactions between stressors morphological alteration and hydropeaking, especially in the Drava River Basin - as described by Schmutz et al. (2014), who found interactive effects between habitat characteristics and ramping rate. Based on these results, we assume that the amount of water bodies affected by hydropeaking in our investigation area is too low to considerably contribute to the models (only 11 water bodies were affected by hydropeaking, with intensity classes C (3) or D (4)). Although related impacts of hydropeaking on fish are well known already (Saltveit et al., 2001; Schmutz et al., 2014; Scruton et al., 2008), this low number of cases leads to a lack of intensity range for stressor hydropeaking, which may also be the reason why this stressor was not contributing to the models. Similarly, only four water bodies with high chemical stress (status class 3) occur in the dataset. However, chemical- and water quality stressors are not a big issue in Austria's rivers any more, thanks to sufficient wastewater treatment and emission regulations. Nonetheless, the response of the biota visually observed in PDPs (Appendix 12.1) always showed degraded conditions with increasing stressor intensity. Also this stressor was selected third by VIMP ranking in ES and FIA.

Further, twenty-two water bodies are impacted by impoundments, with intensities in categories C (3) and D (4). This stressor contributed on average 20% to variable importance of the BRT models. In comparison to other stressors, multiple authors observed strong responses of fish assemblages to impoundments (e.g. Van Looy et al., 2014; Schmutz et al., 2008). Marzin et al. (2013) identified the presence of impoundments as being a significant stress factor driving the response of fish indicators. The impact of impoundments is large, as a lotic system is changed to stagnant waters characterized by reduced flow velocities, bank fixations, reduced channel variations, disconnection of inflows and changes in sediment regime altering river functioning (Baxter, 1977; Tiemann et al., 2004). For Austrian water bodies, Schmutz et al. (2010) clearly showed that an increasing percentage of impoundments per water body leads to a decreasing ecological status (R^2 of 0,97). In another study using regression trees, Schmutz et al. 2007a observed that impoundment length and mean discharge were the most important variables in terms of explained variance of a biotic index. In our study, the PDP results of FIA agree with previous findings of that author, showing a lower FIA for no or short impoundment lengths (<300m in previous findings, <500m in our study) compared to long ones. However, this predictor (I) was not among the most important variables selected for explaining the response of the FIA and neither for ES. Instead, guild metrics, especially metrics associated with reproduction were sensitive to this stressor type where it accounted for the main part in variability explained by the model (see Table 5.8). This may indicate the shift from a lotic to a lentic system. In metric age structure (EVAL_AS), impoundments accounted for 11% of the variable importance and a slight shift from class A (1) and B (2) to C (3) and D (4) in fitted values was detected (Appendix 12.1). This may be due to the parallel occurrence of unsuitable instream habitats expressed by morphological alterations, which might be limiting habitats for juvenile fish as possible reason for bad age structure evaluations.

The impacts of residual flow in combination with other stressors have rarely been addressed in multi-stressor literature (and only in experimental studies, e.g. of Lange et al. (2014)), but studies especially for headwater and medium gradient rivers are missing. Here, the variable importance (VIMP) of residual flow (R) and thus its contribution to the power of the models was often high: e.g. 39% of VIMP in ES or 30% of VIMP in EVAL_AS. We expected an increase in stressor intensity class with increasing indicator value. However this was not the case for the explored indicators and associated PDPs showed no clear trend. These results go in line with another Austrian study conducted by Schmutz et al. (2008). The authors were not able to reveal significant

response of fish metrics to multiple stressors including residual flow, the only reactive component was the mean annual daily low flow (MNJQt) of below or above 40%. This feature approximately corresponds to the separation of stressor intensity classes A (1) and B (2) versus C (3) and D (4) within our study. Reasons for the missing gradients are manifold and some may be explained by the following assumptions: literature describing the development of the FIA (Haunschmid et al., 2006) revealed no evidence of significant metric reaction to residual flow. Thus, the developed index and associated metrics may not be sensitive to this stressor category. Moreover, negative consequences of residual flow depend on many other influences, such as the river type and river-reach morphology as assumed by Holzapfel et al. (2014). Again, a set of more precise predictor variables such as percentage of abstracted residual flow may be worth exploring, as they might better explain the response in biotic indicators.

For stressor connectivity disruption (C), class A indicates that no barriers are present in the water body or barriers are passable without fish migration facilities. In class B of the national impact assessment, passability is limited or only assured by fish migration facilities and in class C there are one or more non-passable barriers occurring in a water body. The variable B provokes high uncertainty due to divergent results. Although ranking of VIMP is sometimes high (e.g. in indicators AS_DS, AS_SDS), PDP patterns don't show the expected results – that were an increasing intensity class (A (1) to C (3)) with decreasing ecological integrity. Nevertheless, migration barriers are known to affect fish communities, as they degrade habitats and fragment populations, which leads to reduced productivity and genetic isolations (Meldgaard et al., 2003; Santucci et al., 2005). As water bodies in this analysis show a huge variation in length (from less than 1 km to over 46 km in the dataset with fish sampling sites), it is questionable whether the considered variable C (i.e. only identifying if there is an impassable barrier or not) is able to detect a fish ecological response to this stressor.

To summarize, most indicators suggest a significant difference between low and high stress- levels for some stressors, i.e. morphological alteration (M), impoundment (I) and chemical status (C). This confirms that the metrics are suitable to identify ecosystem integrity for such stressors. However, others don't contribute sufficiently to the model for reasons of data quantity, predictor unsuitability or characteristics of indicators, which further have to be investigated. An adapted methodological approach may help exploring the situation in the Drava and Mura River Basins and the Austrian RBMPs 2015 further, by improving goodness of fit and interpretability of the contributing predictors and interactions.

5.1.5.1.3 Generic implications for MARS and for Basin management

This study faces several limitations, but also implications for future investigations and improvements. Firstly, we are aware, that the aggregation of data (i.e. the re-coding/simplification of original stressor data) for the investigation of stressors and the descriptively observed response of biotic indicators leads to a loss of information. This was however necessary to conduct an analysis on the categories and quantities of stressors. Available stressor data are described in categories of three to four intensity levels, based on a number of underlying variables. This partially leads to a low gradient of stressor intensity and often makes interpretation difficult. There are several variables available in the present database, which are not considered yet, but potentially relevant for further analyses in Austria. Therefore we propose the consideration of a set of more precise/distinct stressors, such as the number of impoundments per water body, the total length of impoundments per water body and others for further investigations of the Austrian RBMP data. Especially for stressor connectivity disruption we suggest the calculation of variables which account for fragmentation of the riverine ecosystem or for a differentiation of passability of barriers by more detailed specifications (such as e.g. the number of barriers per segment/water body, individual segments contribution to the overall network connectivity or the delineation of segments based on the passability of barriers) as conducted in other studies (Unterberger, 2014; Van Looy et al., 2014).

Another important issue is that the low explanatory power of some models may also result from the assumption that one fish sample is representative for the whole water bodies' stressor status. This approach may not be suitable. In many cases, multiple fish samples were available per water body, however only one was selected. For modelling stressor-indicator relationships it may be advantageous to find a way to link multiple samples to an aggregated evaluation, which better represents the ecological status of a total water body. Here, an alternative method could be the implementation of a buffer approach as additional scale of analysis, as e.g. performed by Mielach (2010) and Schmutz et al. (2007). Moreover, an investigation about the location of the sampling area on a water body could give additional insights.

Finally, the number of water bodies per stressor category. There are only five stressor categories occurring at least 20 times which poses a challenge for statistical analysis, as a minimum sample size is required. For example, a study by Stockwell and Peterson (2002) showing the effects of sample size on the accuracy of species distribution models suggests that for machine-learning

methods, accuracy was near maximum at 50 data points. For finer surrogate models and logistic regression models, a sample size of about 100 data points was necessary for the same accuracy. Our study does not fulfil these criteria for the majority of stressor categories, which limits statistical testing. Thus, statistical testing was not performed for stressor categories and stressor quantities. Instead, patterns were only observed visually. Some limits, especially related to data quantity may be resolved by extending the datasets and by using water bodies from comparable regions in entire Austria.

The stressor analysis can support river basin managers to identify water bodies, which are degraded by the same stressor categories to apply suitable restoration measures. Moreover, future developments in terms of single and multiple stressors can be compared with today's situation.

5.1.6 Conclusions

There are several relevant outcomes of this work, including strong implications for further analysis and research on the relationship of human stressors and fish based indicators at the river basin scale:

- A large amount of different stressor categories, i.e. single and multiple stressors currently occurs in the Austrian Drava and Mura River Basins.
- Most frequent single stressors identified for related water bodies are morphological alteration (M) and connectivity disruption (B).
- In terms of multiple stressors, morphological alteration combined with connectivity disruption (MB), connectivity disruption combined with residual flow (BR) and a combination of all three, i.e. morphological alteration, connectivity disruption and residual flow were most frequent in the Drava and Mura River basins.
- The identification of these single and multiple stressors may help to prioritize future restoration and management actions by informing practitioners and other scientists on the most frequently occurring stressor categories and quantities and their distribution and patterns within different fish zones.
- Fish based indicators and the ecological status reveal contrasting responses to the occurring, mainly hydromorphological stressors. This likely is caused by a limited methodological approach including narrow stressor gradients, aggregated stressor variables leading to

dimension reduction/information loss and the linkage of one single fishing site to an entire water body.

- At the river basin scale, the variable ‘fish zone’ largely drives the response of biotic indicators. We assume that this is mainly due to the unequal distribution of stressors between fish zones and to a certain extent based on the fish zone itself, which incorporates some natural variability.
- Our results confirm necessity of using multiple indicators for assessing the ecological integrity of rivers and streams.

The RBMP data and the BRT approach bear high potential for further fruitful analysis: the updated RBMP data are generated through standardized methods with multiple variables that may still be considered, additional data from other river basins may be included and some BRTs show already promising explanatory power.

5.2 Elbe, Havel and Saale

5.2.1 Introduction

The Middle Elbe basin is located in the North of Germany, and drain about 20% of the country. It ends with the dam Geesthacht about 50 km upstream of the city Hamburg and before any tidal influence. This middle part of the Elbe received about half of its water from the Labe basin in the Czech Republic and is further drained by the water-rich river Saale (30%) and three others (Schwarze Elster, Mulde, and Havel), each with a large basin mainly in the lowlands. The total Middle Elbe basin covers the area of 83,920 km², in which arable land use clearly dominates (55.5%), followed by 30% forests. In the sub-basins Spree (Havel) and Schwarze Elster large scale carbon and metal mining causes pollution and an imbalance of groundwater hydrology. Several urban areas are widely distributed in the Middle Elbe Basin sum up to total 21 million habitants. The most populated region is presented by the cities Berlin and Potsdam in the sub-basin Havel. Other centers are located in the sub-basin of river Saale (Halle and Leipzig) and along the Elbe river with the cities Dresden, Wittenberg and Magdeburg.

Under mean water level conditions the water has already an age of 63 hours (IKSE, 2005), when passing 367 km through the Czech Republic and arriving the main source of the German basin at Elbe station Schmilka. Water flow start in the region of the Giant’s Mountains and has crossed

the Bohemian Cretaceous basin, confluence with river Vltava (Moldau) and cut partially volcanic bedrock. In the first German section (0-96 km) the river Elbe belongs to the Low Mountain region and cross the scenic river canyon in Elbsandsteingebirge with variegated sandstone and loess-covered lowlands. Near the city Meißen the river enters the North German lowlands. The river partially follows ancient glacial valleys formed during the Elster, Saale and Weichsel Glacial periods (Pusch et al. 2009). Active floodplains are to find subsequently in the plains of Middle Elbe (Gierk & de Roo 2008) which contribute to the nitrogen retention in the river system (Natho et al. 2012). Downstream of the city Magdeburg, the Elbe valley widens to about 20km and cross glacial deposits, and then enters a glacial valley partially used by the Havel tributary today (Pusch et al. 2009).

The river basin management plan (RBMP, FGGE 2009) has identified good ecological status only in 4.3% out of all the 2317 surface water bodies investigated. The water quality in the Middle Elbe basin is reduced by diffuse pollution (eutrophication and harmful chemical substances from former mining activities.) The good ecological status is additional disturbed by channelization and water regulation. 51% of total river length is classified as Heavily Modified Water Bodies (HMWB) or Artificial Water Bodies (AWB). Eutrophication is caused mainly via the pathway “diffuse pollution” from agriculture land. The current status of nutrient load is far from background conditions which have been reconstructed in former studies by the nutrient emission and transformation model MONERIS (Venohr et al. 2011; Wechsung et al. 2013; Becker & Venohr 2015). Scenarios were run to simulate the reduction effect of possible management measures listed in a catalog to reduce nutrient emission and to improve nutrient retention (retention ponds in drained agriculture) in the whole basin. According these future simulations the basin wide implementation of almost all measures will not be able to achieve sufficient nitrogen reduction to support high ecological status in coastal waters. Likewise, when applying a set of measures to reduce total phosphorus (TP) a model simulation of Quiel et al. (2011) revealed that also TP will remain on concentration level high enough to allow an enormous algal standing stock in Elbe river, on which grazers such as rotifers can establish a population size known for lakes in the spring bloom (Holst et al. 2002). Currently, high amounts of phytoplankton biomass are transported along the river and settle down in the tidal region, where they cause strong oxygen depletion as a secondary effect, which act as a barrier for diadrom-living fish species.

Therefore, the reduction of the eutrophication remains in the focus of management in the Middle Elbe basin. Supporting measures such as the increase in riparian vegetation is in debate not only

to reduce nutrient input by erosion prevention and by improving denitrification. Furthermore, riparian vegetation can help to reduce effects of climate changes (heating and erosion), and reduce the incoming light for aquatic primary producers. As a support for this idea, a simulation carried out by a model (Hutchins et al. 2010) revealed that riparian tree shading has a high potential to reduce phytoplankton growth in small and mid-sized rivers. Regarding the river network of the Middle Elbe the share of rivers smaller than 10m is high (80%), but most of these naturally shaded rivers lost their riparian buffer zone when agriculture became intensified.

Therefore, we aim to establish a model chain between land use (including loss of riparian vegetation), nutrient emissions, water retention and nutrient transformation processes, to biological responses in a large freshwater river in Central Europe. The model is made to evaluate the ecological effects of multiple stressors acting in concert, e.g. nutrient loading, light increase and alterations in water flow duration. The chain of models is also used to run plausible future scenarios on climate, land use and management changes. As an ecosystem service the Middle Elbe basin provides already a strong nutrient retention in its tributaries which is modelled under improved riparian river conditions and future scenarios.

In this study, the undertaken modelling of Middle Elbe combine all stressors (climate, social, agro-technical measures) into three storylines for 2 future time frames.

5.2.2 Context for modelling and storylines

The scenario concept is imbedded into the EU project MARS (Hering et al. 2015), in which three MARS –storylines are agreed to be implemented in the 16 European basins joining the project.

The projection to Middle Elbe result into the following scenarios:

Techno world (Storyline 1) has intermediate environmental stressor (overuse of resources), partly high technical or political measures are applied which is accompanied with relative high population increase (21.1% until 2050)

Consensus world (Storyline 2) put into practice improved sustainability (sustainable use of resources) and optimal technical or political measures accompanied with shrinking human population (-3.7% in 2050)

Fragmented world (Storyline 3) has the most strong environmental stressor (overuse of resources), and few or even reduced technical or political measures accompanied with strong shrinking human population (-15.9% in 2050)

Nutrient load and concentrations and phytoplankton status, biomass and composition are the modelled variables. The model output is used to evaluate ES and to provide advises for optimal measures under multi-stressor conditions.

5.2.2.1.1 Overall MARS model for the Basin

A statistic empirical model (EM Elbe) is derived from environmental and biological response data of monitoring station and combined with data for landscape morphology and landuse derived from common GIS maps and with WFD typology and status information of water bodies. EM Elbe is to identify the most important influencing factors and their interactions for biological response.

Process-based models are trained with current condition for simulating the MARS future scenarios which are driven by dynamic climate input data (RCP) and simulated discharge with the regional adopted model SWIM (Hattermann et al. 2015, Roers et al. 2016). The regional climate models RCMs RCP4.5 and RCP8.5 are applied in the MARS consortium driven by two global climate models, the ISI-MIP scenarios GFDL-ESM2M and IPSL-CM5A-LR and their results are feed into the hydrological model SWIM (Hattermann et al. 2015) in order to take into account the climate projection uncertainty (Roers et al. 2016).

Nutrient emission and transformation and the phytoplankton biomass of the large catchment Middle Elbe are simulated by MONERIS (Venohr et al. 2011) and the modul PhytoBasinRisk (Mischke et al., Annex 1), respectively driven by provided discharge simulated by the model SWIM (Roers et al. 2016). All three models are structured and computed for the regional scale into analytic units. By using the WFD river network, which designates water bodies, the model outputs can predict also ecological status for large water bodies and selected metrics.

Model applications focus on services for recreation and water purification (N and P-retention).

5.2.2.1.2 DPSIR model for the Middle Elbe Basin

Since the abiotic and biotic state of most water bodies are less than good because of high pressures, the river basin restrict response with management measures (FGGE 2009, 2015 a, b) which aim to improve also the Ecosystem Services (ES, Impact).

Using the Driving forces, Pressures, States, Impacts and Responses (DPSIR) framework (Figure 5.14), the modelling for Middle Elbe focus on the feedback of measures (Response) for reducing nutrient emission in urban waste water treatment plants (UWWTP) and in agriculture practice of the whole catchment with additional applications for the riparian buffer zone along the river net (develop riparian forest).

The observed and improved nutrient retentions in Elbe have a direct financial advantage for the society and can be directly translated as ES “Flow”. Any improvement by lowering “total algal biovolume and chlorophyll a” will improve the water quality and State, and help to maintain drinking water and raw water sources.

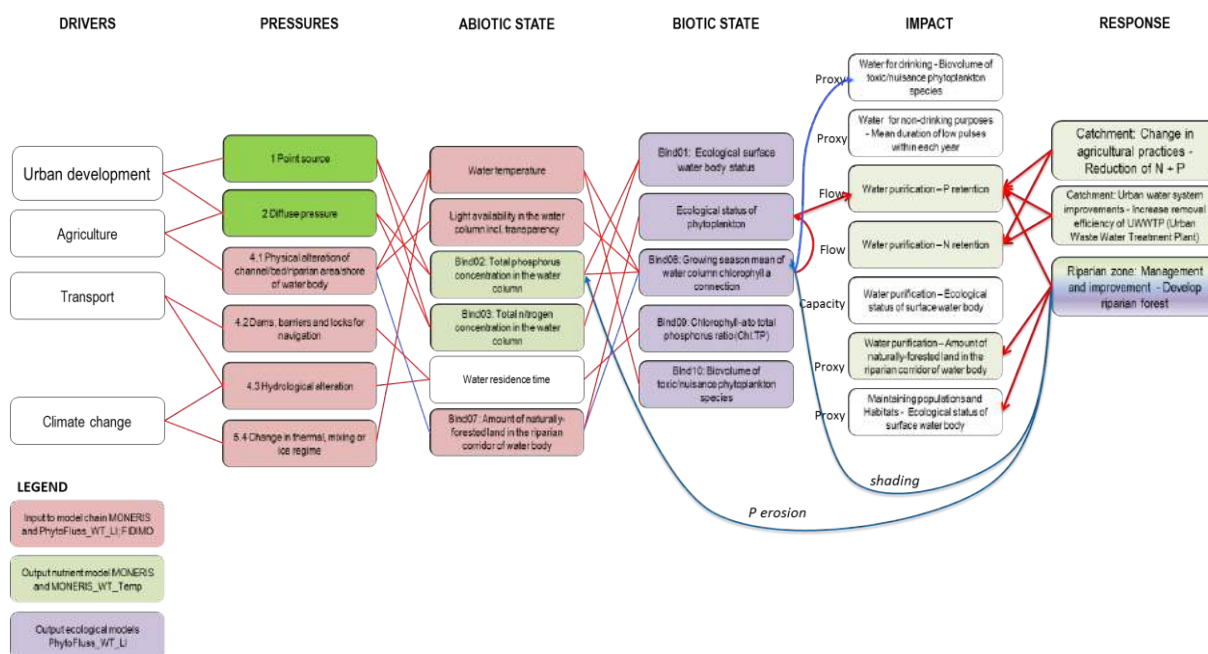


Figure 5.14 DPSIR model for the Middle Elbe basin

5.2.3 Data and

5.2.4 Methods

5.2.4.1.1 Training data

The Middle Elbe basin is an extensively monitored lowland basin (see Table 5.9; FGGE, 2015b, 2nd RBMP). Here we refer only to a small part of all available data, which were selected for to have a nearby gauge station and for covering the period 2005-2010 almost continuously in monthly intervals at least for the vegetation period (April – October). Monitoring data were collected by the basin-sharing German Federal States under cooperation with the River Basin Community Elbe (FGGE). We linked the provided data with GIS information for population, municipal waste water treatment plants, landuse, slope soil type and river morphology and analytic units in a database.

Observation stations are evenly distributed (Figure 5.15) within the four coordination regions and cover 73 different river water bodies.

Table 5.9 Number of rivers and lake water bodies (WB; 1st RBM-Plan (FGGE 2009)) and of observation stations for model fitting in the German coordination regions of Middle Elbe

		River WB	Lake WB	Stations	Analytic units
	Middle Elbe total	2318	344	104	722
River sections in regions	coordination regions				
Elbe - CZ/DE-border to Barby / Elde	MEL	409	69	28	146
Havel/Spree	HAV	982	213	21	210
Saale	SAL	354	35	18	181
Elbe from Barby to Geesthacht / Mulde and Schwarze Elster	MES	573	27	37	185

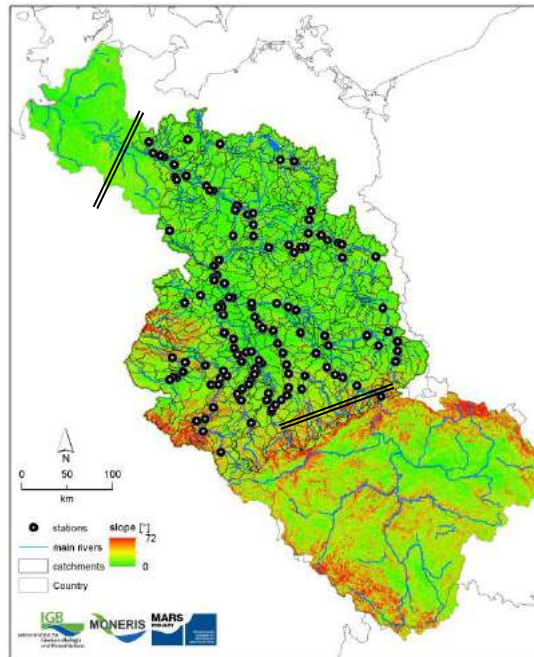


Figure 5.15 Landscape slope classes and observation stations with nearby gauges in the German Middle Elbe Basin with marker lines at main source station Schmilka at the Czech-German border and the basin outlet at dam Geesthacht.

5.2.4.1.2 Description of pre-processing of data

All spatial data for the study (information on land use and soils, and the digital elevation model) were projected to uniform GIS layers. The soil parameters are based on the German Soil Survey Map (BÜK 1000), and land-use data are based on the CORINE landcover classification published in the ATKIS data (© GeoBasis-DE / BKG (2013)) in 10x10m resolution. Watercourses are mapped as polylines, and as polygons when lakes or rivers are wider than 12m (for details see Annex I). The borders of analytic unit areas were taken from data of the Federal Environment Agency, which were used for nutrient emission modelling in former projects (Venohr et al 2015; Roers et al. 2016). The river network was joined to a map for water bodies provided by the river basin commission FGGE 2013 (DLM 5000 / BKG), which is used for WFD reporting (FGGE river network). Here, 3943 individual rivers segments belong to distinct river water bodies (EU_CD_RW) and were processed to extract following parameters for model application: a) borders of analytic unit, b) river category “main river (MR)” or “tributary (TRIB), c) river length, d) river width, e) land use in analytic unit, f) land use in the 10m-buffer at river shoreline and g) surface area of rivers in analytic unit. Also, 1247 lake polygons were analyzed for: i) proportion of lake area tot total water body area in analytic unit, II) total lake lengths. The count of deep lakes

was done by joining WDF reporting lakes (N = 283) to lake attribute list of DLM5000 /BKG. Other topographical parameters (slope in 100m, mean altitude), were derived from digital maps.

Climate data delivered by the external model SWIM were aggregated for each analytic unit for atmospheric conditions (short wave radiation at ground (named here as “global radiation”), air temperature, precipitation), and were additionally transformed to annual and summer means (see **Error! Reference source not found.**) and run-off were cumulated along the river network with the flow-net equation (Venohr et al. 2011). The calculation of incoming-light into the water body based on global radiation and water quality data and its reduction by riparian tree shading is described in Annex I.

5.2.4.1.3 Establishing an empirical model for Middle Elbe Basin

An empirical model (EM) was established in order to identify interactions of stressors, which were included as abiotic variables into the model (**Error! Reference source not found.**).

A data set from monitoring and mapped data were compiled which include a list for environmental and abiotic variables. As a first step, a data screening was performed which follow the cookbook of Segurado et al. (2015a; Feld et al. 2016) and use a provided R script. Variables which show extreme positive skewness in the histogram were log-transformed (see “log” in legend in **Error! Reference source not found.**).

For reducing the number of influencing variables they were checked for correlation to each other (Pearson's product-moment correlation), and dropped in case of correlation factor >0.6. For example, we kept in the two P variables (PO₄ and TP) although they correlate to each other with a coefficient of 0.56, but in the final model they have an opposite sign in the coefficient. When dropping one of both, the model has much higher residuals.

We first established a boosted regression tree (BRT) model and used the selected main explanatory variables to run GLM models (see Feld et al. 2016).

Table 5.10. Variables used to build up the empirical model for Middle Elbe and minimum and maximum of not transformed value in the vegetation period (Apr –Opct) in the years 2006-2010

Type of variable	Legend	Minimum	Maximum
Environmental			
site_PPTyp	river water body type		
Ae	sub-basin size (km ²) log	186	125,413
slope	slope of analytic unit (m 0.1 km ⁻¹) log	0.93	14.16
agri	% basin agriculture landuse	17.2	73.2
urb	% basin urban area	2.69	20.0
fors	% basin forest area	10.7	55.9
Q	Discharge (m ³ s ⁻¹)	0.01	1,126
prec	Precipitation at station (mm m ⁻² y ⁻¹)	0.56	146.5
Abiotic			
TP	total phosphorus (mg/l)	0.04	0.70
PO4	dissolved reactive phosphorus (mg l ⁻¹) log	0.005	0.43
NH4	ammonia (mg l ⁻¹) log	0.005	0.77
abiNO3	nitrate (mg l ⁻¹) log	0.005	8.9
O2	oxygen dissolved (mg l ⁻¹)	3.9	17.5
WTem	water temperature (°C)	6.0	27.3
Response			
Chla	chlorophyll a (µg/L) log	1	375.9

For analyzing the response of the benchmark indicator “chlorophyll a” to multiple stressors a GLM was derived according Segurado et al. (2015b). To reflect the spatial effect of the stations the catchment size (A_e) was included into model. A_e was strongly correlated to discharge at station ($r^2=0.9$), so we drop the latter variable. When including only the months within the vegetation period (April to October) the variable water temperature was less important for the model and was dropped by the GLM simplification step.

5.2.4.1.4 Process-oriented modelling with MONERIS and module PhytoBasinRisk

Nutrient emission, transformation and the phytoplankton biomass of the large catchment Middle Elbe are simulated with MONERIS (Venohr et al. 2009, 2011) in Version 3.0 (Venohr, unpubl.) and with the new module PhytoBasinRisk (Mischke et al. unpubl., Annex 1), respectively. Compared to other nutrient emission and water quality models the MONERIS model (MOdelling Nutrient Emissions in River Systems; BEHRENDT et al., 2000) and Modul PhytoBasinRisk work with a moderate demand of input data, requires only a short computing time and is applicable to large river basins.

In contrast to former model setups of Elbe basin with MONERIS (Behrendt et. al. 2000; Venohr et al. 2005; Becker & Venohr 2015, Wechsung et al. 2013) we have improved the setup with the following updated data: maps for landuse, N- and P-surplus, human population, connectivity to point sources and a new river net map, which is also used for EU-WFD reporting. By using the WFD river network, which designates water bodies, the model outputs can predict also ecological status for large water bodies and for selected metrics. The FGGE river network covers a total length of 33,000 km, to which main rivers contribute 18%. This detailed river network is still partly a simplification when comparing to rivers mapped in ATKIS data, where very small ditches are included, too.

The basin is divided into spatial analytic units and routed through the flow system to the catchment outlet at Elbe dam Geesthacht by a flow net equation (Venohr et al. 2011).

The process-based models are trained with current conditions (baseline runs) for simulating nutrients and phytoplankton biomass under conditions of the MARS future storylines driven by simulated climate variables and discharge conditions (see next chapter).

The MONERIS model simulate the substances total nitrogen (TN), TP and DIN on annual and monthly level as loads and concentrations (Venohr et al. 2011). The emissions are separated into pathways

The nutrient retention in the surface waters is calculated for each analytic unit and is calculated for the basin outlet as the cumulated basin retention by the help of the flow net equation for ecological service interpretations.

Table 5.11. Pathways separating the total emission in the model MONERIS

Pathways emission	Abbrivation for pathway
point sources	PS
urban systems without WWTP	US
ground water	GW
tile drainages	TD
Erosion	ER
surface run-off (dissolved fraction)	SR
atmoshaeric deposition on surface waters	AD

5.2.4.1.5 Climate and hydrological input data for scenario runs

Model MONERIS and module PhytoBasinRisk are driven by provided recently simulated discharge by the ecohydrological model SWIM (Soil and Water Integrated Model, Krysanova et al. 1998; Hattermann et al. 2005), using the integrated module for computing the hydrology (Hattermann et al. 2015).

The baselines and scenarios are driven by external simulated monthly discharges for two different dynamic climate input data (RCP). In our study, we use long term mean (LT) for each month of the periods a) 1971-2001 b) 2020-2030 c) 2045-55 with climate variables precipitation (PP), global radiation (GR), air temperature (AT) and the modelled discharge in each modelled area (Q_AU).

The external simulated discharge data take into account the uncertainty of climate models (Hattermann et al. 2015, Roers et al. 2016) by applying two regional climate models (RCMs choice for MARS-project case studies is RCP4.5 and RCP8.5), driven by two global climate models for our setup (ISI-MIP scenarios GFDL-ESM2M and IPSL-CM5A-LR) and their results were feed into the hydrological model SWIM by several climate variables to calculate the discharge for all spatial analytic units for two training baselines (GFDL 1971-2001; IPSL 1971-2001) and for the future period 2010-2100. The hydrological simulation resulted in a high amount of daily data and further climate variables

In we provide an overview of the discharge data and some climate variables finally used for our modelling and which were extracted for the different future periods.

According our model performance check, the monthly differences of climate variables and discharges are highly relevant for our model outputs. In case of PhytoBasinRisk, discharge fluctuations in the vegetation period can alter phytoplankton biomass strongly (see Annex I), while changes in the winter discharge are not directly relevant for phytoplankton development because of light limitation. As one example out of all 722 analytic units, climate driven differences in the cumulated mean discharges simulated by model SWIM for period April to October are listed at the basin outlet for baseline and for the future periods in **Error! Reference source not found.**

The wettest long term mean is simulated for GFDL around the year 2050 with RCP8.5, and the driest projection is for IPSL around the year 2025 with RCP4.5. In contrast to former SWIM

scenarios based on climate projections by STAR, which predicts dry summers for Elbe river in the future, the GCM-GFDL driven results revealed that summers will become near baseline (100 – 119% of baseline) or would be 86 – 91% of baseline in the future, when simulated discharges is driven with IPSL (Hattermann et al. 2015). Also, focusing on the vegetation mean the calculated water temperatures derived from simulated air temperatures are not very different from baseline simulations with a deviation in the range of 3 – 17% in future (see **Error! Reference source not found.**), while strongest climatic changes are simulated for winter months (not shown here).

Table 5.12. Simulated discharge ($\text{m}^3 \text{s}^{-1}$; cum Q) and water temperature ($^{\circ}\text{C}$; WT) averaged for the vegetation period (Apr-Oct) at station Boitzenburg calculated as longterm means of each period, the baseline period and the two future periods and in two RCP-projections based on data provided by Potsdamer Climate Institute (Roers et al. 2016).

GCM-model ICI-MIP	Parameter as vegetation mean	baseline 71-2001	rcp4p5 2020-2030	rcp8p5 2020-2030	rcp4p5 20545-2055	rcp8p5 2045-2055
GFDL-ESM2M	cum Q	627	633	625	665	745
IPSL-CM5A-LR	cum Q	656	565	639	604	597
GFDL-ESM2M	WT	17,4	17,3	17,5	18,2	17,4
IPSL-CM5A-LR	WT	18,1	18,1	18,7	19,7	18,1

The full range of spatial (722 areas) and temporary differences (monthly for 11 years for 10 scenarios) in discharge and temperature are much stronger and additionally, high and low flow situations not occur synchronic in the whole basin, therefore simulations of specific sub-basins can differ from the overall mean at basin outlet.

5.2.4.1.6 Implementation of the scenarios in Basin Middle Elbe

The quantification of the scenario implementation is summarized in and **Error! Reference source not found.**

Land use: For the implementation of landuse into the MARS storylines 1-3 we followed global models summarized in Sanchez et al. (2015). For riparian buffer zones the current status of area without agriculture use was changed with minus 30% for scenario 1, plus 50% in scenario 2 and minus 80% for each individual analytic unit. The resulting change at all surface waters is provided in.

Human population and social effects: The German Federal Institute for Research on Building, Urban Affairs and Spatial Development (BBSR) analysed population demographic changes and trends in Germany and found a distinct decrease or rural population and increase of urban population (BBSR, 2016; “Rural exodus? Society on the move”). We take this trend into account by implementing it in different degree in the 3 MARS storylines (**Error! Reference source not found.**

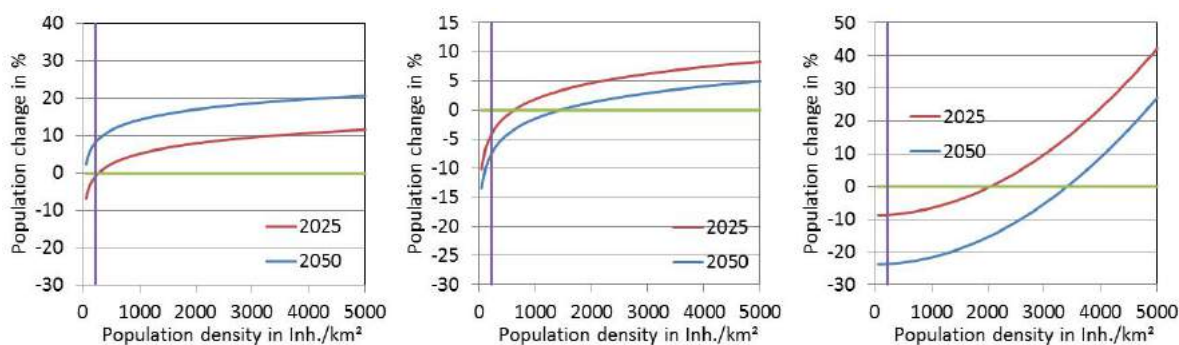


Figure 5.16 Assumed population changes in dependence of population density for Storyline 1 (left), 2 (middle) and 3 (right) for the years 2025 and 2050 compared to the zensus data 2010 for German municipalities.

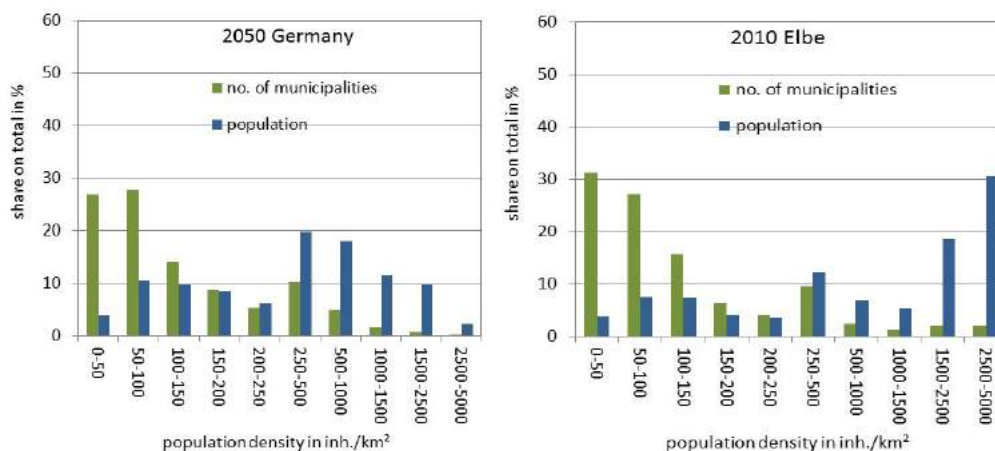


Figure 5.17 Share of municipalities and inhabitants in dependency of population density in Germany and the Elbe catchment according to zensus data 2010.

We assume that people in the cities will also change their nutrition, which will strongly effect the person specific P disposal In a more balanced diet with less meat, the P disposal will decrease strongest in storyline 1, less in storyline 2, but will be negatively change to more meat consumption in storyline 3.

Table 5.13.Final effluent of WWTP of different size classes for N and P assumed for the storylines (SL1 – SL3)

WWTP size class	N			P		
	<GK4	GK4	GK5*	<GK4	GK4	GK5*
SL1	20	18	10	1,5	1	0,5
SL2	10	8	5	1	0,5	0,3
SL3	30	25	20	3	2	1,5

*assumed only for the new connected habitants according population changes

Table 5.14.Change of emission input data to run MONERIS model for validation (2006-2010) and for the 3 MARS storylines in the future time periods 2025 and 2050.

	Story line	2006-2010	1971-2001	1971-2001	1	1	2	2	3	3
					2025	2050	2025	2050	2025	2050
arable land	%	41			23	22	23	22	23	22
Population	Mio. Inhabitants	17.7			18.3	19.9	17.7	17.1	17.6	14.9
connected to WWTP	% of population	90			90	90	90	93	91	91
person specific P disposal	g/inh./day	1.90			1.74		1.31		2.81	
N-surplus TS	kg/ha/yr	50			46		40		63	
P accumulation	kg/ha	730			621	619	555	548	831	824
DPS arable	%	77	77	77	67	67	59	59	80	80
buffer strips	% of surface waters	83			58		100		17	

Table 5.15.Climate input data summarized as longterm mean of the periods: validation period (2006-2010), climate baseline (1971-2001 for GFDL and IPSL) and future MARS storylines in 2020-2030 (2025) and 2045-55 (2050)

	period	2006-2010	1971-2001	1971-2001	2025	2025	2025	2025	2050	2050	2050	2050
	RCP				4.5	4.5	8.5	8.5	4.5	4.5	8.5	8.5
	Climate		GFDL	IPSL	GFDL	IPSL	GFDL	IPSL	GFDL	IPSL	GFDL	IPSL
Precipitation	mm	742	717	732	742	768	750	791	767	787	766	793
summer precipitation	mm	392	392	400	392	423	395	451	403	436	386	448
annual run-off	m ³ /s	769	843	862	867	840	874	862	925	823	971	839
summer run-off	mm	591	552	586	561	524	568	599	611	564	655	563
mean annual water temperature	°C	10.9	10.9	10.9	11.8	12.3	11.6	12.3	12.1	13.2	12.1	13.6
mean summer water temperature	°C	17.9	17.9	17.9	18.3	18.9	18.2	19.2	18.7	19.8	18.9	20.4
annual incoming short wave radiation at ground	w/m ²	120	120	120	122	124	121	126	122	126	119	126
summer incoming short wave radiation at ground	w/m ²	172	172	172	176	179	175	183	177	184	175	184

For emission pathways we keep the population connected to waste water treatment plants (WWTP) on the same level as baseline, but in storyline 2 the technical level is the highest, and in storyline 3 the lowest for WWTP. The final effluent from WWTP was assumed to change according **Error! Reference source not found.**

The climate scenario data provided by Roers et al. (2016) includes the simulated annual run-off for each spatial analytic unit and were used as monthly longterm mean for each future period (annually summarized in **Error! Reference source not found.**).

The climate and abiotic data to run scenarios with module PhytoBasinRisk were taken from the climate model (SWIM) and from the nutrient model (MONERIS). In addition, current status of area with trees or bushes in the 10m buffer was changed with minus 30% for storyline 1, plus 50% in storyline 2 and minus 80% for storyline 3 for each individual analytic unit. In dependency to the mean river widths this results in less strong shading effect, since only a part of tributaries are smaller than 7m, for which optimal shading is assumed (see Annex 1). At tributaries the simulated mean tree shading factor is 0.83 in current status, 0.97 in storyline 1, strongest in storyline 2 with factor 0.53 (the measure response “develop riparian forest” is realized) and no tree shading in storyline 3 (shading factor 1).

5.2.4.1.7 Estimation of ecosystem services

The ecosystems services are calculated for nutrient retention and for improving ecological status.

- (a) Calculation of nutrient retention in tons per year by model MONERIS to costs, which would be necessary to reduce them in WWTP. The cost base is redrawn from a regional study for tributary Havel in Horbat et al. (2016).
- (b) Simulation of chlorophyll a concentration and their relation to ecological status (Mischke et al. 2011).

5.2.5 Results

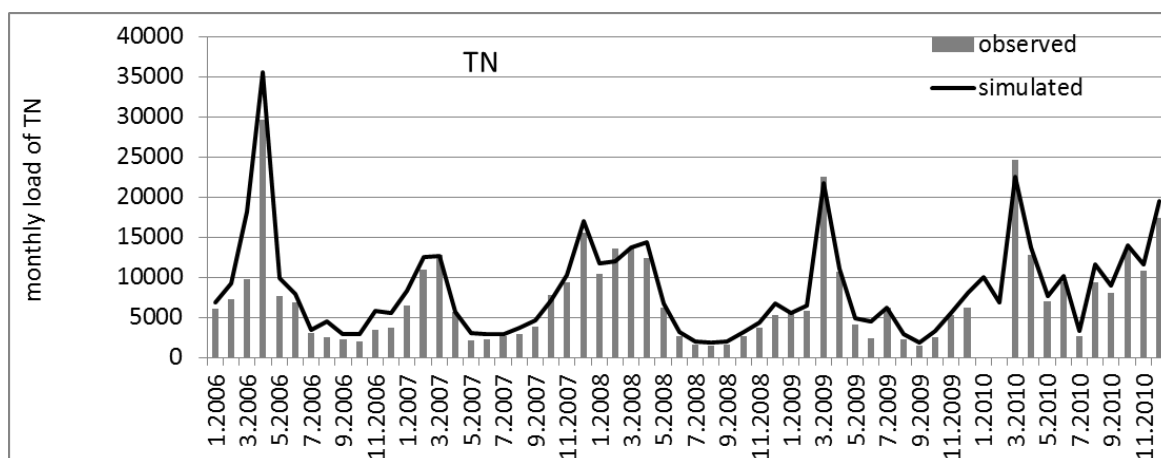
5.2.5.1.1 Performance of nutrient emission modelling by MONERIS

Overall, the output of the MONERIS model was compared to other emission model in several studies and turned out to be in the same range of uncertainty than other (Kronvang et al. 2009; Malagó et al. 2015).

Modelled loads were transformed to nutrient concentration by cumulated discharge (Q). The simulated nutrient results were compared to monitoring data for main stations. The seasonal variation is sufficiently reflected by the model (**Error! Reference source not found.**) and mainly within the $\pm 30\%$ confidence interval (**Error! Reference source not found.**).

When comparing the simulated loads with the expected 1:1 line, there is no systematic under- or overestimation is simulated.

Additionally to the basin outlet the nutrient load for 12 further stations are compared. The correlation coefficient for TN loads for simulated to observed annual means range between 0.85 – 0.99, and for TP between 0.31 – 0.81, respectively. The lowest match is simulated for TP load for the outlet of river Havel, in which the water quantity management for operating a water bypass for a shipping course may have led to unusual discharge conditions in combination with retention in lake-river systems.



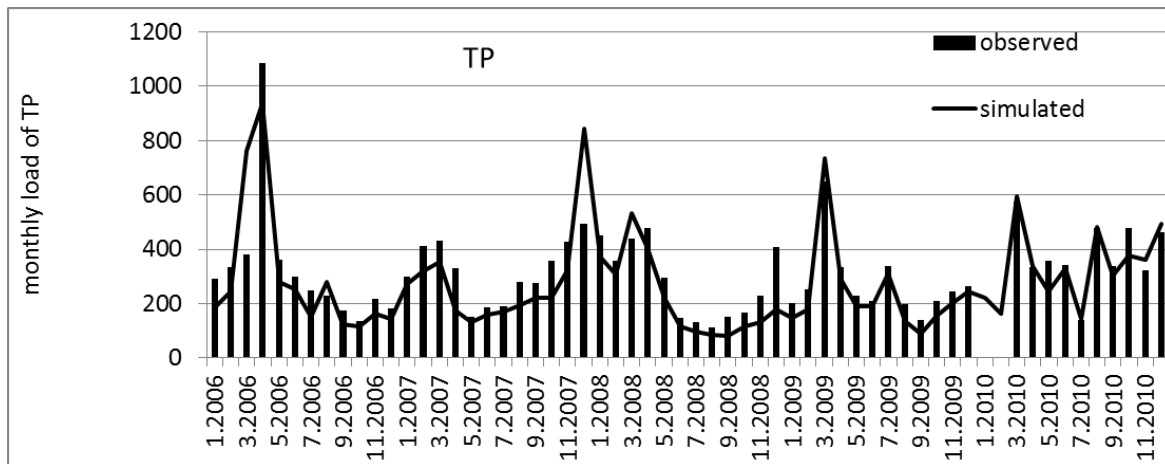


Figure 5.18 Observed and modelled monthly load of TP and TN at station near basin outlet (Neu Darchau)

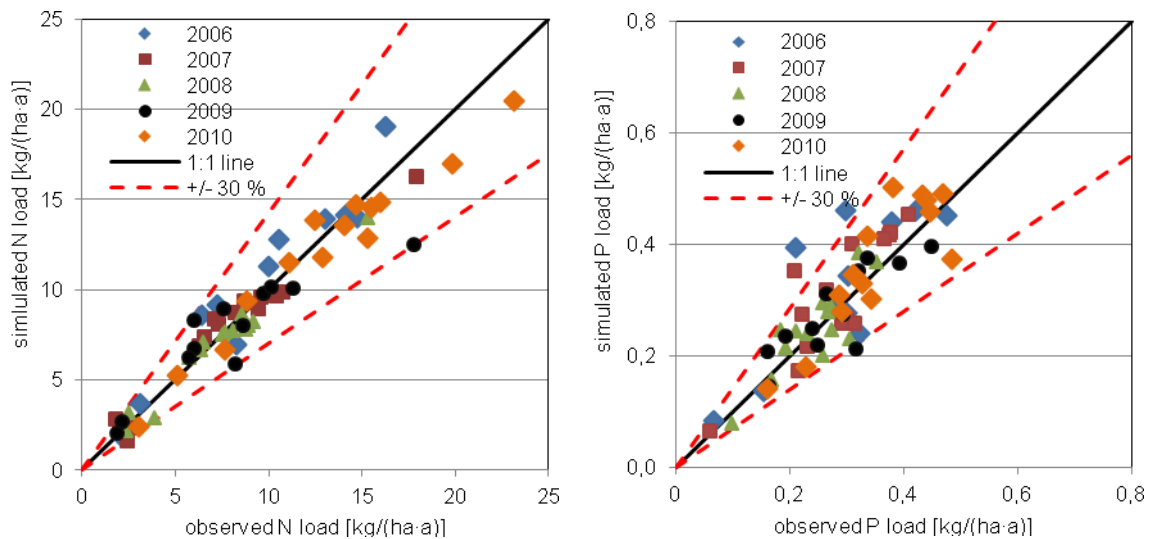


Figure 5.19 Modelled and observed monthly loads for TN (left) and TP (right figure) different colored for the years at basin outlets of Middle Elbe in years of validation period. Hatched lines indicate the $\pm 30\%$ confidence interval.

5.2.5.1.2 Performance analysis for module PhytoBasinRisk

Modelled chlorophyll a concentrations were compared to monitoring data for several main stations (see **Error! Reference source not found.**). The seasonal variation is reflected by the model. For ecological status assessment the vegetation mean of the period April-October is used (**Error! Reference source not found.**), so the low peak match is not in front of the simulation task.

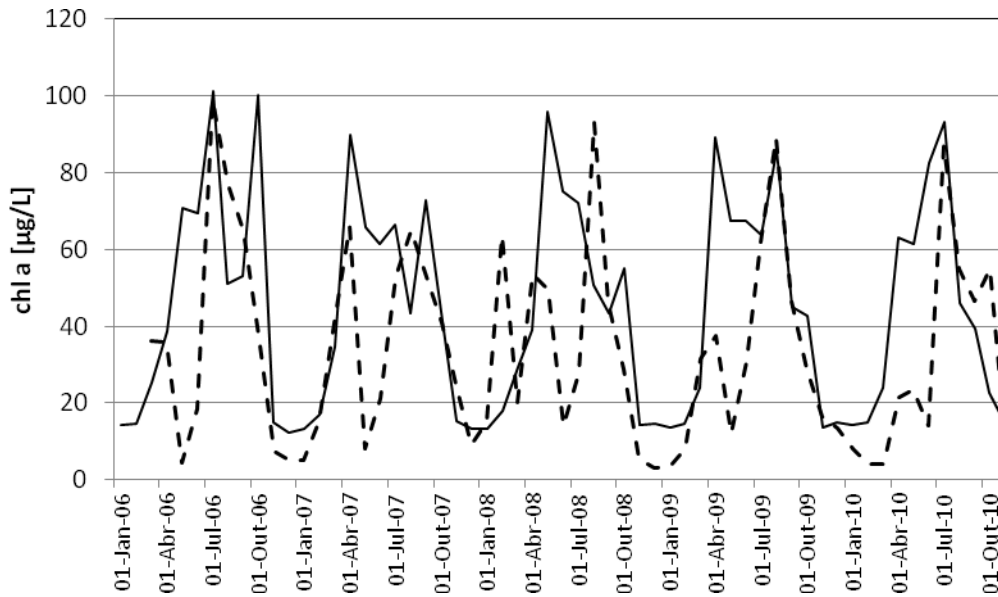


Figure 5.20 Observed (hatched black line) and simulated chlorophyll a concentration as monthly means modeled with PhytoBasinRisk in river Spree at station Jannowitzbrücke

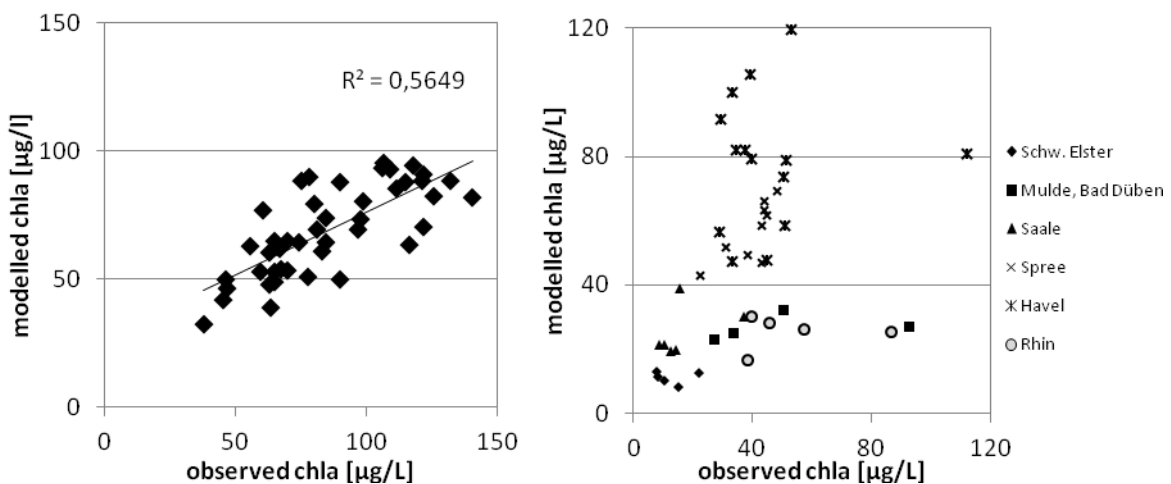


Figure 5.21 Observed and modelled chlorophyll a (chl a) seasonal means in Elbe stations (left figure) and in tributaries (right figure)

A synthetic data set was produced to test sensitivity of the PhytoBasinRisk module for single variables.

The input data of the longterm mean run for period 2005-2010 was altered with reducing P by 20% or 30%, increase water temperature with 2°C (pl2Temp) and run shading effect as assumed for storyline 2 (SL2_shade) for each of the spatial analytic units. The effect on simulated

chlorophyll a is shown for a smaller catchment, in which shading effect can be expected because of smaller rivers (**Error! Reference source not found.**).

The simulated summer concentrations of chlorophyll a do not response to P reduction because 30% reduced concentrations are still above the limitation thresholds. The chlorophyll a output clearly increase with increased temperature and are reduced by riparian shading when high share of trees in the 10m buffer were assumed as implemented for storyline 2 (upper **Error! Reference source not found.**, SL2_shade).

These clear effects by temperature and tree shading vanish in larger catchments, because of biotic regulation: Higher grazing losses are simulated for rivers wider than 35m, when chlorophyll a concentrations > 50µg/L flow in from upstream sections and temperatures are above 14°C (see Annex 1).

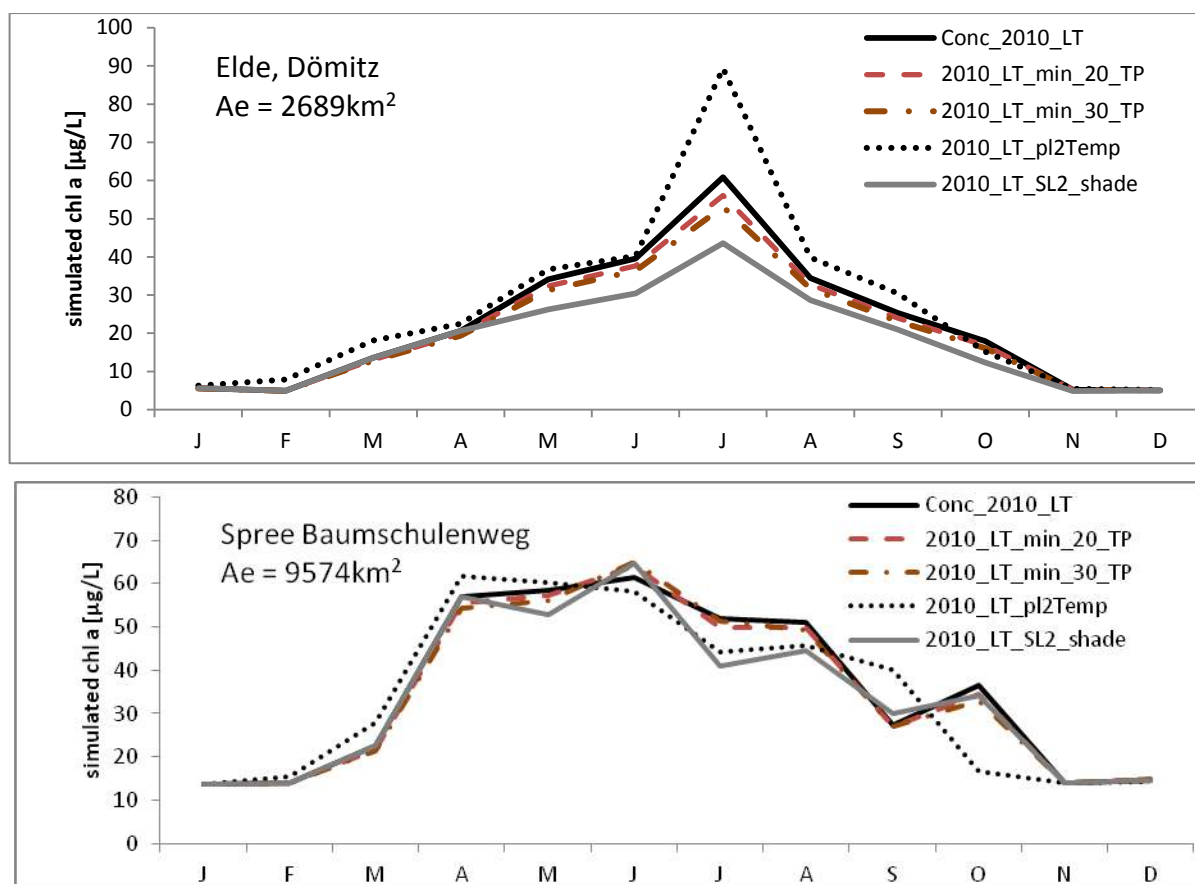


Figure 5.22 Monthly simulated chlorophyll a concentrations in sub-basins Elde (Dömitz) and Spree (Baumschulenweg) under synthetically altered input data (see text) in comparison to simulation for currents means of the period 2006-2010.

5.2.5.1.3 Uncertainty in the PM results

The Middle Elbe basin is large, so for several parameters the data are not available in high spatial resolution. The river net comprises high- and lowland regions to which more than 200 large lakes and reservoirs are connected. Therefore, uncertainties for nutrient emission and transformation result from several sources of the input data, the transformation in the lakes and in the estimation of the concentrations in the groundwater.

The PM model PhytoBasinRisk reflects the best the conditions in the main channel of the Elbe, while the different tributaries are mainly heavily modified by series of dams (Saale), water flow is managed by upstream reservoirs and dams (Spree), a chain of lake-river-systems are connected (Havel) or the river is dominated by macrophytes (Müggelspree). Estimations of water residence time (WRT) for all of these hydrological modified conditions are rough and causes the highest uncertainties in modelling chlorophyll a concentration. Flow times are available for only the main courses of the total river network (IKSE 2005). Uncertainty is also increased by lake outflows which are covered in the model by a common approach so far (sedimentation loss per lake-lengths; inoculum chlorophyll a in analytic units at the beginning of the river net arms, WRT>30d for deep lakes, see Annex 1), but each lake has individual transformation processes (morphology, extent of macrophyte cover, fish-zooplankton interaction).

5.2.5.1.4 Empirical model results: interaction of explanatory variables

The empirical model derived with a GLM model (GLM –model Middle Elbe, Gaussian family) with response variable “chlorophyll_a concentration” based on seasonal data for Middle Elbe was as followed (for abbreviations see **Error! Reference source not found.**):

$$\log_Chla = -2.36253 + -10.99 * \logPO4 + 19.43 * TP + 0.35 * NO3 + 0.65 * Ae + -0.065 * (Ae * NO3) + -1.52 (Ae * TP).$$

The two latter terms of the model are two synergistic interaction terms for catchment size to nutrient variables. No interaction was identified between two stressor variables.

Fitted directly to the training data set, the GLM model Middle Elbe is able to predict what is to expect when nutrient level is lowered by reducing management measures, as for storyline 2 in the

Consensus World of the project MARS. For this purpose, the log-transformations ($\log_{10} + 1$) of variables required for statistical needs, must be converted back.

For example, starting with upstream station with 75,000km² catchment size and current nutrient concentrations (PO₄ 0.01; TP 0.12; NO₃ 1.4 mg/l) the model would predict 319µg/L chlorophyll a, which is occasionally realized in Elbe channel. In a second step, we can test the effect of a TP concentration of 0.085 mg/L in future simulation according to nutrient modelling after setting a bundle of measures to reduce nutrients (see MONERIS in storyline 2): This reduction would restrict chlorophyll a to 53 µg/L, which is at the upper border for good ecological status according to the German assessment method PhytoFluss (Mischke et al. 2011).

The model performance is shown in Figures 5.21-5.22 and summarized in **Error! Reference source not found.** All variables and both interaction terms are highly significant. Also the residual analysis for each of the variables revealed no trend (**Error! Reference source not found.**). The simplified model revealed an r^2 correlation with 0.772. The other model performance indicators are $se = 0.013$; the mean total deviance = 1.228; mean residual deviance = 0.325; estimated cv deviance = 0.5; $se = 0.027$ and training data correlation = 0.859.

The Akaike Information Criteria (AIC) is lowest (AIC 2992.9) when both interaction terms are included in the final GLM model.

To take into account temporary random effect by analyzing several observation years, GLMs were built up for each of the 5 years. Each of the annual GLM revealed the same variables with slightly different influence proportion (for final model see **Error! Reference source not found.**). Facing water residence times of only 8-10 days in main channel of Elbe in the German part and less than month in most of the tributary sections, we assume that the simulated value of the month before had not a strong influence on the next month. Instead, the exchange of the running water implies that for each month new nutrients emissions enter the surface waters and the recently produced algal biomass is washed out by longitudinal transport.

The indicated influence and sign of each of the variables in the GLM can be functionally explained by the following interpretations:

PO4

The negative sign in the coefficient of dissolved phosphorus (PO₄) is functionally produced by algal uptake in our plankton-dominated river system. As in lake systems the PO₄ is consumed up by phytoplankton or other plants, but extreme rapid P recycling from TP and sediment and rapid uptake causes the phenomenon that phytoplankton can still grow at very low concentrations of PO₄, and growth is more depended on TP concentration. The integration of PO₄ in the model operate as an indicator for the presence of algal biomass when low.

TP

Although P is in-cooperated into phytoplankton biomass, and phytoplankton is also a fraction of TP, the Pearson correlation between both variables is low (corr. = 0.1032). As expected from the Vollenweider model, TP is the most positive influencing variable for algal growth.

NO3

Nitrate (NO₃) is available in the basin in surplus, except of river arms with a lake-river-system such as river Rhin or Müggelspree, in which summer denitrification can cause a depletion of NO₃ and NH₄ to critical limitation threshold below 0.15 mg/L. These limiting situation occur in the training data set in 3.7% of all cases.

Ae

The size of the catchment (Ae) at a sampling point trigger the water residence time for algal to grow, increase the risk to receiving larger emissions and is also strongly correlated to the discharge (corr. = 0.899).

Ae * NO3 and Ae * TP

Both interaction terms have a weak negative sign, which indicate that increasing site of the catchment decrease the effect of nutrients (NO3; TP), antagonistic effect (single variables are all positive). The integration of the interaction terms make the model much more realistic and prevent for overshooting for stations with large catchment size, and for overestimating in those with small catchment.

Table 5.16. Model summary for GLM for Middle Elbe with response variable chlorophyll a

Deviance Residuals:				
Min	1Q	Median	3Q	Max
-3.4612	-0.6443	0.0111	0.6175	3.2129
Residual deviance: 839.65 on 1193 degrees of freedom				
Null deviance: 1473.84 on 1199 degrees of freedom				
Coefficients:				
	Estimate	Std. Error	t value	Pr(> t)
(Intercept)	-2.36253	0.41241	-5.729	1.28e-08 ***
PO4	-10.98757	0.57190	-19.212	< 2e-16 ***
TP	19.42877	1.78226	10.901	< 2e-16 ***
NO3	0.35098	0.09160	3.832	0.000134 ***
Ae	0.64658	0.04765	13.571	< 2e-16 ***
NO3 : Ae	-0.06495	0.01044	-6.224	6.71e-10 ***
TP : Ae	-1.52323	0.19823	-7.684	3.20e-14 ***

Significance codes: 0 '***' 0.001 '**' 0.01 '*' 0.05 '.' 0.1 ' ' 1				

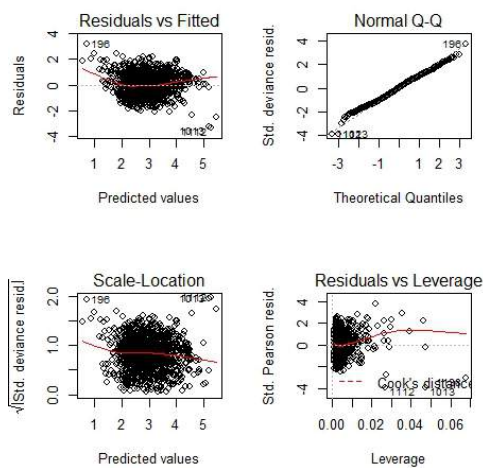


Figure 5.23 Model performance of the empirical model derived from GLM model.

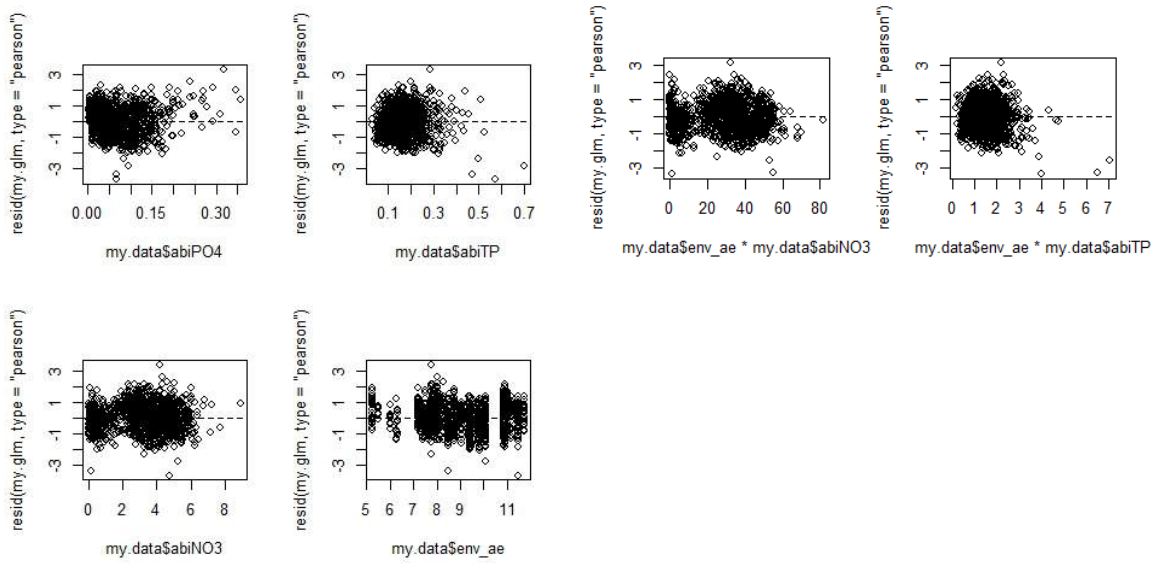


Figure 5.24 Residual for each of the terms used in the GLN model for Middle Elbe for response variable chlorophyll a-

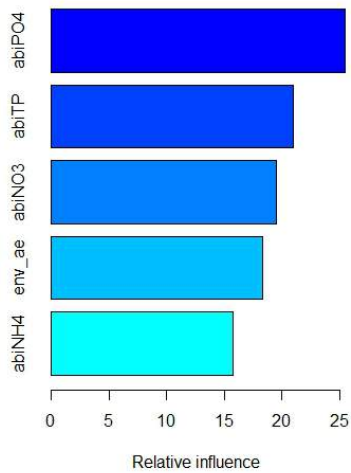


Figure 5.25 Relative influence of each of the variables to the GLM

5.2.5.1.5 Constrains to use the GLM model for predictions in Middle Elbe

The derived empirical model to predict the chlorophyll a concentration is simple in respect to the variables which are known to influence the phytoplankton growth (light exposure, growth time, silicon, nitrogen and phosphorus limitation) and losses (sedimentation, grazing by mussels and zooplankton, etc.).

Climate factors were dropped during the model simplification process such as precipitation and water temperature, but are known to be important. Furthermore, mean monthly conditions were analysed which do not reflect the short dividing rate of the phytoplankton, so uncertainties occur due to unknown interim disturbances and losses within a month.

The model setup suffer also from data limits: a) Especially upstream sites are less continuously monitored than those on the main channel (2005-2010) and b) data are not independent.

For developing a reliable model, the number of independent observations is crucial: Feld et al. (2016) recommend at least ≥ 150 independent observations and main stressors having $\geq 75\%$ of the full gradient's lengths, to achieve low errors and a high goodness of- fit (expressed as R^2) of the final averaged model. We do not have such a high number of independent observations at one site.

Furthermore, phytoplankton is transported along the river network, so upstream station will influence downstream phytoplankton biomass. Therefore, we can expect dependency of catchment size (Ae) to resulting response, but what we found was an low linear correlation (log: $\log r^2 = 0.104$; raw data: $r^2 = 0.21$) using Ae to predict chlorophyll a for our 1,096 observations of 56 sites which partly are subsequently arranged along main channel Elbe or in its tributaries. This is in accordance with distribution of chlorophyll a concentration within the river net: Interim algal blooms in the tributaries Saale and Havel drop down before the confluence with the main river Elbe, and chlorophyll a concentrations not simply increase with catchment size at sub-sequence stations but interim drop downs can be observed (losses; see process- orientated module PhytoBasinRisk).

5.2.5.1.6 Results of modelling nutrient loads with process-orientated model MONERIS

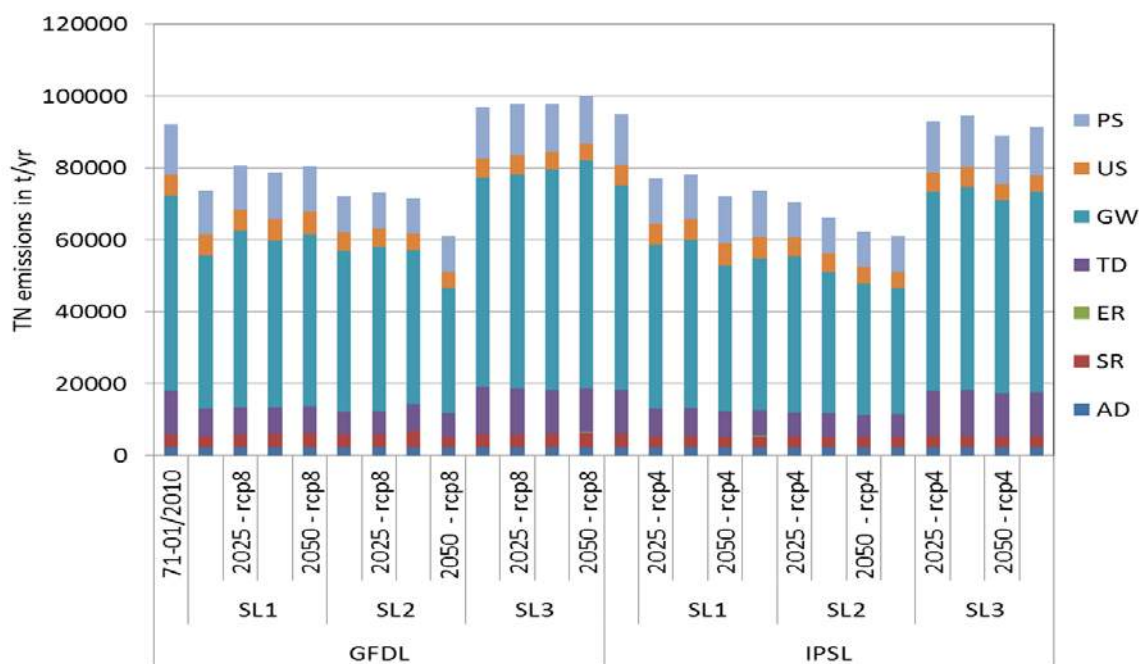
At basin outlet, total nutrient emissions simulated for TP and TN for baseline and future scenarios show clearly the same trends when driven with ISI-MIP scenarios GFDL-ESM2M and IPSL-CM5A-LR (see **Error! Reference source not found.**). In storyline 3 (Fragmented world) the emission is highest, and for storyline 2 (Consensus World) the lowest. Although highest human population is assumed for storyline 1, the implemented technical upgrade of WWTP, less N surplus and more balanced food will compensate human increase in the Techno World.

The GFDL socio-climate scenarios provide overall higher emissions for TN than IPSL. The TP difference is small. TN emission is dominated by the pathway groundwater, TP reach the surface waters from point sources (WWTP) and urban systems.

The nutrient emissions are transformed and retained within the river system (see next chapter) and are diluted by simulated discharge to final concentrations (**Error! Reference source not found.**) which effect the phytoplankton growth when limiting thresholds are surpassed.

While TN emission is reduced up to 33% of baseline, the resulting concentration reduction is less strong (**Error! Reference source not found.**).

The changes in monthly discharge frequently cause peak loads, while the resulting concentration remains low by dilution. This fact is demonstrated in **Error! Reference source not found.**, for which the scenario with the highest TN emission on annual base was selected.



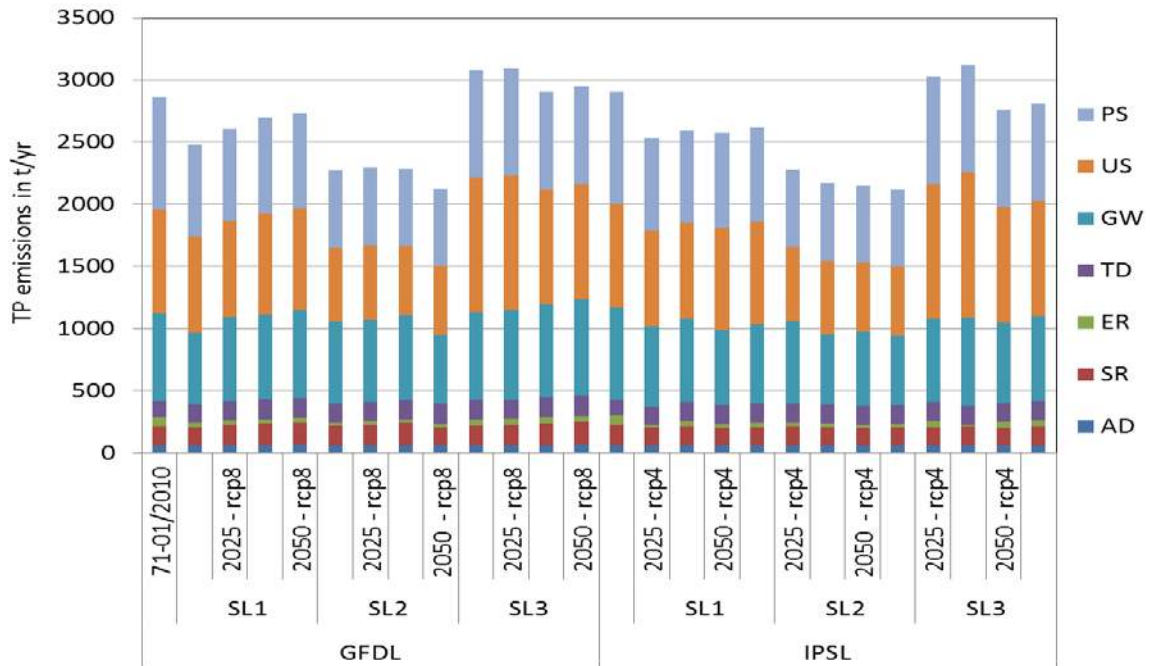


Figure 5.26 Simulated emission of TN (upper graph) and TP (lower graph) at outlet of Middle Elbe basin by model MONERIS (vs. 3.0) for longterm monthly baseline simulation (71-01/2010) and for all three storylines (SL1 – 3) driven by ISI-MAP climate scenarios GFDL or IPSL for RCP 8.5 or 4.5 and as a long term mean for the periods 2025 (2020-2030) and 2050 (2045-2055). The emissions are separated for the pathways listed in

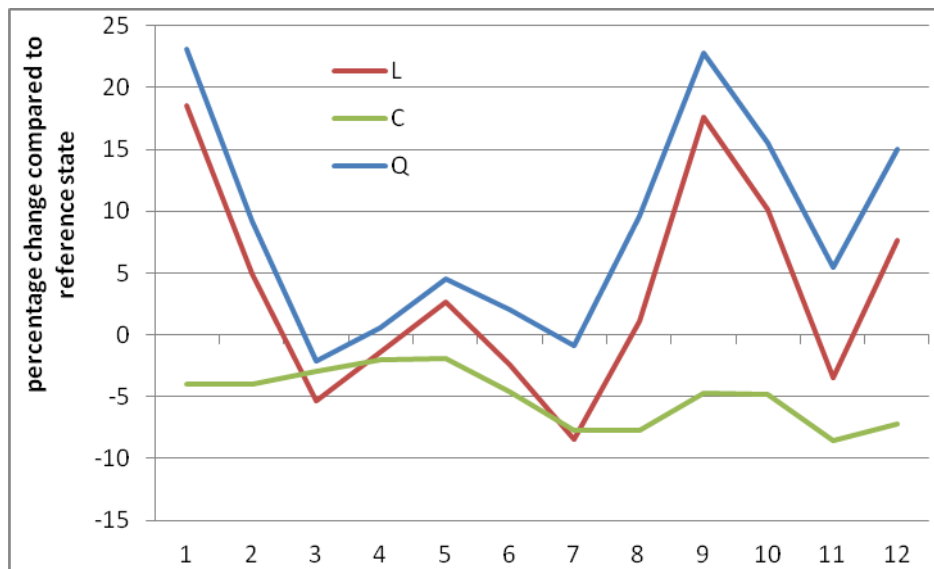


Figure 5.27 Comparison of simulated monthly values of cumulated discharge (Q), TN loads (L) and resulting TN concentration (C) for storyline 3 driven with climate GFDL and RCP 8.5 at basin outlet for the future period 2050.

5.2.5.1.7 Results of modelling phytoplankton biomass with PhytoBasinRisk

On monthly base for longterm means of each future periods, chlorophyll a concentration will decrease under GFDL climate simulation in all storylines and strongest in period 2050 with RCP 8.5 in comparison to GFDL baseline simulation for longterm period 1971-2001 (**Error! Reference source not found.**). Spring bloom in April will be lowered by 40% reduction, while summer months differ from baseline with -10 – 15%. In contrast running the same landuse, population and management option changes for all storylines as in GFDL under IPSL climate simulations; at least for storyline 1 and 3 chlorophyll will increase up to 30-40% in some months (April, September) in comparison to baseline (IPSL 1991-2001).

On annual level, the differences between the two IPS-MIP climate scenarios are stronger than those between the different MARS storylines for station near basin outlet. As so, when a single month is simulated as extreme dry or wet for the longterm mean of a future period, this signal remains visible in all 3 storylines: For example wet month April in GFDL for 2050 in RCP 8 with $300\text{m}^3 \text{ s}^{-1}$ more than in its baseline run reduce simulated chlorophyll a by 40%.

The model was initially run with TP and TN simulated by model MONERIS, and a second run with using simulated dissolved inorganic nitrogen (DIN) instead of TN revealed very similar differences to the baseline, while the seasonal means of chlorophyll a- concentrations change with -5 -10%.

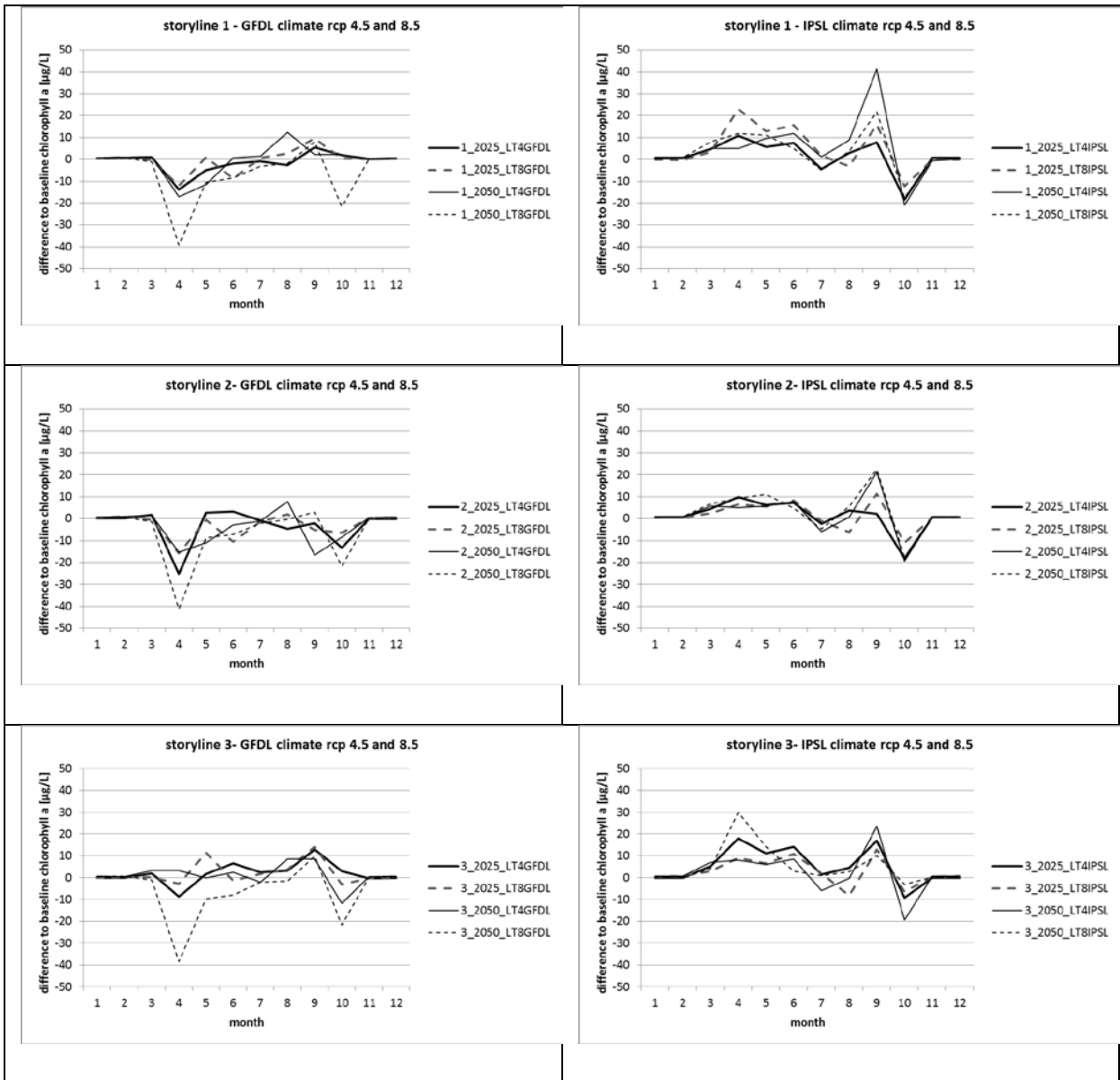


Figure 5.28 Change of chlorophyll a concentration to baseline (zero) for each month at basin outlet (station Boizenburg) modeled by PhytoBasin Risk in the three MARS storyline driven by simulated nutrient concentrations (MONERIS), and discharges (SWIM) for two climate scenarios and two future periods (2025; 2050)

5.2.5.1.8 Ecosystem service derived from nutrient retention and reduction of costs

In the German Middle Elbe basin occurs a strong nutrient retention in the river system. Comparing the emission with final loads, the retention contributes to reduce TP with a share of 39-41 % of the total emission at the basin outlet and TN with 25-26%. While TP retention is high in the tributaries only, the main channels contribute high denitrification rates in summer. Retentions

simulated for all future scenarios are in the same range as the inter-annual variance observed for the period 2006-2010 (first 5 balks in **Error! Reference source not found.**).

In absolute values 38,636 – 40,631 tons TN per year are retained or lost (denitrification) in the river system. To eliminate such high amount in WWTP it would cost the society 1932 – 2031 million Euro, when assuming cost of 50 €kg⁻¹ N (see Horbat et al. 2016).

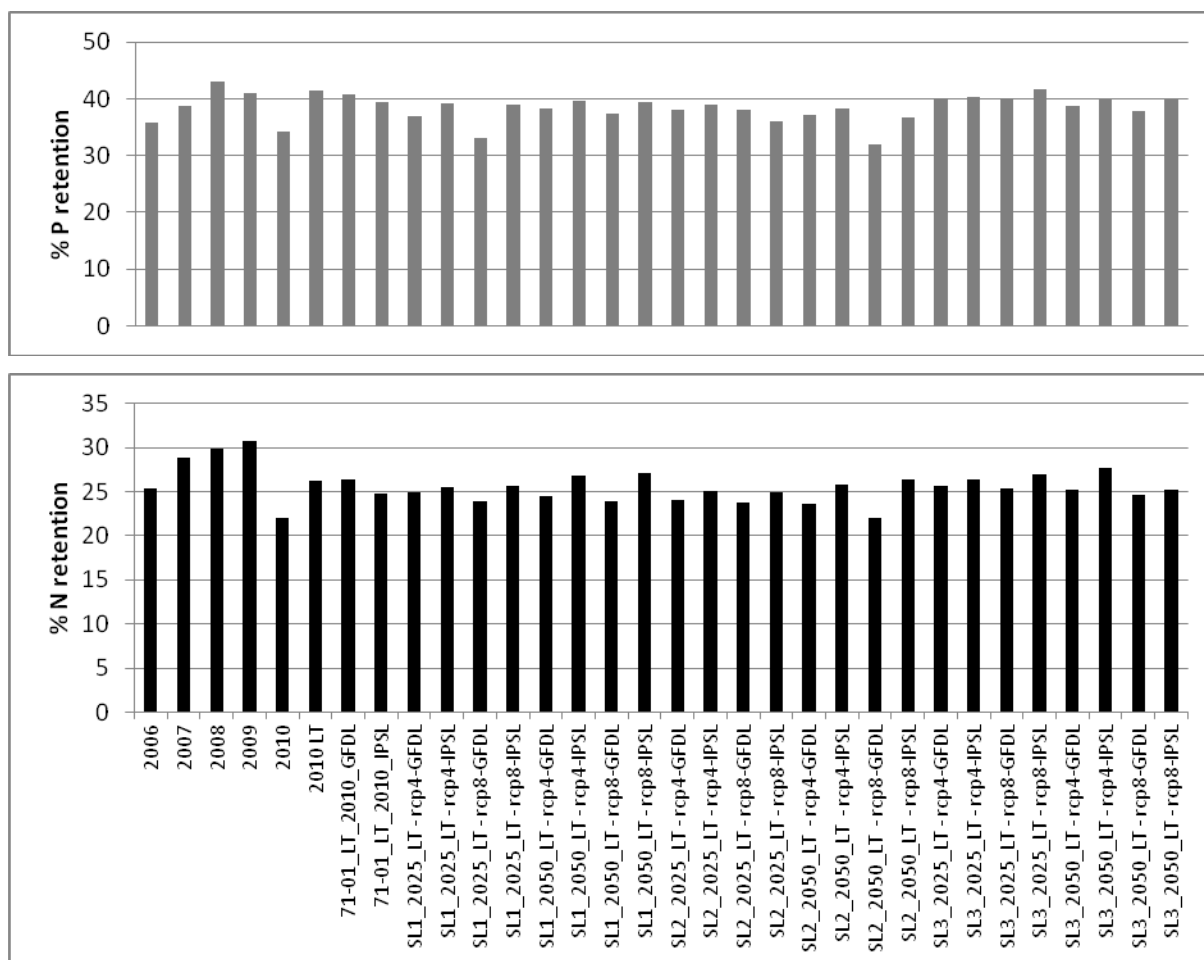


Figure 5.29 Proportion of calculated nutrient retentions (total P; upper graph; total N; lower graph) of total load in German area of Middle Elbe basin.

5.2.5.1.9 Ecosystem services derived from status improvement (chlorophyll a)

For main river Elbe the chlorophyll a concentrations will change in a range of 58 - 81µg/L (near basin outlet; **Error! Reference source not found.**). This range corresponds to an ecological status class of “moderate” or “poor” according the current assessment classification (Mischke et al. 2011). Improvement from status class “moderate” to “good” (<26µg/L chla) is simulated for the

sand – and clay dominated lowland rivers (type 15, 17), so at 3 stations of river Saale in the storyline 2.

TP concentrations higher than 0.075mg/L enable still high algal biomass with 58µg/L according our simulation with PhytoBaslin risk. In contrast, the empirical GML model predicts that resulting algal biomass would already decrease to a level of about 45µg/L chl a at this TP level, which would be in good status.

5.2.5.1.10 Key results of the scenario analysis

The achieved nutrient reduction in the Consensus World (storyline 2) with concentrations below 0.85µg l⁻¹ TP is not long lasting for all months in the vegetation period and is not strong enough to limit vegetation mean of phytoplankton biomass, which is still above 65µg l⁻¹ chlorophyll a in the seasonal mean (**Error! Reference source not found.**). Also, the assumed shading effect by riparian tree vegetation is not affecting the response output in the main channel. Tree shading in the tributaries reduce locally the algal growth (**Error! Reference source not found.**), but as a consequence of optimized higher light availability (when more clear tributaries confluence) downstream, the optimized growth rates in all main channels compensate the regional light limiting effects.

Table 5.17.Key results of the scenario analysis as seasonal mean (Apr-Oct) for station Elbe, Boizenburg near basin outlet for concentrations of chlorophyll a, total phosphorus (TP, mg/l) and total nitrogen (TN). Minima are in shaded fields and maxima are in bolt values.

Var	year	Techno World				Consensus World				Fragmented World			
		RCP4 _G	RCP4 _I	RCP8 _G	RCP8 _I	RCP4 _G	RCP4 _I	RCP8 _G	RCP8 _I	RCP4 _G	RCP4 _I	RCP8 _G	RCP8 _I
chl_a	2025	72.6	74.8	73.5	81.2	69.2	74.3	68.1	75.2	77.9	81.2	76.2	75.9
chl_a	2050	74.0	80.7	64.0	77.4	69.5	75.0	63.8	77.4	78.3	76.8	64.7	81.3
TP	2025	0.088	0.084	0.112	0.086	0.077	0.079	0.077	0.084	0.093	0.096	0.093	0.118
TP	2050	0.083	0.089	0.081	0.089	0.075	0.080	0.079	0.084	0.087	0.093	0.085	0.094
TN	2025	2.88	2.98	3.08	2.96	2.86	2.84	2.86	2.72	3.27	3.25	3.29	3.50
TN	2050	2.85	2.86	2.78	2.77	2.75	2.67	2.45	2.50	3.15	3.14	3.07	3.37

5.2.6 Discussion

The GLM model derived from empirical nutrient and site data from Middle Elbe is able to predict the resulting chlorophyll a concentration with a high confidence within the vegetation period April to October, although it omits any climate dependent variables such as discharge, temperature or global radiation. The interactions of nutrient response with size of catchment improve the model strongly.

The used chain of models implicated a high uncertainty:

The strategy to combine climate and socio-economic future scenarios in the MARS storylines make it necessary to estimate the specific contribution of climate change and socio-economic changes in our simulated output for nutrients and phytoplankton biomass. Climate scenarios applied in our study will change the discharge not as strong as expected (Krysanova et al. 2008), when simulation results for IPSL and GFDL by model SWIM are used as longterm means of each future period, ranging between $565 - 745 \text{ m}^3 \text{ s}^{-1}$ at basin outlet in the vegetation mean (**Error! Reference source not found.**). The relatively small range of climate changes has the lowest share on changes in nutrient concentration simulated by model MONERIS (Roers et al. 2016). We expect that simulation monthly changes for each single year will produce a much higher variability since extreme dry and extreme wet summers will be covered (Huang et al. 2013, 2015).

In contrast, another driver turns out to be much more relevant in the Middle Elbe: a strong shrinking of human population especially in the rural areas is the officially expected change for the modelled future time frames. It has to be recognized that the change of this driver will almost neutralize the effect of overuse of resources, which is realized in our MARS storyline 3 (“Fragmented world”).

According to the results of our models the physical and nutrient conditions in Middle Elbe enable phytoplankton to build up high biomasses ($>20-150 \mu\text{g/L}$ chl a in seasonal mean) in a high share of the modelled spatial units within a wide range of discharge and nutrient conditions, which is in accordance to the observations at monitoring stations. Short time events as floods or nutrient depletion are rapidly compensated in the system by newly emitted inputs, by optimized growth rates when a turbid phase is flushed out of the system (within about 5-10 days) and by strong feedbacks within the food web (grazing). The remobilizing of nutrients from sediments is not fully reflected in the models, but is expected to be important especially in the lake-river chains. The mechanism of channel retentivity proposed by Reynolds and Descy (1996) influences the

phytoplankton development in a strong manner when locations of almost no flow are frequent: Simulation is run here with a main velocity and assuming full mixed water bodies, we overlook the recruitment of phytoplankton from less turbulent areas.

Both models suffer from the fact that silica concentrations are not simulated for seasonal changes in future scenarios, but Si-depletion ($<0.3 \text{ mg l}^{-1}$) is known to occur occasionally at Elbe stations and in the river Havel, when high biomasses of diatoms develop. In consequence we expect that some maxima values of simulated chlorophyll a concentrations are locally and occasionally overestimated. On the other hand, silicon (Si) is supplied by the regular geological wash-out in a amount to carry a high phytoplankton biomass without limitation, since the observed 3-5 mg/L Si enables to build up at least $300 \mu\text{g/L}$ chl_a, when assuming Si content of 0.07 mg/mg in dry matter for planctonic diatoms (Quiel et al. 2011).

Implementing a bundle of measures in MARS scenario 2 (Consensus world) and running for future projections in 2025 and 2050 these measures will be able to compensate for climate change effects, but a level for strong phosphorus (P) nutrient limitation will not be achieved except of short summer periods, when simultaneously high phytoplankton biomasses occur. This is in accordance to future simulations by the process-based model QSIM applied to the main channel of Elbe river (Quiel et al. 2011), which predicts no or few P limitation. Nitrogen (N) is always available in surplus. The main pathway for P is point sources, while N is emitted mainly by diffuse pollution.

Therefore, a wider application of balanced fertilization and measures improving the nutrient retention directly near the agriculture fields such as installation of technically improved tidal drain ponds and much more areas with regular flooded wetlands is needed to achieve a reduction of the eutrophication risk in rivers and in the coastal zones.

The future development of the human population in the Middle Elbe region will lead to reduced emission since up to 19% less population are in the official actual prognoses. Only in combination with higher efforts to reduce nutrient emissions, the pressure relaxing by shrinking population will lead to good ecological status.

We identified antagonistic interactions between nutrients and catchment size when chlorophyll a is the response. Still, the full model predicts that smaller basins are less sensitive to nutrients and stronger eutrophication response is expectable in stations with a large catchment. This finding has

the implication for water managers that a fail of ecological response observed in small sized rivers at high nutrient concentration is still a management problem, since eutrophication risk strongly increase in downstream water bodies or in the connected coastal zone. Much more effort has to be implemented in the Middle Elbe basin to further reduce the nutrient levels for improving ecological status.

5.2.7 Conclusion

The surface waters in the Middle Elbe basin are under high diffuse pollution and hydro-morphological pressure. Supported by specific environmental characters, such as extreme long residence times in reservoirs and river-lake-systems combined with intensive landuse in the riparian zones, the nutrient emissions are transformed effectively to phytoplankton biomass and lower the ecological status to the classes moderate or poor. Climate change will slightly intensify this transformation, if not suitable management options such as further reduction of nutrient surplus and increasing tree shading will be implemented in the whole basin including the smaller tributaries.

5.2.8 Acknowledgements

This work is part of the MARS project (Managing Aquatic ecosystems and water Resources under multiple Stress) funded under the 7th EU Framework Programme, Theme 6 (Environment including Climate Change), Contract No.: 603378 (<http://www.mars-project.eu>). We acknowledge Fred Hattermann and Michael Roers for delivering the modelled discharge data for the chosen socio-climate scenarios and the simulated input-data. Meteorological data were provided by the German Weather Service's Meteorological Observatory called Deutscher Wetterdienst (DWD). We kindly thank the Elbe basin river district (FGG Elbe) and all joining German Federal States for their cooperation and delivery of monitoring data and maps.

5.3 Odense

5.3.1 Introduction

The Odense River basin, Denmark, is an agriculturally dominated lowland catchment draining into an estuary, the Odense Fjord, Figure 5.30. Table 5.18 summarizes the main characteristics of the Odense catchment. Figure 5.31 illustrates the DPSIR model of the basin also indicating the approach of linking a process-based hydrological catchment model to empirically developed ecological models.

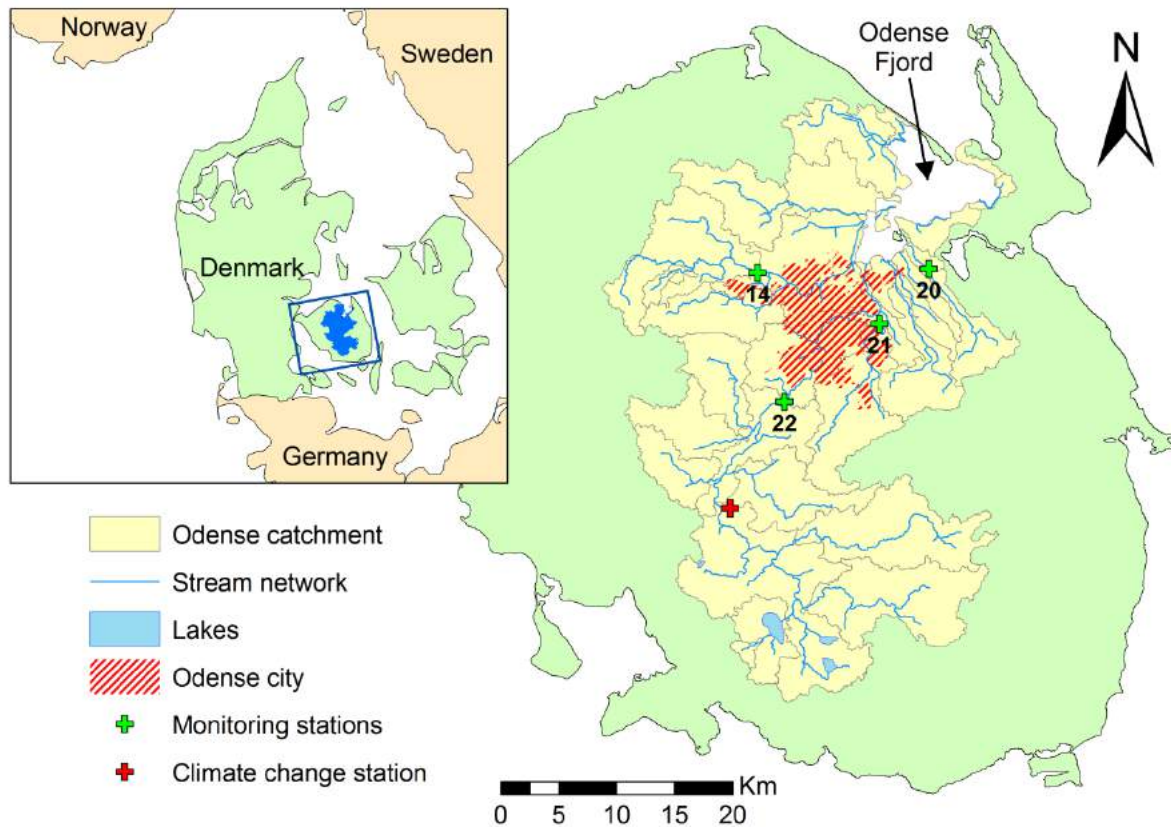


Figure 5.30 Location of the Odense River catchment, subbasin division and location of runoff and nutrients monitoring stations and climate change station.

Table 5.18.Characteristics of the Odense River catchment.

Location	
Basin name	Odense
Source name	Højslunde (Hågerup Å)

Source height	100.8 m
Source coordinates	55° 9' N, 10° 32' E
Mouth or lowest flow gauge name	Mouth: Odense Fjord estuary; lowest flow gauge: Ejby Mølle 450001
Mouth height	sea level
Mouth coordinates	55° 26' N, 10° 26' E
Basic physiography	
Basin area	1061 km ²
Length of main channel	70 km
Geology	Younger clayey moraines from the Weichsel glaciation (the last glaciation)
Land cover distribution	Agriculture 68%; forest 10%; urban 14%
Description of basin physiography	Lowland river basin with gentle topography, predominantly rural with forested headwaters and considerable urbanization around the outlet into the Odense Fjord estuary.
Hydrometry	
Basin average annual rainfall and monthly long-term average totals	672 mm yr ⁻¹ (1961 – 1990) J 55 mm F 39 mm M 44 mm A 40 mm M 49 mm J 54 mm J 63 mm A 63 mm S 62 mm O 67 mm N 74 mm D 63 mm
Flow statistics for lowest flow gauge (Ejby Mølle, not defining the basin)	1977 – present Mean flow: 10.4 m ³ s ⁻¹ Q95: 2.7 m ³ s ⁻¹

	Q10: 22.7 m ³ s ⁻¹
Description of factors affecting measured runoff	Runoff reduced by groundwater abstraction (for households, industry, agriculture)
RBM Plan-type information	
Main pressures on water resources	Wetlands and streams: land drainage, hydromorphological alterations (culverting, channelization, widening/deepening), groundwater abstraction, weed cutting in streams, pesticides, waste water from scattered dwellings not connected to sewers. Lakes: eutrophication. Groundwater: water abstraction, nitrate. Estuary: eutrophication, hazardous substances.
Key ecosystem services	Water supply, nutrient retention, recreation, angling
WFD ecological status	Streams (728 km): 39% good or high (reasons for not complying: waste water, pesticides, poor physical condition) Lakes (16 lakes > 5 ha): 19% good or high (reasons for not complying: excessive external or internal phosphorus loading). Estuary (62 km ²): poor (due to excessive external and internal nutrient loading).
Planned measures (2015 – 2021)	Streams: (main goal to improve physical conditions) river restoration, removing obstacles for fish migration. Lakes: (main goal to reduce external P loading) allowing temporary flooding of riparian areas for sedimentation of P-rich particles, lake restoration, mapping of P-risk areas. Coastal water bodies: (main goal to reduce N loading) wetlands, set-aside, catch crops, reforestation.
Stakeholder summary	
Key stakeholders	The Nature Agency under the Ministry of the Environment (Odense office), responsible for River Basin Management Plans including outline of Programmes of Measures, responsible for the national monitoring of the aquatic environment. The municipalities within the basin, various interests including recreation. Responsible for implementing the Programme of Measures. National and local angling associations.
MARS work in basin	

Aims of work in basin	<p>To establish a model chain between climate, catchment processes and biological response in freshwater and estuarine ecosystems.</p> <p>To run plausible scenarios on climate, land use and management changes with the chain of models.</p> <p>To evaluate the ecological effects of multiple stressors acting in concert, e.g. nutrient loading, temperature increase and alterations in water flow dynamics.</p>
Stressors	Eutrophication, pesticides, water scarcity, land drainage, channelization, mowing of stream macrophytes.
Indicators	<p>Abiotic: TN, TP, SS, flow</p> <p>Biotic: Aquatic macrophyte species and coverage, abundance and number of fish species, composition of macroinvertebrate communities (Danish Stream Fauna Index), phytoplankton (in lakes).</p>
Ecosystem services	<p>Water supply</p> <p>Nutrient retention Recreation</p> <p>Angling (trout).</p>
Data	<p>National data 2004-2012 used for developing empirical abiotic-biotic models:</p> <p>Fish: 100 sites, species level</p> <p>Macroinvertebrates: 130 sites, species level</p> <p>Stream macrophytes: 100 sites, species level</p>
	Catchment hydrological data: 13 fixed gauging stations within the catchment the oldest with nearly 100 years of data. Other stations with only instantaneous discharge measurements (n = 100).
	Catchment morphological data: n = 13 stream stations in surveillance monitoring plus > 100 stream stations in operational monitoring.
	Catchment physico-chemical data: Data from 13 fixed gauging stations and discrete sampling of water quality at other ca. 100 stations.

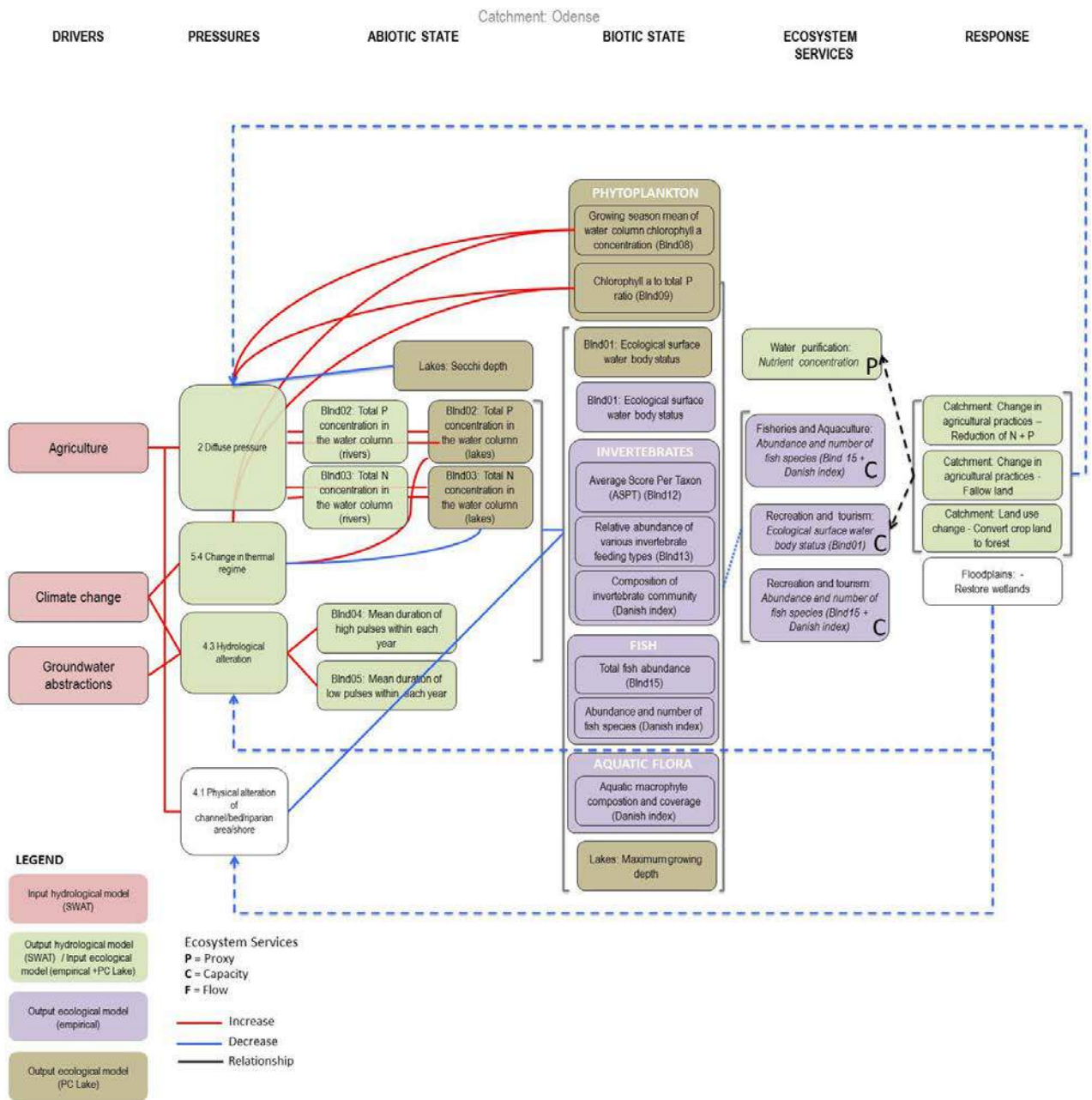


Figure 5.31 The DPSIR model for the Odense River basin. Outputs from a process-based hydrological catchment model are linked to empirical ecological models to assess biotic state and ecosystem services.

5.3.2 Scenarios Definition

Various future climatic and socio-economic scenarios were chosen in the context of the MARS project to define three storylines at the European level. They differ mainly in four main aspects:

main drivers in the economy, economic growth, policies regarding the environment and public concern about the environment and protection of ecosystem services.

Storyline 1, called *Techno world (or economy rules)*, considers that economy grows fast, with high energy demands and increase of CO₂ emissions due to a fossil fueled development. Society shows high awareness about environmental issues but protection regulations are poor and policies are not renewed. Water management strategies are oriented to water needed for economic development and little effort is done on sustainable measurements. Climate change scenario RCP 8.5, a rising scenario with very high greenhouse gas emissions, is assigned to this storyline.

Storyline 2, called *Consensus world*, considers that the economy and the population are growing at the same pace as now. There are regulations to save energy in favor of reducing emissions, environmental awareness and interest for preservation. Current environmental guidelines and policies are continued but in a more integrated manner. First choice in water management strategies is sustainable at mid-long term cheap solutions. RCP 4.5 climate change scenario, a stabilization one, is taken into account.

Storyline 3, called *Fragmented world*, considers a regional rivalry Europe where the economy grows in some countries (included Northern Europe) and decreases in others. Europe suffers a lack of resources and an extended use of fossil fuels. No attention is paid to the preservation of the ecosystems, although rich countries implement some measurements. Environmental policies are broken because of focusing on economic development. Water management actions are restricted to short term effects. Again, climate change scenario RCP 8.5 rules in this storyline.

Detailed information about the development of the storylines can be found in (Faneca Sanchez et al., 2015).

We down-scaled these storylines to the Odense River catchment in order to simulate future scenarios at a basin scale. The time horizons are 2030 (interval 2025-2034) and 2060 (2055-2064). The reasons of these horizons are, first, the update of the Water Framework Directive on 2027 (one of the objectives of MARS is to support managers and policy makers in practical implementation of the update of the WFD) and second, 2060 is chosen to show the impacts of climate change, as by 2030 climate projections show little change of climate variables in comparison with the now (Faneca Sanchez et al., 2015). The period 2011-2020 was chosen as baseline.

Two climate models from the ISI-MIP project (Inter-Sectoral Impact Model Intercomparison Project, www.isi-mip.org) were used to simulate each climate scenario, GFDL-ESM2M and IPSL-CMA-LR, as they offered the best results when representing the median cumulative precipitation over the period 2006-2099 for the different case studies across the MARS project (REF?). The variables selected to force the climate change scenarios in SWAT were maximum and minimum air temperature, precipitation, solar radiation, relative humidity and wind speed. Climate change data for each model were obtained for the period 2006-2099 from the (REF?), which offers daily projections for the required variables in a 30x55 Km network. The network point located inside the Odense catchment (lat 55.25, long 10.25, Figure 5.30) was selected to extract the daily projections and run the scenarios for the abovementioned periods. Previously, we compared the first years of the projections (2006-2014) with observed data and applied the appropriate bias correction for precipitation and temperature in a monthly basis through the ArcSWAT interface.

Regarding land use change, since our study area is eminently agricultural (68% of the basin), we focused on the farming context to design three scenarios corresponding to the storylines:

1. High-tech agriculture: Agricultural area remains similar, with some conversion to permanent grass and willow. Slight increase in livestock density and slight decrease in artificial fertilizer application rates.
2. Agriculture for nature: Agricultural area decreases and changes towards forest and less intensive farming types. Artificial fertilizer application decrease slightly as well.
3. Market driven agriculture: Agricultural area increases and changes towards intensive pig and dairy farm types. Livestock density and fertilizer application increase.

The scenarios are based on a very comprehensive work done by the Centre for Regional change in the Earth System (CRES) (Olesen et al., 2014). Land use changes were applied in SWAT through changes in land use type area, in fertilizer application rates and in timing on crop management operations for the long term scenario (timing in the short term scenario remains as in baseline) (Figure 5.32, Tables 5.21-5.23).

Table 5.19. Absolute area change of the different land use types for the three scenarios (and % of each change regarding total basin surface). In bold those changes involving more than a 5% of total basin area.

FARM TYPE	Manure (KgN ha ⁻¹)	Baseline (ha)	Scenario 1: High-tech agriculture		Scenario 2: Agriculture for nature		Scenario 3: Market driven agriculture	
			Absolute change (ha)	% of total basin area	Absolute change (ha)	% of total basin area	Absolute change (ha)	% of total basin area
Mixed and Plant	<50	3122	-521	0.5	-887	0.8		
Pigs	<70	24973	-7392	7.0	-5394	5.1	-24973	23.5
	>70	21851	-2273	2.1	-10292	9.7	+33077	31.2
Dairy / Cattle	<85	4682	-1447	1.4	+538	0.5	-4682	4.4
	85-170	7804	-1709	1.6	-3278	3.1	-7804	7.4
	>170	3122	+164	0.2	-1545	1.5	+12486	11.8
Mixed + horticulture	>50	12486	-3009	2.8	-5494	5.2		
Permanent grass	-	1969	+2780	2.6	+13714	12.9	-24	0.02
Forest - deciduous	-	5954			+10218	9.6	-4894	4.6
Forest - coniferous	-	4138			+2420	2.3	-3186	3.0
Willow	-	0	+13408	12.6				

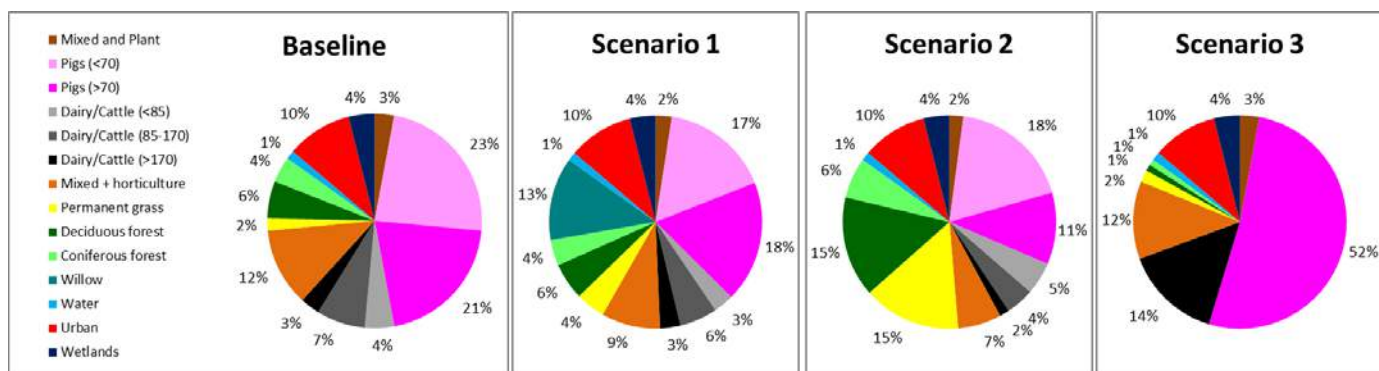


Figure 5.32 Land uses % coverage in the baseline and the three LUC scenarios (1=High-technology agriculture, 2=Agriculture for nature, 3=Market driven agriculture)

Table 5.20. Change in fertilizer application rates (%) for the different scenarios (1=High-technology agriculture, 2=Agriculture for nature, 3=Market driven agriculture). Absolute fertilization rates are shown for willow since it is a new land use in scenario 1.

FARM TYPE	SCENARIOS 1 AND 2			SCENARIO 3	
	Manure N (Kg N/ha)	Animal manure	Artificial fertilizer	Animal manure	Artificial fertilizer
Mixed and Plant	<50	-2%	-13%	+6%	+50%
Pigs	<70	-1%	-2%	-1%	-2%
	>70	+1%	-2%	+18%	+31%
Dairy / Cattle	<85	-2%	-6%	-2%	-6%
	85-170	+1%	+13%	+1%	+13%
	>170	+1%	-17%	+19%	+134%
Mixed + horticulture	>50	-1%	-13%	-1%	-13%
Willow (Kg N/ha)	-	80	60	-	-

Table 5.21. Crop management operation dates for current and long term (2060) scenario.

Crop	Period	Ploughing	Sowing	Manure	Fertilizer	Harvest	Kill/end
W. wheat	Current	18/9	20/9	15/3	1/4, 1/5	20/8	
	2060	24/9	27/9	11/3	26/3, 25/4	12/8	
S. barley	Current	16/3	4/4	15/3	2/4	15/8	
	2060	8/3	22/3	7/3	20/3	6/8	
W. rape	Current	20/8	22/8	15/3, 19/8	1/4	20/7	
	2060	26/8	27/8	5/3, 25/8	20/3	15/7	
Sugar beet	Current	16/3	12/4		10/4	15/10	
	2060	8/3	1/4		30/3	25/10	
Silage maize	Current	2/4	27/4	1/4	25/4	20/10	
	2060	26/3	17/4	25/3	15/4	10/10	
Seed grass	Current		16/8, 21/8	15/3	1/4	15/8	14/3, 15/3, 17/9
	2060		7/8, 13/8	7/3	19/3	6/8	6/3, 7/3, 23/9
Grass (clover)	Current		16/8, 21/8	15/3	16/3, 1/6, 5/7	25/5, 1/7, 10/8, 15/8, 10/10, 1/10	14/3, 15/3, 31/3, 17/9
	2060		7/8, 13/8	5/3	6/3, 1/6, 10/7	25/5, 5/7, 15/8, 20/8, 20/10, 1/10	6/3, 7/3, 24/3, 23/9
Willow	Current			1/4	1/4	1/12	
	2060			1/4	1/4	1/12	
Grain maize	2060	25/3	17/4	24/3	15/4	20/10	

Due to climate change, grain maize was introduced in the long term scenario for all land use change scenarios replacing winter wheat as follows (Table 5.24), with the same fertilization rates.

Table 5.22. Adaptation of pig farms in 2060 to include grain maize.

ROTATION SCHEME						
Farm Type	Manure N (KgN ha ⁻¹)	Year 1	Year 2	Year 3	Year 4	Year 5
Pig	>70	W. Rape	W. wheat	Grain maize	Grain maize	S. barley
		S. barley	Seed grass	S. barley	W. wheat	Grain maize

As a result, 20 scenarios were run in SWAT (Table 5.25):

- 4 scenarios with the last ten years of observed climate data used to calibrate and validate the model (2001-2010), one with the current land use and three with the future land use scenarios. This procedure is necessary to evaluate the isolated effect of land use on hydrology and nutrient load, since in the storylines each land use is run together with different climate models/RCPs.
- 4 scenarios that act as baseline for the MARS storylines (2 RCPs × 2 climate models), running for the first ten years of each climate projection with the current land use.
- 12 scenarios to simulate the described future storylines (2 climate models × 2 time horizons × 3 land uses).

Table 5.23.20 scenarios run in SWAT to analyze the individual effect of land use (a) and the possible effects in MARS storylines (b).

a)

ONLY LAND USE SCENARIOS				
Climate	Present land use	Agriculture for nature	High tech agriculture	Market driven agriculture
OBSERVED	PLU_Observed	AN_Observed	HT_Observed	MD_Observed

b)

		MARS Storylines: Land use + climate change scenarios		
Climate model	Time horizon	Agriculture for nature (Consensus world) + RCP 4.5	High tech agriculture (Techno world) + RCP 8.5	Market driven agriculture (Fragmented world) + RCP 8.5
GFLD-ESM2M	Baseline	PLU_GF_45	PLU_GF_85	
	2030	AN_GF_30	HT_GF_30	MD_GF_30
	2060	AN_GF_60	HT_GF_60	MD_GF_60
IPSL-CM5A-LR	Baseline	PLU_IP_45	PLU_IP_85	
	2030	AN_IP_30	HT_IP_30	MD_IP_30
	2060	AN_IP_60	HT_IP_60	MD_IP_60

5.3.2.1.1 Results

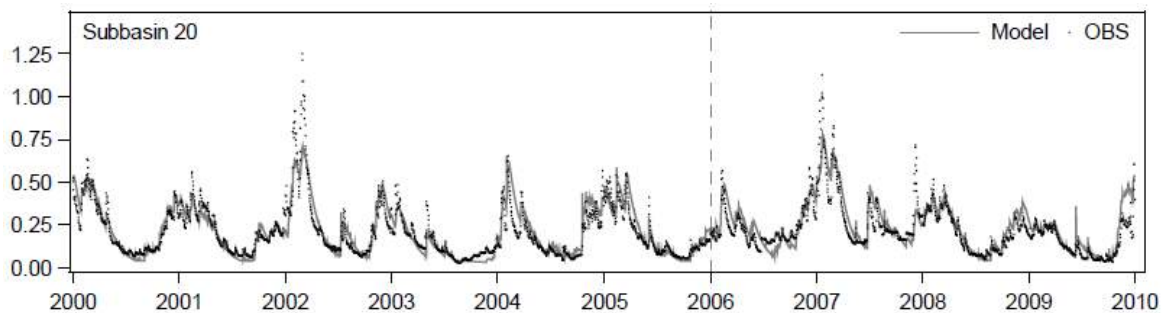
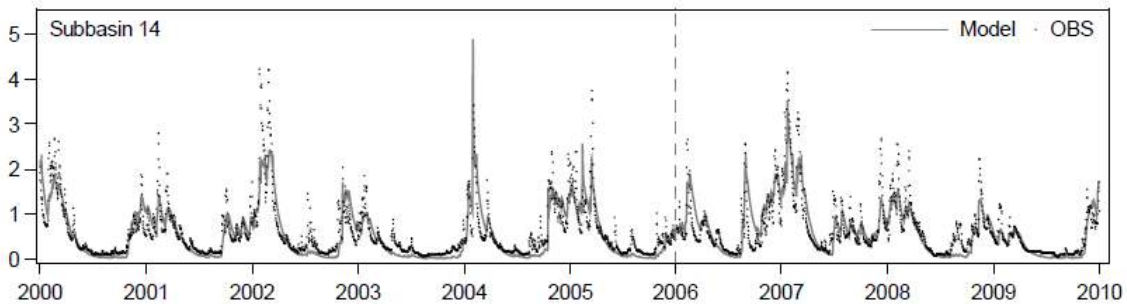
Model Calibration and Validation

The initial and calibrated values of the selected parameters are given in Table 5.26. Figures 5.33-5.37 show the observed and simulated discharges and nutrient fractions in the monitoring stations during calibration and validation periods, and Table 5.27 shows the corresponding performance statistics values.

Table 5.24. Initial range and calibrated values of the selected parameters (IV=Initial value of parameter before calibration).

DISCHARGE PARAMETERS			
Parameter	Level	Initial range (relative change)	Calibrated values
SFTMP.bsn	Basin-wide	-1 - 1	0.94
SMFMN.bsn	Basin-wide	-1 - 2	1.12
SMFMX.bsn	Basin-wide	1.6 - 3.5	2.57
SMTMP.bsn	Basin-wide	-2.3 - 1	-0.14
SURLAG.bsn	Basin-wide	1 - 10	5.23
<hr/>			
ALPHA_BF.gw	Sub-basin	0 - 1.011	0.07 - 0.97
ALPHA_BNK.rte	Sub-basin	0 - 1.1	0.003 - 0.94
CH_K2.rte	Sub-basin	0 - 75	9.68 - 74.31
CN2.mgt	Sub-basin	17.5 - 119.6 (IV·0.7 - IV·1.3)	17.5 - 67.16
DDRRAIN.mgt	Sub-basin	770 - 1430 (IV·0.7 - IV·1.3)	792 - 1331
EPCO.hru	Sub-basin	0.01 - 1.103	0.11 - 0.66
ESCO.hru	Sub-basin	0 - 1	0.31 - 0.98
GDRAIN.mgt	Sub-basin	1.4 - 2.6 (IV·0.7 - IV·1.3)	1.72 - 2.26
GWQMN.gw	Sub-basin	0 - 2000	133.67 - 1735.02
GW_DELAY.gw	Sub-basin	0 - 600	28.19 - 339.88
GW_REVAP.gw	Sub-basin	0 - 0.2	0.06 - 0.13
OV_N.hru	Sub-basin	0.008 - 0.36 (IV·0.8 - IV·1.2)	0.008 - 0.32
REVAPMN.gw	Sub-basin	0 - 2000	368.71 - 1896.40
SOL_AWC.sol	Sub-basin	0.03 - 0.43 (IV·0.2 - IV·1.8)	0.08 - 0.36
SOL_BD.sol	Sub-basin	0.56 - 2.04 (IV·0.8 - IV·1.2)	0.62 - 2.02
SOL_K.sol	Sub-basin	1.28 - 129.03 (IV·0.2 - IV·3)	9.31 - 83.53
TDRAIN.mgt	Sub-basin	33.6 - 62.4 (IV·0.7 - IV·1.3)	46.56 - 60.48
<hr/>			
NUTRIENT PARAMETERS			
CMN.bsn	Basin-wide	0.002 - 0.003	0.0027
PRF_BSN.bsn	Basin-wide	0.5 - 2	0.85
RSDCO.bsn	Basin-wide	0.02 - 0.1	0.058
SPCON.bsn	Basin-wide	0.001 - 0.01	0.0036
SPEXP.bsn	Basin-wide	1 - 1.5	1.18
ADJ_PKR.bsn	Basin-wide	0.5 - 2	1.09
CDN.bsn	Basin-wide	0.02 - 0.3	0.19
NPERCO.bsn	Basin-wide	0.21 - 0.95	0.58
N_UPDIS.bsn	Basin-wide	20 - 100	87.4
SDNCO.bsn	Basin-wide	0.8 - 0.88	0.85
PHOSKD.bsn	Basin-wide	140 - 450	180.8
PPERCO.bsn	Basin-wide	11 - 16	11.2
PSP.bsn	Basin-wide	0.01 - 0.7	0.19
P_UPDIS.bsn	Basin-wide	28 - 95	51.4

ANION_EXCL.sol	Sub-basin	0.1 - 1	0.40-0.87
BC1.swq	Sub-basin	0.1 - 0.99	0.27-0.85
BC2.swq	Sub-basin	0.2 - 2	0.90-1.52
CH_BED_KD.rte	Sub-basin	0.001 - 3.75	1.25-3.44
CH_BNK_KD.rte	Sub-basin	0.001 - 3.75	0.30-2.60
CH_D.rte	Sub-basin	0.58 - 3.57 (IV·0.7 - IV·1.5)	0.81-3.02
CH_L1.sub	Sub-basin	10.83 - 32.21 (IV·0.75 - IV·1.25)	11.92-30.89
CH_L2.rte	Sub-basin	6.10 - 21.51 (IV·0.75 - IV·1.25)	7.30-18.56
CH_N1.sub	Sub-basin	0 - 0.4	0.05-0.30
CH_N2.rte	Sub-basin	0 - 0.4	0.01-0.29
CH_ONCO.rte	Sub-basin	500 - 20000	3850-12293
CH_OPCO.rte	Sub-basin	0 - 3000	435-2388
CH_S1.sub	Sub-basin	0.001 - 0.010 (IV·0.8 - IV·2.0)	0.001-0.009
CH_S2.rte	Sub-basin	0.016 - 0.000 (IV·0.8 - IV·2.0)	0.001-0.150
CH_SIDE.rte	Sub-basin	0 - 5	0.99-4.99
CH_W1.sub	Sub-basin	1.72 - 22.62 (IV·0.75 - IV·1.25)	1.98-22.20
CH_W2.rte	Sub-basin	2.29 - 30.16 (IV·0.75 - IV·1.25)	2.55-25.03
GWSOLP.gw	Sub-basin	0.01 - 0.2	0.05-0.08
HLIFE_NGW.gw	Sub-basin	0 - 600	431-549
USLE_P.mgt	Sub-basin	0 - 0.1	0.02-0.08



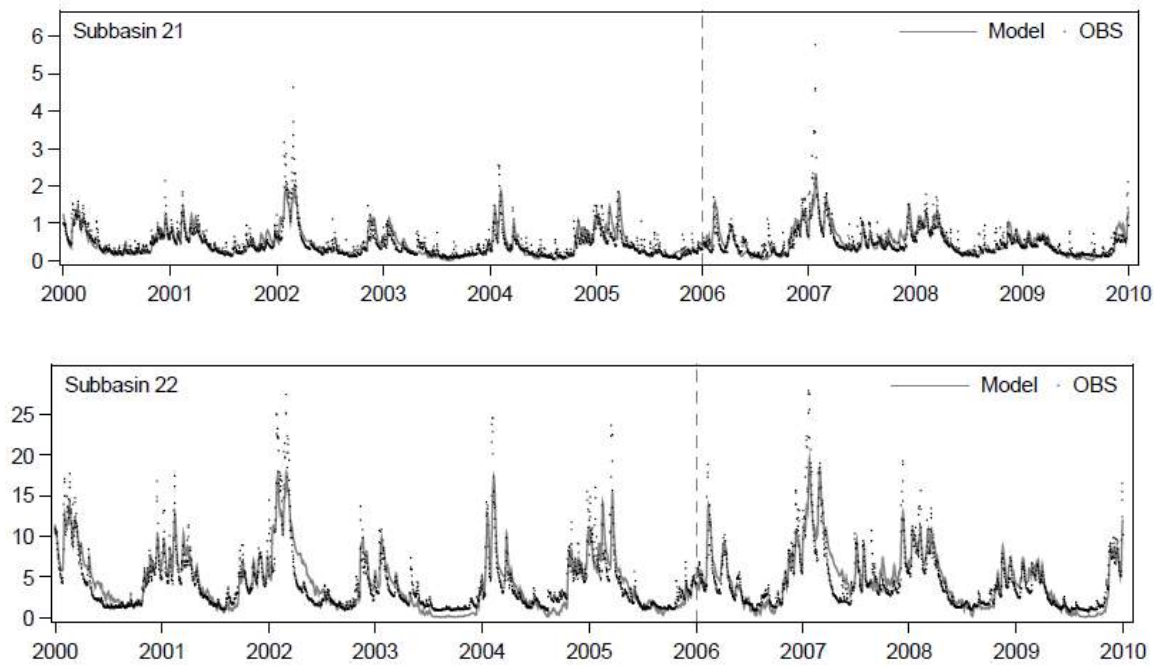


Figure 5.33 Observed (black dots) and simulated (grey line) daily discharge (m^3/s) at the four gauging stations in the Odense River catchment during calibration (2000-2005) and validation (2006-2009) periods.

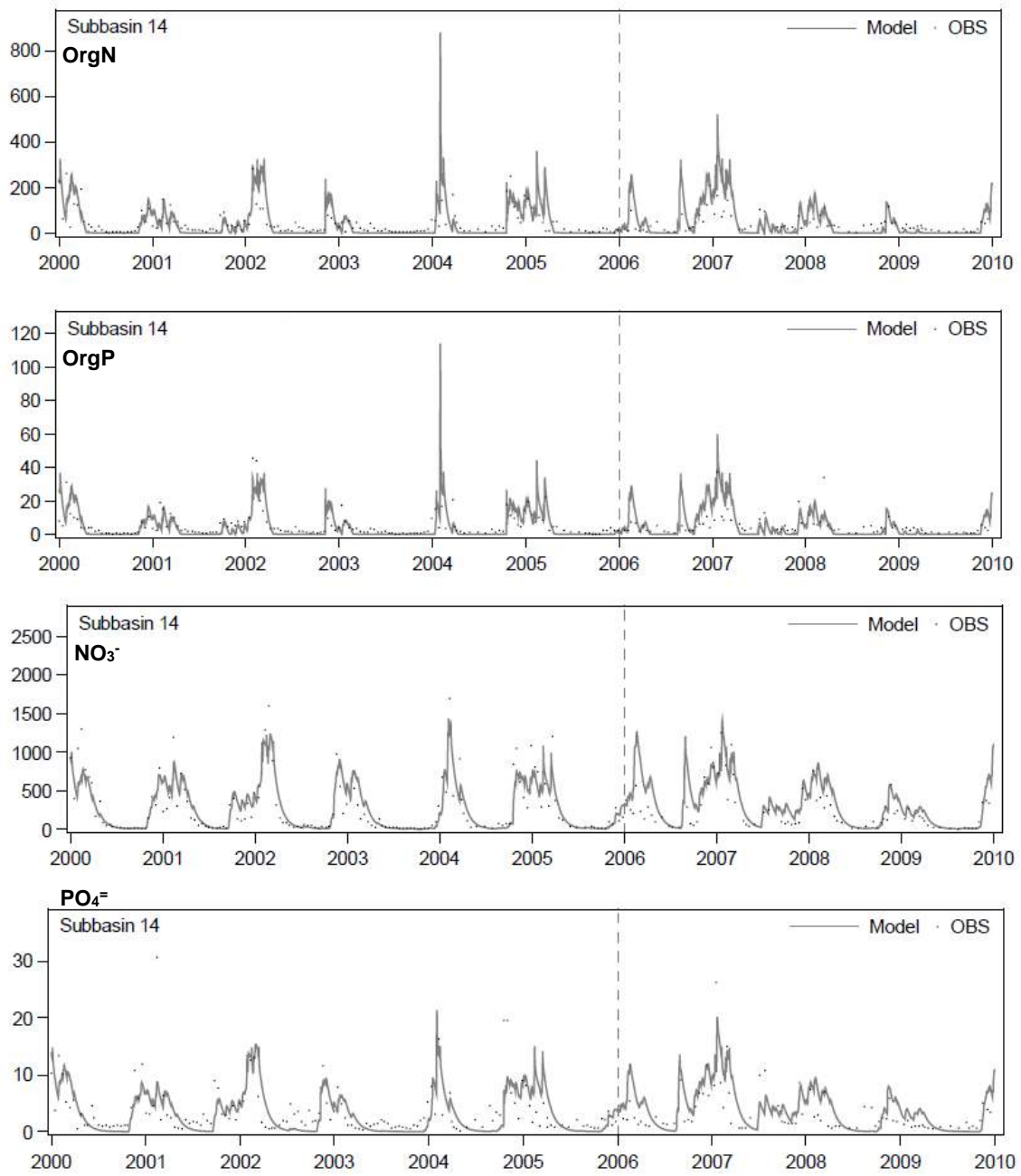


Figure 5.34 Daily nutrient loads (Kg) observed and predicted in sub-basin 14 during calibration (2000-2005) and validation (2006-2009) periods.

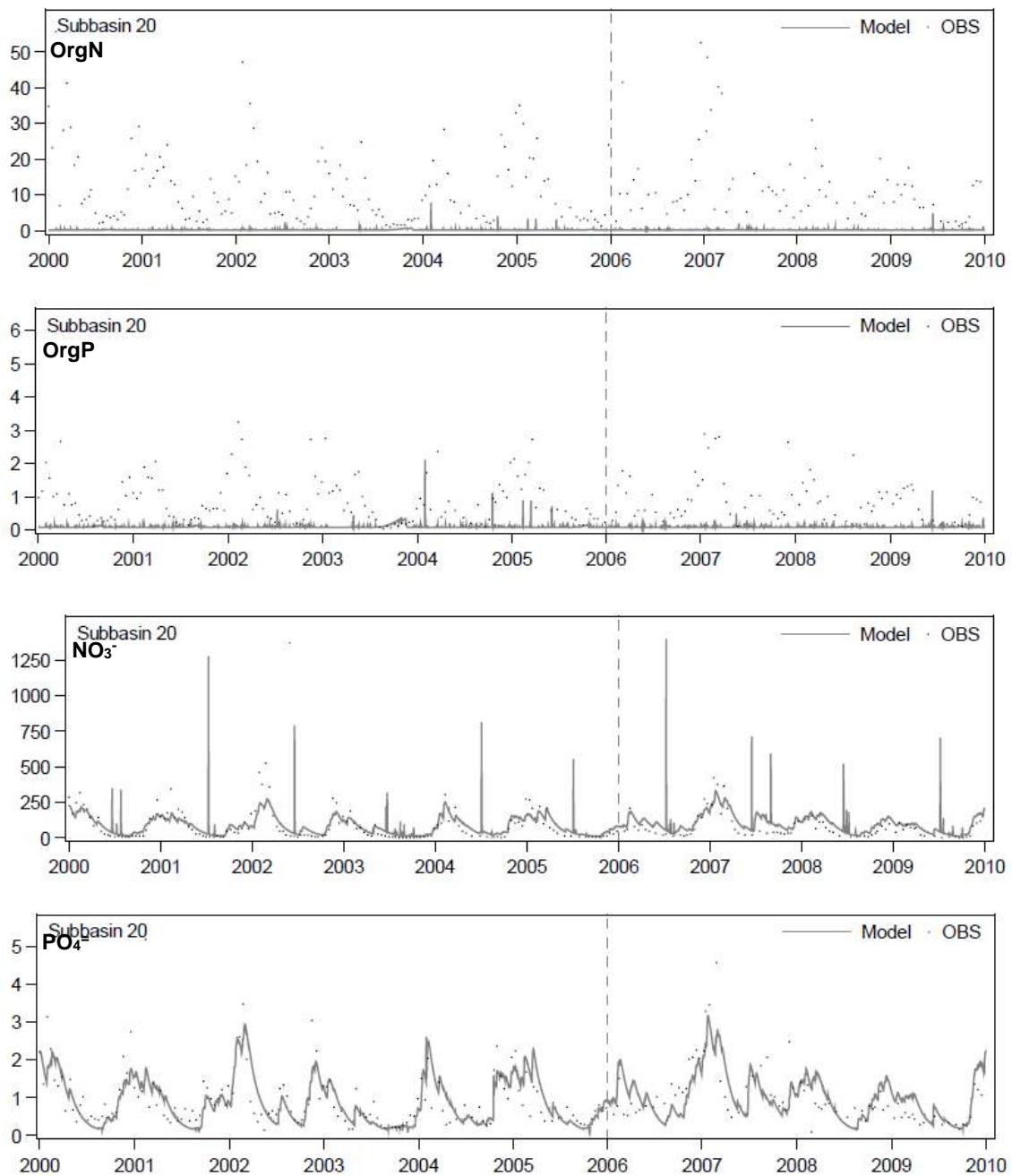


Figure 5.35 Daily nutrient loads (Kg) observed and predicted in sub-basin 20 during calibration (2000-2005) and validation (2006-2009) periods.

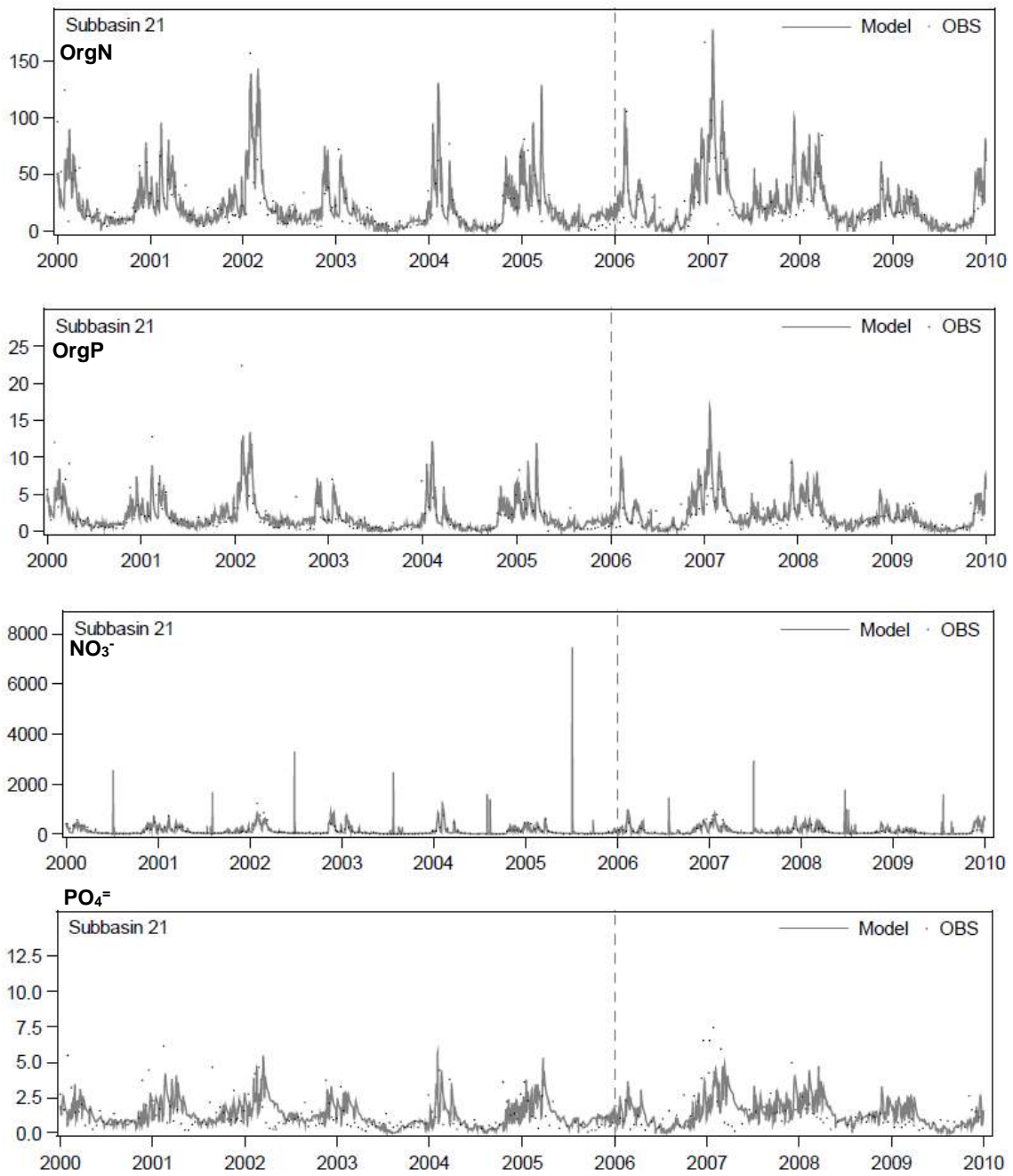


Figure 5.36 Daily nutrient loads (Kg) observed and predicted in sub-basin 21 during calibration (2000-2005) and validation (2006-2009) periods.

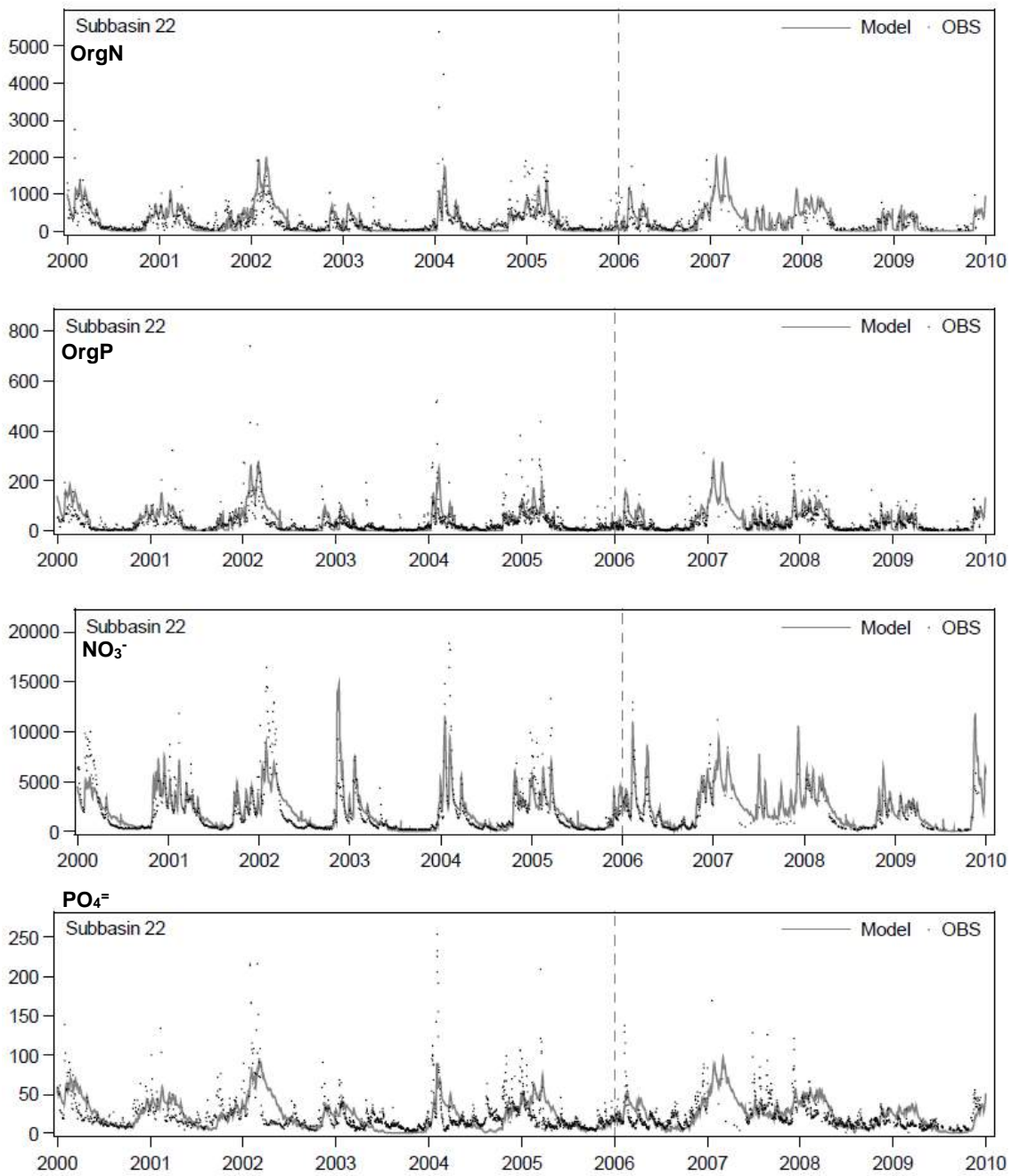


Figure 5.37 Daily nutrient loads (Kg) observed and predicted in sub-basin 22 during calibration (2000-2005) and validation (2006-2009) periods.

Table 5.25. Calibration (2000-2005) and validation (2006-2009, in brackets) performance statistics values for daily runoff and nutrients at the six monitoring points (four for nutrients) in the Odense River catchment.

	Subbasin 14	Subbasin 20	Subbasin 21	Subbasin 22
DISCHARGE				
NSE	0.73 (0.74)	0.82 (0.76)	0.71 (0.67)	0.79 (0.83)
R2	0.74 (0.74)	0.83 (0.79)	0.71 (0.68)	0.79 (0.83)
PBIAS	9.5 (2.6)	-1.9 (-9.2)	0.8 (-1.9)	-0.6 (-2.4)
NO3				
NSE	0.71 (0.40)	0.72 (-2.59)	0.69 (0.42)	0.64 (0.64)
R2	0.71 (0.66)	0.80 (0.09)	0.70 (0.49)	0.64 (0.75)
PBIAS	-1.5 (-45.6)	-3.0 (-62.9)	1.1 (-6.6)	-1.4 (-26.9)
ORG N				
NSE	0.25 (-0.78)	-1.34 (-1.41)	0.32 (0.45)	0.39 (0.16)
R2	0.53 (0.62)	0.00 (0.00)	0.45 (0.50)	0.46 (0.41)
PBIAS	1.4 (-31.5)	98.2 (98.5)	-7.8 (-17.7)	6.6 (3.3)
PO4				
NSE	0.34 (0.24)	0.51 (0.44)	-0.20 (-0.21)	0.22 (0.11)
R2	0.37 (0.42)	0.51 (0.46)	0.00 (0.04)	0.27 (0.23)
PBIAS	6.0 (-34.6)	4.3 (-7.0)	3.9 (-8.7)	6.0 (-1.4)
ORG P				
NSE	0.42 (-0.41)	-1.05 (-1.59)	0.46 (-0.02)	0.33 (0.17)
R2	0.54 (0.33)	0.01 (0.02)	0.46 (0.48)	0.41 (0.43)
PBIAS	7.4 (-20.7)	89.6 (90.5)	2.0 (-29.3)	-0.9 (-7.7)

Scenarios Simulation

CLIMATE PROJECTIONS

Table 5.28 shows the changes in the projected changes -annual averages- for RCP 4.5 and RCP 8.5 scenarios in both climate models.

Table 5.26. Projected changes (annual averages) relative to the baseline period (2011-2020) for the climate variables forced in SWAT.

Period	2025-2034				2055-2064			
	GFLD-ESM2M		IPSL-CMA-LR		GFLD-ESM2M		IPSL-CMA-LR	
	RCP 4.5	RCP 8.5	RCP 4.5	RCP 8.5	RCP 4.5	RCP 8.5	RCP 4.5	RCP 8.5
Precipitation (%)	-0.4	2.8	0.6	5.6	-1.3	-1.0	1.9	13.2
Max. temp. (°C)	1.1	0.5	0.7	0.9	1.4	1.3	1.4	2.5
Min. temp. (°C)	1.0	0.5	0.9	1.1	1.2	1.3	1.7	2.8
Rel. humidity (%)	-2.1	-0.8	-0.1	-0.3	-2.8	-0.7	-0.3	-0.8
Solar radiation (%)	5.0	1.8	-0.3	0.7	6.0	0.2	0.2	-1.7
Wind speed (%)	4.0	1.1	3.9	-0.5	2.5	1.1	2.0	3.0

Although the variation of precipitation in all the projections is small, the tendencies are different between models (Table 5.28). Precipitation is relatively stable across GFLD-ESM2M projections, slightly increasing for RCP 8.5 in the short term and slightly decreasing in the other cases. On the

contrary, for IPSL-CMA-LR model projections precipitation always increases, slightly for RCP 4.5 and more noticeable for RCP 4.5 (up to 13% in the long term). Regarding seasonality, there is not a clear pattern for the different models and pathways (shown).

For temperature (maximum and minimum), both climate models show homogeneous patterns. All the projections show an increase, lower for the first term (between 0.5 and 1.1°C) and higher from the second (between 1.2 and 2.8 °C) (Table 6.11). Especially relevant is the temperature increase expected for the model IPSL-CMA-LR in the long term, which is more than 1°C higher than in the other projections (2.5 and 2.8 °C increase for maximum and minimum temperatures, respectively). Regarding seasonality, temperature increase is higher for winter months in all the projections (not shown), up to 4.5 and 5.3°C increase in maximum and minimum temperatures in February for the IPSL-CMA-LR model in the long term.

Relative humidity experiences a slight decrease, more relevant for GFLD-ESM2M model in the short term. For this model and time horizon, solar radiation increase is higher, up to 6% in annual average, while in other projections slightly increases or decreases. Regarding wind speed, it increases in all the projections but one, and more in the short term for RCP 4.5 (up to 4%) (Table 5.28).

Effects of Isolated Land Use Change (Luc) Scenarios

In order to have an overview of the isolated effects of LUC, LUC scenarios were run with the same (observed) climate and results were obtained. Figure 5.38 shows the effect of LUC scenarios in the water balance components subject to be modified by land use change, i.e. actual evapotranspiration (AET) and water yield (Q). AET slightly decreased in HT and remained almost the same in AN and MD. Q increased in HT and AN, remaining the same in MD. Flow components suffered different alterations across LUC scenarios (Figure 5.39). Although groundwater flow always dominated, compared to PLU, its contribution increased in HT and AN, while decreased in MD, in which tile drain flow contribution increased. Surface and lateral flow contributions remained similar in all the scenarios, both in percentage and absolute contribution.

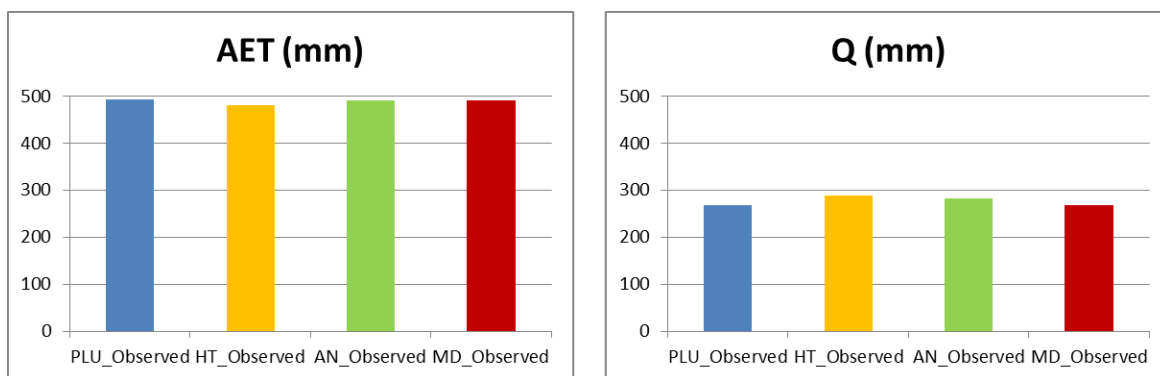
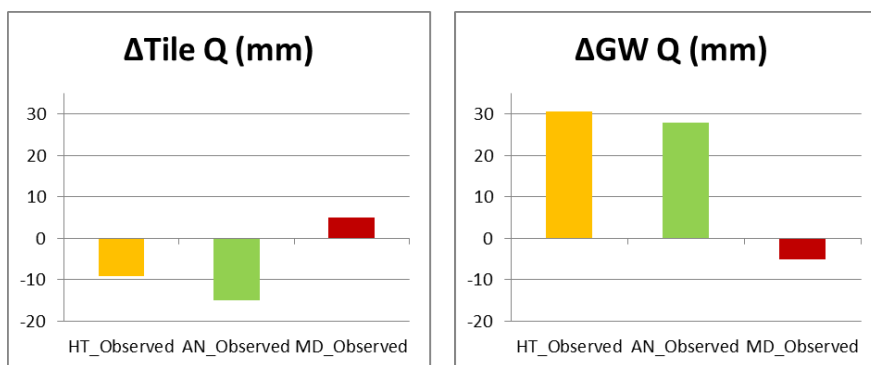


Figure 5.38 Changes expected in water balance components subject to be modified when analyzing the isolated effects of LUC scenarios under observed climate.

a)



b)

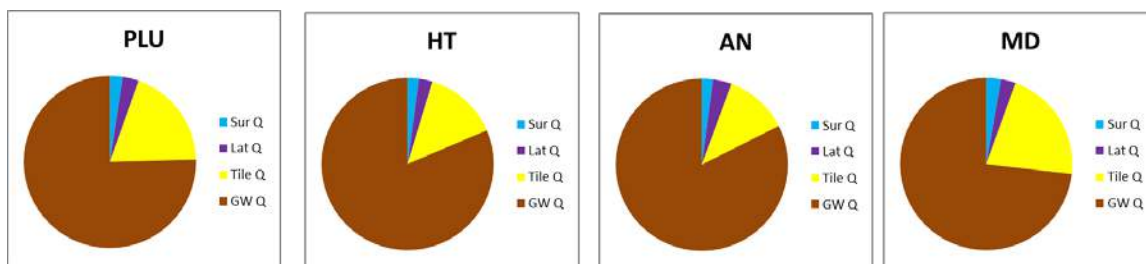


Figure 5.39 Changes in flow components when analyzing the isolated effects of LUC scenarios under observed climate. a) Absolute changes in tile drain flow and groundwater flow with respect to baseline; b) % contribution of the different flow components in all the scenarios.

Fertilization changes described in Table 5.29 yielded the N and P changes in fertilizer depicted in Figure 5.40.

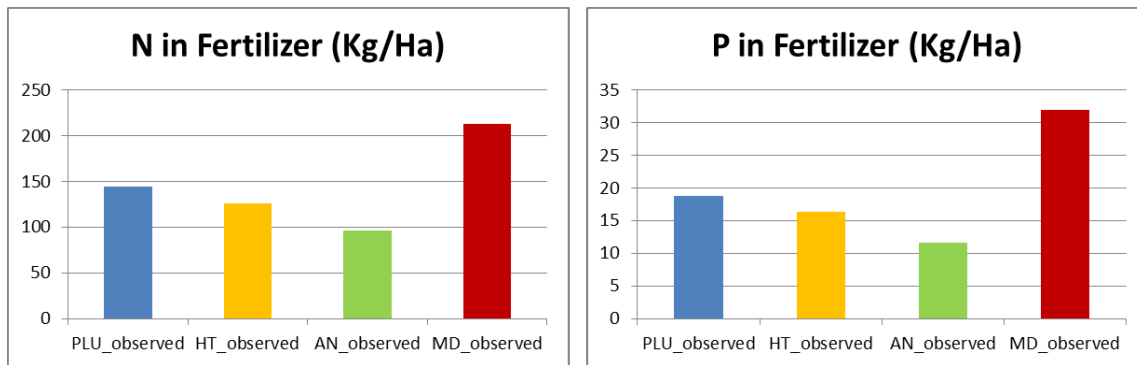


Figure 5.40 Changes in N and P applied in fertilizer for the different scenarios.

Regarding nutrient loads, organic N and P showed a slightly higher load in HT than in the other scenarios. NO₃ decreased in HT and even more in AN while increased in MD. MinP load showed an increase in HT and AN, slightly higher in the first (Figure 5.41).

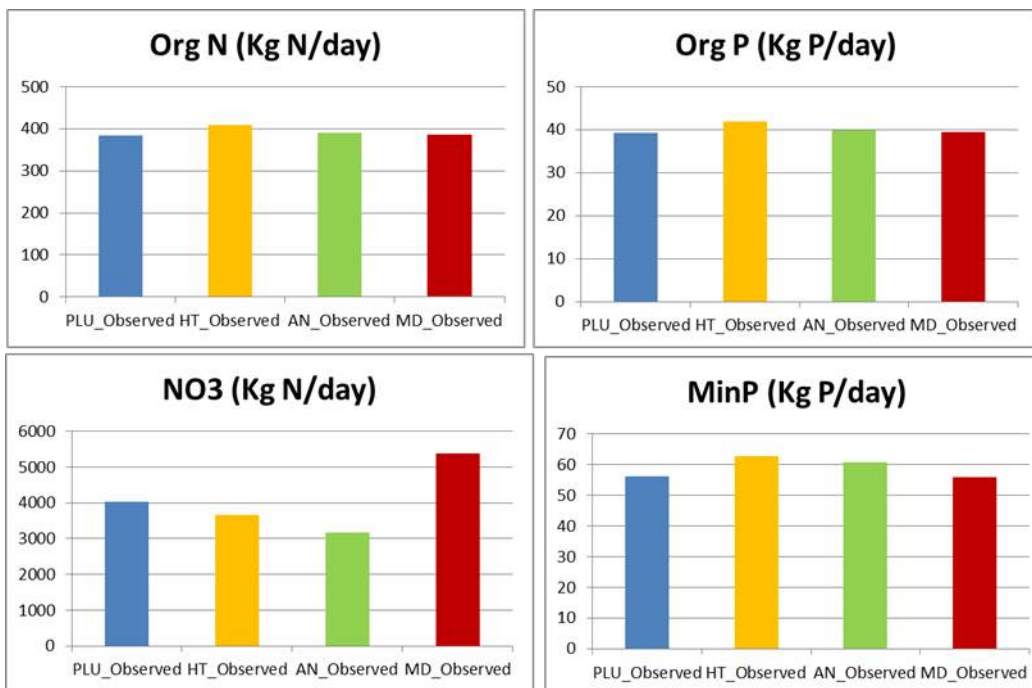


Figure 5.41 Changes expected in nutrient loads when analyzing the solely effects of LUC scenarios under observed climate.

Simulation of Mars Storylines

Since we are simulation scenarios that depart from different baselines (projected climate with different RCPs (8.5 for HT and MD, 4.5 for AN) and two different climate models), results show changes in each scenario with respect to its baseline (Table 5.24b) and not total values, in order to avoid confusion to the reader and to facilitate the subsequent discussion.

Regarding water balance, AET increases in all the scenarios. However, flow decreases in all the scenarios for the GFLD-ESM2M model (except HT in the short term) and increases in HT and MD storylines for the IPSL-CMA-LR model, while in AN remains the same. These changes are showed in Figure 5.42, together with the changes in precipitation to facilitate further discussion.

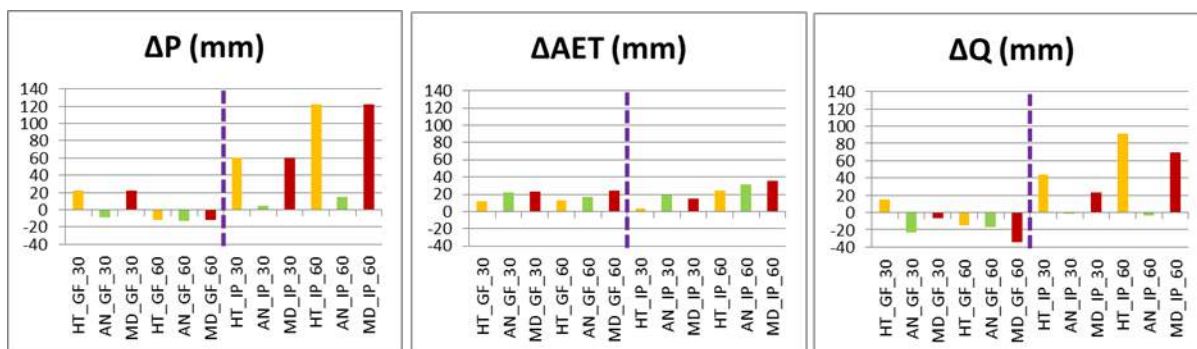


Figure 5.42 Changes predicted in the water balance components for the different scenarios.

Table 5.29 shows the percentage contributions of flow components across the different scenarios, which remained very similar for both climate models. The effect of land use changes over percentage contributions described before was again observed for both climate models and for all time horizons, with MD showing lower groundwater and higher tile drainage contributions than HT and AN. Figure 5.43 shows the absolute changes from baseline expected in tile drainage flow and groundwater flow. Surface and lateral flow did not showed significant absolute changes (maximum absolute variations from baseline were 1.8 mm and 1.6 mm, respectively).

Table 5.27. Contribution (%) of the different flow components to total discharge across scenarios.

	PLU_GF_45	PLU_GF_85	HT_GF_30	AN_GF_30	MD_GF_30	HT_GF_60	AN_GF_60	MD_GF_60
<i>Sur Q</i>	1.8	1.6	1.6	1.5	1.9	1.7	1.5	2.0
<i>Lat Q</i>	3.1	3.3	2.8	4.2	3.1	3.1	4.1	3.4
<i>Tile Q</i>	18.8	19.3	14.1	12.2	21.9	14.4	11.8	22.4
<i>GW Q</i>	76.3	75.9	81.4	82.0	73.0	80.8	82.6	72.2
	PLU_IP_45	PLU_IP_85	HT_IP_30	AN_IP_30	MD_IP_30	HT_IP_60	AN_IP_60	MD_IP_60
<i>Sur Q</i>	3.2	3.2	1.9	2.0	2.3	1.8	2.3	2.1
<i>Lat Q</i>	3.7	4.0	3.2	4.5	3.5	2.9	4.6	3.2
<i>Tile Q</i>	20.1	20.2	15.0	12.7	23.4	14.2	12.6	21.9
<i>GW Q</i>	73.0	72.6	79.9	80.7	70.8	81.0	80.4	72.8

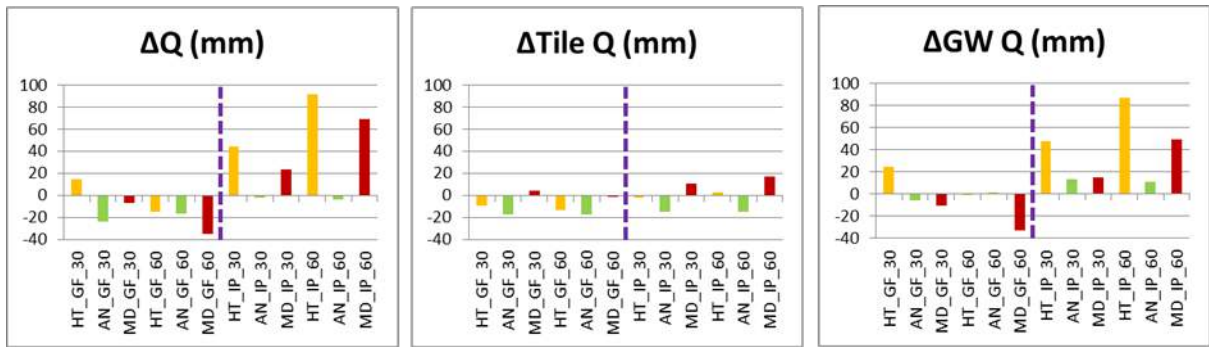


Figure 5.43 Absolute changes from baseline predicted in tile drainage flow and groundwater flow for the different scenarios. Total flow results are showed again to facilitate visualization.

Figure 5.44 depicts the expected changes in nutrient loads. While organic nutrients follow a similar trend, variations in predicted loads are different for the two mineral species modelled.

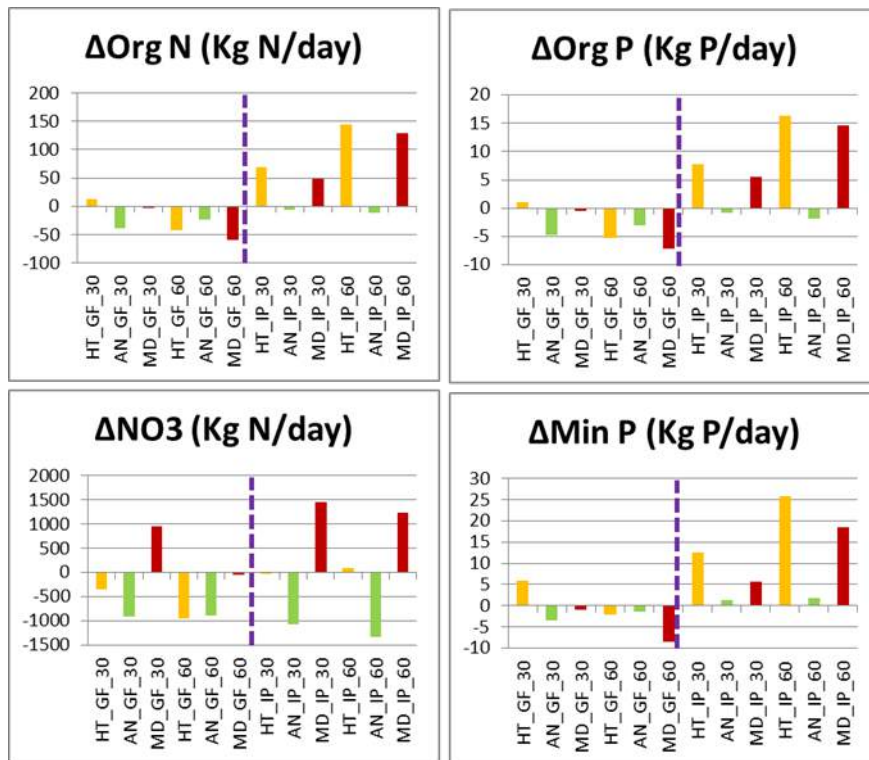


Figure 5.45 Changes predicted in nutrient loads for the different scenarios.

5.3.2.1.2 Discussion

Model calibration and validation

The observed discharges and their tendency in time were well reproduced in all the stations during the calibration period (Figure 5.33). Statistically, the model showed a better performance than in the previous calibration by Thodsen et al. (2015) (Table 5.27), which proves the convenience of including more parameters at a sub-basin level even though it slows the calibration process. Subbasins 20 and 22 showed a better performance, while Subbasin 4 performance was slightly worse. Nevertheless, it can be considered a very good daily calibration overall, compared to the performance statistics for daily data in the literature (e.g. Gassman, Reyes, Green, & Arnold, 2007; Moriasi et al., 2007). Visual inspection of the model performance during the validation period also displayed a model capable of encompassing the observed heterogeneity in magnitudes (Figure 5.33) and the statistical performances were also very good (Table 5.27), sometimes better than during calibration. This demonstrates the ability of the model to reproduce the discharge in the Odense catchment, which then serves as a good starting point when initiating the calibration of nutrient fractions.

Dynamics of the different nutrient fractions were adequately represented by the model in most of the cases (Figure 5.34-5.37). Statistical performance also reflects a good calibration (Table 5.27) (Moriasi et al., 2007), especially considering that our model was calibrated with daily values, which usually show lower ratings (Gassman et al., 2007), and that it was a spatial (4 stations) and multi-variable (4 nutrients species) calibration, which makes much more difficult to obtain satisfactory results for all the variables. Nevertheless, unsatisfactory results were obtained for organic N and P in sub-basin 20 (Figure 5.35). It is the smallest sub-basin among those monitored and located in the border of the catchment (Figure 5.30). Discharge might be too low for SWAT to produce a realistic organic nutrients load (which in a low-land catchment may be largely a result of riverbank erosion or collapses). NSE and R^2 values were also unsatisfactory for PO₄ in sub-basin 21. In this case magnitudes are right, as the good PBIAS denotes, but not the timing of the peaks. NO₃ calibration in sub-basins 20 and 21 showed some outlying values much higher than the observed dynamics, but they are rather exceptional.

During the validation period, the model also showed a good reproduction of the observed nutrient loads in the majority of the cases, keeping the abovementioned imprecisions (Figures 5.34-5.37). Statistical metrics performance decreased during validation (lower R^2 and NSE, higher absolute

PBIAS), which is expected in this kind of models (Gassman et al., 2007). The lowest performance of NSE and PBIAS in certain sub-basins was especially noticeable (Table 5.27). Nevertheless, the majority of the values are suitable for a multi-site and multi-variable daily calibration. With the exception of organic fractions in sub-basin 20, absolute PBIAS is always lower than 70, in most cases lower than 40 and many times lower than 25, which would indicate a “satisfactory”, “good” or “very good” performance for a monthly calibration (Moriassi et al., 2007). These results guarantee the ability of the model to reproduce nutrient loads in the Odense catchment, especially the overall average loads as the good PBIAS values reveal.

A robust and realistic catchment model for hydrology and nutrient loads for the Odense River basin is ready for further work such as scenarios simulation and empirical models coupling.

Scenario simulation

EFFECTS OF SOLELY LUC SCENARIOS

SWAT modelled a slight decrease in AET in HT scenario (13.3 mm) due to a lower ET of willow (Figure 5.38) compared to the other crops that it is replacing (Table 5.21 and Figure 5.32). Conversely, HT showed an increase of Q up to 20.9 mm, so it was additionally favoured by the land use change. Despite not decreasing AET, AN also favoured a small increase in Q (14.2 mm), while in MD remained the same than in the present land use. The flow increase in HT and AN was ruled by an increase in groundwater flow (Figure 5.39), which might be a response to higher tree coverage (willow in HT, forest in AN, Figure 5.32) that facilitates infiltration. Despite the global increase, tile drainage flow decreased in these scenarios (Figure 5.39) due to the surface reduction of drained agriculture (Figure 5.32). The opposite trend, but less pronounced, was observed in MD scenario (Figure 5.39), where current farmed surface increases (Figure 5.32).

Regarding nutrients, it seems that fertilization was the main source of NO₃ in the basin, since NO₃ load changes followed exactly the same pattern as the variation in fertilization within scenarios (Figures 5.40 and 5.41). However, the load in the other three fractions did not showed the same dynamics. Mineral P load showed the same variation as groundwater flow, increasing in HT and AN and slightly decreasing in MD (Figures 5.39 and 5.41), which may indicate that groundwater is the main source of this fraction in the Odense catchment. Changes in organic nutrient loads were minimal, showing basically a slight increase in HT (Figure 5.41) which did not respond to the variations in fertilization. An explanation could be found in a higher in-stream

sediment change in HT (1.45 T/ha) than in the other scenarios (1.38, 1.40 and 1.41 T/ha in PLU, AN and MD respectively), which can be also related with the higher total flow.

To sum up, isolated land use change effects on nutrient loads were more noticeable in NO₃ due to the changes applied in fertilization, while in the other three fractions the changes in loads were less pronounced and seemed to be related with changes in flow and in-stream sediment change.

Simulations of MARS storylines

AET increased in all the scenarios (Figure 5.42) following the pattern of temperature change (Table 5.27), but increased less in HT due to the land use change effect showed in Figure 5.38. The AET increase was the main driver of the Q increase in those scenarios where precipitation was slightly increasing or decreasing (Figure 5.42). Despite the fact, precipitation increase was higher in certain scenarios (Figure 5.42), especially in those using the IPSL-CMA-LR model projections and the 8.5 RCP (HT and MD), showing a final increase on discharge (Figure 5.42). The additional effect of HT and AN yielding a higher Q was again observed in those scenarios where Q was predicted to decrease or slightly increase considering the P-AET balance. However, in those scenarios with high P increase the opposite effect was observed and the increase of Q was not as high as the P-AET difference (Figure 5.42).

Groundwater remained as the dominant flow component. The changes in relative contributions of groundwater and tile drainage flow observed for solely LUC remained in the storylines (Table 5.41), and ultimately affected the absolute variations. Thus, in those scenarios for HT and AN where total Q decreased, it was tile drainage flow the main component decreasing, while groundwater flow decreased less or even increased, despite being the dominant contributor. Conversely, in those HT scenarios where total flow increased, only groundwater flow did it, while tile drainage flow remained similar or even decreased (Figure 5.43). Again, the opposite effect was observed in MD scenarios: when total flow decreased, only groundwater flow decreased while tile drainage flow remained similar; when total flow increased the effect was not that obvious and both increased (groundwater flow was still the main component in MD scenarios despite its lower contribution compared with HT and AN).

It must be noticed that in the previous analysis of solely LUC scenarios, total flow variation was just due to LUC effects since climatic inputs were the same in all the scenarios, while in the

storylines climate change is also taken into account. Thus, the results showed that LUC was also able to modulate the total flow variations derived from a different climate input.

The choice of climate model (especially due to different precipitation inputs) showed the strongest influence on water balance and total Q. While the scenarios run with the climate projections from the GFLD-ESM2M model showed a general decrease of discharge in the Odense River basin, the scenarios using IPSL-CMA-LR showed an increase for HT and MD, while Q in AN remained the same. This difference could not be attributed to the effect of land use, but it was a result of using a different RCP in the climate projections (4.5 in AN, 8.5 in HT and MD). Nevertheless, it has been discussed how discharge in every scenario was ultimately modulated by LUC, so it was the combination of all these different stressors which yielded final values of Q and its component contribution subject to have a subsequent effect on nutrient loads.

The analysis of nutrient loads results becomes more complex when climate change effects and land use changes are combined. Regarding organic nutrients, both N and P followed the same pattern (Figure 5.44), which was very similar to the variation in total flow (Figures 5.42 and 5.43) and thus can be related to variations on in-stream sediment change, which also followed the pattern of total flow (data not shown). Fertilization in the future storylines remained as showed in figure 5.39 when the effects of solely LUC were analyzed. Combining them with climate change, results showed a NO₃ load which was a combination of effects of both stressors (Figure 5.44). As an example, in the MD_GF_60 scenario, despite the fertilization increase, NO₃ load remained as in baseline due to the flow decrease. On the contrary, in HT_IP_60 scenario, despite the fertilization decrease, NO₃ load slightly increased because this scenario showed the highest Q rise. Regarding MinP, its variation within scenarios showed again a very similar pattern to those in groundwater flow (Figures 5.43 and 5.44), which confirmed that this component might be the main source of this nutrient fraction in the Odense catchment.

These analyses showed that river discharge (and its components) was the main driver for organic nutrients and MinP loads, and discharge variations were mostly ruled by the different climate inputs observed. Among those, the choice of climate model showed big differences on final discharge even for the same storylines, being the main factor conditioning the final load of these fractions. Thus, while in a hypothetical future under the GFLD-ESM2M model projections these loads are more likely to decrease, under the IPSL-CMA-LR model projections are expected to increase in HT and MD storylines, remaining stable in AN storyline. Regarding NO₃, both LUC

(because of differential fertilization) and river discharge were seen as drivers of its load. Fertilization showed a strong influence and NO₃ load decreased in most of the scenarios with lower fertilizers input (HT and AN), increasing in those with higher inputs (MD). However, there are exemptions: although fertilization changes are the same across scenarios irrespective to climate model and RCP, different climate inputs ultimately modulated the NO₃ loads (e.g. MD_GF_60 and HT_IP_60 scenarios). Thus, the choice of climate model becomes also very relevant for final NO₃ load results.

It must be noticed that organic N contribution to total N load is much lower than NO₃ contribution, while P contribution is similar in both organic and mineral fractions (Figure 5.41). Thus, for the N case, especial attention must be placed on the mineral fraction regarding its ultimate effects over aquatic ecosystems.

5.3.2.1.3 Conclusions of the process-based modelling of the Odense Basin

The three MARS storylines were downscaled to the Danish Odense River basin focusing on changes in land use and agricultural management. The future scenarios involved adaptation to a warmer climate by changes in crops, fertilization levels and timing of field operations.

Isolated changes in land use affected total catchment runoff, albeit only to a small degree. The groundwater flow component increased on behalf of the tile drain flow component in the high-tech agriculture (storyline 1) and agriculture for nature (storyline 2) scenarios and vice versa in the market driven agriculture (storyline 3) scenario. Land use change affected losses of organic nutrients and of inorganic P only to a small degree, however the increased N fertilization in the market driven agriculture scenario resulted in a considerable increase in the loss of inorganic N.

When introducing climate change on top of land use changes it becomes apparent that the choice of climate model is crucial: the GFLD-ESM2M model decreases catchment runoff in all storylines (except in storyline 1 in the short term) whereas the IPSL-CMA-LR model increases runoff in storylines 1 and 3 and remains the same in storyline 2.

The analyses of combined land use change and climate change showed that river discharge (and its components) was the main driver for organic nutrients and inorganic P loads, and discharge variations are mostly ruled by the different climate inputs observed. Regarding inorganic N both

land use change (via inputs of fertilizer) and river discharge were seen as drivers of the load. Fertilization showed a strong influence and inorganic N load decreased in most of the scenarios with lower fertilizers input (storyline 1 and 2), and increasing in those with higher inputs (storyline 3).

Our analysis revealed that the choice of climate model has a strong influence on nutrient load results. From the two climate models selected by the MARS work team, IPSL-CMA-LR was seen to represent better the future behavior of climate in Denmark (Ref: MARS internal document: Choice of the MARS climatic model for the case studies), so scenario simulation results using this climate model might be prioritized when using them for decision making or to link further models.

5.3.3 Development of empirical models for ecological indicators in Danish streams

A range of both national Danish indices and MARS benchmark indicators of ecological quality of streams have been calculated. Subsequently it was tested if performance of these indices could be explained by abiotic variables. The list of tested indicators comprises: DFFV (the Danish fish index for the WFD); DVPI (the Danish macrophyte index for the WFD), DVFI (the Danish macroinvertebrate index for the WFD); Bind12 (average score per taxon, macroinvertebrates); Bind13 (abundance ratios of functional feeding groups, macroinvertebrates); Bind14 (relative abundance of invasive alien species, macroinvertebrates); Bind15 (total fish abundance).

In our work we compare the abiotic-biotic equations developed following the MARS approach to models previously developed using the EUREKA software and we test the EUREKA developed models using the recommended MARS approach. Based on a national Danish dataset (see Introduction, above) we end up with four statistically significant models for respectively DFFV, DVPI, DVFI and Bind12. Development and test of the abiotic-biotic models is described below.

5.3.3.1.1 Data description and pre-selection of key stressors

Input data used for the analysis is from a national Danish data set and comprises 263 variable and 131 observations (stored locally in “Stream_chem_traits_2004_2011_all_data.xlsx”). All data were imported and processed in the program R.

First, the stressors that have a correlation (R) higher than 0.35 or lower than -0.35 with each ecological indicator were pre-selected for the variable ranking. The result of the preselection are listed below (Table 5.30). For other MARS ecological indicators, e.g. BInd13 and BInd15, no variable fit the preselection criteria.

Table 5.28. Variables that have high correlation (R2) with each ecological indicator.

DFVQ_EQR		DVPI_EQR		DVFI_EQR		BInd12	
Variables	R	Variables	R	Variables	R	Variables	R
NO23_min	0.56	drain_tot	-0.51	sin	0.55	sin	0.56
BI5_max	-0.47	drain_2m	-0.49	q90	0.45	TP_mean	-0.46
drain_tot	-0.45	pH_mean	-0.48	TP_std	-0.44	q90	0.45
q90	0.45	dur3	-0.46	TP_mean	-0.43	DRP_std	-0.42
TN_min	0.44	pH_max	-0.42	DRP_std	-0.42	drain_2m	-0.41
bfi	0.43	frst_2m	-0.39	bfi	0.40	TP_std	-0.40
Temp_std	-0.41	q90	0.38	drain_2m	-0.38	BI5_mean	-0.39
BI5_std	-0.41	Temp_std	-0.37	dur3	-0.38	Q_min	0.39
dur3	-0.40	pH_min	-0.37	BI5_mean	-0.37	drain_tot	-0.39
Temp_min	0.37			wet_nat_2m	0.36	DRP_max	-0.38
sin	0.36			Temp_std	-0.36	wet_nat_2m	0.38
wet_nat_2m	0.36			DRP_max	-0.35	bfi	0.38
DRP_max	0.36			agri_2m	-0.35	agri_2m	-0.38
BI5_mean	-0.35			drain_tot	-0.35	imp_tot	-0.37
						Q_mean	0.36
						Width	0.35
						NO23_std	-0.35

5.3.3.1.2 Variable ranking with Boosted Regression Trees (BRT)

Following the MARS WP4 recommendation, we followed the procedure:

BRT ranking with all preselected variables

BRT ranking results are quite different from the correlation matrix ranking, especially for DVFI and BInd12, sin, q90 and TP_mean dropped from the top ranking list in Table 5.31 (marked in green).

Table 5.29. Ranking and relative influence of the pre-selected variables for each indicator calculated by the BRT

DFVQ_EQR		DVPI_EQR		DVFI_EQR		BInd12	
var	rel.inf	var	rel.inf	var	rel.inf	var	rel.inf
bfi	28.982	drain_2m	21.730	drain_2m	20.625	drain_2m	17.650
NO23_min	26.650	pH_max	19.438	wet_nat_2m	18.169	TP_std	17.462
BI5_mean	12.026	pH_mean	17.497	TP_std	10.306	agri_2m	8.441
dur3	10.217	dur3	11.068	sin	9.390	TP_mean	8.341
BI5_std	6.626	Temp_std	10.500	TP_mean	6.856	Q_mean	7.996
drain_tot	5.664	q90	8.972	bfi	6.088	wet_nat_2m	6.689
wet_nat_2m	4.627	pH_min	4.169	BI5_mean	5.036	BI5_mean	5.309
Temp_min	2.004	frst_2m	3.767	DRP_max	4.852	drain_tot	3.890
DRP_max	1.138	drain_tot	2.859	q90	4.567	bfi	3.588
Temp_std	1.073			Temp_std	4.418	sin	3.498
BI5_max	0.477			drain_tot	3.899	q90	3.236
TN_min	0.255			agri_2m	3.397	imp_tot	2.994
q90	0.229			dur3	1.355	Width	2.683
sin	0.032			DRP_std	1.043	Q_min	2.624
						NO23_std	2.291
						DRP_max	2.075
						DRP_std	1.235

The predictions from the full BRT model were not much better than the GLM’s originally developed using EUREKA (Figure 5.52). The number of observations (n) were much less than in Figure 5.52, because there were more variables and hence more missing values.

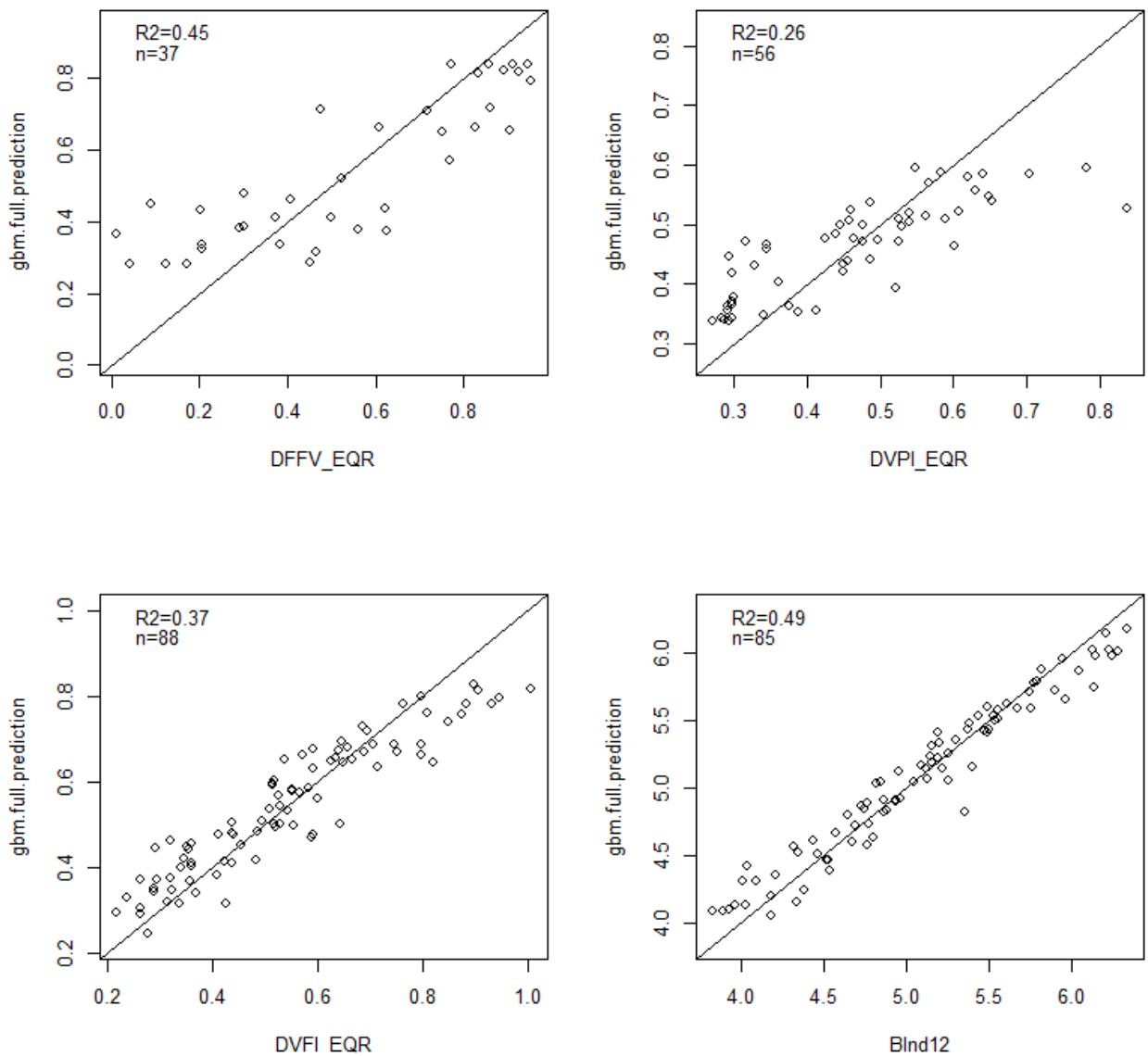


Figure 5.46 Predictions of BRT models with all pre-selected variables for each ecological indicator.

BRT Simplification to reduce the number of variables

We can choose how many variables we would like to drop for further analysis, based on the result of BRT simplification. For the fish index DFFV_EQR, the number of observations was not large enough ($n < 50$) for BRT to simplify the analysis and therefore no results were presented.

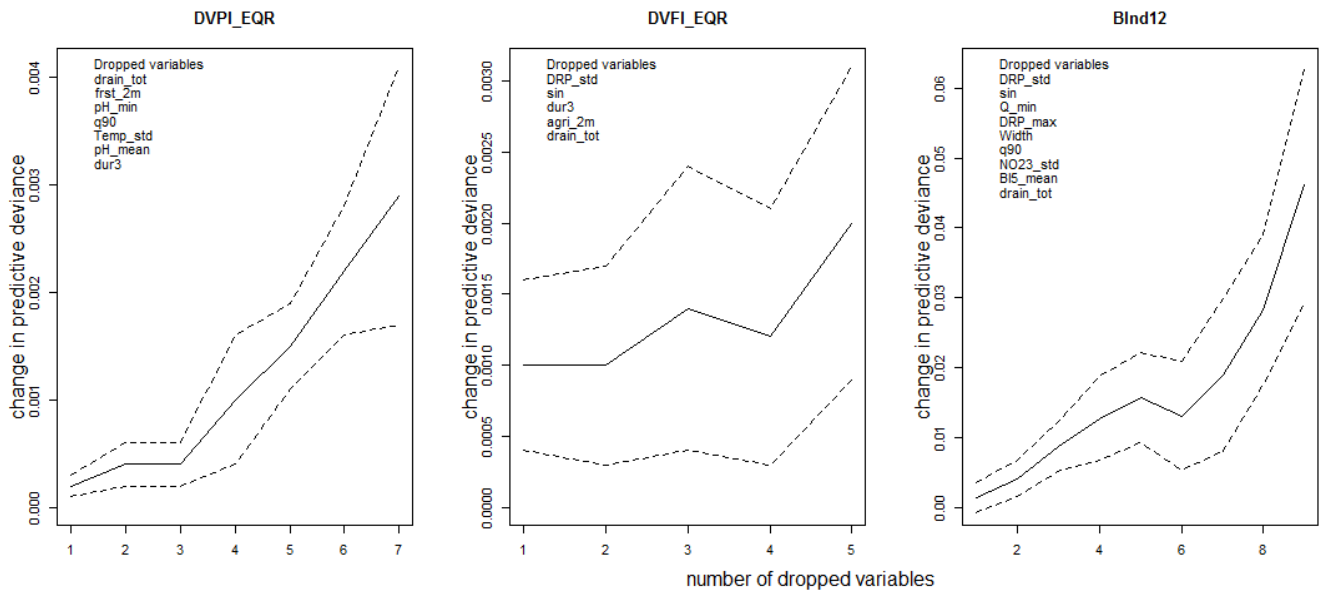


Figure 5.47 Chang in predictive deviance by dropping variables

BRT interaction

The following figures indicate how each variable interacts with the prediction of the ecological indicator. This may aid in the understanding of the relationships between variables and indicators.

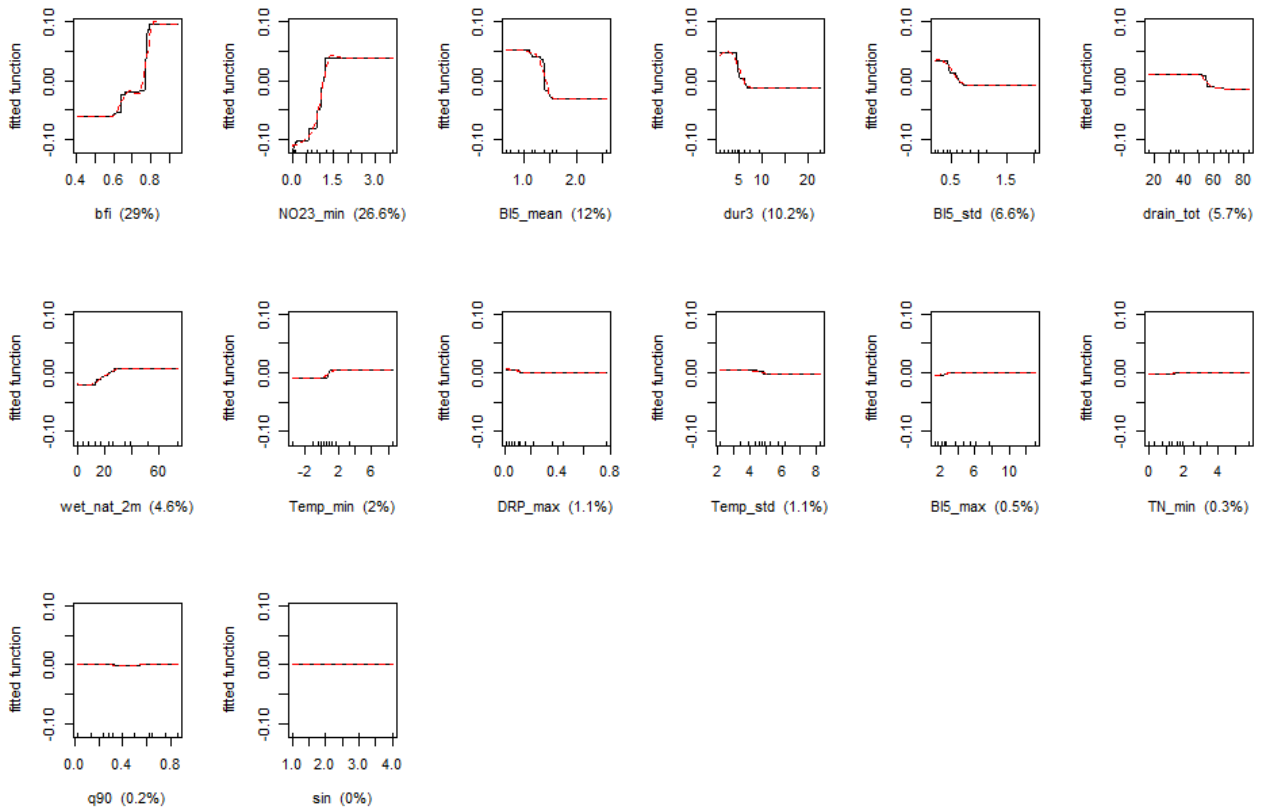


Figure 5.48 Partial interaction of all the variables against the fish index `DFFV_EQR`.

For the fish index `DFFV_EQR`, unfortunately the observations are too few for the simplification procedure. Yet we can see from the figures that except the first three variables, the rest of the variables do not change the model output much. Therefore, we might only include the first three variables for the general linear analysis.

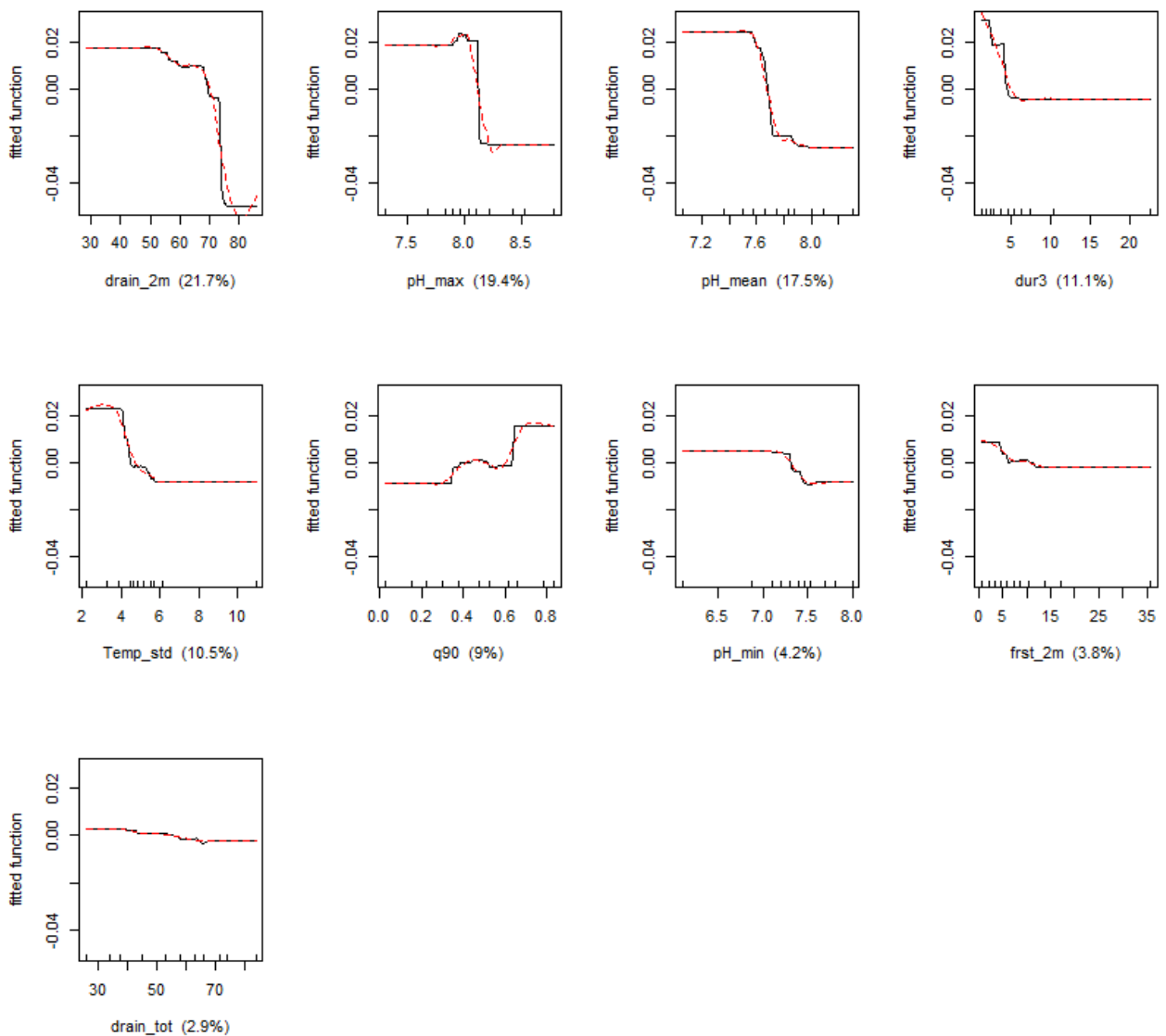


Figure 5.49 Partial interaction of all variables in the plant index DVPI_EQR

For the plant index DVPI_EQR, except the least influential variable “drain_tot” in Table 5.31, the other variables change the model output quite a bit. Though simplified results indicated excluding variables will worsen the model output (Figure 5.46), BRT models with fewer variables provide better correlation with DVPI observations (Table 5.44). This might be due to the random effect of BRT method and each time a new model is made, results are different. Two pH variables ranked high in the results, which closely co-relate to each other.

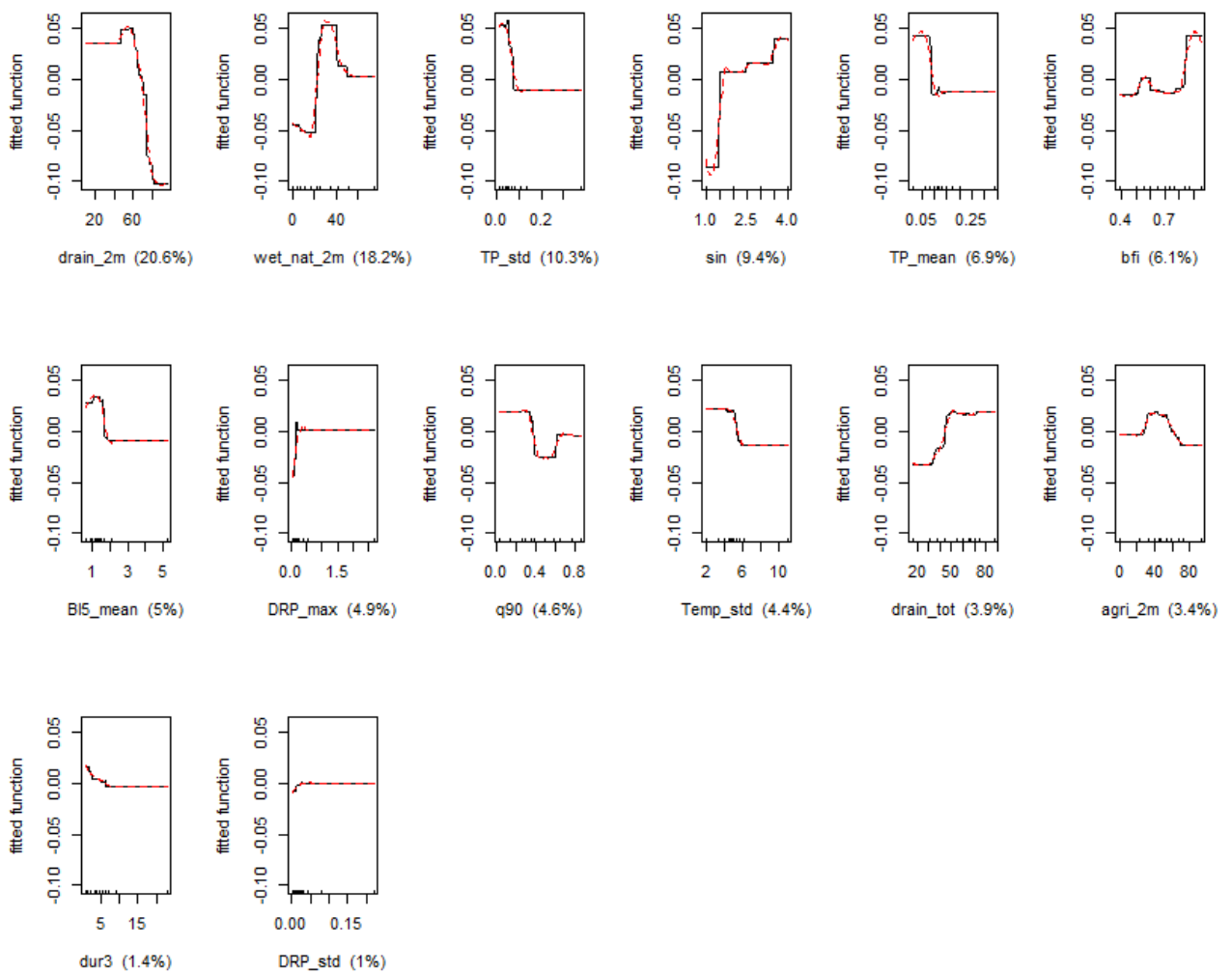


Figure 5.50 Partial interaction of all variables in the macro-invertebrates index DVFI_EQR

Results for the macro invertebrate index DVFI_EQR are quite similar to the MARS indicator Bind12 (Average score per taxon ASPT), except the most influential variable for DVFI is TP_std, whereas for ASPT it is drain_2m. Effect of reducing variable numbers on DVFI prediction is linear, less variable numbers, worse the correlation (Table 5.32), though the drop of the least influential variable DRP_std did not change the prediction much (Figure 5.46 and Table 5.32). There are also two TP variables in high rank, mean and std values not necessarily co-relate with each other.

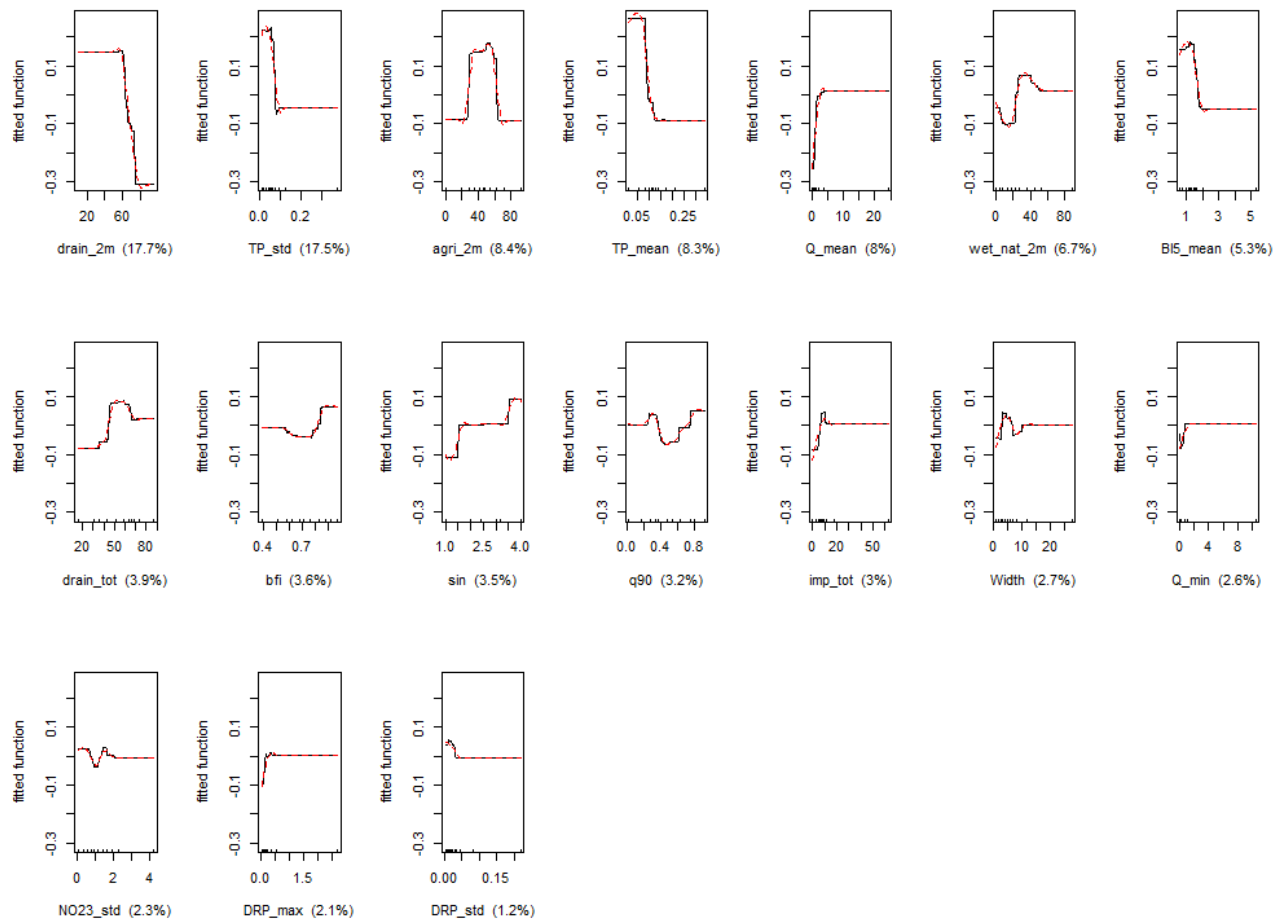


Figure 5.51 Partial interactions of all variables in the MARS index BInd12 (Average score per taxon ASPT)

The BRT model without the least influential variable DRP_std resulted quite well (Table 5.32), even though the simplification results indicated that the drop of DP_std might worsen the model output (Figure 5.46).

5.3.3.1.3 General linear model (GLM)

Exploring data

1. Identify the percentage of zeros in response variable (indicators)

There are no zeros in any of the selected response variable

2. Categorical covariates – check if there are enough of observations per level of a categorical covariate

None of the indicators was categorical, therefore it's fine.

3. Histograms: check the normality and distribution of the indicators.

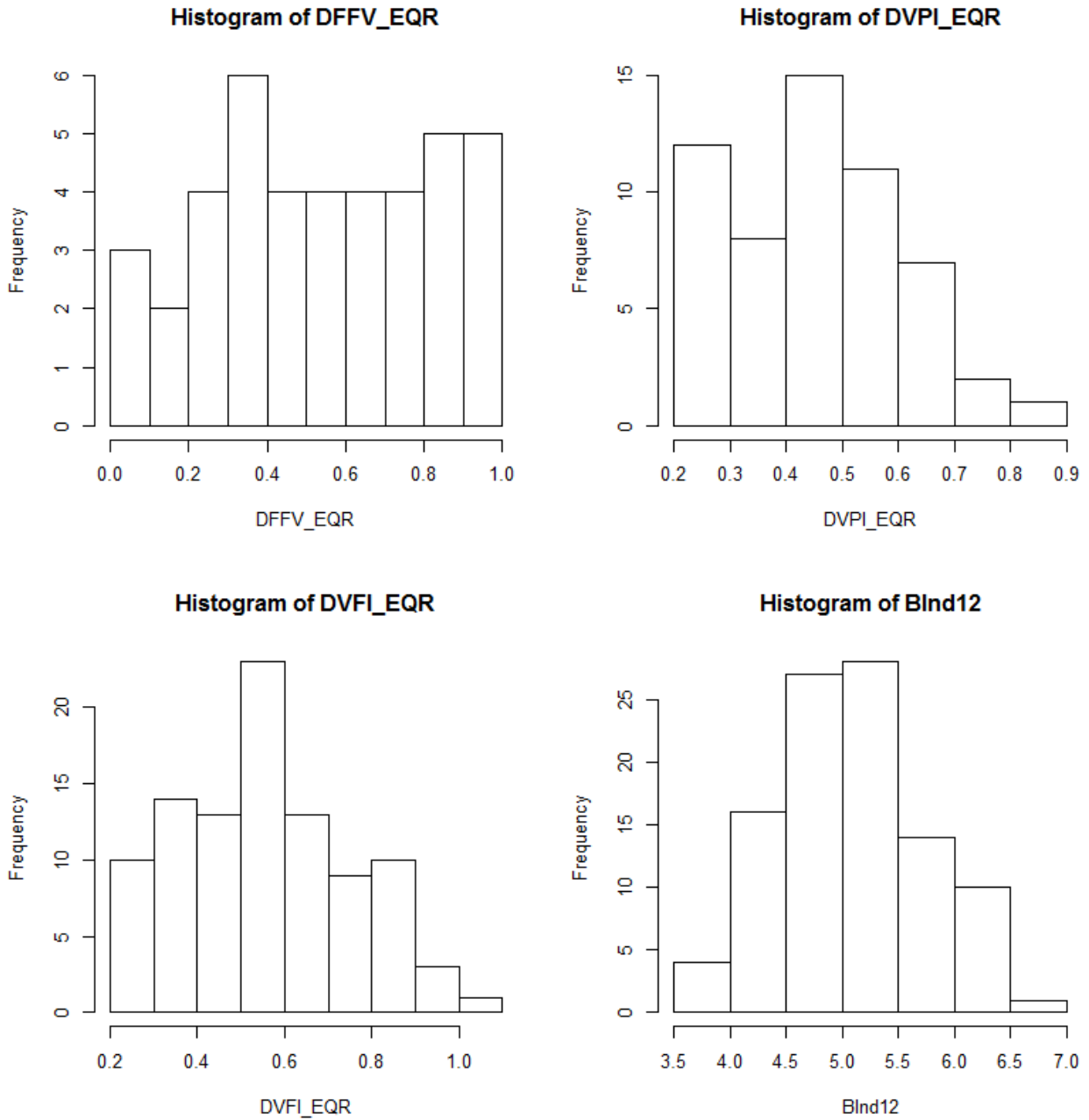


Figure 5.52 Histograms of the response variables (ecological indicators)

4. Check collinearity (strong correlation between two or more predictor variables) with VIF

The VIF function calculate the correlations of predictor variables and when the VIF values are higher than 10, the model has a collinearity problem.

Some of the variables have VIF values higher than 8 marked in yellow and should be excluded for GLM analysis.

Table 5.30. maximum correlation of the predictor variables and the correlation coefficient for each response variable (Indicator)

DFFV_EQR		DVPI_EQR		DVFI_EQR		BInd12	
Variables	VIF	Variables	VIF	Variables	VIF	Variables	VIF
Sin	1.79	q90	4.30	sin	1.26	Width	5.95
q90	6.23	dur3	2.25	q90	6.12	sin	1.48
dur3	4.39	frst_2m	1.32	dur3	2.27	q90	5.16
Bfi	2.76	drain_2m	3.91	bfi	2.76	bfi	3.06
wet_nat_2m	4.00	drain_tot	7.31	agri_2m	2.29	agri_2m	2.68
drain_tot	4.10	pH_mean	8.75	wet_nat_2m	3.98	wet_nat_2m	3.97
BI5_mean	5.43	pH_max	4.37	drain_2m	6.21	imp_tot	1.87
BI5_max	5.03	pH_min	3.51	drain_tot	9.90	drain_2m	6.57
DRP_max	3.54	Temp_std	1.34	BI5_mean	2.27	drain_tot	10.58
Temp_min	2.40			TP_mean	5.69	Q_mean	24.75
NO23_min	10.69			DRP_max	12.02	BI5_mean	3.00
TN_min	8.04			Temp_std	1.63	TP_mean	6.41
Temp_std	3.52			DRP_std	15.41	DRP_max	12.83
BI5_std	10.75			TP_std	3.66	Q_min	18.87
						NO23_std	2.41
						DRP_std	15.68
						TP_std	4.83

GLM analysis

GLMS DEVELOPED FROM PREVIOUS EUREKA ANALYSIS.

Table 5.31. Equations estimated by EUREKA and the interactions among variables

	Estimate	Std. Error	t value	Pr(> t)	Significant level
DFFV_EQR = 0.199 - 0.020·q90 + 0.562·BFI - 0.041·BI5_max + 0.018·Fre25					
<i>R</i> ² = 0.35					
q90:bfi	-6.669	6.555	-1.017	0.314	
q90:BI5_max	-0.084	1.202	-0.070	0.945	
bfi:BI5_max	-1.088	0.721	-1.508	0.139	
q90:fre25	-0.534	0.607	-0.879	0.384	
bfi:fre25	-0.498	0.454	-1.097	0.279	

	Estimate	Std. Error	t value	Pr(> t)	Significant level
BI5_max:fre25	-0.076	0.067	-1.131	0.264	
q90:bfi:BI5_max	0.309	1.525	0.203	0.840	
q90:bfi:fre25	0.562	0.789	0.713	0.480	
q90:BI5_max:fre25	0.044	0.144	0.302	0.764	
bfi:BI5_max:fre25	0.061	0.101	0.607	0.547	
q90:bfi:BI5_max:fre25	-0.018	0.195	-0.090	0.929	
DVPI_EQR = 0.634 - 0.011·Dur3 - 0.024·Temp_Std - 0.013·DRP_mean + 0.020·Fre25 - 0.026·Fre75					
$R^2 = 0.41$					
dur3:Temp_std	-0.166	0.087	-1.900	0.064	.
dur3:DRP_mean	-6.094	6.164	-0.989	0.328	
Temp_std:DRP_mean	-14.226	10.615	-1.340	0.187	
dur3:fre25	-0.107	0.050	-2.162	0.036	*
Temp_std:fre25	-0.131	0.062	-2.096	0.042	*
DRP_mean:fre25	-10.642	5.278	-2.016	0.050	*
dur3:fre75	-0.122	0.082	-1.499	0.141	
Temp_std:fre75	-0.162	0.082	-1.988	0.053	.
DRP_mean:fre75	-4.564	6.615	-0.690	0.494	
fre25:fre75	-0.074	0.029	-2.533	0.015	*
dur3:Temp_std:DRP_mean	1.826	1.242	1.471	0.148	
dur3:Temp_std:fre25	0.023	0.011	1.993	0.053	.
dur3:DRP_mean:fre25	1.281	0.921	1.391	0.171	
Temp_std:DRP_mean:fre25	2.564	1.224	2.095	0.042	*
dur3:Temp_std:fre75	0.033	0.019	1.695	0.097	.
dur3:DRP_mean:fre75	0.963	1.178	0.818	0.418	
Temp_std:DRP_mean:fre75	1.807	1.450	1.246	0.219	
dur3:fre25:fre75	0.016	0.008	1.945	0.058	.
Temp_std:fre25:fre75	0.019	0.008	2.549	0.014	*
DRP_mean:fre25:fre75	1.143	0.594	1.926	0.061	.
DVFI_EQR = 0.40 + 0.085·Sin + 0.144·q90 - 0.920·TP_mean					
$R^2 = 0.38$					
sin:q90	-0.166	0.234	-0.710	0.480	
sin:TP_mean	-1.217	0.975	-1.247	0.216	
q90:TP_mean	-2.877	5.084	-0.566	0.573	
sin:q90:TP_mean	1.271	1.784	0.713	0.478	
ASPT(BInd12) = 4.54 + 0.261·Sin + 0.658·q90 - 3.311·TP_mean					
$R^2 = 0.42$					
sin:q90	-0.849	0.736	-1.153	0.252	
sin:TP_mean	-5.428	3.073	-1.766	0.081	.
q90:TP_mean	-15.580	16.015	-0.973	0.333	
sin:q90:TP_mean	7.858	5.619	1.398	0.165	

Even though the interaction term for some variables in DVPI_EQR indicated significant interaction (marked in yellow), the VIF test for the variables showed no covariant problem ($VIF < 5$).

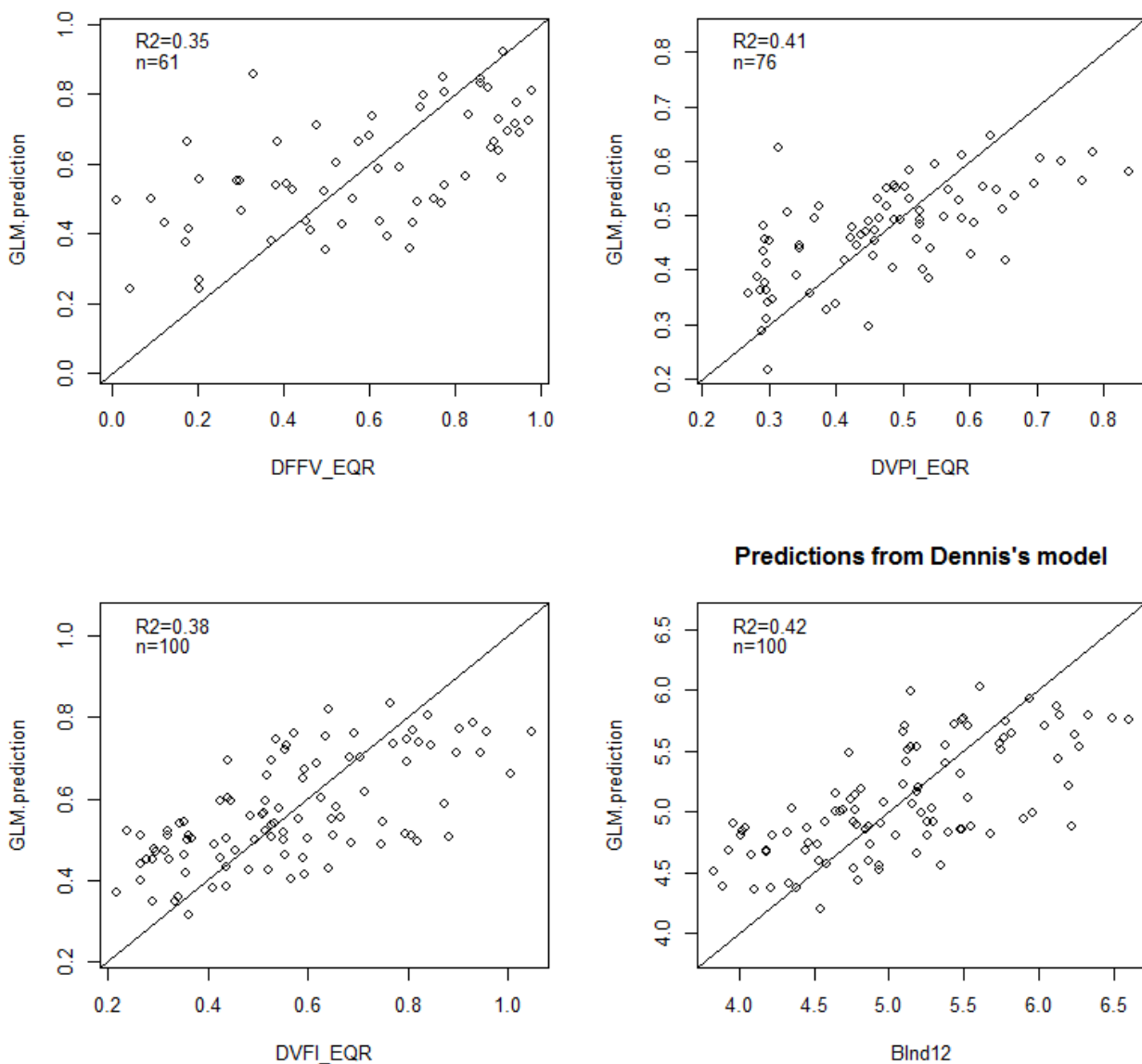


Figure 5.53 Predictions verses input indicators from the previous models developed by EUREKA.

The drop test was performed to check the impact of each variable on the model prediction. Except for DFFV_EQR, the rest of the equations were fairly sensitive to the variables, Table 5.34.

Table 5.32. Result for the drop test on the EUREKA models to view the change in deviance when dropping each variable

	Deviance	AIC	scaled dev.	Pr(>Chi)	Significant level
DFFV_EQR ~ q90 + bfi + BI5_max + fre25					
q90	2.943	-1.807	0.008	0.929	
bfi	3.094	1.253	3.068	0.080	.
BI5_max	3.509	8.925	10.740	0.001	**
fre25	3.087	1.115	2.930	0.087	.
DVPI_EQR ~ dur3 + Temp_std + DRP_mean + fre25 + fre75					
dur3	0.922	-107.610	6.219	0.013	*
Temp_std	0.916	-108.160	5.671	0.017	*
DRP_mean	0.850	-113.830	0.001	0.976	
fre25	0.951	-105.310	8.523	0.004	**
fre75	1.008	-100.890	12.947	0.000	***
DVFI_EQR ~ sin + q90 + TP_mean					
sin	2.922	-61.506	20.236	0.000	***
q90	2.474	-78.135	3.607	0.058	.
TP_mean	2.653	-71.153	10.589	0.001	**
BInd12 ~ sin + q90 + TP_mean					
sin	29.110	168.380	18.972	0.000	***
q90	25.901	156.700	7.292	0.007	**
TP_mean	27.536	162.820	13.414	0.000	***

New GLMs following the MARS procedure

We selected three variables based on the ranking from the BRT analysis in Table 5.31 and the R2 ranking in Table 5.30, marked in green. The selected variables have no covariance problem according to Table 5.32.

For DVFI_EQR and BInd12, the variables were chosen based on R2 ranking, because GLMs from the high ranked variables in BRT analysis were worse. The selection for BInd12 was the same as for the previous EUREKA model, so results are not presented (see Table 5.35).

Table 5.33. Equations and interactions estimated with new variable ranking

	Estimate	Std. Error	t value	Pr(> t)	Significant level
DFFV_EQR = 0.356 + 0.416·bfi + 0.118·NO23_min - 0.144·BI5_mean					
<i>R² = 0.44</i>					
bfi:NO23_min	-0.920	0.504	-1.827	0.073	.
bfi:BI5_mean	-0.452	0.620	-0.728	0.470	.
NO23_min:BI5_mean	-0.265	0.267	-0.992	0.326	.
bfi:NO23_min:BI5_mean	0.314	0.347	0.905	0.370	.
DVPI_EQR = 1.700 - 0.004·drain_2m - 0.117·pH_max - 0.006·dur3					
<i>R² = 0.44</i>					
drain_2m:pH_max	0.012	0.010	1.216	0.230	.
drain_2m:dur3	0.031	0.018	1.708	0.094	.
pH_max:dur3	0.256	0.153	1.677	0.100	.
drain_2m:pH_max:dur3	-0.004	0.002	-1.669	0.102	.
DVFI_EQR = 0.384 + 0.080·Sin + 0.111·q90 - 1.075·TP_std					
<i>R² = 0.36</i>					
sin:q90	0.029	0.168	0.173	0.863	.
sin:TP_std	0.261	1.025	0.255	0.800	.
q90:TP_std	-1.258	5.380	-0.234	0.816	.
sin:q90:TP_std	0.319	2.077	0.154	0.878	.
DVPI_EQR = 0.830 - 0.003·drain_2m - 0.020·Temp_std - 0.010·dur3 - 0.005·frst_2m					
<i>R² = 0.48</i>					
drain_2m:dur3	-0.003	0.004	-0.676	0.502	.
drain_2m:Temp_std	-0.006	0.006	-0.954	0.344	.
dur3:Temp_std	-0.062	0.078	-0.800	0.427	.
drain_2m:frst_2m	-0.002	0.002	-1.031	0.307	.
dur3:frst_2m	-0.023	0.040	-0.583	0.562	.
Temp_std:frst_2m	-0.047	0.042	-1.123	0.266	.
drain_2m:dur3:Temp_std	0.001	0.001	0.805	0.424	.
drain_2m:dur3:frst_2m	0.000	0.001	0.570	0.571	.
drain_2m:Temp_std:frst_2m	0.001	0.001	1.056	0.295	.
dur3:Temp_std:frst_2m	0.006	0.009	0.750	0.456	.
drain_2m:dur3:Temp_std:frst_2m	0.000	0.000	-0.732	0.467	.

The interactions among variables were not significant and there were no covariance problems.

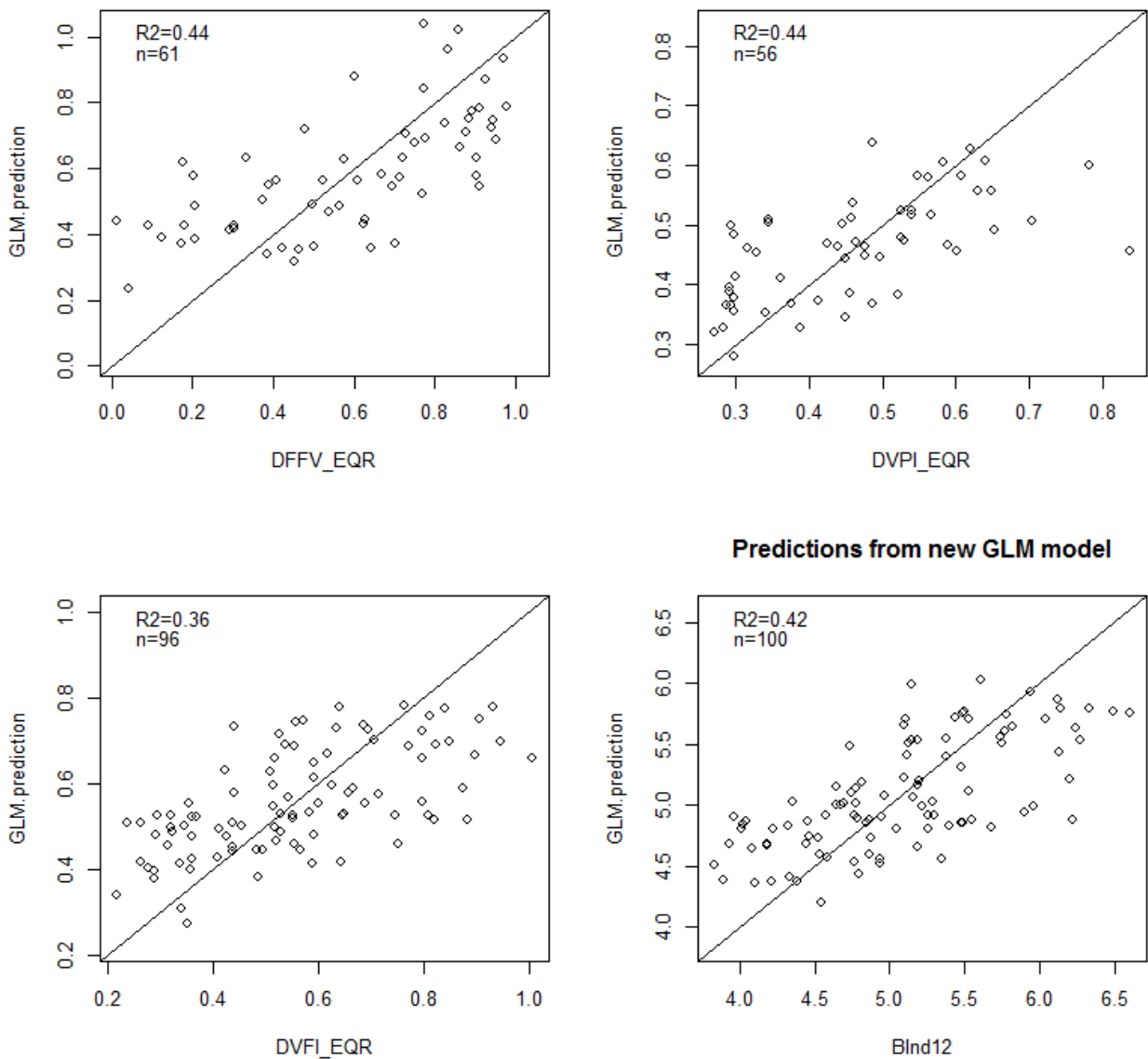


Figure 5.54 Predictions verses input indicators from the new GLM analysis

The new equations for DFFV_EQR and DVPI_EQR were better than the original analysis, with less number of variables (Figure 5.52), whereas new equation for DVFI_EQR was worse than the original analysis.

For DVPI_EQR, however, the variable pH_max was not measured frequently and not an output from SWAT model. Therefore, we developed another model without the pH component, and included in total four variables (marked in yellow in Table 5.30 and 5.31). The equation is listed at the end of Table 5.35 and the prediction is better ($R^2 = 0.48$, Figure 5.54) than the GLM with 3 variables and better than the EUREKA model.

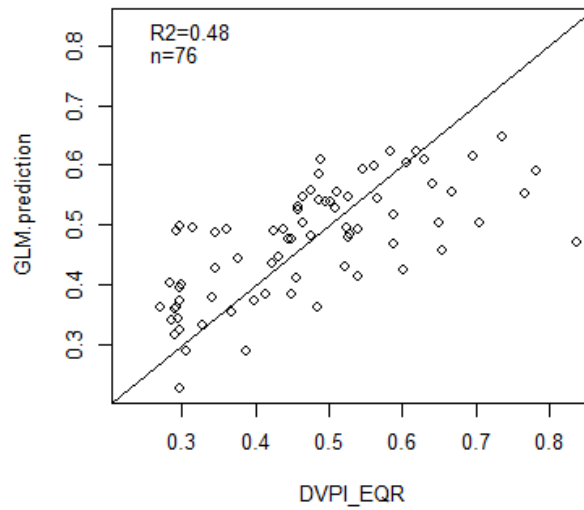


Figure 5.55 Predictions versus input indicators from the new GLM analysis for DVPI_EQR without pH variables.

Final GLM's

After discussion, we decided that for DFFV_EQR (the fish index), the nitrogen variables should be excluded from the analysis, and for DVPI_EQR (the macrophyte index), the forest variable should be excluded from the analysis since we could not biologically explain the effects of these two variables. This resulted in a model for DFFV which was worse than the original EUREKA model, hence we keep the EUREKA model. For DVPI we removed the forest variable and substituted drain_2m with drain_tot and additionally included q90. This model has an $R^2 = 0.42$ which is better than the EUREKA model. For DVFI and Bind12 the EUREKA models were superior and we keep them. The final abiotic-biotic equations are summarized in Table 5.36. Table 5.37 holds a description of the independent abiotic variables.

Table 5.34. The final recommended equations and the interactions among variables

	Estimate	Std. Error	t value	Pr(> t)	Significant level
DFFV_EQR = $0.199 - 0.020 \cdot q90 + 0.562 \cdot BFI - 0.041 \cdot BI5_max + 0.018 \cdot Fre25$					
$R^2 = 0.35$					
q90:bfi	-6.669	6.555	-1.017	0.314	
q90:BI5_max	-0.084	1.202	-0.070	0.945	
bfi:BI5_max	-1.088	0.721	-1.508	0.139	
q90:fre25	-0.534	0.607	-0.879	0.384	
bfi:fre25	-0.498	0.454	-1.097	0.279	
BI5_max:fre25	-0.076	0.067	-1.131	0.264	
q90:bfi:BI5_max	0.309	1.525	0.203	0.840	
q90:bfi:fre25	0.562	0.789	0.713	0.480	

	Estimate	Std. Error	t value	Pr(> t)	Significant level
q90:BI5_max:fre25	0.044	0.144	0.302	0.764	
bfi:BI5_max:fre25	0.061	0.101	0.607	0.547	
q90:bfi:BI5_max:fre25	-0.018	0.195	-0.090	0.929	
<hr/>					
DVFI_EQR = 0.887 - 0.004·drain_tot - 0.025·Temp_std - 0.009·dur3 - 0.100 q90					
$R^2 = 0.42$					
drain_tot:Temp_std	0.007	0.006	1.036	0.304	
drain_tot:dur3	0.004	0.004	1.213	0.230	
Temp_std:dur3	0.108	0.063	1.722	0.090	
drain_tot:q90	-0.024	0.042	-0.571	0.570	
Temp_std:q90	0.362	0.549	0.660	0.512	
dur3:q90	0.061	0.414	0.148	0.883	
drain_tot:Temp_std:dur3	-0.001	0.001	-1.364	0.178	
drain_tot:Temp_std:q90	0.005	0.009	0.506	0.615	
drain_tot:dur3:q90	0.005	0.007	0.781	0.438	
Temp_std:dur3:q90	-0.022	0.091	-0.239	0.812	
<hr/>					
DVFI_EQR = 0.40 + 0.085·Sin + 0.144·q90 - 0.920·TP_mean					
$R^2 = 0.38$					
sin:q90	-0.166	0.234	-0.710	0.480	
sin:TP_mean	-1.217	0.975	-1.247	0.216	
q90:TP_mean	-2.877	5.084	-0.566	0.573	
sin:q90:TP_mean	1.271	1.784	0.713	0.478	
<hr/>					
ASPT(BInd12) = 4.54 + 0.261·Sin + 0.658·q90 - 3.311·TP_mean					
$R^2 = 0.42$					
sin:q90	-0.849	0.736	-1.153	0.252	
sin:TP_mean	-5.428	3.073	-1.766	0.081	
q90:TP_mean	-15.580	16.015	-0.973	0.333	
sin:q90:TP_mean	7.858	5.619	1.398	0.165	

Table 5.35. Description of independent variables in the final recommended equations. All variables are based on a time series 2004-2011 from 131 stream water stations.

Variable	Description
Q90	90 th percentile from the flow duration curve divided by Q50
BFI	Baseflow index; baseflow volume divided by total volume
BI5_max	Annual maximum biological oxygen demand
FRE25	Frequency of flow events above Q25
Drain_tot	Percentage artificial drainage in catchment
Temp_std	Standard deviation of stream water temperature
Dur3	Mean duration of flow events above 3*Q50
Sin	Sinuosity of the stream
TP_mean	Annual mean concentration of total phosphorus.

5.3.4 Linking process-based and empirical models: assessing the impact of multiple stressors on stream water quality

5.3.4.1.1 Introduction

When analysing the results of the process-based modelling it became clear that the choice of climate model has a strong influence on nutrient load results. Further, from the two climate models selected by the MARS work team, the IPSL-CMA-LR model was seen to represent better the expected future behaviour of climate in Denmark (i.e. this model gave the median cumulative precipitation of an ensemble of five different climate models, Ref: MARS internal document: Choice of the MARS climatic model for the case studies). For these reasons it was decided to only use outputs from the process-based model calculated with inputs from the IPSL-CMA-LR climate model when linking process-based and empirical models.

5.3.4.1.2 Methods and materials

Time series of daily flow and nutrient transport at the subbasin level were extracted from the process-based model simulations for the scenarios listed in Table 5.38. Subsequently, the hydrological indices needed as inputs for the empirical models were generated (Table 5.38). Temp_std, the standard deviation of stream water temperature, was calculated from daily time series of stream water temperature at the catchment level generated by the process-based model. The degree of artificial drainage and the sinuosity of streams were extracted per subbasin in GIS (variables Drain_tot and SIN, Table 5.38). As biological oxygen demand is not an output from the SWAT model, we used the average value for BI5_max calculated from the data set on which the empirical models were developed as an input.

Table 5.36.Scenarios considered when assessing the impact of multiple stressors on stream water quality.

<i>Scenario</i>	<i>Short name</i>
Present land use, observed climate 2001-2010	PLU_obs
Present land use, climate projection RCP4.5 2011-2020 (baseline ¹ for RCP4.5)	PLU_4.5
Present land use, climate projection RCP8.5 2011-2020 (baseline ¹ for RCP8.5)	PLU_8.5
Techno world (High-tech Agriculture) ² , observed climate 2001-2010	HT_obs
Consensus world (Agriculture for Nature) ² , observed climate 2001-2010	AN_obs
Fragmented world (Market Driven Agriculture) ² , observed climate 2001-2010	MD_obs
Techno world (High-tech agriculture) ² climate projection RCP8.5 2025-2034	HT_2030
Techno world (High-tech agriculture) ² climate projection RCP8.5 2055-2064	HT_2060
Consensus world (Agriculture for nature) ² climate projection RCP4.5 2025-2034	AN_2030
Consensus world (Agriculture for nature) ² climate projection RCP4.5 2055-2064	AN_2060
Fragmented world (Market driven agriculture) ² climate projection RCP8.5 2025-2034	MD_2030
Fragmented world (Market driven agriculture) ² climate projection RCP8.5 2055-2064	MD_2060

¹The time series for the climate model starts in 2006. The hydrological model needs a 5 year warm-up period, hence a 10 years period is 2011-2020.

² Name of the MARS storyline, in parenthesis is the name of the interpretation of the storyline to the context of the Odense catchment

5.3.4.1.3 Results and discussion

Table 5.39 lists the values of the input variables for the empirical models. To improve the overview the values are presented as averages for the 31 subbasins. The first four rows compares the effect of land use only by comparing the effect of present land use and observed climate (2001-2010) to the effects of three storylines also simulated using observed climate (2001-2010). The hydrological effects of the land use changes are modest. Most remarkable is the decrease in DUR3, the annual duration of extreme flows (flows above 3 times the median flow) from 13.0 days/year to 10.9 and 11.6 days/year in the High-technology Agriculture and Market Driven Agriculture scenarios, respectively. The stream water phosphorus concentration which is to a large extent driven by hydrology is unaffected by the land use scenarios. Stream water nitrogen concentration, on the other hand, is strongly affected with concentration values 33% higher in the market driven agriculture scenario due to the higher inputs of fertilizer and manure. Both the Agriculture for Nature and the High-technology Agriculture scenarios have lower inputs of fertilizer and manure compared to present land use and stream water nitrogen concentrations are thus lower for these two scenarios.

The combined effects of land use change and climate change must be studied within a given climate model projection: HT_2030 and HT_2060 using PLU_85 as baseline; AN_2030 and AN_2060 using PLU_45 as baseline; and MD_2030 and MD_2060 using PLU_85 as baseline.

Table 5.37. The variables needed for the empirical models, average values for the 31 subbasins for each scenario.

Scenario	Q90	BFI	DUR3	FRE25	TP_mean	TN_mean	Temp_std	BI5_max	SIN	DRAIN_TOT
	(-)	(-)	(days/yr)	(events/yr)	(mg P/l)	(mg N/l)	(°C)	(mg O ₂ /l)	(-)	(%)
AN_obs	0.18	0.85	13.0	4.0	0.083	3.975	5.0	3.7	1.2	60.2
HT_obs	0.20	0.85	10.9	4.2	0.084	4.435	5.0	3.7	1.2	60.2
MD_obs	0.17	0.82	11.6	4.5	0.083	7.326	5.0	3.7	1.2	60.2
PLU_obs	0.17	0.83	13.0	4.3	0.083	5.518	5.0	3.7	1.2	60.2
PLU_45	0.17	0.81	11.6	3.9	0.079	6.080	5.3	3.7	1.2	60.2
PLU_85	0.14	0.85	11.6	3.7	0.081	6.033	5.2	3.7	1.2	60.2
HT_2030	0.16	0.89	12.0	3.3	0.081	6.033	5.2	3.7	1.2	60.2
HT_2060	0.15	0.89	8.4	3.2	0.082	4.259	4.6	3.7	1.2	60.2
AN_2030	0.16	0.88	13.7	3.3	0.081	4.489	4.9	3.7	1.2	60.2
AN_2060	0.18	0.89	22.4	2.8	0.080	3.983	4.8	3.7	1.2	60.2
MD_2030	0.14	0.86	14.4	3.6	0.081	7.980	5.2	3.7	1.2	60.2
MD_2060	0.15	0.88	11.3	3.7	0.082	6.244	4.6	3.7	1.2	60.2

The frequency of high flow events (above the 25th percentile, FRE25) decreases in all scenarios relative to the baseline and the proportion of groundwater flow (BFI) increases. The duration of high flows (DUR3) decreases in the High-Tech Agriculture scenario from 11.6 events/year to 8.4 events/year, whereas it increases in the Agriculture for Nature from 11.6 to 22.4 events/year and remains the same in the Market Driven Agriculture scenario. The concentration of total phosphorus, TP_mean, is virtually unaffected by the combined land use and climate change scenarios. A stronger effect is seen in the concentration of nitrogen, TN_mean, which decreases in the Agriculture for Nature and the High-Tech Agriculture scenarios relative to the baseline, whereas the value in 2060 in the Market Driven Agriculture scenario is slightly higher than the baseline value (6.244 mg N/l compared to 6.080 mg N/l).

All scenario results for all four ecological quality indices are summarized in Table 4.3 as averages for the 31 subbasins in the Odense catchment, and illustrated at the subbasin level in figs. 4.1 – 4.4. For the fish index (DFFV_EQR), the macroinvertebrate index (DVFI_EQR) and for the Average Score Per Taxon (ASPT) the effects of combined land use change and climate change are minor when evaluated as averages for the entire catchment. However, as illustrated by Figs. 4.1 – 4.4 there is large inter-subbasin variation. Figure 4.5 illustrates using DVFI_EQR as an example the effect of changes in land use evaluated in 2055-2064 at the subbasin level. The effect of land use change is small, also at the subbasin level, and not consistent between subbasins. A

similar low response to land use change is observed for the fish index (DFFV_EQR) and for ASPT (not shown). The Danish macrophyte index, DVPI_EQR, has the strongest response both to land use change and to climate change, Table 4.3 and Fig.4.2. Figure 4.6 illustrates the combined effect of land use and climate changes on DVPI_EQR at the subbasin level for storyline 1 (High-tech agriculture): for all subbasins a positive impact of land use and climate change is observed, however the effect varies between subbasins. Figure 4.7 compares the effect of land use change by illustrating the macrophyte index per subbasin in 2055-2064 for the three land use scenarios (storylines). It should be noted that the scenarios are run with different climate projections, Table 4.1. The response to the imposed changes is mixed between scenarios and between subbasins, however for all subbasins the lowest macrophyte index values are found for the Agriculture for Nature scenario.

Table 5.38. Ecologic quality indices, average values for the 31 subbasins for each scenario.

	DFFV_EQR	DVPI_EQR	DVFI_EQR	ASPT
PLU_obs	0.59	0.39	0.45	4.70
AN_obs	0.59	0.38	0.46	4.71
HT_obs	0.60	0.40	0.46	4.72
MD_obs	0.59	0.40	0.45	4.70
PLU_85	0.57	0.39	0.46	4.72
PLU_45	0.59	0.40	0.45	4.69
HT_2030	0.61	0.39	0.45	4.70
HT_2060	0.61	0.44	0.45	4.69
AN_2030	0.60	0.39	0.45	4.70
AN_2060	0.60	0.31	0.46	4.72
MD_2030	0.60	0.37	0.45	4.69
MD_2060	0.61	0.41	0.45	4.69

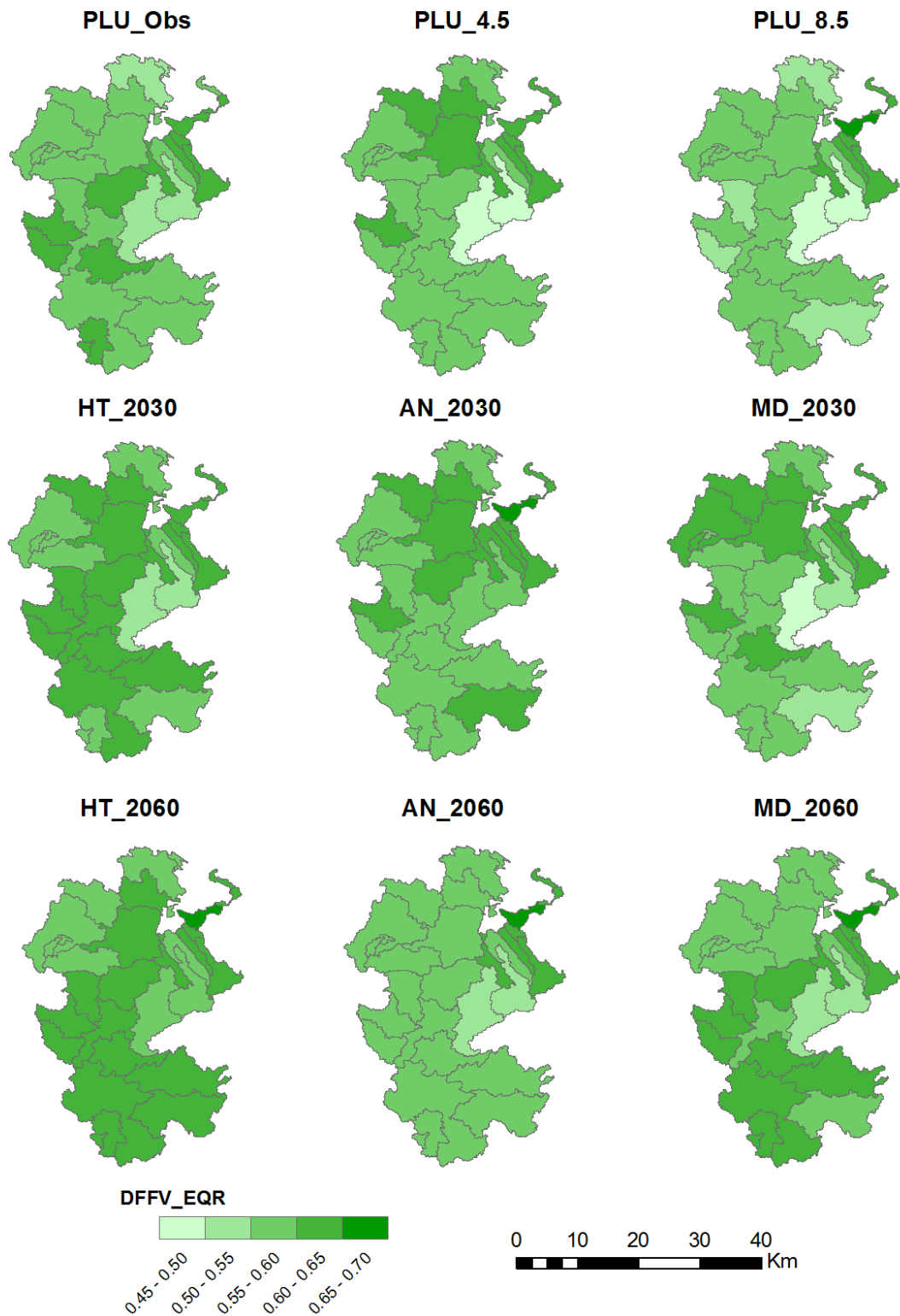


Figure 5.56 DFFV_EQR, the Danish fish index, calculated for three combined climate change-land use change scenarios for 31 subbasins in the Odense catchment.

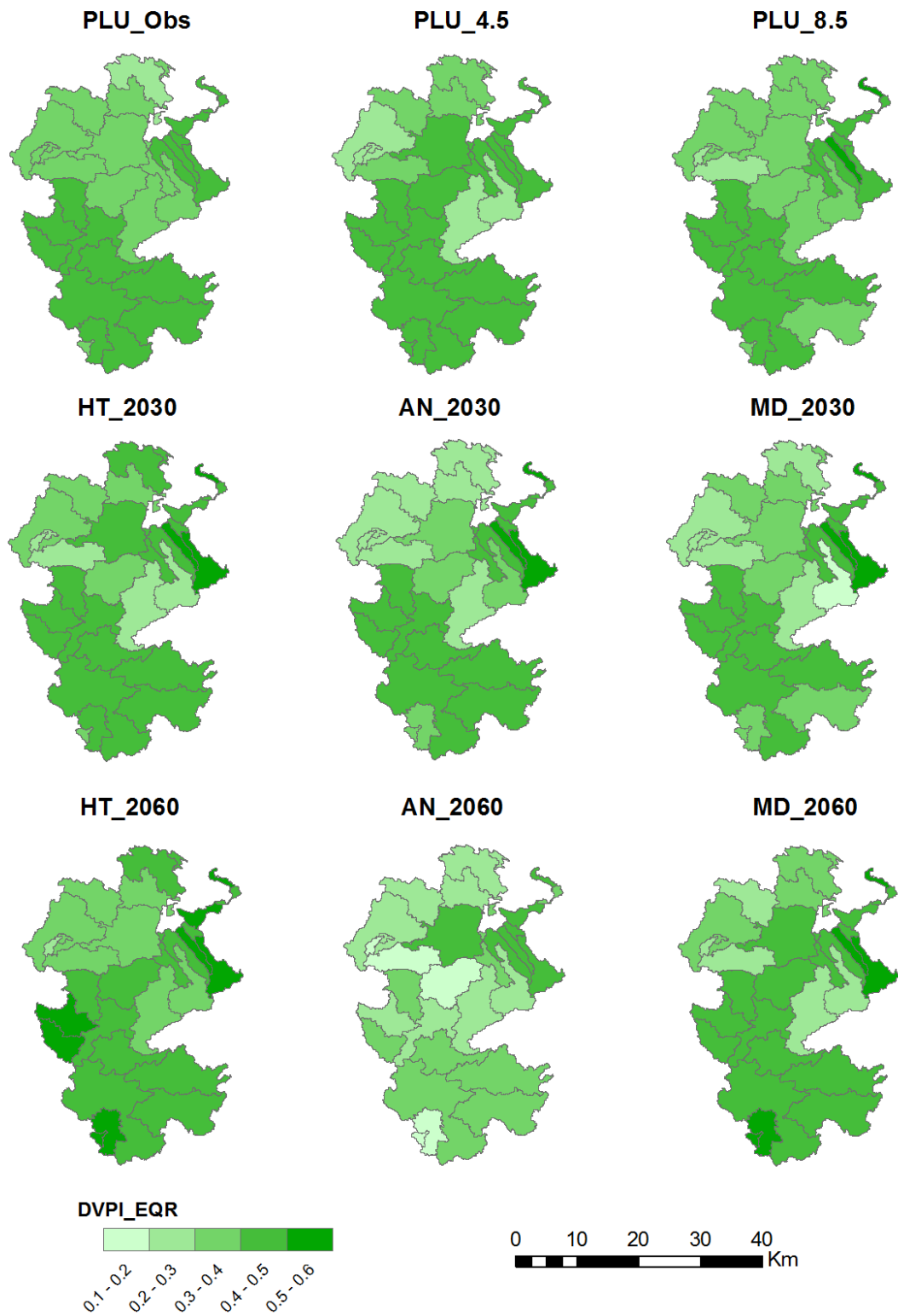


Figure 5.57 DVPI_EQR, the Danish macrophyte index, calculated for three combined climate change-land use change scenarios for 31 subbasins in the Odense catchment.

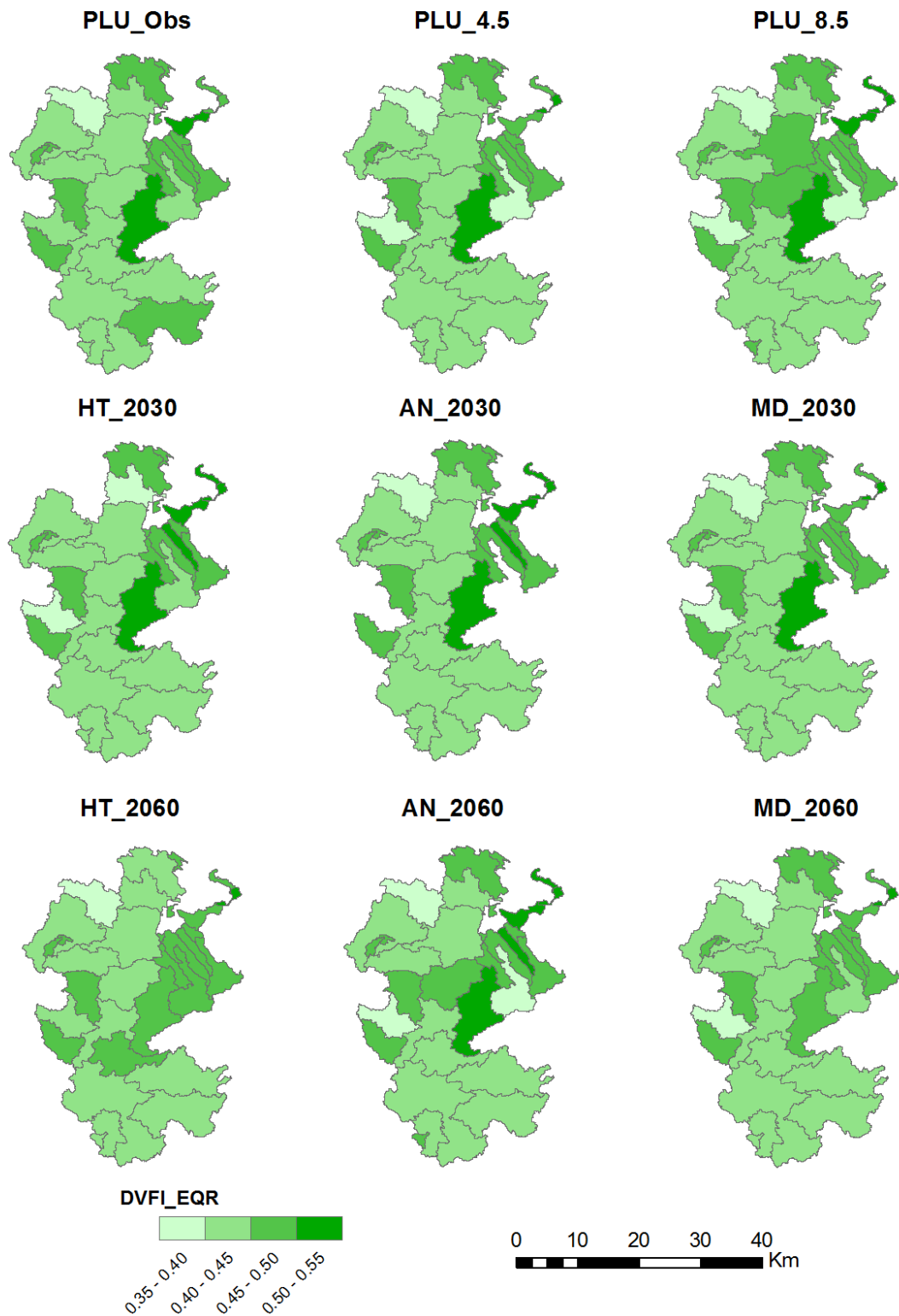


Figure 5.58 DVFI_EQR, the Danish macroinvertebrate index, calculated for three combined climate change-land use change scenarios for 31 subbasins in the Odense catchment.

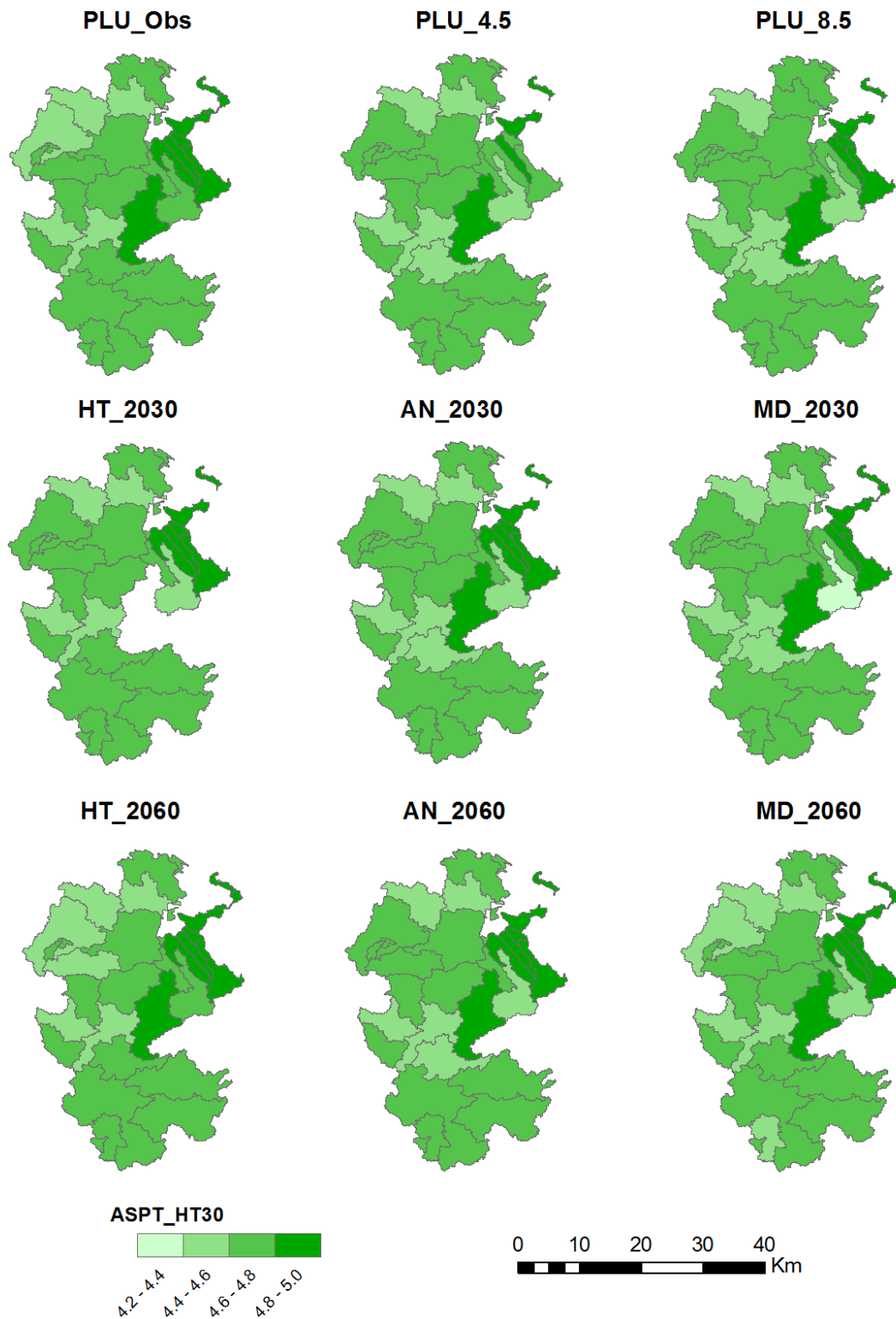


Figure 5.59 ASPT, average score per taxon, calculated for three combined climate change-land use change scenarios for 31 subbasins in the Odense catchment.

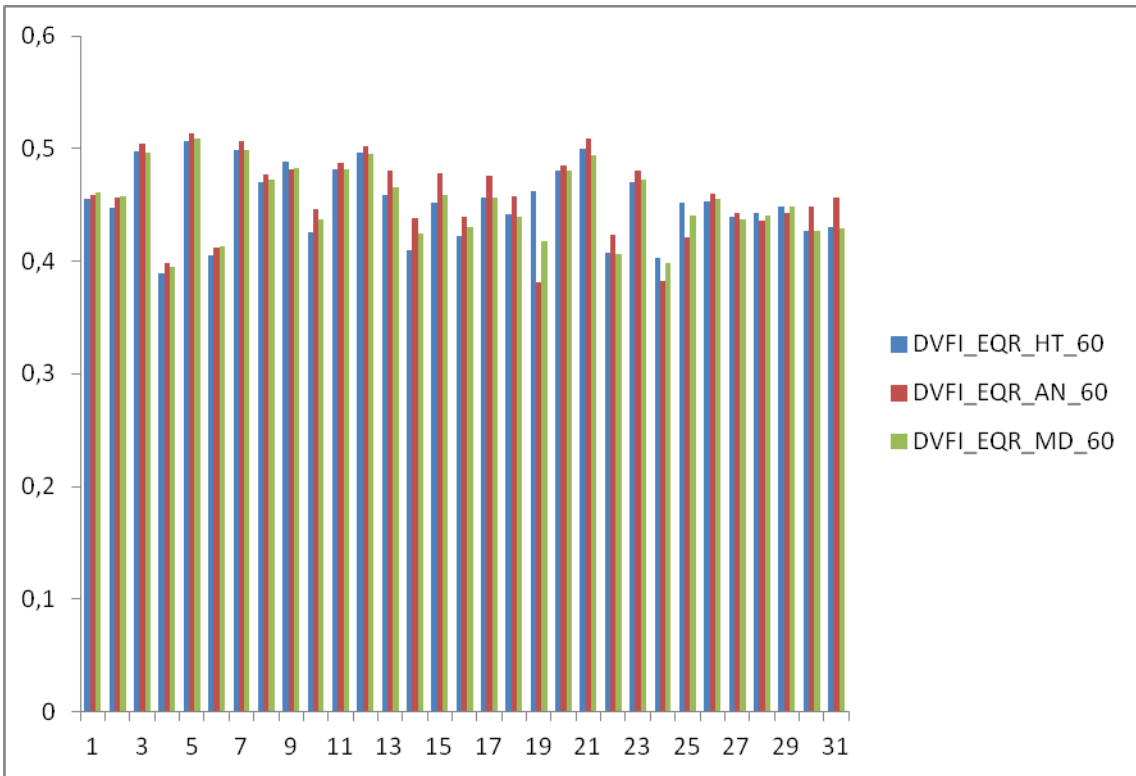


Figure 5.60 DVFI_EQR, the Danish macroinvertebrate index, calculated for three combined climate change-land use change scenarios for 31 subbasins in the Odense catchment.

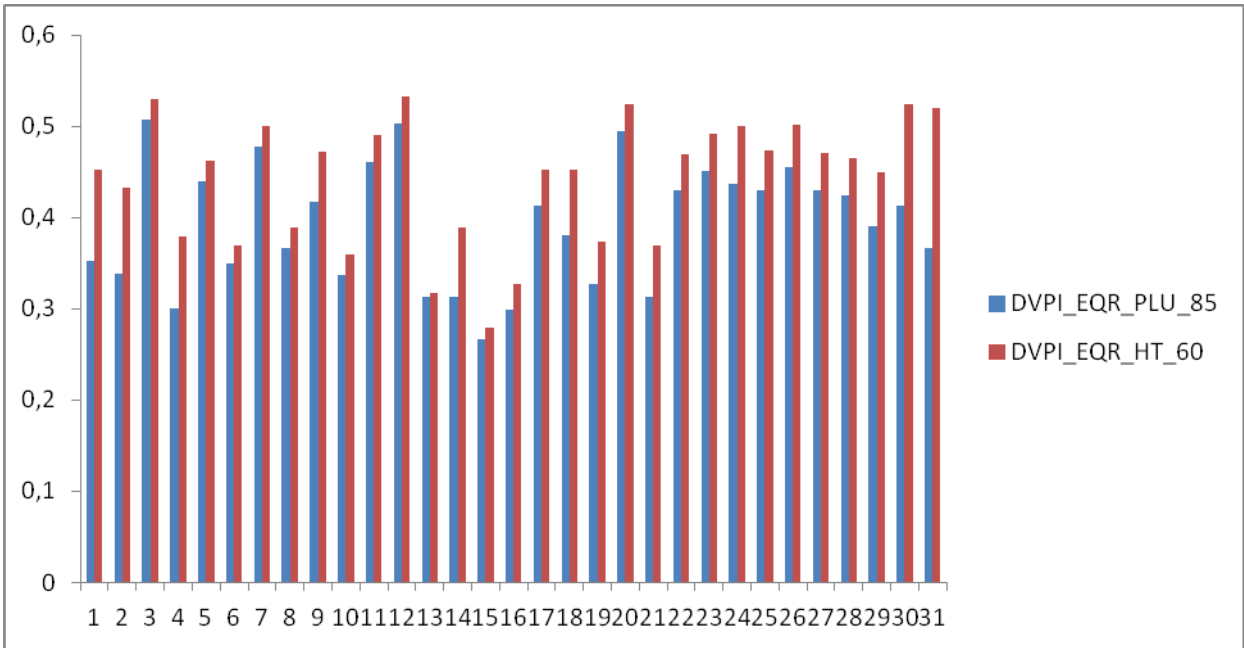


Figure 5.61 DVPI_EQR, the Danish macrophyte index, comparing baseline (DVFI_EQR_PLU_85) to MARS storyline 1 (high-tech agriculture, DVFI_EQR_HT_60, situation 2055-2064) for 31 subbasins in the Odense catchment.

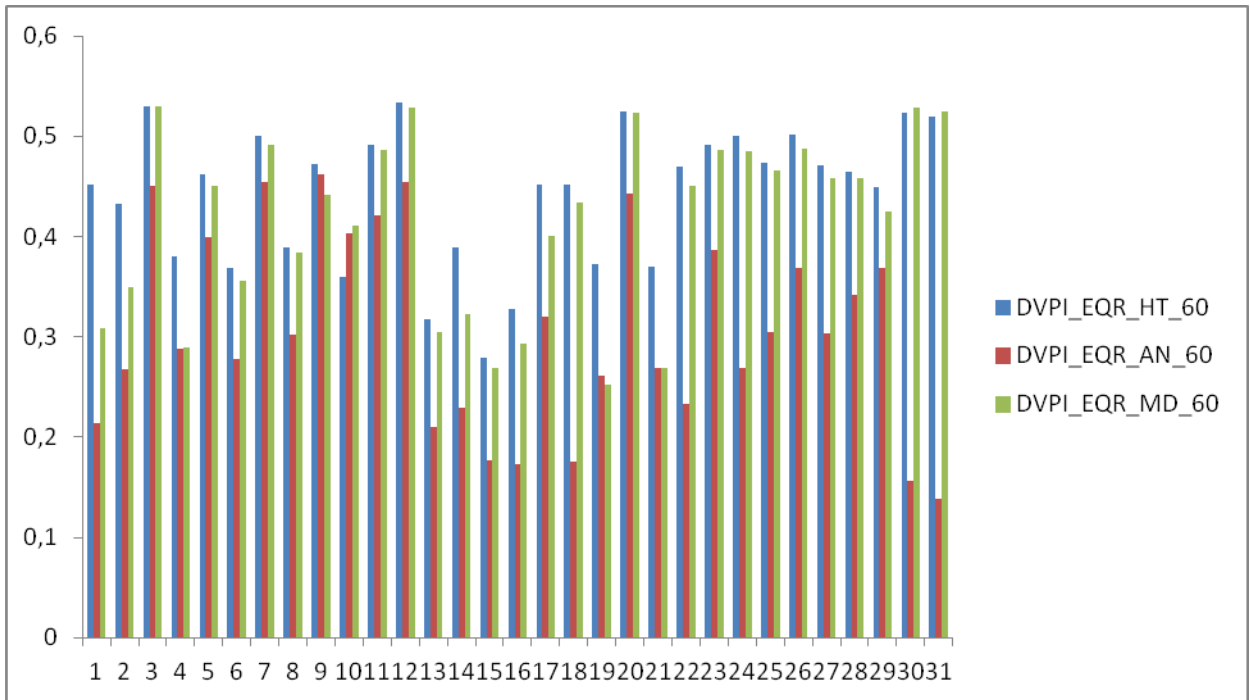


Figure 5.62 DVPI_EQR, the Danish macrophyte index, calculated for three combined climate change-land use change scenarios for 31 subbasins in the Odense catchment.

5.3.5 Conclusions

The effects of land use change and climate change were evaluated at the Danish Odense catchment by calculating the values of four ecological quality indicators for three different storylines which combined land use and climate changes. The ecological indices were calculated by linking outputs from a process-based biophysical model (SWAT) to empirical abiotic-biotic models. Three indices, the Danish fish index, the Danish macroinvertebrate index, and Average Score Per Taxon (ASPT) responded very moderately to the imposed changes. A larger, and negative, effect of combined land use change and climate change was observed for the macrophyte index, however only in the Consensus World/Agriculture for Nature scenario. The main reason is an increase in the duration of high flows resulting from the climate change.

5.4 Regge and Dinkel

5.4.1 Introduction

The Dinkel catchment falls within the authority of Waterboard Vechtstromen and is part of the River Basin Management Plan (RBMP) of the Rhine (Figure 5.63). The Dutch part of the Rhine catchment covers 479 surface water bodies, of which the Dinkel catchment (Figure 5.62) covers 9 (Ministry of Infrastructure and the Environment, 2015).

An overview of the status and other important characteristics of these surface water bodies is presented in Table 5.41 and Figure 5.64. Most of the surface water bodies of the Dinkel catchment do not meet the objectives for chemical status (Figure 5.64) and only one of the water bodies has a good ecological status (Table 5.41).

The river Dinkel, although classified as heavily modified according to the Water Framework Directive, is one of the few (semi)natural meandering stream systems in the Netherlands. The river is fed by tributaries such as the Glanerbeek, Geelebeek, Elsbeek, Puntbeek, Tilligterbeek, and Ruenbergerbeek. To regulate water levels of the Dinkel, especially during winter, a channel ‘Omleidingskanaal’ was dug, which has been in use since 2001. If the water level of the Dinkel reaches a certain threshold, part of the water will be rerouted via this channel.

The Dinkel catchment has a temperate marine climate with annual precipitation of 800 to 850 mm per year, mean evaporation of 560 mm per year and a mean annual air temperature of round 9.9 °C (KNMI, 2016). The Dinkel flows through a valley between ice-pushed ridges which originate from the Saalien ice age. On top of these clayey moraines, shallow aquifers are present from which the tributaries originate. The Dinkel valley is mainly filled with sandy deposits.

Land use in the Dinkel catchment consists primarily of agriculture (60-70%), for which an extensive system of watercourses and drainage is present. Apart from agriculture, water chemistry is influenced by four waste water treatment plants located near the largest villages: Glanerbeek (17.3 k inhabitants), Losser (13.3 k inh.), Denekamp (8.6 k inh.) and Ootmarsum (4.5 k inh.). These urban areas are scattered throughout the Dinkel catchment. Ground and surface water are intensively used for irrigation, industry, drinking water and recreation. Parts of the Dinkel have been straightened or deepened for flood prevention; the same applies to its tributaries.

The groundwater in the Dinkel catchment is intensively drained and abstracted, mostly for agriculture, flood protection and urban development. Streams are straightened and often over dimensioned. As such, the main drivers⁴ of the Dinkel catchment are: groundwater abstraction, groundwater drainage, urban development, flood protection, agriculture and climate change.

The most important reasons for not reaching a good ecological status are combinations of insufficient water flow, unnatural stream bed, insufficient connectivity for fish and moderate to poor chemical status (nutrients and other pollutants). So far, it is unclear to what degree problematic substances (a substance above its threshold according to the WFD) contribute to the ecological functioning of these surface water bodies (Waterboard Regge and Dinkel, 2010).

The river Dinkel originates in Nordrhein-Westfalen (Germany) between Coesfeld and Ahaus. Its catchment is 63,000 ha large, of which 23,000 ha lies within the Netherlands. The Dinkel flows from Germany into the Netherlands at Losser and from the Netherlands back into Germany near Oosterzand. The river has a length of 93 km, of which 46 km is located within the Netherlands and 38 and 9 km are located upstream and downstream in Germany respectively. The focus of this report is the Dutch part of the Dinkel catchment (Figure 7.1), which will be referred to as ‘the Dinkel catchment’.

The structure of this report is as follows. Section 7.1 contains an overview of the conceptual MARS model, the process based model and the empirical model. Section 7.2 shows which data, data preparations and models were used. In Section 7.3 methods of the different model applications are presented and in Section 7.4 the results are shown and discussed. Section 7.5 discusses progress in the work focussing on the influence of groundwater contribution to stream ecology. Section 7.6 contains the conclusions, recommendations from the Regge and Dinkel case study.

⁴ The definition of a driver within the MARS project is: an anthropogenic activity or climate change phenomenon that may have an environmental effect (Birk et al., 2015).

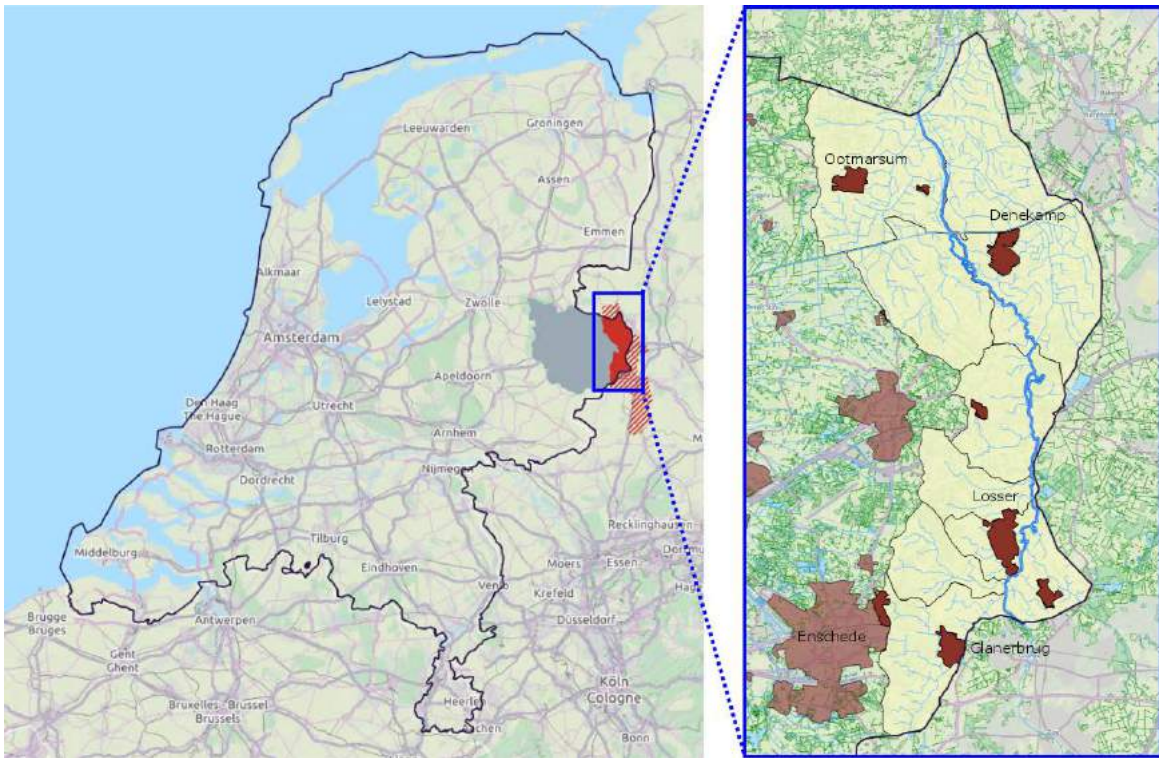


Figure 5.63 Maps of the case study area. Left: The Dinkel catchment in red, with the German part hatched and the Dutch part solid red, and the Regge catchment in grey. Right: The Dinkel catchment in yellow and the Dinkel river and its tributaries in the Netherlands in blue. The main cities and villages in the Dinkel catchment in the Netherlands are shown in red.



Figure 5.64 River basins according to the RBMP in the Netherlands.

Table 5.39.Characteristics of the Water Framework Directive water bodies in the Dinkel catchment (Waterboard Vechtstromen, 2015b).

Name	Type	Status	Status due to	Land use (%)			Subcatchment size (ha)	Water body length (km)	Ecologic status
				Agriculture	Forest/Nature	Urban			
Boven Dinkel	R6	Heavily modified	Drainage	65	18	17	2152	9.5	Moderate
Midden Dinkel	R6	Heavily modified	Drainage	69	27	4	4830	30.4	Poor
Beneden Dinkel	R7	Heavily modified	Drainage Weirs, dams, reservoirs	75	18	7	3355	2.4	Bad
Tilligterbeek	R5	Heavily modified	Drainage Weirs, dams, reservoirs	76	20	4	6032	10.7	Bad
Puntbeek	R5	Heavily modified	Drainage Weirs, dams, reservoirs	56	43	1	436	3.4	Good
Geelebeek	R5	Heavily modified	Drainage Weirs, dams, reservoirs Channelization, normalisation, stabilization waterway and river bank stabilization	82	16	2	1321	9.6	Bad
Glanerbeek	R12	Heavily modified	Drainage Weirs, dams, reservoirs	62	24	14	2281	5.6	Moderate
Ruenbergerbeek	R5	Heavily modified	Drainage	71	14	15	384	5.1	Poor
Elsbeek	R5	Heavily modified	Drainage	69	28	35	1310	3.1	Moderate

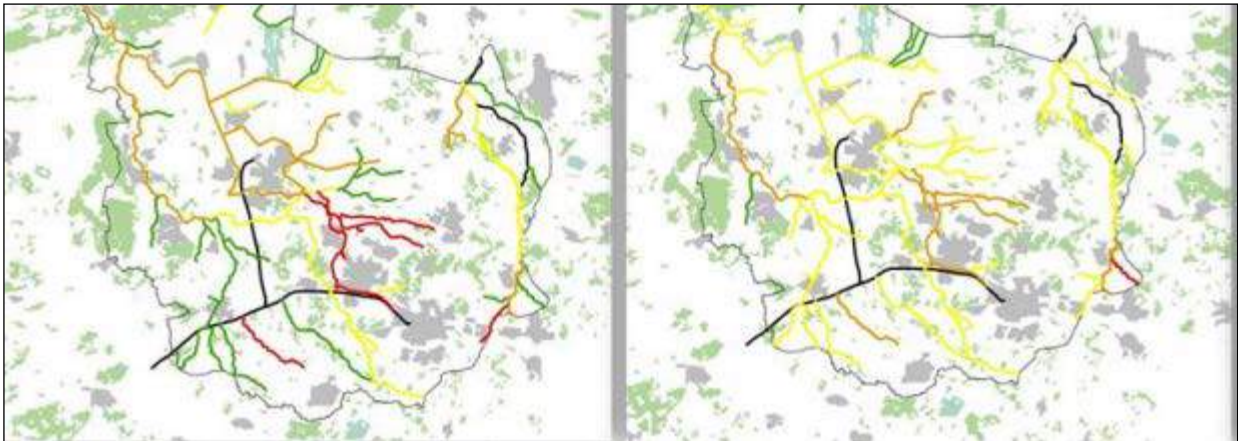


Figure 5.65 Chemical status of surface water bodies in the Regge and Dinkel catchments (from Waterboard Vechtstromen, 2015). Left: Total Phosphate, Right: Total Nitrogen. Green: good, yellow: moderate, orange: poor and red: bad status. Blue: no WFD water body.

5.4.2 Models

Two different overarching models were developed for the MARS project. The first is a conceptual model, based on the MARS conceptual model in the DOW. This model gives a graphical overview of the drivers, pressures, abiotic and biotic states, the ecosystems services and responses relevant, and their assumed interconnections, in the Dinkel surface water body. For an explanation of the terminology, see Birk et al. (2015).

The second model is a combination of numerical and statistical models. This model suite was made based on the conceptual MARS model. The goal of this model is to calculate the effects of the drivers and pressures on the abiotic and biotic states in the Dinkel catchment. This second model consists of a process-based model (PM) to calculate the effect of changes in the drivers and pressures on the abiotic states and an empirical model (EM) to estimate the effect of the changes in abiotic variables on the biotic variables and ecosystem services.

5.4.2.1.1 The MARS model

To conceptualize the processes in the catchment, a conceptual model was made of the Dinkel catchment (Figure 5.65), based on the MARS model in the MARS DOW. In the MARS project some changes have been made in the conceptual model schematisation. First, the conceptual model has mainly been built on the DPSIR components of the MARS model. Second, the column

for 'State' was split into an abiotic and biotic state. And third, the column for 'Impact' was replaced by the term 'Ecosystem Services' of the surface water body (a subset of impacts from the ecosystem services cascade of the MARS model in the DOW).

The MARS model has to be read from left to right. On the left hand side, the drivers are shown which were discussed in chapter 1. The related pressures are shown in the second column and lines are drawn indicating the effect of the drivers on each pressure (increase in red, and decrease in blue). Pressures are for example 'Diffuse pressure' (Diffuse pollution) which in this case is caused by the drivers 'urban development' and 'agriculture', and 'Physical alteration of streams' which, in this case, indicates the deepening and straightening of water bodies, for the purpose of flood protection.

The pressures influence certain abiotic states, which are shown in the third column and are connected to the pressures by lines indicating the type of relationship. For instance, 'Diffuse pressure' is connected with red lines to total phosphorus and to total nitrogen, showing that this pressure generally increases the total amount of nitrogen and phosphorus. Most of the abiotic states are output from the process-based model.

The abiotic parameters are combined and used as input for the empirical models to calculate the biotic state. Indicators of the biotic states are such as the Average Score per Taxon (ASPT) and the total fish abundance. The biotic states can then be related to certain ecosystem services. In this case the ecosystem services are in the form of capacities. A capacity gives an indication of the capacity of the system to provide a certain service. For instance, the 'Total fish abundance', the capacity of the system for fish, is positively related with 'Recreation' due to recreational fishery.

Responses in the MARS model are the responses, i.e. measures, of river basin management. These responses are connected back-wards showing their influence on drivers, pressures or states. For instance, waste water treatment plants can be improved (this is the response) thereby reducing the 'Point pressure' or Groundwater abstractions can be reduced, reducing the driver 'Groundwater abstractions'.

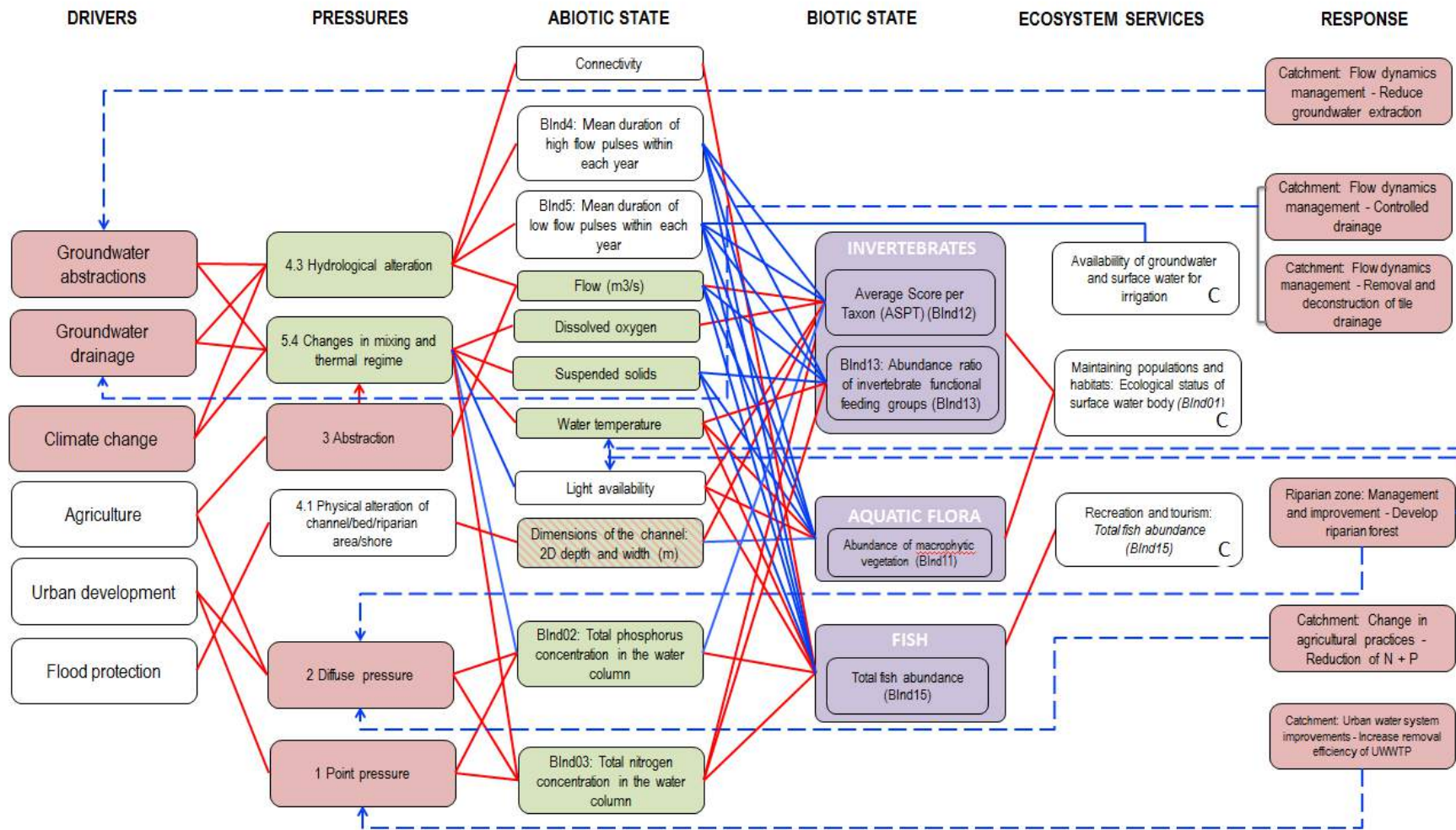


Figure 5.66 MARS model of the Dinkel catchment. Boxes have been given a colour according to the model they belong to: red = input for the process models, green = output of the process models and input for the empirical models, purple = output of the empirical models. The solid lines indicate the relationships between the different elements of the MARS model: red = positive correlation, blue = a negative correlation. The capital letter C shows that the 'capacity' of the ecosystem service is modelled. The dashed arrows indicate on which MARS model element the response element has an effect

5.4.2.1.2 Combining process- based and empirical models

In order to model both the abiotic and biotic environment, process-based and empirical models were combined. The process model is the key to the abiotic conditions in the Dinkel catchment under different scenarios, while the empirical model connects these abiotic conditions (such as total phosphorus and total nitrogen) to ecological response variables (such as macroinvertebrates and fish).

The abiotic process-based model consists of three components:

- A rainfall-runoff model (LGSJ) to calculate the amount of groundwater and surface water flowing from the tributaries into the Dinkel catchment (Kuijper et al., 2013).
- A 1D hydrodynamic model (SOBEK) for the calculation of the direction, flow velocity and water levels in the Dinkel river (Hydrologic and Deltares, 2014).
- The 1D water quality module (built in DELWAQ, Deltares 2014a) for the calculation of water quality processes in the surface water of the Dinkel catchment, including the modelling of water temperature and chlorophyll-a.

Basic principle in our empirical modelling is that we aimed a model that could use the output (abiotic variables) of the process model as input for the empirical models. The empirical model consists of:

- Boosted Regression Trees (BRT), to calculate the most important abiotic variables that influence the biotic variables. As explained by Elith et al. (2008): BRT's combine regression trees and boosting. Regression trees are models that relate a response to their predictors by recursive binary splits. Boosting is an adaptive method for combining many simple models to give improved predictive performance. BRT's are insensitive to outliers and can handle missing data in the predictor variables.
- Generalized Linear models (GLM), to calculate the relationships between the abiotic variables and the biotic variables. A GLM is a flexible generalization of linear regression that allows for a non-normal error distribution of the response variable.

See Figure 5.66 for a graphic overview of how the process and empirical models are connected. Inputs and outputs of the models are indicated. Currently the models have not yet been physically connected. This is the aim for MARS WP7.3.

For the empirical models a larger dataset than that of the Dinkel catchment alone turned out to be necessary to obtain more meaningful statistical relationships between the biotic and abiotic parameters. Therefore, additional data from the Regge catchment (Waterboard Vechtstromen), was included in the dataset to retrieve the statistical relationships. The Regge catchment lays adjoined to the Dinkel catchment and is roughly five times as large as the Dinkel catchment. Its hydro-geological, hydrological and ecological characteristics are comparable to those of the Dinkel catchment.

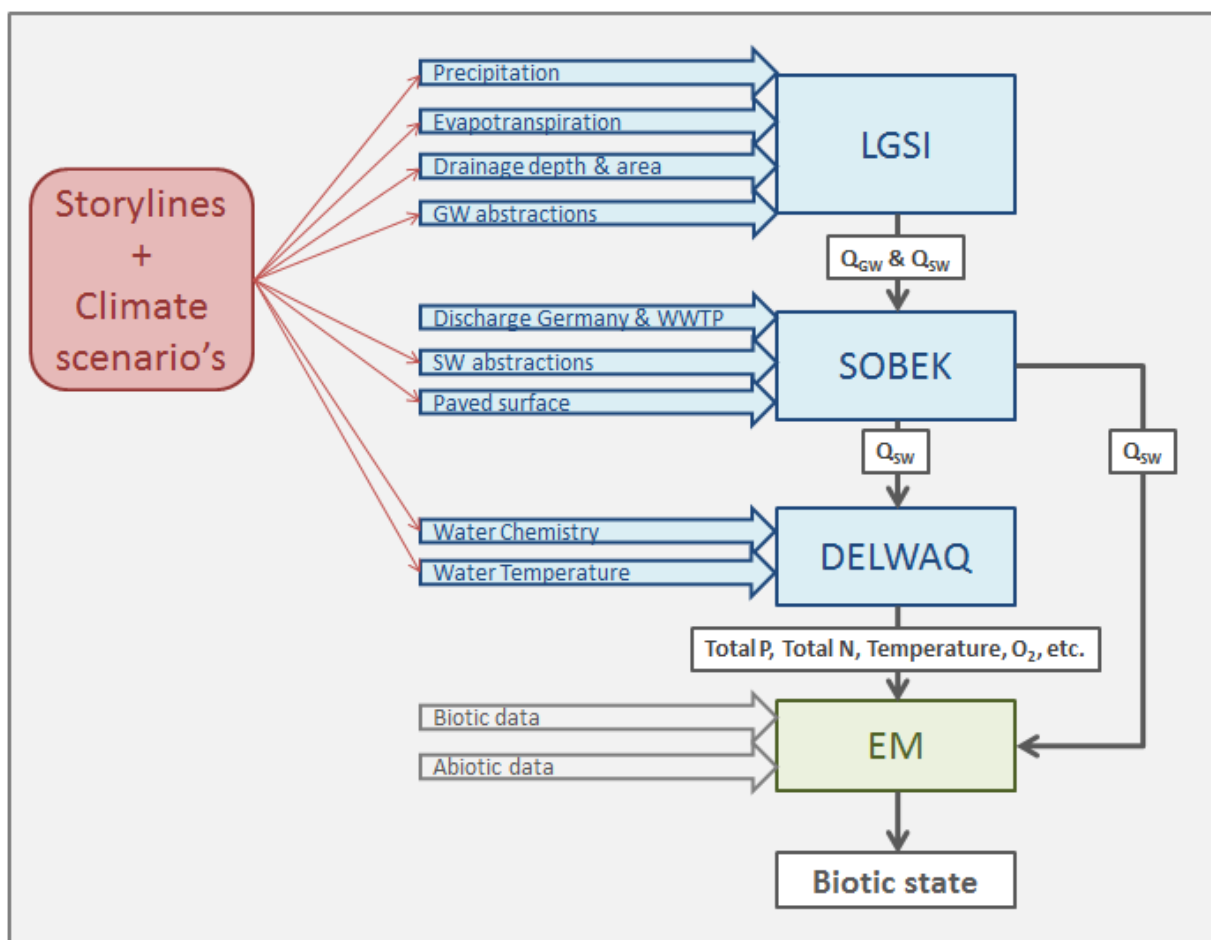


Figure 5.67 Modelling chain for the Dinkel catchment. The elements in which the calculations take place are indicated by rectangular boxes. Blue boxes for the process model chain and green boxes for the empirical model (EM). The most important inputs for each calculation element have been displayed as thick arrows. The inputs that were used to make the EM are indicated by thick grey arrows. The most important outputs have been indicated by thin arrows. The inputs that were changed in the scenario runs are indicated by red arrows. The abbreviations stand for: GW = ground water, SW = surface water, EM = empirical model, P = phosphorus, N = Nitrogen, WWTP = waste water treatment plant.

5.4.2.1.3 The scenarios

Scenarios were prepared in WP 2.6 of the MARS project for use in all MARS case studies. These scenarios consisted of a combination of climate models and climate model scenarios for the periods 2030 and 2060 and three storylines. WP2.6 advises to use the ISIMIP climate scenarios.

The scenarios are based on storylines and are called Techno world / MARS ad hoc world, Consensus world / MARS world, and Survival of the fittest world / No MARS world in the MARS project (Sanchez et al, 2015). These storylines are based on a combination of shared socioeconomic pathways (SSP5 – Conventional development, SSP2 – Middle of the Road, and SSP3 – Fragmentation), climate model scenarios (representative concentration pathways RCP 8.5 and RCP 4.5, Sanchez et al. 2015), and combinations of measures fitting the rationale of each storyline.

In Survival of the fittest world each country cares only for itself and no attention is paid to the preservation of ecosystems. There are no water management strategies, but only short term actions. In Consensus world the economy keeps on growing as it is now. There is an eye for preservation and everyone tries to comply with the regulations for water management. In Techno world the focus is on economy, which therefore grows fast. There is awareness in society of the environment, but most actions are taken ad hoc and environmental policies won't be renewed. Water management is focussed on flooding and drought. Each of the MARS storylines has a specific climate model scenario related to it, Techno world and Survival of the fittest world are connected to RCP 8.5, while Consensus world is related to RCP 4.5 (Sanchez et al., 2015).

Sanchez et al. (2015) formed a set of storyline elements to make the storylines more applicable to the process-based models. A selection of these elements was made for the Dinkel case study according to their suitability for the Dinkel catchment and the process-based model. Subsequently, the amount of change for each storyline element was estimated based on stakeholder and expert knowledge. The absolute amounts of change were implemented according to a baseline model. This baseline model was the process-based model calibrated on the historical period 2000-2012.

Different parts of the model required different kind of information. The following section describes which variables were used in each model. All data was acquired for the period 2000-2012. This period is based on the years for which the hydrodynamic part of the process based model was available.

5.4.2.1.4 The Data

This section explains which parameters were collected per model, including some general statistics on these parameters.

Process-based model

The data for the process-based model consisted of a set meteorological data, abiotic and biotic data.

METEOROLOGICAL DATA

For the meteorological data the following parameters were used for the baseline model:

- surface irradiance (hourly)
- relative air humidity (hourly)
- percentage sunshine (daily)
- air pressure (hourly)
- air temperature (hourly)
- rainfall (daily)
- evaporation (daily)

The time series for these parameters were taken from the meteorological station closest to the Dinkel catchment: meteorological station Twenthe (KNMI station 290; roughly 6 km North of Enschede). These data were obtained from the website of the Royal Netherlands Meteorological Institute (KNMI): <http://www.knmi.nl/nederland-nu/klimatologie>

For the scenarios daily values for rainfall, irradiance, air pressure and air temperature from the GFDL-ESM2M and IPSL-CM5A climate models were downloaded from the Deltares ftp servers for the periods 2006-2015, 2024-2036 and 2054-2066.

ABIOTIC AND BIOTIC DATA

Table 5.42 shows an overview of the abiotic and biotic parameters that were used in the process-based model. These data were supplied by Waterboard Vechtstromen.

The data that was used to determine the water quality of the boundaries⁵ was measured at 40 locations in the Dinkel catchment. For the exact coordinates of the boundary monitoring locations see Appendix 12.4. The monitoring frequency of the measurements differed per parameter and location from once every couple of years to biweekly.

The data used to determine the water quality of the effluent of the waste water treatment plants (WWTP) Glanerbrug, Denekamp, Losser and Ootmarsum had monthly data for suspended particulate matter, total nitrogen, and total phosphorus for 2000 and 2001. No data was available for 2002, while only monthly data was available for all parameters between 2003 and 2012.

Table 5.40. Data availability of parameters at monitoring locations and at WWTP outfalls

Parameter	Unit	Monitoring locations (Diffuse source)	WWTP effluent (Point source)
Ammonium	mg/l	Yes	Yes
Chloride	mg/l	Yes	Yes
Chlorophyll-a	mg/l	Yes	No
Discharge	m ³ /d	Already available from hydrodynamic process based model	Yes
Kjeldahl nitrogen	mg/l	Yes	Yes
Nitrate	mg/l	Yes	Yes
Oxygen	mg/l O ₂	Yes	No
Phosphate	µg/l	Yes	Yes
Suspended particulate matter	mg/l	Yes	Yes
Total nitrogen	mg/l	Yes	Yes
Total phosphorus	µg/l	Yes	Yes
Water temperature	°C	Yes	No

Empirical model

Table 5.43 shows the abiotic and biotic parameters used in the empirical model. The data used in the Empirical Model (EM) was measured at 93 locations in the Dinkel catchment and at 342 in the Regge catchment with the same hydrodynamical and geomorphological characteristics. The

⁵ A boundary is the location where water discharges enter the model system. These boundaries are based on the location where tributaries enter into the main channel.

monitoring frequency of the measurements differed per parameter and location from once every several years to biweekly, but was most often very low.

Table 5.41. Abiotic and biotic parameters used for the empirical model.

Parameter	Unit
Depth	m
Flow speed	m/s
Oxygen	%
Secchi depth	m
Suspended particulate matter	mg/l
Total nitrogen	mg/l
Total phosphorus	µg/l
Water temperature	°C
Width	m
Emergent, floating, and submerged macrophytes composition	%
Fish species composition	n
Macroinvertebrate species composition	n

5.4.3 Data pre-processing

Some data conversions were necessary in order to use the data in the PM and EM. In this section these conversions are discussed.

5.4.3.1.1 Process model

The data for the process based model needed to be pre-processed both for the input of the baseline of the model and for the different scenarios. This section describes which data transformations were used for both the baseline and the scenario models.

BASELINE MODEL

The units of the meteorological data were transformed to the units of SOBEK, see Appendix 12.4.

Not all water quality data had the same resolution, which is necessary in order to fill the missing values. The following pre-processing steps were applied:

- If there was no data in a certain year, the data of the nearest previous year was used to fill in the gap.
- If there was no data on a certain boundary, the nearest upstream monitoring location was used to fill in the gap.
- If a parameter needed to be calculated the following formulas were used:
 - Adsorbed phosphate AAP = 0.8 * (Total Phosphorus – Phosphate)
 - Detrital Carbon = Chlorophyll-a * 0.03
 - Detrital Nitrogen = Kjeldahl Nitrogen - Ammonium
 - Detrital Phosphorus = 0.2 * (Total Phosphorus – Phosphate)

Very little chlorophyll-a data was available. Therefore, monthly chlorophyll-a values from monitoring location 36-003 were used for all locations (Table 5.44). These monthly values were only available between April-September, for the other months a value of 0.001 was assumed.

Table 5.42. Chlorophyll-a values from monitoring location 36-003

	Chlorophyll-a (mg/l)
April	0.008
May	0.015
June	0.024
July	0.018
August	0.013
September	0.012

The boundaries of the model did not overlap completely with the monitoring locations. Therefore, the monitoring locations were handpicked based on their closeness to the boundary (but preferably not in the main stream itself) and data availability. If more than one location was available, the values of both locations were averaged per month as an input value for the boundary. Finally, the values were interpolated with a block interpolation over time. This means that the missing values were filled with the last available value. For the exact coordinates of monitoring locations per boundary see Appendix 12.4.

SCENARIOS

A linear scaling method was used to translate the data from the coarser scale of the climate models to the finer scale of the process-based model, based on an example excel script by Shrestha (2015). In Shrestha's excel script monthly correction factors are calculated for climate model data, based on differences in monthly averages between real and modelled over a historical time period. Accordingly, for the Dinkel catchment the data of the meteorological station Twente and each of the two climate models were compared for the period 2006-2015 and monthly correction factors were calculated for air temperature, air pressure, rainfall and irradiance. These correction factors were subsequently applied to the climate model data of the periods 2024-2036 and 2054-2066.

The evaporation for the scenarios was calculated based on the Makkink method as described in Elbers et al. (2009).

The land use change from grassland to agricultural area was calculated by taking the Top10NL map with terrain identification from <https://www.pdok.nl/nl/producten/pdok-downloads/basis-registratie-topografie/topnl/topnl-actueel/top10nl>, after which the percentages of available grassland per LGSI area could be calculated from these maps. Finally the amount of change in each MARS scenario was calculated from this value and subtracted from the non-drained area percentages in the LGSI model. The assumption here was that all arable land is drained, only grassland is not drained. The percentage of change was subtracted proportionally from both high and low areas in the LGSI model.

The drainage depth was calculated by subtracting 20 cm of the current drainage level in the high areas in the baseline LGSI model.

The amount of surface water abstraction in each scenario was determined per LGSI area and based on the amount of ground water abstraction (parameter Q_{wout}) per LGSI area in the baseline model. The surface water abstraction nodes were placed downstream from the LGSI nodes.

The amount of urban area that was specified in the model was calculated as a fraction, based on maps of the current urban area in the baseline model. The increase in urban area was calculated per LGSI area and the run off from each paved area entered the system slightly downstream of each LGSI node. For the water quality substances and concentrations of the run off see Appendix 12.4.

5.4.3.1.2 Empirical model

The data for the empirical model needed to be pre-processed. This section describes which methods were used to make the data suitable for the empirical modelling.

Biotic and abiotic parameters were often not measured in the same year or at the same time. Therefore, ten year averages (2000-2010) were calculated for each parameter to create a full dataset.

The abiotic parameters for the empirical model were averaged per summer period (May-September) and per year if there were at least two data points available. These summer and yearly averages were then used to calculate ten year averages.

Benchmark indicators 4 and 5 (mean duration of high and low flow pulses within each year) were calculated based on SOBEK model results. First the hourly data was aggregated to daily averages, after which the 10th or 75th percentile was calculated within each year. Then the amount of days for each uninterrupted period was calculated and averaged for 2000-2010.

The ecological variables such as fish, macroinvertebrates and macrophytes, each had their own transformation:

- For fish, the data was filtered on the sampling method electrical fishing and net fishing. Subsequently, the species abundance at each site was summed to reach a total fish abundance per site.
- For macroinvertebrates, the species data was transformed into average score per taxon (ASPT) values and the functional feeding group ratio (FFGr) of grazers and scrapers to shredders, gatherers and collectors. The ASTERICS software was used to calculate the ASPT, while the freshwater ecology database was used to determine the functional feeding groups. The species data had to be linked to the two databases using the Latin names of the species. This meant that for many species the data had to be checked manually, since not all species names were recognized. In these cases the following method was applied:
 - If the unrecognized species had a slightly different spelling (nigrum - nigra) or abbreviation to indicate a clade, then the suggestion of the database was copied.
 - If the unrecognized species were not in the database, but the family of the species was there, they were appointed to the family.

- If the unrecognized species was not in the database, nor was its family, then this species was removed from the dataset.

The ASPT, FFGr, fish abundance and macrophyte coverages were averaged over a ten year period (2000-2010).

For the ranges, spatial distribution and histograms of these data see Appendix 12.4.

5.4.4 Methods

This section explains how the process-based and empirical models work, how their performance was checked and what some of the considerations are in regard to the modelling results.

5.4.4.1.1 Processed based model

Model settings

For the processed based modelling, a SOBEK-model including Lowland Ground water Surface water Interaction (LGSI) model was used. The overall model comprised both hydrology and water quality. The hydrological part of the model described the hydrology of the Dinkel catchment and its main streams. The water quality part of the model described the water temperature and nutrient concentrations of the system.

SOBEK is a 1D-2D modelling suite that can model (amongst others) flood forecasting, optimization of drainage systems and surface water quality. It allows for the simulation of the interaction of water and water related processes in time and space. The SOBEK-model that was used in this project consisted of:

- A rainfall-runoff model (LGSI) to calculate the amount of ground- and surface water flowing from the tributaries into the Dinkel catchment (Kuijper et al., 2013).
- A 1D hydrodynamic model (SOBEK) for the calculation of the direction and flow velocity of the water in the Dinkel (Deltares, 2014b).
- The 1D water quality module (DELWAQ) for the calculation of water quality processes in the surface water of the Dinkel catchment, including the modelling of water temperature (Deltares, 2014a).

An overview of the model schematization is shown in Figure 5.66. A catchment overview of the model is shown in Figure 5.67.

LGSI models are lumped rainfall runoff models for which the knowledge is derived from a more complex semi 3D groundwater model. In this case the WRD-2012-model was used (Kuijper et al., 2012; Hendriks et al. 2014). LGSI models calculate the groundwater head and groundwater discharge and are especially suited to take into account groundwater baseflow. The LGSI model of the Dinkel catchment is used as a boundary condition for SOBEK, thereby connecting groundwater flow to surface water flow.

A detailed description of the hydrological SOBEK model and the LGSI implementation can be found in Kuijper et al. (2013) and Hydrologic and Deltares (2014).

The output from the LGSI model, together with the pre-processed water quality measurements formed the model input at the SOBEK/DELWAQ model boundaries (inflow points). The black dots in Figure 5.68 show these inflow points in the SOBEK/DELWAQ model.

For simulation of the baseline situation the LGSI/SOBEK/DELWAQ model was run for the years 2000-2012. The input data consisted of:

Hydrological modelling

- Rainfall (mm/hour)
- Evaporation (mm/day)
- Profiles of the water channels (m)
- Catchment areas (m²)
- Discharges (m³/s)
- Hydraulic resistance: k-Strickler (20 m^{1/3}/s)
- Information on water control structures
- Land use data
- Digital terrain model
- Soil data
- Groundwater depth data
- Drainage and abstraction data

Water quality modelling

- Water temperature (°C)
- Surface irradiance (W/m²)
- Relative air humidity (%)
- Percentage sunshine (%)
- Air pressure (mbar)
- Air temperature (°C)
- Chloride (mg/l)
- Oxygen (mg/l)
- Ammonium (mg/l)
- Nitrate (mg/l)
- Phosphate (mg/l)
- Inorganic matter (mg/l)
- Adsorbed phosphate (mg/l)
- Detrital Carbon (mg/l)
- Detrital Nitrogen (mg/l)
- Detrital Phosphorus (mg/l)
- Chlorophyll-a (mg/l)

The model was run with the numerical solver 15 and a simulation time step of 1hour. The numerical solver determines how the equations of DELWAQ are solved. Numerical solver 15 is an iterative solver based on the generalised minimal residual method. A detailed explanation of this solver can be found in the DELWAQ (D-WAQ) User Manual (Deltares, 2014a).

For an overview of all activated surface water quality processes see Appendix 12.4.

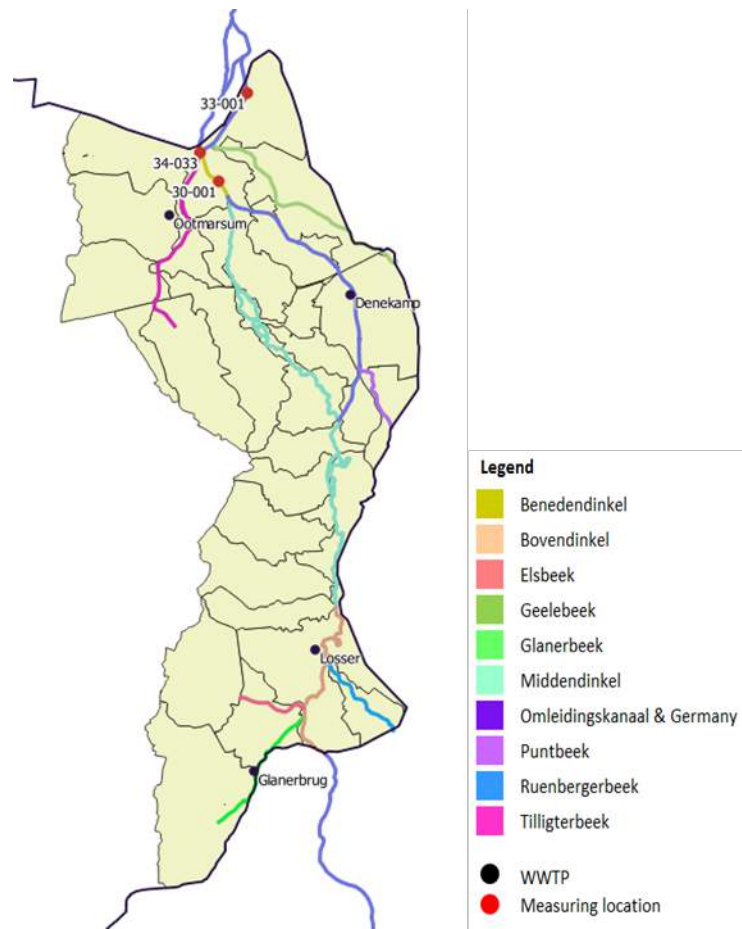


Figure 5.68 Overview of the LGSI areas (light brown), SOBEK/DELWAQ model schematization (coloured lines), calibration monitoring locations (red dots) and waste water treatment plants (black dots) in the process-based model. More than three calibration points were used for building the LGSI-model and the SOBEK model. The monitoring locations shown are used to calibrate the DELWAQ model.

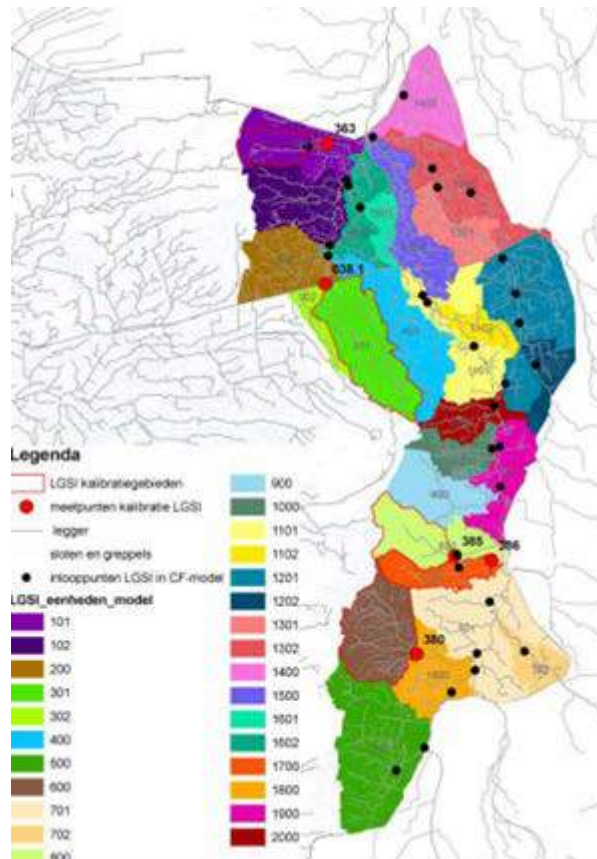


Figure 5.69 LGSi areas (coloured areas) and inflow points (black dots) into the SOBEK/DELWAQ model. Red dots are the calibration points of the of the corresponding red-rimmed areas in the LGSi model.

Calibration

Calibration and validation of the hydrological LGSi/SOBEK part of the model (water levels and discharges) was described by Hydrologic and Deltares (2014).

The output of the baseline of the LGSi/SOBEK/DELQAQ model was checked visually by comparing the model output at the monitoring locations 30-001, 33-001 and 34-033 for the substances chloride, chlorophyll-a, nitrate, phosphate, water temperature, total phosphate, total nitrogen, oxygen and suspended particulate matter between 2000-2012 with the measurements that were available for these substances and locations in this period (Figure 5.67; see results in chapter 4). Monitoring locations 30-001 and 33-001 were chosen based on the fact that they are the locations positioned most downstream in the Dutch part of the Dinkel catchment and that they

contain different water ways of the Dinkel catchment⁶. Monitoring location 34-033 was chosen for the fact that it is a downstream location that does not receive water from Germany.

Furthermore, for the same substances and locations the outputs were checked via target diagrams (Joliff et al., 2008; Los & Blaas, 2010). Target diagrams are a more objective way to check the performance of a model. They show the differences between the model and the measurements by plotting the difference in mean (bias) and the amount of deviation (root-mean-square deviation, RMSD).

Confidence

There are some points which should be kept in mind while looking at the results of the process-based model. These are:

- Not all biological processes were activated in this model application. The model has been kept as simple as possible, while still obtaining good results. This might mean that some important processes have been overlooked.
- Since the goal of the model was to run scenarios and use the output to indicate a percentage of change, the calibration was less stringent.
- The resolution of the input data was not optimal for all boundaries. Still, some assumptions and corrections had to be made on the data. For the current time period this is the best there is.
- Water quality was not modelled in the LGSI-model. This means that the different flow routes distinguished in the LGSI-model were not given different water quality characteristics. This means that changes of loads of substances that can be expected by changes in flow processes, such as more phosphorous outflow caused by increase in the occurrence of overland flow events, are not included in the process model. As a result, changes in climate and in water management scenarios will change total water fluxes, dynamics of water fluxes and concentrations of substances (e.g. dilution) at the model boundaries. Measures and changes in nutrient management will change loads of substances.

⁶ Water from the Tilligterbeek and Geelebeek will flow to location 33-001, while all other streams will flow to location 30-001.

5.4.4.1.2 Empirical model

Model setup

First, a selection of environmental variables was made for each ecological response variable. The selection of variables was based on their relation to the four key questions mentioned in the Introduction (total nitrogen, total phosphorus, flow velocity, water temperature, width/depth ratio), their ecological relevance (oxygen, suspended particulate matter, light availability) and on the possibility to model these parameters with the process-based model.

Then, these environmental parameters were checked visually on outliers with boxplots and histograms. Outliers were further inspected, but only removed if their presence seemed highly unlikely (~ 4 times the standard deviation).

After this, the correlation between the environmental parameters was checked visually in plots and by their variance inflation factor value (VIF). A VIF above 8 indicates multicollinearity and should be avoided. Therefore, the abiotic indicators with a VIF value above 8 were removed one by one. Each time checking the correlation plots to see which interaction was taking place and removing the parameter that seemed least likely to influence the biotic indicator.

The remaining set of parameters was used for further analysis of their importance for describing the ecological response variable with BRT's, as described in the MARS WP4 data analysis cookbook by Segurado et al. (2015). The bag fraction⁷ was set on 0.5 and the tree complexity⁸ on 2, as advised in Segurado et al. (2015). The learning rate⁹ of the model was chosen iteratively as to get a number of trees between 1000-1500, according to the rule of thumb of Elith et al. (2008) to allow for at least a 1000 trees. For submerged, emergent and floating macrophytes the learning rate was set to 0.002, 0.0025 and 0.001 respectively. For the ASPT and the FFGr the learning rate was set to 0.005 and 0.0028 respectively. For the fish abundance the learning rate was set to

⁷ Some stochasticity usually improves the accuracy and speed of a model. In addition to this it can also reduce overfitting. The stochasticity of the BRT is controlled by the bag fraction. The bag fraction specifies the proportion of data to be selected at each step. This means that with a bag fraction value of 0.5, 50% of the data is drawn at random from the full data set at each iteration. Elith et al. (2008).

⁸ Tree complexity indicates the number of nodes in a tree (Elith et al., 2008).

⁹ The learning rate determines the amount of contribution of each tree as it is added to the model. A smaller learning rate shrinks the contribution of each tree to the model. Elith et al. (2008).

0.0007. The parameters and interactions that came out of the BRT's were then used for the general linear models (GLM).

Before calculating the GLM's all abiotic variables were log-transformed ($\log(x+\min(x)+0.01)$) and scaled, to create a more normal distribution and standardize the environmental variables.

After calculating each GLM the Akaike information criterion (AIC) value was determined. The AIC value is a measure of the relative quality of a statistical model and provides a way for model selection. The model with the lowest AIC value chosen as the most suitable model to connect the abiotic to the biotic variables.

The GLM's were build according to the following steps:

- GLM 1: All interactions and parameters as suggested by the BRT modelling.
- GLM 2: All parameters as suggested by the BRT modelling.
- GLM 3: Only the parameters that were significant in GLM 1 and 2.
- GLM 4, 5 and 6: only the parameters and interactions as suggested by the main questions.
- GLM 7: If applicable, including parameters and/or interactions to GLM 3 that turned out to be significant in model 4, 5, and/or 6.
- GLM 8: If applicable, including spatial filters to the GLM (1-7) with the lowest AIC value.

The GLM's residuals were checked for normality and the variance was checked for homogeneity, to see if the model was fit for general use. The GLM was also tested with the Moran's I test for effects due to spatial differences. If these effects were present in the model, the model was updated with spatial filters that removed this spatial dependence.

The specifics of the GLM modelling procedure can be found in Segurado et al (2015).

The analysis was done with statistical software R (R Core Team, 2016).

Confidence

- The macrophyte models do not have a normally distributed set of residuals. This means that they might not be suitable for general use. For macrophytes, the data on submerged, emergent and floating macrophytes contained many zero's (16, 18, and 24 % for submerged, emergent and floating macrophytes respectively), which may have influenced the outcomes of their GLM models unduly. Further analysis could try to split the data into a presence and

absence component and a without-zero's component and try to see if the overall results remain the same if these two datasets are analysed.

- The analysis of the data would have been more robust if the biotic data would have been recorded around the same time as the abiotic data. This could be an improvement for the monitoring in the Dinkel catchment.
- Due to the averaging, it is possible that the water temperature effect that we see could be due to changes in seasonality. The period of April – September is quite long.
- Connectivity, substrate and shading also play an important role in the ecosystem. It would be good to try to include these in further analysis.

Due to the limited availability of discharge data it was not possible to include Bind 4 or 5 in the empirical models.

5.4.4.1.3 Scenario implementation

The scenario implementation was done according to the changes indicated in Table 5.45 and 5.46. Table 5.45 shows an overview of the storyline elements and their translation into model parameters. Table 5.46 shows the total amount of change per model parameter.

For the climate change input, data from five ISIMIP climate models were available. To facilitate the choice of one of these climate models, we analysed which model gives median results for each climatic model cell (Kuijper & Sanchez, 2015). The methodology followed consisted of finding the model that gave the median cumulative precipitation over the period 2006-2099 per model cell of 0.5 degrees. For all case studies it appeared that either model GFDL-ESM2M or model IPSL-CMA-LR are amongst the models that represent the median cumulative precipitation for that case study. It was therefore decided to apply the outcomes of GFDL-ESM2M and model IPSL-CMA-LR for each climate scenario in each case study. In the Dinkel models the climate change parameters that were changed based on these two models and the three scenarios were: rainfall, evaporation, irradiance and air temperature.

For each scenario the inputs for rainfall, evaporation and irradiance were adjusted in the SOBEK model. The LGSI adjustments in the form of the groundwater abstraction, area size, drained area fraction, and drainage depth were adjusted via the SACRMNTO.3B file. The adjustments in water temperature, total nitrogen and total phosphorus for the boundaries and WWTP inputs were changed in the BOUNDWQ.DAT file.

For the period of 2030 the years 2024 – 2036 were calculated, for the period of 2060 the years 2054 – 2066 were calculated. An overview of the scenarios that were run is presented in Table 5.47

Table 5.43. Storyline interpretation for the Dinkel case study

Storyline element	Techno World -		Consensus World -		Survival of the fittest -		Translation to model	Model
	MARS ad hoc World		MARS World		No MARS World			
	I D	Description of change	I D	Description of change	ID	Description of change		
Agricultural areas for crops	+ +	50% grassland to agriculture/horticulture. +20% GW abstraction	+ +	25% grassland to agriculture/horticulture. +1 0% GW abstraction	++ +	100% grassland to agriculture/horticulture. +40% GW abstraction	Changes in land use are not part of the process-based model. Therefore, the change from grassland to agriculture / horticulture has been translated to an effect on the amount of drained area. The assumption is that grassland is not drained and agricultural area is always drained.	LGSI
Use of fertilizers (NOT manure)	+	+25% fertilizer use. Increase of agricultural production but in an efficient way.	+ +	+10% fertilizer use. Agricultural production is increased, but 'green cycle' techniques are used and measures are taken to prevent leakage to the environment.	++ +	+50% fertilizer use due to increase of agricultural production.	The use of fertilizer is not a parameter in the process-based model. This change has therefore been translated into a change in diffuse total nitrogen and total phosphorus concentrations.	DELWAQ
Nutrient load (due to manure)	+ +	+50% livestock	+ +	+25% livestock	++ +	+100% livestock	Livestock is not a parameter in the process-based model. This change has therefore been translated into a change	DELWAQ

Storyline element	Techno World -		Consensus World -		Survival of the fittest -		Translation to model	Model
	MARS ad hoc World		MARS World		No MARS World			
	I D	Description of change	I D	Description of change	ID	Description of change		
							in diffuse total nitrogen and total phosphorus concentrations.	
WWTP load	+ +	+25% load due to population growth	+ +	+10% load due to population growth	++ +	+50% load due to population growth	Population growth is not a parameter in the process-based model. This change has therefore been translated into a change in total nitrogen and total phosphorus concentrations coming from WWTP's.	DELWAQ
Urbanization	+ +	+25% urban area	+ +	+10% urban area	++ +	+50% urban area	An increase in urban area has been translated into an increase surface runoff due to a larger paved area.	SOBEK
Overexploitation of water resources by industry & urban areas	+ +	+50% water use	+ +	+20% water use	++ +	+100% water use	Groundwater abstractions	LGSI
Control drainage (water retention in fields)	0	No measures are taken to store water, water is taken from the surface water: +25% surface	+ +	Water retention and EFN measures. 100% of drainage is controlled drainage.	---	No measures are taken to store water or for EFNs. Water is taken from the groundwater: +25%	Drainage depth to increase GW levels for controlled drainage. Qwout LGSI & SOBEK SW abstraction	LGSI & SOBEK
Environmental flow needs covered	+	water abstractions	+ +		---	groundwater abstractions.		

Storyline element	Techno World -		Consensus World -		Survival of the fittest -		Translation to model	Model
	MARS ad hoc World		MARS World		No MARS World			
	I D	Description of change	I D	Description of change	ID	Description of change		
Natural water retention measures (holding onto water for use in dry periods)	+		+ +		--			
(Loss of)riparian zones (in favour of touristic areas, agriculture, etc.)	+	-25% riparian zones. +5% NP. Small water temperature increase.	0	Restoration of riparian zones +10%. -2% NP. Small water temperature decrease.	++ +	-100% riparian zones. All riparian zones are removed. +20% NP. Water temperature increase.	Less riparian zones means more light and a higher water temperature in the stream (less shadow), also more overland inflow of nutrients: decrease loss coefficient for NP	DELWAQ
Restoration of riparian zones	-		+ +		---			

Table 5.44. Model implementation of the storylines. The changes are relative according to the baseline situation.

Model	Location	Parameter name	Parameter description	Techno World	Consensus World	Survival of the fittest world
				MARS ad hoc World	MARS World	No MARS World
LGS1	SACRMNTO.3B	fAsdN & fAsdG	Fraction non drained area in infiltrating and draining areas	50% of grassland becomes drained	25% of grassland becomes drained	100% of grassland becomes drained
		DdrG	Drainage depth of infiltrating areas	No change	Drainage raised by 20 cm	No change

		Qwout	Infiltration and/or groundwater abstraction	+75%	+30%	+165%
SOBEK	Schematization	Paved surface node	Paved surface	+25%	+10%	+50%
		Lateral node	Surface water abstraction	+25%	No change	No change
DELWAQ	Boundary files	AAP, PO4, DetP, DetN, NO3, and NH4 for all boundaries	Total Nitrogen and Total Phosphorus concentration from a diffuse source	+80%	+37%	+170%
		AAP, PO4, DetP, DetN, NO3, and NH4 for all boundaries	Total Nitrogen and Total Phosphorus concentration from WWTP	+25%	+10%	+50%
		Temperature for all boundaries & WWTP	Water temperature	-25% riparian zones: +0.5°C	+10% riparian zones: -0.2°C if 12.5°C+	-100% riparian zones: +2°C

Table 5.45. Overview of the scenario runs.

Name	Climate model	RPC scenario	Storyline	Horizon*
Baseline	None	None	None	2006
Scenario_NO_stT_2000	None	None	Techno world	2006
Scenario_NO_stS_2001	None	None	Fragmented world	2006
Scenario_NO_stC_2002	None	None	Consensus world	2006
Scenario_G8_O_2030	GFDL-ESM2M	8.5	None	2030
Scenario_G4_O_2030	GFDL-ESM2M	4.5	None	2030
Scenario_I8_O_2030	IPSL-CM5A-LR	8.5	None	2030
Scenario_I4_O_2030	IPSL-CM5A-LR	4.5	None	2030
Scenario_G8_O_2060	GFDL-ESM2M	8.5	None	2060
Scenario_G4_O_2060	GFDL-ESM2M	4.5	None	2060
Scenario_I8_O_2060	IPSL-CM5A-LR	8.5	None	2060
Scenario_I4_O_2060	IPSL-CM5A-LR	4.5	None	2060
Scenario_G8_stT_2030	GFDL-ESM2M	8.5	Techno world	2030
Scenario_G8_stS_2030	GFDL-ESM2M	8.5	Fragmented world	2030
Scenario_G4_stC_2030	GFDL-ESM2M	4.5	Consensus world	2030
Scenario_I8_stT_2030	IPSL-CM5A-LR	8.5	Techno world	2030
Scenario_I8_stS_2030	IPSL-CM5A-LR	8.5	Fragmented world	2030
Scenario_I4_stC_2030	IPSL-CM5A-LR	4.5	Consensus world	2030
Scenario_G8_stT_2060	GFDL-ESM2M	8.5	Techno world	2060
Scenario_G8_stS_2060	GFDL-ESM2M	8.5	Fragmented world	2060
Scenario_G4_stC_2060	GFDL-ESM2M	4.5	Consensus world	2060
Scenario_I8_stT_2060	IPSL-CM5A-LR	8.5	Techno world	2060
Scenario_I8_stS_2060	IPSL-CM5A-LR	8.5	Fragmented world	2060
Scenario_I4_stC_2060	IPSL-CM5A-LR	4.5	Consensus world	2060

* 'Horizon' refers to the following modelling periods: 2006: 2000-2012, 2030:2024-2036; 2060: 2054-2066.

5.4.5 Results

This section contains the results from the process-based model and the empirical models.

5.4.5.1.1 Process based-model

The process-based model was first calibrated and validated for the baseline period of 2000-2012. After which twenty-two scenario runs were done. This section shows the results for the baseline period and the twenty-two scenario runs.

Baseline model validation

The process-based model was calibrated and validated for the locations 30-001, 33-001 and 34-033 for the 13-year period between 2000-2012 (see Figure 5.67 for locations). Monitoring point 30-001 is located in the main river Dinkel. At this location the discharge of the entire upstream catchment, of which roughly 75% originates from Germany, converges. Monitoring point 33-001 has a much smaller upstream catchment but also receives water from Germany. The discharge at monitoring point 34-033 is all generated in the Dutch part of the Dinkel catchment. The three monitoring locations are used for validation, however, since the scenarios in this case study are chosen to only affect the Dutch part of the Dinkel catchment (to reflect the amount of influence of the Dutch waterboard), the results of the different scenarios will only be discussed for point 34-033 (WFD surface water body Tilligterbeek).

With respect to the comparison between the model results and the measurements, the following observations can be made based on graphs and target diagrams of Figures 5.69, 5.70, 5.71 and 5.72:

- The modelled chloride concentrations fit the measurements at all locations quite well, for both average absolute values as well as the dynamics. Modelled Cl-concentrations at location 33-001 are on average a little bit too high, but within the same order of magnitude as the measurements.
- Chlorophyll-a measurements were not present for the more recent years or for location 34-033, the validation was therefore based on the earlier years and only on location 30-001 and 33-001. For location 30-001 the chlorophyll-a concentration is reasonably modelled according to the target diagram. At location 33-001 the chlorophyll-a

concentration is underestimated which is likely to be the result of a too low input of chlorophyll-a at the LGSi-nodes. Real chlorophyll-a data was lacking for many locations, therefore the only available signal was used for all locations.

- The water temperature at all locations is modelled very well for both average absolute values as well as the seasonal fluctuations.
- The average concentrations of total nitrogen and nitrate are a little bit too high at all locations. However, they follow the yearly pattern quite well. Location 30-001 shows a much better fit than locations 33-001 and 34-033.
- The total phosphorus and phosphate concentrations fit the data on average quite well. However, based on the target diagrams it appears that some of the variation in both concentrations is missed.
- The oxygen concentrations fit the data at all locations reasonably to good. With the exception of the oxygen concentrations at the beginning of 2000, which fit the measured data for location 30-001 and 34-033 quite poorly.
- The solid particulate matter is modelled on average reasonably well to good at location 33-001 and 34-033. At location 30-001 the model frequently underestimates the amount of variation (RMSD), but fits the data on average quite good.

The water levels and discharges of the entire Dinkel catchment were well calibrated and validated in a previous study. These results can be found in Hydrologic & Deltares (2014) and are not be repeated in this report.

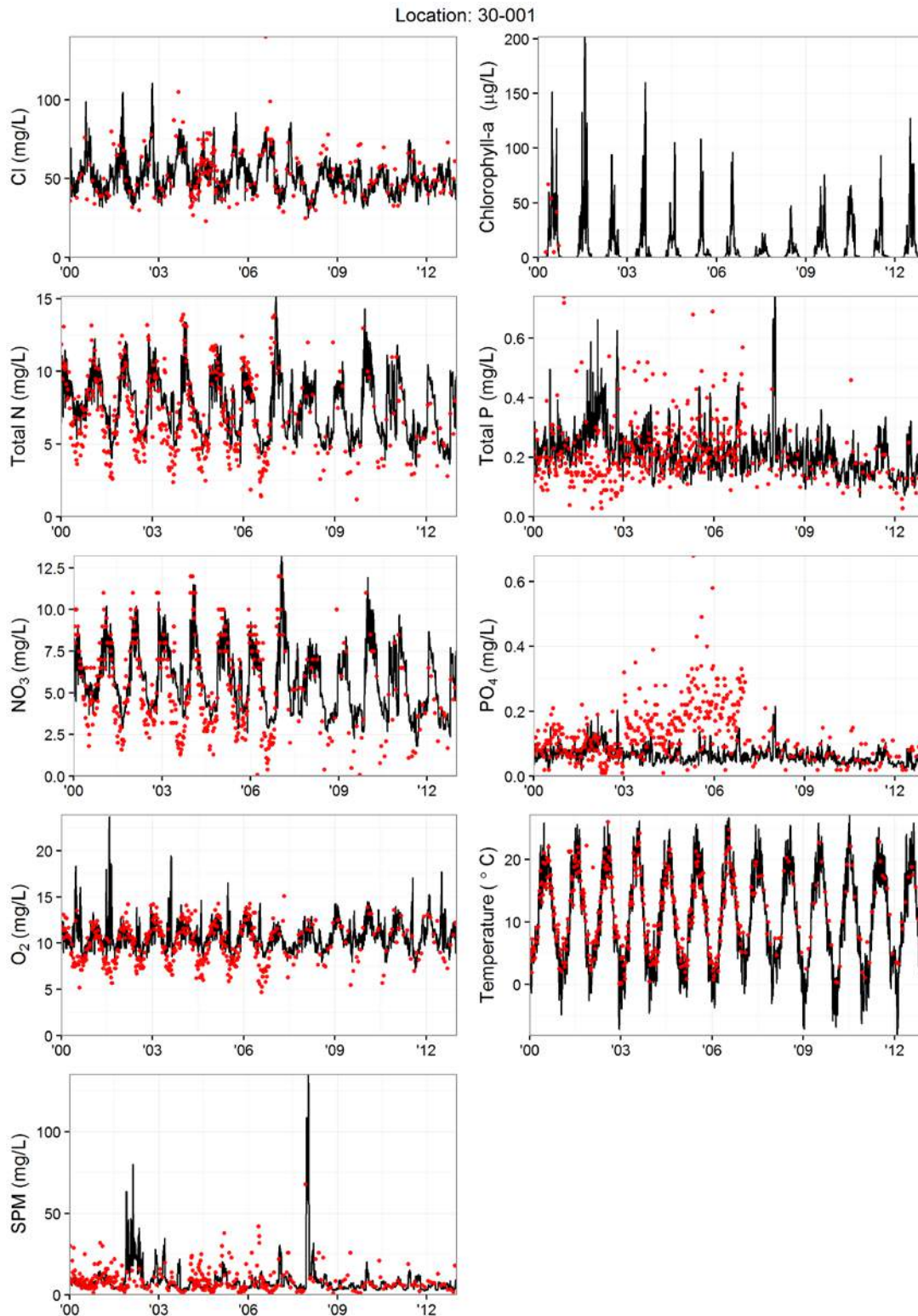


Figure 5.70 Modelled and measured data for 2000-2012 for location 30-001. The modelled data are indicated by the solid black line and the measured data are indicated by the red dots. From top to bottom and from left to right: Chloride, chlorophyll-a, total nitrogen, total phosphorus, nitrate, phosphate, oxygen, water temperature and solid particulate matter.

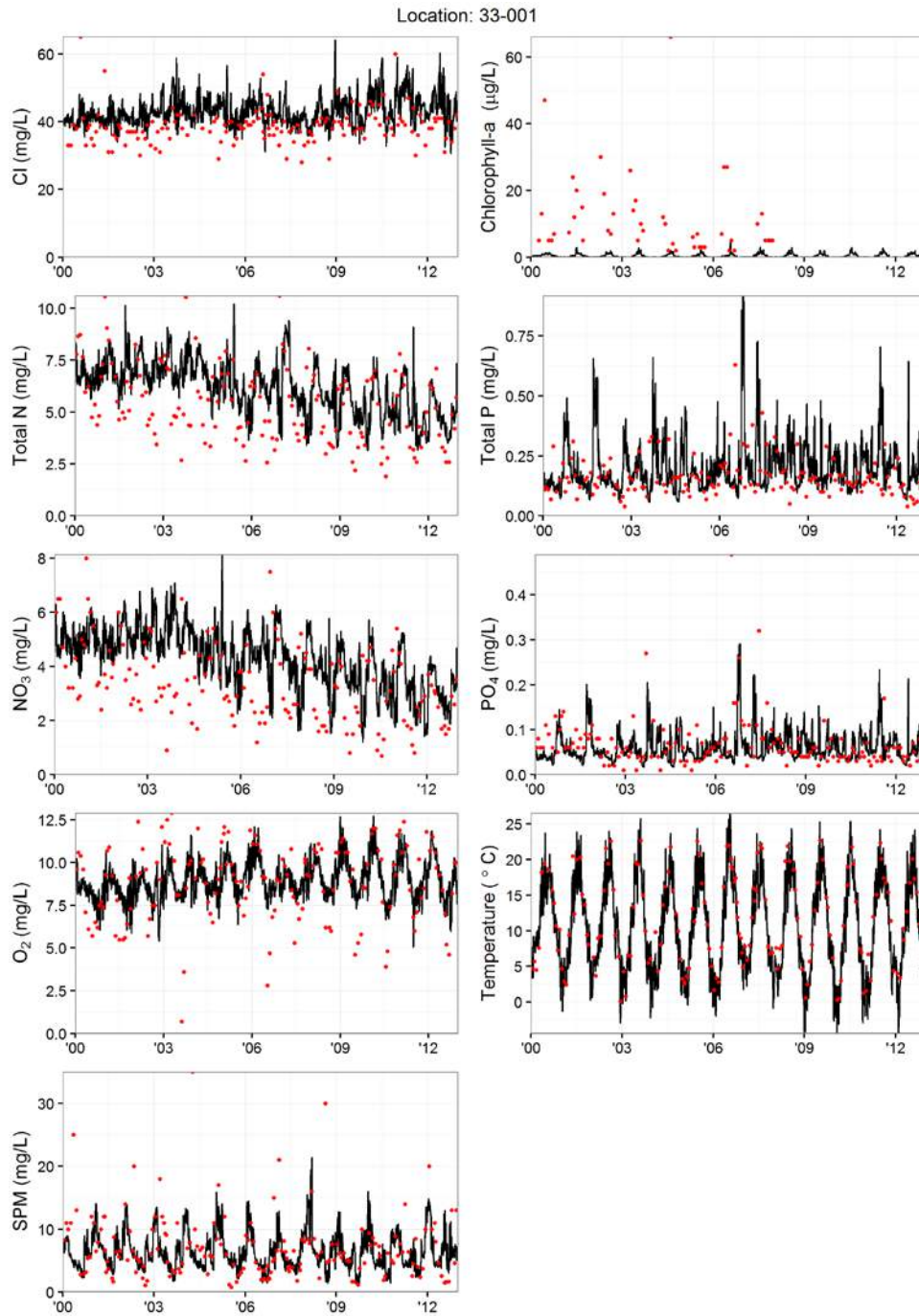


Figure 5.71 Modelled and measured data for 2000-2012 for location 33-001. The modelled data are indicated by the solid black line and the measured data are indicated by the red dots. From top to bottom and from left to right: Chloride, chlorophyll-a, total nitrogen, total phosphorus, nitrate, phosphate, oxygen, water temperature and solid particulate matter.

Location: 34-033

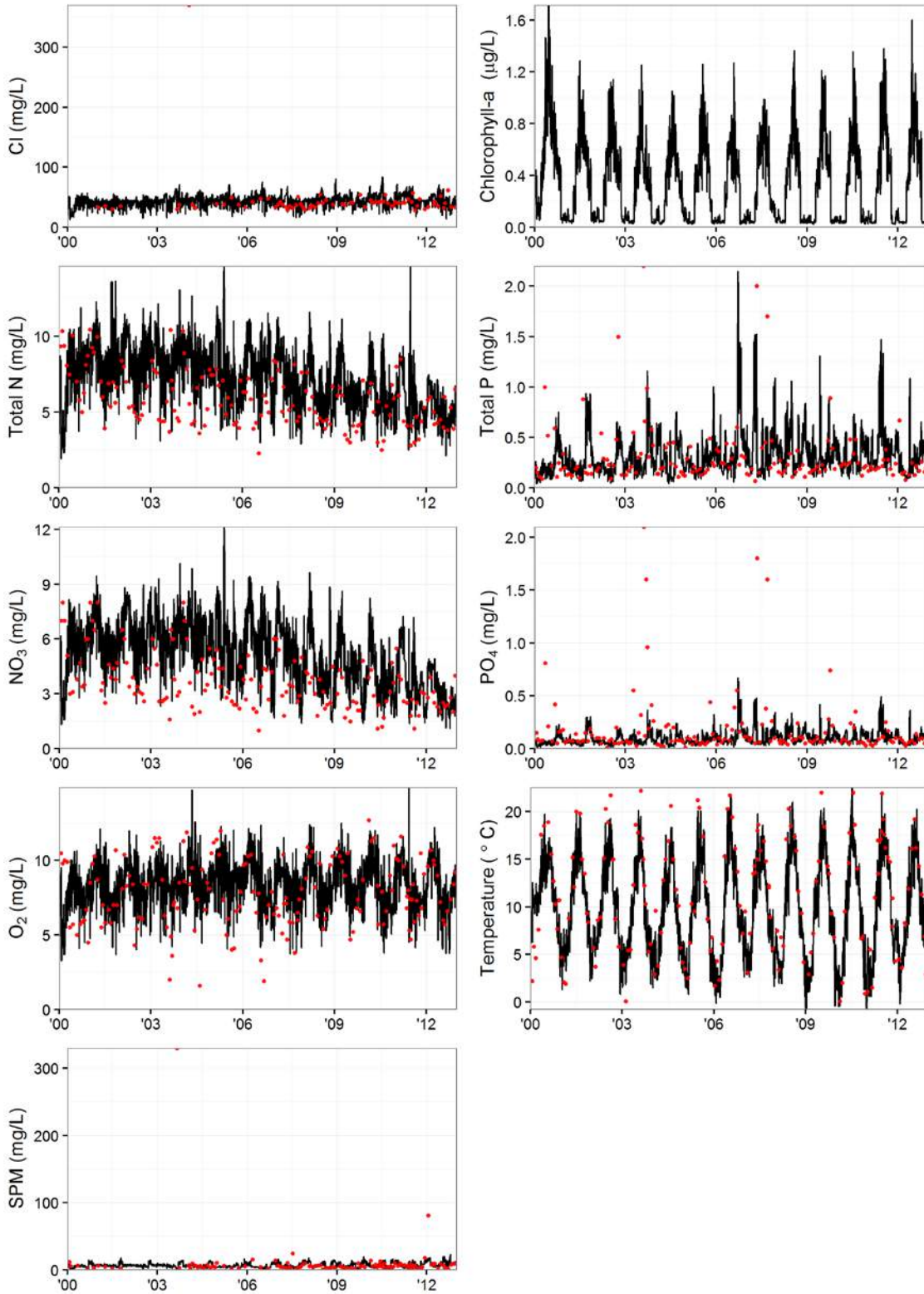


Figure 5.72 Modelled and measured data for 2000-2012 for location 34-033. The modelled data are indicated by the solid black line and the measured data are indicated by the red dots. From top to bottom and from left to right: Chloride, chlorophyll-a, total nitrogen, total phosphorus, nitrate, phosphate, oxygen, water temperature and solid particulate matter.

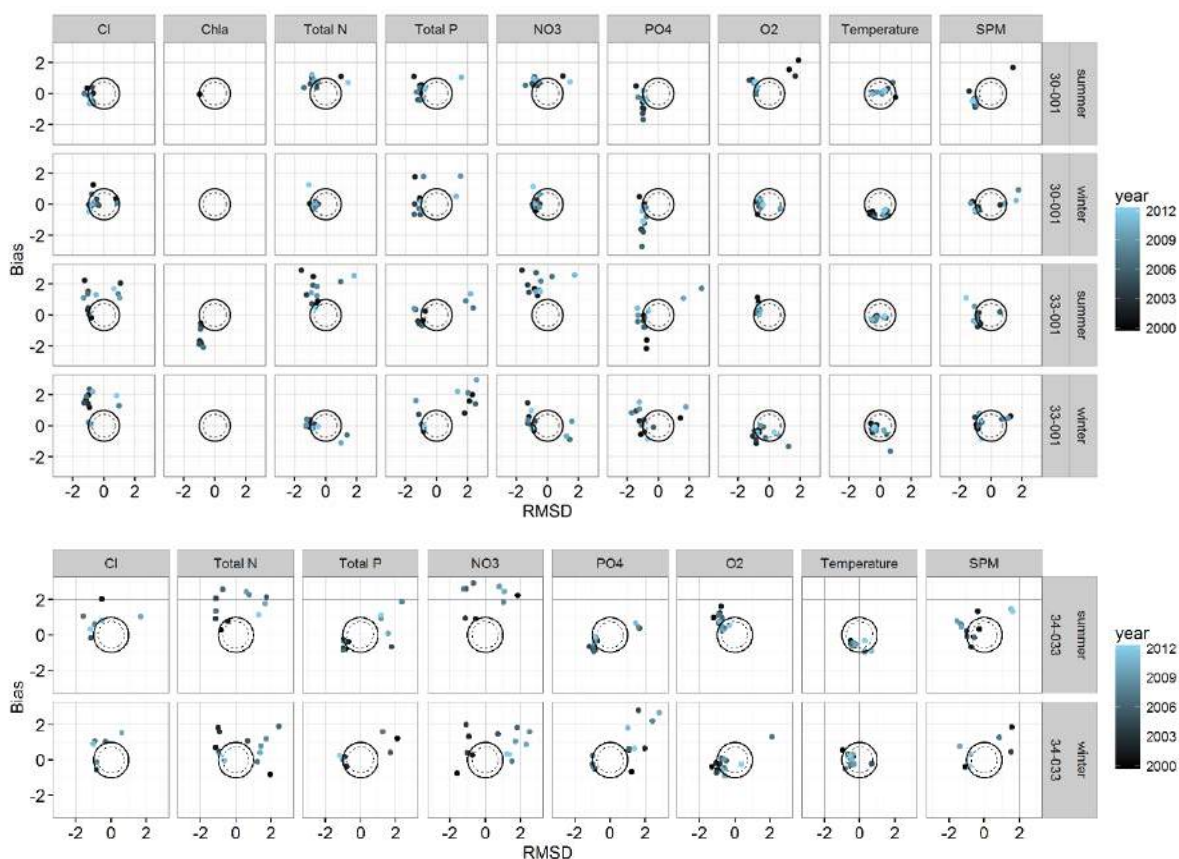


Figure 5.73 Target diagram showing the normalized bias and signed, normalized, unbiased root-mean square deviance of the model results with respect to the observations. The results are shown for the locations 30-001, 33-001 and 34-033 for the winter and summer months between 2000 and 2012. The years are indicated by colour. From left to right: chloride, chlorophyll-a, total nitrogen, total phosphorus, nitrate, phosphate, oxygen, water temperature and suspended particulate matter. The x axis shows the root mean-squared-deviance (RMSD), which tells us whether the pattern of the model matches the pattern of the data, and the y axis shows us the bias, which tells us whether the mean of the model matches the mean of the data. Results within the drawn circle with overall score RMSD = 1 score at least 'reasonable', while results within the dashed circle RMSD = 0.74 score 'good'.

Baseline abiotic status

For location 34-033 (Tilligterbeek) the calculated abiotic state variables are summed in Table 5.48. For the Tilligterbeek the water framework directive (WFD) standard for total nitrogen and total phosphorus for a good ecological status are respectively 2.3 and 0.11 mg/l (summer averages). From Table 5.48 it can be seen that considering both total nitrogen and total phosphorus the Tilligterbeek is far from a good ecological status. According to the WFD standards the status for both abiotic states is classified as poor. For comparison: in the river basin management plan (RBMP) total phosphorus in 2009 was reported as bad in the

Tilligterbeek (i.e. more than 0.44 mg P/l) and total nitrogen was reported as moderate (2.3 - 4.6 mg N/l). The same modelling results are found for almost all streams in the Dinkel catchment. It is clear that diffuse pollution from agriculture are responsible for these high nutrient concentrations.

For flow conditions there are no official WFD-standards available and instead Dutch-standards are used (Van der Molen and Pot, 2007 and Hendriks et al., 2014). According to these standards, the minimum summer flow velocity should be between 0.1 and 0.5 m/s, whereas the Tilligterbeek has average flow velocities of 0.05 m/s in summer and 0.11 m/s in winter. This is probably due to low discharges and the presence of weirs in the stream which slow down the flow velocity significantly.

From the modelled and measured abiotic states it can be concluded that multiple stressors are active resulting in too low flow velocities and too high nutrient loads, affecting the ecological status of the streams in the Dinkel catchment. How much each of the stressors contributes to the poor ecological status and how they interact cannot be derived directly from the current process model results.

Table 5.46. Calculated abiotic state variables for monitoring location 34-033. The values are averaged for the 13-year period 2000-2013.

Variable	Unit	summer	winter	Year
AAP	mg/l	0.19	0.21	0.20
Chlfa	mg/l	0.51	0.14	0.33
Cl	mg/l	45.2	43.3	44.2
DetN	mg/l	1.3	1.4	1.3
DetP	mg/l	0.02	0.03	0.03
IM1	mg/l	6.1	8.2	7.1
NH4	mg/l	0.7	0.8	0.8
NO3	mg/l	5.2	5.3	5.2
OXY	mg/l	8.4	8.6	8.5
PO4	mg/l	0.09	0.11	0.10
SaturOXY	mg/l	10.5	12.5	11.5
TotN *	mg/l	7.1	7.5	7.3
TotP *	mg/l	0.30	0.35	0.32
Temp	°C	13.4	6.1	9.8
TempAir	°C	14.8	5.3	10.1
Discharge	m ³ /s	0.32	0.66	0.49
Flow velocity	m/s	0.05	0.11	0.08
Water Level	m AD	17.6	17.6	17.6
bind4	number			6.2
bind4.length	days			15.9
bind5	number			4.1
bind5.length	days			9.8

* WFD standards:

Tot-N: good <= 2.3 mg/l, moderate 2.3-4.6 mg/l, poor 4.6-9.2 mg/l, bad >-9.2 mg/l.

Tot-P: good<= 0.11 mg/l, moderate 0.11-0.22 mg/l, poor 0.22-0.44 mg/l, bad >=0.44 mg/l.

Scenarios

The scenarios are a combination of climate change scenarios and storylines. In this section, the effects of the different climate change scenarios will be described first, followed by the differences between the storylines (without climate effects). Subsequently, the effects of the combinations of climate change and storylines are discussed.

Only effects on water temperature and flow conditions are discussed since the calculations for solute concentrations are still underway. These effects will be described in a supplementary report.

DIFFERENCES BETWEEN CLIMATE MODELS

Figure 5.73 shows the average yearly rainfall and air temperature for the different climate models and the baseline model, during the period around 2000 (baseline), 2030 and 2060. A large fluctuation can be seen between the different years and it becomes directly visible that individual years cannot be compared with each other. Changes of rainfall patterns, air temperature, evaporation and irradiance in the different climate models are reflected over periods longer than one year (e.g. due to different recurrence intervals of extreme drought events). Thus, comparing individual years is not meaningful. We therefore averaged the results of the different climate models over periods of 13 years before comparing them with each other. The same is done for all scenarios (storylines and climate-storyline-combinations).

The average values over the 13-year period (summer, winter, and yearly) of the climate characteristics rainfall, evaporation, air temperature and irradiance are given in Table 5.49. The table shows that compared to the current baseline situation the average rainfall will decrease for all climate models. However, there are large differences between summer and winter for the different climate models. For example, all climate models produce a lower rainfall in summer but an increase in winter rainfall is found for models G4 and I8. The summer evaporation rates increase for all climate models compared to the current situation. The air temperature will increase significantly for all climate models, for both winter and summer with the highest increase of 2.6 °C for model I8. The irradiance will increase for all climate models during summer and a decrease is found for the winters.

Table 5.47. Characteristics of the baseline climate (year 2000) and the four climate change scenarios for 2060 horizon (all characteristics are averaged over a period of 13 years).

Climate element	season	unit	Baseline	G4	G8	I4	I8
rainfall	summer	mm/d	2.2	1.9	1.9	2.1	1.8
rainfall	winter	mm/d	2.1	2.2	2.0	1.9	2.2
rainfall	year	mm/d	2.1	2.0	1.9	2.0	2.0
evaporation	summer	mm/d	2.6	2.8	2.7	2.7	2.8
evaporation	winter	mm/d	0.6	0.6	0.6	0.6	0.6
evaporation	year	mm/d	1.6	1.7	1.6	1.7	1.7
air temperature	summer	°C	14.9	15.9	16.3	16.2	17.0
air temperature	winter	°C	5.3	6.6	6.9	6.8	8.3
air temperature	year	°C	10.1	11.2	11.6	11.5	12.7
irradiance	summer	W/m ²	181.0	194.6	184.7	185.0	188.0
irradiance	winter	W/m ²	50.0	48.4	48.5	55.4	47.0
irradiance	year	W/m ²	115.7	121.6	116.7	120.3	117.6

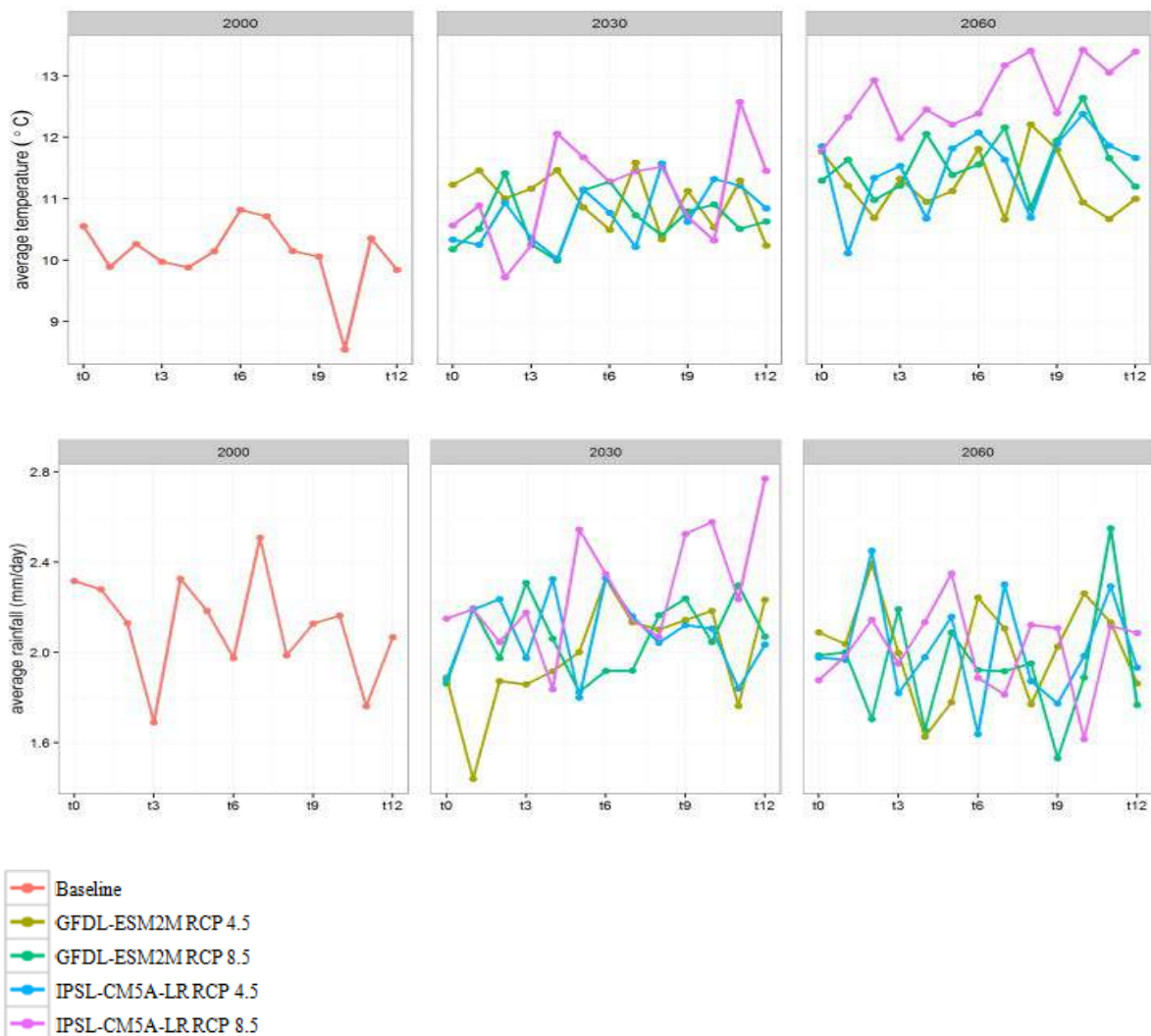


Figure 5.74 Yearly average rainfall and air temperature per climate model and climate scenario for the periods 2000, 2030 and 2060. T0-T12 (2000) = 2000-2012, T0-T12 (2030) = 2024-2036, T0-T12 (2060) = 2054-2066.

To compare the effects of the different climate scenarios, the baseline model was run with the climate model's input for the 2060 time horizon. Figure 5.74 shows the different cumulative frequency discharge (Q-cum) diagrams at location 34-033. The four climate models produce more or less comparable Q-cum diagrams whereas the deviation with the baseline model is very large. The calculated discharges are much higher for the baseline model and also the peak discharges are more frequent for the baseline model than for the climate models. From this result, one could conclude that this is the result of climate change. However, since the results of the four climate models are very similar to each other, it is more likely that the explanation must be found in the methodology of applying the climate models. In this case, for the baseline model, real meteorological data provided by a local meteorological station of The Royal Netherlands Meteorological Institute (KNMI) is used, whereas the climate models are the result of calculations on a very large scale. A linear scaling method is used to correct the climate model input for the local situation. This linear correction was applied on monthly data, neglecting the variations on daily and hourly time scale. This could explain the large deviations in calculated discharge between the baseline model and the climate models, since the responsible processes (like rainfall, drainage, run-off, evaporation) are acting on a much smaller timescale (daily to hourly). Therefore, comparisons between the baseline model and the climate models may not be appropriate and should be done with care. Comparisons between the different climate models can be done without any doubt, since the method of generating input data was equal.

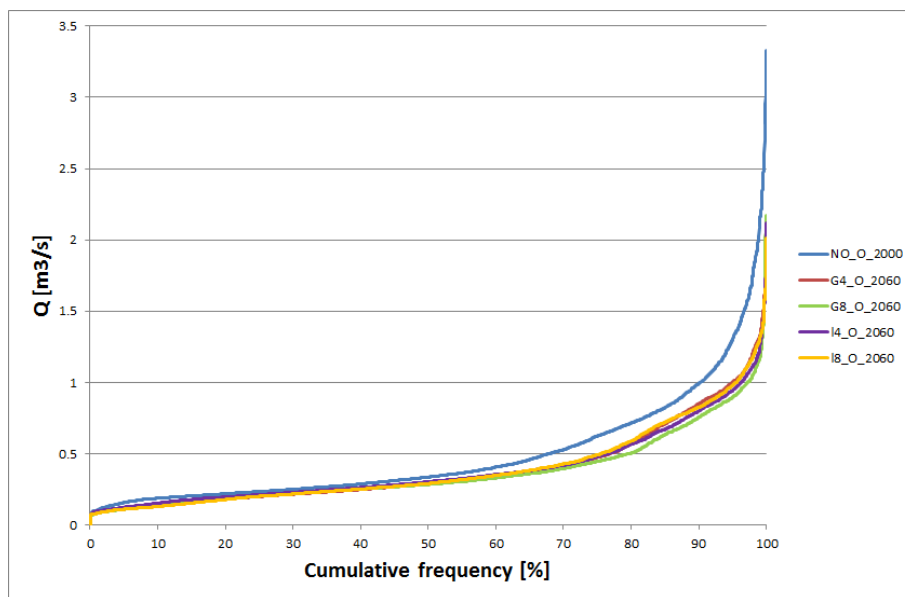


Figure 5.75 Cumulative frequency diagrams of the calculated discharge (for 13 years) at location 34-033 for the four different climate models (horizon 2060) and the baseline model (NO_O_2000).

In Table 5.50 and 5.51 the state variables with respect to water temperature and flow conditions are summed for the different climate scenarios. For all climate models, the water temperature increases both in winter and summer. As described above, drawing conclusions based on absolute increases compared to the baseline may not be appropriate.

Remarkable is that the increase in temperature is almost twice as high for stream water temperature than for air temperature. This is probably the result of a decrease in stream discharge and flow velocity which makes it easier to warm up the stream water. Decreases in groundwater base flow are not reflected in the model results, as the LGSI model does not calculate water quality and water temperature changes, but might further enhance the warming effect (see also chapter 5).

The decrease of the yearly average stream discharge is in the order of 20% for all climate models which is due to less rainfall and higher evaporation rates. Flow velocities only decrease slightly. The change in the benchmark indicators Bind4 and Bind5 show that high flow conditions as well as low flow conditions will occur more frequently with consequently shorter duration.

In general, the results show that climate model IPSL-CM5A-LR (indicated with I in tables) has a stronger effect than climate model GFDL-ESM2M (indicated with G in tables) and that RCP scenario 4.5 (indicated with 4 in tables) has a lighter effect than RCP scenario 8.5 (indicated with 8 in tables), which is to be expected. Furthermore, the differences between the climate models IPSL-CM5A-LR and GFDL-ESM2M are larger than the differences in the RCP 4.5 or RCP 8.5 climate scenarios.

Table 5.48.The calculated abiotic state variables for temperature and flow conditions (average values over period of 13 years), for the different scenarios (climate, storylines and combination of climate and storylines).

variable	period	baseline	climate				storey line			combi cs					
		NO_O	G4_O	G8_O	I4_O	I8_O	NO_C	NO_S	NO_T	G4_C	G8_S	G8_T	I4_C	I8_S	I8_T
		2000	2060	2060	2060	2060	2000	2000	2000	2060	2060	2060	2060	2060	2060
Temp (°C)	summer	13.44	15.78	16.01	15.81	16.69	13.45	14.39	14.05	15.93	17.23	16.85	15.92	17.96	17.52
TempAir (°C)	summer	14.84	15.88	16.24	16.19	16.99	14.84	14.84	14.84	15.88	16.24	16.24	16.19	16.99	16.99
Discharge (m³/s)	summer	0.32	0.23	0.24	0.26	0.23	0.28	0.23	0.18	0.21	0.17	0.11	0.23	0.16	0.10
Velocity (m/s)	summer	0.05	0.04	0.05	0.05	0.04	0.05	0.04	0.03	0.04	0.03	0.02	0.05	0.03	0.02
Water Level (m AD)	summer	17.64	17.50	17.50	17.50	17.50	17.64	17.63	17.63	17.50	17.50	17.50	17.50	17.50	17.50
Temp (°C)	winter	6.11	7.76	7.98	8.15	9.47	5.86	6.22	6.10	7.61	8.57	8.15	8.01	10.05	9.65
TempAir (°C)	winter	5.33	6.58	6.91	6.80	8.36	5.33	5.33	5.33	6.58	6.91	6.91	6.80	8.36	8.36
Discharge (m³/s)	winter	0.66	0.55	0.50	0.53	0.56	0.60	0.48	0.48	0.51	0.36	0.35	0.49	0.40	0.40
Velocity (m/s)	winter	0.11	0.10	0.09	0.10	0.10	0.10	0.08	0.08	0.09	0.07	0.06	0.09	0.07	0.07
Water Level (m AD)	winter	17.55	17.52	17.52	17.52	17.52	17.55	17.54	17.54	17.52	17.51	17.51	17.52	17.51	17.51
Temp (°C)	year	9.78	11.78	12.00	11.99	13.09	9.66	10.31	10.08	11.78	12.91	12.51	11.97	14.01	13.59
TempAir (°C)	year	10.09	11.24	11.58	11.50	12.68	10.09	10.09	10.09	11.24	11.58	11.58	11.50	12.68	12.68
Discharge (m³/s)	year	0.49	0.39	0.37	0.39	0.39	0.44	0.36	0.33	0.36	0.26	0.23	0.36	0.28	0.25
Velocity (m/s)	year	0.08	0.07	0.07	0.07	0.07	0.07	0.06	0.05	0.07	0.05	0.04	0.07	0.05	0.05
Water Level (m AD)	year	17.59	17.51	17.51	17.51	17.51	17.59	17.59	17.59	17.51	17.51	17.50	17.51	17.51	17.51
bind4 (nr)	year	6.17	7.15	6.66	7.33	8.00	5.71	5.12	5.60	6.30	4.35	5.52	6.14	6.08	6.64
bind4.length (d)	year	15.92	13.85	14.31	14.15	12.00	16.62	18.69	17.15	15.54	21.85	17.23	16.00	16.46	14.38
bind5 (nr)	year	4.14	4.40	4.66	5.04	5.14	4.40	4.38	4.99	4.85	4.21	4.59	5.47	4.46	4.95
bind5.length (d)	year	9.77	9.38	8.62	8.38	7.77	9.77	9.31	9.46	8.85	9.38	8.54	8.69	8.77	7.92

Table 5.49.The calculated change in abiotic state variables for temperature and flow conditions, for the different scenarios (climate, storylines and combination of climate and storylines): blue increase, red decrease, compared to the baseline.

variable	period	baseline	climate				storey line			combi cs					
		NO_O	G4_O	G8_O	I4_O	I8_O	NO_C	NO_S	NO_T	G4_C	G8_S	G8_T	I4_C	I8_S	I8_T
		2000	2060	2060	2060	2060	2000	2000	2000	2060	2060	2060	2060	2060	2060
Temp	summer	13.44	2.34	2.58	2.37	3.25	0.02	0.95	0.61	2.49	3.79	3.41	2.48	4.52	4.08
TempAir	summer	14.84	1.05	1.40	1.35	2.15	0.00	0.00	0.00	1.05	1.40	1.40	1.35	2.15	2.15
Discharge (m³/s)	summer	0.32	-0.09	-0.08	-0.06	-0.09	-0.03	-0.09	-0.14	-0.11	-0.15	-0.21	-0.08	-0.16	-0.21
Velocity (m/s)	summer	0.05	-0.01	0.00	0.00	-0.01	0.00	-0.01	-0.02	-0.01	-0.02	-0.03	0.00	-0.02	-0.03
Water Level (m AD)	summer	17.64	-0.14	-0.14	-0.13	-0.14	0.00	0.00	0.00	-0.14	-0.14	-0.14	-0.13	-0.14	-0.14
Temp	winter	6.11	1.65	1.87	2.04	3.36	-0.25	0.11	-0.01	1.50	2.46	2.04	1.90	3.94	3.54
TempAir	winter	5.33	1.25	1.58	1.47	3.04	0.00	0.00	0.00	1.25	1.58	1.58	1.47	3.04	3.04
Discharge (m³/s)	winter	0.66	-0.11	-0.16	-0.14	-0.11	-0.06	-0.18	-0.18	-0.15	-0.31	-0.32	-0.18	-0.26	-0.26
Velocity (m/s)	winter	0.11	-0.01	-0.02	-0.02	-0.01	-0.01	-0.03	-0.03	-0.02	-0.05	-0.05	-0.02	-0.04	-0.04
Water Level (m AD)	winter	17.55	-0.03	-0.03	-0.03	-0.03	0.00	-0.01	-0.01	-0.03	-0.04	-0.04	-0.03	-0.04	-0.04
Temp	year	9.78	2.00	2.22	2.21	3.31	-0.12	0.53	0.30	2.00	3.13	2.73	2.19	4.23	3.81
TempAir	year	10.09	1.15	1.49	1.41	2.59	0.00	0.00	0.00	1.15	1.49	1.49	1.41	2.59	2.59
Discharge (m³/s)	year	0.49	-0.10	-0.12	-0.10	-0.10	-0.05	-0.13	-0.16	-0.13	-0.23	-0.26	-0.13	-0.21	-0.24
Velocity (m/s)	year	0.08	-0.01	-0.01	-0.01	-0.01	-0.01	-0.02	-0.03	-0.01	-0.03	-0.04	-0.01	-0.03	-0.03
Water Level (m AD)	year	17.59	-0.08	-0.08	-0.08	-0.08	0.00	-0.01	-0.01	-0.08	-0.09	-0.09	-0.08	-0.09	-0.09
bind4 (nr)	year	6.17	0.98	0.50	1.16	1.83	-0.46	-1.04	-0.56	0.13	-1.81	-0.64	-0.02	-0.08	0.48
bind4.length (d)	year	15.92	-2.08	-1.62	-1.77	-3.92	0.69	2.77	1.23	-0.38	5.92	1.31	0.08	0.54	-1.54
bind5 (nr)	year	4.14	0.25	0.52	0.90	0.99	0.25	0.23	0.84	0.70	0.06	0.45	1.32	0.31	0.80
bind5.length (d)	year	9.77	-0.38	-1.15	-1.38	-2.00	0.00	-0.46	-0.31	-0.92	-0.38	-1.23	-1.08	-1.00	-1.85

DIFFERENCES BETWEEN STORYLINES

The individual effects of the three different storylines (without climate change effects) can be seen in Table 5.50. Since the storylines were also run for the present climate (without the climate change models), they can be compared with the baseline results (in Table 5.50 compare NO_C, NO_S and NO_T with the baseline NO_O). The results show that the effects of the storylines on water temperature and flow are small compared to the calculated climate change effects. However, since the absolute values of the climate models are uncertain and probably

not valid, the conclusion that climate change has a larger effect than the storylines on flow and water temperature cannot be drawn. For water temperature it is more likely that climate has a much more pronounced effect than the storylines. The mechanisms which could affect water temperature in the storylines are a change in flow conditions (discharge, water depth, velocity) and the change in riparian zone area. A decrease of the riparian zone leads to an increase in water temperature. The water in the ‘consensus world’ (NO_C) is slightly cooler than that of the baseline, while the water temperature in both ‘techno’ (NO_T) and ‘survival of the fittest’ world (NO_S) has become more than 0.5 degrees warmer. Only for the ‘consensus world’ storyline, an increase of the riparian zone is implemented which explains the calculated small decrease of water temperature. For both Techno world and Survival of the fittest world the water temperature was expected to increase due to the loss of riparian zones.

For all storylines, the discharge and flow velocity are influenced by an increase of run off from the urban areas and an increase of water abstractions (both surface water and groundwater), and to a smaller degree a raise of drainage level (only consensus world). Figure 5.75 and Table 5.51 shows that the net effect for every storyline is a significant decrease in stream discharge. For the summer period the discharge decreases with 10% for the consensus world, 28% for the survival of the fittest world and more than 40% for the ‘techno’ world. Consequently, a comparable decrease is calculated for flow velocity.

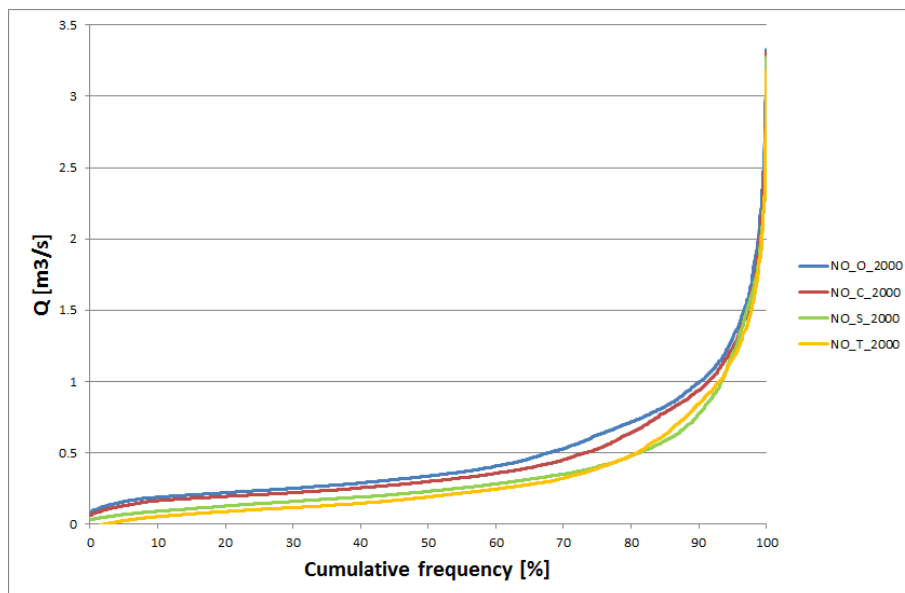


Figure 5.76 Cumulative frequency diagrams of the calculated discharge (for 13 years) at location 34-033 for the three storylines (period 2000) and the baseline model (NO_O_2000)

COMBINATION OF CLIMATE CHANGE AND STORYLINES

Six combinations of climate models and storylines are calculated with the model and results are summarized in Table 5.50. As already mentioned, the calculated impact of climate change cannot be compared with the baseline, and therefore a comparison between the combination-scenarios and the baseline is also not possible. However, the combi-scenarios can be compared with each other. Table 5.50 shows that combinations of the ‘techno world’ storyline with RCP 8.5 climate model output leads to the lowest discharge and lowest flow velocities during the summer period. Since climate has a much more pronounced effect on temperature than the storylines, the combination with the RCP 8.5 has the largest effects on both air and water temperature.

The results also show that the combination of climate change and storylines leads to a larger increase in water temperature than the summed single effects of climate and storyline. This is probably due to a non-linear response of water temperature to changes of stream discharge and flow velocity. The same, although to a much lesser degree, is valid for flow velocity. For discharge the opposite is found; the increase in discharge (Figure 5.76) is smaller for the combi-scenarios than when the single effects are summed. Further analysis of field data and model results is recommended to gain a better understanding of these non-linear processes.

According to the calculations, the decreases of stream discharge and flow velocity are in the same order of magnitude for the storylines and for the climate change models, keeping in mind that climate change effects may not be quantified correctly. Notwithstanding this climate change uncertainty, the combination of climate change and the storylines will certainly lead to a decrease of discharge and flow conditions. Climate change and the storylines thus show a *synergic effect* on the future discharge, deteriorating the ecological status of the streams.

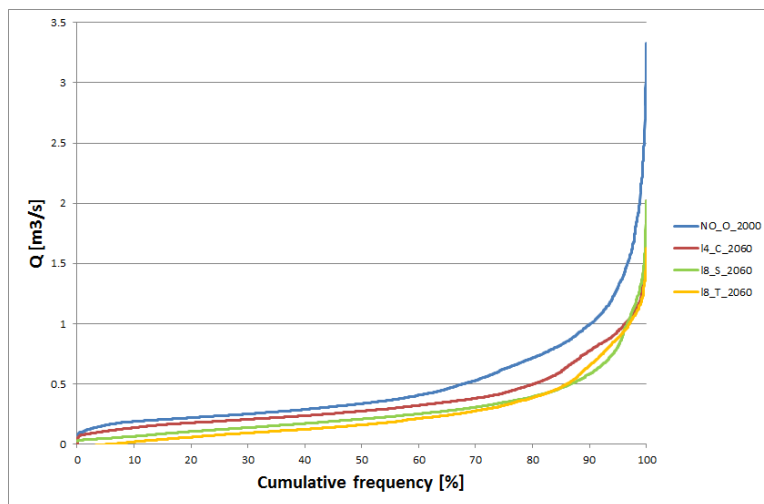
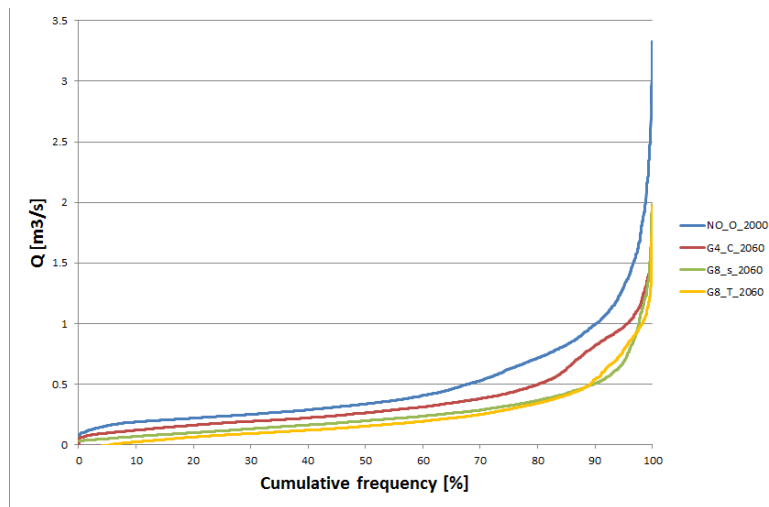


Figure 5.77 Cumulative frequency diagrams of the calculated discharge (for 13 years) at monitoring location 34-033 for the different scenarios comprised of a combination of a climate model and a storyline (period 2060) and the baseline model (NO_O_2000)

5.4.6 Empirical models

The empirical models were made for different biological quality elements, namely macrophytes (submerged, emergent and floating macrophyte cover), macroinvertebrates (ASPT and FFGr) and fish (total fish abundance). This section shows the results of the BRT's and GLM's grouped per element.

5.4.6.1.1 Macrophytes

Table 5.52 shows the BRT results for the submerged, emergent and floating macrophytes. The chosen abiotic parameters explain between 15.1% and 5.8% of the variance in the models, with cross validation variance varying between 7.7% and 1.8%. The variables that have an influence on the macrophyte cover, differ per macrophyte cover type. The relatively low explained variances for these abiotic parameters leave room for improvement. It would be advisable to widen the range of parameters in future studies.

For submerged macrophyte cover influential variables are: particulate matter (23%), water temperature (20.9%), width-depth ratio (16.6%), total P (15.7%), flow velocity (13.8%) and total N (9.7%). For emergent macrophyte cover, only flow velocity (66.9%) and water temperature (33%) are found to be influential.

For floating type macrophyte cover, flow velocity is most influential (42.5%), followed by total N (20.7%), total P (18.7%) and water temperature (18.1%).

Table 5.50. BRT results of macrophyte cover per macrophyte type. PM = particulate matter, T = Water temperature, WDR = Width-Depth ratio, TP = Total phosphorus, F = Flow velocity, TN = Total nitrogen. Based on summer decadal means of the abiotic variables.

	Macrophyte cover type					
	Submerged		Emergent		Floating	
Number of trees (-)	1500		1150		1000	
Explained variance of model	0.151		0.108		0.058	
Explained variance cross validation	0.077		0.046		0.018	
Relative influence (%)	PM	23.035	F	66.903	F	42.522
	T	20.969	T	33.097	TN	20.702
	WDR	16.627			TP	18.685
	TP	15.702			T	18.091
	F	13.873				
	TN	9.792				
Interactions (Top 3 and > 10) (%)	T * F	61.15	T * F	439.88	T * F	28.29
	PM * T	38.59				
	T * WDR	10.74				

For all macrophyte types an increase in macrophyte cover correlates with an increase in summer average *water temperature* (within the range of 10 to 22 °C) and a decrease in summer

average *flow velocity* (within the range of 0 to 0.2 m/s), see Figure 5.77 and 5.79. This does however not necessarily mean that an increase of water temperature and a decrease in flow velocity lead to an increase of macrophyte cover. In this case the relationship may well be the other way round: an increase in vegetation cover leads to a decrease in flow velocity, thereby increasing stream water temperature.

Furthermore, the data show relatively *low summer average flow velocities*, i.e. most below 0.2 m/s. Flow velocities for this type of surface water bodies (R5, continuously slow flowing middle and lower reaches on sand) are recommended between 0.1 and 0.5 m/s (Van der Molen and Pot, 2007). It may thus very well be possible that most macrophyte types in our database are the types that are currently adapted to low flow conditions and not the flow preferring types. A decrease in flow may then lead to a decrease in this type of macrophyte cover in favour of other submerged macrophyte types. The scatter plot in Figure 5.78 shows that the decrease in submerged macrophyte cover with decreasing flow velocity is mainly determined by the measured flow velocities below 0.2 m/s. For the measured flow velocities above 0.2 m/s an increase in submerged macrophyte cover could be concluded. For the emergent macrophytes this effect is not seen in Figure 5.78. Further analysis of the data behind the BRTs is recommended to determine the relevance of the higher flow velocity data points and to analyse if this part of the measurements indeed involves an increase of the flow preferring types due to increased flow velocities.

No measurements were available of water temperatures higher than 23 °C, making the current models unreliable for use with higher water temperatures.

The foremost interaction effect between *two* abiotic parameters was the same for all macrophyte type, i.e. the interaction between *water temperature and flow*. This could support our theory above. For submerged macrophyte cover also an interaction effect between particulate matter and water temperature and an interaction effect between water temperature and width-depth ratio was indicated by the BRT. The 3D plots of these interactions are shown in Figure 5.80.

The BRTs for nutrients (TN and TP) require further analysis. This analysis will be part of the work in MARS WP7.3.

None of the GLM's for macrophyte cover contained an interaction effect. All of the GLM's had a significant Moran's I value, which was corrected for with spatial filters. These spatially

corrected GLM's had a McFadden R^2 of 0.42, 0.26 and 0.21 for submerged, emergent and floating macrophytes respectively. An overview of the GLM's, their coefficients and their McFadden R^2 values can be found in Table 5.53. The residual plots (Appendix 12.4) show a distinct line. This line is probably due to several zero values present in the data. This line could be an indication that the GLM might not be suitable for general applications and that the results from this model should be interpreted with caution.

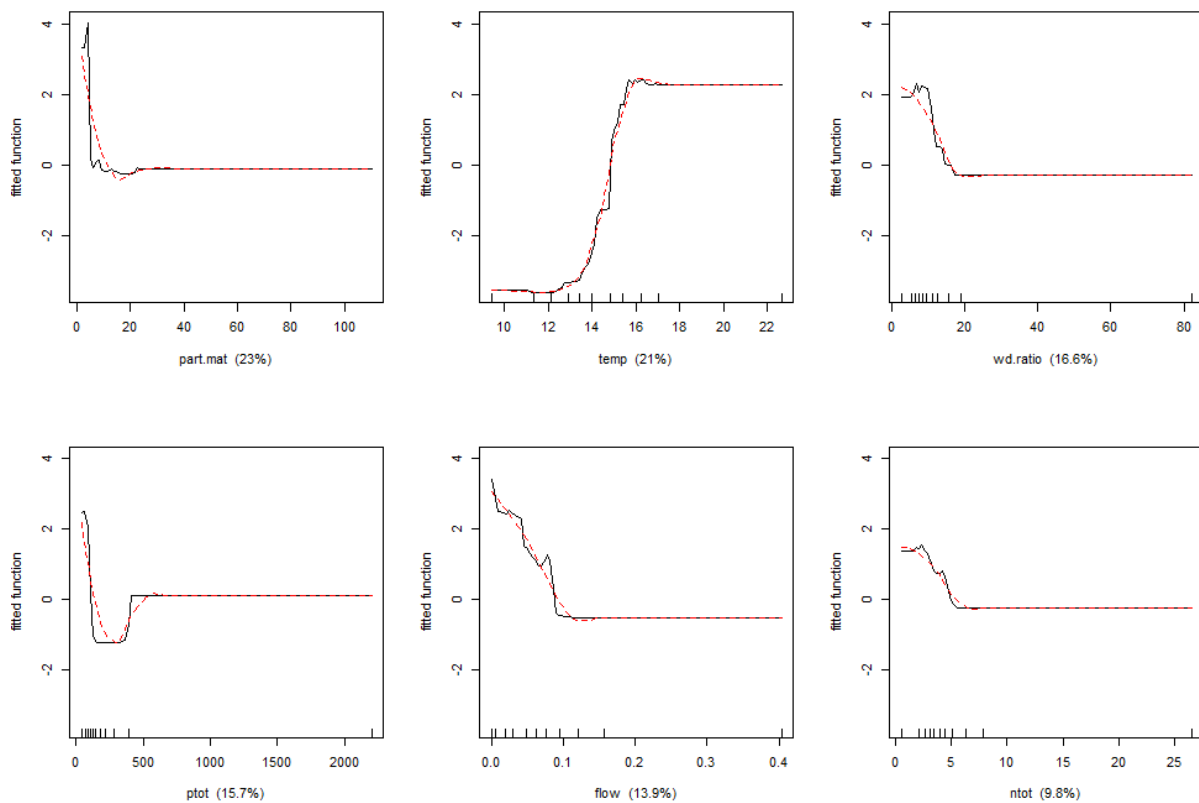


Figure 5.78 Partial dependence plots showing the BRT-fitted functions for submerged macrophyte cover. Y axis are on the log scale and centred to have a zero mean over the data distribution. The X axis indicates the data range of (from left to right and from top to bottom) particulate matter (mg/l, summer decadal mean), water temperature ($^{\circ}\text{C}$, summer decadal mean), width-depth ratio, total phosphorus ($\mu\text{g/L}$, summer decadal mean), flow velocity (m/s, summer decadal mean), and total nitrogen (mg/l, summer decadal mean). The tick marks give an indication of the data distribution.

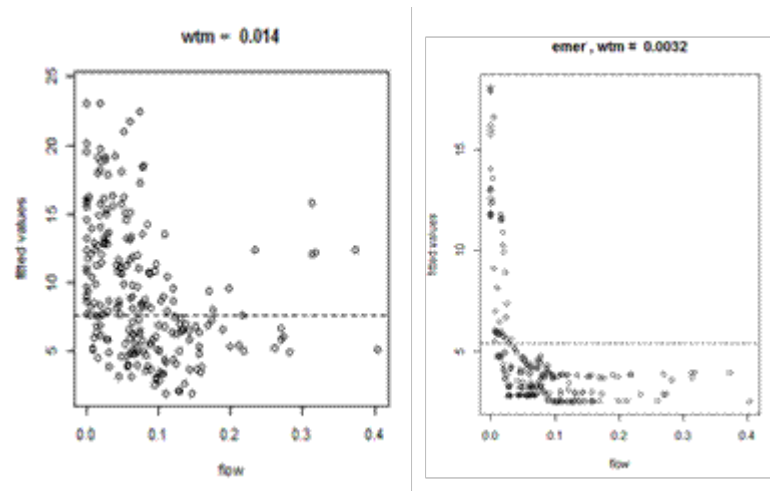


Figure 5.79 Partial responses of the BRT for flow velocity, for submerged (left) and emergent (right) macrophyte cover.

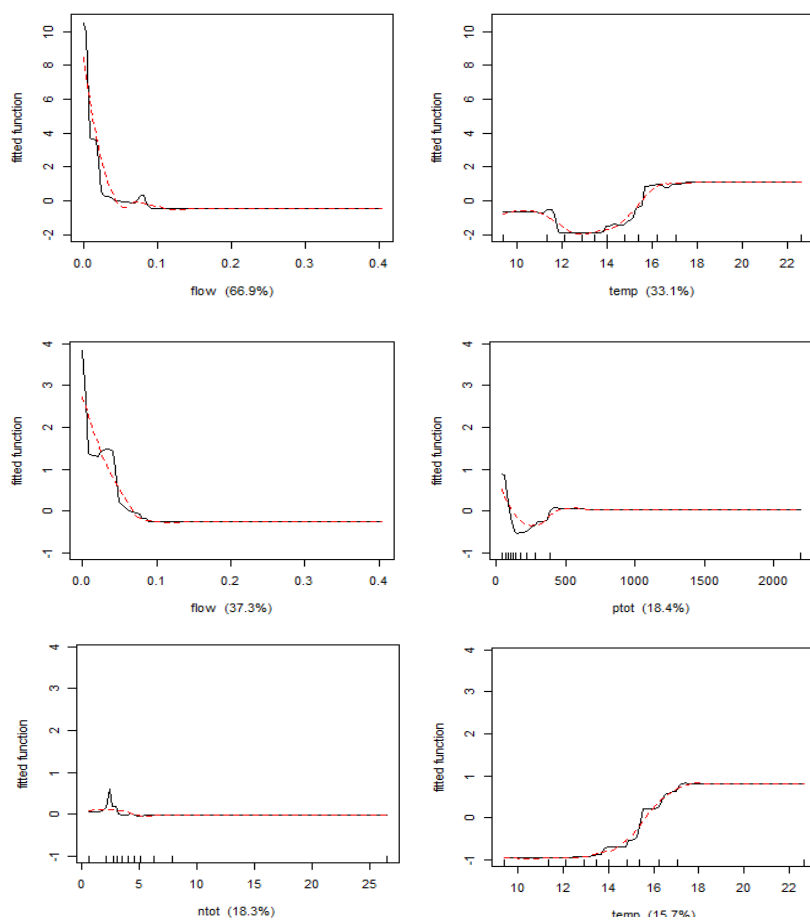


Figure 5.80 Partial dependence plots showing the BRT-fitted functions for emergent and floating macrophyte cover. The Y axis are on the log scale and centred to have a zero mean over the data distribution. The X axis indicates the data range of (from left to right and from top to bottom) emergent macrophytes for flow velocity (m/s, summer decadal mean) and water temperature ($^{\circ}\text{C}$, summer decadal mean) and for floating macrophytes for flow velocity (m/s, summer decadal mean), total phosphorus ($\mu\text{g/L}$, summer decadal mean), total nitrogen (mg/l , summer decadal mean), and water temperature ($^{\circ}\text{C}$, summer decadal mean). The tick marks give an indication of the data distribution.

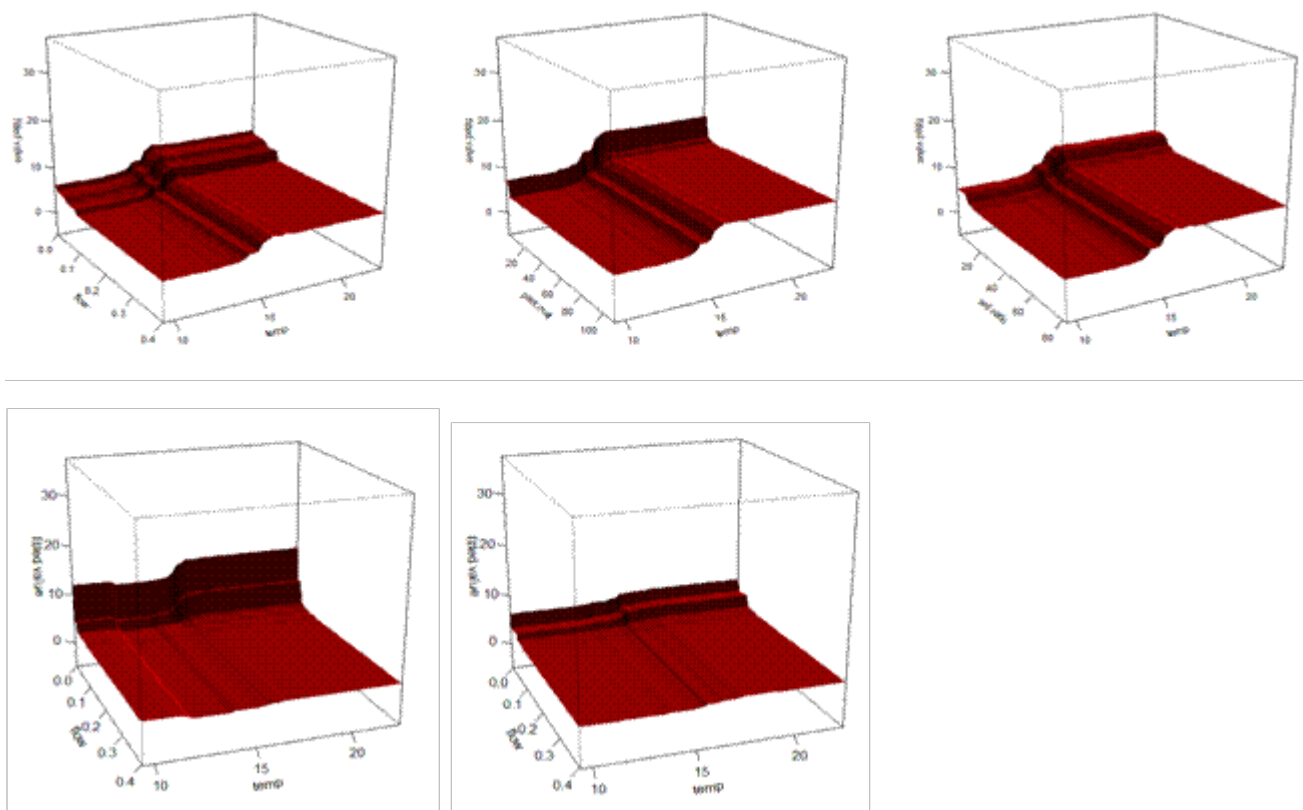


Figure 5.81 From left to right and from top to bottom: Interaction effects for submerged macrophyte cover for flow velocity (m/s, summer decadal mean) * water temperature (°C, summer decadal mean), particulate matter (mg/l, summer decadal mean) * water temperature (°C, summer decadal mean) and width-depth ratio (-) * water temperature (°C, summer decadal mean). Interaction effects for emergent macrophyte and floating macrophyte cover for flow velocity (m/s, summer decadal mean) * water temperature (°C, summer decadal mean).

Table 5.51. GLM results for macrophyte cover. Subm = submerged macrophytes, emer = emergent macrophytes, floa = floating macrophytes, SPM = suspended particulate matter, T = Water Temperature, WDR = Width-Depth ratio, TP = Total phosphorus, F = Flow velocity, TN = Total nitrogen, SF [n]= spatial filter and eigenvector value, Intc. = intercept at y-axis.

	Submerged macrophytes		Emergent macrophytes		Floating macrophytes				
Formula	subm ~ SPM + T + WDR + F + SF 16 + SF 35		emer ~ F + T + SF 2 + SF 15 + SF 35		floa ~ F + T + SF 1 + SF 3				
	Coef.	P-value		Coef.	P-value	Coef.	P-value		
	Intc.	0.266	0.060	Intc.	-0.586	0.000	Intc.	-0.586	0.000
	SPM	-0.342	0.019	F	-0.717	0.000	F	-0.642	0.000
	T	1.045	0.000	T	0.788	0.000	T	0.531	0.001
	WDR	-0.589	0.000	SF 2	-6.243	0.005	SF 1	6.549	0.006
	F	-0.614	0.000	SF 15	-6.341	0.004	SF 3	-6.404	0.005
	SF 16	-7.850	0.000	SF 35	-8.091	0.000			
	SF 35	-5.439	0.010						
McFadden R²	0.415		0.260		0.211				
AIC	924.208		950.245		961.827				

5.4.6.1.2 Macroinvertebrates

Table 5.54 shows the results for the ASPT (average score per taxon) and the FFGr (functional feeding group ratio). The chosen abiotic parameters explain between 33.8% and 20.7% of the variance in the models respectively, with cross validation variances of 21.2% and 6.8%.

No interaction effects were suggested by the BRT analysis for either the ASPT or the FFGr.

Table 5.52. BRT results for macroinvertebrates. O = oxygen, TN = total nitrogen, TP total phosphorus, WDR = width-depth ratio, T = water temperature, SPM = suspended particulate matter, F = flow velocity.

	Macroinvertebrates ASPT		FFGr	
Number of trees		1350		1450
Explained variance of model		0.338		0.207
Explained variance cross validation		0.212		0.068
Relative influence	O	31.068	F	37.170
	TN	21.050	O	22.471
	WDR	15.965	SPM	12.0356
	TP	9.804	WDR	10.067
	T	8.270	TN	9.840
	F	7.373	T	8.415
	SPM	6.471		
Interaction effects (Top 3 and > 10)		< 1		< 1

The BRT partial response plots for the ASPT show that oxygen, total nitrogen, width-depth ratio, water temperature and flow velocity are all positively related to the ASPT. Meaning that an increase in these variables correlate with an increase in the ASPT. Total phosphorus on the other hand shows a negative relationship with the ASPT (Figure 5.81).

The BRT partial response plots for the FFGr (Figure 5.82) show that an increase in particulate matter and width-depth ratio are associated with a decrease in FFGr, while an increase in water temperature is associated with an increase in FFGr. Oxygen concentration shows an optimum for the FFGr around 32 % (Figure 5.82).

For water temperature and flow we refer to the discussion and uncertainties described in the previous section. Besides influencing flow velocity and water temperature, the presence of vegetation itself is also likely to influence macroinvertebrates. However, the effect of the presence of vegetation on the macroinvertebrates in this dataset has not been studied.

The GLM with the lowest AIC value for ASPT includes oxygen, total nitrogen, total phosphorus, flow and the interaction effect between flow and total nitrogen. Since the Moran's I value turned out to be significant, the model was spatially corrected. The McFadden R² value for this model was 0.435 (Table 5.55). The interaction effect of this model appears to be *synergistic*, since the coefficients for *flow*, *total nitrogen* and the interaction effect are all positive, meaning that a higher total nitrogen and a higher flow velocity are related to a higher ASPT. This interaction effect is visualised in Figure 5.83.

The best GLM for the FFGr turned out to be a model that included flow, particulate matter, total nitrogen and water temperature. No interaction effects turned out to be significant. The McFadden R^2 value of this model was 0.127 (Table 5.55).

The residuals of both models are nicely distributed, indicating that the GLM's for ASPT and FFGr could be good models (Appendix 12.4). Although the low McFadden R^2 values are an indication that there might be other parameters, that were not included in this study, which play a role in this system.

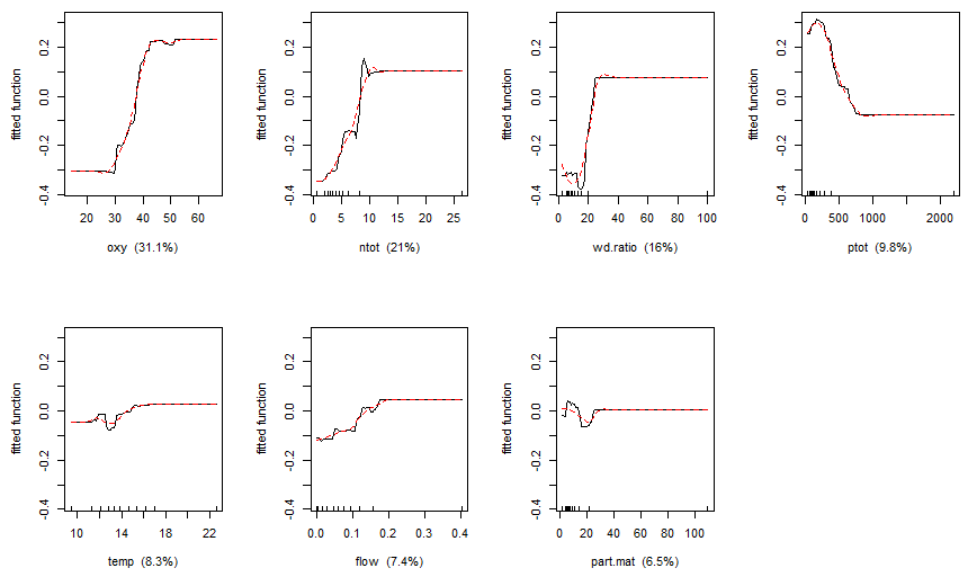


Figure 5.82 Partial responses of the BRT for the ASPT. From left to right and top to bottom: oxygen (mg/l, decadal summer mean), total nitrogen (mg/l, summer decadal mean), width-depth ratio, total phosphorus ($\mu\text{g/L}$, summer decadal mean), water temperature ($^{\circ}\text{C}$, summer decadal mean), flow velocity (m/s, summer decadal mean), and suspended particulate matter (mg/l, decadal summer mean).

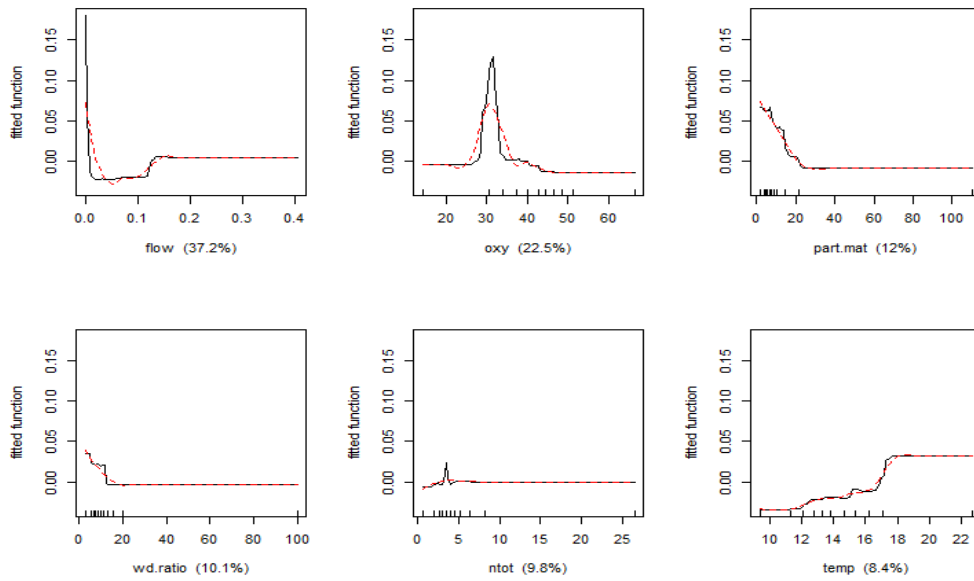


Figure 5.83 Partial responses of the BRT for the function feeding group ratio (FFGr). From left to right and top to bottom: flow velocity (m/s, summer decadal mean), oxygen (mg/l, decadal summer mean), particulate matter (mg/l, decadal summer mean), width-depth ratio , total nitrogen (mg/l, summer decadal mean), and water temperature (°C, summer decadal mean).

Table 5.53. GLM results for ASPT and FFGr. ASPT = ASPT, FFGr = functional feeding group ratio, SPM = suspended particulate matter, T = Water temperature, WDR = Width-Depth ratio, TP = Total phosphorus, F = Flow velocity, TN = Total nitrogen, O = Oxygen, SF [n]= spatial filter and eigenvector value, Intc. = intercept at y-axis, * = interaction

	ASPT		FFGr	
Formula	aspt ~ O + TN + WDR + TP + F * TN + SF 6 + SF 7 + SF 43		FFGr ~ F + PM + TN + T	
Model results	Coef.	P-value	Coef.	P-value
Intc.	4.502	0.000	Intc.	-1.748 0.000
O	0.151	0.000	F	-0.155 0.001
TN	0.088	0.006	SPM	-0.145 0.002
WDR	0.113	0.000	TN	0.117 0.017
TP	-0.081	0.006	T	0.144 0.002
F	0.087	0.019		
SF 6	1.592	0.001		
SF 7	-1.563	0.001		
SF 43	1.587	0.000		
TN * F	0.107	0.002		
McFadden R²		0.435		0.127
AIC		279.852		495.472

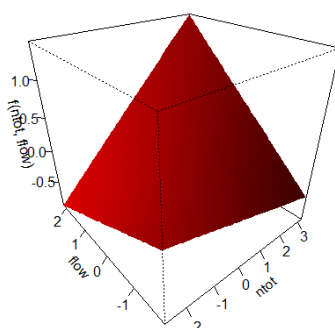


Figure 5.84 Visualisation of interaction effect of Ntot and flow for the ASPT.

Fish

The BRT results for the fish abundance show that water temperature has the highest influence on the fish abundance (35.5%), after which flow velocity (22.7%), total phosphorus and total nitrogen concentration follow (19.7 and 9.7% respectively), see Table 5.56. The least influential are particulate matter and oxygen concentration. There were no suggested interaction effects above a value of 1. The explained variance of the model was 0.126 and the explained variance of the cross validation was 0.021.

The partial response plots show that an increase in water temperature, flow velocity and total phosphorus might be related to an increase in fish abundance, while a decrease in total nitrogen might be related to an increase in fish abundance (Figure 5.84). It is not clear from this analysis if flow velocity and water temperature directly affect fish abundance or indirectly via the presence of macrophytes. As discussed in the previous 2 subsections, flow velocity and water temperature may be affected by the presence of macrophytes.

The GLM with the lowest AIC for fish abundance had a McFadden R^2 of 0.215 (Table 5.57). This model includes water temperature, total phosphorus, flow velocity, total nitrogen, particulate matter and the interaction between water temperature and total phosphorus. Since the coefficients of *water temperature and total phosphorus* both have a positive sign, while the interaction effect has a negative sign this could indicate that the interaction effect is *antagonistic*.

The residuals of this model seem slightly skewed. This could be an indication that the model is not optimal for general applications.

Table 5.54. BRT results for fish abundance. O = oxygen, TN = total nitrogen, TP total phosphorus, T = water temperature, PM = particulate matter, F = flow velocity.

Fish abundance		
Number of trees		1450
Explained variance of final model		
		0.126
Explained variance cross validation		
		0.021
Relative influence	T	35.535
	F	22.745
	TP	19.739
	TN	9.754
	PM	6.329
	O	5.898
Interaction effects (Top 3 and > 10)		
		< 1

Table 5.55. GLM results for fish abundance. Fish = fish abundance, SPM = Suspended Particulate Matter, T = Water Temperature, WDR = Width-Depth ratio, TP = Total phosphorus, F = Flow velocity, TN = Total nitrogen, O = Oxygen, * = interaction.

Model 3			
Formula	fish ~ T + TP + F + TN + PM + T*TP		
Model results	<i>Var.</i>	<i>Coef.</i>	<i>P-value</i>
	Intc.	0.081	0.309
	T	0.332	0.000
	TP	1.639	0.000
	F	-0.163	0.000
	TN	0.043	0.000
	SPM	-0.223	0.000
	T * TP	-0.099	0.000
McFadden	0.215		
R²	0.215		
AIC	25365.870		

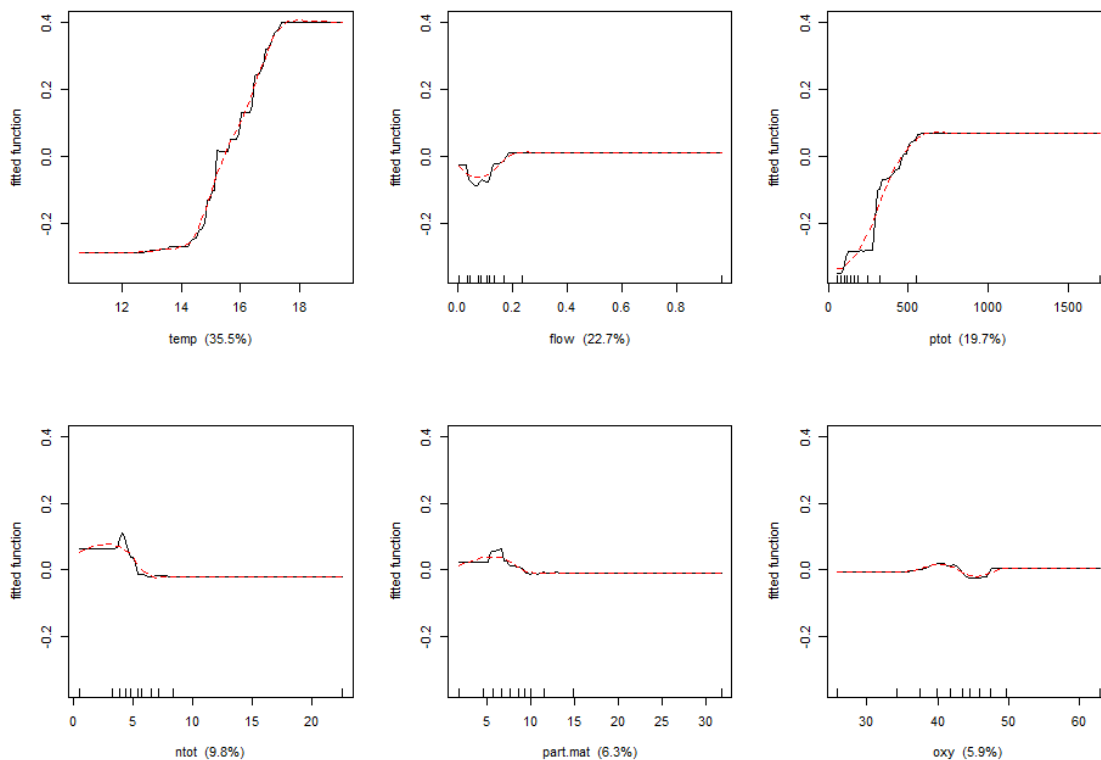


Figure 5.85 Partial responses of the BRT for fish abundance. From left to right and top to bottom: water temperature (°C, summer decadal mean), flow velocity (m/s, summer decadal mean), total phosphorus (µg/L, summer decadal mean), total nitrogen (mg/l, summer decadal mean), particulate matter (mg/l, decadal summer mean), oxygen (mg/l, decadal summer mean).

5.4.7 Contribution of groundwater flow to stream ecology

To gain more insight in the role of groundwater-surface water interaction for aquatic ecology in multiple stressor systems, a MARS PhD project was started within the Regge and Dinkel case study. This study contributes to filling the knowledge gap about the contribution of different groundwater flow routes towards the stream. This process is currently not fully understood and not simulated in existing models. In sandy lowland catchments, like the Regge and Dinkel catchments most water passes through the groundwater system. The travel times through the groundwater system vary from hours up to centuries. In this chapter we share first results relevant for the Regge and Dinkel case study.

Groundwater discharge influences surface water in different ways. First, discharge of regional groundwater flow systems is often important for stream base flow (Hendriks et al., 2014). Streams with a constant regional groundwater flow component are less susceptible to drying during summers. Second, groundwater has a large influence on the nutrients dynamics in streams (Wriedt et al., 2007; van der Velde et al., 2010). Through deep and shallow groundwater flow, the subsurface system connects several stressors in a catchment with its streams. Groundwater chemistry is influenced by all activities in the recharge areas of the catchment. Through diffuse discharge for example diffuse pollutions are transported towards surface water bodies. On the other hand, groundwater base flow can provide a constant source of relatively unpolluted input to the stream as opposed to water discharged through shorter flow routes like overland flow, interflow and tile drainage. Third, groundwater also has a relatively constant temperature and consequently functions as a temperature buffer. The temperature of groundwater roughly approximates the yearly mean air temperature, which for the Netherlands is between 11 and 13 degrees Celsius. When this water flows into a stream during a hot summer it provides a cool input, while in winter this water is a warm input. This way, groundwater provides thermal refugia for fish (Power et al., 1999; Hayashi and Rosenberry, 2002). It is well known that groundwater influences multiple abiotic habitat factors (Hendriks et al, 2015), but how exactly and how groundwater fits in the multi-stress concept has not yet been well researched.

First objective of the study was to characterize the groundwater contribution to streams. It was decided to focus on three tributaries of the Dinkel because the contribution of groundwater to streams is more apparent on smaller scales. These streams are the Springendalse Beek, Roelinksbeek and Elsbeek. These streams were selected based on available data and differences

in catchment and discharge characteristics (Table 5.58). Table 5.58 also shows the Base flow Index (BFI) which is the amount of base flow divided by the total amount of stream flow (Gustard et al., 1992). A stream with a value near 1, such as the Springendalse Beek, has a stable discharge and probably a high groundwater component. The knowledge gained by studying these three streams is used to assess the contribution of groundwater on bigger scales.

Table 5.56. Characteristics of the three studied tributaries of the Dinkel.

	Springendalse Beek	Roelinksbeek	Elsbeek
Catchment size	4 km ²	12 km ²	11 km ²
Length of stream	3 km	5.5 km	5.5 km
Elevation (m NAP)	70 -> 24 m	50 -> 23 m	60 -> 34 m
Average discharge	0.043 m/s	0.093 m/s	0.104 m/s
Falls dry?	No	Yes	Yes
Weirs?	No	Many	Some (upstream)
Base flow Index (BFI)	0.8	0.4	0.4
Main land use	Forest	Agriculture	Agriculture
Value	N2000, WFD	-	WFD

Groundwater can discharge to a stream in different ways. For instance, it can seep up through the streambed either locally or over larger areas, it can be discharged through tile drains or contribute to a stream via springs, which are often very local. Part of the groundwater originates from deeper layers and is therefore often a lot older than the water that flows from shallow layers, for instance through macro pores and tile drains. Not only is groundwater discharged through different mechanisms, the water also differs in age. The age or travel time of groundwater, i.e. the time it takes for the water to flow through the ground from the point of infiltration to the point of discharge, is related with the distance of flow and the layers the water is in contact with. As a result, travel time is also related with water chemistry. Deep groundwater is often low in nitrate due to denitrification and low in other pollutants due to its pre-industrial time of infiltration. Shallow groundwater, on the other hand, is often high in nitrate. Because of the distinction and importance of the age of groundwater, the groundwater travel time is used as a parameter to characterize the groundwater contribution to the three tributaries of the Dinkel. This way, not only the amount of groundwater is assessed, but also the different contributions of old and young groundwater.

The groundwater travel times were calculated with a MODFLOW groundwater model of the Regge and Dinkel catchment. Particle tracking and water balances were combined to calculate the age of the groundwater contributing to the streams for each month during the period 2000

to 2010. Figure 5.85 shows the result for the Springendalse Beek and the Roelinksbeek. It is apparent that the contribution of groundwater with different age fluctuates during the year. During high flow peaks, young groundwater increases in contribution due to high groundwater levels which activate shallow flow paths. In addition, the contribution of older water also increases with high discharge due to the effect of piston flow. Piston flow is a process where high groundwater levels upstream push the older water through the subsurface towards the stream. The blue parts in the graphs of Figure 5.85 indicate groundwater older than 25 years old. This part of the discharge appears to be quite stable during the year in the Springendalse Beek (left hand side). In the Roelinksbeek (right hand side), however, the contribution of this water also fluctuates strongly between the wet and dry seasons.

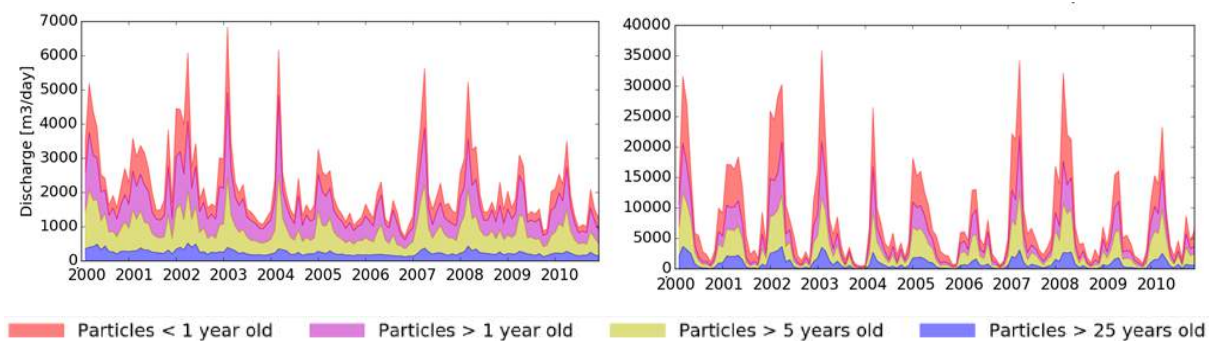


Figure 5.86 Result of the Travel Time modelling for the Springendalse Beek (left) and Roelinksbeek (right). Note the difference in scale of the y-axis.

The shape of the cumulative discharge curve is distinctive for a catchment and gives more information than a mean travel time, which is often used in literature. Using our model, we can make monthly cumulative discharge curves showing the variation throughout the years. Figure 5.86 shows these graphs for the Springendalse Beek (left) and Roelinksbeek (right). The monthly curves of the Springendalse Beek don't show as much variation as the curves of the Roelinksbeek. This is explained by the fact that the Roelinksbeek has a bigger component of young groundwater (Figure 5.85) and shallow flow paths with a lot of variation in travel time throughout the year. The Springendalse Beek on the contrary has a stable baseflow of relatively old groundwater.

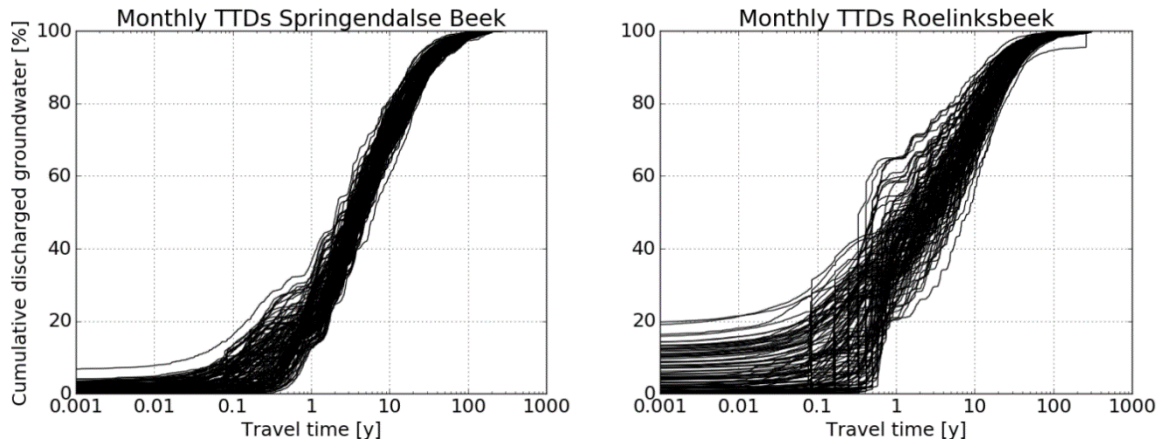


Figure 5.87 Cumulative discharge versus Travel time (log-scale). Left: Springendalse beek. Right: Roelinksbeek.

Because the temperature and temperature dynamics of groundwater are distinctive from the surface water, temperature can be used as a tracer to find locations with groundwater discharge. Measurements with glass fibre cables provide a method to measure temperature along a stream reach with high spatial and temporal resolution. Glass fibre cables were installed in stretches of 1.5 km in the Springendalse Beek and Elsbeek, to localize the locations with significant groundwater discharge. In addition, the data will be used to study the temperature dynamics of the surface water in both streams related to groundwater travel times. Measurements are done every 30 minutes for each meter of stream. First measurements have shown the effect of local springs and drain outlets.

Water quality samples are also taken regularly from the three streams to be combined later with the modelling outcomes and temperature measurements. Some components, such as Mg and Fe will be used as groundwater tracers and combined with the modelling. Furthermore, special attention is also given to nutrient and their relation with groundwater flow paths and travel times because of their importance for stream ecology in the Dinkel catchment. Radon222 isotopes have been measured in the Springendalse Beek and will be analysed in order to provide a direct indicator of groundwater. Groundwater is enriched in Radon222 due to its release from aquifer material. As soon as groundwater seeps up this process is stopped and the Radon222 decays with a very short half-time (days) and thus indicated recent groundwater upwelling. Sampling of macroinvertebrates will be done based on the locations of groundwater upwelling found with the temperature measurements. Sampling and determination of the species composition will be done upstream of discharge zones, in discharge zones and downstream to shown how groundwater influences the distribution of macroinvertebrates species.

5.4.8 Conclusions and recommendations

The goal of this study was to appraise how multiple stressors affect the water quantity, quality and ecology of the Dinkel catchment under a range of multi-stressor scenarios. The focus of this study was on the following drivers: groundwater abstractions and drainage, climate change, agriculture and urban development. These drivers lead to the following pressures: hydrological alterations, changes in mixing and thermal regime, abstractions, diffuse and point sources pressures.

Three models were developed to answer the research questions. First a conceptual MARS model, based on the DPSIR approach, was developed to visualise the different factors that play a role in the water system. Subsequently a process based model and an empirical model were developed to simulate the effects of changes of the drivers and pressures on the abiotic and biotic states of the Dinkel surface water body.

The scenarios for which the models were run included two climate models (GFDL-ESM2M and IPSL-CM5A-LR) and three storylines (Consensus world, Techno world and Survival of the fittest world) for the period 2054-2066 (horizon 2060). Besides these scenario's a baseline for the period 2000-2012 (horizon 2000) was also run.

This section describes the most important conclusions and discusses a number of recommendations resulting from this study.

5.4.8.1.1 Multiple stressors in the baseline (2000-2012)

- From the abiotic status of the Tilligterbeek it can be concluded that multiple stressors are active resulting in *low flow velocities and high nutrient loads*, negatively affecting the ecological status of the streams in the Dinkel catchment. The low flow velocities are driven by groundwater and surface water abstractions for agriculture and urban development. The high nutrient concentrations are caused by diffuse pollution from agriculture and, especially during summer, point source pollution from waste water treatment plants.
- The baseline calculations for the Tilligterbeek show that the summer average concentration of total N and total P (7.1 and 0.3 mg/l respectively) are far above the WFD standards (2.3 and 0.11 mg/l for total N and total P, respectively). Also, the

average summer flow velocities (0.05 m/s) are far below the Dutch-standard for minimum summer flow velocity (0.1-0.5 m/s) for a good ecological status.

- From the empirical model, it appeared that for fish, flow velocity and temperature (measured in the 14 - 18°C range) are most important, followed by total N and total P. Flow appears to be relatively unimportant (7.4%) for ASPT but most important (37.2%) for FFGr.
- From the empirical modelling, *two interaction effects* turned out to be significant:
 - *Water temperature and total phosphorus* show an antagonistic relationship with fish abundance.
 - *Flow velocity and total nitrogen* show a synergistic relationship with ASPT.
- Further analysis of the data behind the BRTs is recommended to fully understand the relationship and feedback mechanisms between flow velocity, water temperature and macrophyte cover.
- The BRTs involving nutrients (TN and TP) require further analysis.

5.4.8.1.2 Multiple stressors under climate change (horizon 2060)

- The decrease of the yearly average stream *discharge* over 45 years is in the order of 20% for all climate models which is due to less rainfall and higher evaporation rates. *Flow velocities* only decrease slightly. This may be because velocities in the baseline model are already very low.
- The change in mean duration of high and low flow pulses within each year (benchmark indicators *Bind4* and *Bind5* respectively) show that in all climate scenarios *high flow conditions* as well as *low flow conditions* will occur more frequently with consequently shorter duration.
- The modelled increase in *water temperature* is almost twice as high for stream water temperature than for air temperature. This is probably the result of a decrease in stream discharge and flow velocity which makes it easier to warm up the stream water.

5.4.8.1.3 Multiple stressors in the storylines (horizon 2060)

- The net effect for every storyline is a large *decrease in stream discharge*. For the summer period the discharge decreases for horizon 2060 with 10% for the consensus world, 28% for the survival of the fittest world and more than 40% for the ‘techno’ world, in comparison to horizon 2000. *Flow velocities* only decrease slightly. This may be because velocities in the baseline model are already very low.
- Model results show that the combination of climate change and storylines leads to a larger increase in water temperature than the summed single effects of climate change and storylines. This is probably due to a non-linear response of water temperature to changes of stream discharge and flow velocity.
- Climate change and the storylines show a synergic effect, decreasing future discharges.

5.4.8.1.4 Baseline model

- The Tilligterbeek is a representative stream in the Dinkel catchment and conclusions from this stream can be extrapolated to the rest of the Dinkel catchment.
- The current models do not distinguish between flow routes and travel times (e.g. overland flow, inter flow, shallow and deep groundwater flow) of nutrients that enter the main channel. Distinction is necessary, because for example N and P are influenced by different processes in the catchment and transported in different ways towards the stream. This distinction could not be made in the currently available models. First results of modelling experiments in the Dinkel catchment, to determine flow routes and travel time distributions (Kaandorp et al., in prep.), show that travel time distributions vary a lot within the Dinkel catchment, depending on geohydrology and other catchment specific characteristics, like slope, drainage intensity and land use. Consequently, programs of measures at the catchment scale are expected to change the relative portions of water over different flow routes and thus travel time distributions of the water entering the main channel. This is expected to further change as a result of climate change and storylines (increasing overland flow, decreasing base flow). It is recommended that in future modelling studies this change in travel paths and travel times is taken into account.

5.4.8.1.5 Model scenarios

- The current method of linear scaling of climate model outcomes with monthly correction factors appears not to provide reliable results. Comparisons between the baseline model (with measured weather input) and the climate scenario runs may therefore not be appropriate and should be done with care. Comparisons between the different climate scenario runs can be done without any doubt, since the method of generating input data was equal.
- To compare outputs of the (baseline model and) climate model scenarios, we need to use long-term yearly, or seasonal, averages. Comparing on a day-to-day basis is not meaningful because changes in the different climate model scenarios, like changes in the recurrence intervals of extreme events, are reflected over periods longer than one year. We therefore averaged the results of the different climate models over periods of 13 years before comparing them with each other.
- The choice of climate model appears to be more important than expected. Differences between the climate models IPSL-CM5A-LR and GFDL-ESM2M are larger than the differences in the RCP 4.5 or RCP 8.5 climate scenarios.
- The scenarios modelled in this case study, typically are a combination of climate change and measures/storylines. Distinction between storylines and climate change scenarios proved to be very helpful in understanding and distinguishing the effects of both types of changes in the catchment. However, as not all measures were modelled independently, stressor-response relationships could not be specified. The current results should therefore be seen as:
 - A quantification and sensitivity analysis of the current multiple stressor situation in the Dinkel catchment, from driver to biotic state indicator.
 - A bandwidth of what the future of the Dinkel catchment could look like under different climate and water management scenarios.
- Changing all stressors independently, including experimenting with different combinations of measures, can further improve the understanding of the multiple stressor gradients and the effect of specific (programs of) measures.

5.5 Ruhr

5.5.1 Introduction

5.5.1.1.1 Overview of the Ruhr Basin

Location

The river Ruhr is an important right-bank tributary of the lower Rhine and is situated in Central German Uplands. The source of the River Ruhr is in the north of Winterberg in the Hochsauerland District, at an elevation of approximately 674 m a.s.l. The Ruhr descends from the mountains in northward direction for about 25 km and then flows westwards to the River Rhine. The mouth is in Duisburg at 17 m a.s.l.

Basin physiography

The Ruhr Basin covers a surface area of 4485 km², with a main channel length of 219 km and a total length of all watercourses of about 7000 km (www.ruhrverband.de and MUNLV 2005). The area of the Ruhr belongs predominantly to the Rhenish Slate Mountains except the far west, which physiographical allocates to the Lower Rhine Embayment. The northern part of the Basin borders on the Westphalian Lowlands. As the basin almost exclusively locates in the Rhenish Slate Mountains, the watercourses consist primarily of mid-sized fine to coarse substrate-dominated siliceous mountain rivers (www.ruhrverband.de). Slate and shist of the Devonian and Carboniferous predominantly occur in the Basin while in the river valleys of the lower Ruhr area Quaternary sediments prevail (MUNLV 2005). In a small area of the catchment carbonate rocks dominate.

With regard to the land use the southern and north-eastern upper parts of the Basin are dominated by agriculture and forestry, whereas the lower northwest is a highly urbanized and industrialized area (www.ruhrverband.de). According to MUNLV (2005) the land cover distribution of the Ruhr Basin can be summarized as follows

- forest: 53%
- arable land: 12%
- pasture: 18%
- urban areas: 15%
- others: 2%

The major urban areas (Figure 5.87) are located in the northwest of the Ruhr Basin.

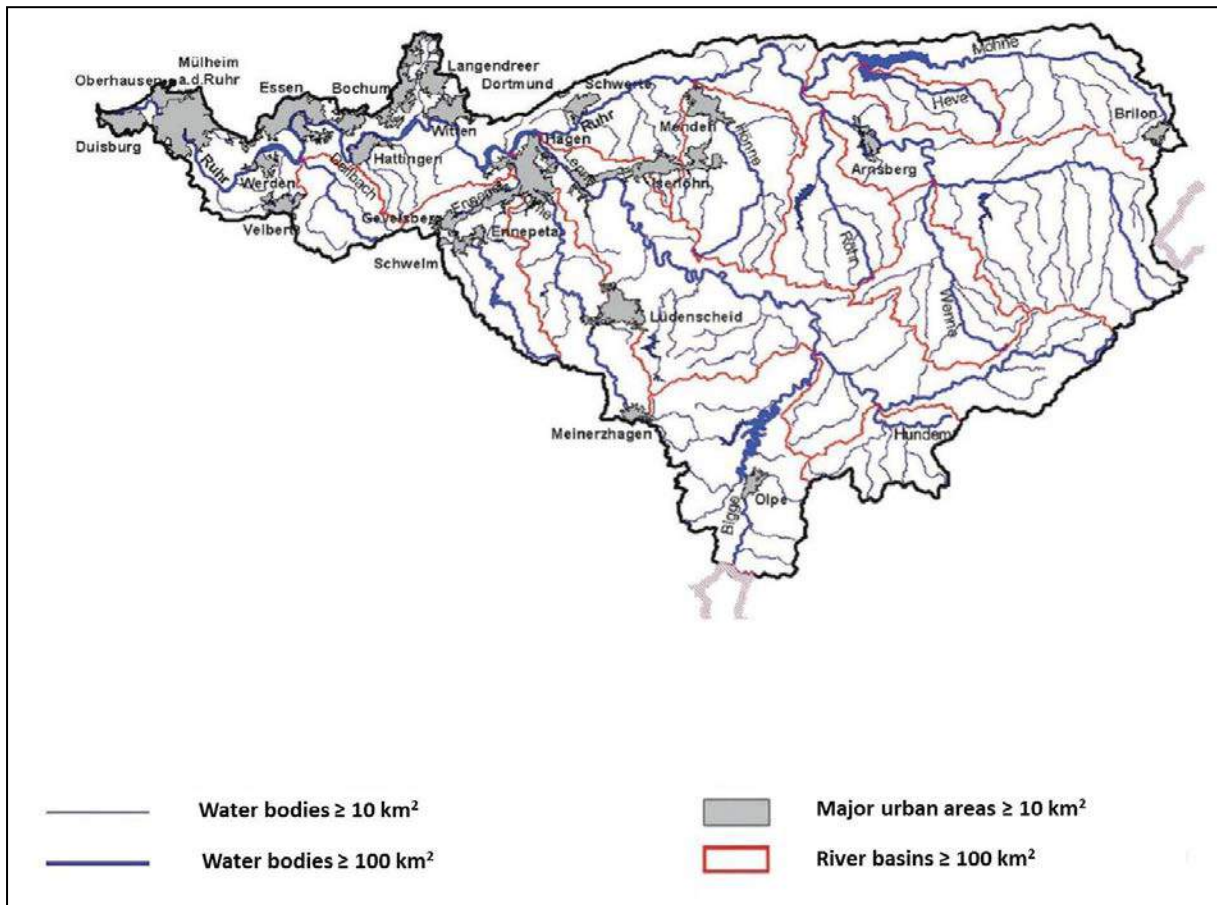


Figure 5.88 Major urban areas within the Ruhr Basin (modified after MUNLV 2005)

5.5.1.1.2 Brief description of current RBMP, water body status, identified reasons for failure and key stakeholders

RBM Plan-type information

According to the North Rhine-Westphalia State Environment Agency (LANUV NRW) 243 waterbodies have been assessed for the WFD ecological status. The distribution of the status classes is as follows:

WFD status classes	% approximate
high	< 1
good	17
moderate	39
poor	24
bad	19

Maps showing the classification of status for the Ruhr Basin can be found on www.elwasweb.nrw.de.

There are many reported reasons for moderate or worse status. According to MKULNV (2014) the main reasons for failure for waterbodies are:

1. Physical modification
 - a. Urban and industrial uses of waterbodies by bank fixation, straightening and deepening lead to a lack of habitats.
 - b. Lack of linear connectivity by many barriers e.g. weirs, ground sills, dams → constraints to the migration of fishes and other aquatic organisms.
 - c. Operation of hydropower plants withdraws a substantial portion of the water and the reservoirs above the dams change the waterbody character considerably.
2. Diffuse and point source pollution
 - a. Diffuse source pollution (nutrient discharges) from farming and agriculture.
 - b. Diffuse and point source pollution from municipal and industrial discharges → nutrient and metal pollutants from wastewater discharges and mixed and rainwater drainage.

Stakeholder Summary

We identified three main (key) stakeholders with an interest in the Ruhr Basin.

1. Ruhrverband

The Ruhrverband is a water management company based on public law and responsible for the source and supply of water for drinking and industrial purposes. It regulates and balances the water runoff of the whole Ruhr basin. In addition, it fulfils responsibilities for secure flood water flow, treats sewage and analyses water management conditions. The Ruhrverband holds various information about biological, chemical and hydrometric data.

<http://www.ruhrverband.de/>

2. Regional authorities

- a. Bezirksregierung Arnsberg
- b. Bezirksregierung Düsseldorf

The regional authorities Arnsberg and Düsseldorf, called “Bezirksregierungen” (District Governments) act as mid-level agencies with a wide range of regulatory responsibilities. Bezirksregierung Arnsberg covers the upper and middle parts of the Ruhr River Basin and Bezirksregierung Düsseldorf is responsible for the lower north-western part of the Ruhr.

<http://www.bezreg-arnsberg.nrw.de/>

<http://www.brd.nrw.de/>

3. Environment Agency

The North Rhine-Westphalia State Environment Agency is a state supervising authority and deals with the technical aspects of environmental protection for industry, trade and the municipalities in the fields of water, soil, air, solid wastes and contaminated sites. LANUV NRW holds information systems and databases with a wide range of detailed water data (biotic and abiotic data).

<http://www.lanuv.nrw.de/>

5.5.1.1.3 Main pressures in the Ruhr Basin

Following specific pressures on surface waters have been identified in the evaluation report for the Ruhr River Basin (MUNLV 2005):

- Municipal discharges
- Industrial discharges
- Diffuse pollution
- Extraction and transfers of water
- Hydromorphological changes
- Flow regulation

Detail information on each of the pressures can be found in MUNLV 2005. A summary analysis showed that the status of the surface waters in the Ruhr catchment is affected by the combination of these pressures. Barely a watercourse segment is solely exposed to one pressure, so that a heterogeneous high stress status was determined. In addition, other pressures like recreation, shipping, mining activities or acidification play an important role which had not been included in the evaluation report.

5.5.1.1.4 Questions to be addressed by the modelling

Many experimental studies contributed to the unravelling of the combined stressor effects. However, there is a lack of tackling the multiple stressor effects using monitoring data. This collected biological and environmental data is available in huge numbers due to many monitoring programmes across Europe. The difficulty of using this data for multiple stressor analyses consists in the fact that the collected environmental data (stressors) is very heterogeneous. This means, there is a mix of real stressor variables (e.g. nutrient concentrations) and, for example, drivers (e.g. land cover). Besides that, biological metrics resulting from datasets of national monitoring programmes (e.g. EQR, ASPT or EPT) are not stressor-specific. They were developed to integrate multiple stressor effects rather than unravelling them. However, these metrics are the main sources of national decision making for implications for River Basin Management. Against this background we thus aimed to disentangle the multiple effects of heterogeneous stressor data on metrics of three aquatic organism groups by using appropriate analytical methods.

Following questions should be answered:

Q1: How do different organism groups respond to natural and anthropogenic predictors in multiple stress conditions? Do the three organism groups show different responses? Do the different metrics show consistent response patterns?

Q2. Which predictor group and which single predictor have the greatest influence on the different organism groups?

Q3. Are we able to identify, quantify and interpret interactions?

5.5.1.1.5 Ecosystem services to be modelled for the Basin

Two ecosystem services (i) the provisioning service “Total biomass of commercially relevant fish species” and the regulating service (ii) “Carbon sequestration” were assessed for the Ruhr Basin.

5.5.1.1.6 Variables to be modelled in the scenario analysis

Under contrasting scenarios we based our predictions on scenarios of future riparian land use on ecological status using empirical models. Two storyline elements (i) Loss of riparian zones and (ii) Restoration of riparian zones were selected to be implemented in the Basin. For the storyline element “Restoration of riparian zones” (increase of naturally-forested land in riparian areas) pasture, arable land and non-native coniferous forest areas were turned into naturally-forested land. For the second element “Loss of riparian zones” we decreased the amount of naturally-forested land in riparian areas.

5.5.2 Context for modelling

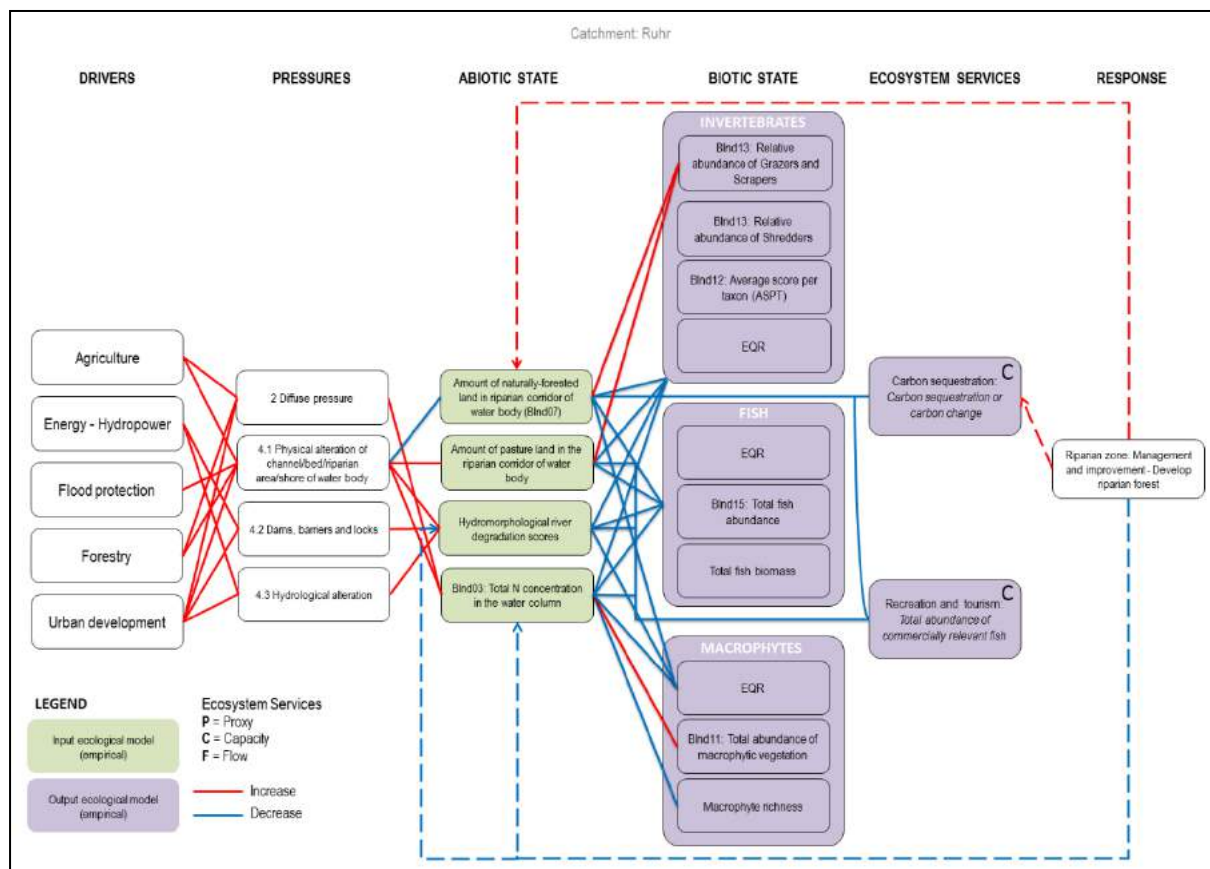
5.5.2.1.1 Overall MARS model for the Basin

			- Land use (urban, agriculture, non-native forestry)	
Multi-Stress		Spatial distribution of stress intensities	- Hydromorphological degradation/changes - Loads to surface water (diffuse/point sources)	
Indicators	Abiotic	National threshold values for Total nitrogen	- Amount of natural land use in riparian corridor of water body - Structural water quality status - Total nitrogen concentration in the water column	Area occupied by riparian forests (Carbon sequestration)
	Biotic	Saprobic Index Type-specific German Fauna Index* ¹	<ol style="list-style-type: none"> Benthic invertebrates <ul style="list-style-type: none"> - Average Score per Taxon (ASPT, BInd 12) - Relative abundance of various invertebrate feeding types BInd13) - Saprobic Index - Type-specific German Fauna Index*¹ - EQR (PERLODES assessment*²) Macrophytes <ul style="list-style-type: none"> - Species richness - Abundance of submerged, emergent and floating-leaved vegetation (BInd11) - EQR (PHYLIB assessment*²) Fish <ul style="list-style-type: none"> - Total fish abundance (BInd15) - Total fish biomass - Biomass of commercially-relevant fish species - EQR (FIBS assessment*²) 	Biomass of commercially-relevant fish species
	Functions & Services	No resilience reserves	- Climate protection	- Carbon sequestration
				Economic Benefits
				Monetary Value
Enhancement of riparian buffer zone				

*1 German Fauna Index is a multimetric Index for stream assessment, which is mainly focussed on the impact of hydromorphological degradation on the macroinvertebrate fauna.

*2 PERLODES, PHYLIB and FIBS are the official WFD compliant assessment systems for rivers and streams in Germany.

5.5.2.1.2 DPSIR model for the Basin



5.5.3 Data and methods

5.5.3.1.1 Data

Anthropogenic predictors

This study addressed the main anthropogenic stressors present in the Ruhr basin. This includes the impact of different land use types, hydromorphological alteration and diffuse nutrient input. Overall, we investigated 14 environmental factors belonging to three predictor groups: (i) riparian land use, (ii) physical habitat quality and (iii) nutrients (Appendix 12.5). In addition, two natural predictors (“altitude” and “distance from source”) were included in the analyses.

Riparian land use

Riparian land use was evaluated in a 10 m wide (left and right along the watercourse) and 1000 m long buffer strip upstream of each sampling site. Buffer strips were generated by

delineating polygons along the river network including the main river course above a sampling site as well as its tributaries. Sites with buffer distances less than 750 m were excluded from the analyses. For each buffer strip, percentage of land use derived from ATKIS®-Basis-DLM (Official Topographical Cartographic Information System) was calculated using a GIS system. Land use data was grouped into the following categories: arable land, pasture, urban areas, naturally-forested land and non-native coniferous forest. For all sites, land use categories with a share less than five percent within a buffer strip were set to zero.

Hydromorphological data

Physical habitat quality data was based on a large hydromorphological data set which has been evaluated according to the German river habitat survey method described in Gellert et al. (2013) by regional authorities. This method assesses local-scale habitat variables which are grouped into 31 single parameters at a resolution of 100 m reaches. These single parameters are combined into six main parameters (channel development, longitudinal profile, bed structure, cross profile, bank structure, and adjacent land zone) and further aggregated to the zones “streambed”, “bank” and “adjacent land” and finally to the “overall evaluation”. The classification of these aggregated parameters is based on a seven-step scale ranging from 1 (reference conditions) to 7 (completely altered stream segments). For each sampling site, we evaluated the mean value of the physical habitat quality of 100 m stretches lying within 1000 m section upstream. For the analysis eight parameters were used: main parameters “channel development”, “longitudinal profile”, “bed structure”, “cross profile”, the zones “streambed”, “bank” and “adjacent land” and the “overall evaluation”.

Nutrients

As nutrient predictor total nitrogen (TN) was included in the analysis. Data for TN derived from national Water Framework Directive (WFD) monitoring. For each site, we calculated mean values of concentrations measured during one year back from the sampling of different organism groups analysed in this study.

Natural predictors

We used the two variables “altitude” and “distance from source” as natural predictors. Both originated from digital maps using a GIS System. “Altitude” represents topographical

variability and “distance from source” accounts for changes in characteristics of a river channel (e.g. different river types).

Response variables

Site-specific biotic data originated from national WFD monitoring surveys and the local water board (Ruhrverband) and followed national monitoring standards for field sampling procedure. In total, data from 1096 sites were used, comprising taxa lists of three organism groups: (i) benthic invertebrates, (ii) macrophytes and (iii) fish.

We used samples collected between 2006 and 2014, whereby only one sample per site was considered. If multiple-annual samples for a site in the period from 2006 to 2014 were available, then the most recent sampling, close to the date of the assessment of the physical habitat quality (2011-2012) was preferred. This was done in order to adapt the temporal comparability of biotic samples and physical habitat quality assessment. If an invertebrate site was sampled several times a year, then those samples were selected, which were taken within the seasonal sample period recommended by the German protocols for the different stream types (e.g. for small and mid-sized streams with catchment sizes below 1000 km² spring samples were preferred).

In total, 21 metrics for the three organism groups (11 benthic invertebrates, seven macrophytes and three fish metrics) were calculated to address the anthropogenic impact (Appendix 12.5).

Before calculating the metrics, raw taxa lists were taxonomical adjusted to exclude inconsistency and regarding benthic invertebrates to eliminate species-poor sites (sites with less than 5 taxa) and differences between processor-dependent identification levels (e.g. Chironomidae and Oligochaeta).

5.5.3.1.2 Methods

EM approach

Boosted Regression Trees (BRT) were applied to identify the individual strength of each predictor and predictor group, the predictors' hierarchy and interactions among predictors. BRTs were constructed mainly according to the procedure provided by Elith et al. (2008) and

Elith & Leathwick (2011) and run in R using the libraries “gbm” (version 2.1.1, Ridgeway 2015) and “dismo” (version 1.0-15, Hijmans et al. 2011). For each BRT model, the optimum number of trees was set between 1000 and 1500 by varying the learning rate and using the default 10-fold cross-validation. Besides that, models were fitted by setting tree complexity to ‘5’ and bag fraction to ‘0.5’. Error was assumed to fit a Gaussian distribution.

In total, 21 BRTs were run for each possible combination of organism group and response variable using all natural, riparian land use, physical habitat quality and nutrient variables as predictors. Model performance was expressed as percentage of explained deviance (R^2) in the BRT and calculated as $\{[1 - (\text{mean residual deviance} / \text{mean total deviance})] \times 100\}$. The relative contribution of each predictor variable to the overall deviation explained by the single full models is scaled so that the sum adds to 100. Higher numbers demonstrate stronger influence on the response variable.

To quantify and to compare the importance of single predictors between different metrics and organism groups, we converted the contribution values of each predictor relative to the total deviation explained by the full single model, following by determining mean values of the relative contributions of a single predictor across all models within an organism group. The importance of each anthropogenic predictor group was evaluated by summing the mean values of predictors for each predictor group.

In the final step, we first identified interaction effects between predictor variables using BRTs and the routine function “gbm.interactions” of the package “dismo”. This function allowed us to assess the level to which pairwise interactions exist in the stressor data (Elith & Leathwick, 2011). Further, the relative strength of each identified pairwise interaction fitted by BRT is reported, so that the outputs inform us about important interaction terms. Pairwise interactions were considered solely among predictors of different anthropogenic predictor groups. Thus, for each of 21 metrics there were 48 pairwise meaningful interactions possible. Due to the high number of possible interactions, we have chosen to account for the top three pairwise interactions for each individual metric based on interaction value determined via BRT. Second, using this top three most influential and meaningful interactions, we estimated the magnitude of single predictors and interaction terms in a Generalized Linear Model (GLM). We therefore ran first an additive GLM including only the two single predictors of the interaction term and second an interactive GLM containing the single predictors and the interaction term. As our data is heterogeneous, we used standardised regression coefficients of the GLMs to identify

and to compare the directions of the effects and the effect sizes of individual predictors and interaction terms. If the effect sizes were <0.1 , we interpreted that this relationship is not biologically relevant (see also Lange et al. 2014). Running an additive and interactive model separately ensures that there is no influence of the interaction term on the single stressor effect sizes. We considered only significant interaction terms in the models. Our interpretation of interaction types and classification was based on the studies of Lange et al. (2014), Nakagawa & Cuthill (2007), Piggott et al. (2015) and Feld et al. (2016).

Modelling of ecosystem services

In this study we assessed two ecosystem services: (i) “Fisheries and aquaculture” and (ii) “Carbon sequestration”. To quantify the ecosystem services we used (i) “Total biomass of commercial fish species” and (ii) “Total carbon stored in the riparian zone” as indicators of natural capacity.

Total biomass of commercial fish species

To address the multiple anthropogenic impact on the provisioning service “Total biomass of commercial species” we applied the same modelling procedure using BRTs as described above. As commercial relevant fish species in the Ruhr Basin we identified the brown trout (*Salmo trutta fario*). For each site, we calculated the total biomass as biomass of caught brown trout per hectare using literature values for mean weights of different brown trout size classes. As the brown trout primarily populate the small stream in mountain areas, we exclude the large mountain rivers from the analysis and used solely the small stream types (available number of sites = 160).

Total carbon stored in the riparian zone

In the case of the service “Carbon sequestration” our aim was (i) to assess the current amount of stored carbon in riparian zones in the entire Ruhr Basin, (ii) to demonstrate which amount of carbon could be additionally stored in riparian area by reforestation of pasture land and (iii) to value the additionally stored carbon due to reforestation. As forested area is capable in fixing more carbon compared to pasture, an increase in carbon sequestration is to be expected from before to after reforestation. To determine the amount of carbon sequestered in the riparian zone we evaluated in a first step riparian land use in a 10m wide buffer strip (left and right along the watercourse) for the entire basin. Percentage of land use derived from ATKIS land cover data was calculated using a GIS system. Land use data was grouped into eight categories

(Table 5.59). In a second step, we assigned vegetation types to the land use categories. According to LUA NRW (2001) dominant tree species in the riparian area of the reference river in the Ruhr Basin are *Alnus glutinosa*, *Carpinus betulus* and *Quercus robur*. Based on the classifications of Cierjacks et al. (2010) these species are classified as hardwood forest. Further, we classified non-native coniferous forest characterized by *Picea* sp. as softwood forest and pasture land as the vegetation type meadows and reeds. To estimate the current amount of stored carbon in riparian zones we used specific values of total carbon stocks of above ground and belowground in tons per hectare estimated by Cierjacks et al. (2010) (Table 5.59). For the land use category mixed forest we used an averaged value of total C stocks of softwood and hardwood vegetation units. Land use categories arable land, urban area, water body and others were not considered for the calculations.

In the next step, we assumed a reforestation of available pasture land areas (these areas may offer better opportunities for reforestation projects) in the riparian zone by deciduous forest and estimated benefits of C stocks sequestered in fully developed deciduous forest compared with pasture land. We considered a reforestation of 10, 25, 50 and 100% of pasture areas. Hereafter, we used the average price for the emission of one ton CO₂ (approx. 13 Euro, source: www.investing.com) since 2005 of the European Union Emission Trading Scheme (EU ETS) as a proxy for the value of the carbon sequestration service. EU ETS was launched in 2005 to fight Global warming. The amounts of sequestered carbon were converted into the corresponding CO₂ values. The ratio of CO₂ to C is 3.67. Therefore, to determine the weight of sequestered carbon dioxide, we multiply the weight of carbon by 3.67.

Table 5.57. Land use categories, assigned vegetation types and total carbon stocks of above ground and belowground (modified after Cierjacks et al. 2010)

(*averaged value of softwood and hardwood vegetation type)

Land use categories	Vegetation type	Total C stocks of above ground and belowground / t•ha ⁻¹
Non-native coniferous forest	Softwood forests	356
Deciduous forest	Hardwood forests	474
Mixed forest	Mixed (softwood/hardwood)	415*
Pasture	Meadows and Reeds	212
Arable land		
Urban area	Others	0
Water body		
Others		

Implementation of the scenarios in the Basin

We based our predictions on scenarios of future riparian land use on ecological status using empirical models. Ecological Quality Ratios (EQR) for benthic invertebrates were used as the response variable characterizing ecological status. The investigation of the impact of changes in riparian land use on the ecological status was performed solely for the largest stream type in the Ruhr Basin, which is “Large mountain streams”. The reasons for this (revealed by a preliminary data mining) are as follows: (i) Weak relationships between land use variables and EQR were found using the entire data set. (ii) Strong influence of natural predictors (altitude and distance from source) was detected (both data are not shown here). We therefore divided the data set in the stream types which occurred in the Ruhr Basin. With the exception of the stream type “Large mountain streams” very weak relationships were identified for the remaining stream types (results are not shown here). Due to small number of sampling sites for the large stream type (N = 62), modelling future riparian land use using the BRT technique was not feasible. We therefore used GLM. To investigate the response of EQR to different amounts of riparian land use in a multi-stressor condition we included all natural and anthropogenic predictors used in EM approach (see Appendix 12.5) in the GLM model. We mainly applied the procedure described in Feld et al. (2016). Among others, this procedure includes the assessment of collinearity between predictor variables using the Variance Inflation Factor (VIF) to avoid biased parameter estimates. We excluded highly collinear variables, defined as those with a VIF > 6. Final GLM model was those, which included only significant predictor variables. After performing stepwise GLM analyses using non-collinear predictors, the final model identified altitude, longitudinal profile and naturally-forested land as significant variables explaining 83% ($R^2=0.83$) of the total variance. Other land use categories were not significant. Therefore, for the implementations of our scenarios of future riparian land use we were able to consider solely the amounts of naturally-forested land.

We selected two contrasting storyline elements (i) Loss of riparian zones and (ii) Restoration of riparian zones to be implemented in the Ruhr Basin. For the first storyline element we replaced pasture, arable land and non-native coniferous forest areas by naturally-forested land. For the second element, the amounts of naturally-forested land were decreased. As pasture, arable land and non-native coniferous forest may offer better opportunities for reforestation projects, urban areas were regarded as dedicated for long term usage. We do not expect that a sizeable portion of these areas will be available for restoration projects and therefore urban areas were not replaced by naturally-forested land in our scenarios. The qualitative change and

estimated quantification of values for an increase or decrease of naturally-forested land in the three different storylines (Techno, Consensus and Fragmented World) are shown in the Table 5.60. In addition, we transformed the EQR values into ecological status classes to investigate for how many sites, an improvement of ecological status class could be achieved.

It should be noted that increasing naturally-forested land e.g. by 50% in a Consensus World scenario not always resulted in a net 50% increase. This level of increase occurred only for those sites with availability of corresponding pasture, arable land and non-native coniferous forest areas in the riparian zone. For sites with no adequate available areas in the riparian zone the level of increase is unavoidable smaller.

To investigate the effects of changed amounts of naturally-forested land on the EQR we used the function “predict”.

Table 5.58. Selected storyline elements to be implemented in the case study of the Ruhr and their qualitative change and quantification for a decrease (-) or increase (+) of naturally-forested land in the three different worlds

Qc = Qualitative change, Q = Quantification

Criteria	Element of storyline	Techno world		Consensus World		Fragmented world	
		Qc	Q	Qc	Q	Qc	Q
Environment and Ecosystems	Loss of riparian zones	+	-25%	0	+10%	+++	-100%
Eutrophication and water treatment	Restoration of riparian zones	-	-10%	++	+50%	---	-50%

5.5.4 Results

5.5.4.1.1 EM results

Importance of single predictors and predictor groups for the three organism groups

Three organism groups were analysed resulting in 21 biological responses to anthropogenic and natural predictors. The single percentages of explained deviance in the BRT models varied between metrics and organism groups (Appendix 12.5). Overall, the models for invertebrates performed best with regard to the explained deviance (mean value over the eleven metrics: 60%). Fish metrics performed less well; on average anthropogenic and natural predictors explained 40% of the total deviance in the three fish metrics. The models for macrophytes performed worst, on average, about 21% of the variance in the six metrics was explained by

natural and anthropogenic predictors. The response of the three organism groups to natural predictors was inconsistent. Natural predictors showed more influence on invertebrate metrics compared with fish and macrophyte metrics. Similar, anthropogenic predictors were more influential on invertebrate metrics (mean over the eleven metrics: 33%) in comparison with fish (mean: 26%) and macrophytes (mean: 17%). Across all organism groups and considering solely anthropogenic predictors, physical habitat quality variables explained larger parts of the variance in the metrics compared with riparian land use predictors and TN. The contribution of TN to the overall variance explained was negligible. The explained deviance of trait-based invertebrate metrics (functional feeding groups) was on average lower compared with general invertebrate metrics (e.g. EQR, ASPT and SI). The response of the three fish metrics was comparably similar. Besides the macrophyte metric SAC, the remaining metrics (EQR, SNe, SNs, SACe, and SACs) showed no or the weakest response across all groups and metrics. If separated by different growth form types of aquatic vegetation, models for submerged macrophytic species (SNs and SACs) performed better compared with models for emergent species (SNe and SACe).

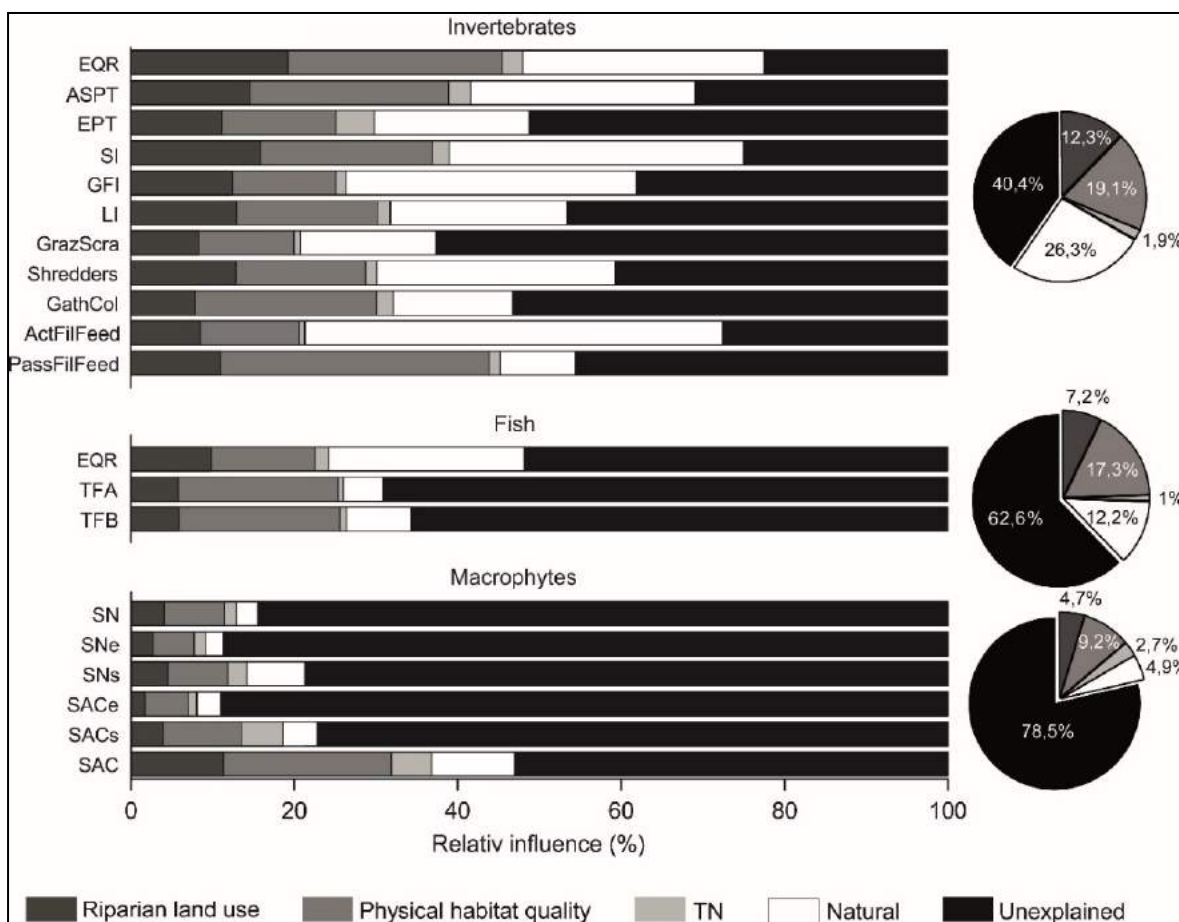


Figure 5.89 Relative influence of natural and anthropogenic predictor groups on the metrics of the three organism groups

No model could be computed for the macrophyte metric EQR. Pie charts on the right side show mean values of relative importance of natural and each anthropogenic predictor groups summarized for all metrics of each organism groups.

Considering the importance of single predictors, BRT results revealed that out of the physical habitat quality variables bed structure and adjacent land showed the greatest contribution to the overall deviance explained comprising all organism groups (Figure 5.89). Regarding riparian land use variables alone across all organism groups, on average more than 80% of metric variance was accounted for the variables pasture, naturally-forested land and urban areas, whereas the variables arable land and non-native coniferous forest explained only minor portions of the overall variance in the models. TN had the highest relative effect on macrophytes compared with invertebrates and fish.

(Top three out of riparian land use and physical habitat quality and TN; To make the predictors comparable among metrics and organism groups, we converted the contribution values of each predictor relative to the total deviation explained by the full single model, following by determining mean values of the relative contributions of a single predictor across all models within an organism group)

Interactions

In freshwater ecosystems stressors often co-occur. However, if these stressors are highly correlated, then the response cannot be related to individual stressor or combination of them. Therefore, in a previous analysis we investigated the relationships between our anthropogenic predictor variables among different predictor groups. The results showed weak correlations between the anthropogenic variables (data not shown here), which provides a good base to evaluate interaction effects.

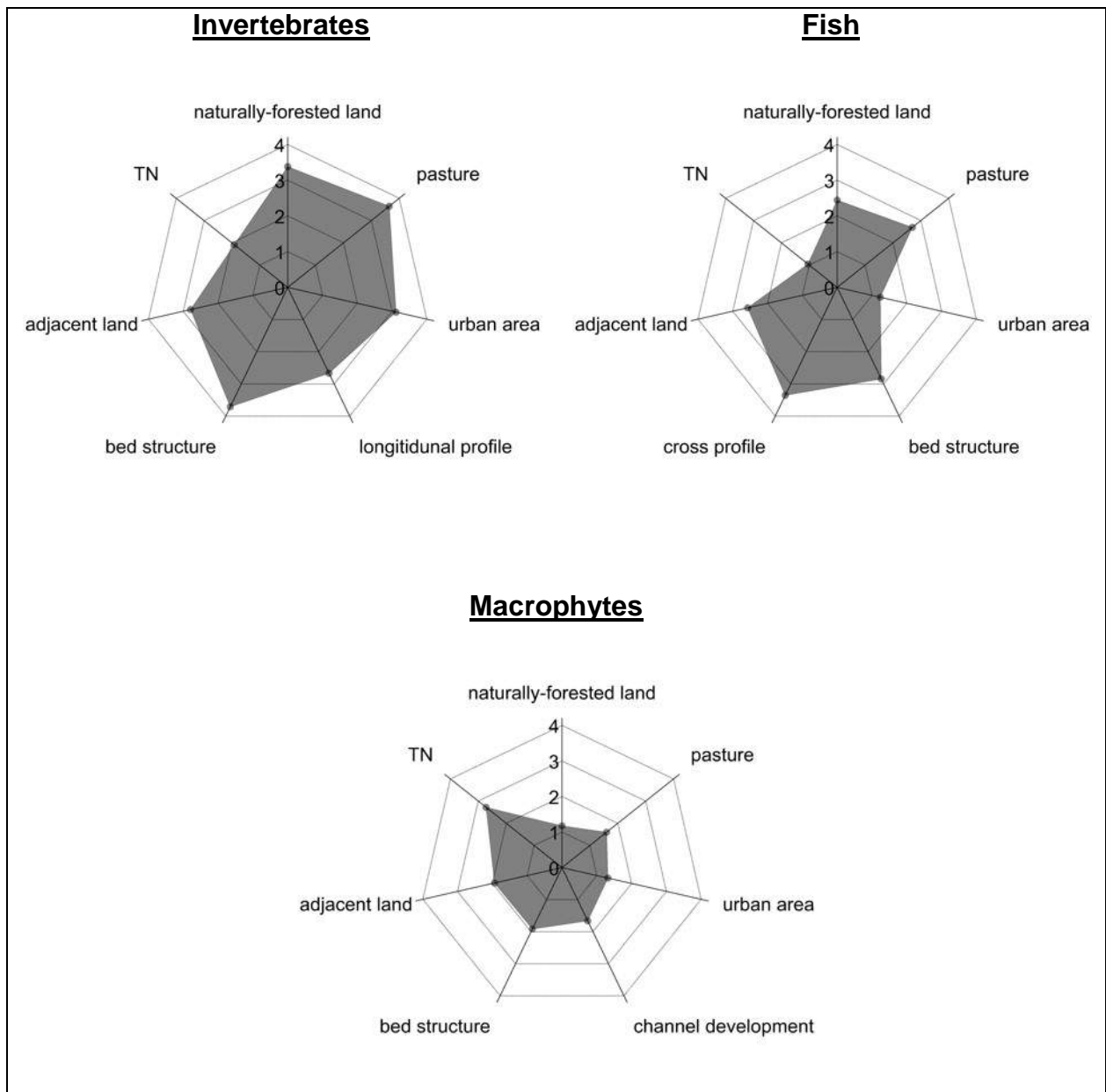


Figure 5.90 Relative influence (%) of the most important anthropogenic predictors on the three organism groups

In total, 17 different pairwise interactions were identified via BRT for invertebrate metrics, ten for macrophyte and four for fish metrics. However, only six interaction terms for invertebrates and one for macrophytes were significant in a GLM and showed an effect size <0.1 . No significant interaction terms could be identified for the fish metrics. Using standardised regression coefficients we compared the directions of the effects and the effect sizes of individual predictors and interaction terms and classified the interactions according Piggott et al. (2015). The results are summarized in Table 5.61. Variables of all predictor groups were involved in interaction terms. Overall, only opposing and synergistic interaction types were

determined. Three of the opposing interaction terms were classified as positive antagonistic and one as negative synergistic. Regarding the invertebrate metrics, we demonstrated that mostly for the trait-based metrics (Filter feeders, Grazers and Scrapers) significant interaction terms were classified compared with sensitivity and tolerance metrics (e.g. EQR, EPT or ASPT).

Table 5.59. Significant interaction terms, potential interaction types and directional classifications determined for the metrics of invertebrates and macrophytes

No significant interaction terms could be identified for the fish metrics.

Interaction types are: Opp = Opposing; S = Synergistic; The direction of individual predictors (a) or (b) and interaction effect (a + b) are coded as positive (+) or negative (-). Double symbols (--) or (++) indicate that the cumulative effect (a + b) is greater than the sum of individual predictor effects (in absolute terms); Classes are: negative / positive antagonistic (-A) / (+A), negative / positive synergistic (-S) / (+S)

Organism group	Interaction term (a + b)	Metric	Interaction type	Direction of the effects			Classification
				a	b	a + b	
Invertebrates	bed structure + urban area	PassFilFeed	Opp	-	+	-	+A
	TN + naturally-forested land	PassFilFeed	Opp	-	+	--	-S
	streambed + pasture	ActFilFeed	S	+	+	+	+S
	TN + bed structure	EPT	S	-	-	-	-S
	channel development + urban area	PassFilFeed	Opp	-	+	-	+A
	longitudinal profile + urban area	GrazScra	Opp	-	+	-	+A
Macrophytes	bed structure + pasture	SAC / SACs	S	+/+	+/+	++/++	+S / +S

5.5.4.1.2 Ecosystem service modelling results

Total biomass of commercial species

The BRT model explained 52.5% of the variance in the biomass of brown trout (Table 5.62). Physical habitat quality predictors alone accounted for approx. 46% of the variation in the metric, followed by natural and riparian land use predictors and TN. Within anthropogenic descriptors, pasture and the quality of adjacent land and longitudinal profile showed the greatest contribution to the overall deviance explained (Figure 5.90).

Table 5.60.Explained deviance derived from BRT and relative influence of predictor groups

Explained deviance (%)	Relative influence (%)			
	Natural	Riparian land use	Physical habitat quality	TN
52.5	26.4	23.6	46.1	3.9

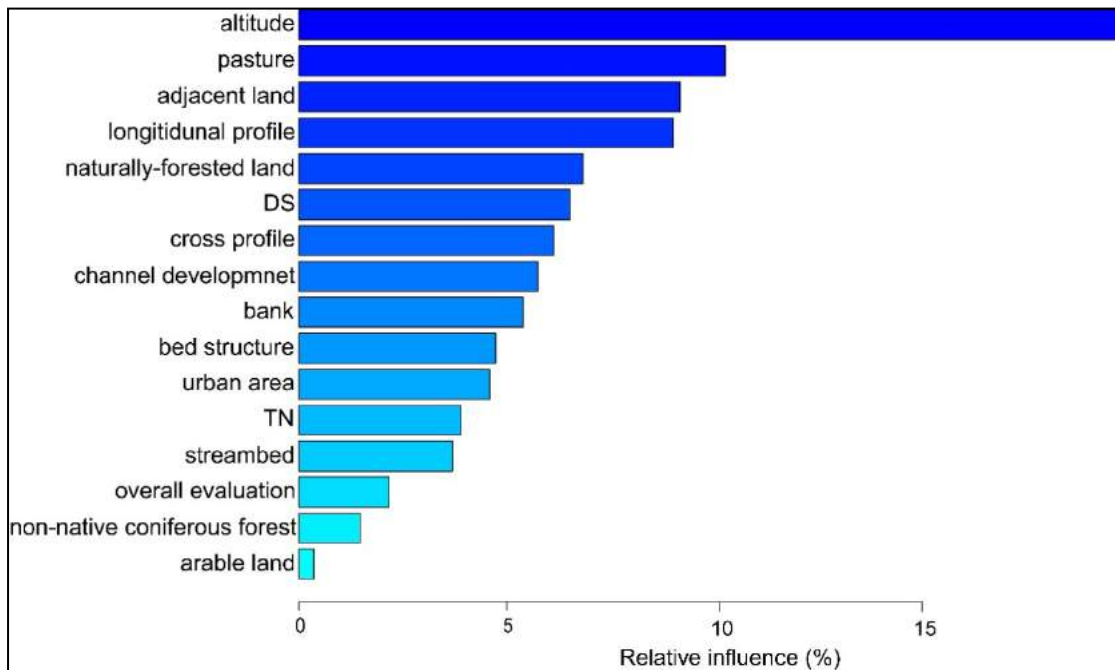


Figure 5.91 Summary of the relative influence of predictor variables to the full BRT model

As part of the outcome of the BRT analysis, Partial Dependence Plots display the influence of each of the sixteen predictor variables on the biomass of brown trout taken that every other variable has been kept to its mean value (Figure 5.91). The plots show that the abundance of brown trout increased up to an elevation of 400m above sea level with a nearly linear association. Anthropogenic predictors, however, showed weaker influence on the biomass of brown trout. Pasture land and the quality of the adjacent land and the longitudinal profile were the most influential anthropogenic predictors. Higher amounts of pasture land in the riparian zone resulted in a decline of the biomass of brown trout, whereas decreasing quality of adjacent land and longitudinal profile were linked with a slight increase of the biomass of brown trout.

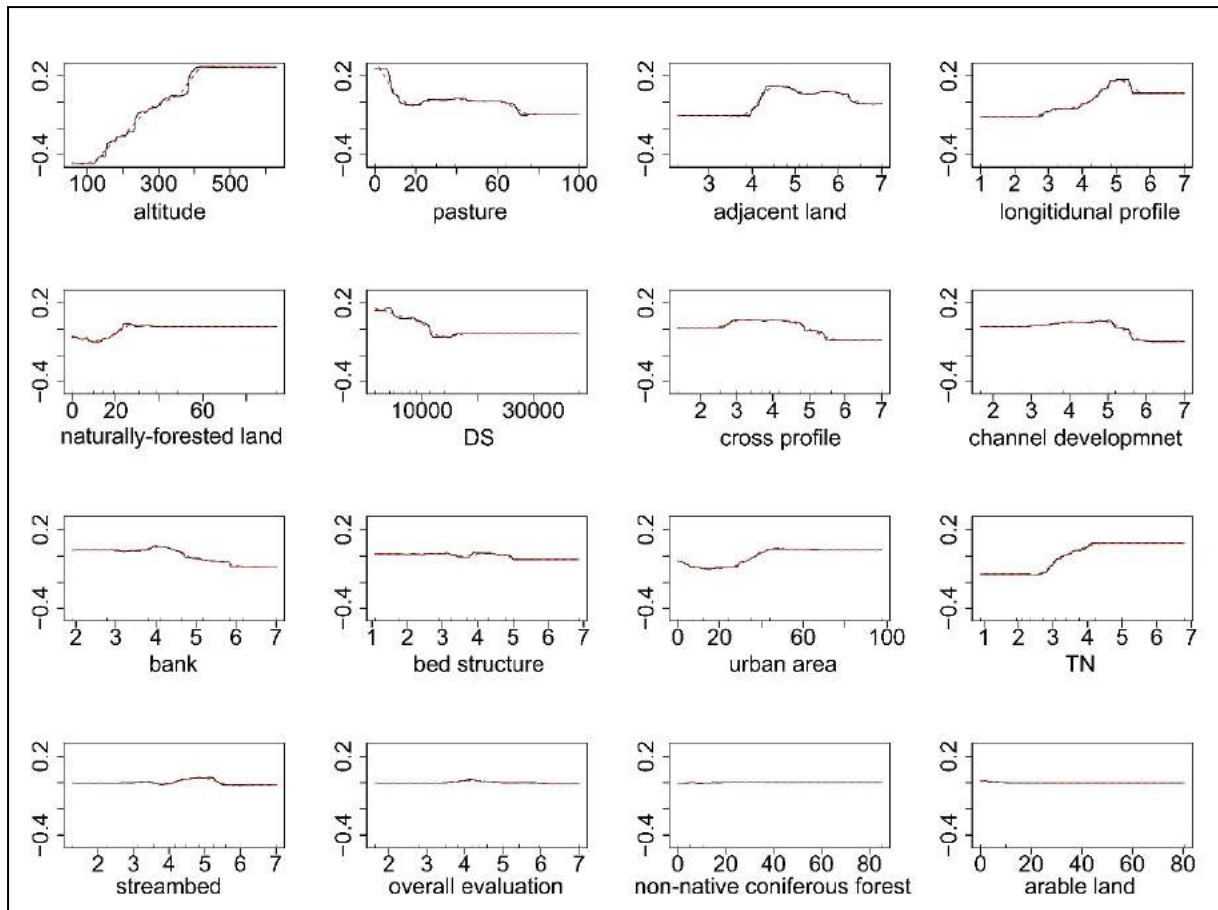


Figure 5.92 Partial Dependence Plots showing the fitted values for “Total biomass of brown trout” along selected predictor gradients

Interactions between anthropogenic predictors were identified, quantified and classified according to the procedure applied for the EM analysis as described before. We investigated the top five most influential and meaningful pairwise interactions determined via BRT. As this interaction terms were not significant in the GLM, no estimation of the magnitude and classification of the interaction terms could be performed. This means interactions were not relevant for the provisioning service “Total biomass of commercial species”.

Total carbon stored in the riparian zone

We calculated a total riparian area in the Ruhr Basin of approx. 10400 hectare, which is approx. 2.3% of the entire Ruhr Basin area. Pasture land which could be potentially reforested covers approx. 34% of the riparian area.

According to the surface area of each vegetation unit and its specific value of total C stocks per hectare (Table 5.59), we estimated a total C amount of 2.8 million tons accumulated in soil and vegetation for the entire riparian area in the Ruhr catchment. The land use category with the highest value of C stocking was deciduous forest which covers about 20% of the riparian area in the catchment (Table 5.63).

The amount of carbon which could be sequestered in fully developed reforested areas in excess of what is sequestered in pasture areas is given in the Table 5.63. Given that, 100% of available pasture areas in riparian zones would be reforested, up to approx. one million tons of carbon could be additionally sequestered.

Calculated prices for the additional sequestered CO₂ are shown in Table 8.6. Assuming a reforestation of 100% available pasture areas approx. up to 3.4 million tons CO₂ with a value of 44 million Euros could be additionally sequestered.

Table 5.61. Percentage cover and total carbon stocks of different vegetation units in the riparian area of the Ruhr Basin

Land use types	Vegetation units	Area / ha	Percentage of study area	Total C stocks / t
Non-native coniferous forest	Softwood forests	2185.3	21.0	777,968
Deciduous forest	Hardwood forests	2070.4	19.9	981,349
Mixed forest	Mixed (softwood/hardwood)	749.3	7.2	310,973
Pasture	Meadows and Reeds	3558.3	34.1	754,360
Arable land				
Urban area				
Water body	Others	1849.5	17.8	0
Others				

Table 5.62. Estimated benefits of C and CO₂ and prices for additional sequestered CO₂ for the four different reforested amounts of pasture land

Percentage of reforested pasture land	10	25	50	100
Reforested area / ha	356	890	1779	3558
Benefits of C stocks in fully developed reforested area / t*	93,227	233,069	466,137	932,275
Benefits of CO ₂ stocks in fully developed reforested area / t	341,800	854,500	1,708,999	3,417,999
Price for the additional sequestered CO ₂ / EUR	4,443,399	1,110,8496	2,2216,993	44,433,985

5.5.4.1.3 Results of the scenario analysis

In a first step, before modelling the effects of changed naturally-forested land on EQR, we predicted the EQR scores without changing the amounts of naturally-forested land to compare the goodness of fit of predicted and observed EQR values. The predicted and observed EQR values were highly correlated in the GLM model (Figure 5.92). These predicted EQR values were used as baseline condition.

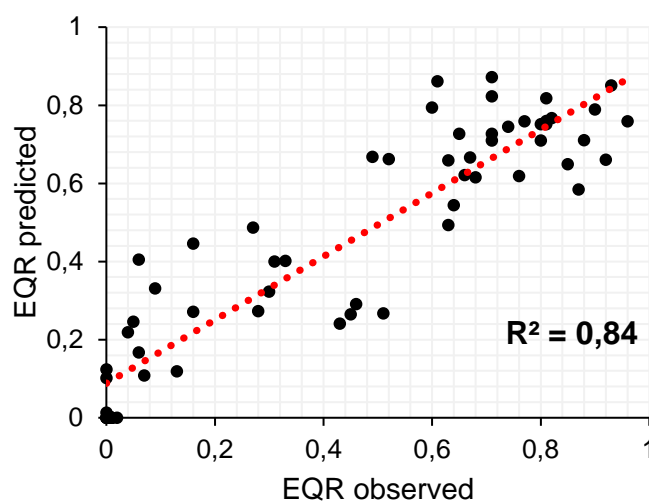


Figure 5.93 Scatter plot of observed vs predicted values of EQR

The results of the predicted mean values of EQR and the corresponding number of sites with an improvement or decline of ecological status class for the 62 sites in the three different scenarios are summarized in Table 5.65.

Increasing naturally-forested land in the riparian zones by 50% in a Consensus World scenario improved the mean overall EQR by 22%. In this case, the ecological status could be improved by one class for 23 of 62 sites. In a Fragmented World scenario removing 100% of naturally-

forested land areas led to a decrease of 18% in EQR and deterioration of ecological status for 27 sites by one class.

Table 5.63. Predicted invertebrate mean EQR values for the storyline elements “Loss of riparian zones” and “Restoration of riparian zones” in the three different scenarios

EQR = predicted mean values of EQR under baseline conditions (no land use changes) and in the three different worlds; Q = Quantification; ESC = Number of sites with an improvement (+) or decline (-) of ecological status by one class

Element of storyline	Baseline	Techno World		Consensus World		Fragmented World				
	EQR	Q	EQR	ESC	Q	EQR	ESC	Q	EQR	ESC
Loss of riparian zones	0.45	-25%	0.40	-15	+10%	0.47	+4	-100%	0.37	-27
Restoration of riparian zones	0.45	-10%	0.43	-8	+50%	0.55	+23	-50%	0.38	-22

5.5.5 Discussion

5.5.5.1.1 Q1: How to different organism groups respond to natural and anthropogenic predictors in multiple stress conditions? Show the three organism groups different responses? Do the different metrics show consistent response patterns?

Differences between organism groups

In the first part of this study, we aimed to address the response of selected metrics of three aquatic organism groups (flora and fauna) in a multi-stressor environment to anthropogenic (riparian land use, physical habitat quality and TN) and natural predictors. Simultaneous analysis of three organism groups enabled us to compare organism group-specific response patterns within an ecosystem. The results of our BRT models showed that the three organism group differ in their response to anthropogenic and natural characteristics. Among the three organism groups tested, benthic invertebrates showed on average the strongest relation to both natural and anthropogenic predictors compared with fish and macrophytes. A possible reason for the weak response of fish and macrophyte metrics might be the stream typology of the Ruhr Basin. The Ruhr river system consists primarily of small and mid-sized mountain streams. In contrast to mostly diverse invertebrate assemblages in these stream types, fish and macrophyte

assemblages are usually species-poor. In addition, macrophytes are often patchily distributed and even under natural conditions riparian shade may inhibit macrophyte growth. This applies in particular for the small mountain streams in the Ruhr Basin, where the height of the riparian vegetation exceeds the width of the streams. Thus, the relatively species-poor fish and macrophytes assemblages may limit the use of these groups for investigating multiple stress impacts in small mountain streams.

Differences between metrics

Differences in response to the anthropogenic and natural predictors were found not only among the three organism groups, but also between the metrics of one organism group analysed, in particular for invertebrate and macrophyte metrics. These findings implicate that attention should be given not only to one organism group but to the metrics selected to identify anthropogenic impacts.

5.5.5.1.2 Q2. Which predictor group and which single predictor have the greatest influence on the different organism groups?

Our results of the BRT models indicate that in contrast to fish and macrophytes, invertebrates were shown to be strongly affected by natural predictors. Consequently, leaving natural predictors unconsidered in empirical modelling would first lead to an incorrect interpretation of natural patterns as being anthropogenic impacts on invertebrate assemblages and would second increase the proportion of unexplained variance. In order to solve this problem a potential approach might be to separate the data in more homogeneous subsets, in our case in different stream types. On the one hand, an advantage of this approach could be that the natural gradient would be shorter and hence the explained variance by natural predictors could be reduced. But on the other hand, splitting the data reduce the number of available sites, which will necessarily affect the analytical approach negatively. To be able to rank the predictor's importance and to detect relevant interactions a minimum number of 150 independent sites are recommended (Feld et al. 2016). This is (among other things) why we decided to use the entire data set and not to divide the data.

Regarding the anthropogenic predictors, all three organism groups were more strongly related to the physical habitat quality predictors together compared with riparian land use and TN. For describing the riparian land use impacts we selected narrow buffer width and short buffer

length (1000m) for our investigations because we think, that narrow “natural” forested riparian buffer zones could be an applicable and practical land use management objective to improve the ecological quality of running waters, compared with land use in large buffers or even entire catchment land use. The weak response of the organism groups to riparian land use may be explained by the following factors:

(i) The amount of arable land and non-native coniferous forest seemed to play no role in characterizing the three organism groups, although negative effects of these land use categories are estimated, e.g. nutrient enrichment, habitat degradation, hydrologic alteration or reduced leaf-litter. However, this weak response of organism groups may be mainly due to the short gradients of these land use variables in upstream riparian area of the Ruhr Basin.

(ii) The short buffer length of 1000m may be not enough to indicate the influence of upstream riparian land use. For instance, Feld (2013) showed stronger impacts of riparian land use with increasing buffer lengths from one to ten kilometres upstream.

For all organism groups the quality of the bed structure appeared as an important predictor. The quality of the bed structure is characterized by following features: substrate diversity, special bed pressures (waste, sand drift erosion etc.), special bed features (pools, runs, riffles, wood debris etc.) and bed fixation. The importance of good quality of the bed structure for the three organism groups could be explained by the following facts:

(i) Benthic invertebrates are largely limited to the conditions of the stream bed, which depends on substrate quality.

(ii) Higher substrate quality and diversity increase the availability of spawning habitats for the fish and consequently enhance the density of the fish.

(iii) An increased quality of the bed structure provide a more suitable habitats for rooting macrophytes. This results in higher macrophyte abundances.

The weak role of TN may primarily be attributable to the short gradient. The highest measured concentrations of TN of 10.4 mg L⁻¹ (mean over all sites: 3.4 mg L⁻¹) may have not stress triggering effect on the organism groups analysed.

5.5.5.1.3 Q3. Are we able to identify, quantify and interpret interactions?

Although we were able to identify many pairwise interaction terms in our monitoring and heterogeneous predictor data set using BRTs, however, only in subordinate percentage of possible cases we could classify these interactions in a GLM.

The most pairwise interactions were identified and classified for the invertebrate metrics. Only one interaction term could be classified for the macrophyte metrics and none for the fish metrics. Therefore, we conclude that interactions appear to be also organism group specific and play a marginal role for fish and macrophytes, at least using monitoring data and heterogeneous predictors.

Even though many interaction terms were identified for invertebrates, the investigations strongly suggest that even based on a tremendous high sampling data (790 sites), very few interactions could be classified. As a consequence, we conclude that interactions were detectable, but they play a minor role in monitoring data using heterogeneous predictor variables.

Further, our findings emphasise that interactions were not equally relevant for all metrics. The generally minor influence of the interaction terms on specific metrics can be explained by the metric types/calculations process. Invertebrate metrics e.g. EPT, ASPT and EQR are metrics which integrate the influence of multiple factors and are not stressor specific and thus potentially not capable to detect interactions. As the most interactions could be classified for the trait-based invertebrate metrics (Filter feeders, Grazers and Scrapers) we conclude that trait-based metrics are potentially more suitable to differentiate the effects of multiple stressors. These findings are supported by the investigations of Lange et al. (2014).

Attention need to be given to the fact, that predictors with relative weak single influence on biota could be also involved in interaction terms. For instance, we identified a weak single role of TN, but the interaction analysis showed that TN interacts with both riparian land use and physical habitat quality predictors. Therefore, we should consider that these interactions exist.

Generic implications

As we could quantify and classify interactions at least for trait-based invertebrate metrics, we conclude that more detailed investigations are needed. For the future analysis we suggest that on the one hand available monitoring data should be included in the investigations to reveal

more about interactions, but on the other hand, however, national monitoring measures should also target direct stressors. It seems to be not sufficient to determine land use effects using land cover data, but rather we need direct effects resulting from land use, e.g. concentration of nutrients.

5.5.5.1.4 Ecosystem services

Total biomass of commercial fish species

Biomass of brown trout was shown to be mainly explained by physical habitat quality predictors, whereas the influence of riparian land use predictors together was lower. However, the amount of pasture land in the riparian area as single descriptor was the most influential anthropogenic predictor. On the one hand, the biomass of brown trout was negatively related to higher amounts of pasture land, but on the other hand worse quality of the two most influential structural predictors (i) longitudinal profile and (ii) adjacent land showed slight positive relation to the biomass of brown trout. The remaining structural predictors showed a slightly negative or not clear influence. This inconsistent influence of anthropogenic impacts could potentially be explained by the following:

(i) Brown trout need woody streamside vegetation, which provides the shade necessary to keep water temperature cool. In stream sections with high amounts of pasture land less woody vegetation is available, explaining negative influence of pasture land on the trout biomass. The slightly positive influence of worse quality of some structural predictors can be explained by the fact that adult brown trout prefer boulders, undercut banks, deep stream sections and velocities that they primarily find in degraded and straightened sections.

(ii) A further reason could be the extensive stocking measures with brown trout in the Ruhr Basin. The stocking practices may mask the human-induced impacts.

These facts may be also the reason why relevant interactions among anthropogenic predictors could not be identified. However, human-induced impacts e.g. pollution and habitat destruction exert stress on fish populations and might cause impacts at the ecosystem and endanger ecosystem services generated by fish.

Total carbon stored in the riparian zone

In our study we estimated the current amount of stored carbon in different vegetation types in the riparian zone by using specific values of total carbon stocks of above ground and below ground. The results showed that by replacing pasture land areas by mature deciduous forest, approx. 35% of carbon could additionally be stored, in excess of what is currently sequestered. Considering the relevance of woody riparian zones in preventing nutrient and sediment input to streams and rivers, the reforestation of available pasture areas by deciduous forest has the potential not only to sequester a huge amount of atmospheric carbon but also simultaneously to enhance ecosystem services such as water and habitat quality.

Additionally, we estimated the monetary value of the carbon sequestration service. As the carbon price has been very volatile to date, we used the average price for the emission of one ton CO₂ since 2005 (approx. 13 Euro) on the EU emission trading market. We calculated that in fully developed reforested areas up to 3.4 million tons CO₂ with a value of 44 million Euro could be additionally sequestered in excess of what is currently sequestered in pasture areas. These estimations demonstrate that besides other benefits of reforested riparian areas, carbon sequestration can be considered as an effective way for immediately mitigating significant shares of CO₂ emissions and furthermore it provides a financial incentive of addressing climate change. Regarding the forecast of the European Commission (Capros et al. 2013) the prices for carbon emission will follow a slowly increasing trend until 2025 and stronger increases thereafter. It is projected that the prices will increase more than tenfold. Higher prices could become an important point when companies start to think differently on the decision to include carbon sequestration in their considerations.

Nevertheless, there are several limitations of the applied approach in our study. We do not account for a number of factors included in estimation of carbon stocks and in cost studies. The applied method of estimating carbon sequestration using cover-related vegetation types provides a rapid way to figure out current carbon stock, estimate sequestration capacity and calculate the potential for additional sequestration. However, the estimations of stored carbon in the riparian area are based on a broad scale. Further, we did not include costs associated with conversion of pasture land to developed deciduous forest.

5.5.5.1.5 Scenario analysis

Our results of the scenario analysis suggest that EQR scores in the large mountain streams of the Ruhr Basin are affected by the amount of naturally-forested land implying that higher amount will have a positive effect on benthic invertebrate communities. Regarding the effects of the applied scenarios we showed that solely by increasing naturally-forested land in riparian zones in favour of pasture, arable and non-native coniferous forest areas, EQR changes are profound. For instance, increasing naturally-forested land by 50% in Consensus World lead to an improvement of mean overall EQR by 22%. This improves the ecological status by one class for 23 of 62 analysed sites. These positive effects are explained by the many benefits which woody riparian vegetation provides for invertebrate communities, like habitats (root wads, shade) or organic matter (large wood, leafs) and furthermore mitigation of anthropogenic influences (e.g. fine sediment input or temperature increase). These findings emphasise the potential of reforestation measures for river management, in particular for the aim of WFD to achieve the good ecological status.

5.5.6 Conclusion

1. Benthic invertebrates showed the strongest relation to anthropogenic predictors. They are more suitable to analyse multiple stressor effects in small and mid-sized mountain streams of the Ruhr area. The relatively species-poor fish and macrophytes assemblages may limit the use of these groups for investigating multiple stressor effects.
2. Differences in response to the anthropogenic predictors between the metrics of one organism group were determined. Hence, attention should be given to the metrics selected to identify multiple anthropogenic impacts.
3. Natural patterns need to be considered in analysing multiple stressor effects.
4. Enhancing stream physical habitat quality, particularly the diversity/quality of channel substrates should be considered as the first measure to improve the ecological quality in the Ruhr Basin.

5. Interactions play a minor role in monitoring data using heterogeneous predictor variables. However, invertebrate trait-based metrics were shown to be potentially more suitable to differentiate the interaction effects compared with general metrics (e.g. ASPT or EQR).

6 Analysing interaction effects using land cover data was shown to be not sufficient. Direct effects resulting from land use are needed. Thus, national monitoring measures should also target direct stressors.

7. Enhancement of naturally-forested riparian zone were shown to be relevant for both achieving a good ecological status and sequestering a huge amount of carbon.

8. Carbon sequestration can be considered as an effective way for mitigating significant shares of CO₂ emission. Additionally, it provides a financial incitement of addressing climate change.

5.6 Thames

5.6.1 Introduction

5.6.1.1.1 Location, geology and land use of the Thames basin

The river Thames (Figure 5.93) is the second largest river in the United Kingdom, with a total length of 354 km from its source in the Cotswold Hills to its tidal limit at Teddington Lock in south west London, and a catchment area of 9948 km² (Marsh and Hannaford, 2008). The western parts of the Thames Basin are predominantly rural, whereas the highly urbanized area of Greater London is located in the central and eastern part of the basin and is home to about 14 million people. The Thames Basin contains many other major urban centres, including Swindon, Oxford, Slough and Reading (Figure 5.93), and in total houses a fifth of the UK population.

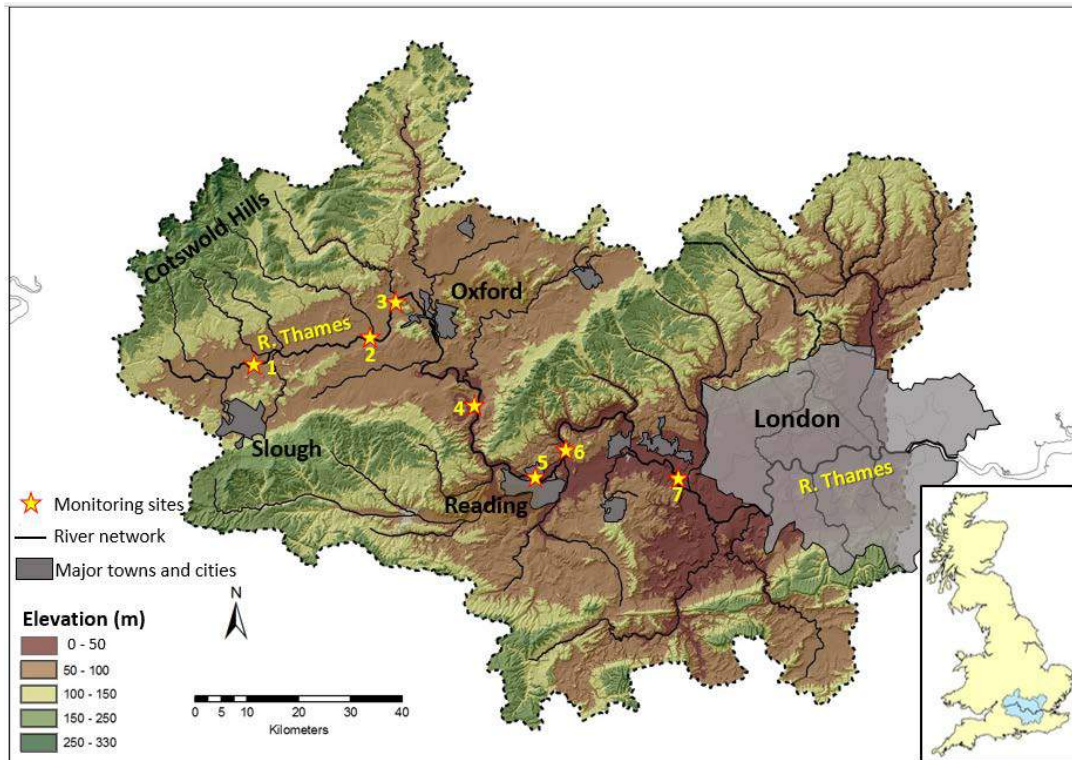


Figure 5.94 Map of Thames basin, showing location of some of the monitoring sites. Site 1 = Hannington Wick; Site 2 = Newbridge; Site 3 = Swinford; Site 4 = Wallingford; Site 5 = Reading; Site 6 = Sonning; Site 7 = Runnymede / Egham. Source: Bowes et al. (in press)

Despite its high human population density of approximately 960 people km² (Merrett, 2007), approximately 45 % of the Thames area is classified as arable, 11 % woodland, 34 % grassland, and only 6% classed as urban and semi-urban development (Fuller et al., 2002). The geology of the basin is complex, summarised in Table 5.66 the catchment is predominantly underlain by Cretaceous Chalk geology, with Oolitic Limestones in the upper catchment. The River Thames at Reading has a mean annual flow of 38.9 m³ s⁻¹, a base flow index of 0.68 and a mean annual rainfall of 744 mm (Marsh and Hannaford, 2008).

Table 5.64.Permeability (%) of the Thames basin

	Bedrock	Superficial deposits
High	43.2	14.0
Moderate/ mixed	9.7	7.2
Low	37.1	7.4

5.6.1.1.2 River Basin Management Plan of the Thames basin

For the Thames River Basin District, a number of specific pressures have been identified as significant water management issues (Environment Agency, 2009b, page 6) as follows:

- Abstraction and other artificial flow pressures
- Invasive non-native species
- Nitrate in surface and groundwater
- Phosphorus in rivers and standing waters
- Physical modification morphology
- Sediment (rivers and lakes)
- Urban and transport pressures
- Faecal indicator organisms
- Organic pollution (ammonia and biochemical oxygen demand)

Key ecosystem services are not identified in the Thames River Basin Plan (Environment Agency, 2009a), but public water supply and recreational services (e.g. fishing, boating, bathing) are identified as important.

Based on Environment Agency (2009a), 571 surface water bodies (including 76 lakes and reservoirs and 11 estuarine or transitional water bodies) have been assessed for ecological status and 46 groundwater bodies have been assessed for chemical and quantitative status; they show that 23% of assessed surface waters are at good or better biological status; 35% of groundwater bodies are at good quantitative status; and 43% of groundwater bodies are at good chemical status.

For the surface water bodies, Environment Agency (2009a) states that the main reasons for failure of good status are:

- point source discharges from water industry sewage works,
- diffuse source pollution from agriculture,
- abstraction and physical modifications to the channels.

For groundwater quality, Environment Agency (2009a) states that the main reason for poor status is high or rising nitrate concentrations, with some failures for pesticides and other chemicals. Poor groundwater quantitative status is caused by high levels groundwater

abstraction – mainly for drinking water / public supply – that exceeds the rate at which aquifers are recharged.

Environment Agency (2009a) also notes the key ecosystem elements affected by specific causes of poor or failing status of rivers, as follows (Table 5.67):

Table 5.65. Causes for poor environment status of water bodies of the Thames basin. Source: Environment Agency, 2009a

Reason for failure	Key ecosystem elements affected
Point source pollution (water industry sewage works)	Diatoms, invertebrates, phosphate
Physical modification flood protection and coastal erosion protection	Mitigation measures for morphology
Diffuse source agricultural	Diatoms, invertebrates, phosphate
Physical modification urbanisation	Fish, invertebrates, mitigation measures for morphology
Physical modification wider environment	Fish, invertebrates, mitigation measures for morphology
Abstraction	Hydrology (flows)
Physical modification land drainage	Fish, invertebrates, mitigation measures for morphology
Physical modification barriers to fish migration	Fish
Diffuse source mixed urban run-off	Ammonia, dissolved oxygen, fish, invertebrates, phosphate,
Physical modification water storage and supply	Fish, invertebrates, mitigation measures for morphology

There is no consensus with respect to specific knowledge gaps in understanding of causes of poor or failing status of surface or groundwater. However, the Environment Agency (2009a) do note that because “*many of the key pressures are complex and occur in combination, we often do not know the reason for a failure. For many water bodies either, the reasons for failure are unknown, or it is uncertain whether there is a failure or whether pressures really are causing an impact.*”

5.6.1.1.3 Main drivers and stressors in the Thames basin

Based on previous assessment of possible cause for water body status failure, **Error! Reference source not found.** lists the drivers and stressors identified for the Thames.

Table 5.66. Main drivers and stressors identified in the Thames basin

Drivers	Stressors
Urban development	Point pressure
Agriculture	Diffuse pressure
Industry	Change in thermal regime
Climate change	Hydrological alteration
Groundwater abstraction	Physical alteration of riparian area
Flood protection	Abstraction/ flow diversion

5.6.1.1.4 Research questions for the Thames basin

The following research questions have been addressed by the empirical modelling:

1. What are the ecological responses to extreme temperature to nutrient stress? [CB]
2. What are the ecological responses to extreme low flow and nutrient stress? [CB]
3. What are the ecological responses to extreme high flow and nutrient stress? [CB]
4. What are the ecological responses to extreme temperature and extreme low flow? [Thames]
5. What are the ecological responses to extreme temperature and extreme high flow? [Thames]

No ecosystem service is directly modelled in the Thames; however, changes in flow might have consequences for public water supply.

5.6.1.1.5 Indicators and variables used for the Thames basin analysis

The variables were modelled in the empirical and scenario analysis are summarised in **Error! Reference source not found.**

Table 5.67. Variables modelled in the Thames basin

Acronym	Description	Unit
BInd2	Total phosphorus concentration in the water column	mg l ⁻¹
BInd9_TotalP	Total phosphorus concentration in the water column during the growing season (water temperature above 9°C)	mg l ⁻¹
BInd3	Total nitrogen concentration in the water column	mg l ⁻¹
DO	Dissolved Oxygen	mg l ⁻¹
Temp	Water temperature	°C
ExtremeTemp	Water degree days above 9°C	°C
BInd4	Mean duration of high pulses (periods with mean daily flow above Q25/ 75%ile) within each year	day
NbBInd4	Number of high pulses (periods with mean daily flow above Q25/ 75%ile) within each year	
BInd5	Mean duration of high pulses (periods with mean daily flow below Q90/ 10%ile) within each year	day
NbBInd5	Number of high pulses (periods with mean daily flow below Q90/ 10%ile) within each year	
BInd8	Growing season (water temperature above 9°C) water column chlorophyll-a concentration	mg l ⁻¹
BInd9_Chla-TotalP	Growing season (water temperature above 9°C) water column chlorophyll to Total P ratio	
Run	Mean annual runoff	mm
Q25	High flow indicator	m ³ s ⁻¹
Q90	Low flow indicator	m ³ s ⁻¹
10 th %ile DO	Low DO statistic typical of summer conditions	mg l ⁻¹
BInd3	Mean total N concentration	mg l ⁻¹
90 th %ile Temp	High water temperature statistic typical of summer conditions	°C

5.6.2 Context for the modelling

Considering the available data, the modelling capacity and the identified drivers and stressors, the DPSIR model of **Error! Reference source not found.** has been defined for the Thames.

Catchment: Thames

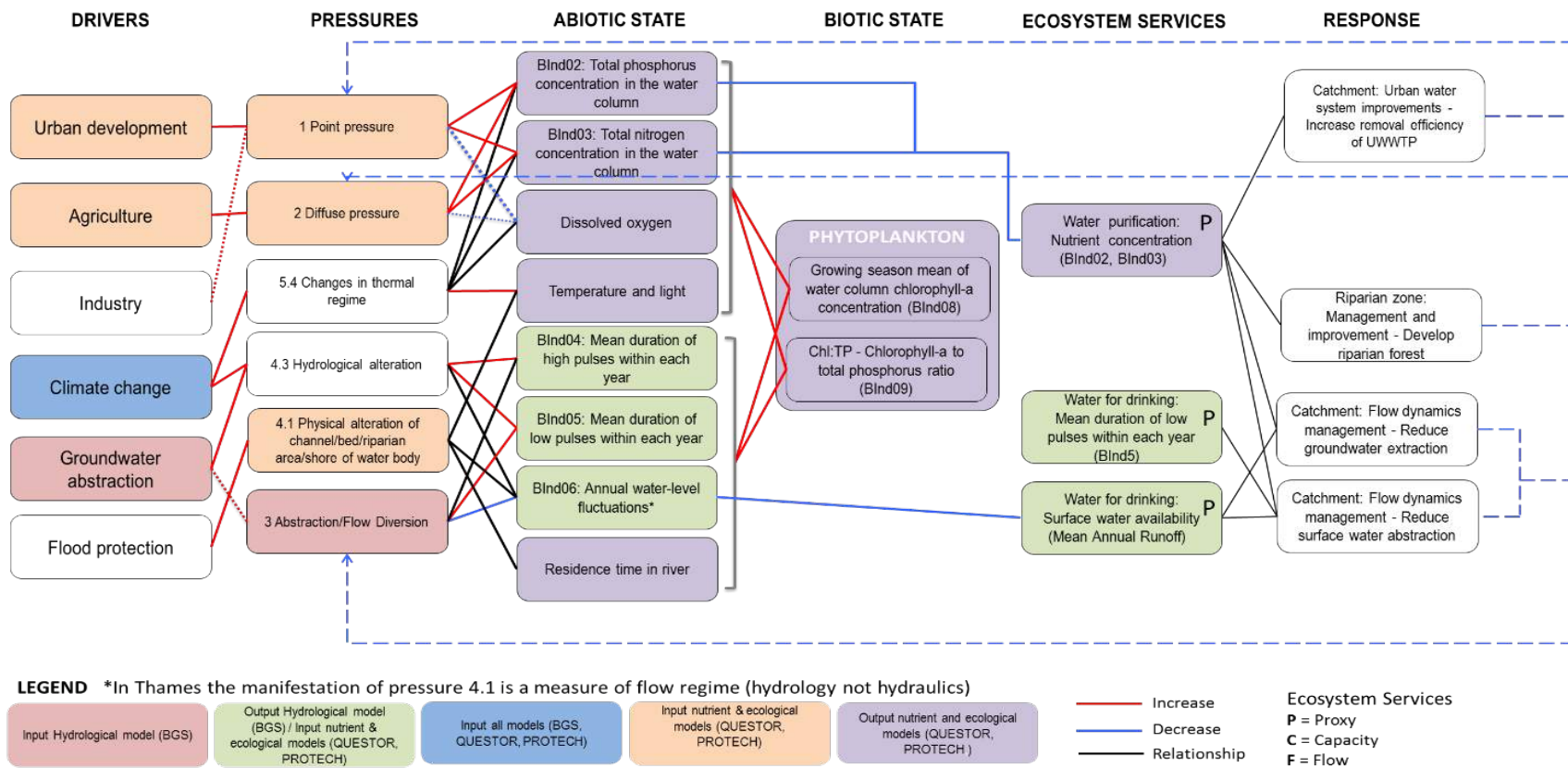


Figure 5.95 DPSIR model for the Thames basin

5.6.3 Data and methods

5.6.3.1.1 Data

The Thames basin benefits from a relatively dense network of hydro-climatic, chemistry and biotic gauges, summarised in **Error! Reference source not found., Error! Reference source not found.** and **Error! Reference source not found.**. Data were used to calibrate and evaluate models under baseline conditions.

Table 5.68. Thames basin observational data network used for the analysis

Variable	Network density	Measurement frequency	Period of record
Precipitation	1-km grid from high density raingauges	day	1961-2014
Potential Evapotranspiration	1-km grid from variety of climatic records, based on Penman-Monteith equations	day	1961-2014
River flow	19 river gauges across the basin including 9 on the main channel. For 6 sites, simple relationships with gauged flow and known influence (abstraction or return) were used to derive daily flow representative of the sampling site	day	Variable; up to 2014
Groundwater levels	Groundwater levels from 207 observation boreholes were used for the calibration of the fully-distributed Chalk groundwater model (MABSWEC). The semi-distributed Cotwolds model was calibrated to river flows at 10 gauging stations located at the outlet of selected model cells.	variable	1971-2013
Water temperature	21 sites cross the basin including 6 on the main channel	hourly	2009-2014
NO ₃	21 sites cross the basin including 6 on the main channel	weekly	2009-2014
Total Phosphorus	21 sites cross the basin including 6 on the main channel	weekly	2009-2014
Chlorophyll-a	21 sites cross the basin including 6 on the main channel	weekly	2009-2014

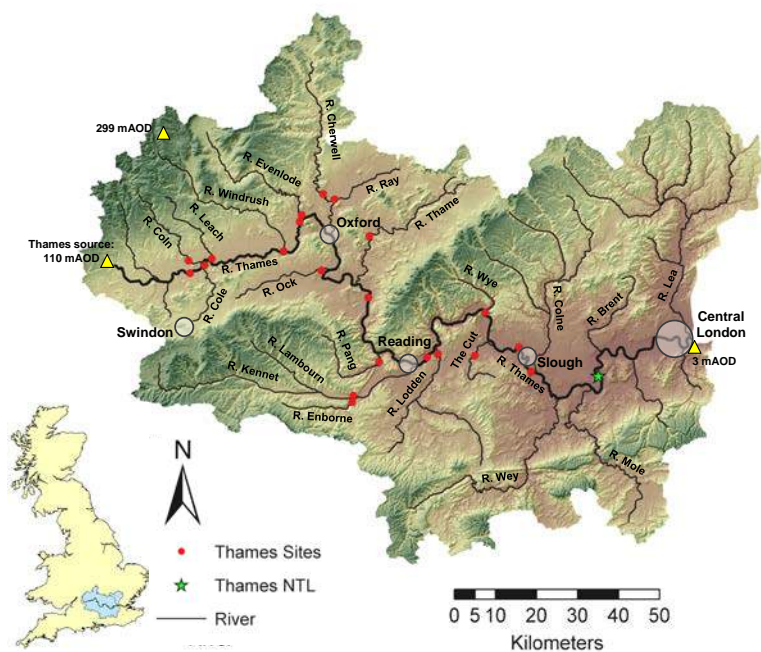


Figure 5.96 Chemistry and chlorophyll sampling sites on the Thames basin (Thames Initiative data)

Table 5.69. Thames basin sampling sites information

Site code	River at gauging site	Distance_source	Size catchment	Altitude	River_slope	Mean Temperature (year)	Total Precipitation (year)	Agriculture	Forestry	Urban develop
		km	km ²	masl	%	°C	mm	over 20%	over 15%	over 5%
TC1	Thame at Wheatley	53.2	532	55.4	0.5	10.5	654	Yes	No	Yes
TC2	Ray at Islip	31.7	290	59.3	0.4	10.5	725	Yes	No	Yes
TC3	Cherwell at Hampton Poyle	68.9	566	60.8	0.5	10.5	690	Yes	No	Yes
TC4	Evenlode at Cassington Mill	58.4	427	60.9	1.1	10.5	721	Yes	No	No

Site code	River at gauging site	Distance_source	Size catchment	Altitude	River_slope	Mean Temperature (year)	Total Precipitation (year)	Agriculture	Forestry	Urban develop
TC5	Thames at Swinford	89.2	1623	60.7	0.4	10.5	804	Yes	No	Yes
TC6	Thames at Newbridge	78.4	1229	64.5	0.3	10.5	765	Yes	No	Yes
TC7	Windrush at Newbridge	63.0	362	64.4	1.6	10.5	765	Yes	No	No
TC8	Leach at Lechlade	29.0	77	72.8	2.5	10.5	737	Yes	No	No
TC9	Cole at Lyte Bridge	28.9	141	71.9	0.3	10.5	702	Yes	No	Yes
TC10	Coln at Whelford	43.6	136	78.0	1.6	10.5	874	Yes	Yes	No
TC11	Ock at Abingdon	33.3	255	49.9	0.3	10.5	658	Yes	No	Yes
TC12	Pang at Tidmarsh	27.6	175	41.8	1.5	10.5	707	Yes	Yes	No
TC13	Thames at Sonning	166.1	5790	33.6	0.2	10.5	721	Yes	No	Yes
TC14	Lodden at Charvil	49.6	584	32.4	0.7	10.5	755	Yes	No	Yes
TC15	The Cut at Paley Street	19.5	63	31.8	7.0	10.5	680	No	Yes	Yes
TC16	Thames at Runnymede	221.7	7192	15.0	0.4	10.5	722	Yes	No	Yes
TC17	Wye at Bourne End	17.3	134	24.7	3.8	10.5	772	Yes	Yes	Yes
TC18	Thames at Wallingford	134.0	4213	42.6	0.2	10.5	717	Yes	No	Yes

Site code	River at gauging site	Distance_source	Size catchment	Altitude	River_slope	Mean Temperature (year)	Total Precipitation (year)	Agriculture	Forestry	Urban develop
TC19	Thames at Hannington	46.5	567	74.0	0.4	10.5	757	Yes	No	Yes
TC20	Kennet at Woolhampton	71.3	842	58.2	1.3	10.5	782	Yes	No	No
TC21	Enborne at Brimpton	25.5	142	60.6	1.4	10.5	814	Yes	Yes	Yes

5.6.3.1.2 Methods

Process modelling

GROUNDWATER AND RIVER FLOW MODELLING

Two principle aquifers are present within the study area: the Chalk and the Oolitic limestones of the Jurassic. These aquifers provide the main source of flow to the River Thames and its tributaries. They are separated by impermeable clay deposits and are connected only by the surface river network. Simulation of this complex system and its interaction with the rivers required the constructions of a series of hydrogeological models. These models were developed using different modelling codes, reflecting the degree of complexity of the part of the system being considered. Since the MARS study focusses on the upper and middle reaches of the River Thames, the model set up of **Error! Reference source not found.** was used to simulate daily river flows. This included:

- 1) gridded recharge models (green and red outlines in Error! Reference source not found.) that simulate run-off and recharge across the Chalk and Limestone catchments, based on the distributed recharge model code ZOODRM (Mansour and Hughes, 2004). The models simulate rainfall recharge to the water table and were used drive the groundwater models of the limestone and chalk aquifers and to calculate surface runoff.

- 2) the Cotswolds model: a semi-distributed model of the Oolitic limestone aquifer (blue outline in Error! Reference source not found.) where flows in and out of each cell are calculated from the hydraulic gradients between neighbouring cells, using Darcy's law (Darcy, 1856). Time-variant groundwater levels and flows are calculated for every time step from the overall water balance in each cell, including: recharge due to rainfall, river leakage (water exchanges between the river and the aquifer), flows in and out of the cell due to groundwater flow, and abstractions.
- 3) the MABSWEC model: a gridded groundwater model of parts of the Chalk aquifer (red outline in Error! Reference source not found.), a fully distributed groundwater model based on finite difference modelling code ZOOMQ3D (Jackson and Spink, 2004).

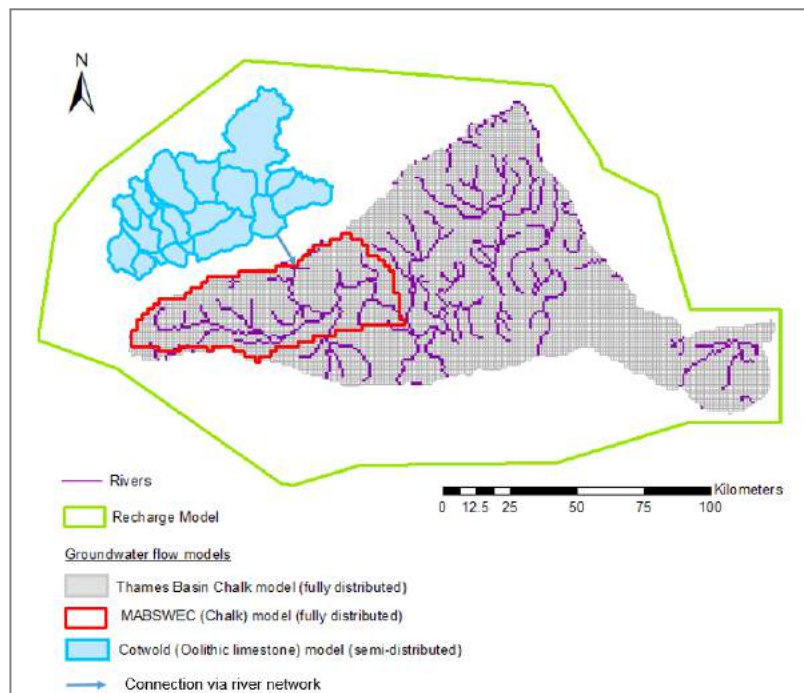


Figure 5.97 Thames Basin Groundwater Models

All three models were run for the period Jan 2009-Dec 2012. The Cotswolds model calibration was carried out by adjusting hydraulic conductivity, transmissivity/ base elevation, storage coefficients and river bed conductance within a Monte Carlo framework and comparing the resulting river flows at selected cell outlets to observations. Its performance on river flow simulation (based on the Nash and Sutcliffe Efficiency criterion) varies between 0.46 and 0.88. The calibration of the MABSWEC model

included comparison of model results with observations of river flows at 20 gauging stations, groundwater levels at 207 observation boreholes and a number of river flow accretion profiles. Generally, the model reproduced the observed data well, both groundwater hydrographs and river baseflows. Baseflow in the River Wye were less well simulated. Groundwater abstraction appears to dominate the catchment and to reduce baseflow. This catchment is near to a model boundary, which is delineated along the estimated location of a groundwater divide.

RIVER WATER QUALITY MODELLING

River water quality modelling for the Thames to Wallingford (3445 km²) used the 1-D model QUESTOR which represents flow routing and chemical reactions in the river channel in the upper Thames basin divided into 41 reaches (33 on the 92 km main Thames between Hannington and Wallingford, and a further 3 and 4 reaches representing 15 km of the Cherwell and 19 km of the Thames respectively). Output was generated at TC6 (Thames at Eynsham, upper reach) and TC18 (Thames at Wallingford, middle reach).

The version of the model used and its performance under 2009-12 daily conditions is described elsewhere (Hutchins et al., *in press*). As a foundation for the storylines the 2009-12 period was used to provide a baseline of meteorological fluctuation (e.g. notably water temperature and sunlight) and a reference point for present day land-use and environmental management as reflected in concentrations of pollutants in sewage effluents, magnitudes of those effluents and water abstractions.

Under present day conditions nine effluents of total flow 1.335 m³ s⁻¹ directly influence the river network. Likewise there are two abstractions removing 2.71 m³ s⁻¹ (one for water supply 1.62, the Farmoor reservoir, the other 1.09 for industry, the Didcot power station).

As input the model requires daily data on flow and water quality from 22 tributaries. For the baseline run, observed data was used for the 10 sites considered in the groundwater modelling; for the other tributaries, flows were translated and scaled from one of the same 10 gauging stations. Monthly mean river temperature and pollutant concentration in tributaries were calculated from observed data and used as inputs in the baseline run (representing a combination of the effects of 2009-12 meteorological conditions and environmental management). A single time-series of solar radiation was used upon which

a single network-wide estimate of the effect of shade from riparian canopies was applied (20%).

RESERVOIR WATER QUALITY MODELLING

Farmoor reservoir is located in the Thames catchment 6 km west of Oxford and is an important part of the water supply network in the catchment, supplying water to Swindon and north Oxfordshire, including Oxford. The model PROTECH (Phytoplankton RespOnses To Environmental Change; Elliott et al., 2010), which simulates the responses of up to 8 species of lake phytoplankton to seasonal changes at a daily time step, was applied to simulate the phytoplankton abundance in the reservoir, with particular reference to the potentially harmful cyanobacteria types which can so readily cause problems to drinking water supply. PROTECH has been applied in over 35 peer reviewed studies and is one of the most cited lake models in the world (Trolle et al., 2012). Although mainly used for lakes studies, it can also be applied to reservoirs as was the case in this study.

PROTECH was set-up to simulate the observed data collected from Farmoor reservoir in 2014 using meteorological data from Brize Norton and weekly observed river nutrient data from the Thames Initiative. Thames Water, who own the reservoir, provided inflow and outflow discharges and their qualitative data on phytoplankton species were used to select the eight most representative types from PROTECH's phytoplankton library. After some minor adjustments to the observed relative humidity values, which needed increasing, the model captured well the annual changes in phytoplankton biomass measured as total chlorophyll *a* ($R^2 = 0.63$; **Error! Reference source not found.**).

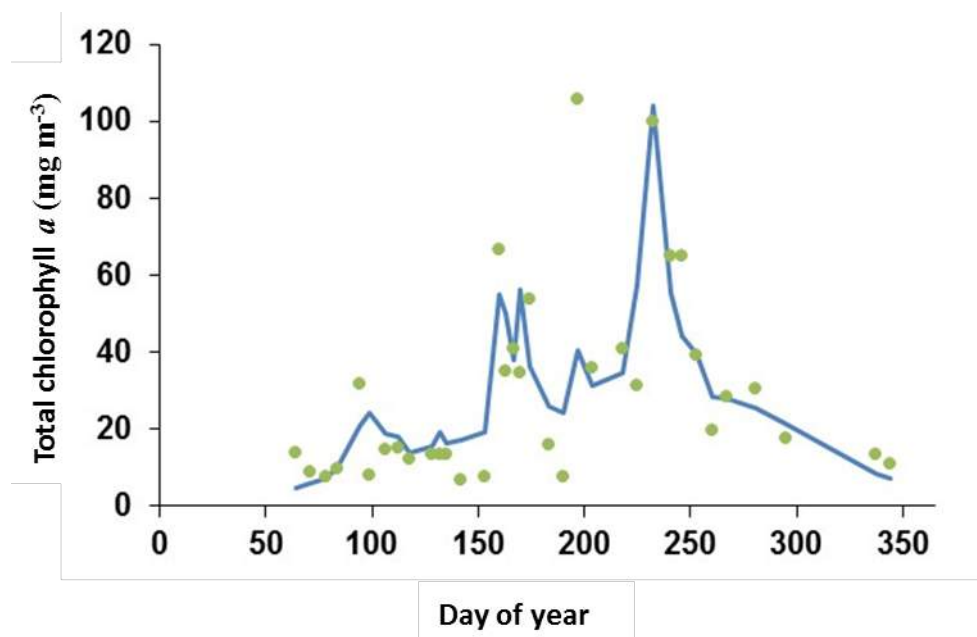


Figure 5.98 PROTECH modelling performance: Comparison between observed and simulated total chlorophyll a in Farmoor Reservoir for 2014.

EMPIRICAL MODELLING APPROACH

The empirical modelling followed protocols and methodology described in MARS guidance documents including ‘A cookbook for data handling and screen in R’, ‘a cookbook for analysing the response of benchmark indicators to multiple stressors’ and ‘Analysing stressor-response relationships and interactions in multi-stressor situations’. The following r-scripts were adapted for the Thames basin analysis:

- R_script_data_screening_Tulcea_v2.r
- ExampleAnalysisForWP6Synthesis.r
- MARS_GLMM_functions.r

Owing to the relatively limited number of sites (21 with complete data) and record length (maximum of 6 years between 2009 and 2014), a Generalised Linear Mixed Modelling with two stressors was conducted to answer each research question using site and year as random effects (multi-site, multi-year, spatio-temporal analysis). The ‘Growing season mean of water column chlorophyll-a concentration (BInd8) was used as response variable, with the stressor variables presented in Table 5.72.

Table 5.70. Research question and stressor combinations considered for the Thames basin (BInd8 is always the response)

Question	Stressor 1	Stressor 2
1. What are the ecological responses to extreme temperature to nutrient stress? [CB]	BInd9_TotalP	ExtremeTemp
2. What are the ecological responses to extreme low flow and nutrient stress? [CB]	BInd9_TotalP	BInd5 NbBInd5
3. What are the ecological responses to extreme high flow and nutrient stress? [CB]	BInd9_TotalP	BInd4 NbBInd4
4. What are the ecological responses to extreme temperature and extreme low flow? [Thames]	BInd5 NbBInd5	ExtremeTemp
5. What are the ecological responses to extreme temperature and extreme high flow? [Thames]	BInd4 NbBInd4	ExtremeTemp

Following data screening and testing for normality and collinearity, all variables were transformed following the Box-Cox transformation (estimateBC and applyBC R functions). The GLMM analysis for multisite, multiyear was conducted using the script written by Dan Chapman and adapted as a function ‘MARS_GLMM_functions.r’. Models with and without interactions were considered. Evaluation metrics are summarised in **Error! Reference source not found.**

Table 5.71. GLMM analysis results for research questions of Table 6.

Question	Interaction	AIC	R ² Marginal (fixed effects)	R ² Conditional (random effects)	Residual correlation p value	Shapiro- wilk normality test pvalue
1	Without	167.5	0.322	0.875	0.38	0.41
	With	169.1	0.325	0.877	0.38	0.41
2a	Without	201.4	0.143	0.851	0.31	0.09
	With	202.3	0.137	0.851	0.31	0.05
2b	Without	201.8	0.140	0.851	0.31	0.09
	With	203.8	0.142	0.851	0.31	0.10
3a	Without	201.1	0.147	0.853	0.31	0.10
	With	202.4	0.170	0.851	0.31	0.07
3b	Without	200.6	0.138	0.850	0.31	0.21
	With	196.8	0.172	0.880	0.33	0.19
4a	Without	169.3	0.240	0.863	0.37	0.25
	With	166.5	0.282	0.870	0.38	0.32
4b	Without	170.0	0.243	0.864	0.37	0.27
	With	168.3	0.272	0.870	0.38	0.29
5a	Without	170.7	0.245	0.862	0.37	0.28
	With	172.5	0.251	0.864	0.37	0.21
5b	Without	170.5	0.249	0.862	0.37	0.19
	With	172.3	0.250	0.861	0.37	0.21

MARS storyline scenarios implementation in the Thames basin

Using the suite of process models illustrated in **Error! Reference source not found.**, a set of 12 model runs was conducted to produce total river flow, river and reservoir water quality indicators for the MARS storyline scenarios defined in Table 5.74

Those simulations were compared with a baseline simulation of 2009-2012 to quantify the impact of the MARS storylines on the abiotic and biotic systems.

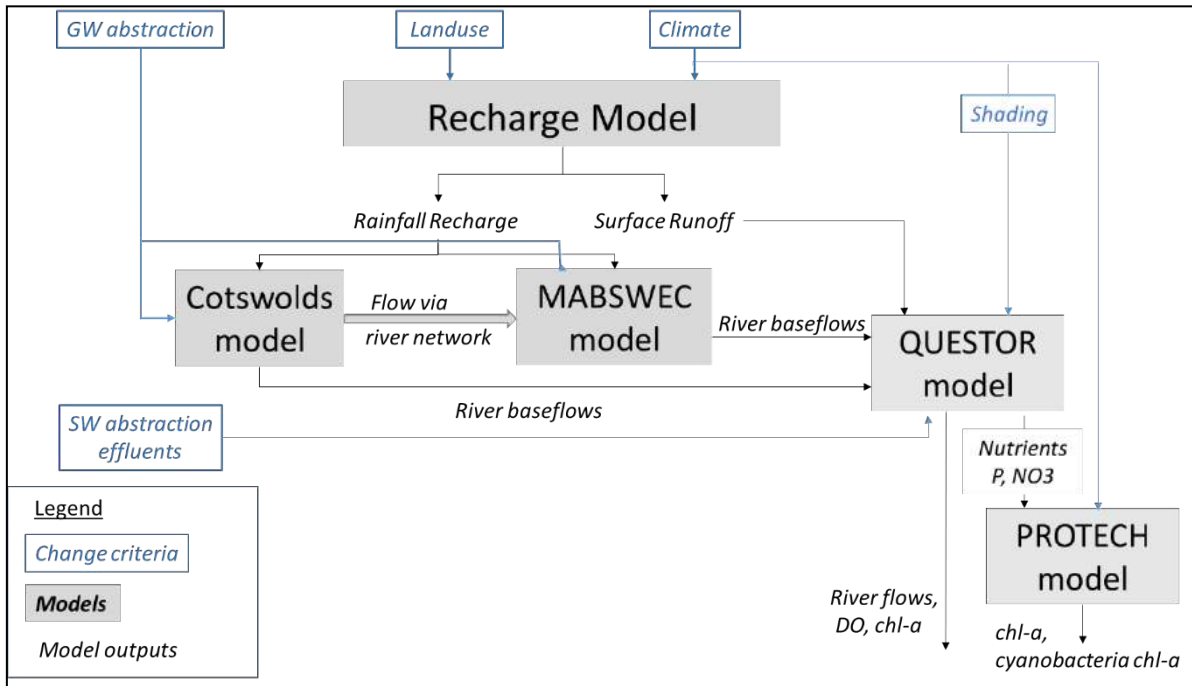


Figure 5.99 Flow diagram of the modelling process for the MARS storylines simulations

Land use changes were implemented through the recharge model by changing the proportion of land use in the catchment area as defined in Table 5.74.

Climate change scenarios were implemented through the recharge model, QUESTOR and PROTECH using the change factor method (Hay *et al.*, 2000). Climate change factors were first calculated following the MARS protocol, using 10-year mean monthly averages of bias-corrected catchment average daily extracted from climate model projections for the time periods of 2006-2015 (baseline TH_{present}), 2036-2045 (2030s) and 2056-2065 (2060s) (both TH_{future}). The monthly change factors were expressed as absolute change (for temperature) and percentage change (for all other climate variables) between TH_{future} and TH_{present} as $(TH_{\text{future}} - TH_{\text{present}}) (*100/ TH_{\text{present}}$ for percentage change). Monthly change factors were calculated for temperature (tas), potential evapotranspiration (PET), surface wind speed (wind), shortwave radiation (rsds), long wave radiation (rlds) and precipitation (pr). The climate change factors were applied multiplicatively to observed daily time series for precipitation, potential evapotranspiration and solar radiation, and additively to air temperature to produce time series input to the process based models as shown in **Error! Reference source not found.** for each time horizons. Following MARS protocol, two climate models and two Representative Concentration Pathways (RCPs) were considered to describe the MARS

storylines, as described in Table 5.74. The recharge model produced the rainfall recharge required to drive the groundwater models as well as the surface runoff component required for the calculation of total river flows.

Table 5.72.MARS story line scenarios and criteria applied to the Thames basin

Criteria	Techno world				Consensus World				Survival of the Fittest			
Climate	RCP8.5				RCP4.5				RCP8.5			
	GFDL 2030	GFDL 2060	IPSL 2030	IPSL 2060	GFDL 2030	GFDL 2060	IPSL 2030	IPSL 2060	GFDL 2030	GFDL 2060	IPSL 2030	IPSL 2060
Land use change	1.5 (50% Increase of all urban areas within catchments)				1.2 (20% Increase of all urban areas within catchments, but not taken from arable land)				1.5 (50% Increase of all urban areas within catchments)			
	0.9 (10% reduction in arable - Change to grass/ pasture and forest)				Present day / no change				0.7 (30% reduction in arable - Change to grass/ pasture and forest)			
Water levels	0.9 (10% reduction in groundwater abstraction)				0.8 (20% reduction in groundwater abstraction)				0.75 (25% increase in groundwater abstraction)			
Total P	0.9				1.5				1.5			
Urbanisation (i.e. abstractions and effluents)	0.96				1.35				1.875			
Shade	2 (to 40%)				0.75 (to 15%)				0 (to 0%)			
Invertebrate grazers (impact of pesticide runoff)	0.9				0.5				0.5			

Flows and water temperature scenarios were calculated by first deriving monthly flow factors for all simulated river reaches, and then applying them to the observed baseline flows (2009-12), so that any bias in the flow simulation does not affect the water quality simulation, which is very sensitive to low flow periods. Temperature change factors were applied additionally to each tributary's monthly mean observed water temperature.

For the *non-climatic variables*, Total Phosphorus concentration, abstraction and effluent rates, percentage of shading and percentage of invertebrate grazers, multiplier factors related to environmental change factors described in Table 5.74 were applied to baseline values. Farmoor *nutrient concentration (NO₃, P)* scenarios were taken from the QUESTOR simulations (baseline and 12 storyline runs). All other categories of input were held constant at present day levels (e.g. BOD, DO, nitrogen species, suspended sediment, pH). Although some of these have the potential to be influenced by management it was assumed these would not change significantly.

Water level change scenarios were implemented in the groundwater flow models by applying the percentage change to all groundwater abstractions within the model. The two aquifer systems are connected by the surface river network, with river flows from the Cotswolds recharging the downstream Chalk aquifer. To account for this, river baseflow at the outlet of the Cotswold model (Thames at Eynsham) were used to define river inflows at the top of the MABSWECC model (Thames at Wallingford). Simulated river baseflow data from the groundwater models and surface runoff from the recharge model were then used to calculate total river flows at selected river stations throughout the Thames Basin catchment.

Changes to water management regime: Application of the TW and SoF scenarios resulted in the river drying up. As a consequence alternative configurations were built in which changes had been implemented to represent

- 1) new alternative reservoir storage further downstream to meet abstraction demand. To increase abstraction rates beyond capacity of the existing reservoir is unsustainable in the upper part of the basin. It was assumed that the existing reservoir storage is at 80% of capacity
- 2) a constant water transfer into the basin entering in the upper reaches of the network. The transfer was assumed to be either at a minimum level to ensure sustainability of water resources in the Thames (Techno World: $2 \text{ m}^3\text{s}^{-1}$) or to comfortably exceed requirements (Survival of the Fittest: $4 \text{ m}^3\text{s}^{-1}$).

5.6.4 Results

5.6.4.1.1 Impact of MARS storylines on the Thames basin based on Process Modelling

The process modelling suite was applied to the 12 MARS storylines to identify the potential impact of climatic and environmental stressors on the abiotic and biotic systems of the Thames. This section summarises the results as a set of tables, Table 5.75 to 5.78, and Figures 5.99 to 5.101.

Table 5.73. Modelled mean baseline conditions modelled (2009-12) for the MARS indicators for the Thames Basin

	Newbridge	Eynsham	Abingdon	Wallingford
BInd2 (mg l ⁻¹)	0.484	0.424	0.536	0.546
BInd4 (day)	30.417	28.077	24.333	24.333
BInd5 (day)	36.500	36.500	24.333	24.333
BInd8 (mg l ⁻¹)	0.013	0.018	0.033	0.038
BInd9_TotalP (mg l ⁻¹)	0.528	0.456	0.580	0.583
BInd9_Chla-TotalP (unit)	0.025	0.045	0.072	0.086
DegreeDays_Above9/yr (°C year ⁻¹)	1671.495	1691.976	1755.439	1941.340
Q25 flow exceeded 25% of time (m ³ s ⁻¹)	14.490	17.520	31.580	34.800
Q90 flow exceeded 90% of time (m ³ s ⁻¹)	2.271	1.495	3.943	3.750
10th %ile DO ()	9.676	9.711	9.633	8.937
BInd3 (mg l ⁻¹)	6.801	6.372	6.386	6.355
90th %ile Temp (°C)	19.500	19.850	20.450	21.810

Nutrients (Bind2, Bind3 and Bind9) are in excess at all sites. Algal blooms (Bind8) only develop to a persistent extent downstream of Oxford (at Abingdon and Wallingford TC18). The Thames becomes increasingly slow flowing downstream and this is reflected in warmer summer water temperatures and higher degree days.

Table 5.74. Percentage change associated with the MARS storylines for the Thames basin at site: TC6 (Thames at Eynsham, upper reach) and TC18 (Thames at Wallingford, middle reach). Cells are shaded in red for changes greater than 25%, white for changes between +/- 25%, and blue for changes lower than -25%

		TC6 Thames at Eynsham						TC18 Thames at Wallingford					
		Consensus World		Techno World		Survival of the Fittest		Consensus World		Techno World		Survival of the Fittest	
		GFDL 4.6	IPSL 4.6	GFDL 8.5	GFDL 4.6	IPSL 4.6	GFDL 8.5	IPSL 8.5	GFDL 8.5	IPSL 8.5	IPSL 8.5	GFDL 8.5	IPSL 8.5
BInd2	2030	-57	-61	27	-50	-49	5	0	24	15	15	46	34
	2060	-63	-65	31	-52	-50	6	-8	26	16	16	50	38
BInd4	2030	44	8	18	-12	7	-6	7	0	0	18	0	30
	2060	30	18	-7	-17	-6	-12	15	-12	7	-7	-7	30
BInd5	2030	-50	100	-50	-25	-33	-40	-40	-40	-46	-33	-20	-33
	2060	-50	-20	-20	-14	-46	-50	-25	-50	0	-50	-1	-20
BInd8	2030	3	-17	67	-15	-16	138	114	136	110	53	28	28
	2060	8	-29	87	-15	-14	136	121	138	127	46	35	34
BInd9_ TP	2030	-58	-62	31	-51	-50	7	4	27	21	23	52	44
	2060	-65	-66	34	-54	-50	6	-7	28	19	14	53	39
BInd9_ch ITP	2030	169	139	11	82	77	95	84	50	43	12	-22	-18
	2060	260	112	21	106	96	99	98	50	51	2	-20	-18
DegreeDa y	2030	16	37	2	15	31	17	7	10	4	1	-3	-3
	2060	65	43	13	42	36	30	30	20	19	15	5	8
Q25	2030	-5	-9	1	10	-2	2	22	4	25	5	10	16
	2060	-29	-24	-11	-13	-14	-6	5	-4	27	12	-1	19
Q90	2030	-27	-22	38	-10	-12	-17	44	16	77	109	189	260
	2060	-76	-53	32	-60	-49	-25	-1	8	37	97	182	221
	2030	-2	-4	4	-9	-12	-5	4	8	8	1	1	-1

		TC6 Thames at Eynsham						TC18 Thames at Wallingford					
		Consensus World		Techno World		Survival of the Fittest		Consensus World		Techno World		Survival of the Fittest	
		GFDL 4.6	IPSL 4.6	GFDL 8.5	GFDL 4.6	IPSL 4.6	GFDL 8.5	IPSL 8.5	GFDL 8.5	IPSL 8.5	IPSL 8.5	GFDL 8.5	IPSL 8.5
10th %ile													
DO	2060	-4	-3	4	-41	-24	-14	-12	6	5	-1	1	-1
BInd3	2030	-3	-6	1	3	2	-5	0	2	4	2	5	5
	2060	-14	-9	-1	-2	-1	-7	-7	0	0	3	5	4
90th %ile													
	Temp	2030	7	10	-3	7	10	6	2	2	0	-1	-5
	2060	26	7	2	25	14	13	14	6	7	3	-2	0

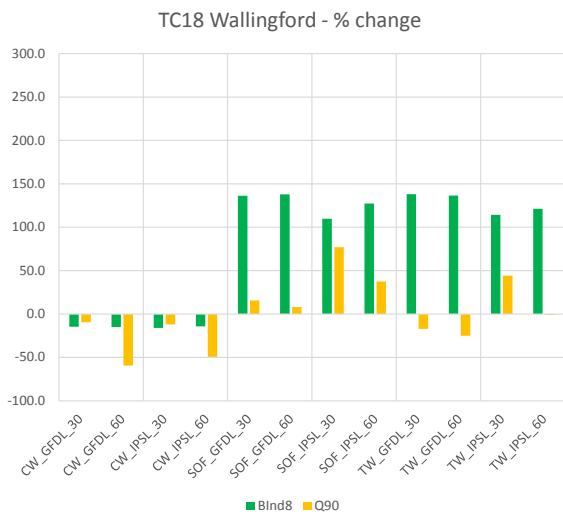
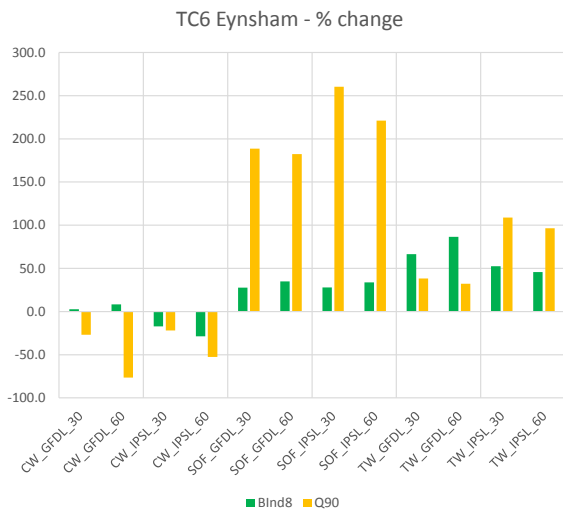


Figure 5.100 Percentage changes associated with the MARS storylines for the Thames basin at site TC6, the Thames at Eynsham in the upper reaches (left) and at site TC18, the Thames at Wallingford in the middle reaches (right) for the growing seasonal chlorophyll-a concentration (days above 9°C) (BInd8) and a low flow indicator, the flow exceeded 90% of the time Q90.

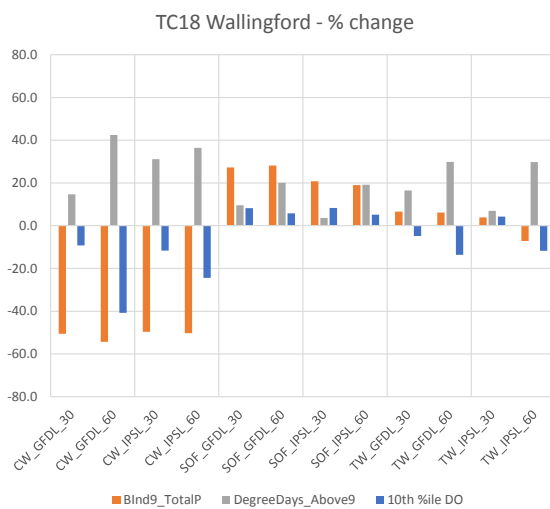
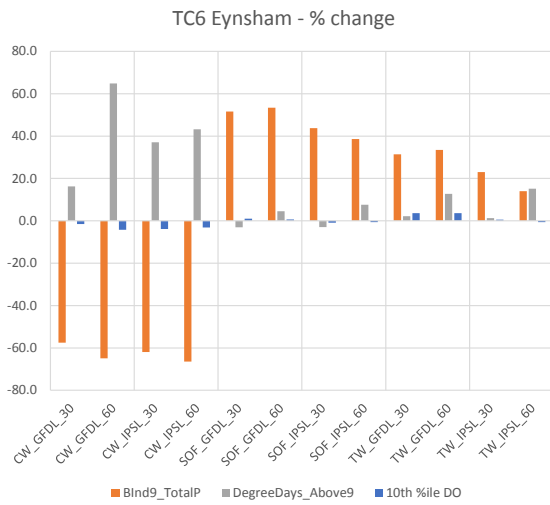


Figure 5.101 Percentage changes associated with the MARS storylines for the Thames basin at site TC6, the Thames at Eynsham in the upper reaches (left) and at site TC18, the Thames at Wallingford in the middle reaches, for the Total Phosphorus concentration during the growing seasonal (days above 9°C) (Blind9_TotalP), extreme temperature the water degree days above 9°C (DegreeDays_Above9) and a low Dissolved Oxygen indicator, the 10th percentile DO (10th %ile DO).

For the *reservoir simulations* two key metrics were simulated: mean total and cyanobacteria (i.e. potentially toxic species) chlorophyll *a* during the growing season; the latter is a useful measure of water quality with high values representing a decline in quality. The growing season was defined as days where the water temperature was > 9 °C. The relative percentage change in these metrics from their respective baseline values were calculated Table 5.77. The baseline values were total chlorophyll *a* = 47.2 mg m⁻³ and cyanobacteria chlorophyll *a* = 25.5 mg m⁻³.

Table 5.75. Percentage change associated with the MARS storylines for the Farmoor reservoir for the mean total (total chl a) and cyanobacteria chlorophyll a (Cyanobacteria chl a) concentration during the growing season (days above 9°C). Cells are shaded in red for changes greater than 25%, white for changes between +/- 25%, and blue for changes lower than -25%

		Consensus World		Techno World		Survival of the Fittest	
		GFDL 4.6	IPSL 4.6	GFDL 8.5	IPSL 8.5	GFDL 8.5	IPSL 8.5
Total chl a	2030	-28.4	-29.0	5.3	14.6	15.0	20.5
	2060	-23.1	-13.8	17.3	11.9	27.2	19.0
Cyanobacteria chl a	2030	-29.1	-26.9	11.4	27.2	18.2	33.1
	2060	-15.6	6.1	32.9	33.2	42.1	38.9

Differences between the storylines

Only by implementing a radical change in management of catchment water demand can the Techno World and Survival of Fittest World support a sustainable River Thames.

Implementing shading to 40% as defined under Consensus World is very effective at preventing accelerated algal growth particularly in the downstream reaches. However it is markedly less effective at keeping the river cool. This is only achieved (i.e. maintaining temperatures at present day levels) by limiting abstractions and including incoming water transfers (as in TW and SOF). Even then the benefits are only seen in upstream reaches (above Oxford) and start to be overcome by effects of climate change by 2060.

Light is the dominant factor limiting algal bloom development in all storylines. However CW differs from the other storylines and the present day baseline in that algal blooms are also strongly limited by phosphorus. This limitation, which develops during midsummer, causes algal population crashes which lower DO concentrations. As phosphorus concentrations, by definition due to photosynthetic algal uptake, are also low at this time the large negative percent change relative to the baseline is apparent.

In the SoF and TW storylines phosphorus supply is higher and algal growth continues unconstrained to very high concentrations. A substantial crash was not simulated and DO levels did not dip during the simulation period beyond that expected from high temperatures. If the combination of conditions were to have come together to cause a

population crash the consequences would have very likely been considerably more severe than that following the crash under CW. That this did not happen during the somewhat limited 4 year period of simulation available for the model applications is likely due to chance and it should not be concluded that SoF or TW storylines are in relative terms beneficial for DO.

For the Farmoor reservoir, the worst deterioration in phytoplankton-based water quality was under SoF where there was as much as a 46% increase in cyanobacteria. Under CW, phytoplankton abundance is reduced although this reduction generally lessened with time. The TW presents an intermediate response that, whilst still producing an increase in phytoplankton, was not as severe as that seen under SoF.

Differences between the climate scenarios

Only two climate models were used to explore the uncertainty due to climate change, with a drier signal from GFDL compared with IPSL under the RCP 8.5 (SoF and TW). Despite being drier, water temperature is slightly higher by 2060s under IPSL 8 climate at TC6. At TC18 differences in water temperature are not apparent. For the CW, the differences between the two climate models appear fairly similar. The largest difference is between DO at TC18. However, differences in water quality are intractable and cannot be attributed in absence of statistical interpretation and sensitivity analysis.

Differences between the time horizons

Future conditions lead to a decrease in low flows. This hydrological change is apparent for all climate models and is a trend that is pervasive along the river system. Changes in low flows in the summer growing season exacerbate any trends in increasing water temperature which may be brought about solely by an increase in air temperature. Higher water temperature leads to a decrease in DO although this is only substantial downstream (at TC18) by which point there may be impacts from eutrophication.

There is a consistent general pattern of deterioration of the water quality in the Farmoor reservoir across all three storylines between the earlier period (2030s) and the later period (2060s), attributed to an increase in temperature. Regardless of storyline, cyanobacteria

biomass changes tended to be relatively greater than total chlorophyll changes, the difference increasing later in the century, also attributed to warmer conditions.

5.6.4.1.2 Empirical Modelling results

The empirical modelling between chlorophyll-a concentration (response) and a number of stressors on the Thames basin was conducted on 21 sites across the basin, 6 of them on the main channel and 15 on tributaries near the confluence.

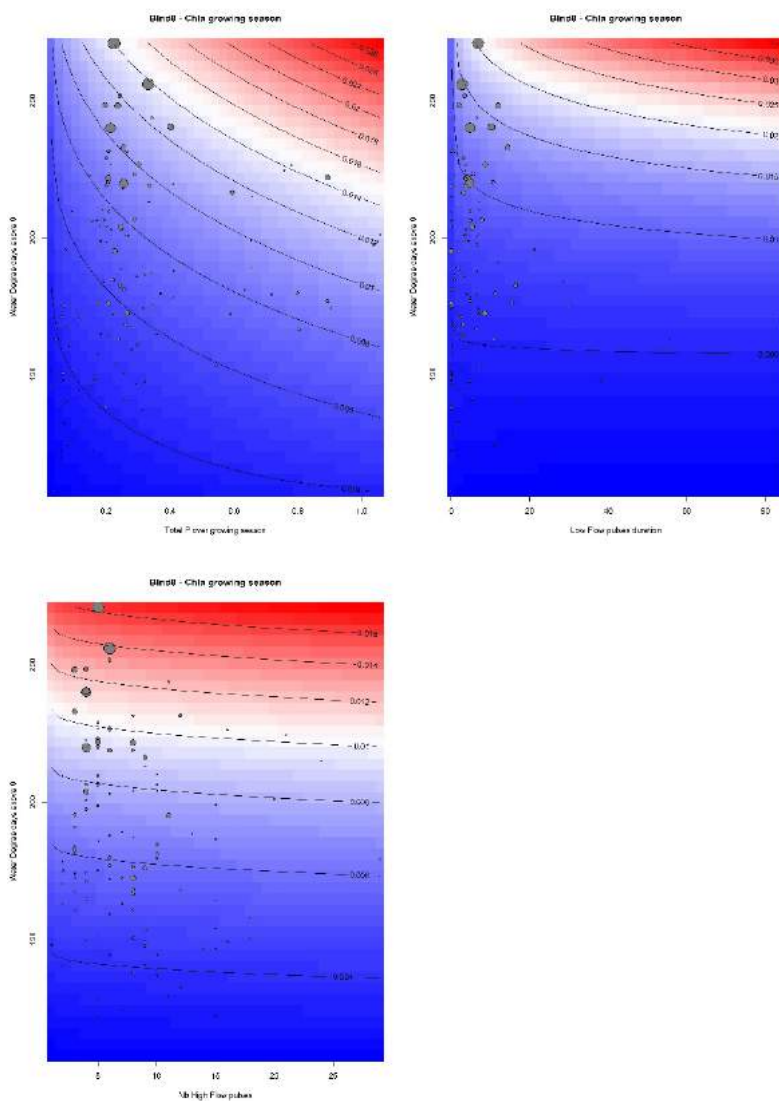


Figure 5.102 Observed and modelled response of chlorophyll-a to left: nutrient and extreme temperature (AIC: 167.5); middle: extreme temperature and length of extreme low flow pulses (AIC: 166.5); right: extreme temperature and number of extreme high flow pulses (AIC: 170.5). Observations are shown as circle, radius

being proportional to BInd8. Modelled response are shown as colour gradient shows (blue low to red high) and contour lines. Note difference in scale in the colour gradients.

Whilst none of the models show good performance (see for example **Error! Reference source not found.** modelled and observed response for the 3 best models), some commonality can be found:

- Including random effects improves the modelling. This is likely to be due to the high variability in biotic and abiotic variables both in space (i.e. tributaries do not experience as high levels of chlorophyll-a as the main channel) and time (2009 and 2011 have very different levels of chlorophyll-a whilst both showing marked low flow signal)
- Including interactions have marginal effect. Models including/ excluding interactions between the two stressors show very similar performance.
- Ecological responses (algal blooms) are complex. At the annual scale, water temperature, nutrient or flow do not explain the magnitude of chlorophyll-a concentration in the Thames basin.

All models show a strong underestimation of the highest algal bloom (**Error! Reference source not found.**), which shows highest mean concentration of chlorophyll-a (BInd8) during the growing season in the Thames in 2009. This might be due to the fact that relatively similar hydro-climatic conditions in 2011 resulted in lower chlorophyll-a concentration (Table 5.78), and an annual model not being able to capture the dynamics of algal bloom development.

Table 5.76. Ecological and stressor indicators for the sampling sites of the Thames basin for the year 2009 and 2011. Sites on the main channel are marked with *

	2009					2011				
	BInd8	Total P	DegDays_A bove9	BInd5	NbBInd4	BInd8	Total P	DegDays_A bove9	BInd5	NbBInd4
TC1	0.0315	0.8922	221.9	4.45	5	0.0114	1.0357	197.3	6.60	4
TC2	0.0230	0.5942	216.4	3.14	9	0.0040	0.9031	173.9	6.93	4
TC3	0.0344	0.2077	221.6	4	8	0.0211	0.2425	182.5	16.44	3
TC4	0.0199	0.2880	206.5	8	5	0.0088	0.3451	175	30.20	5
TC5*	0.0268	0.1962	248.5	2.14	4	0.0163	0.2056	220.2	10.69	5
TC6*	0.0197	0.242	251.8	3.5	6	0.0179	0.2878	223.2	5.64	5
TC7	0.0053	0.1471	222.6	1	4	0.0052	0.1912	183.7	28.50	3
TC8	0.0030	0.0393	194.9	1.86	3	0.0021	0.0422	162.7	55.33	2
TC9	0.0103	0.3432	243.7	6.6	11	0.0069	0.4116	187.9	6.74	6
TC10	0.0037	0.0926	209.3	0	2	0.0036	0.1144	170	84.00	2
TC11	0.0057	0.3328	212.91	7.20	9	0.0045	0.4298	190.8	12.00	3
TC12	0.0032	0.0687	132.1	2	12	0.0040	0.0471	147.4	38.25	1
TC13*	0.0607	0.2136	240.1	4.83	4	0.0297	0.2525	233	14.40	3
TC14	0.0057	0.2523	217.7	NA	NA	0.0035	0.1896	210	7.17	10
TC15	0.0051	0.7806	226.3	3.91	16	0.0043	0.7572	224.6	3.69	21
TC16*	0.0772	0.2240	271	6.86	5	0.0357	0.2357	248.2	12.00	3
TC17	0.0043	0.2138	226.8	2	5	0.0038	0.4096	178.1	5.00	2
TC18*	0.0744	0.3309	256	2.86	6	0.0413	0.4022	240.5	10.31	4
TC19	0.0076	0.2927	NA	0	4	0.0051	0.4097	219.5	5.38	5
TC20	0.0047	0.0947	NA	10.6	12	0.0088	0.0723	195.5	21.14	3
TC21	0.0027	0.2010	NA	10.17	7	0.0036	0.2225	171.7	7.36	6

5.6.5 Discussion

5.6.5.1.1 Discussion of modelling process

The QUESTOR model reveals there is an iterative and circular dependency between chlorophyll and phosphorus. Phosphorus is present at levels that do not limit algal growth until the algal populations increase above a threshold. It is unclear what this threshold is but it appears to be over 0.1 mg l⁻¹. Above this level P controls chlorophyll and then chlorophyll starts controlling P. This change in control is complex in particular when decay and recycling of P starts to occur.

Further empirical analysis of high-frequency water quality data on the Thames was conducted, showing that chlorophyll-a concentration responds to environmental factors at a sub-daily time scale, demonstrating the complexity of the Thames system (Bowes et al., *in press*). This behaviour is very difficult to be captured by a multi-site, multi-year empirical modelling that does not resolve the time-varying dynamics, as the MARS indicators such as Bind4 and Bind5 are ill-suited to capture between-year and between-site differences in chlorophyll-a.

The number of storylines tested (3) is very limited and does not enable to identify the relative impact of each individual stressor. Instead, systematic sensitivity analyses of multiple stressors would be more appropriate to clearly quantify the individual and combined impacts of the considered stressors. Under a modelling framework, a comprehensive and robust design would need to use alternative model structures so that uncertainty in process modelling could also be accounted for; for example known limitations of the QUESTOR structural model uncertainty include a tendency to underestimate peak algal levels and simulated blooms last longer than observed.

5.6.5.1.2 Basin-specific discussion of results

It is clear that the process modelling applied here supports in part existing understanding of the dynamics observed in the Thames. It has confirmed for example that for algal biomass, shading and residence time (flow) are the sensitive stressors. Phosphorus is secondary, but it is largely only when the phosphorus stressor becomes important that DO becomes vulnerable. This P stress will be fairly transient, more consistently temperature will put some (secondary) stress on DO.

Only under the Consensus World the quality of the Farmoor reservoir is projected to improve due to less nutrient rich river influent, with severe deterioration found under Survival of the Fittest (and to a lesser extent, under the Techno World) which would have damaging consequences to drinking water supply in the basin.

5.6.6 Conclusion

The application of the MARS storylines to the Thames basin has highlighted a number of key messages summarised here:

- The complex dynamics of algal blooms in the Thames cannot be represented at the coarse resolution of annual indicators using empirical modelling.
- Reduction of low flow and increase in water temperature can increase the risk of algal blooms. It is hence critical to maintain low flows to a minimum level, and to keep the river channel cool, which could be achieved through shading in the Thames upper reaches.
- Because the Thames is not nutrient limited, there is little need to keep P levels low although in upstream reaches this would probably be beneficial.
- There is some evidence that low P levels further down the river system may actually be detrimental to river health.
- Reduction of nutrients in rivers could help reduce the total phytoplankton biomass in reservoirs, but this might be mitigated by an increase in the dominance of that biomass by the toxic cyanobacteria species as the century progresses and becomes warmer.
- Projected climatic changes under the most extreme RCPs might result in drying of the river part of the year which could only be mitigated with drastic changes in water management through building a new reservoir or water transfer from outside the catchment. They would be associated with severe deterioration of the water quality both in the river and the existing reservoir.
- The limited number of storylines with simultaneous changes of multiple stressors does not allow a robust identification of stressor-response relationships. A sensitivity analysis where stressors are changes independently of each other, including combinations, would be more appropriate

6 Northern Basins

6.1 Vorstjäv, Estonia

6.1.1 Introduction

Overview of Võrtsjärv basin. Lake Võrtsjärv is a large (270 km²) lake located in southern Estonia (north-eastern Europe) which belongs to the southern boreal (or hemiboreal) forest zone. It is a shallow (average depth: 2.8 m) and eutrophic water body: mean total phosphorus (TP) is 48 µg l⁻¹, total nitrogen (TN) 0.91 mg l⁻¹, and chlorophyll *a* concentration (Chl *a*) 36 µg l⁻¹ (Cremona et al., 2016). The lake is dominated by planktonic primary producers, especially cyanobacteria (Cremona et al., 2014a). During the last decade, Lake Võrtsjärv has been ice-covered 135 days per year on average (from mid-November to mid-April) and has been mostly turbid during the ice-free period (Secchi depth < 1 m) owing to frequent sediment resuspension. As the

flat relief restricts outflow during water rich periods the lake experiences several water level changes yearly, in particular during the snow melt at the end of winter (Nõges et al., 2003). The main tributary of Võrtsjärv and contributor of 40% of its total inflow on average is the River Väike Emajõgi (Figure 6.1). It is a medium-sized (length: 82 km) river with a 1173 km² large catchment that is roughly equally divided between forested (51%) and agricultural areas (46%) with marginal settlements (3%) and wetlands (1%). The flow regime of the Väike Emajõgi is natural.

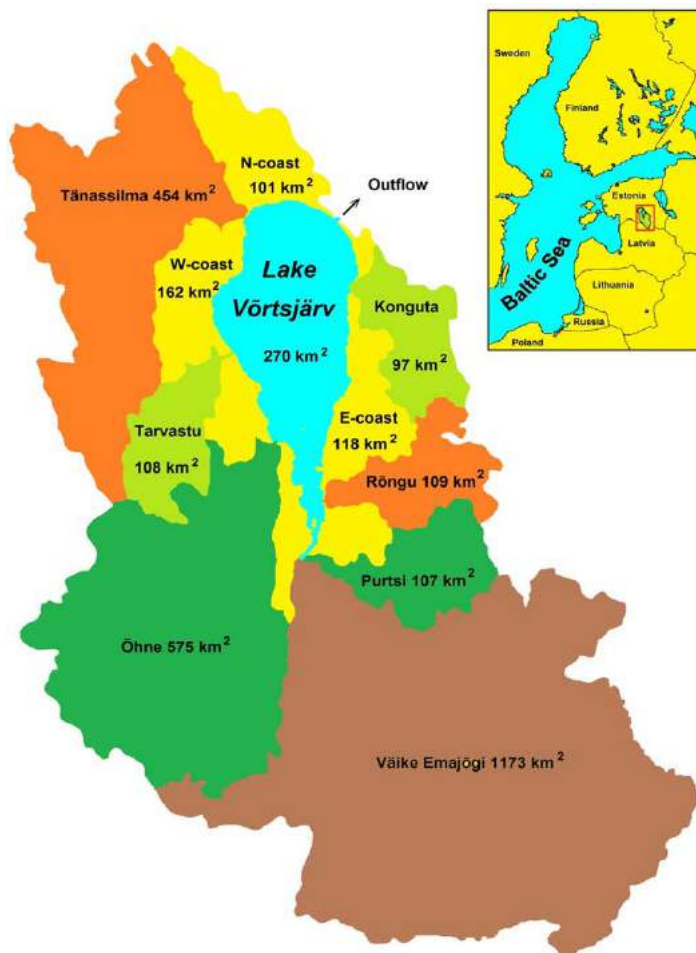


Figure 6.1 Location and surface area of Võrtsjärv and its tributary basins.

Ecological status. Lake Võrtsjärv water body status in the last decades could be classified from high to moderate depending on the index chosen. Generally, the status has been better when assessed with hydromorphology, macroinvertebrate abundance and fish composition indicators than with planktonic or macrophyte-related indicators. If we consider that ecological status is determined by the biological quality element, which shows the greatest anthropogenic disturbance, Võrtsjärv falls into the moderate category. High phosphorus and nitrogen concentrations from basin agriculture are indeed responsible for persistent cyanobacteria presence, food web and metabolism alterations (Cremona et al., 2014a, 2014b).

Main drivers and pressures in Vörtsjärv basin:

drivers: agriculture, climate change.

pressures: diffuse pollution, hydrological alteration.

Modelled variables:

abiotic indicators: air temperature (T_{air}), Väike Emajõgi flow (Q) and dissolved inorganic carbon concentration (DIC)

biotic indicators: Vörtsjärv Chl-a, cyanobacteria (B_{cyan}) and rotifer biomass (B_{roti})

Main ecosystem services

water for non-drinking purposes: PROXY

biovolume of toxic phytoplankton species (cyanobacteria): CAPACITY

number of visitors to Vörtsjärv museum: FLOW

General objectives. Our main goal was to forecast the combined influence of climate change, land use and water abstraction on the phytoplankton (cyanobacteria) and zooplankton (rotifer) biomass of Lake Vörtsjärv, for the mid-21st century (2030-2060). Our main working hypothesis was that the magnitude of the stressors would be positively correlated with the rise of cyanobacteria and decline of rotifers. To test this hypothesis, we used a chain modelling approach consisting in a succession of climate, process-based and empirical models.

6.1.2 Methods

Scenario construction. The regional to basin downscaling for climate-related variables was proceeded for us by Raoul-Marie Couture (NIVA). The basin to river downscaling, corresponding to a switch of climate-related to river-related variables, was done with process-based model INCA-C, using land use in the Väike Emajõgi catchment and water

abstraction as the two main pressures. The output variables of this INCA-C modelling were DIC concentration and river flow which have both strong connections to lake-related variables (Cremona et al., 2014b). Then, for further downscaling from river-related variables to lake-related variables, we employed two empirical models: Boosted Regression Trees (BRT) and Random Forests (RF) models as recommended by our modellers in the Tulcea meeting. However, further analysis showed that BRT provided the best estimates and we thus used mostly this method. The outputs of INCA-C were used as inputs for this BRT in order to predict eventually lake-related variables (Chl *a*, cyanobacteria and rotifer biomass). Each of the three storylines was coupled with one of the two selected climate change models: ESM2M from the Geophysical Fluid Dynamics Laboratory (USA, later on “GFDL model”), and CM5A-LR from the Institut Pierre Simon Laplace Modelling Centre (France, later on “IPSL model”) totalling six possible scenarios. To each climate change model and radiative forcing scenario – the Representative Concentration Pathways (RCP) – were associated air temperature and precipitation predictions, meaning that four climate forecasts (IPSL 4.5, IPSL 8.5, GFDL 4.5, GFDL 8.5) were used in this study. The RCP 8.5 was associated with the two storylines (Techno and Fragmented) that predicted increased radiative forcing whereas the lower RCP 4.5 was linked with a stabilization of radiative forcing described in the Consensus storyline (van Vuuren et al., 2011, 2014). The water abstraction and land use changes concurrent to each scenario were assessed according to storyline environmental impacts described by the stakeholders in 2014. In other words, the percentage of water abstracted from the Väike Emajõgi and forest terrains replaced by agriculture was raised in the following pattern: Consensus < Techno < Fragmented. The six scenarios were all run for a near future (2030-2060) estimate. To summarize, the scenarios were constructed according to the following diagram (Figure 6.2).

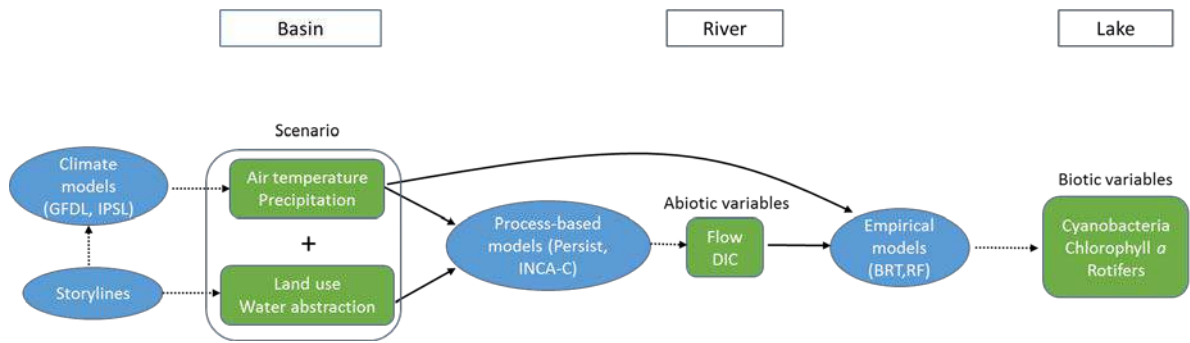


Figure 6.2 Conceptual diagram of study design, with downscaling from basin to lake, from stressors to biotic indicators. Models and storylines are in ellipse-shaped boxes whereas variables are in polygon-shaped boxes. Solid and dashed arrows represent model inputs and outputs respectively

DPSIR model for the Basin. The last version of the DPSIR model of the Basin (dating July 2016) is enclosed below (Figure 6.3).

Catchment: Vörtsjärv

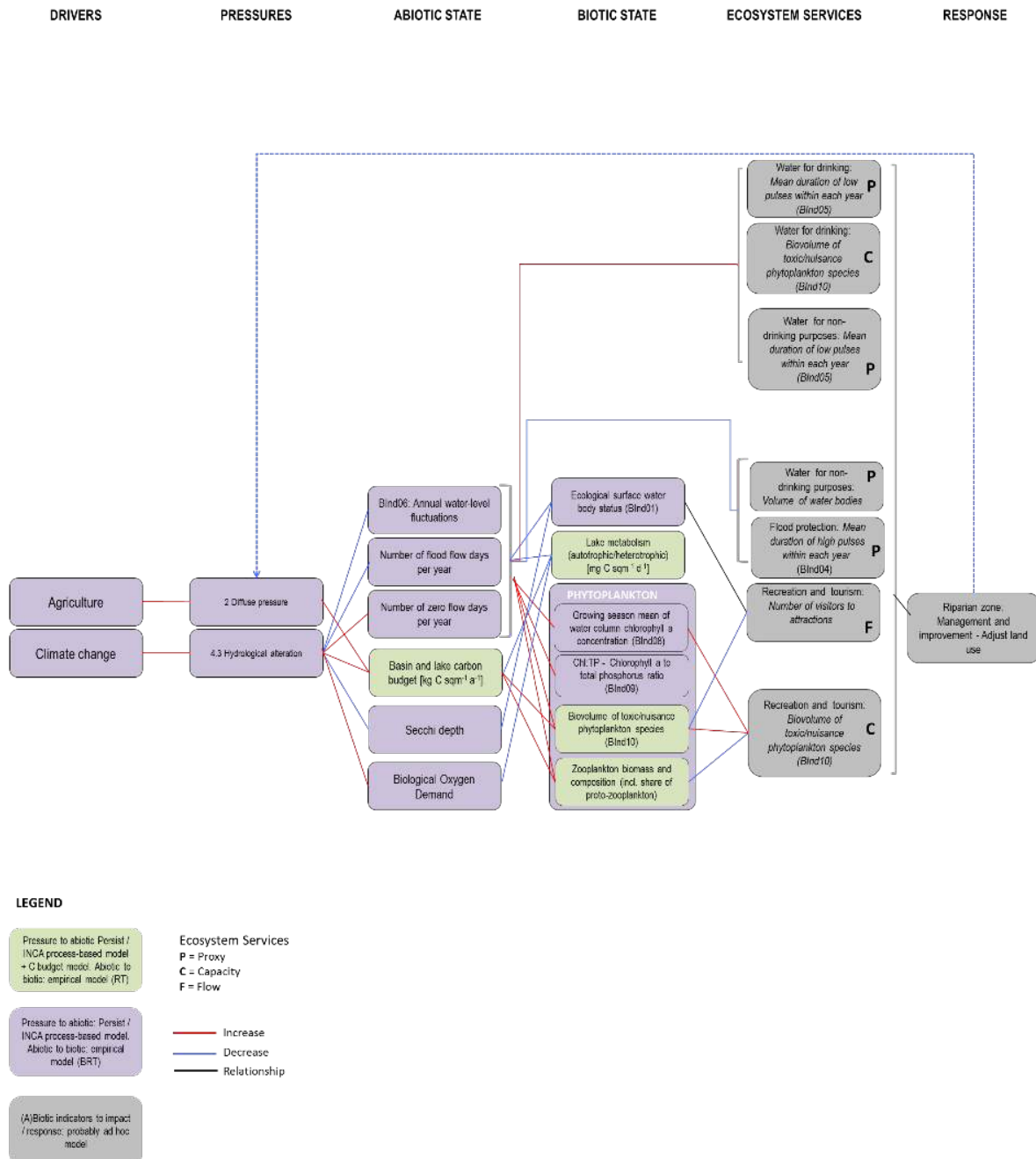


Figure 6.3 DPSIR model of Vörtsjärv basin, as designed in collaboration with Deltares.

Data overview. Data for model input variables was gathered on a monthly basis during 10 years (2005-2014) with the exception of DIC concentrations which were measured during 6 years (2008-2013) and air temperature, precipitation and river flow which were measured daily. Air temperature ($^{\circ}\text{C}$), precipitation (mm), and stream flow values of the River Väike Emajõgi ($\text{m}^3 \text{s}^{-1}$) were obtained from Estonian Environment Agency. Since precipitation was measured at Valga and Tõlliste stations both located within the Väike Emajõgi catchment area, we averaged these two time-series in order to better represent conditions prevailing in the catchment.

The concentration of DIC were determined at the Institute of Agricultural and Environmental Sciences of Estonian University of Life Sciences (Tartu) using the TOC analyser and standard methods (ISO 8245, 1987; EN 1484, 1992). An exhaustive description of the method is available in Pall et al., (2011) and in Cremona et al., (2014b).

Phyto- and zooplankton were collected from the monitoring station near the eastern shore where the water depth corresponded to the mean lake depth. Sampling was conducted using standardized methods described in Cremona et al. (2014a). Chlorophyll a concentration (96% ethanol extract) was analysed spectrophotometrically and calculated according to Lorenzen (1967).

For characterizing cultural services, we used the number of visitors of the Lake Museum and the Visiting Centre drawn from the Lake Võrtsjärv Foundation's homepage (<http://www.vortsjarv.ee/en>).

Description of process-model (PM) used. The Integrated Catchment model for Carbon (INCA-C) was employed for simulating river flow and DIC fluxes in the River Väike Emajõgi. INCA-C is based on the INCA-N model (Whitehead et al., 1998) and comprises four components that we have employed in the present study (Futter et al., 2007): (1) a semi-distributed module that defines sub-catchment boundaries and land cover uses, (2) an external rainfall-runoff model called Persist (Rankinen et al., 2004) that is used to calculate hydrologically effective rainfall (HER) and soil moisture deficit (SMD), (3) a land-phase hydrochemical model simulating material fluxes through the soil column and transformations between chemical stocks and (4) an in-stream model simulating the

transformations in the aquatic phase. The mathematical model in INCA-C and its conceptual diagram are described more thoroughly in Futter et al., (2007). For summarizing, the model represents the main terrestrial, soil and in-stream stocks of organic and inorganic carbon and the transfer of carbon between them. Each land-cover class consists of two soil boxes which are organic and mineral layer respectively. The stream is modelled as a single continuously mixed system.

Time series of observed air temperature and precipitation and calculated SMD and HER are required for running the model, which operates on a daily time-step. Measured DIC concentrations are also necessary for calibrating INCA-C although they do not need to be on a daily time-step. Soil and stream water temperatures are modelled as functions of air temperature whereas solar radiation is estimated as a function of site latitude and day of year. Model outputs consist of carbon stocks and fluxes in, between and from organic and mineral pools, stream flow, and stream DIC concentrations. The INCA-C model is calibrated by adjusting rate coefficients and parameter values to minimize differences between observed and simulated stream flow and DIC (Futter et al., 2007).

Calibration process for PM. We selected data from 2005 to 2014 as the baseline of our simulation after which scenarios would be constructed. Before starting to calibrate the INCA-C model *per se*, four input parameters (SMD, HER, air temperature, precipitation) must be obtained, otherwise the model cannot be employed. For calculating SMD and HER we employed Persist model which has the same daily time step as INCA-C and provides reliable outputs through Bayesian framework (Rankinen et al., 2004) by comparing observed flow data to predicted outputs. The posterior flow values predicted by Persist were considered to match successfully the observed data ($r^2 = 0.7$, $n=3652$) and we were thus able to employ predicted HER and SMD as INCA-C inputs parameters.

We used the latest version of INCA-C (version 1.1 beta 7) and calibrated it using the observed flow in the Väike Emajõgi, air temperature, precipitation, and DIC concentrations, and calculated values of SMD and HER. The calibration process was carried out in two phases: (1) selection of fixed values for some parameters as explained by Ledesma et al. (2012), (2) manual calibration of both hydrological and carbon sub-models using an iterative method. A base flow index of 0.7 was calculated for the Väike

Emajõgi based on the 2005-2014 flow values. As a rule of thumb, a gradient of decreasing soil organic carbon (SOC) and dissolved organic carbon (DOC) in the three INCA-C boxes (direct runoff organic layer, mineral layer) was to be kept, with the following gradient between land uses: wetland > forest > farmland > settlement. For DIC, the gradient was the following: farmland >= settlement > forest > wetland. These assumptions were constructed on previous research that linked larger DIC export to the ocean by agricultural and urbanized catchments compared to forested catchments (Barnes & Raymond 2009). We employed starting parameter values for initial conditions described in Futter et al. (2007). The calibration was considered successful when at least half (r^2 of 0.5 or higher) of the variance of both flow and DIC were explained by the model and no iteration could increase the r^2 anymore.

Linkages between PM and empirical modelling (EM). INCA-C output values (DIC, river flow) in addition to air temperature were used together as input values for predicting lake-related ecological variables with BRT model. Empirical modelling consisted of two steps. Firstly, we numerically explored the possible dependence between DIC concentration in the Väike Emajõgi, river flow and air temperature on one hand and three Võrtsjärv-specific ecological variables (cyanobacteria biomass, Chl a, rotifer biomass) on the other hand, using the monitored values in 2005-2014 as a baseline. Secondly, once the numerical relationship was assessed, the empirical model was run for predicting the ecological variables based on the outputs of process-based model INCA-C described above (Figure 6.1). We ran BRT under the R environment (R Core Team, 2015) using “gbm”, “dismo”, and “usdm” statistical packages. Tree complexity was set to 2, learning rate to 0.001, and bag fraction to 0.6.

One-way Analysis of Variance (ANOVA) was done on the model outputs to test scenario and seasonal differences. Tukey’s Honestly Significant Difference (HSD) test completed the analysis by outlining which groups were differing from each other. These analyses were performed with JMP (version 10; SAS Institute Inc., Cary, North Carolina).

Linkages between EM and Ecosystem Services. To analyse the environmental factors influencing the ESS of Võrtsjärv, we used the data for the period 2006--2013. The physico-chemical and eutrophication parameters were measured within the Estonian National Monitoring Programme. We used the annual mean values of water transparency (Secchi depth), electrical conductivity (Cond), pH, chemical and biological oxygen demand (COD_{Mn} , BOD_5), concentrations of dissolved oxygen (DO), chlorophyll a (chl a), TN, TP, and dissolved silica (DSi). The data on water discharge, water level, and duration of the ice cover were obtained from the Estonian Environment Agency.

Principle Component Analysis (PCA) and Spearman rank correlation coefficients provided by STATISTICA for Windows 7 (Dell Inc., 2015.) were used to link the environmental factors with the indicators of ESS. The PCA of the environmental factors was performed to identify the main gradients of the factors affecting the ESS. Thereafter the variables of the ESS indices were introduced.

6.1.3 Results

PM results

Calibration - Persist: The output time-series from the hydrological model Persist matched well with the observed flow in the Väike Emajõgi ($r^2 = 0.7$, $RMSE = 89.3$, $n = 3652$, Figure 6.4) during the studied decade (2005-2014). Especially, the occurrence of spring floods was well captured by the model although the magnitude of these floods was exaggerated by Persist. Similarly, the calculated values exceeded the observed ones during the interflood period as well.

Calibration - INCA-C: Small adjustments in INCA-C flow parameters improved slightly the predictive power of the persist outputs (r^2 increase from 0.7 to 0.72, not shown). For DIC we obtained a relatively robust time-series calibration ($r^2 = 0.65$, $N-S = -0.77$, $RMS = 26.27$, $RE = -4.84$, $n = 71$) although the amplitude of DIC variation was greater (Figure 6.4).

BRT: Using Boosted Regression Trees, strong relationships were found between lake-related and river-related variables. Chl a concentration was the best predicted variable as BRT explained nearly two-thirds (65%) of its variance, followed by cyanobacteria biomass (60%) and rotifer biomass (47%). For all the three lake-related variables, air temperature was the best predictor of posterior distribution, followed by river flow and DIC concentration. Since all three variables were significant (although DIC displayed much less predictive power than the two others) we decided to use them for the following step – running the six climate change scenarios described previously.

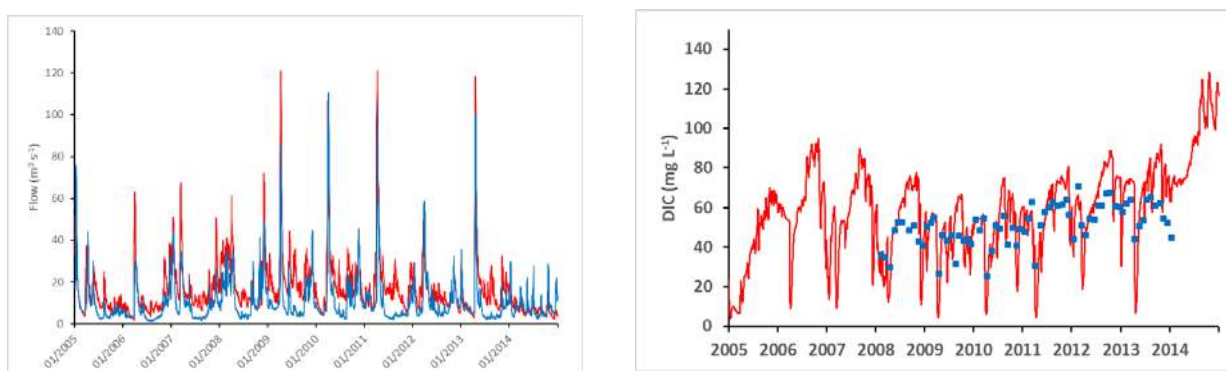


Figure 6.4 Calibration results for the Väike Emajõgi flow (left) and DIC concentrations (right) using respectively Persist and INCA models. Time-series of observed (blue solid line or dots) and predicted (red solid line) values comprise also statistical results of the model run.

Flow: All six simulations predicted a dramatic decrease of river flow in the Väike Emajõgi during the 2030-2060 period compared to the reference period (Figure 6.5). The disparity between reference and predicted periods was the strongest during autumn and spring months. Simulations performed with the IPSL model consistently predicted lower mean flow than simulations which employed GFDL climate data. For each model, annual mean flows were higher for the consensus scenarios (M5) than for the Techno (M4) and Fragmented (M6) scenarios. As scenarios using the Techno and Fragmented storylines were constructed with the same climate data predictions their output values were more similar to each other than they are to Consensus outputs. Thus, the lower flow values of Fragmented scenarios compared to Techno ones can only be attributed to greater water abstraction and less water retention by agricultural soils in Fragmented scenarios.

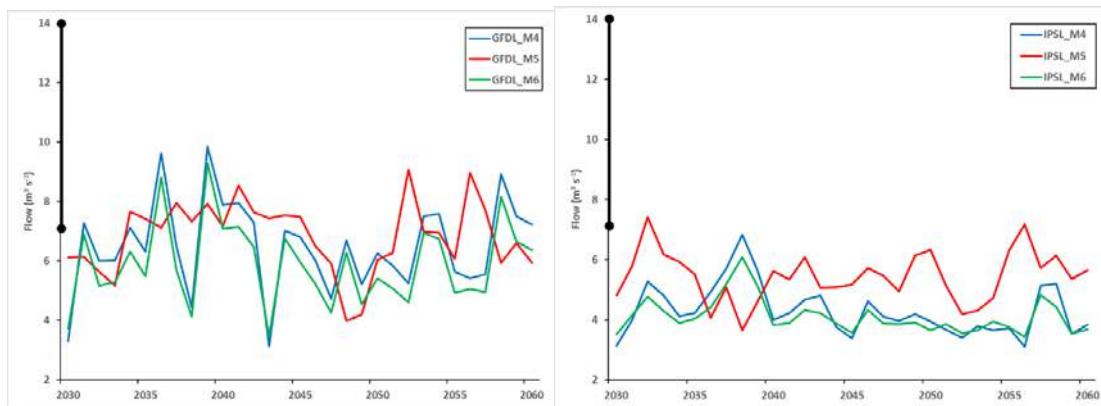


Figure 6.5 Annually-averaged time series of the Väike Emajõgi flow ($\text{m}^3 \text{s}^{-1}$) as modelled by INCA-C for predictive scenarios using GFDL (left) and IPSL (right) climate models data as input values. Thicker double-headed arrow on the y axis corresponds to the flow range in reference conditions.

DIC: INCA-C predicted a strong increase in the Väike Emajõgi DIC concentrations during the 2030-2060 period compared to reference values of 2005-2014 (Figure 6.6), with no scenario exhibiting DIC concentrations that would be within the range of reference. DIC concentrations in the future were supposed to increase three- (Consensus M5 scenarios with both climate models) to six-fold (Fragmented M6 scenario with IPSL). Similarly to flow, DIC simulations that were ran with IPSL climate data predicted larger deviation from the reference (i.e. higher DIC concentrations) than those employing GFDL data. As there is an inverse relationship between flow and DIC in the Väike Emajõgi, the average lower flow in the future would concentrate the amount of mineral carbon that is in the water column.

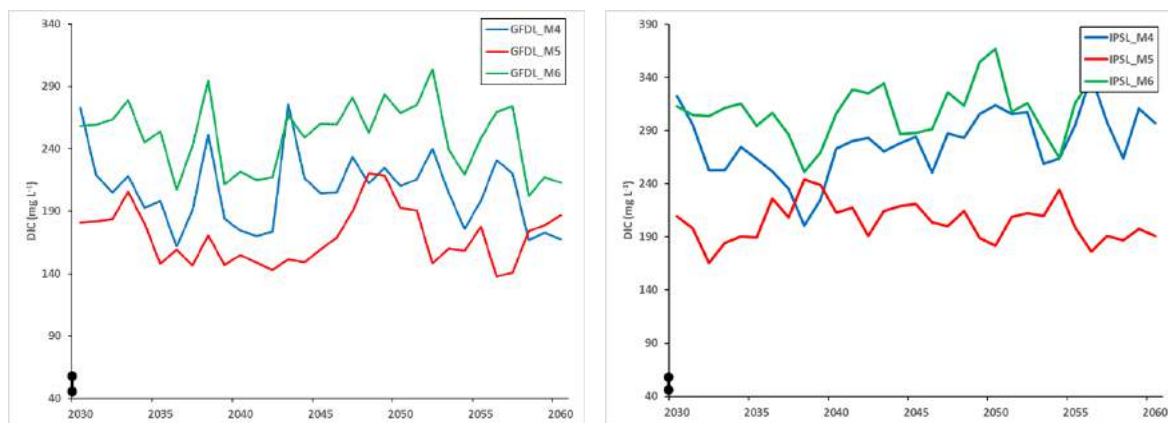


Figure 6.6 Annually-averaged time series of the Väike Emajõgi DIC concentrations (mg L⁻¹) as modelled by INCA-C for predictive scenarios using GFDL (left) and IPSL (right) climate models data as input values. Thicker double-headed arrow on the y axis corresponds to the DIC range in reference conditions.

EM results

Chl a: Boosted Regression Trees predictions for *Chl a* diverged between GFDL and IPSL groups of scenarios. *Chl a* predicted based on GFDL climate data did not significantly differ from the reference value (Tukey HSD test, $\alpha = 0.05$, $q = 2.95$) and was even slightly lower in the case of Techno and Consensus storylines (GFDL_M4, M5, Figure 6.7). Only the *Chl a* values for the Fragmented storyline (GFDL_M6) marginally exceeded the reference (mean $39 \mu\text{g L}^{-1}$ compared to 38 in reference conditions). However, using the IPSL model data yielded significantly higher *Chl a* for Techno and Fragmented conditions (mean values, respectively, $43 \mu\text{g L}^{-1}$ and $44 \mu\text{g L}^{-1}$) although Consensus conditions resulted in *Chl a* values similar to the reference.

Although comparisons of yearly data did not show large differences in *Chl a* concentrations between reference and future conditions, comparisons of monthly values revealed dramatic changes between reference conditions and scenarios. Significantly higher phytoplankton biomass was forecasted for late winter and spring and significantly lower for late summer/early autumn while remaining more or less stable for the rest of the year.

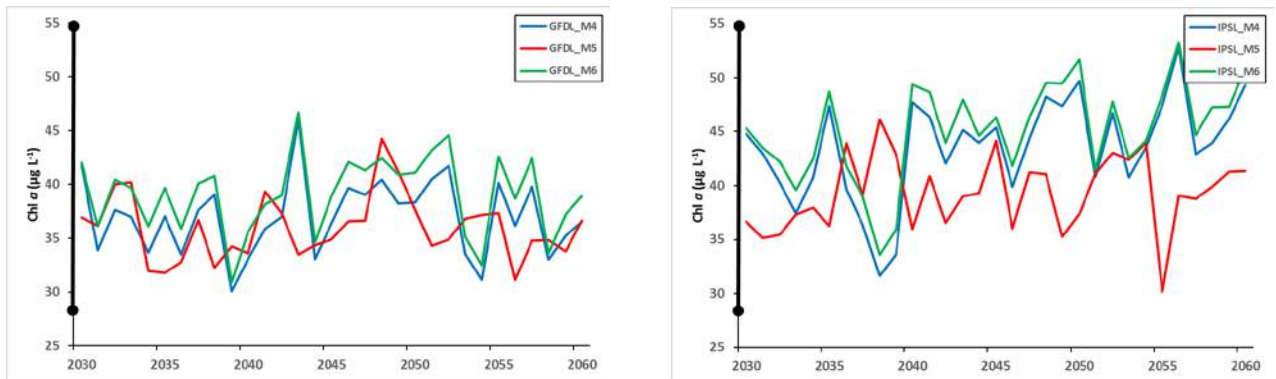


Figure 6.7 Annually-averaged time series of Lake Vörtsjärv Chl a ($\mu\text{g L}^{-1}$) which was modelled by BRT for predictive scenarios using GFDL (left) and IPSL (right) climate models data as input values. Thicker, double-headed arrow on the y axis corresponds to the Chl a range in reference conditions.

Cyanobacteria biomass: Mean cyanobacteria biomass in Lake Vörtsjärv showed modest (6% GFDL_M5) to strong (34% IPSL_M6) rise according to the prospective scenarios (Figure 6.8). As for Chl a, the increase of B_{cyan} relative to the annual mean reference value ($\approx 11 \text{ mg ww L}^{-1}$) was much stronger in the case of IPSL Techno and Fragmented scenarios than in their GFDL counterparts. The phenology of cyanobacteria is predicted to follow the same dynamics as the whole phytoplankton community, i.e. increasing in late winter/early spring, and decreasing in late autumn. These temporal trends were consistent with the predicted decrease of river flow during the same parts of the year.

Rotifer biomass: All scenarios predicted B_{roti} to decline well below the $0.1 \mu\text{g ww L}^{-1}$ average reference value (Figure 6.9) as the differences between reference values and simulation time-series were significant ($p < 0.0001$). Only under Consensus scenario calculated with GFDL data (GFDL_M5), B_{roti} exceed the average reference values in one year. Interestingly, there were significant but rather small differences between monthly averages of reference and scenario values, except for May. The B_{roti} reference value for May ($0.35 \mu\text{g ww L}^{-1}$) exceeded nearly three times the predicted values for the six scenarios ($0.09\text{-}0.13 \mu\text{g ww L}^{-1}$) showing that, according to the simulations, the spring peak of B_{roti} is predicted to disappear over the next decades.

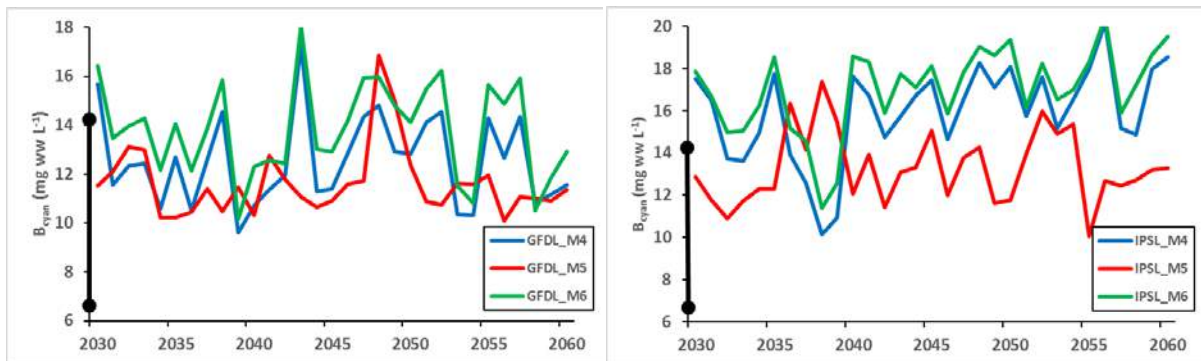


Figure 6.8 Annually-averaged time series of Lake Vörtsjärv cyanobacteria biomass (B_{cyan} mg ww L^{-1}) which was modelled by BRT for predictive scenarios using GFDL (left) and IPSL (right) climate models data as input values. Thicker, double-headed arrow on the y axis corresponds to the range of B_{cyan} in reference conditions.

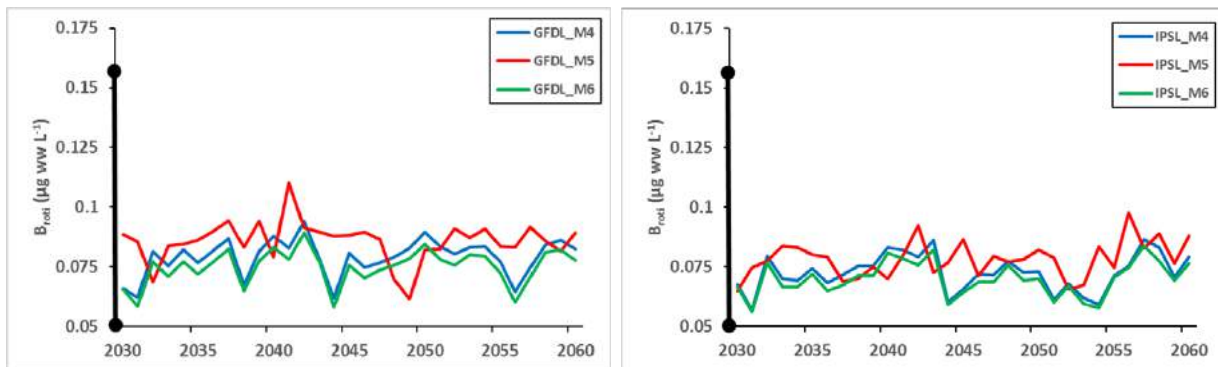


Figure 6.9 Annually-averaged time series of Lake Vörtsjärv rotifer biomass (B_{roti} μg ww L^{-1}) which was modelled by BRT for predictive scenarios using GFDL (left) and IPSL (right) climate models data as input values. Thicker, double-headed arrow on the y axis corresponds to the range of B_{roti} in reference conditions.

Ecosystem service results. River flow and cyanobacteria biomass correspond respectively to “water for non-drinking purposes” and “biovolume of toxic phytoplankton species (cyanobacteria)” ecosystem services. The former is, under MARS classification system a “proxy” while the latter is a “capacity”. They can be used as such by stakeholders. The third ecosystem service (number of visitors) was not correlated to any of our variables ($p > 0.05$).

6.1.4 Discussion

Chl-*a*. According to half of the predictive scenario runs, Lake Vörtsjärv will experience a slight net increase of annual mean phytoplankton Chl *a* in the next decades caused in particular by more favourable conditions (higher temperature, lower tributary flow) in winter, while algal biomass will slightly decrease in summer compared to reference conditions. However, three other scenarios predict either a small decrease in Chl *a* or no quantitative change. Consensus scenarios from GFDL and IPSL, which both rest on an environmental-friendly policy-making point to equilibrium or decrease of algal biomass which is at odds with the published literature. Paleolimnological, modelling studies and mesocosm experiments generally describe a positive relationship between anthropogenically driven climate change and phytoplankton biomass in shallow lakes (Jeppesen et al., 2014). Smol et al. (2005) reported that shallow arctic water bodies exhibited greater productivity under global warming conditions. Sorvari et al. (2002) observed that reduced ice-cover duration and extended thermal stability in Lapland lakes favoured year-long growth of planktonic algae community. In a review of Dutch lakes, Mooij et al. (2005) noted that climate change will improve the carrying capacity of phytoplankton and trophic state of shallow lakes. Using a modelling approach Malmaeus et al. (2006) hinted at a stronger release of nutrients and augmented phytoplankton biomass in lakes under warmer conditions, even for lakes with short water residence times, which is the case for Vörtsjärv. A study conducted in that lake by Nöges et al. (2010) has demonstrated that warmer periods (which are associated with lower tributary flow and lake water levels) were positively correlated with in-lake total phytoplankton biomass and also with cyanobacteria. In the light of the literature on the topic and our scenario results it is safe to assume that a rise of planktonic algae biomass in Lake Vörtsjärv in the next decades is very likely.

Cyanobacteria biomass. Although the total Chl *a* will increase only modestly according to our forecast, the cyanobacteria biomass might rise up to 30% compared to reference conditions. Consequently, the relative contribution of cyanobacteria to phytoplankton community biomass will increase in the future. These findings are consistent with the literature on the topic as global warming is expected to promote a net increase of

cyanobacteria biomass in shallow lakes (Jeppesen et al., 2009; Kosten et al., 2012). The decadal, steady increase in cyanobacteria biomass in Vörtsjärv that Jeppesen et al. (2015) observed for the 1978-2012 period is thus expected to continue. Furthermore, although the models we have employed are not able to trace or forecast cyanobacteria bloom episodes, there is a strong presumption that an increase in the annual cyanobacteria biomass will be linked to the advent of harmful cyanobacteria blooms (O'Reilly et al., 2015) with dire consequences for the whole lake ecological processes such as dissolved oxygen concentration, metabolic balance and carbon cycling (Cremona et al., 2014a).

Rotifer biomass. All the scenarios forecasted a significant decline of Vörtsjärv rotifer biomass in the future ranging from 14 to 30%. The linkages that we observed between zooplankton metrics and climate conditions are broadly in agreement with the existing literature. According to Gyllström et al. (2005), climate was the most important predictor of general zooplankton biomass although they did not observe any conclusive relationship between rotifer share of the biomass and climate-related variables. Adrian et al. (1999) observed a strong relationship between ice phenology in temperate lakes and the magnitude of the peak abundance of rotifers in spring. Indeed, the gradual increase of air temperature will certainly result in a steady reduction of ice cover duration in Vörtsjärv (Jeppesen et al., 2015) which in turn might cancel the spring peak of rotifer abundance. Although they are dominant in abundance (up to 99%) rotifers do not constitute the main body of zooplankton community biomass in Vörtsjärv, this position is occupied by ciliates which make up to 60% of the lake zooplankton biomass (Zingel and Haberman, 2008). However, as written previously rotifers are a useful indicator of a detrital food-web behaviour. A decline of rotifer total biomass and a concomitant rise of cyanobacteria would signify a selective pressure for smaller-bodied rotifer species as it is observed during more eutrophic summer conditions (Haberman and Virro, 2004). It could also correspond to a concomitant rise of ciliates abundance which are rotifer main competitors for detritus and bacteria as hinted by a recent study¹⁰. It is thus suggested that Vörtsjärv will be pursuing its decadal shift from a grazing to a detrital food-web behaviour.

¹⁰ Nöges, T., Järvalt, A., Haberman, J., Zingel, P. & Nöges, P. Is fish able to regulate filamentous blue-green dominated phytoplankton? *Hydrobiologia* (in press).

Differences between scenarios. In the two scenarios of the Consensus storyline (GFDL-M5, IPSL-M5) where the anthropogenic pressures were only marginally different from nowadays, we observed that the deviation from reference was evident for flow, DIC, cyanobacteria and rotifer biomass. Changes in air temperature and precipitation are thus the principal cause of ecosystem alteration in the case of Vörtsjärv basin. Further it is useful to compare Techno and Fragmented set of scenarios to each other as these two storylines use the same climate data and differ only by the magnitude of water abstraction and land use. We notice that GFDL-M4 and GFDL-M6 (and IPSL-M4 compared to IPSL-M6) point to the same direction: reduction of flow, increase of DIC, increase of cyanobacteria, decrease of rotifer biomass. The only disparity is that GFDL-M4 predicts a modest decline of Chl *a* while GFDL_M6 forecasts the opposite. These findings suggest that anthropogenic pressures further pushed the deviation from references conditions regarding river- and lake-related variables that were already caused by climate-related factors.

Model issues. The INCA-C model enabled forecasting long-term dynamics of the Väike Emajõgi flow and DIC concentrations with a high temporal resolution and a strong statistical robustness. Furthermore, the simulated river flow by INCA-C proved crucial for assessing ecological variables such as cyanobacteria biomass which was less dependent on air temperature than the other variables. INCA-C has limited data-requirements, is relatively easy to use thanks to a built-in interface and possesses many of the best features of existing carbon models (Futter et al., 2007). However, the model calibration by manual means alone is a very laborious process. Considering the hundreds of parameters involved, it is impossible (1) to test manually multiple parameter sets simultaneously and assess for equifinality, (2) to calibrate several reaches and basins at the same time considering the complexity of the process. Fortunately, the gradual advent of Bayesian calibration methods using Markov Chains Monte-Carlo (MCMC) runs would shorten greatly this time-consuming part of model-use, solving equifinality and multiple-reach issues (Ledesma et al., 2012). With a MCMC calibration method available, running

INCA-C for Võrtsjärv basin tributaries in addition to the Väike Emajõgi would have been greatly facilitated and the overall precision of the estimates would have been improved.

Boosted Regression Trees are considered a versatile tool for ecological modelling (Elith et al., 2008) and provided valuable outputs in this study: the BRT model explained up to two-thirds of the variance in ecological variables, which is substantial considering the large number of observations in our time-series data. Furthermore, the built-in forecast function of BRT enabled reliable, decadal-based predictions of phytoplankton and protozooplankton biomass.

Besides model-specific uncertainties, the main pitfall of our study design resides in the error magnification which is inherent to chain modelling (Fowler et al., 2007). Indeed, in the present study error accumulates first when downscaling climate variables to river-related variables and another time when the latter are converted to lake-related variables. However, this uncertainty is mitigated by the variety of ecological conditions that are covered under our six scenarios. The scenarios constructed from Consensus and Fragmented storylines represent, respectively, the lower and upper ranges of output data distribution for GFDL and IPSL. The credible data distribution is thus represented by the values remaining between these two extreme scenario outputs.

6.1.5 Conclusion

Our main working hypothesis was validated as the modelling approach forecasted an increase of cyanobacteria and a decrease of rotifer biomass in Lake Võrtsjärv during the 2030-2060 period. The models also predicted a surge of dissolved inorganic carbon concentrations in the main tributary water column. These changes are all clearly indicative of a degradation of the ecological status of the lake. Furthermore, they will trigger other feedback mechanisms on the lake ecosystem and food webs that are beyond the scope of this research but are well described in the existing literature. The anthropogenic pressures taking place in the lake catchment and tributaries whether they are already existing (land use) or projected (water abstraction) will further increase the degradation of the lake ecological status that will be mostly driven by climate-related changes. We recommend to Estonian policy makers and stakeholders to adopt the

“Consensus” storyline described in this article and in MARS project in order to reduce as much as possible the damages done to Vörtsjärvi and the ecosystem services this lake provides to the community.

Capsule:

River flow of Vörtsjärvi main tributary is expected to decline steadily in every scenario.

Inorganic carbon concentration in Vörtsjärvi main tributary will be multiplied by three at minimum.

Cyanobacteria biomass in Lake Vörtsjärvi will increase from 6 to 34% compared to reference conditions.

Protozooplankton biomass will follow the opposite pattern and will decrease.

Multiple stressors will magnify ecosystem degradation which is mostly caused by climate change.

Indicator's value is deviating more from reference in Fragmented > Techno > Consensus
st

6.2 Lepsämäenjoki, Finland

6.2.1 Area description

Lepsämäenjoki catchment (214 km²) is a sub-basin of the Vantaanjoki river basin in southern Finland. The river Vantaanjoki discharges to the Gulf of Finland outside Helsinki (Figure 6.10) and the area is very important for outdoor recreation. River Vantaanjoki is the secondary drinking water source for the capital Helsinki.

The mean discharge in the river Lepsämäenjoki was 2.2 m³s⁻¹ in 2000's (Korhonen and Haavanlammi, 2012). The mean annual precipitation in the area is 650 mm, and mean annual temperature is +4 °C (Data from Finnish Meteorological Institute). Main soil types in the Lepsämäenjoki catchment are clay (*Vertic Cambisol*) and rocky soils (*Dystric Leptosol*) (Lilja et al., 2006). Arable fields cover 23% of the area the rest being mainly

forest. Arable fields are located on clay soils. Main crops are spring cereals barley (*Hordeum vulgare* L.), spring wheat (*Triticum aestivum* L.) and oat (*Avena sativa* L.), but at the upper reaches of the catchment there is also some cabbage (*Brassica oleracea var. capitata*) cultivation (about 3% of the area). In 2005 animal density was 0.08 animal units (AU) per hectare of field (Mattila et al., 2007).

The ecological status of the river Lepsämäenjoki is moderate, and that of the tributary Härkäläjoki is poor. In the river basin plan the river Lepsämäenjoki is estimated to achieve good ecological status by 2021 (Joensuu et al., 2010). Most of the farmers are committed to fulfill environmentally sound cultivation practices included in the Finnish agri-environmental support scheme, the main tool for the Water Framework Directive (Mattila et al., 2007).

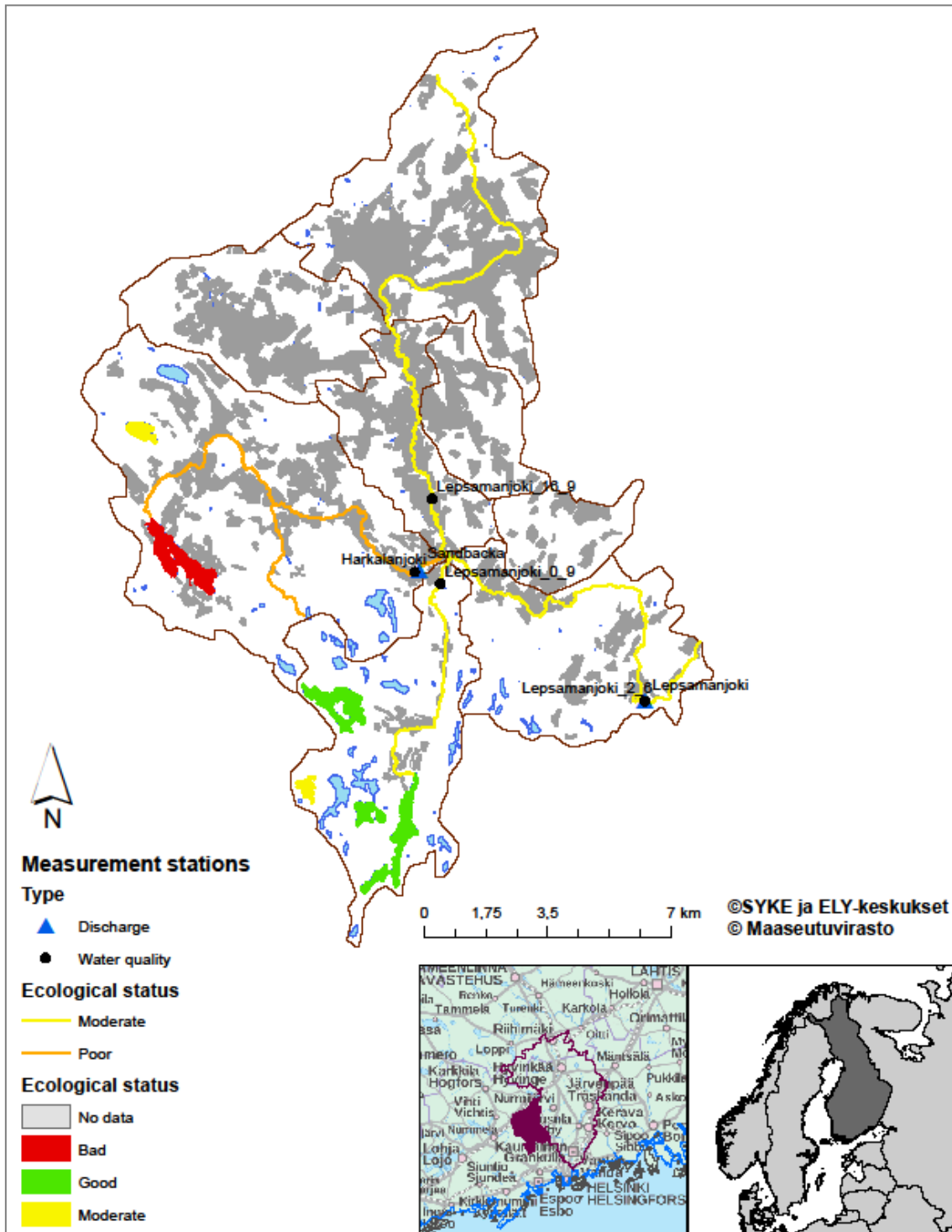


Figure 6.10 Location of the Lepsämäenjoki catchment. Field areas are marked by gray color.

6.2.2 Conceptual Model

The research question of the Lepsämäenjoki case is eutrophication of the river due to human activities, mainly agriculture (Figure 6.11). Dissolved and total nutrient loading from the catchment were simulated by the INCA model according to different climate change scenarios and storylines. Effect of climate, runoff and nutrient concentrations on summer time phytoplankton (Chl- α) growth in river were estimated by empirical models.

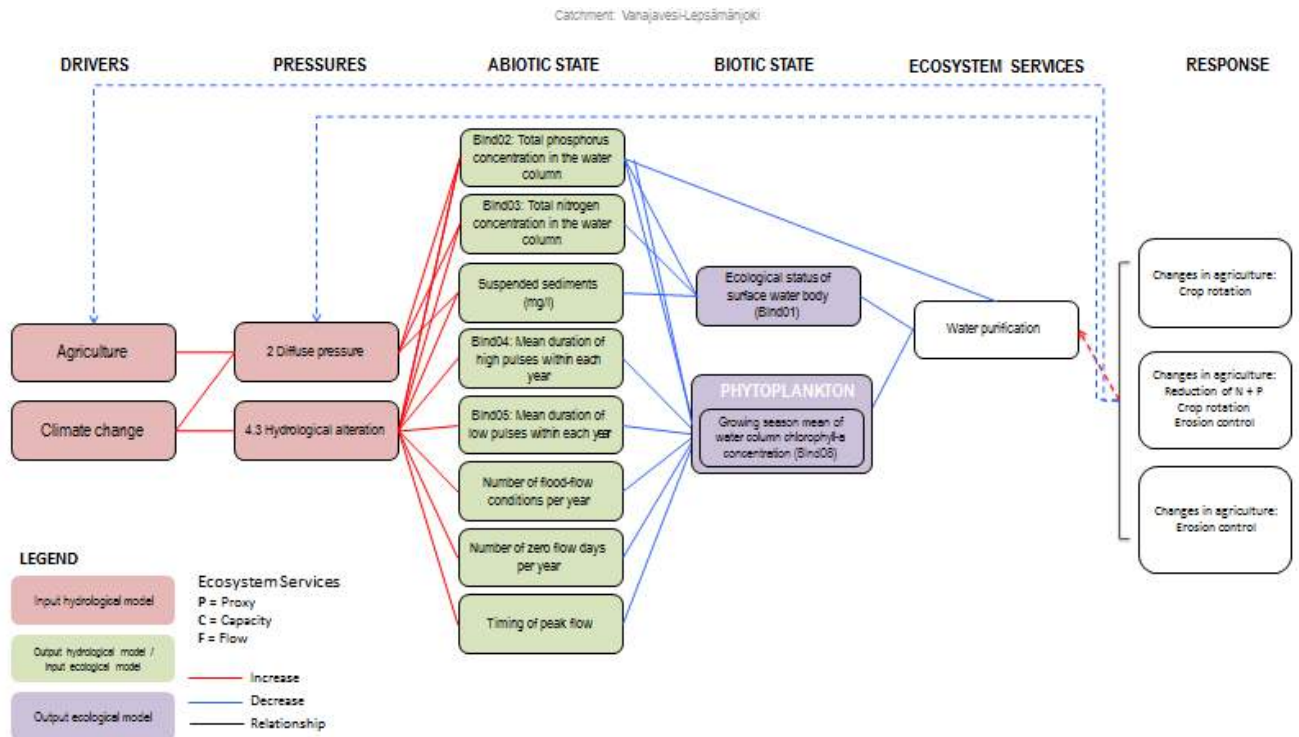


Figure 6.11 Conceptual model of the Lepsämäenjoki case.

6.2.3 Data

The Lepsämäenjoki catchment has two discharge gauging stations and several water quality sampling sites. The data set was extended by including data from surrounding river basins that has similar climate, soil types and land cover than Lepsämäenjoki catchment (Figure 6.12, Table 6.1). The dataset contained all together 175 observations (summer means) from years 1985-2014. From direct discharge data (m^3/s) also runoff (mm) and minimum and maximum 1 day and 7 day runoff (mm) were calculated. Relationship between total phosphorus (TP) and turbidity (Turb) was calculated as a proxy for soluble reactive phosphorus.

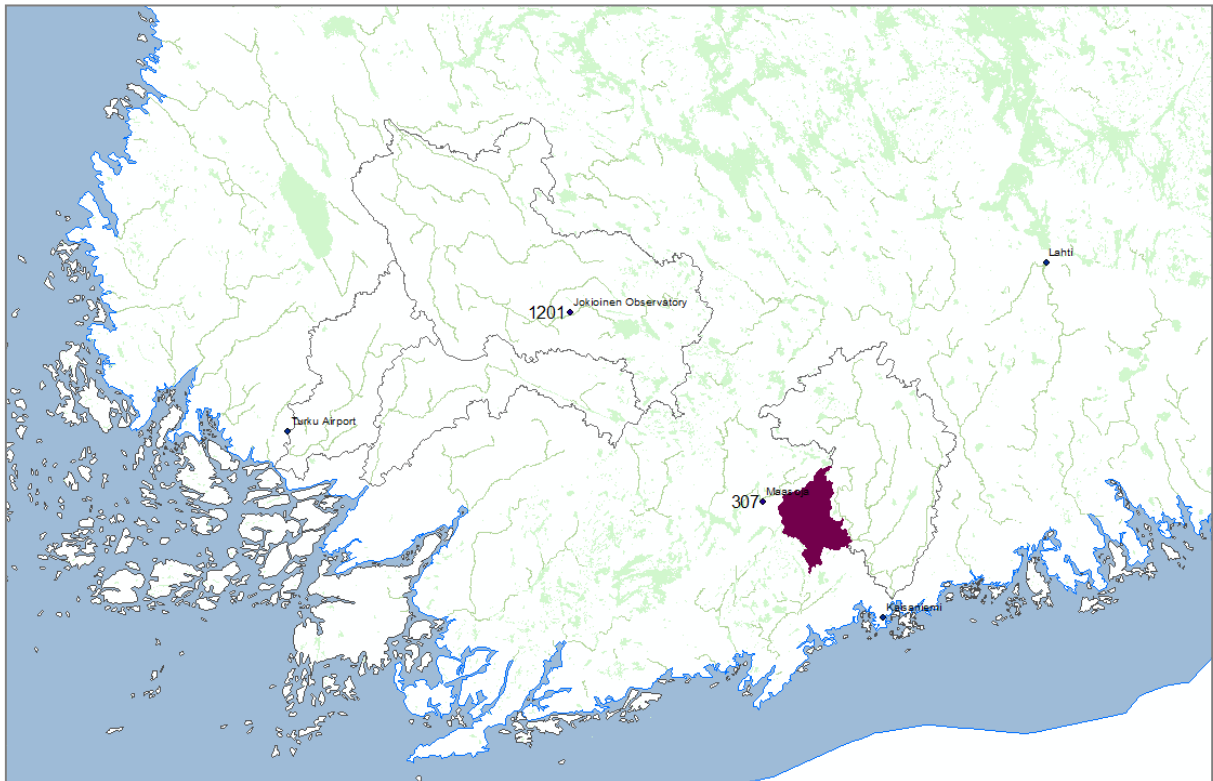


Figure 6.12 Location of the river basins with Chl- α observations, and location of the weather stations.

Table 6.1.Origin of the data.

Catchment	Site	Discharge gauging station	Weather station	Global radiation
Lepsämäenjoki	Lep	Lepsämäenjoki	Lohja Porla	Vantaa lentoasema
Lepsämäenjoki			Lohja Porla	Vantaa lentoasema
Lepsämäenjoki	Harka	Sundsbacka	Lohja Porla	Vantaa lentoasema
Loimijoki	Lojo68	Maurialankoski	Jokioinen Observatorio	Jokioinen Observatorio
Loimijoki	Lojo64	Maurialankoski	Jokioinen Observatorio	Jokioinen Observatorio
Loimijoki	Lojo40	Sallilankoski	Jokioinen Observatorio	Jokioinen Observatorio
Loimijoki	Loimi92	Sallilankoski	Jokioinen Observatorio	Jokioinen Observatorio
Loimijoki	Loimi113	Kuhalankoski	Jokioinen Observatorio	Jokioinen Observatorio
Loimijoki	Lojo58	Kuhalankoski	Jokioinen Observatorio	Jokioinen Observatorio
Aurajoki	Aura54	Aurajoki	Turku lentokenttä/Artukainen	Kaarina Yllöinen
Paimionjoki	Pajo44	Halistenkoski	Turku lentokenttä/Artukainen	Kaarina Yllöinen

6.2.4 Physical Models

INCA and PERSiST models. INCA is a dynamic mass-balance model, and as such attempts to track the temporal variations in the hydrological flowpaths and nutrient transformations and stores, in both the land and in-stream components of a river system. INCA provides as an output of daily and annual land-use specific organic and inorganic-nutrient fluxes for all transformation processes and stores within the land phase, and daily time series of land-use specific flows, and organic and inorganic-nutrient concentrations in the soil and ground waters and in direct runoff. The nitrogen model solves traditional nitrogen cycle in different land use classes. In phosphorus model the phosphorus reactions are based on equilibrium equations, and transport as soluble substances or as attached on soil particles. Erosion sub-model describes the erosion and suspended sediment transportation processes from land use classes to river water. The model equations are described by (Whitehead et al., 1998b; Wade et al., 2002a; Wade et al., 2002c; Wade, 2004; Lazar et al., 2010; Jackson-Blake et al., 2016a).

Spatial data describing the major land use types are required. INCA also requires time series inputs describing the hydrology, namely the Soil Moisture Deficit, Hydrologically Effective Rainfall, Air Temperature and Actual Precipitation. These data are usually obtained from analysis of meteorological data and rainfall gauges and derived from a hydrological model.

PERSiST is a flexible rainfall-runoff modelling toolkit for use with the INCA family of models (Futter et al., 2014b). PERSiST (the Precipitation, Evapotranspiration and Runoff Simulator for Solute Transport) is designed for simulating present-day hydrology; projecting possible future effects of climate or land use change on runoff and catchment water storage. PERSiST has limited data requirements and is calibrated using observed time series of precipitation, air temperature and runoff at one or more points in a river network.

Calibration and validation. The Persist model and the INCA models were calibrated and validated against measured data at the Lepsämäenjoki catchment. There were several water quality measurement stations and two discharge gauging stations, so the multi branch structure of the model was used. Main stream was divided into three subcatchments with tree tributaries (Härkälänjoki, Lakistonjoki and Hangasjoki). Calibration period was 2004-2006 and validation period 2007-2009. The goodness-of-fit values are listed in Table 6.2.

Table 6.2. Goodness-of-fit values for calibration and validation periods.

Parameter	Site	CALIBRATION				VALIDATION			
		R2	N-S	RMSE	NO	R2	N-S	RMSE	NO
Q	Härkälänjoki	0.615	0.608	69.250	1039	0.542	0.516	60.802	731
	Lepsämäenjoki-middle	-	-	-	-				
	Lepsämäenjoki-outlet	0.640	0.540	92.361	261	0.612	0.528	57.346	672
NO3-N	Härkälänjoki	0.654		348.102	7				
	Lepsämäenjoki-middle	0.034		129.451	13	0.145		112.801	35
	Lepsämäenjoki-outlet	0.112		96.032	64	0.126		78.376	61
NH4-N	Härkälänjoki	0.028		70.755	6				
	Lepsämäenjoki-middle	0.003		115.666	13	0.141		87.396	36
	Lepsämäenjoki-outlet	0.148		113.713	63	0.020		117.006	61
Susp. Sed.	Härkälänjoki	-		-	-	0.020		103053	9
	Lepsämäenjoki-middle	-		-	-	0.01		583.857	22
	Lepsämäenjoki-outlet	0.195		97.315	63	0.008		104.079	60
Tot-P	Härkälänjoki					0.396		51.106	9
	Lepsämäenjoki-middle	0.047		83.31	19	0.004		217.402	45
	Lepsämäenjoki-outlet	0.285		70.325	64	0.173		61.097	71
SRP	Härkälänjoki	-		-	-	-		-	-
	Lepsämäenjoki-middle	0.379		118.111	6	0.09		483.064	46
	Lepsämäenjoki-outlet	0.037		111.065	63	0.103		242.127	91

Storylines. The following storylines were simulated:

- Storyline1 – Consensus world: In the storyline 2 the main objective of the government and citizens is to stimulate economic activity but also to promote sustainable and efficient use of resources. The current guidelines and policies are continued. As future climate is assumed to favour agricultural production by increasing yields in Finland (Peltonen-Sainio et al., 2009; Peltonen-Sainio et al., 2010), field percentage is assumed to increase, limited only by soil types and field slopes (>10%) which are not suitable for cultivation.
- Storyline2 – Techno world: This storyline is based on high awareness but poor regulation of environmental protection. Most actions are the result of individual or commune interest on protecting the environment and they are based on technical solutions. Cultural services like recreation opportunities are locally important. In the Lepsämäenjoki River basin this storyline is based on the improvement of sewage treatment. Moderate increase according to (Haakana et al., 2015) in urban land cover (human settlements) is assumed.
- Storyline3 – Fragmented world: The focus of this storyline is to survive as a country instead of as part of Europe. National institutions focus on economic

development and no attention is paid to the preservation of the ecosystems. In this storyline field area is assumed to increase up to 90% of the sub-catchment area as future climate favour agricultural production. As current environmental guidelines are not valid, the main production type will be monoculture of cereals with increased fertilization level. As the catchment is located relatively close to Helsinki, also increase in human settlements is assumed.

The implementation of the storylines is listed in the Table 6.3. The qualitative storylines were included into the model application by making a quantitative change in the relevant parameter value.

Table 6.3.Implementation of the storylines.

Storyline	Sector	Type of measure	Specific measure
Consensus	Agriculture	Increase in agricultural land; up to 50%	Forest turned into fields
		Less intensive agriculture	30% increase in yields
		CAP greening crop rotation	40% spring cereals- 30% winter cereals, 15% grass, 15% fallow
		Fertilisation	No change
		Increase in erosion control	80% on stubble in spring cereals fields
Techno	Agriculture	No change	No change in population
		Increase in agricultural land	Forest turned into fields
		More intensive agriculture	20% increase in yields
		Moderate crop rotation	50% spring cereals- 50% winter cereals, no change in grass and fallow
	Urban	Increase in fertilisation	20% increase in N- and P fertilizer application
Fragmented	Agriculture	No change in erosion control	50% in stubble on spring cereal fields
		Increase in urban areas	1.5% of forest areasturned into urban
		Improvement in waste water treatment	New central sewage system (outside the area), decrease in sewage by 50%
		High increase in agricultural land	up to 90% of forest areas (soil type limited) turned into fields
		More intensive agriculture	25% increase in yields
		Monoculture	Mainly barley
		Increased fertilisation	30% increase in N and P fertilizer application
		No erosion control	No erosion control
		Urban	Increase in urban areas
		Increase in population and waste water	Effluents from scattered dwellings and sewage treatment plants are increased by 10%

6.2.5 Results of the physical model

Temperature and discharge. Future climate scenarios provided increase in both temperature and precipitation. Around 2030 the mean temperature was be almost +6 °C,

and around 2050 6.5 °C. Also precipitation increased up to 20%, depending on the scenario. Precipitation increased especially in spring and late autumn.

As a result current peak runoff due to snow melting in April occurred earlier in spring (Figure 6.13). Some scenarios would provide also increase in runoff in late autumn. On the other hand, summer runoff decreased according to all of the climate scenarios. There were no major changes in duration of high and low pulses. Duration of high pulses decreased by couple of days, and duration of low pulses might increase by couple of days (Figure 6.14).

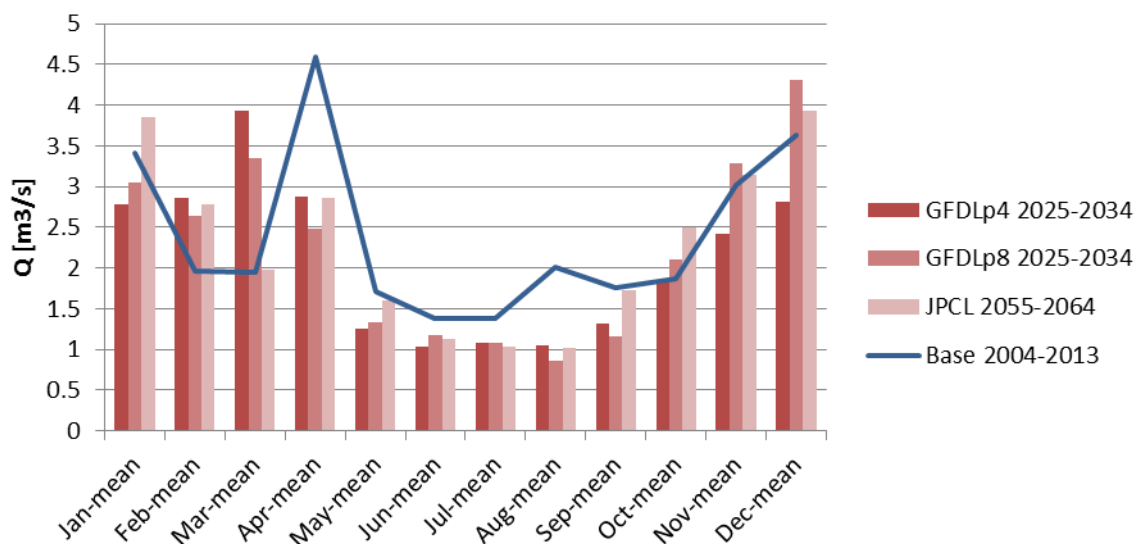


Figure 6.13 Change in peak flow according to the climate scenarios.

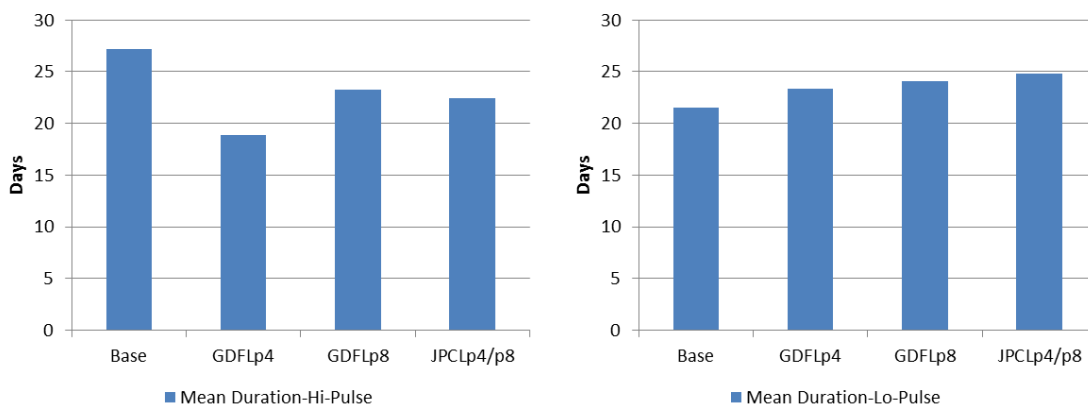


Figure 6.14 Mean duration of high and low pulses within each year.

Nutrient concentrations. Nutrient concentrations would increase in the river according to all storylines (Figure 6.15). Increase of field area is highest at the middle reaches of the river, and there also the increase in nutrient concentrations is highest. Increase in suspended sediment concentrations occurs only in snow-free periods, but concentrations of nitrate increases also during winter. According to Finnish standards (Table 6.4) the ecological status of the river became bad or poor.

Table 6.4. Finnish classification of the ecological status.

Type	WFD class	Ecological status	TP ($\mu\text{g/l}$)
Small or medium size river on clay soils	0	Bad	>130
Small or medium size river on clay soils	1	Poor	130-100
Small or medium size river on clay soils	2	Moderate	100-60
Small or medium size river on clay soils	3	Good	60-40
Small or medium size river on clay soils	4	Excellent	<40

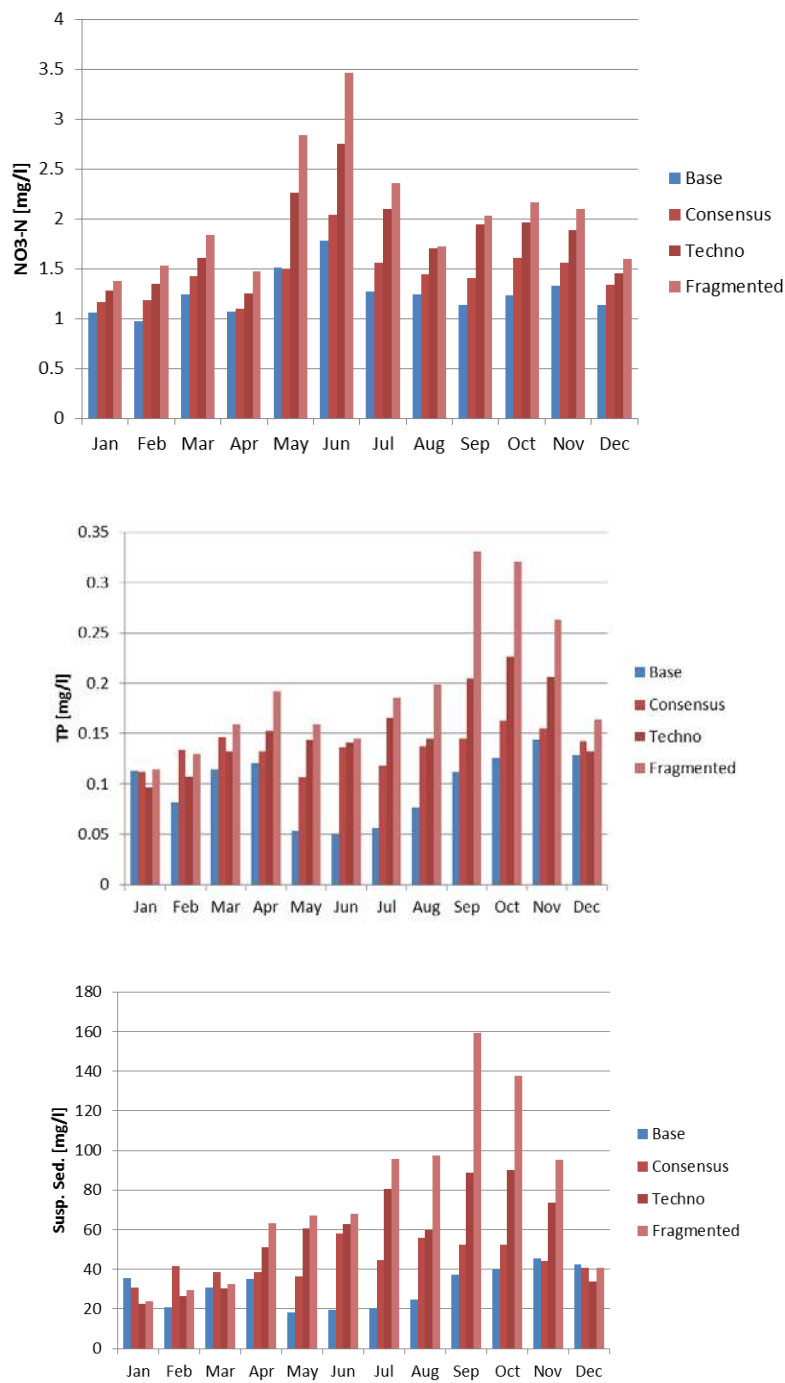


Figure 6.15 Suspended sediment and nutrient concentrations at the middle reaches on the river.

6.2.6 Empirical Models

GLMM. Mixed models were used instead of linear models, because the data set contained random effects: year and site. Most of the variables were biased, so they were log-

transformed to better follow normal distribution. Main single effects of parameters on Chl-a concentration are plotted in Figure 6.16.

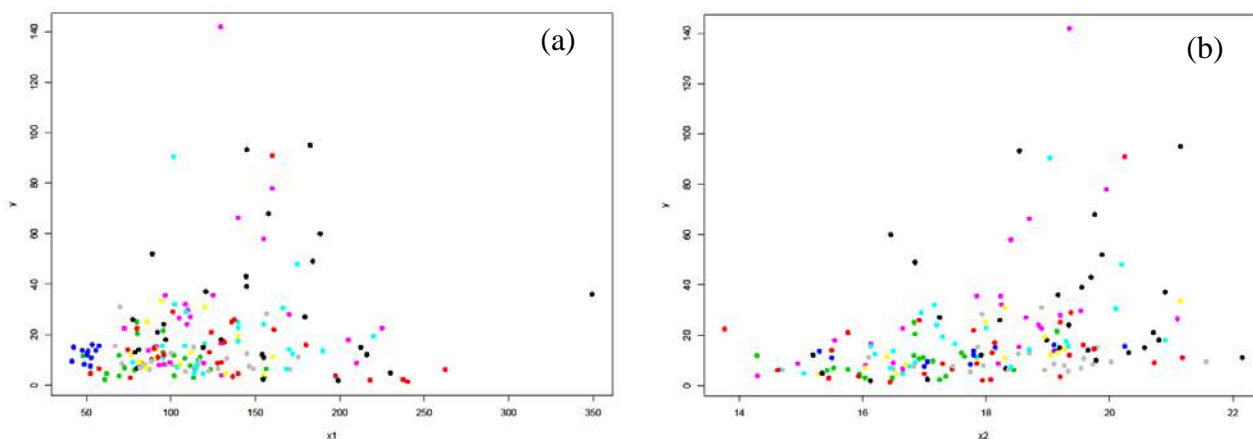


Figure 6.16 The single effects for Chl- α concentration; (a) TP, (b) T_w. Different colors represent different measurement points.

Observed summer-time Chl- α concentration in agricultural rivers flowing through clay soils was relatively well explained by a simple model including only total phosphorus (TP) concentration and water temperature (T_w):

$$\log\text{-Chl}\alpha \sim \log.\text{TP} + \log.\text{TP:T}_w + (1 \mid \text{site}) + (1 \mid \text{year})$$

Goodness-of-fit values of the model are in Table 6.5, residuals are shown in Figure 6.17 and partial responses in Figure 6.18. There is also interaction between water temperature and TP concentration, so that increasing temperature enhances the effect of TP (Figure 6.19).

Table 6.5. Goodness-of-fit values of the GLMM model

	Single influence	Interaction	Estimate	Significance	R ² m	R ² c
Model					0.212	0.409
	Intercept		0.758	*		
	log.TP		-0.68	**		
		log.TP:T_w	0.047	***		

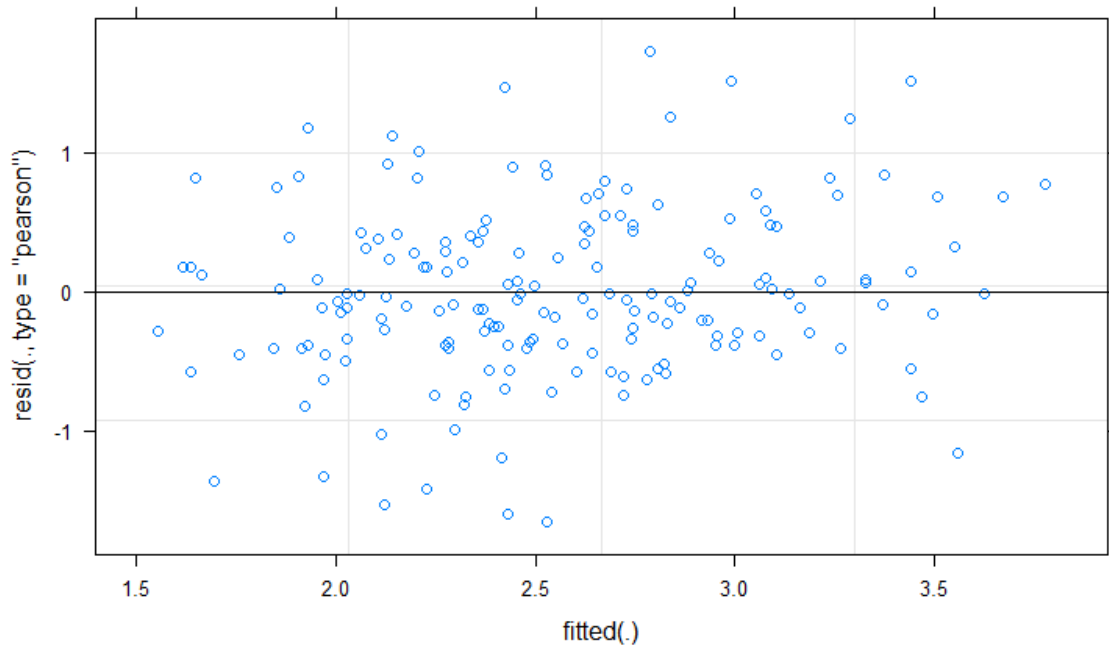


Figure 6.17 Residual of the GLMM model.

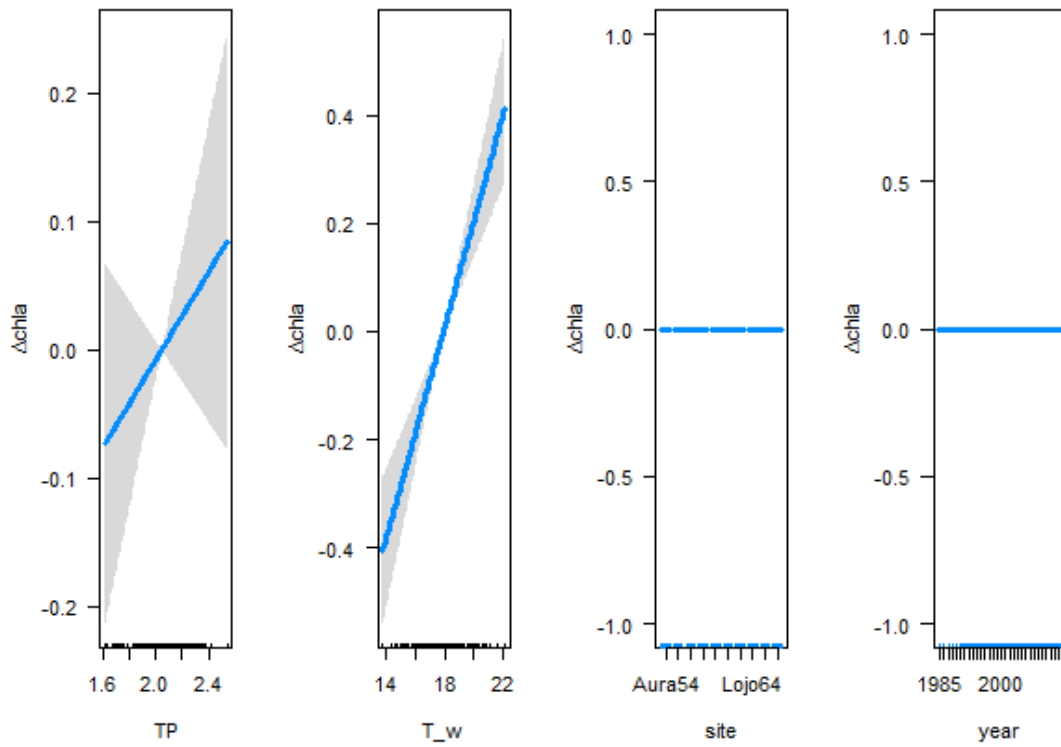


Figure 6.18 Partial responses of the parameters in GLMM model.

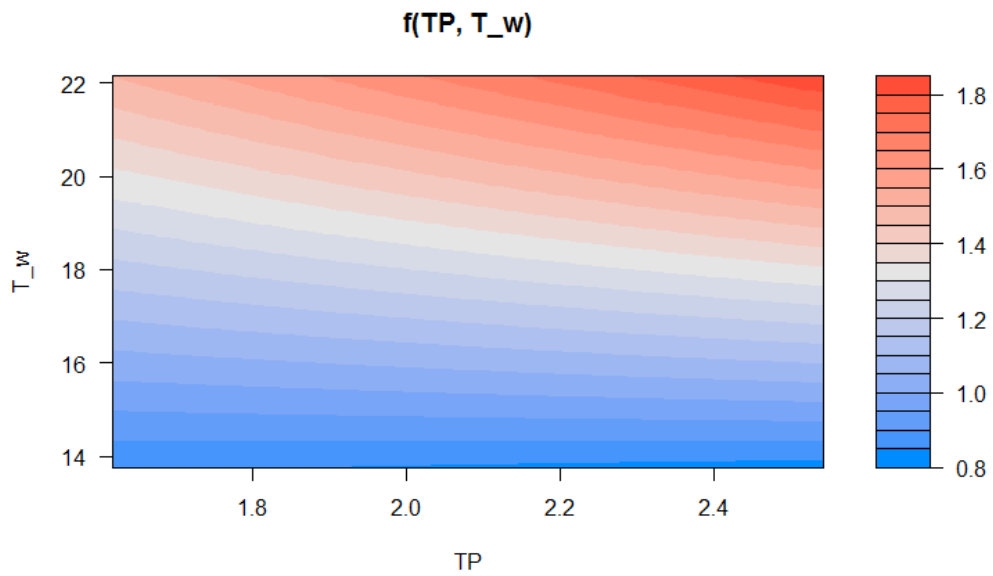


Figure 6.19 Interactions between total P (TP) and water temperature (T_w) in the GLMM model.

Boosted Regression Trees (BRT). The simplified BRT model contains five parameters: total P concentration (TP), nitrate concentration (NO₃-N), proxy for soluble reactive P (TP/Turb), water temperature (T_w) and 7-day minimum runoff (r_{7day_min}). It explains 60% of the variance. Partial responses are in Figure 6.20. There were also in this model a clear interaction between water temperature and TP concentration (Figure 6.21).

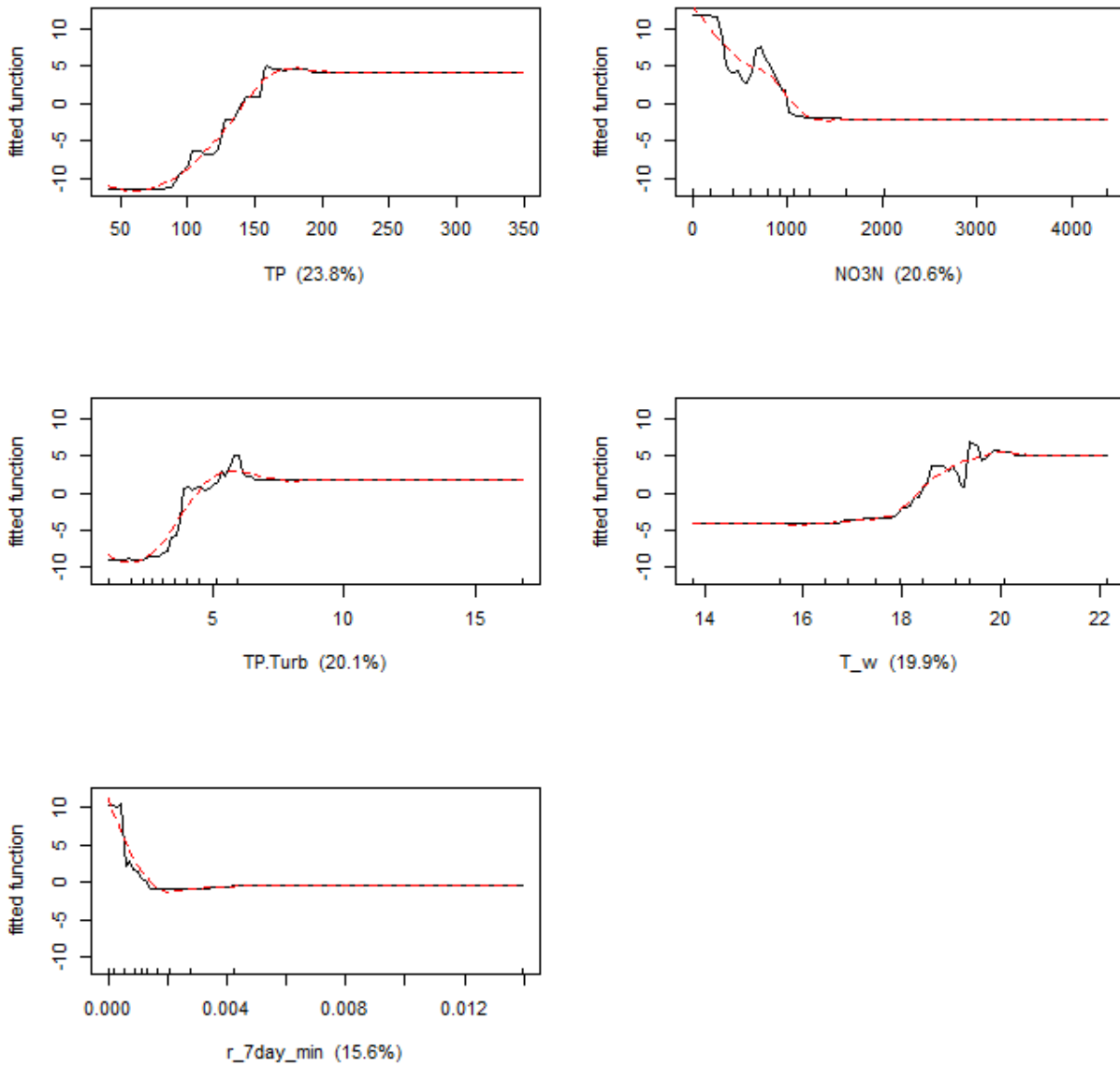


Figure 6.20 Partial responses in BRT model.

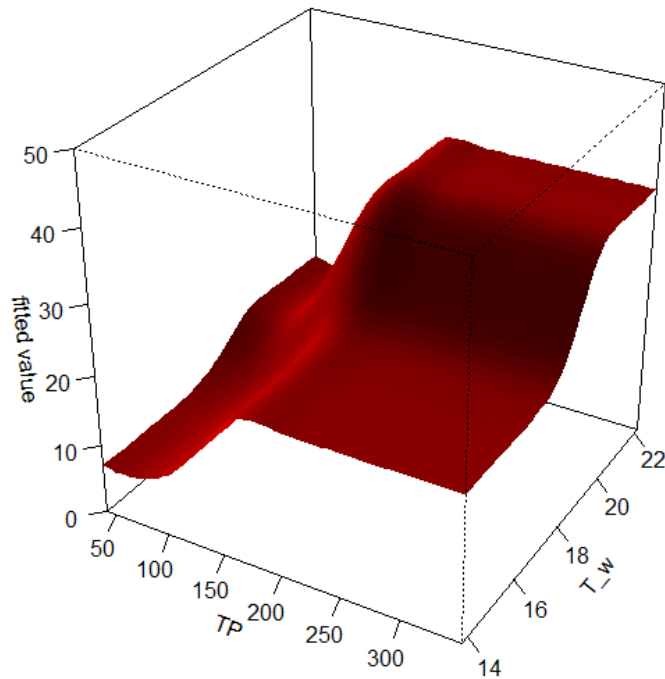


Figure 6.21 Interactions in the BRT model.

6.2.7 Results of the empirical models

GLMM. Empirical glm-model predicted increased chl- α concentrations according to all scenarios. Statistical values for chl- α concentrations in the whole river basin are listed in Table 6.6. The shift of peak concentration at the middle reaches of the Lepsämäjoki and the Härkälänjoki tributary are shown in Figure 6.22.

BRT model. Empirical brt-model predicted similar results with glmm, so that chl- α concentrations increased according to all scenarios. Statistical values for chl- α concentrations in the whole river basin are listed in Table 6.7. The shift of peak concentration at the middle reaches of the lepsämäjoki and the härkälänjoki tributary are shown in Figure 6.23. In general the increase was slightly smaller than by the glmm, probably because brt took into account also concentrations of soluble reactive nutrients.

Table 6.6. Statistics from the GLM-model.

	Min.	1st Qu.	Median	Mean	3rd Qu.	Max.
Consensus_2534	6.498	13.280	18.300	19.510	22.240	47.500
Techno_2534	5.059	28.220	28.410	26.160	28.520	43.330
Fragmented_2534	5.924	14.060	23.250	22.740	28.940	47.800
Consensus_5564	5.924	14.060	23.250	22.740	28.940	47.800
Techno_5564	9.135	20.170	28.370	29.450	37.940	66.240
Fragmented_5564	10.50	22.91	29.74	31.32	39.19	70.08

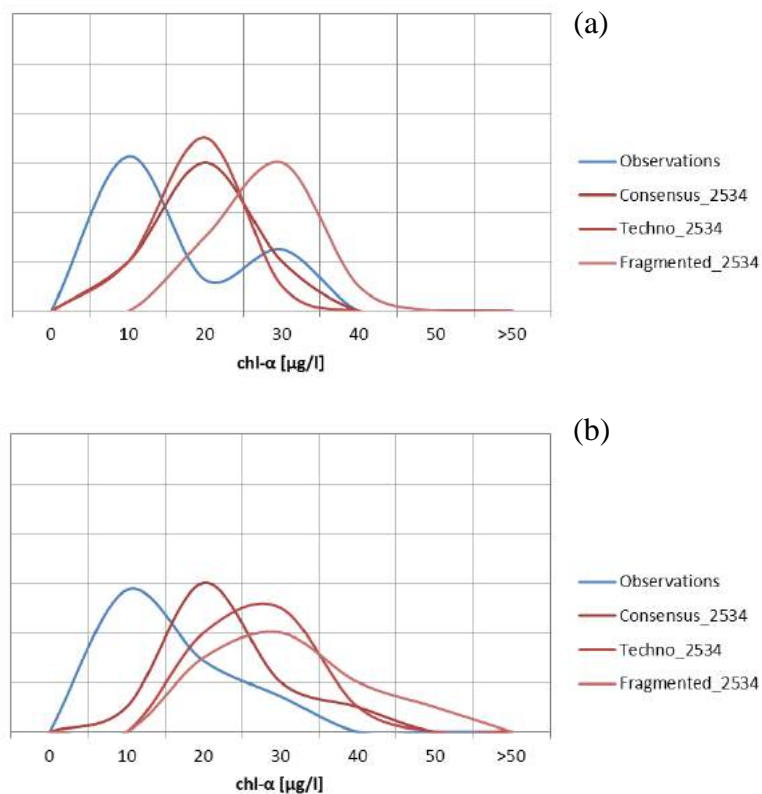


Figure 6.22 Shift in peak concentrations of Chl-a according to different story lines from current situation to years 2025-2034. (a) Härkälänjoki tributary, (b) middle reaches of the river Lepsämänjoki.

Table 6.7. Statistics from the BRT model.

	Min.	1st Qu.	Median	Mean	3rd Qu.	Max.
Consensus_2534	11.77	16.51	17.63	19.24	22.61	33.87
Techno_2534	12.89	17.35	20.02	20.45	24.33	34.21
Fragmented_2534	11.77	19.81	22.57	21.43	23.72	34.14
Consensus_5564	12.76	17.87	23.37	23.25	28.18	36.71
Techno_5564	11.94	17.59	23.34	23.40	27.94	36.79
Fragmented_5564	12.76	19.10	24.37	24.39	28.57	36.71

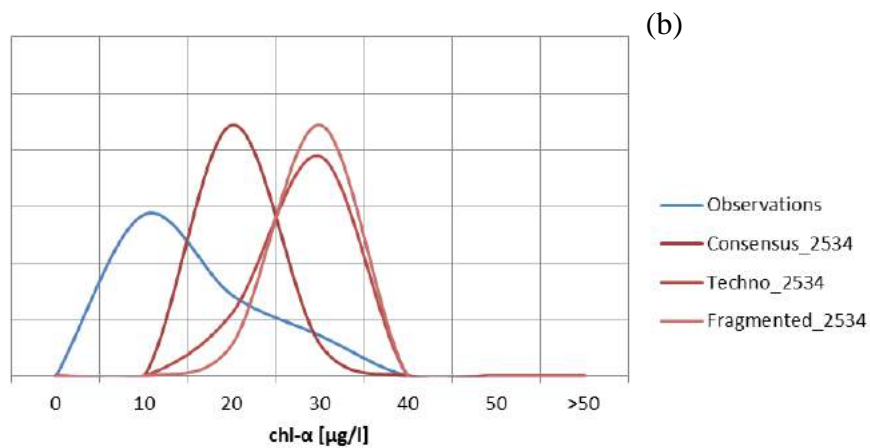
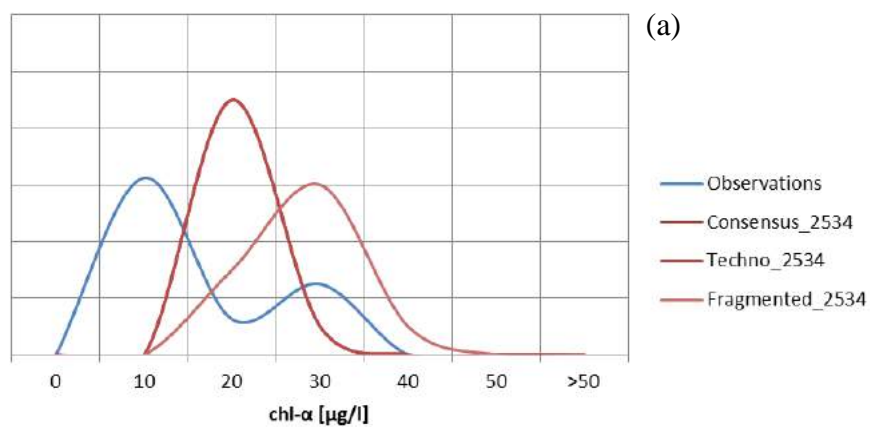


Figure 6.23 Shift in peak concentrations of Chl-a according to different story lines from current situation to years 2025-2034. (a) Härkälänjoki tributary, (b) middle reaches of the river Lepsämänjoki.

6.2.8 Ecosystem services

Multiple pressures and their changes can result in the alteration of both the status and the services of aquatic ecosystems. To structure the analysis of ecosystem services and select appropriate indicators, we used the conceptual framework proposed by (Grizzetti et al., 2016), based on the cascade model. The framework includes the capacity of the ecosystem to deliver the service, the actual flow of the service, and the benefits. Capacity refers to the potential of the ecosystem to provide ecosystem services, while flow is the actual use of the ecosystem services.

For water purification we considered the rate of nutrient removal ($\text{kg}/\text{km}^2/\text{yr}$), which is an indicator of the actual flow of the service. To assess the capacity of the ecosystem to provide clean water for drinking and recreational purposes (Table 6.8) we referred to the Finnish Standards for ecological status (Table 6.4).

On a catchment scale the rate of nutrient removal is negative (Figure 6.24) according to all storylines. In the main sector agriculture, agri-environmental regulations according to storyline Consensus may provide increased nutrient removal when comparing to current situation (Figure 6.25).

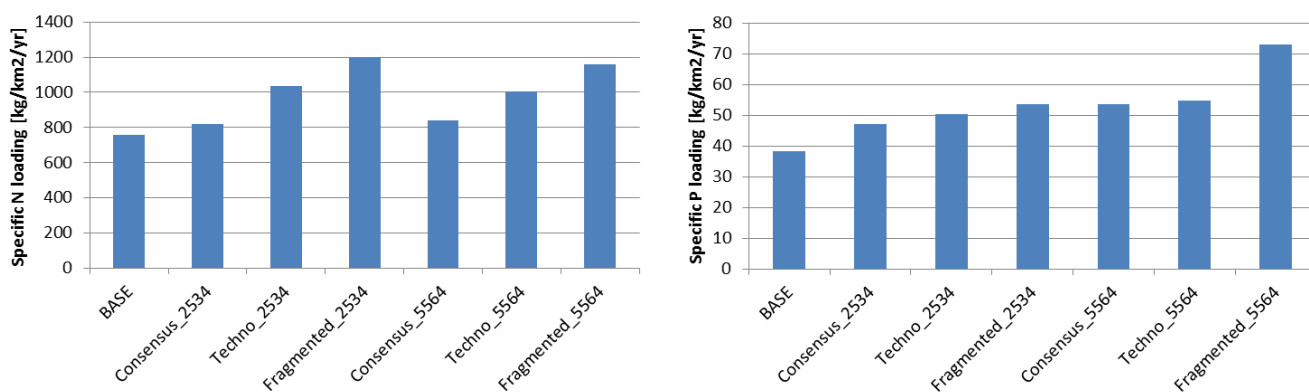


Figure 6.24 Catchment scale nutrient production/removal rate.

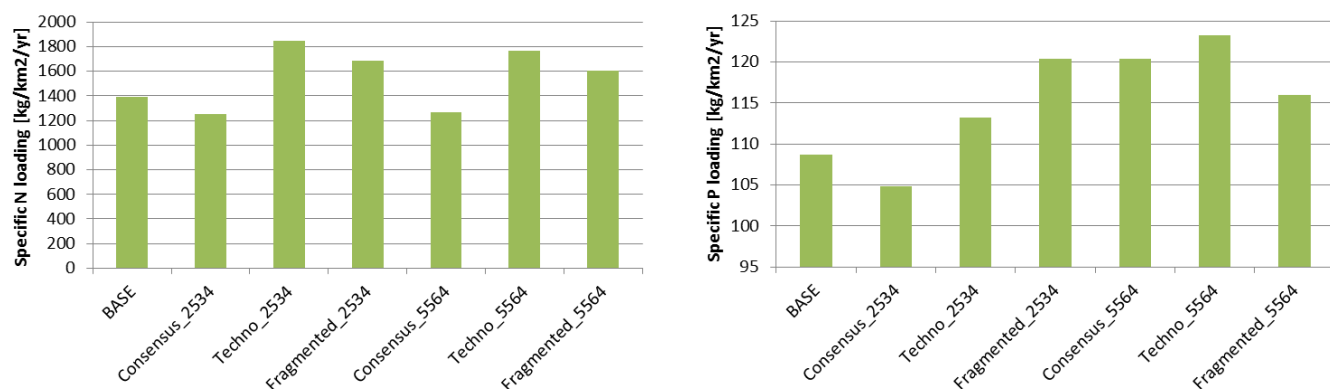


Figure 6.25 Nutrient production/removal rate in agriculture.

Table 6.8.Capacity of the ecosystem.

Storyline	Sub-Catchment	NO3-N [mg/l]	Susp. sed. [mg/l]	TP [mg/l]	Ecological status
Base_0413	Lepsamanjoki_mid	1.25	30.90	0.10	Poor
Base_0413	Harkalanjoki	1.27	18.50	0.09	Moderate
Consensus_2534	Lepsamanjoki_mid	1.44	44.59	0.14	Bad
Consensus_2534	Harkalanjoki	1.52	27.62	0.11	Poor
Techno_2534	Lepsamanjoki_mid	1.79	56.82	0.15	Bad
Techno_2534	Harkalanjoki	1.71	30.26	0.11	Poor
Fragmented_2534	Lepsamanjoki_mid	2.04	76.00	0.19	Bad
Fragmented_2534	Harkalanjoki	1.99	49.72	0.16	Bad
Consensus_5564	Lepsamanjoki_mid	1.40	53.06	0.15	Bad
Consensus_5564	Harkalanjoki	1.47	30.34	0.11	Poor
Techno_5564	Lepsamanjoki_mid	1.73	60.17	0.16	Bad
Techno_5564	Harkalanjoki	1.66	32.68	0.11	Poor
Fragmented_5564	Lepsamanjoki_mid	1.80	65.09	0.18	Bad
Fragmented_5564	Harkalanjoki	1.71	42.79	0.14	Bad

6.2.9 Lessons Learned

GLMM explains changes on Chl- α concentrations efficiently by TP concentration and water temperature. As it does not take soluble nutrients into account, it may give more

pessimistic predictions than BRT. TP and Suspended Sediment concentrations correlate and thus erosion control methods are the only measure that controls TP loading in this model. Lepsämäenjoki catchment is very erosion sensitive area, so reductions in TP are seen rapidly but not very much potential to increase erosion control methods (Rankinen et al., 2015). Reductions in P fertilization is seen on SRP concentrations slowly, but only BRT model takes them into account. Water temperature depends not only air temperature but smaller amount of water flowing slowly warms probably faster. Runoff is included into BRT but not in GLMM.

In earlier climate change studies (e.g. (Rankinen et al., 2013), changes in nutrient concentrations were smaller than in this study, and mitigation by agricultural water protection methods or changes in cultivation practices were an option. Previous studies focused only on agricultural areas, and increase of field area was not assumed, which now masks the positive development in the Consensus storyline.

6.3 Mustajoki/Teuronjoki, Finland

6.3.1 Area description

The Mustajoki catchment belongs to the drainage basin of Lake Pääjärvi (212 km²) of the larger Teuronjoki basin located in southern Finland. It is a part of the Vanajavesi route in the Kokemäenjoki river basin, discharging finally to the Bothnian sea (Figure 6.26). It is the largest sub-catchment and has an area of 76.8 km². The drainage area lies in the southern boreal vegetation zone. During winter, precipitation typically falls as snow and the soil is frozen. Annual mean temperature is 4.0 °C and annual mean runoff 234 mm.

The forests are dominated by Norwegian spruce, Scots pine and birch with some European aspen. In the Mustajoki basin the land use is divided into forest (67% of total area), peatlands (20%) and agricultural land (13%). In the basin 48% of the near-surface deposits are characterized by moraine, with some highly permeable sand and gravel deposits, and organic peat layers (*Haplic Podzols* and *Eutric Regosols*).

There are no point pollution sources of nutrients in the catchment and the area is sparsely populated. The main human influence comes through forestry and agriculture. Agriculture is mainly cereal cultivation but a low proportion of sugar beet is included.

The drainage basin of Lake Pääjärvi was used to study evaporation from the lake surface in connection with the International Hydrological Decade in 1965-1974 when both discharge and water quality measurements started (Tikkanen et al., 1985). Observations continued in several research projects after that, but measurements do not form a continuous time series (Arvola et al., 2002). Samples for DOC (Dissolved Organic Carbon) concentration detection have been taken weekly at the Mustajoki river outlet (6180404100N; 2581204700E; 102ma.s.l.) since the year 2000 by the Lammi Biological Station (LBS) of the University of Helsinki. Sampling started in 1995 but before 2000 the winter-time sampling took place on a monthly basis only.

Ecological status of the Lake Pääjärvi is good, and the rivers Teuronjoki and Mustajoki moderate.

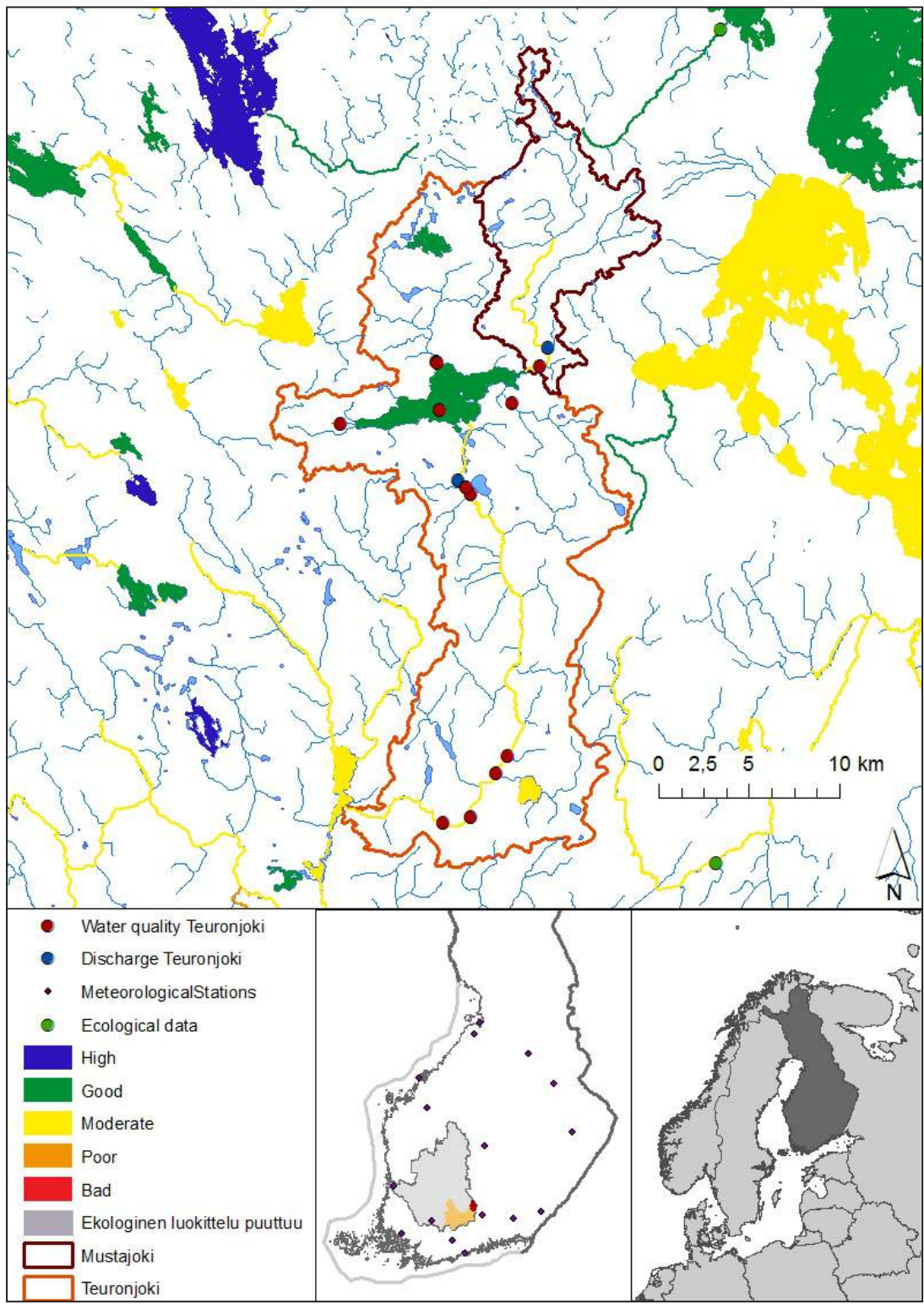


Figure 6.26 Location of the Mustajoki/Teuronjoki catchment with different monitoring sites.

6.3.2 Conceptual model

The research question of the river Mustajoki-lake Pääjärvi combination is brownification of the lake, and influence of water colour on submerged macrophyte depth distribution (Figure 6.27). Dissolved organic carbon (DOC) loading from the catchments were simulated by the INCA model, and the DOC concentration in the lake was calculated by the MyLake model. Simulated DOC concentration was transformed to water colour and light climate of the lake by empirical equations.

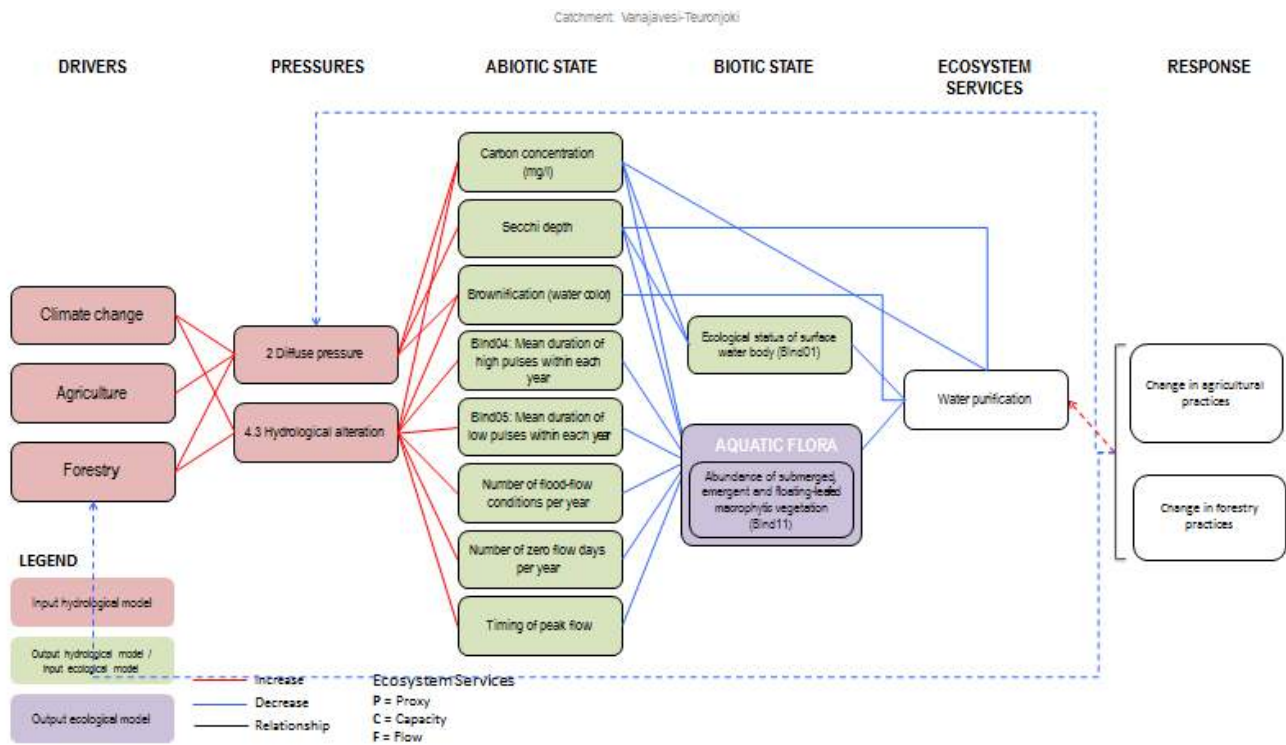


Figure 6.27 Conceptual model of the Mustajoki case.

6.3.3 Scenarios and storylines

Increasing temperature may influence both land use and agricultural production. In 2025-2034 the climate change scenarios provide annual mean temperature around 4.9 °C and in 2055-2064 around 5.5 °C. The following storylines were designed:

- Storyline 1 – Consensus world: In the storyline 2 the main objective of the government and citizens is to stimulate economic activity but also to promote sustainable and efficient use of resources. The current guidelines and policies are continued.
- Storyline 2 – Fragmented world: The focus of this storyline is to survive as a country instead of as part of Europe. National institutions focus on economic development and no attention is paid to the preservation of the ecosystems. In this storyline field area is assumed to increase up to 23% of the area as future climate favour agricultural production. As current environmental guidelines are not valid, the main production type will be monoculture of cereals.

The implementation of the storylines is listed in Table 6.9. The qualitative storylines were included into the model application by making a quantitative change in the relevant parameter value.

Table 6.9.Implementation of the storylines.

Storyline	CC scenario	Sector	Type of measure	Specific measure
SSP2 - Consensus (green focus)	GDFLp4 2025-2034	Agriculture	No change in field area	No change in growing season
SSP2 - Consensus (green focus)	JPCL 2055-2064	Agriculture	No change in field area	Increase by 14 days in growing season in spring and in autumn
SSP3 - Fragmented (intermediate)	GDFLp8 2025-2034	Agriculture	Increase in agricultural land 23% of forest areas turned into field	No change in growing season
SSP3 - Fragmented (intermediate)	JPCL 2055-2064	Agriculture	Increase in agricultural land 23% of forest areas turned into field	Increase by 14 days in growing season in spring and in autumn in 2055-2064

6.3.4 Physical Models

INCA and Persist models. INCA is a dynamic mass-balance model, and as such attempts to track the temporal variations in the hydrological flowpaths and nutrient transformations and stores, in both the land and in-stream components of a river system.

INCA provides as an output daily and annual land-use specific organic and inorganic-nutrient fluxes ($\text{kg ha}^{-1} \text{ yr}^{-1}$) for all transformation processes and stores within the land

phase, and daily time series of land-use specific flows, and organic and inorganic-nutrient concentrations in the soil and ground waters and in direct runoff.

Spatial data describing the major land use types are required. INCA also requires time series inputs describing the hydrology, namely the Soil Moisture Deficit (mm), Hydrologically Effective Rainfall (mm day^{-1}), Air Temperature ($^{\circ}\text{C}$) and Actual Precipitation (mm day^{-1}). These data are usually obtained from analysis of meteorological data and rainfall gauges and derived from a hydrological model

.The Integrated Catchments model for Carbon (INCA-C) describes the major factors and processes controlling DOC in surface waters that have been reported in the literature. Organic carbon is added soil to SOC through litter fall. Both SOC and DOC can be mineralized to DIC in the soil. Organic carbon in the soil is transformed between SOC and DOC through dissociation and association. In both the soil and stream, DIC is lost to the atmosphere. DOC and DIC in the soil water are transported to the stream through diffuse runoff. DOC and DIC in the stream are also lost through the stream outflow. The model equations are described by (Futter et al., 2007).

PERSiST is a flexible rainfall-runoff modelling toolkit for use with the INCA family of models (Futter et al., 2014b). PERSiST (the Precipitation, Evapotranspiration and Runoff Simulator for Solute Transport) is designed for simulating present-day hydrology; projecting possible future effects of climate or land use change on runoff and catchment water storage. PERSiST has limited data requirements and is calibrated using observed time series of precipitation, air temperature and runoff at one or more points in a river network.

MyLake. Calculations of DOC concentration in the lake were made with MyLake (Multi-year simulation model for Lake thermo- and phytoplankton dynamics) model. It is a one-dimensional process-based model code for simulation of daily vertical distribution of lake water temperature and thus stratification, evolution of seasonal lake ice and snow cover, and phosphorus-phytoplankton dynamics and it is described in (Saloranta and Andersen, 2007b).

The FOKEMA submodule was used with MyLake model to calculate dissolved organic carbon in the lake water (Aarnos, unpublished). The focus of the FOKEMA-module is on dissolved organic carbon (DOC) and its mineralization (both microbial and photochemical). Based on observations, the DOC pool in the model is divided into three sub pools that have different bacterial mineralization coefficients. They are denoted by DOC1, DOC2 and DOC3 and the bacterial decay coefficients and initial distributions are shown in Table 6.10. The first pool has the fastest decay rate, the second pool has a lower rate and the third pool is not affected by the bacterial mineralization. The third pool however constitutes the largest fraction of the DOC. The DOC input into the MyLake model is divided into these 3 pools and they are treated separately in the FOKEMA module. After each FOKEMA calculation, the DOC pools are summed up to form the total DOC concentration. FOKEMA calculates both photochemical and microbial mineralization of the DOC (Aarnos, H, unpublished).

Calibration and validation of the models. Input data of the models consisted of daily weather data collected from the weather stations of Finnish Meteorological Institute. Global radiation and cloudiness data were measured at the Jokioinen Observatory. Air temperature, humidity, precipitation and wind speed were measured at Lahti Laune station. In the MyLake model for air pressure a stationary value of 1000 were used. Calibration period was 1995-2003 and validation period 2004-2006. Measurement data was available from date 31.5.1995 to set the initial conditions in the model.

The Persist model and the INCA models were calibrated and validated against measured discharge and DOC concentrations at the outlet of the river Mustajoki. Land cover data was Corine 2000, and more detailed data of agricultural land use was derived from field parcel database. Goodness-of-fit values for discharge were 0.728 (R^2) in calibration period and 0.200 in validation period. R^2 -values for DOC were 0.41 in calibration period and 0.219 in validation period.

Output from INCA Watershed Model (daily inflow and DOC concentrations) was used as input in MyLake model. INCA model offered results for the subcatchment of River Mustajoki. Therefore the inflow values were multiplied by coefficient 2.6 to correspond

the inflow from the whole catchment area to Lake Pääjärvi and these corrected inflow values were used in MyLake. The coefficient was calculated according to the surface areas of the whole catchment and the River Mustajoki subcatchment.

Initial DOC value in the lake was 10 mg/l in each water layer. Temperature profile was set so that temperature was 13,8°C in the uppermost water layer (0-1m depth) and 4,4°C in lowest layer (85-86 m). Initial values were got from observations made in 19.5.2005. Initial DOC value in the lake was 12.4 mg/l in each water layer. Temperature profile was set so that temperature was 6.4°C in the uppermost water layer (0-1m depth) and 5.8°C in lowest layer (85-86m). Weather data were collected similar way as for the calibration period. The bacterial decay coefficient for the 3 different DOC pools of the MyLake model is shown in Table 6.10. It is a constant for temperatures above 5°C and decreases linearly for temperatures below that so that it becomes 0 at 0°C. For depths below 0.5 m the photobleaching term becomes zero. (Aarnos, H, unpublished).

Table 6.10. Properties of the different DOC pools in Pääjärvi MyLake Application.

Pool	Bacterial decay B_B (d^{-1})	Initial fraction
DOC1	0.012	0.045
DOC2	0.0012	0.050
DOC3	0.0	0.905

The bacterial decay coefficients and initial fractions of the three DOC pools can be used for calibration of the FOKEMA model. For the initial fractions of the very labile (DOC1) and labile (DOC2) pools a total value of 0.095 was used. It is an average fraction of consumed DOC in oligotrophic lakes of differing humic content found by (Tranvik, 1988). The initial fraction for the third, recalcitrant pool was therefore 0.905. The bacterial decay coefficients 0.012 for the very labile DOC1-pool and 0.0012 for the labile DOC2-pool were found with calibration since they offered a good fit for the model result and the measured DOC values in the surface water of Lake Pääjärvi. (Hopkinson et al., 2002) and (Ogura, 1972) have conceptualized a three-pool model for DOC in ocean areas. Hopkinson found that, on average, DOC was 16% very labile, 13% labile and 71% recalcitrant for the middle Atlantic bight. The decay rates for the very labile pool ranged

from 0.05 to 1.51 d⁻¹, so there was high variability in the values. Ogura (1972) reported rate constants between 0.01 and 0.09 d⁻¹ for the very labile pool and an order of magnitude lower for the labile pool. The decay rates used in this work are included to the range reported by Ogura, but they are smaller than those reported by Hopkinson.

MyLake model calculated the temperature stratification well during the calibration period (Figures 6.28-6.30). Lake Pääjärvi has quite a simple bathymetry with one deepest point and not many islands or different basins. Therefore MyLake model is a good choice for calculating long time periods in Lake Pääjärvi.

After calibrating the bacterial decay coefficients, the calculated DOC concentrations fit well to observations during the calibration period (Figure 6.31) and the fit was quite good also during the validation period (Figure 6.32).

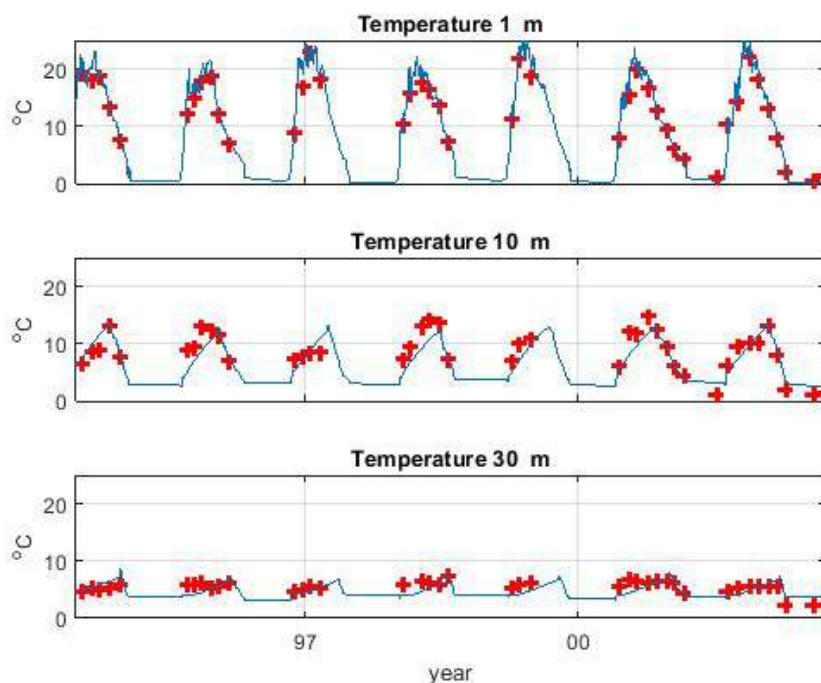


Figure 6.28 Temperature in model results and observations in Lake Pääjärvi during the calibration period 31.5.1995-27.11.2003.

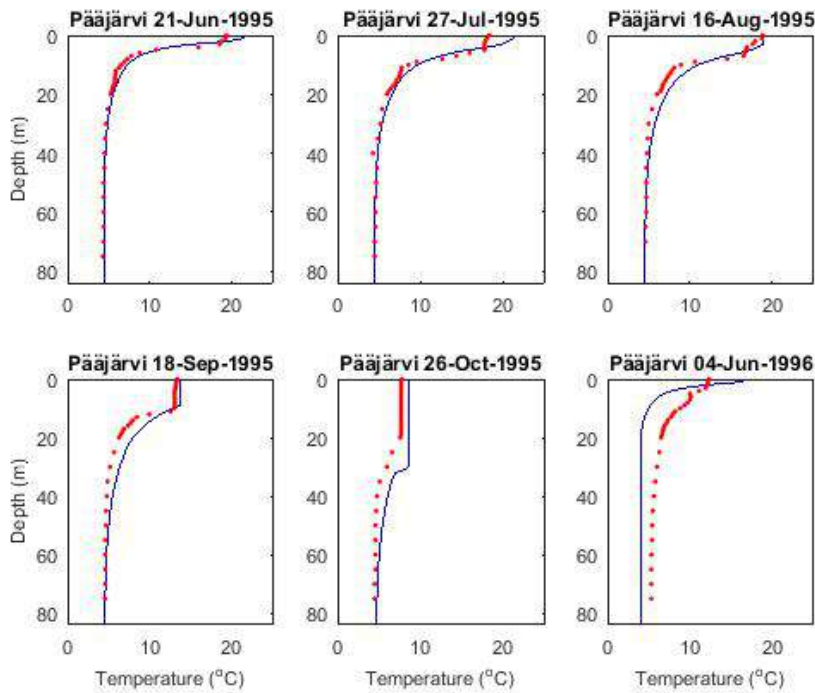


Figure 6.29 Temperature profiles in Lake Pääjärvi during the calibration period 31.5.1995-27.11.2003.

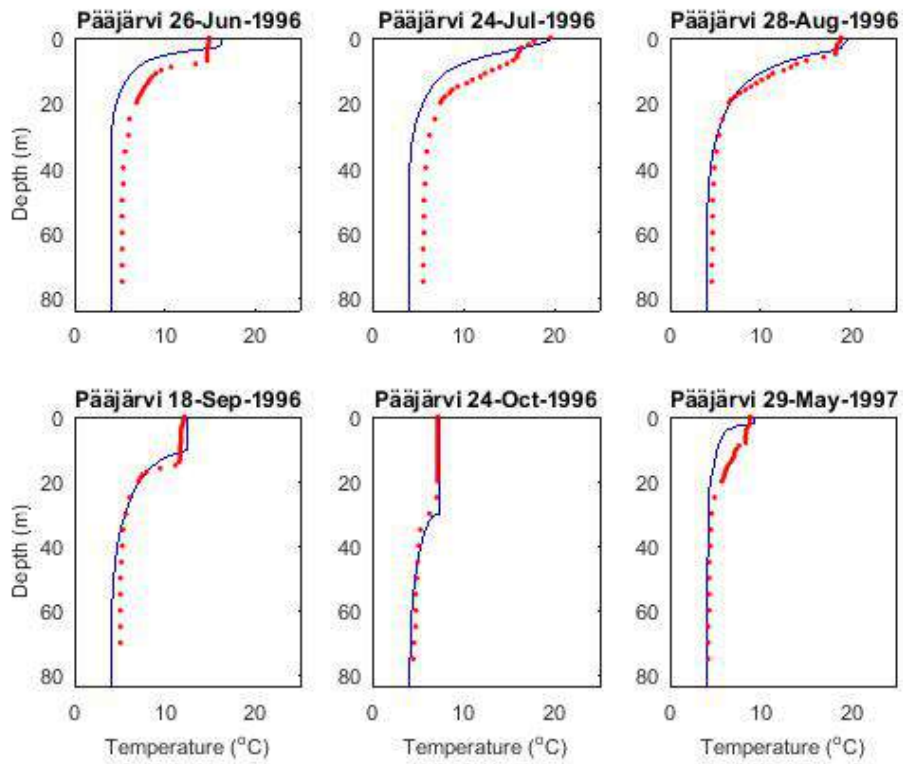


Figure 6.30 Temperature profiles in Lake Pääjärvi during the calibration period 31.5.1995-27.11.2003.

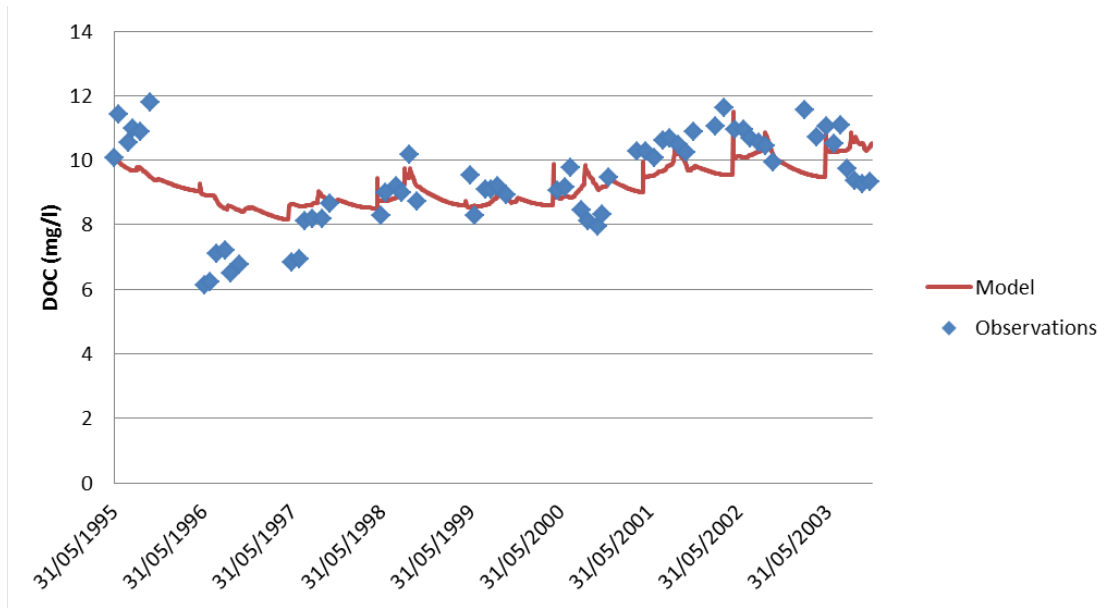


Figure 6.31 Dissolved organic carbon in surface water of Lake Pääjärvi during the calibration period 31.5.1995-27.11.2003. Observations are from depth layer 0-15m and model result is from depth layer 7-8m.

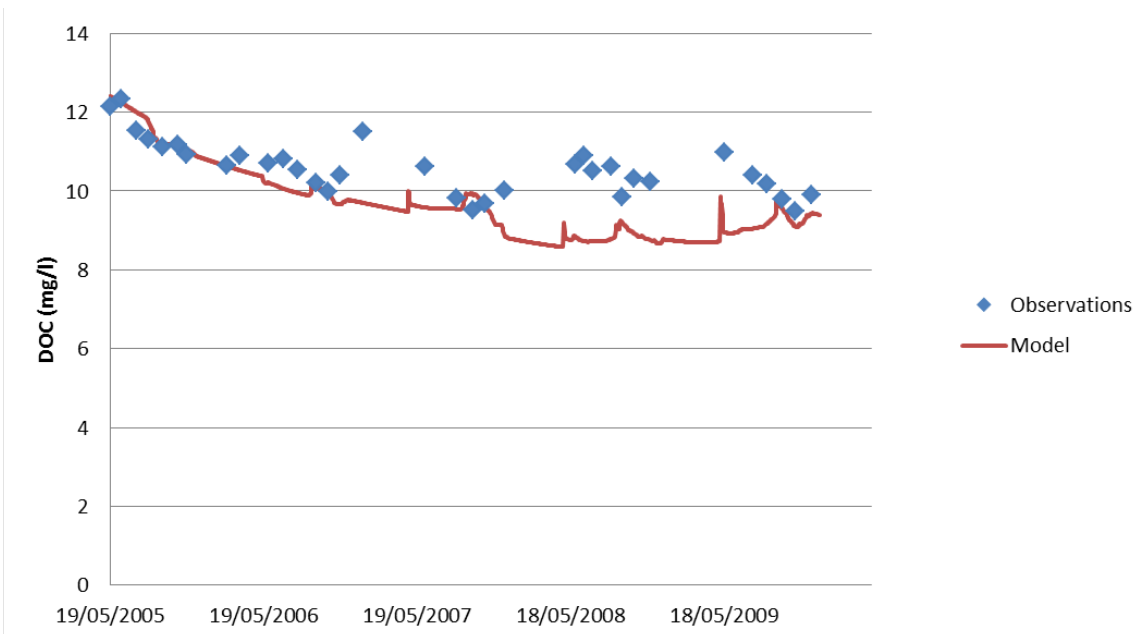


Figure 6.32 Dissolved organic carbon in surface water of Lake Pääjärvi during the validation period 19.5.2005-29.12.2009. Observations are from depth layer 0-15m and model result is from depth layer 7-8m.

6.3.5 Results of the physical models

Changes in hydrology. In the Mustajoki catchment the current snow-melting peak was placed by more continuous runoff in winter according to all scenarios (Figure 6.33). Runoff increased also in some autumn months. Duration of both high and low pulses decreased (Figure 6.34), especially according to GFDL scenarios for period 2025-2034.

DOC loads from the catchment and DOC concentrations in the lake Pääjärvi. DOC loads from the catchment were simulated by INCA-C model as transient runs, e.g. continuous runs from 2015 to 2099. There were obvious increasing trend in DOC concentrations at the outlet of the river Mustajoki (Figure 6.35). This increase was driven by the climate rather than by the land use change. In the model there were increasing trend in decay of soil organic carbon. Correspondingly, DOC concentrations in the Lake Pääjärvi were increasing (Figure 6.36).

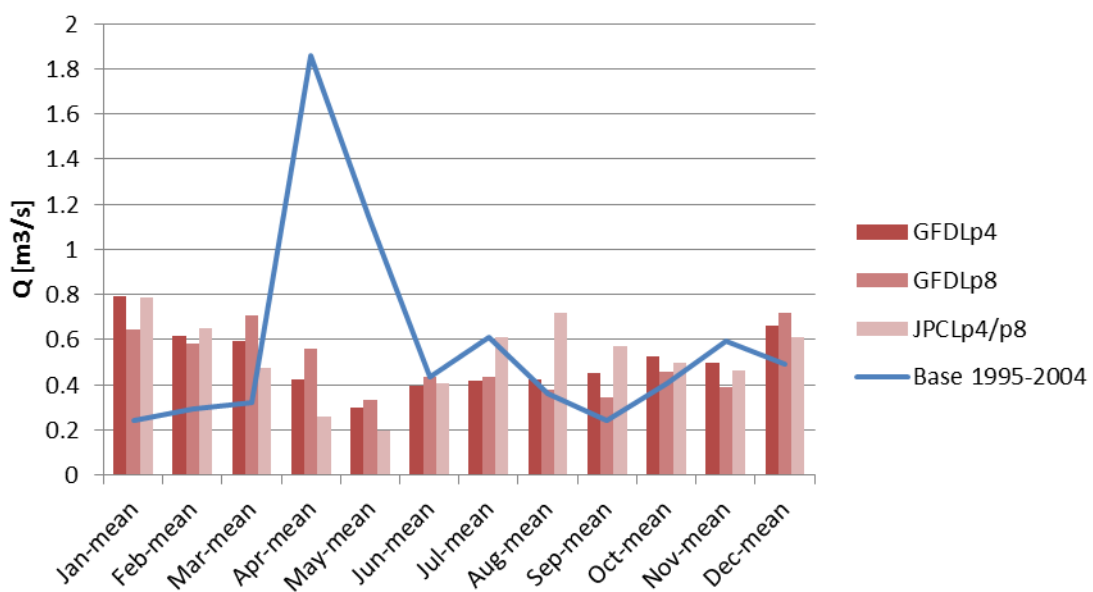


Figure 6.33 Monthly average flows of the river Mustajoki in different scenarios.

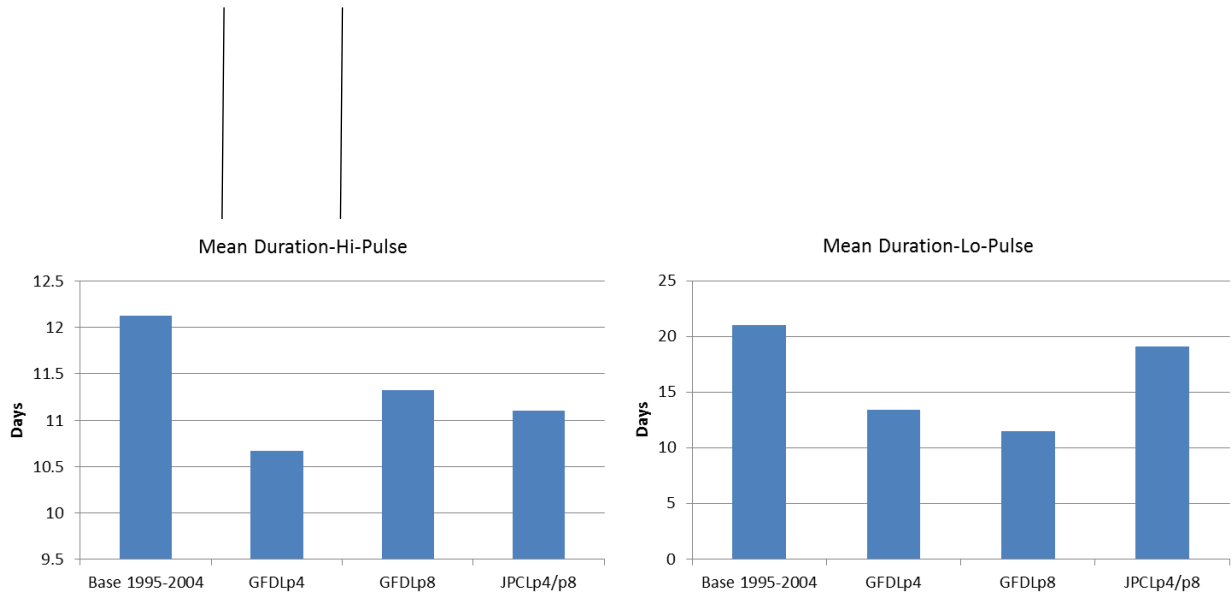


Figure 6.34 Changes in duration of high (over 75th percentile) and low (less 25th percentile) pulses.

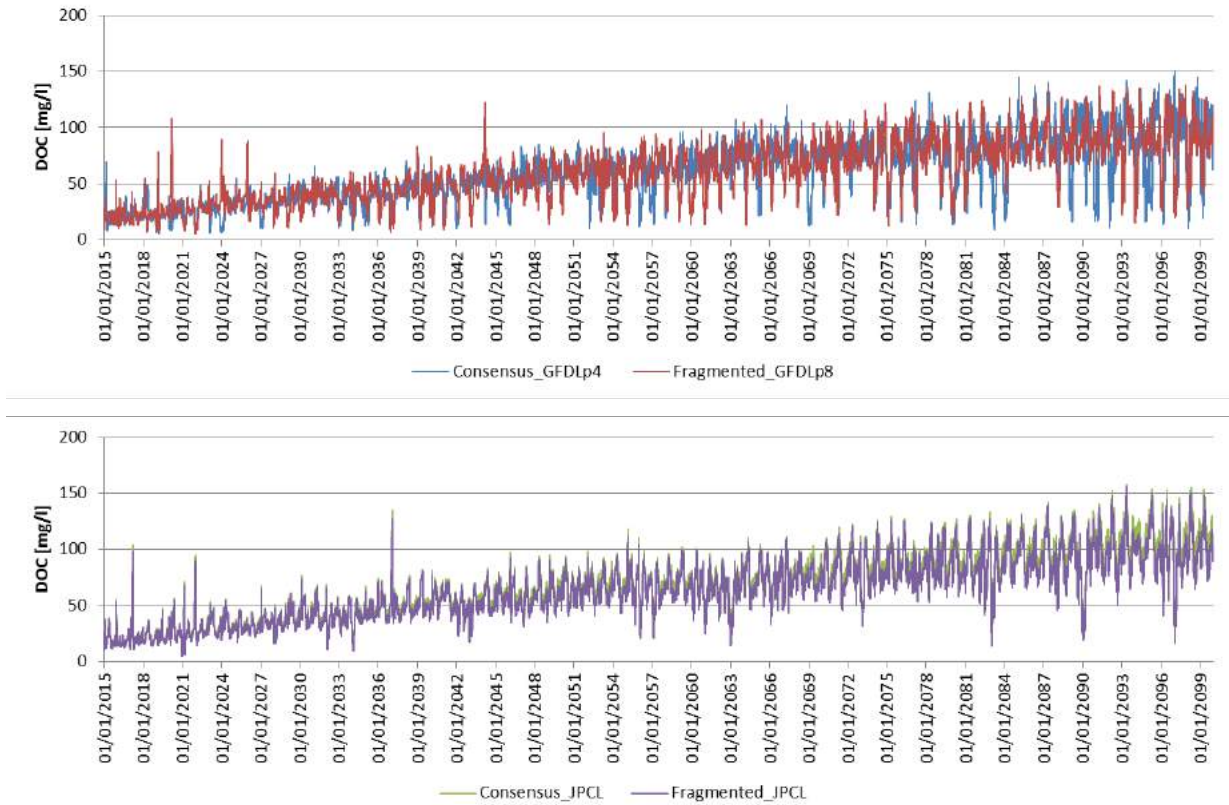


Figure 6.35 Simulated DOC concentrations at the outlet of the river Mustajoki. The periods of interest are marked by black bars.

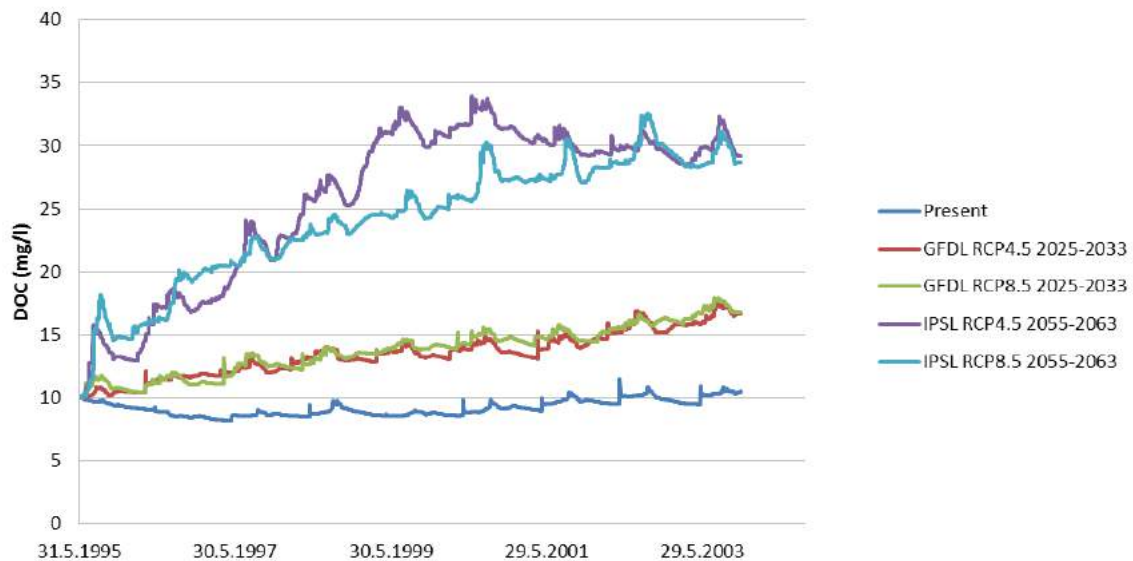


Figure 6.36 Dissolved organic carbon in surface water of Lake Pääjärvi in present situation (31.5.1995-27.11.2003) and in four scenario situations.

6.3.6 Empirical Models

Specific properties of light climate in humic lakes. Light climate in humic lakes differs from clear water lakes significantly. Humic substances reduce light penetration. (Eloranta, 1978) investigated 30 Finnish lakes and found marked difference in depth of euphotic (1% of incident light) productive zone by increase of humic content of water. Euphotic zone describes more production of phytoplankton whereas penetration of red light describes better maximum growing depth of aquatic macrophytes. Based on surveys of (Eloranta and Marja-aho, 1982) lowest limit of macrophytes lies at the level 4,5 % of incident red light.

Water colour and red light extinction relationships were calculated from the original measurements of light penetration presented by Eloranta (1978);

$$E_r = 0.25 A^{0.42}, \quad (\text{with } r = -0.82, n = 30) \quad (1)$$

where: E_r = extinction coefficient of red light, A = water colour (mg Pt l^{-1}).

(Hellsten, 1997) applied 4,5 % of incident red light as an indicator of the lowest limit of productive littoral. The depth of the zone (D_r) reached by 4.5 % of incident red light (627 nm) can be calculated from the Lambert-Beer law;

$$D_r = - \ln (0.045) / E_r. \quad (2)$$

The light zones can be assessed according to the Lambert-Beer law;

$$L_D = L_0 \exp(-E_r D) \quad (3)$$

where: L_D = intensity of red light at a depth of D , L_0 = intensity of red light just below the surface.

(Kortelainen, 1993) described the relationship between DOC and water colour as

$$\text{TOC} = 0.0872 \text{ colour} + 2.79 \quad (4)$$

Calculated and observed maximum growing depth. Large isoetids such as *Isoetes echinospora*, *Isoetes lacustris* and *Lobelia dortmanna* forms often deepest stands of aquatic macrophytes in soft water lakes. These plants are perennial and therefore they reflect relatively well also long term ecological status development of lakes. Large isoetids are key habitats providing shelter for large zoobenthos and acting as breeding ground for fishes. Kanninen et al. (2009) investigated several polyhumic (colour 40 – 100 mgPt⁻¹) small lakes in Central-Finland representing large variety of humic content and nutrient enrichment (Table 6.11). In addition to water quality parameters, deepest growing depth of large isoetids was measured by main belt transect method carefully by using rake or subaquatic drop-down video equipment.

Calculated maximum growing depth based on assumption that 4.5 % of incident red light (D_r) defines border, is plotted against observed growing depth in Figure 6.37. Developed equation describes relatively well potential growing area of aquatic macrophytes showing reduced light climate caused by humic substances.

Average maximum growing depth in reference lakes was 2.28 m whereas it was in impacted lakes only 1.43 m. However, it should be noted that that also humic content of water was slightly higher in impacted lakes (average 72 mgPtl-1) compared to reference one (average 63 mgPtl-1).

Table 6.11. Investigated lakes in Central-Finland (Kanninen et al. 2009).

Lake	Status	Maxgrow (m)	TotP ug/l	Colour Pt/l
Valkeinen	Ref	2,6	8,0	40
Pieni-Myhi	Ref	2,1	14,0	80
Ahveninen	Ref	2,4	19,0	80
Mataroinen	Ref	2,7	7,0	55
Haukijärvi	Ref	2,45	10,0	45
Härkäjärvi	Ref	1,8	15,5	85
Viipperonjärvi	Ref	2,1	12,5	60
Löytönen	Ref	2,2	7,5	50
Harvanen	Ref	2,2	10,0	75
Suurijärvi	Imp	1,1	21,0	40
Pieni-Varpanen	Imp	1,2	29,5	65
Oinasjärvi	Imp	1,3	12,0	95
Syväjärvi	Imp	1,2	25,5	90
Liesjärvi	Imp	1,4	22,0	90
Niskajärvi	Imp	1,5	19,0	100
Vihtanen	Imp	1,5	14,0	80
Korppinen	Imp	2,4	11,5	40
Pieni Säittäjärvi	Imp	1,3	18,0	50

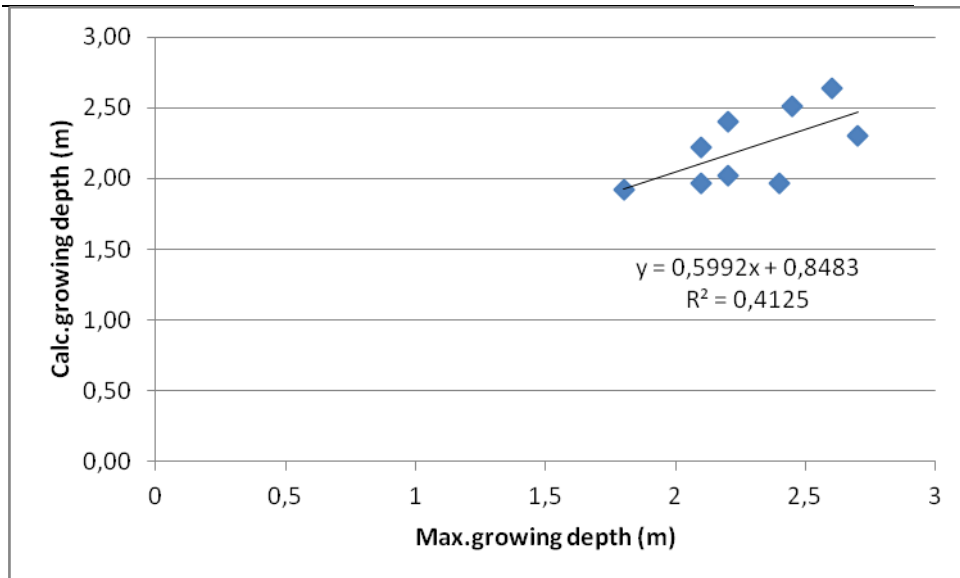


Figure 6.37 Observed and calculated max. growing depth of large isoetids in some humic reference lakes (n = 9).

Effect of brownification on macrophyte depth distribution. Simulated DOC concentrations were transformed to growing depths by equations 1-4, assuming relationship of 0.9 between TOC and DOC concentrations. Growing depths decrease from 2 m to 1.2 m according to different storylines (Figure 6.38). This change corresponds to observed shift from reference lakes to impacted lakes. In worst scenario almost half of large isoetids population is disappearing causing dramatic change in whole ecosystem. (Liu et al., 2016) instead used the ratio of euphotic depth to water depth as indicator for macrophyte growth in Lake Taihu. They found a value 0.8 to be critical threshold for the growth of macrophytes.

Change in land use did not seem to have any effect on growing depth, but it was driven only by the change in climate. The mean annual temperature at the Lahti Laune meteorological station has increased by 1.91 °C since 1961.

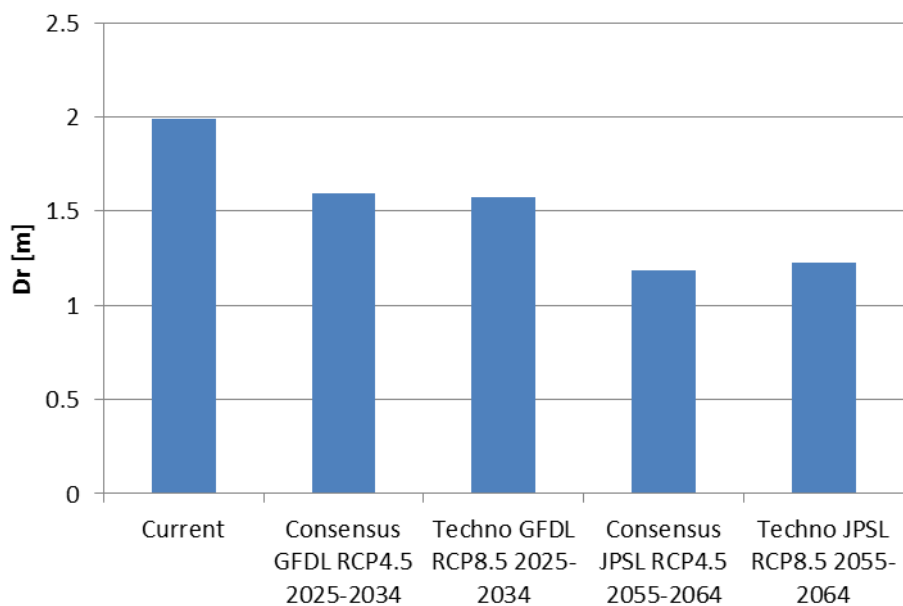


Figure 6.38 Maximum growing depth (m) of large isoetids according to different storylines.

6.3.7 Ecosystem Services

There is already on-going increase in DOC concentrations in the lake Pääjärvi and the river Mustajoki. That change is strongly driven by some other factor than land use change, probably by climate change. In future the DOC concentration of the river water may increase from current 10 mg/l to 15 mg/l (2025-2034) and up to 25 mg/l by 2055-2064. The rate of increased DOC concentration in the river is about 0.8 mg/yr.

6.4 Otra, Norway

6.4.1 Introduction

Basin overview. The Otra River is the largest in southernmost Norway and drains 4000 km² of forests and alpine uplands. The catchment is long and narrow and runs about 240 km north to south to the North Sea at Kristiansand. The upper part is a deep valley surrounded by a high plateau. Beginning in 1905 the Otra River has been extensively developed for production of hydro-electricity. In the lower part of the river a number of dams have laid short stretches of the river dry and exploit vertical drops in the river for electricity production. In the upper Otra modifications began in 1964 and comprise a series of dams and tunnels that collect water from tributary streams in the headwaters and along the western side, store the water in several large and deep basins, lead the water 10s of km south, and use the 600-700 m vertical drop to run several power stations of which Brokke is the largest (Figure 5.39).

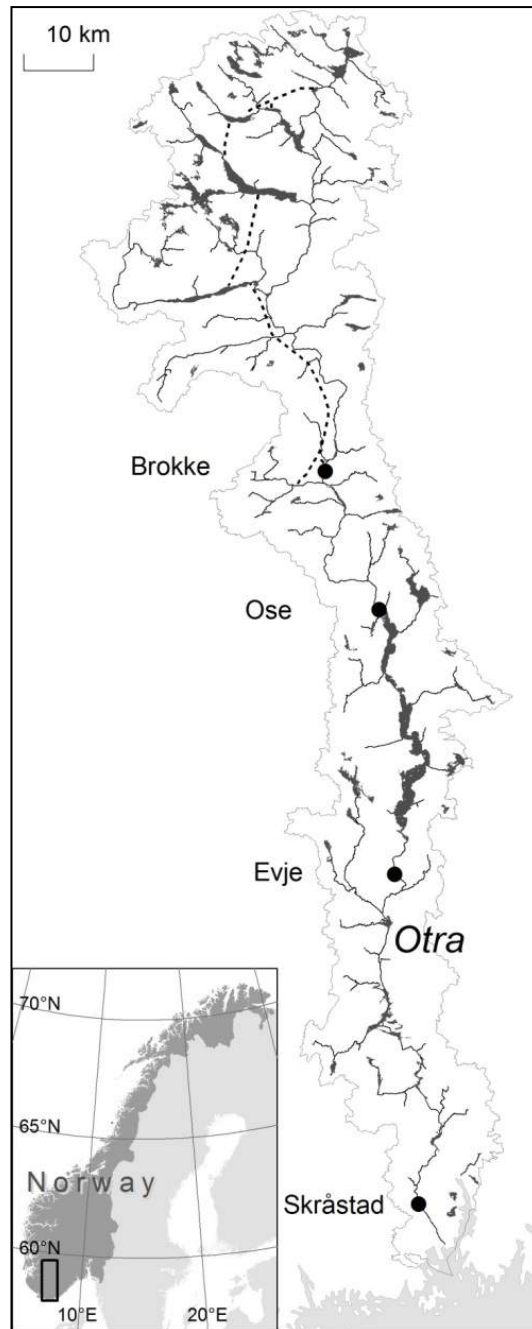


Figure 6.39 Map of the Otra River, southernmost Norway, showing the locations of the Brokke hydropower station, and the three points on the river (Ose, Evje, and Skråstad) for which the modelling simulations were made. Ose and Evje are habitat for the landlocked salmon (bleke) while Skråstad is located on the reach for anadromous salmon near the river mouth. The dashed line in the upper part of the catchment depicts the dams and tunnel used to conduct water from the high-lying areas to the power plant at Brokke. Insert: map of Norway showing location of the Otra River.

Current River basin management plan. Otra is currently at the start of the second plan period (2016-2021). The current status (2013) is that of 249 streams only 32% had good or very good ecological status, and of 77 lakes only 34% had good or very good ecological status (Agder, 2014).

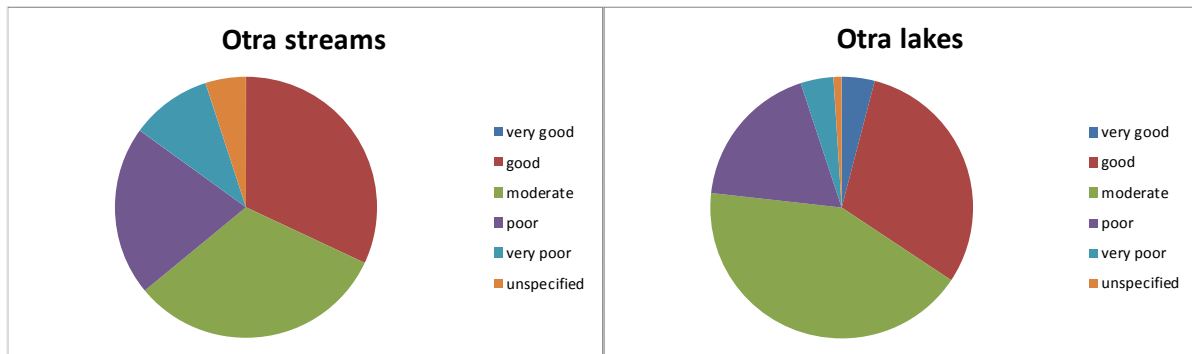


Figure 6.40 Ecological status as of 2013 of streams and lakes in the Otra River basin (Agder, 2014).

The major challenges are related to acid deposition, hydropower development and to a lesser extent growth of nuisance water plants (*Juncus bulbosa*) and invasion of exotic species (the European minnow, *Phoxinus phoxinus*). It is foreseen that fully 95 water bodies will not meet the WFD “good ecological status” by 2021, these include 52 water bodies classified as strongly modified (all due to hydropower operations). Current remedial measures are: i) liming of acidified water bodies; ii) continued international negotiations to reduce emission of air pollutants – precursors to acid deposition; iii) modification of operating procedures in conjunction with upcoming renewal of operating permits to the hydropower companies; iv) mapping and research on possible remedial measures to reduce the impact of excessive growth of macrophytes; v) more research on possible measures against invasive species. The key stakeholders in the Otra river basin are the electricity companies, the sport and commercial fishermen, the general public (tourism and recreational activities), forest owners and farmers, drinking water suppliers, and waste water plant owners.

Main stressors:

- **acid deposition**
- **hydropower development**
- **climate change**

Questions to be addressed by the modelling. The main research question here is how will future acid deposition and climate change affect the current water chemistry and fish populations in the Otra River.

Variables to be modelled in the scenario analysis

- **air temperature**
- **precipitation**
- **discharge**
- **water chemistry (major ions, pH)**
- **fish catch**

Context for the modelling

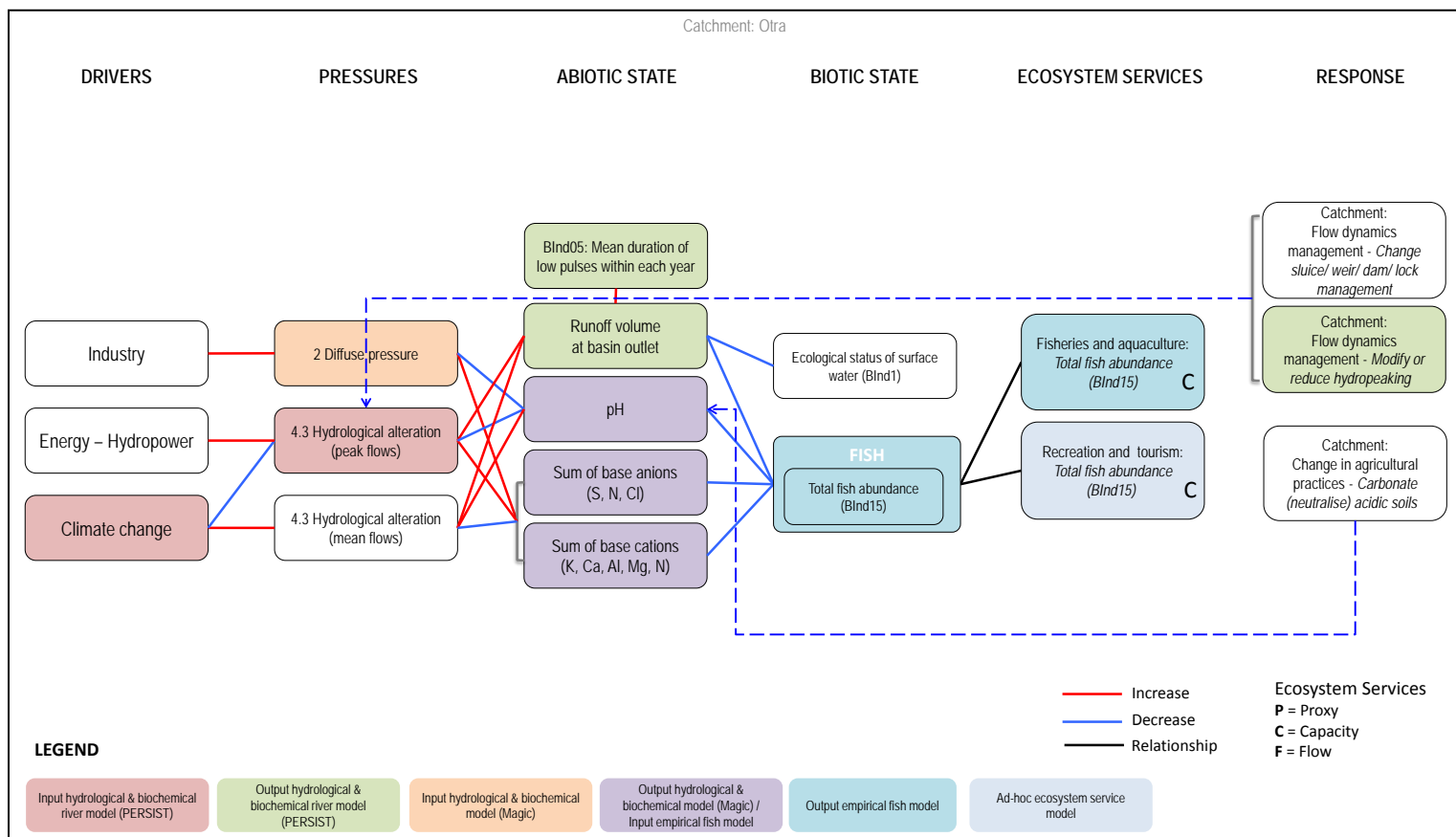


Figure 6.41 Conceptual model for the modelling at Otra following the DPSIR approach.

6.4.2 Data and methods

Data overview

Hydrology: Daily mean discharge at 5 sites 50+ years. Not all data was directly observed but was instead modelled using a simple rainfall-runoff model, calibrated in a nearby basin and scaled to a representative area. Furthermore, regulated discharge data (outflow from power stations) were not available and natural conditions were assumed when computing discharge at such locations.

Water chemistry: Monthly, semi-annual or once annual samples at 5 stations 30+ years.

Fish catch: Number of individual annual test fishing land-locked salmon, annual total catch in kg anadromous salmon.

Meteorological data: Precipitation and temperature data (daily mean values) gridded estimates were provided by the Norwegian Water Resources and Energy Directorate (NVE.no). These are based on measured values obtained from stations in or near the Otra river catchment operated by the Norwegian Meteorological Institute (met.no).

Discharge data: Discharge data (daily values) came from measurements at stations operated by NVE, four on the Otra River, one on a small tributary near the headwaters (Lislefjødd), and one (Austenå) on the adjacent Tovdal River. Austenå and Lislefjødd have no hydropower installations in the catchment; all the other stations are influenced by hydropower operations. For Brokke the discharge was calculated as the difference between Hovet minus Valle. The four tributary sections used scaled discharge from the NVE station Austenå, located in the Tovdal River basin adjacent to the east of the Otra River. Austenå has no hydropower installations. Byglandsfjord was modelled as a fully mixed basin with water retention time 0.6 years.

Chemistry data: Come from monitoring programmes and research projects conducted in the Otra River since the 1960s. Only samples with complete major ion analyses were used as these parameters are required for calibration of the MAGIC model. Parameters used were pH, Ca, Mg, Na, K, SO₄, Cl, NO₃, total organic carbon (TOC), and labile inorganic Al (LAI). Most of these data are held by the Norwegian Institute for Water Research (NIVA).

Soil data: The MAGIC model requires specification of a number of soil chemical and physical parameters. There are no soil data available from the Otra River catchment itself. We took data from two well-studied small catchments in the area, Storgama and Birkenes. Data for these two sites are given by (Larssen et al., 2002)

Atmospheric deposition data: Deposition of major chemical components is measured by the Norwegian Institute for Air Research (NILU.no) in daily or weekly samples taken at two stations within or near the Otra River catchment (Aas, 2013). The station Vatnedalen (N-273) for was used for upper Otra (Flåni, Brokke, Mykle, and Grimsdal) and the station Birkenes (N-01) for lower Otra (Drivenes). Data were aggregated to month. The measured data were scaled to each sub-catchment to account for the fact that the

precipitation measured at one point may not be representative for the entire sub-catchment. This is due to such factors as orographic effects and dry deposition.

Deposition sequences: Long-term historical trends in deposition of non-marine S, NO_x and NH_y for the period up to when the NILU measurements start in 1974 are necessary to calibrate the MAGIC model. Such estimates have been made for all of Europe and specified for each 50 x 50 km grid square. This is part of the work conducted by the Coordinating Center for Effects (CCE), part of the United Nations Economic Council for Europe's (UN-ECE) Convention on Long Range Transboundary Air Pollution (LRTAP) (UNECE, 2014). Data used here were supplied by the CCE in conjunction with the "ex-post" scenario analyses conducted in 2012-14 (Wright, 2011).

Fish data: Water quality requirements for Atlantic salmon (*Salmo salar* L.) have been studied in detail with respect to acidification, and in particular at the Otra River (Kroglund et al., 2008a; Kroglund et al., 2008b). The toxicity of acid water is primarily caused by elevated concentrations of labile inorganic aluminium (LAI). Aluminium is mobilised from soils and surface waters in low pH conditions. In the absence of data for LAI, pH (and ANC) is a good surrogate. Kroglund et al. (2008b) suggest a pH threshold of 5.6 below which there is potential damage to juvenile salmon (parr), and pH 5.95 below which there is potential damage to salmon smolt. These limits are for 10-day exposure.

Data treatments prior to modelling. For this modelling study we divided the river basin into five sub-catchments (Figure 6.44), and calibrated the models individually for each sub-catchment using observed data from the river (Flåni) or from representative monitored lakes in the sub basin (Myklevatn, Grimsdalsvatn, Drivenesvatn). We then combined the simulated discharge and water chemistry from these five sub-catchments to obtain estimates of discharge and water chemistry in the Otra River at three key points: (1) inflow at Ose to Lake Byglandsfjord, (2) outflow of Lake Byglandsfjord at Evje, and (3) mouth of the river at Skråstad. The inflow and outflow of Lake Byglandsfjord are habitats for bleke, while the river at Skråstad is the habitat for the anadromous salmon.

Bias corrections had to be made to the climate data. For the period 2006-2014 the discharge outputs (PERSiST results) from the climate scenarios gave much lower discharge values than the observed (the extrapolated and interpolated discharge values based on Austenå and Lislefjødd) (Figure 6.42). This difference was largest for the autumn months. The climate scenario outputs were thus scaled to be consistent with the observed. We used a linear scaling factor under the assumption that the cumulative difference in discharge between scenarios and hindcasts (observed discharge) was zero for the period in which there was concurrent data (2006-2013). A separate linear scaling factor was calculated for each sub-catchment and for each climate model (Figure 6.43).

This bias correction method might seem simplistic, the general assumption being that the total quantity of water (for the period with observed data) is the same for the hindcasts and the scenarios. A common procedure when performing bias correction for discharge is to correct the precipitation output from Regional Climate Models (RCM) and feed these corrections to a hydrological model. It is generally accepted that precipitation generated by RCM might significantly differ from observation and that the hydrological models introduce systematic biases themselves (van Pelt et al., 2009). There exists a wealth of methods for correcting RCM precipitation (Teng et al., 2015), aiming at preserving one or other statistic in the precipitation field. Evaluating the most adequate bias correction method for this application was beyond the scope of this project, especially considering the uncertainty in the modelling of discharge. Instead, direct correction of the predicted discharge was preferred.

Finally, in order to have a baseline discharge against which to compare the different scenarios, seasonal ARMA models of varying degrees were tested and calibrated using the observed discharges at all stations. The best performing model according to the Akaike information criterion was then selected to model future discharge, after removing the trend from the model.

Model chain. Outputs from two global climate models were used to generate temperature and precipitation data for the period 2006-2099. The first of these was developed by the Geophysical Fluid Dynamics Laboratory (GFDL) run by the National Oceanic and

Atmospheric Administration at Princeton, New Jersey, USA. Here the earth system model 2M (ESM2M) was used. The second was developed by the Institute Pierre Simon Laplace (IPSL) climate modelling centre, a consortium of several organisations in France. Here the climate model 5 (CM5) was used.

Rain fall-runoff model PERSIST. We used the PERSIST (the Precipitation, Evapotranspiration and Runoff Simulator for Solute Transport) (Futter et al., 2014d) model to simulate daily discharge amounts at the five sub-catchments in the Otra River basin. PERSIST takes daily air temperature and precipitation amounts and generates daily discharge at the catchment scale. It includes a snowmelt routine.

PERSIST requires specification of the land cover in each catchment to be modelled. Land cover data were downloaded from www.skogoglandskap.no at the 50x50 km grid scale and clipped the area distribution files according to catchment area to estimate the distribution in each catchment (Table 6.12).

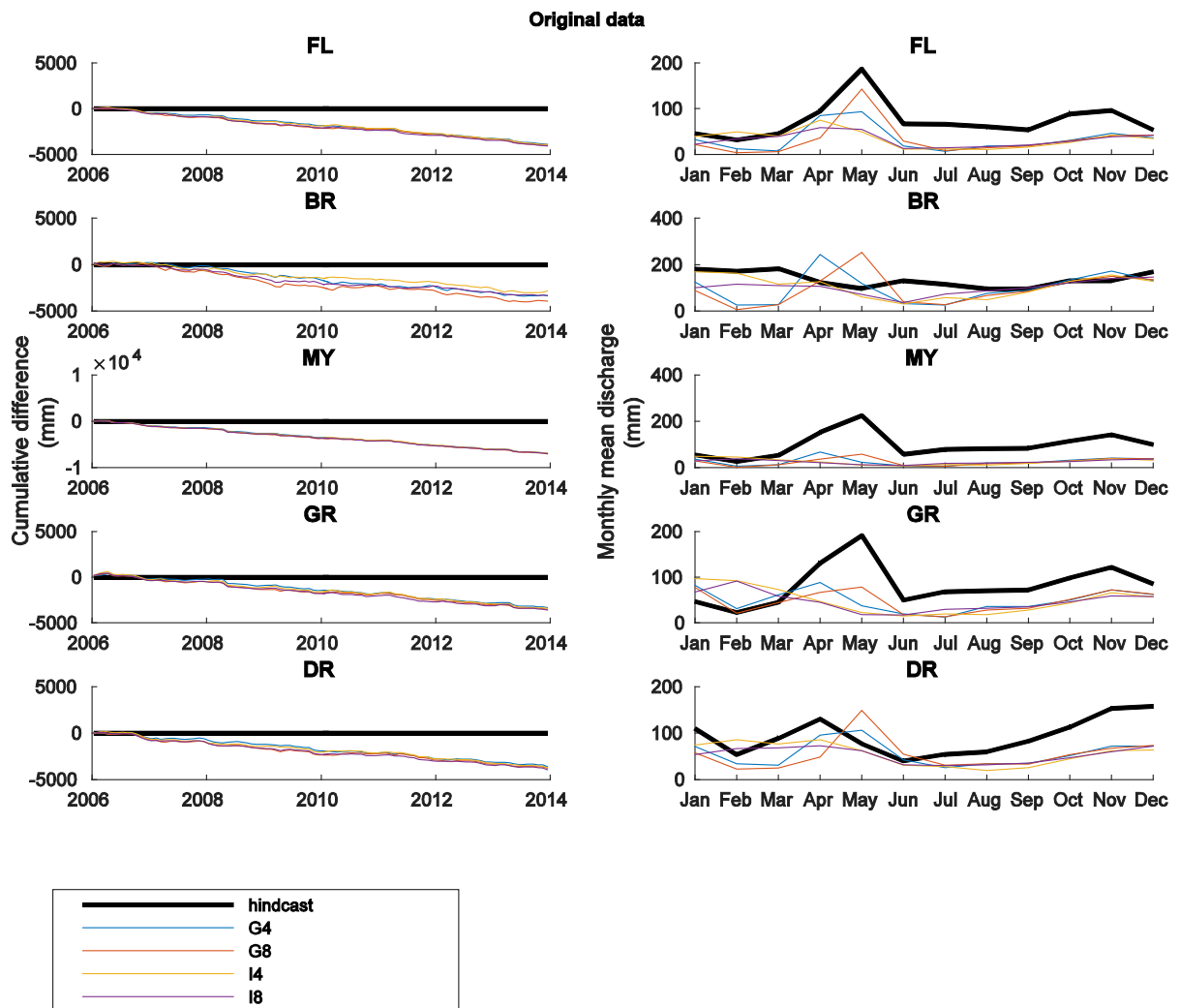


Figure 6.42 Difference between the observed discharge and the discharge scenarios.

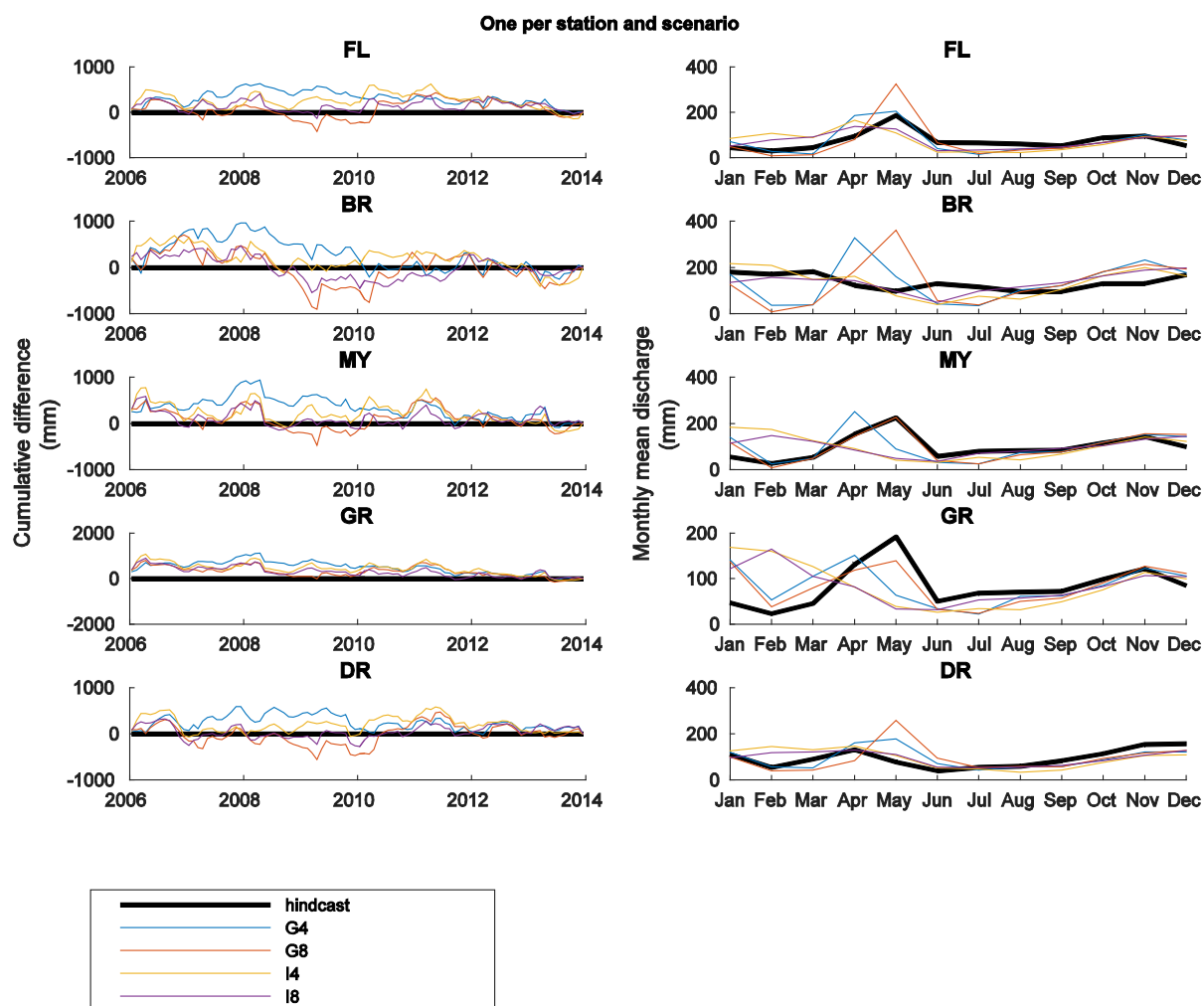


Figure 6.43 Bias correction of the discharge scenarios.

Table 6.12. Distribution of land cover types in each of the sub-catchments in the Otra River basin.

	Area [km ²]	Urban [%]	Cropland [%]	Forest [%]	Mountain [%]	Moor [%]	Lake [%]	Specific discharge [mm/year]
Brokke	1606	0	0	25	60	5	9	1488
Flåni	235	0	4	67	17	6	4	856
Mykle	326	0	2	66	20	3	8	674
Grimsdal	519	0	1	64	17	4	13	815
Drivenes	876	1	3	78	5	8	6	1128

PERSIST was then calibrated to the daily observed (and interpolated) discharge data for the period 1965-2014 at each sub-basin using the Monte-Carlo tool described by Futter et al. (2014d).

Biogeochemistry model MAGIC. The MAGIC model was developed to predict long-term effects of acid deposition on soil and surface water chemistry (Cosby et al., 1985; Cosby et al., 2001). MAGIC calculates annual or monthly concentrations of ions in soil solution and surface water using mathematical solutions to simultaneous equations describing sulphate adsorption, cation exchange, dissolution–precipitation speciation of aluminium, and dissolution–speciation of inorganic and organic carbon. The model accounts for the mass balance of major ions by simulating ionic fluxes from atmospheric inputs, chemical weathering, net uptake in biomass, and loss to runoff.

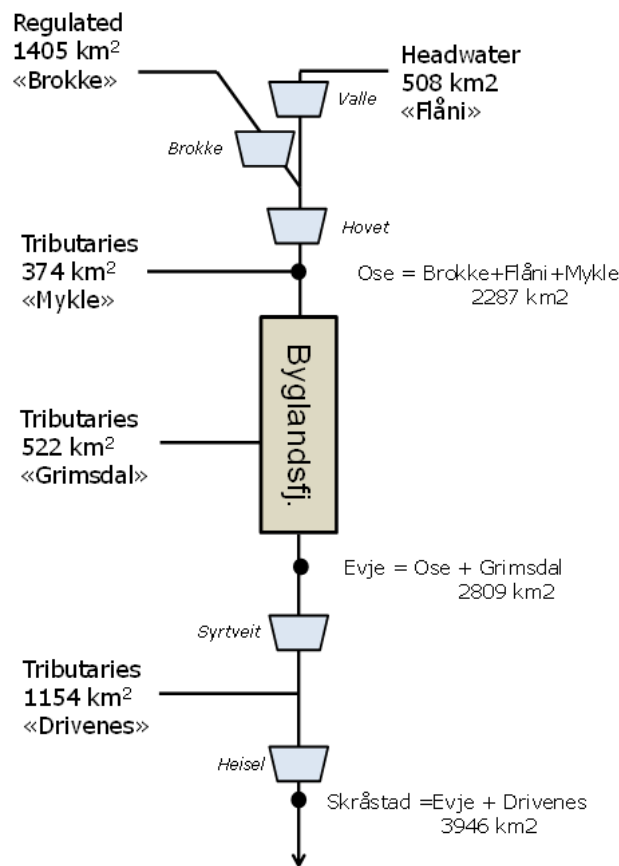


Figure 6.44 Modelling scheme for the Otra River with the five sub-catchments (boxes) and Lake Byglandsfjord, and the three key points at Ose, Evje and Skråstad. The solid circles denote discharge stations.

MAGIC was calibrated at monthly timesteps to each of the five sub-catchments (Figure 6.44) in steps such that the simulated matched the observed concentrations in streamwater for the calibration year(s). First the strong acid anions (SAA) were calibrated. Both Cl

and SO_4 were assumed to come solely from deposition, and the values set in the input file for deposition thus gave the correct concentrations in streamwater. For NO_3 the percent retention in the soil was adjusted such that the simulated NO_3 concentrations matched the observed. Second the four base cations were calibrated simultaneously in a trial and error procedure. Two sets of parameters were adjusted (weathering rates and the initial amounts on the ion exchange complex) until the simulated concentrations in soil and water matched the observed. With the SAA and SBC calibrated, the resulting ANC values also matched. Third step was calibration of pH, Al^{+3} , and organic anions. We used the observed concentration of total organic carbon (TOC) and assumed charge density of 4.5 $\mu\text{eq}/\text{mg}$ TOC to set the total organic charge in MAGIC. Similarly we used the observed LAI concentrations and pH to set the solubility of inorganic Al in MAGIC.

The MAGIC calibrations produced monthly mean fluxes and concentrations of major ions and pH. These were interpolated linearly to give daily values. The fluxes at Ose were assumed to be the sum of fluxes of Brokke+Flåni+Mykle. The daily fluxes were divided by daily discharge to give daily concentrations. The simulated concentrations at Ose were then compared with the observed for those days with samples.

The inputs to Lake Byglandsfjord were assumed to be the sum of the fluxes of Ose (=Brokke+Flåni+Mykle) + Grimsdal. Byglandsfjord was modelled as a well-mixed “bathtub” with water retention time of 0.6 years. The fluxes at Evje were taken as the concentrations in Byglandsfjord times the discharge at Syrtveit.

The fluxes at Skråstad were assumed to be the sum of the fluxes at Evje + Drivenes.

Because the lakes in each of the sub-basins are not exactly representative of all the water in the tributaries an empirical adjustment was made for Brokke, Grimsdal and Drivenes such that the simulated Ose, Evje and Skråstad agreed with the observed.

The models were linked by taking the outputs from one model and feeding them into the next model in the chain (Figure 6.45). PERSIST and MAGIC were calibrated separately for each of the five sub-catchments.

Performance metrics. For the calibration of discharge the Nash-Sutcliffe (N-S) measure was used. For the calibration of water chemistry parameters the Pearson's coefficient of correlation was used (r^2) in addition to N-S

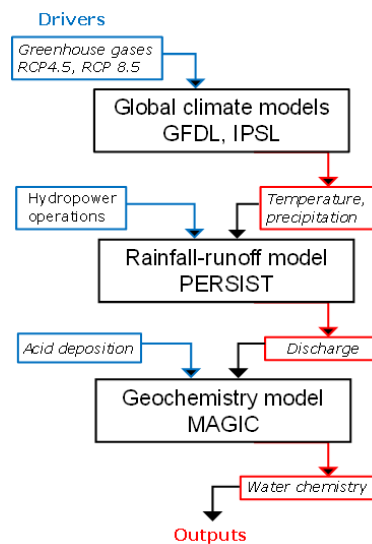


Figure 6.45 Linked model scheme used in this study. Drivers are combined with model outputs time-series to serve as inputs for the next model in the chain.

Empirical modelling approach. The MARS consensus for the empirical modelling was to use at least three different methods to analyse the datasets and to compare the results between these. Based on preliminary results from the empirical analysis of other catchments in the project the method Boosted Regression Trees (BRT) was often able to explain the highest percentage of variation in the analyses. However, BRT requires at least 100 samples (data points) to work properly and both Otra datasets were much smaller than this and it was therefore not possible to use BRT on them. We did try other methods recommended by the MARS consortia - Random Forests (RF), Linear Models (LM) and Generalized Additive Models (GAM). We had two datasets from the Otra system available where it was possible to analyse biological response variables – anadromous salmon catch in Otra river and proportion of land-locked salmon, “Bleke” in catches in lake Byglandsfjorden – as response variables to water chemistry.

For both GM and GAM the number of data points in each dataset was only sufficient to include one explanatory variable in the models. The rule of thumb is that you should not be trying to fit more than, at most, $N/10$ parameters, where N is your number of data points.

Scenarios

Climate scenarios: Both of the global climate models were driven by two separate trajectories of greenhouse gas concentrations, representative concentration pathways RCP4.5 and RCP8.5. These RCPs are moderate and extreme four greenhouse gas concentration trajectories adopted by the IPCC for its fifth Assessment Report (Moss et al., 2008; Meinshausen et al., 2011; Stocker, 2014).

Data for daily surface air temperature and precipitation 2006-2099 for these two models driven by the two RCPs were downloaded from the database of The Inter-Sectoral Impact Model Intercomparison Project (ISI-MIP) at the Potsdam Institute for Climate Change Research (<https://www.pik-potsdam.de/research/climate-impacts-and-vulnerabilities/research/rd2-cross-cutting-activities/isi-mip>) and are specified for grid size 0.5 x 0.5 degrees latitude-longitude (Sanchez, 2015).

Table 6.13. Median values for prognoses of future changes in climate parameters for Norway. Annual values are given for the period 2071-2100 relative to the reference period 1971-2000. RCP: relative concentration pathway; ΔT : change in temperature; ΔP : change in precipitation; ΔQ : change in runoff. Source: Hanssen-Bauer et al. (2015)).

RCP	ΔT °C	ΔP %	ΔQ %
4.5	+2.7 °C	+8%	+3%
8.5	+4.5 °C	+18%	+7%

Acid deposition scenarios: We used three scenarios for future deposition of non-marine S (S^*), oxidised nitrogen species (NO_x) and reduced nitrogen species (NH_y) (Figure 6.46). The NAT scenario comprises national and international agreements for future emissions of acidifying compounds; the MFR scenario reflects maximum feasible reductions in

emissions and the CONST scenario is simply deposition at levels observed in 2010. Data for these scenarios were supplied by the Coordination Centre for Effects (CCE), Bilthoven, the Netherlands, for grid squares in Norway ($0.5^\circ \times 0.5^\circ$ latitude-longitude) as part of work under the UN-ECE Convention on Long-Range Transboundary Air Pollution (UNECE, 2014).

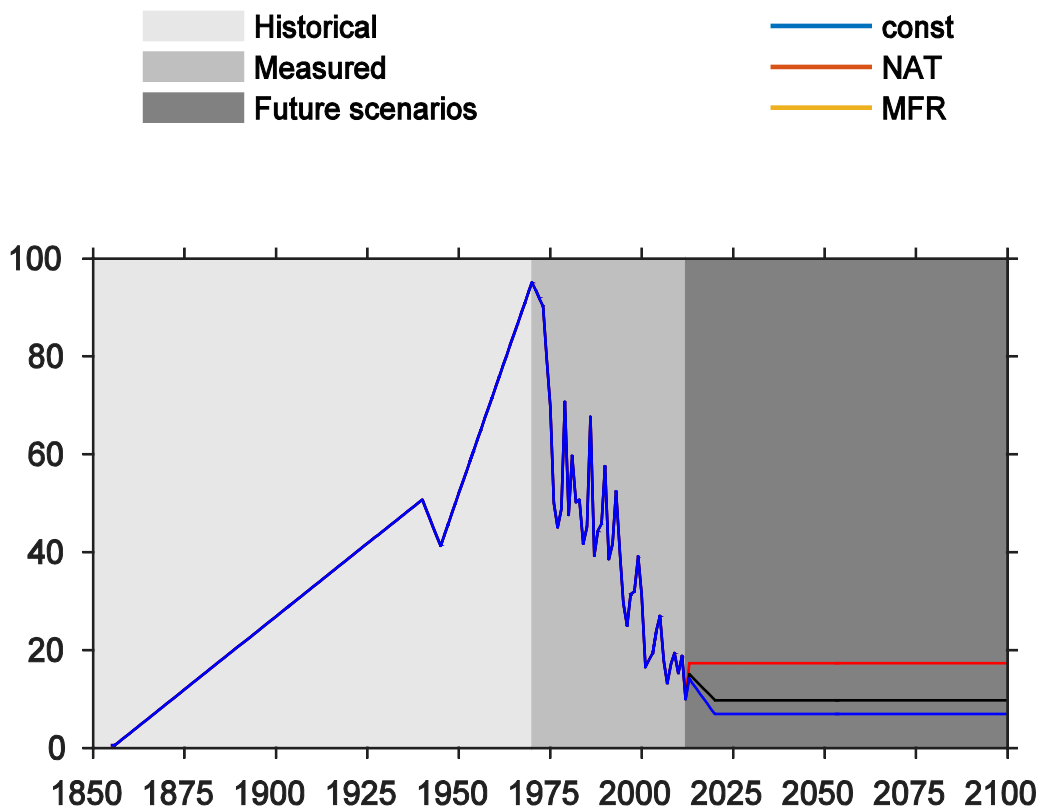


Figure 6.46 Deposition sequences used for non-marine SO₄ (S*). Future scenarios are constant amounts at 2010 levels (CONST), agreed national and international legislation (NAT), and maximum feasible reduction (MFR). Factors are relative to amounts measured in 1995 (average for 1994-1996) at NILU stations, adjusted with SO₄ factors (see text for details).

Table 6.14. Summary of scenarios run for the Otra River for the period 2014-2099. Present-day refers to the period 2008-2014.

Scenario	Climate change	Acid deposition	Hydropower
base	Present-day	NAT=agreed legislation	Present-day
G4	G4	NAT	Present-day
G8	G8	NAT	Present-day
I4	I4	NAT	Present-day
I8	I8	NAT	Present-day
CONST	Present-day	Constant at 2010 levels	Present-day
MFR	Present-day	Maximum feasible reduction	Present-day

6.4.3 Results

PM results

Comparison of predicted hydrology under climate change: Both climate models projected increased runoff in the upper Otra river basin over the next 90 years. The change increases with time. The larger RCP gave a larger increase in runoff (Figure 6.47).

Also the seasonal pattern of runoff was projected to change. Winter runoff was projected to increase while summer runoff was projected to decrease. The two climate models differed in that the GFDL model indicated higher runoff in April and May (spring snowmelt) whereas the IPSL model indicated higher runoff in mid-winter (Figure 6.48).

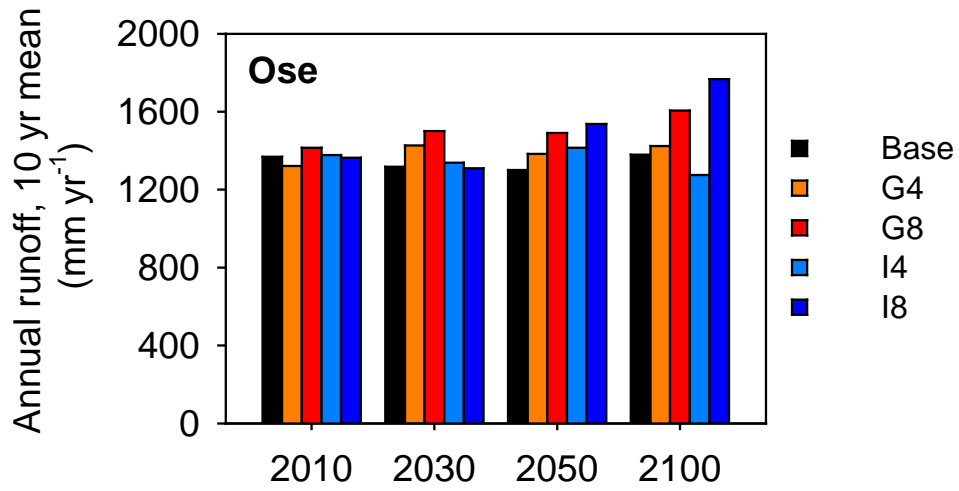


Figure 6.47 Annual mean runoff (mm/yr) at Ose for four 10-year periods under five future climate scenarios. Periods are 2010 (2006-2015), 2030 (2025-2034), 2060 (2055-2064), and 2100 (2090-2099). Scenarios are base (no change in climate), G4 (global climate model GFDL with representative concentration pathway RCP4.5), G8 (GFDL with RCP8.5), I4 (global climate model IPSL with RCP4.5), and I8 (IPSL with RCP8.5).

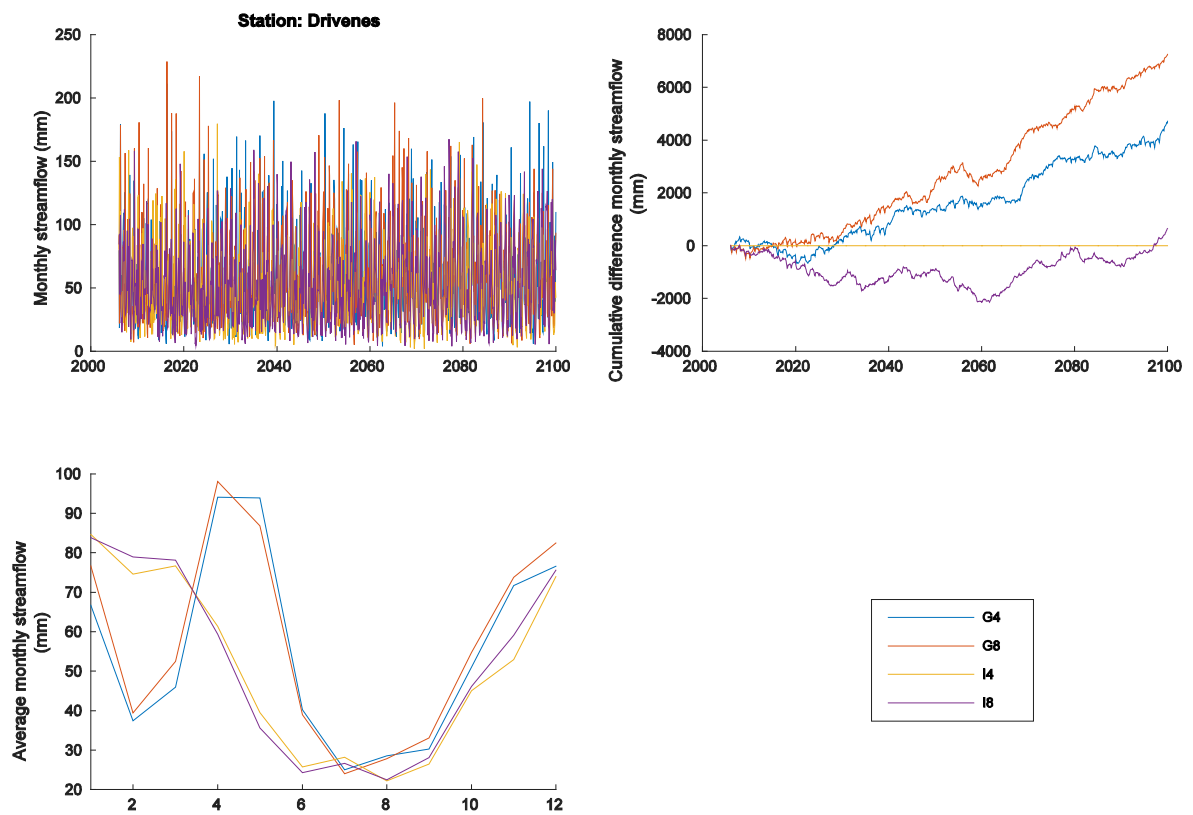


Figure 6.48 Comparison of projected discharge for the different climate scenarios at Drivenes.

Comparison of projected water chemistry under scenarios of acid deposition and climate change: Projections of water chemistry at Ose (inflow to Lake Byglandsfjord, upper Otra River) indicated that future climate change will give a small but measurable improvement over the next decades (Figure 6.49). This was the case for MAGIC driven by the outputs of both the global climate models and for both the RCPs relative to the water chemistry projected with no change in climate (base case). Here all the projections were run with the same acid deposition scenario, the NAT scenario which assumes future emissions of acidifying compounds to decrease according to agreed national and international legislation. The NAT scenario entails a moderate decrease in acid deposition over the period 2010-2020 with no change subsequently.

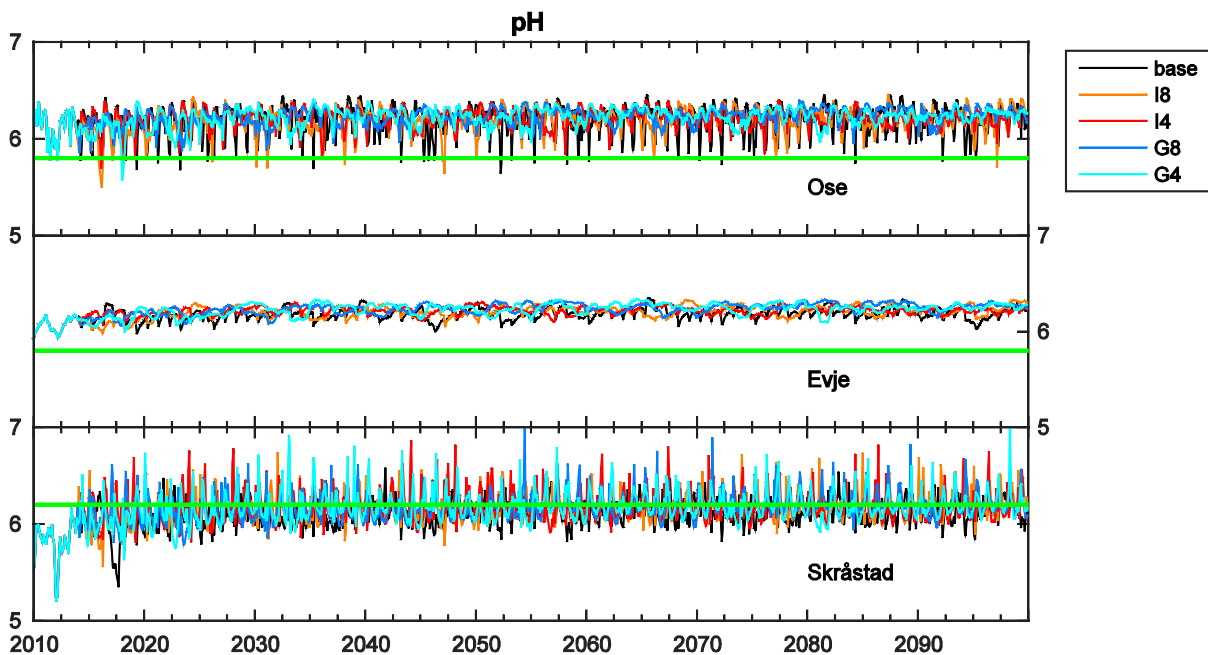


Figure 6.49 Mean monthly pH at Ose, Evje and Skråstad in the Otra River, as simulated by MAGIC under five climate scenarios. Scenarios are base (no change in climate), G4 (global climate model GFDL with representative concentration pathway RCP4.5), G8 (GFDL with RCP8.5), I4 (global climate model IPSL with RCP4.5), and I8 (IPSL with RCP8.5).

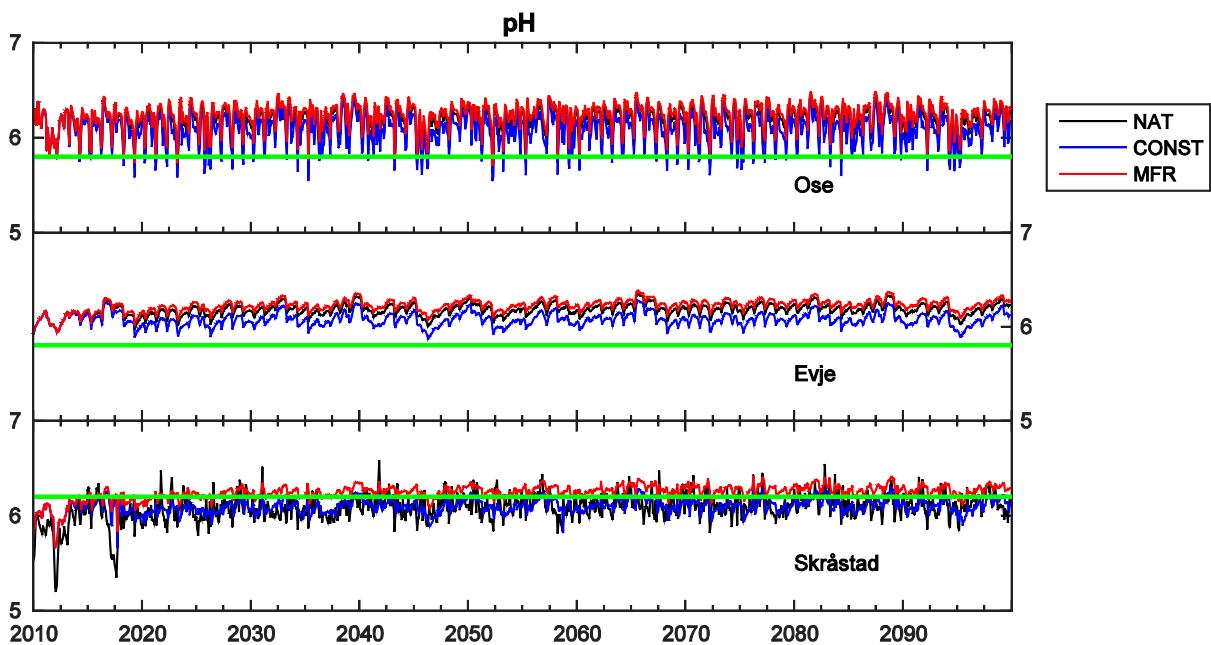


Figure 6.50 Mean monthly pH at Ose, Evje and Skråstad in the Otra River, as simulated by MAGIC under three acid deposition scenarios. Scenarios are NAT (agreed legislation), CONST (constant at 2010 levels), and MFR (maximum feasible reduction). Climate was assumed not to change.

Alternative acid deposition scenarios, on the other hand, had a larger impact on water chemistry at Ose (Figure 6.49). The CONST scenario (constant acid deposition at 2010 levels) gave the highest concentrations of SO_4 , and the lowest ANC and pH, whereas the MFR scenario (maximum feasible reduction) gave the lowest concentrations of SO_4 , ANC and pH. Projections of water chemistry at Evje (outflow of Lake Byglandsfjord, Otra River) were similar to those at Ose, but the monthly variations at Evje were considerably damped due to the integrating effect of the Lake Byglandsfjord (Figure 6.49). Again the scenarios with climate change gave slightly better water chemistry conditions, relative to the base case of no climate change.

The three acid deposition scenarios showed the same general pattern at Evje as at Ose, with the CONST scenario having the highest SO_4 concentrations and lowest ANC and pH, and the MFR scenario yielding the best water quality (Figure 6.50).

The results at Skråstad, near the mouth of the Otra River, showed trends similar to those at both Ose and Evje. Water chemistry at Skråstad had higher SO_4 and lower ANC and

pH compared with that at Evje, due to the input of more acidic water from tributaries in the lower part of the Otra River basin. The climate change scenarios indicated slightly better future water chemistry (Figure 6.49), and the acid deposition scenarios gave poorest water quality under CONST, and best water quality under MFR (Figure 6.50).

Comparison of projected fish populations under scenarios of acid deposition and climate change: Both the landlocked salmon in Lake Byglandsfjord and the anadromous salmon in the lower reaches of the Otra River have been impacted by acid water. The various life stages of salmon have different thresholds for damage. The most sensitive life stages are juvenile salmon (parr) and the smoltification period in the spring (Kroglund et al., 2008b).

A comparative measure of the various scenarios with respect to possible effects on salmon populations is the frequency of months with pH levels in the river water below a given threshold. We used the thresholds indicated by Kroglund et al. (2008b) but increased by 0.2 pH units to account for the difference between episodic pH and monthly mean pH; pH 5.8 for parr (bleke at Ose and Evje) and 6.2 for smolt (anadromous salmon at Skråstad). The frequency of months below these thresholds in the future varied among the various scenarios and also differed between the three stations on the Otra River (Figure 6.51).

At Ose at present about 8% of months have mean pH below the threshold of 5.8. In the future the modelling results indicated that for all the climate scenarios there will be only a few months with mean pH below the threshold. For the acid deposition scenarios as expected the constant 2010 scenario was projected to give 5-8% of months with pH below the threshold. The NAT threshold will improve the situation somewhat, but the modelling results indicated that there will still be months with mean pH below the threshold. The MRF scenario appeared to completely solve the acidification problem.

At Evje at present only about 3% of months have pH below the pH 5.8 threshold. The modelling results indicated that in the future for all the climate and acid deposition scenarios the monthly mean pH will always be above the threshold.

At Skråstad at present nearly 100% of months have pH below the 6.2 threshold for smolt. The modelling results indicated that climate change will improve the situation somewhat, but further reductions beyond the NAT scenario would be needed to reduce the toxicity of water to anadromous salmon.

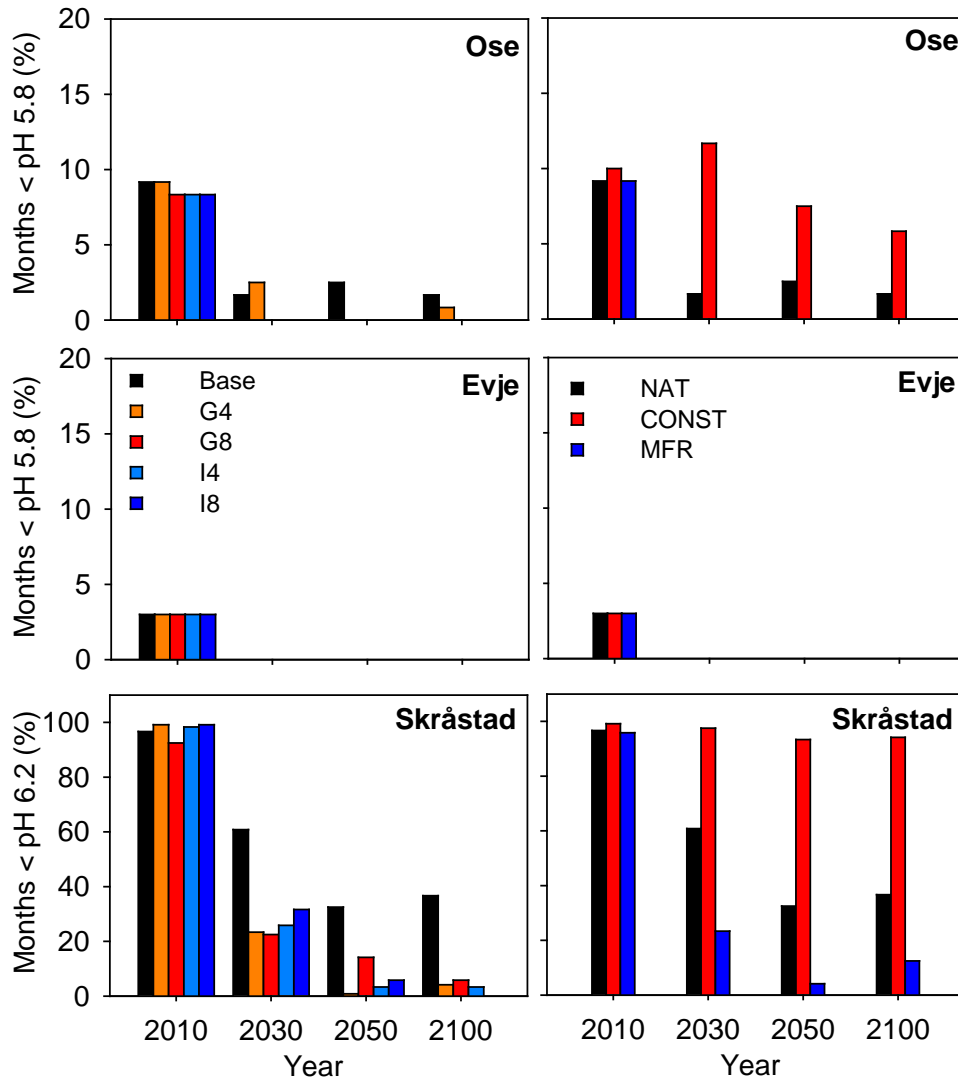


Figure 6.51 Simulated frequency of months with mean pH below the threshold for salmon for 10-year periods 2010 (2006-2015), 2030 (2025-2034), 2050 (2045-2054) and 2100 (2090-2099) at three stations on the Otra River. Left-hand panels: baseline (no climate change) and four climate change scenarios; right-hand panels: three acid deposition scenarios. The “base” scenario assumes no future change in climate, but with the NAT scenario of acid deposition.

6.4.4 EM results

Forests: Random forests (RF) was to be used on the full dataset (all available explanatory variables) in order to identify those that best explained the variability in the response variables. The RF analyses were done in R 3.2.3 (R Core Team, 2015), using the package “randomForestSRC” (Ishwaran and Kogalur, 2016).

The RF analysis on the salmon catch gave nonsense results (e.g. a goodness of fit of -12.6%; Table 6.15), no variables were identified as important by the “Variable importance” or “Minimal depth” functions. This was most likely caused by the number of data points being only nine and too few for this method.

RF on the Bleke dataset worked better and gave a goodness of fit of 55% (Table 6.15). Variable importance identified SO_4^{2-} , pH and Mg^{2+} as the three best explanatory factors (in falling order of importance) in the dataset.

Linear models: SO_4^{2-} ($p=0.0079$) explained 66% of the variability in the salmon catch data (Figure 6.52a), and the residuals look ok.

SO_4^{2-} ($p<0.0001$) explained 55% of the variability in the Bleke proportion data (Figure 6.52b). But there are clear trends in the residuals indicating that a non-linear model is required for this dataset.

Generalized additive models: The GAM analyses were done in R 3.2.3 (R_Core_Team, 2015) using the package “mgcv”. SO_4^{2-} ($p=0.0074$) explained 66% of the variability in the salmon catch data (Figure 6.53a), and the residuals look ok. The degrees of freedom for the model is set to 1 by the GAM function and the GAM model is almost identical to the linear model and it is not clear that it improves on the linear model.

After excluding an outlying data point from the analysis SO_4^{2-} ($p<0.0001$) explained 89% of the variability in the Bleke proportion data (Figure 6.53b), and the residuals look ok and better than in the linear model.

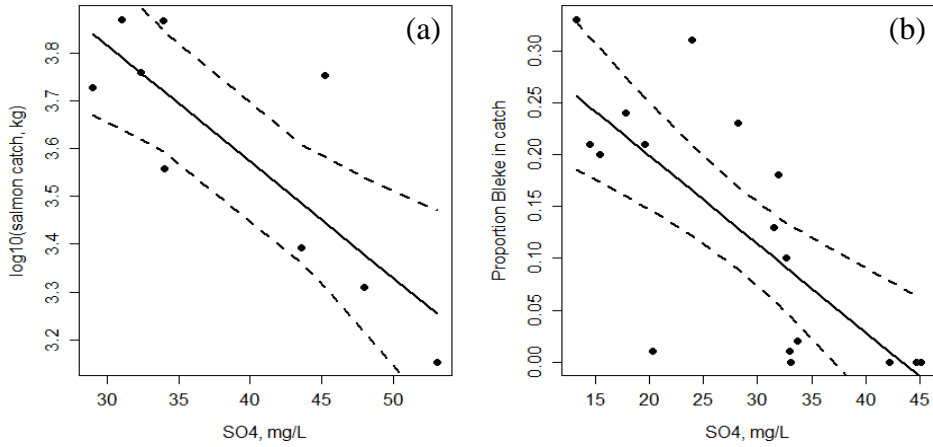


Figure 6.52 Linear models for the salmon dataset (a) and b) Bleke dataset (b). The original data points (black dots), model predictions (solid lines) and the model prediction 95% confidence interval (dashed lines) is shown. See Table 5.4 for R2 and variable significance.

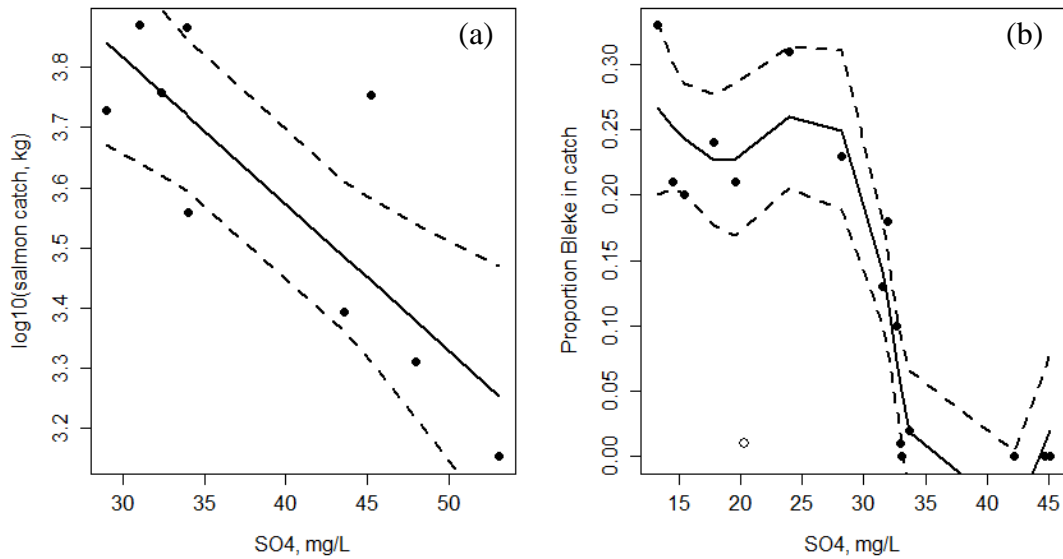


Figure 6.53 Generalized additive models for the salmon dataset (a) and Bleke dataset (b). The original data points (black dots), model predictions (solid lines) and the model prediction 95% confidence interval (dashed lines) is shown. For the Bleke dataset an outlier datapoint was excluded from the analysis but it is shown as an empty point. See Table 5.4 for R2 and variable significance.

Table 6.15. Summary table for the methods used for the empirical modelling of the Otra datasets. RF = Random forests, LM=Linear model, GAM=Generalized additive model.

	SALMON CATCH (kg, n=9, pH n=18)			PROPORTION BLEKE (n=17)		
	RF	LM	GAM	RF	LM	GAM
Goodness of fit	- 12.60 %	R ² =0.66	R ² =0.66	55 %	R ² =0.5 5	R ² =0.89*
Variable interactions	n.a.	n.a.	n.a.	n.a.	n.a.	n.a.
Sign (+/-) of descriptor variables	n.a.	SO ₄ ²⁻ (-), p=0.0079	SO ₄ ²⁻ (-) p=0.0074	SO ₄ ²⁻ (-), pH (+), Mg ²⁺ (-)	SO ₄ ²⁻ (-) p<0.00 01	SO ₄ ²⁻ (-) p<0.0001
Partial dependence plots (BRT, RF)	n.a.	n.a.	n.a.	yes	n.a.	n.a.
3D-plot interactions	n.a.	n too small	n too small	n too small	n too small	n too small
Functions (GLM)	n.a.	log ₁₀ (salmon)=4.55- 0.024*SO ₄ ²⁻	n.a.	n.a.	Bleke= 0.37- 0.0085* SO ₄ ²⁻	n.a.

* One outlier removed (n=16)

Confidence in EM results: The datasets are small; this limits the modelling as only one predictive variable can be included. The salmon dataset is especially small and has a “gap” in SO₄ observations from 35 to 43 mg/L, this “gap” could potentially hide non-linear trends.

6.4.5 Discussion

Notes on river-basin modelling. Prognoses made with global climate models and downscaled to Norway suggest that by the end of the 21st century temperature will rise, precipitation will increase and annual and seasonal patterns of runoff will be affected (Hanssen-Bauer et al., 2015). The change in runoff entails more runoff in the winter and less runoff in the summer. The study of Hanssen-Bauer et al. (2015) is based on an exhaustive analysis of the results from 107 model runs under RCP4.5 and 77 model runs under RCP 8.5, downscaled by both empirical and regional methods.

In our study of the Otra River we used two climate models each driven by two RCPs. The results for annual and seasonal patterns of runoff at Ose for three time intervals in the future showed that there is a model effect and a RCP effect. For the same RCP the GFDL

model gave smaller variations in future annual and seasonal runoff as compared to the IPSL model (Figure 6.45); the scenarios indicated a small increase in annual precipitation. The models differed in the projected future seasonal pattern of precipitation. The GFDL model indicated more runoff in the spring and less in the summer relative to present day, while the IPSL model indicated more runoff especially in the winter and less in the spring. As expected model runs driven by RCP8.5 projected larger changes than those driven by RCP4.5.

The projected changes in climate produced only small changes in river water chemistry. Slight improvements can be ascribed to dilution of strong acid anions by more precipitation. The base case with no climate change assumed that future acid deposition follows the NAT scenario, which entails decreased acid deposition to the year 2020 relative to 2010. Thus all the climate change scenarios in the future showed improvements in water quality during this time interval (Figure 6.46).

Not all possible climate change effects were considered in these model results. Warmer temperatures and longer growing season can be expected to increase vegetation activity in the catchments with greater uptake of base cations and nitrogen. Soils could be affected by increased weathering rates of soil minerals and increased mineralisation of soil organic matter with release of cations, nitrogen and organic carbon to surface waters. The changes forecast in snowmelt accumulation and snowmelt can be expected to alter the seasonal pattern of water chemistry in the river. The MAGIC model can simulate some, but not all of these possible effects, but that requires quantitative information on the changes in rates of various processes due to climate change, and such information is generally lacking (Wright et al., 2006).

Acid deposition to the Otra River basin has decreased substantially from the peak years in the late 1970s. Consequently, sulphate concentrations in the river have decreased, ANC and pH have increased, and concentrations of labile Al have decreased. The river water has become less toxic to salmon and other organisms. Indeed the landlocked population of salmon in Lake Byglandsfjord has had successful natural reproduction since the early 2000s (Barlaup, 2009), and the anadromous salmon has come back to the lowermost stretches of the river (Kroglund et al., 2008a; Kroglund et al., 2001).

Our modelling results suggest that future further reductions in acid deposition will give additional improvements in water quality (Figure 6.47). The problem of acid river water will be helped at Ose, essentially solved at Evje, but remain substantial at Skråstad. Acid deposition will become less important, but still not negligible, and the river will probably always have pH levels near the critical pH thresholds. The differences between Ose and Evje are largely explained by the action of the large and deep Lake Byglandsfjord, which damps the variations in water chemistry of the inflowing river at Ose to the outflow just upstream Evje.

Our study focused on the possible changes in water chemistry and subsequent effects on salmon in the Otra River due to the combined influence of acid deposition, climate change, and hydropower operations. These three environmental stressors can affect fish populations by altering the chemical and/or physical habitat. Climate change is thought to influence several temperature-sensitive aspects of salmon physiology and ecology (Graham & Harrod 2009; Jonsson & Jonsson 2009). In addition to temperature-dependent effects, hydropower development may also increase the deterioration of the habitat through dewatering, introduction of new migratory barriers (Johnsen et al. 2010), and with the release of supersaturated water downstream of turbines (Johnson et al. 2007). The cumulative effects from these three stressors can be seen in the river Otra.

Studies have shown that landlocked salmon, including the Bleke, has low genetic variation compared to anadromous populations of Atlantic salmon (Bourrett et al. 2012). This is the combined result of the founder effect, isolation from other populations and genetic drift. Furthermore, genetic drift has probably increased during the early 1970s when the Bleke population was close to extinction and subsequently rescued by a cultivation program. Consequently, the genetic history of the Bleke has reduced the population's potential to adapt to new conditions imposed by anthropogenic stressors, and it is also unable to migrate out of the current distribution area to colonize less impacted habitats.

In a conservation context, the Bleke is considered biologically important due to its genetic and ecological uniqueness. As a result there has been an ongoing effort to restore the physical habitat impacted by hydropower. However, with the combined effects of multiple stressors, it is important to define long-term strategies for maintaining the

population with a more holistic view. In this perspective, the present results point to a specific need to mitigate the acidification at Ose, where there will be months with mean pH below biological thresholds unless the MRF scenario is reached. Mitigation by continuous liming has the potential to restore the water quality and thereby improving the important spawning and nursing habitats for the Bleke population in the Otra River upstream of Lake Byglandsfjord. Also, the salmon is considered an umbrella species and securing the water chemical conditions for the salmon will also benefit a variety of acid-sensitive species at lower trophic levels (Sandøy & Romundstad 1995), including phytoplankton and zooplankton (Blomqvist et al., 1995; Yan et al. 1996) and zoobenthos (Raddum et al. 1998). The present study is therefore an example of how modelling long-term environmental change is an important means for management decisions that may be pivotal to protect susceptible biota with a high conservation value such as the Bleke population.

Our study focussed on the possible changes in water chemistry and subsequent effects on fish in the Otra River due to the combined influence of climate change, acid deposition and hydropower operations. These three environmental stressors can in addition affect fish populations in ways other than by changing water chemistry. Hydropower operations alter river water temperature and discharge which in turn affects the migration, spawning and hatching phases of the salmon life cycle (Crisp, 1996; Fjeldstad et al., 2014; Harby et al., 2016; Johnson et al., 2007; Jonsson and Ruudhansen, 1985). Water passing through turbines at high pressure can be supersaturated with gases that can damage fish downstream (Johnson et al., 2007). All these factors may affect the bleke population in the upper Otra River.

The anadromous salmon in the lower Otra River are affected by many other factors as well. Fishing pressure both in the marine as well as the freshwater environment, aquaculture, and other factors are all important (Hindar, 2003). Our study indicated, however, that acid deposition remains an important environmental factor for the anadromous salmon in the lower Otra River.

Generic implications for MARS and for Basin management. The Otra River is typical of many rivers in Europe (Schinegger et al., 2012) in that it fails to achieve the good ecological status target of the EU Water Framework Directive (Vest-Adger, 2009), and it

is plagued by the adverse effects of multiple stressors. The programme of measures needed in the river basin management plan (RBMP) for the Otra River necessarily must consider the multiple stressors of acid deposition and hydropower, and now in the second version of the RBMP also climate change. This is difficult, however, as the synergistic and antagonistic effects are complex and challenging to address with modelling tools currently available.

6.4.6 Conclusion

- The empirical modelling indicated that for both the salmon (catch) and bleke (% in catch) datasets SO4²⁻ was the best predictor.
- Both climate models projected increased runoff in the upper Otra river basin over the next 90 years.
- The seasonal pattern of runoff was projected to change.
- Future climate change will probably cause only small but measureable improvement in water chemistry over the next few decades.
- Alternative acid deposition scenarios had a larger impact on water chemistry.
- Future water quality in the Otra River will probably always be near the “edge” for both fish populations.
- Hydropower operations can exacerbate problems with the fish.

6.5 Vansjø, Norway

6.5.1 Introduction

Basin overview. The Vansjø-Hobøl catchment (area = 690 km²), also referred to as the Morsa catchment, is located in south-eastern Norway (59°24'N 10°42'E). The Hobøl River, with a mean discharge of 4.5 m³ s⁻¹, drains a sub-catchment of 301 km² into Lake Vansjø, the catchment's main lake. Lake Vansjø has a surface area of 36 km² and consists of several sub-basins, the two largest being Storefjorden (eastern basin, L1 in Figure 6.54) and Vanemfjorden (western basin, L2 in Figure 6.54). The water-column of both basins remains oxygenated throughout the year. In addition, there are six smaller lakes which together represent less than 15% of the lake surface area. The Storefjorden basin drains to the Vanemfjorden basin through a shallow channel. The outlet of Vanemfjorden discharges into the Oslo Fjord (Figure 6.54).

Land cover of the Vansjø-Hobøl catchment is dominated by forestry (78%), agriculture (15%) and water bodies (7%). The agricultural land-use is dominated by cereal production (89%), with a smaller production of grass (9.8%), vegetables (0.6%) and potatoes (< 0.1%). Together, agricultural practices contribute an estimated 48% of the total P input to the river basin, followed by natural runoff (39%) and WWTPs (5%) and scattered dwellings (8%). It is estimated that these external sources of P contribute to the majority of the P loads to Lake Vansjø (Skarbøvik and Bechmann, 2010).

Current River basin management plan. Because of the problems of eutrophication in the western part of Lake Vansjø, a comprehensive integrated effort has been done to reduce diffuse pollution (especially phosphorus losses) from agricultural areas. The strategy has consisted of information campaigns, farmers' meetings, field trips, environmental planning on individual farms, farms visits, and legal contracts with the farmers combined with economic incentives. During the last decade a great effort has been made to improve water quality in Lake Vansjø by implementing various measures in all sectors contributing to the pollution of the lake. Several small-scale waste water treatment plants have been installed during the last years to reduce pollution from single households.

Agriculture is one of the main contributors of nutrients to the lake and within this sector a comprehensive implementation of measures has been carried out (Skarbøvik and Bechmann, 2010). Several mitigation measures have been applied within the agricultural sector in the entire catchment area. These include reduced tillage and reduced P fertiliser application, vegetated buffer zones and constructed wetlands. Buffer zones have been established amongst others in the eastern part of the basin. The zones are intended to stop the surface runoff from the fields to the rivers, and may also protect against river bank erosion depending on vegetation used. Further, 60 constructed wetlands were built during the last decade, which have been shown to remove between 21 to 44% of stream TP, but only 5% of the orthophosphate (Skarbøvik and Bechmann, 2010). In the Morsa catchment, the most effective change in tillage practice in Norway is to avoid ploughing of sloping fields in the autumn, so that the fields are covered with residue vegetation during the winter, and soil erosion is reduced. The relevant mitigation methods within the area have been described by Bechmann and Deelstra (2006)). Effects of these mitigation measures have been estimated both by modelling and from monitored data through studies.

As of 2015, Lake Vansjø is classified as of moderate ecological status. The river reach Mjær (Figure 6.54) is of poor ecological status due to high cyanobacterial counts (Skarbøvik et al., 2013). The environmental objective at Vansjø-Hobøl is defined as the threshold between moderate and good ecological status, as assessed here using phytoplankton, total phosphorus (TP), total nitrogen (TN) and light penetrating in the lake. According to a recent assessment, only two streams had total phosphorus (TP) concentrations below the environmental objective (Haande et al. 2011), the remaining streams and the main stem of the Hobøl river having TP, nitrogen and coliform above thresholds. In the status classification, phytoplankton along with TP and TN are used.

Using a DPSIR approach, the situation and challenges prevailing before the MARS project at Vansjø can be summarized as follows (Skarbøvik and Bechmann, 2010):

Drivers: In the Vansjø-Hobøl Catchment, the main socio-economic and socio-cultural forces that drive human activities include: (i) food production, including the results of Norwegian policies regarding agriculture and remote settlements, (ii) scattered dwellings (without satisfactory sewage treatment systems), (iii) economic drivers linked to the

requirements for sufficient water flow at the outlet of the lake for purposes such as industry and hydropower, (iv) requirements for drinking water extraction from the eastern basin, (v) requirements for water clean enough for swimming and other recreational use.

Pressures: (i) Water quality pressures: High nutrient and particle loads to the lake from the tributaries deriving mainly from wastewater and agricultural runoff, (ii) Hydrological pressures: Water level fluctuations in Lake Vansjø that are at least partly due to the regulation of the lake. (iii) Flooding during spring/autumn (results in risk of overflowing sewage treatment plants, flooded fields with increased nutrient runoff; damage on infrastructure), (iv) Climate change pressures: May give increased frequency of flooding; increased erosion of river banks; more unstable winters with increased nutrient runoff.

State: High nutrient and particle concentrations in tributaries and lakes.

Impact: Eutrophication of the lake, including: (i) Harmful algal blooms in Lake Vansjø, the most harmful algae is *Microcystis* sp. with the toxin microcystin, (ii) Swimming restrictions in Western Vansjø.

Main stressors. Building on the overview presented above, the following main stressors have been identified:

- **climate change**
- **nutrient loads**
-

Questions to be addressed by the modelling. The main research question here is: How will future climate and land-use change affect water chemistry in the Hobøl river and phytoplankton blooms at Lake Vansjø.

Variable to be modelled in the scenario analysis. INCA-P uses daily air temperature ($^{\circ}\text{C}$) and precipitation (mm) as well as land-use (%) and time-series of fertilizer and point-source effluents to produce daily estimates of discharge (Q , $\text{m}^3 \text{d}^{-1}$), concentration of

suspended solids (SS, mg L^{-1}), soluble reactive P (SRP; $\mu\text{g L}^{-1}$) and total phosphorus (TP; $\mu\text{g L}^{-1}$).

MyLake uses daily meteorological input data such as global radiation (MJ m^{-2}), cloud cover, air temperature ($^{\circ}\text{C}$), relative humidity (%), air pressure (kPa), wind speed (m s^{-1}) and precipitation (mm), as well as inflow volumes and P fluxes to produce daily temperature (T, $^{\circ}\text{C}$) profiles in the water column, concentration profiles and outflow concentrations of SS, dissolved inorganic P ($\text{PO}_4\text{-P}$, $\mu\text{g L}^{-1}$), particulate inorganic P (PIP, $\mu\text{g L}^{-1}$), dissolved organic P (DOP, $\mu\text{g L}^{-1}$), chlorophyll- α (Chl, $\mu\text{g L}^{-1}$) and TP.

Context for the modelling

Catchment: Vansjø-Hobøl

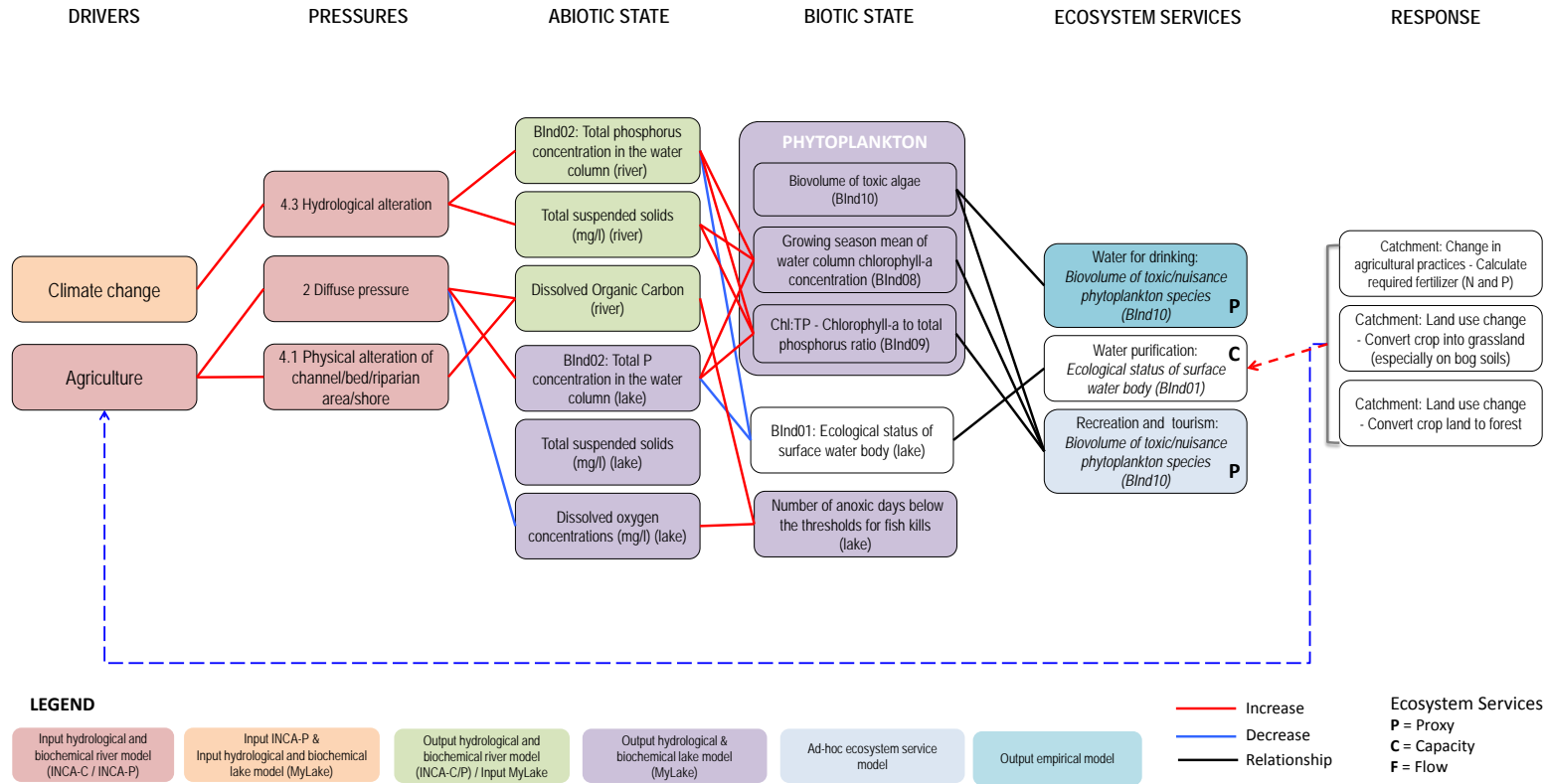


Figure 6.54 Conceptual DPSIR model for the MARS project at Vansjø-Hobøl.

6.5.2 Data and Methods

Data overview

Hydrology: Catchment hydrology was constrained using daily flow over a 10 yr period (01.01.1983 – 31.12.2013) measured at the gauging station at Høgfoss (Station #3.22.0.1000.1; Norwegian Water Resources and Energy Directorate, NVE).

Meteorological data: Observed climate, precipitation, temperature and wind data at Lake Vansjø were obtained from daily weather data at the Norwegian Meteorological Institute stations (1715 Rygge; 1750 Fløter; 378 Igsi) located between the Vanemfjorden and Storefjorden basins (59°38'N, 10°79'E)

Water quality: Water chemistry and temperature data were provided by the Vansjø-Hobøl monitoring program, conducted by Bioforsk and by the Norwegian Institute for Water Research (NIVA). Suspended sediment (SS) in the Hobøl river was sampled weekly from February 1996 to December 2000 and bi-weekly from January 2001 to December 2004. TP was sampled ~weekly from 1990 to 2004 and in 2007. Water-column sampling was conducted weekly from 1990 to 2004, and bi-weekly from 2004 on, at the deepest-site of both basins using a depth-integrating pipe water-column sampler positioned at 2-4 m depth. Values of TP, PP, Chl and PO₄ water-column concentrations for both basins are accessible through NIVA's online database (<http://www.aquamonitor.no>).

Land cover data: The land cover structure for the Vansjø-Hobøl catchment was constructed from GIS digital terrain elevation maps provided by the Norwegian Forest and Landscape Research Institute and complemented by a recent report on the fertilization regimes of agricultural fields (Skarbøvik and Bechmann, 2010). Historical nutrient outputs from waste-water treatment plants (WWTPs) were obtained from the online database KOSTRA, maintained by Statistics Norway (<http://www.ssb.no/offentlig-sektor/kostra>). TP and SS data were analysed downstream of Høgfoss, at Kure (Skarbøvik et al., 2013). P loadings from scattered dwellings are provided by the online GIS information system GISavløp maintained by the Norwegian Institute for Agricultural and Environmental Research (Bioforsk; <http://www.bioforsk.no/webgis>). Land cover of the Vansjø-Hobøl catchment is dominated by forestry (78%), agriculture (15%) and water bodies (7%). The agricultural land-use is dominated by cereal production (89%), with a smaller production of grass (9.8%), vegetables (0.6%) and potatoes (< 0.1%). Together,

agricultural practices contribute an estimated 48% of the total P input to the river basin, followed by natural runoff (39%) and WWTPs (5%) and scattered dwellings (8%). It is estimated that these external sources of P contribute to the majority of the P loads to Lake Vansjø (Skarbøvik and Bechmann, 2010).

Phytoplankton data: Bi-weekly chlorophyll-a (Chl-a) data was downloaded from NIVA's monitoring database (<http://www.aquamonitor.no>) for the years 1990-2012. The data originates from integrated water samples from 0-4 meters. Only data from the months of May to October were included (following the national classification system; section 2.2.4).

Model chain

The model network consists of four separate models: a climate model, a hydrological model, a catchment model for P, and a lake model. The model network is first calibrated to present-day observed data, then run with four storylines to simulate conditions in the future. The model network, described in detail in (Couture et al., 2014) and shown in Figure 6.55, is summarized below.

Outputs from two global climate models were used to generate temperature and precipitation data for the period 2006-2099. The first of these was developed by the Geophysical Fluid Dynamics Laboratory (GFDL) run by the National Oceanic and Atmospheric Administration at Princeton, New Jersey, USA. Here the earth system model 2M (ESM2M) was used. The second was developed by the Institute Pierre Simon Laplace (IPSL) climate modelling centre, a consortium of several organisations in France. Here the climate model 5 (CM5) was used.

Catchment models: The outputs of the RCMs, together with basin characteristics, were used as inputs for the hydrological PERSiST model to produce daily estimates of runoff, hydrologically effective rainfall and soil moisture deficit. Previously, external time series of runoff, hydrologically effective rainfall and soil moisture deficits have been obtained from rainfall-runoff models such as HBV (Sælthun, 1996). Here, we use instead the new model PERSiST v. 1.0.17 (Futter et al., 2013), a daily-time step, semi-distributed rainfall-runoff model designed specifically for use with INCA models. Although PERSiST shares many conceptual characteristics with the HBV model, such as the temperature index

representation of snow dynamics and evapotranspiration, it differs in its description of water storage (Futter et al., 2013). PERSiST uses the same conceptual representation of water storage as the INCA models. Coupling PERSiST with INCA allows a consistent conceptual model of the runoff generation process for both hydrological estimations and water chemistry simulations.

Water chemistry models: Daily hydrological outputs from PERSiST, and weather forcing from the RCMs, were used as inputs for INCA-P. The catchment P-dynamic model INCA-P(Wade et al., 2002b), one of the iterations of the INCA-suite of models, is a process-based, mass balance model that simulates temporal variation in P export from different land-use types within a river system. It has been used extensively in Europe and North America to simulate P dynamics in soils and surface waters and to assess the potential effects of climate and land management on surface water quality (Wade et al., 2002b; Dean et al., 2009; Whitehead et al., 2011; Baulch et al., 2013; Crossman et al., 2013; Farkas et al., 2013; Jin et al., 2013). We use a recent fully-branched version of INCA-P (Branched-INCA-P v. 1.4.11), in which reaches are defined as stretches of river between two arbitrarily defined points, such as a gauging station, a topographic feature or a lake basin (Jackson-Blake et al., 2016b). INCA-P is so-called semi-distributed, that is, soil properties are spatially averaged within user-defined sub-catchments branches. It produces daily estimates of discharge (Q , $\text{m}^3 \text{d}^{-1}$), concentration of suspended solids (SS, mg L^{-1}), soluble reactive P (SRP; $\mu\text{g L}^{-1}$) and total phosphorus (TP; $\mu\text{g L}^{-1}$). The application here (Figure 6.54) simulates the 7 catchment reaches: five reaches of the Hobøl River catchment, each with defined land-use and hydrology (R1-R5); the local Storefjorden sub-catchment (R6); and the Vanemfjorden sub-catchment (R7).

The multi-branch reach structure was established using GIS and land-use maps for the area and the location of monitoring stations and discharge point into lake basins (Whitehead et al., 2011).

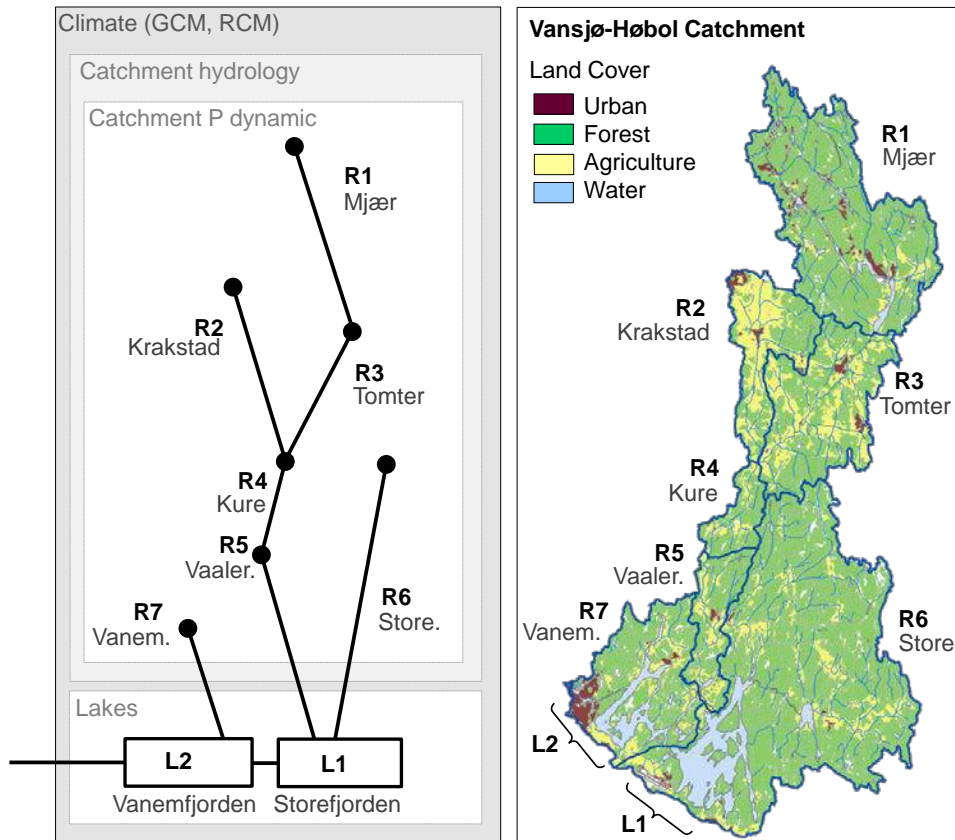


Figure 6.55 Catchment land-use map and model chain schematics. Land-use distribution of the Vansjø-Høbol catchment (right panel) and corresponding schematic representation of the catchment-lake model network (left panel) indicating river reaches (R) modelled with INCA-P and lake basins (L) modelled with MyLake. The hydrological model PERSiST provides input for the catchment model, and the climate models provide forcing for all models.

MyLake model: The lake model used, MyLake v. 1.2.1, is a one-dimensional process-based model designed for the simulation of seasonal ice-formation and snow-cover in lakes, as well as for simulating the daily distribution of heat, light, P species, and phytoplankton abundance in the water column (Saloranta and Andersen, 2007a). MyLake has been successfully applied to several lakes in Norway, Finland and Canada (Saloranta and Andersen, 2007a; Dibike et al., 2012; Gebre et al., 2013) to simulate lake stratification and ice formation (Saloranta and Andersen, 2007a; Dibike et al., 2012; Gebre et al., 2013). It uses daily meteorological input data such as global radiation (MJ m^{-2}), cloud cover, air temperature ($^{\circ}\text{C}$), relative humidity (%), air pressure (kPa), wind speed (m s^{-1}) and precipitation (mm), as well as inflow volumes and P fluxes to produce daily temperature (T , $^{\circ}\text{C}$) profiles in the water column, concentration profiles and outflow concentrations of SS, dissolved inorganic P ($\text{PO}_4\text{-P}$, $\mu\text{g L}^{-1}$), particulate inorganic P (PIP,

$\mu\text{g L}^{-1}$), dissolved organic P (DOP, $\mu\text{g L}^{-1}$), chlorophyll- α (Chl, $\mu\text{g L}^{-1}$) and TP. The biogeochemical processes linking these state variables in the water-column are the mineralisation of DOP and of Chl to PO_4 , and the removal of PO_4 through phytoplankton growth (yielding Chl) or through sorption onto SS (yielding PIP). In the sediments, mineralisation of organic-P and equilibrium partitioning of PIP to the pore water governs the fluxes of PO_4 to the water-column, while resuspension allows Chl and PIP to return to the bottom water. Details on the equations governing these processes are given in Saloranta and Andersen (Saloranta and Andersen, 2007a). In the MyLake model, phytoplankton has a constant C:P ratio of 106:1 and an organic-P:Chl ratio of 1:1, such that particulate organic-P is a proxy for Chl. Similar stoichiometries and constant P:Chl ratios can be found in other models for lake plankton dynamics, such as PROTECH(Reynolds et al., 2001). Finally, total particulate P ($\text{PP} = \text{TP} - \text{PO}_4$; $\mu\text{g L}^{-1}$) was calculated offline and compared to field observations (see section 2.3) to calculate performance metrics.

MyLake was set-up for 2 lake basins (Figure 6.54), Storefjorden (L1) and Vanemfjorden (L2). The outputs of the R1 to R6 simulations from INCA-P are combined and used as inputs for L1. L1 and R7 are then combined and used as inputs for L2. The MyLake setups L1 and L2 are at the end of the model chain, because the lake Vanemfjorden (L2) discharges in the Oslo fjord. However, for the sake of clarity we report only on results at the inlet (i.e. Hobøl river outlet) and outlet of L1.

Performance metrics. For the calibration of PERSiST and INCA-P, the Nash-Sutcliffe (N-S) metric and the correlation coefficient (R^2) were used. For the calibration of MyLake the root-mean square deviation (RMSD) and the correlation coefficient (R^2) were used.

Empirical modelling approach. Data used for empirical modelling are from Lake Vansjø, basin Vanemfjorden, 2000-2012 (Figure 6.54). Cyanobacteria data are only from 2004 onwards (Figure 6.54e). The temporal resolution is bi-weekly during the growing season (May - October). In total four biological response variables were analysed: Chl-a, Chl-a:TP, Cyanobacteria, Microcystin. The three first are MARS benchmark indicators (MARS Deliverable 2.1, part 3). Microcystin is a toxin produced by certain strains of

cyanobacteria, with potentially negative effects on ecosystem services such as drinking and bathing water quality. Predictor variables were TP, Secchi depth, water temperature and Colour (representing TOC). The selection of predictor variables was limited to those that are predicted by MyLake (TP, Secchi depth and water temperature). In addition, colour was included because increased colour (TOC) is an effect of climate change and reduced acid deposition in Nordic countries.

The major part of the empirical modelling for Lake Vansjø was done in the context of Bayesian Network (BN) modelling. The purpose of the BN model (Figure 6.55) was to link future climate and land-use scenarios to biological responses (primarily cyanobacteria) and ecological status via process-based hydrological, catchment and lake models. The development of a BN model for Lake Vansjø started during the former EU project REFRESH (Moe et al. 2014, Chapter 4.3). During MARS, new data analyses were performed with an updated dataset from Lake Vansjø to improve the link from abiotic to biotic variables in the BN. This work been reported in a recent publication of this BN model (Moe et al., 2016). The methods used were GAM and LM/GLM (not reported here) and regression trees. The regression tree analyses were performed with the packages `rpart` and `party` in the software R (R Core Team, 2015). A larger set of abiotic predictor variables have been tested; here we only report on the final predictor-response relationships that were selected for the BN model. The BN model can also be used for predicting abundance of cyanobacteria and ecological status under the MARS future storylines (MARS Deliverable 2.1, part 4), based on the output of the process-based modelling reported here.

In addition, we tried two other methods recommended by the MARS cook book for analysing multiple stressors (Feld et al., 2016): boosted regression trees and random forest. The procedure and the scripts provided by Feld et al. (2016) were followed in these analyses.

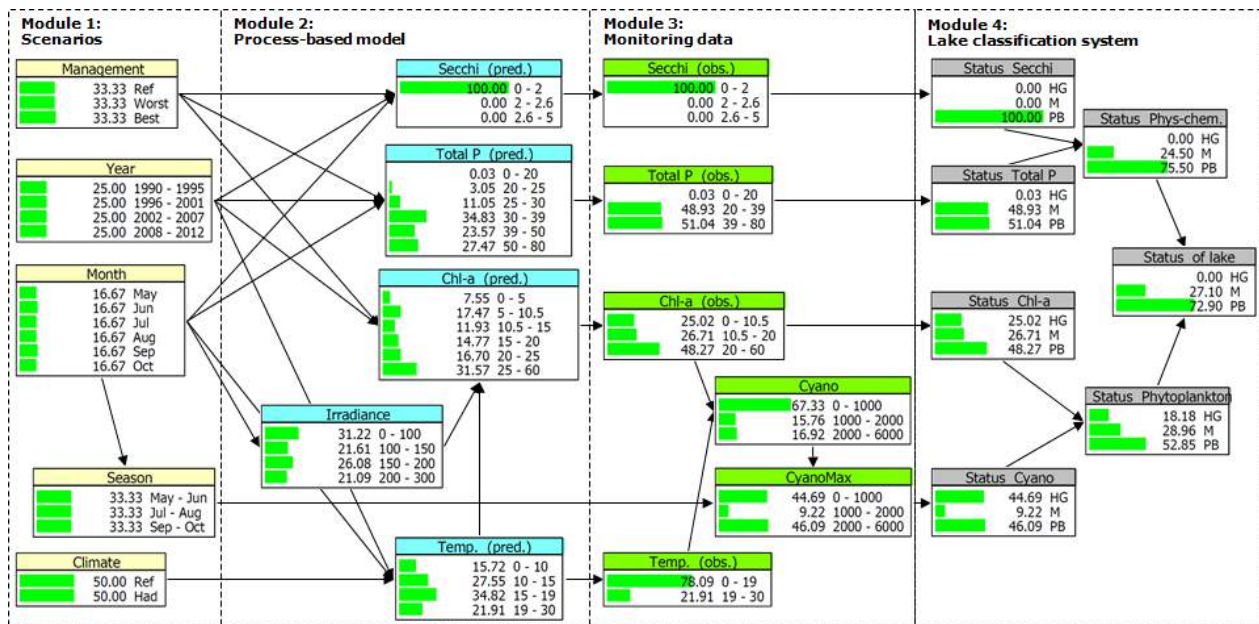


Figure 6.56 Structure of the Bayesian Network (BN) model for ecological status of Lake Vansjø, basin Vanemfjorden. The model consists of four modules: (1) Climate and management scenarios (2), output from the process-based lake model MyLake; (3) monitoring data from Lake Vansjø (1990-2012); (4) the national classification system for ecological status of lakes. The prior probability distribution for each node is displayed both as horizontal bars and by percentages (the first column in each node), across the states (the second column). The set of arrows pointing to one node represents the conditional probability table for this node. Status classes: HG = High-Good (required by the WFD), M = moderate, PB = Poor-Bad. From Moe et al. (2016).

Scenarios

Climate scenarios: Both of the global climate models were driven by two separate trajectories of greenhouse gas concentrations, representative concentration pathways RCP4.5 and RCP8.5. These RCPs are moderate and extreme four greenhouse gas concentration trajectories adopted by the IPCC for its fifth Assessment Report (Moss et al., 2008; Meinshausen et al., 2011; Stocker, 2014).

Data for daily surface air temperature and precipitation 2006-2009 for these two models driven by the two RCPs were downloaded from the database of The Inter-Sectoral Impact Model Intercomparison Project (ISI-MIP) at the Potsdam Institute for Climate Change Research (<https://www.pik-potsdam.de/research/climate-impacts-and-vulnerabilities/research/rd2-cross-cutting-activities/isi-mip>) and are specified for grid size 0.5×0.5 degrees latitude-longitude (Sanchez, 2015).

Table 6.16. Median values for prognoses of future changes in climate parameters for Norway. Annual values are given for the period 2071-2100 relative to the reference period 1971-2000. RCP: relative concentration pathway; ΔT : change in temperature; ΔP : change in precipitation; ΔQ : change in runoff. Source: Hanssen-Bauer et al. (2015)).

RCP	ΔT °C	ΔP %	ΔQ %
4.5	+2.7 °C	+8%	+3%
8.5	+4.5 °C	+18%	+7%

Land-Use scenarios: The modelling scenarios that we employed were constructed along three narratives called “storylines”. According to the MARS definition “a storyline is (...) about a fictive sequence of events that could take place in the near future. (...) storylines describe several aspects of economic, environmental, political and climatic developments and are mainly defined focusing on the different fashions to manage and regulate drivers and pressures impacting aquatic systems”. Three storylines have been outlined in MARS project, each corresponding to a different set of economic, environmental, policy-making, and water management conditions. They are described in full length on MARS website (www.mars-project.eu/index.php/fact-sheets.html). We briefly summarize them here:

- **Storyline 1: Techno world: economy is growing fast. Despite civic society high awareness, regulation of environmental protection by governments is poor. Current environmental policies and guidelines are not renewed after they expire in the next decade and no new environmental policies are set. Water resources management is focusing on getting the water needed for economic development and production of drinking water. This storyline is based on a combination of Shared Socioeconomic Pathway (SSP) 5. (See Kriegler et al. (2012) for a description of SSP’s) and a predicted radiative forcing of 8.5 W m-2 (e.g., van Vuuren et al., 2011)**
- **Storyline 2: Consensus world: the economy is growing at the same pace as now. The current guidelines and environmental policies are continued after 2020 but in a more integrated manner. Sustainable and efficient use of resources is promoted. Water management strategies are set to comply with**

the regulations. This world is based on a combination of SSP2 (Kriegler et al. 2012) and a radiative forcing of 4.5 W m^{-2} .

- **Storyline 3: Fragmented world: economic growth differs markedly between industrialized countries and the developing ones. No attention is paid to the preservation of the ecosystems as the focus is set on the exploitation of natural resources. Current environmental policies and guidelines are broken in 2020-2025. Each country sets its own rules. This world is based on a combination of SSP3 (Kriegler et al. 2012) and a predicted radiative forcing of 8.5 W m^{-2} .**

The downscaling of these the socio-economic factors and anticipated land-use change for the three abovementioned storylines for Norway and the Vansjø-Hobøl river basin was performed together with stakeholders involved in the catchment's land-use and water management during the REFRESH EU-project (Couture et al. 2014). As a result, the following scenarios represent realistic actions that the stakeholders have the capacity to implement.

The main source of phosphorus to the river and lake are agricultural activities and effluent point sources. These two stressors were first modulated individually (Table 6.17) to test their effect in the absence of other drivers. Then, for all three storylines the stressors were modified by applying specific measures as described in Table 6.18.

Table 6.17. Multiple stressor matrix and scenarios run for the Vansjø-Hobøl River basin under the three storylines for future development outlined in the MARS project. Control period: 1996-2012; scenario period: 2030-2060.

Storyline	Agriculture	Domestic Wastewater	Climate
Stressor matrix	Stressor/Pressure 1	Stressor/Pressure 2	Stressor/Pressure 3
Extended baseline (no CC)	Unfert grass only	No effl discharges	Obs data/ctrl period
Agricult-no effluents (no CC)	As present	No effl discharges	Obs data/ctrl period
Effluents - no agricult (no CC)	Unfert grass only	As present	Obs data/ctrl period
Historical (no CC)	Current legislation	Current regulation	Obs data/ctrl period
<hr/>			
RCP 4 Model GDFL	Current legislation	Current regulation	AR5 - 4.5 W/m2
RCP 4 Model ISPL	Current legislation	Current regulation	AR5 - 4.5 W/m2
RCP 8 Model GDFL	Current legislation	Current regulation	AR5 - 8.5 W/m2
RCP 8 Model ISPL	Current legislation	Current regulation	AR5 - 8.5 W/m2
<hr/>			
Storylines-MARS			
SSP5 - Techno	More intensive	Population increase	¹)AR5 - 8.5 W/m2
SSP2 - Consensus	Env. Focus	Stable population	¹)AR5 - 4.5 W/m2
SSP3 - Fragmented	Intermediate	Intermediate	¹)AR5 - 8.5 W/m2
SSP5 - Techno	More intensive	Population increase	²)AR5 - 8.5 W/m2
SSP2 - Consensus	Env. Focus	Stable population	²)AR5 - 4.5 W/m2
SSP3 - Fragmented	Intermediate	Intermediate	²)AR5 - 8.5 W/m2

¹ Model GDFL

² Model ISPL

Table 6.18. Summary of possible measures within the agriculture and wastewater sectors that can be associated with the three storylines for future development outlined in the MARS project. Column 3 specifies how the measures are implemented in the model chain.

AGRICULTURAL MEASURES		
Storyline	Type of measure	Specific measure
SSP5 - Tech	More agricultural land	10% of forest areas turned into grassland (change *.par file)
SSP5 - Tech	More intensive agriculture	30% of grasslands turned into crop production (change *.par file)
SSP5 - Tech	More intensive agriculture	30% of grasslands turned into vegetable production (change *.par file)
SSP5 - Tech	Increased fertilisation	30% increase in N- and P fertilizer application (all agricultural fields) (change *.sfs file)
SSP5 - Tech	Less erosion control	30% increase in erosion parameters to simulate increased erosion risk
SSP5 - Tech	Longer growing season	Growing season extended by 2 months due to climate change
SSP5 - Cons.	Reduction of agricultural land	10% of grassland turned into forest (change *.par file)
SSP5 - Cons.	Less intensive agriculture	30% shift from vegetables to unfertilised grasslands
SSP5 - Cons.	Less intensive agriculture	30% shift from crops to unfertilised grasslands
SSP5 - Cons.	Less fertilisation	50% decrease in N and P fertilizer application (all agricultural fields)
SSP5 - Cons.	More erosion control	50% decrease in erosion parameters (catch crops, buffer strips, sedimentation ponds)
SSP5 - Cons.	Longer growing season	Growing season extended by 2 months due to climate change
SSP3 - Frag.	More agricultural land	5% of forest areas turned into grassland
SSP3 - Frag.	More intensive agriculture	15% of grasslands turned into crop production
SSP3 - Frag.	More intensive agriculture	15% of grasslands turned into vegetable
SSP3 - Frag.	Increased fertilisation	15% increase in N and P fertilizer (all agricultural fields)
SSP3 - Frag.	Less erosion control	15% increase in erosion parameters to simulate increased erosion risk
SSP3 - Frag.		Growing season extended by 2 months due to climate change
WASTEWATER MEASURES		
		Population increase by 30%:
Storyline	Type of measure	Specific measure
SSP5 - Tech.	Less focus on water treatment	Effluents from scattered dwellings and WWTP are increased by 40%
SSP2 - Cons.	Improved WWTP	Effluents from scattered dwellings etc. are reduced by 50%
SSP3 - Frag.	Intermediate	Effluents from scattered dwellings and WWTP are increased by 25%

6.5.3 Results

Process-based modelling results

Catchment modelling

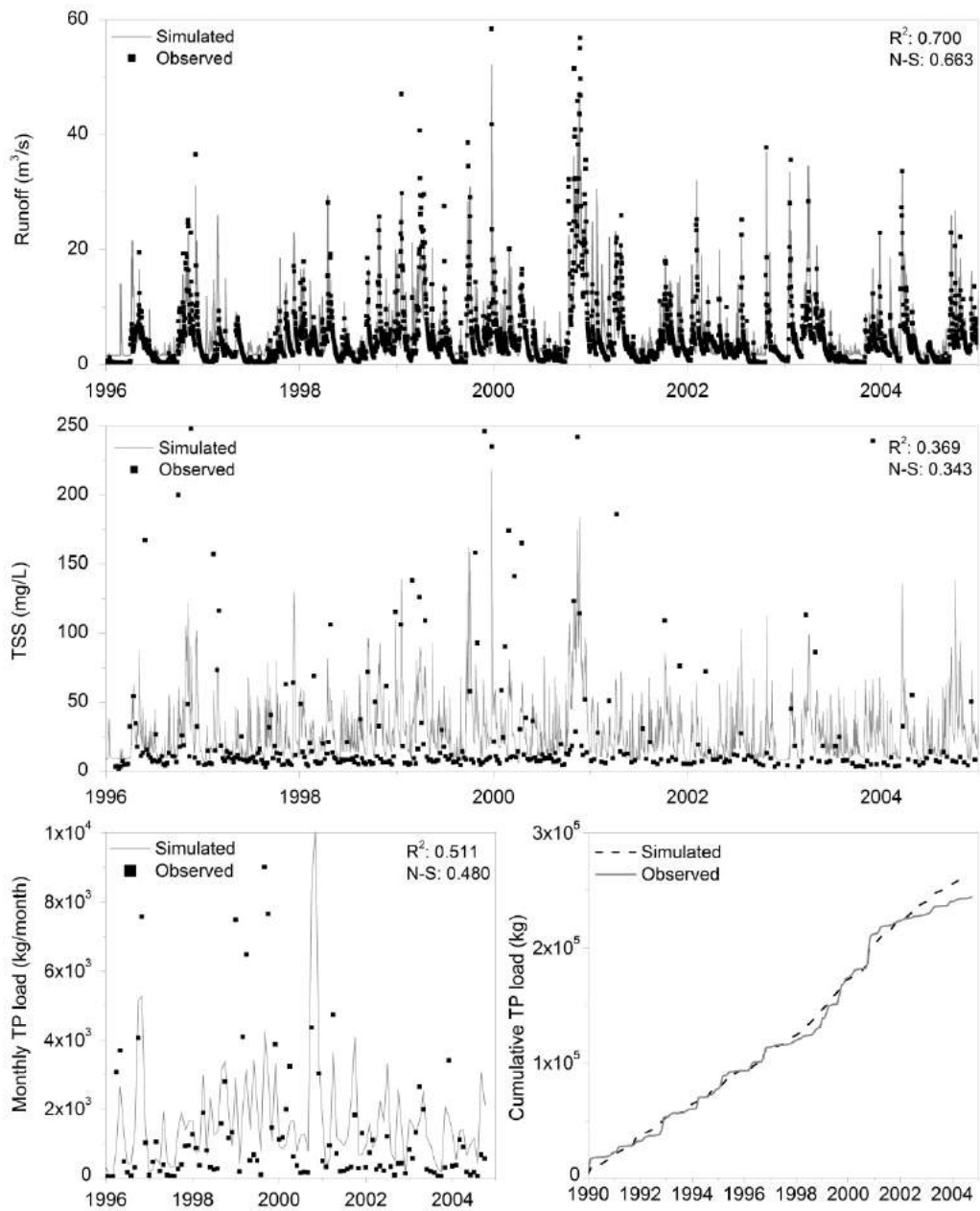


Figure 6.57 Calibration of the INCA-P model. Simulated (line) and measured (squares) runoff (top panel), total suspended solids (middle panel) and monthly TP loads (lower left panel) along with cumulative TP loads simulated (dashed line) and calculated from observations (solid line) using INCA-P at the Hobøl river during the calibration period.

Table 6.19. Outcome of INCA-P calibration assessed against the coefficient of determination (R^2), the Nash-Sutcliffe metric (N-S), the normalized bias (B^*) and the normalized root-mean square deviation (RMSD*) targeting best performance against TP.

	R^2	N-S	B^*	RMSD*
Q	0.700	0.663	0.008	-0.030
TSS	0.369	0.343	-0.001	-0.110
TP	0.007	-0.223	-0.007	-0.150
Monthly_TP load	0.438	0.214	0.201	1.207

Table 6.20. Outcome of INCA-P calibration assessed against the coefficient of determination (R^2), the Nash-Sutcliffe metric (N-S), the normalized bias (B^*) and the normalized root-mean square deviation (RMSD*) targeting best performance against TP loads.

	R^2	N-S	B^*	RMSD*
Q	0.700	0.663	0.008	-0.030
TSS	0.369	0.343	-0.001	-0.110
TP	0.009	-2.051	0.632	1.745
Monthly_TP	0.511	0.480	-0.015	-0.719

These simulations improve on previously performed model setup on the same catchment during the EU-REFRESH project (Couture et al., 2013; Couture et al., 2014). N-S coefficient for Q improved from 0.48 to 0.66 and for TP from -0.51 to +0.22. In addition to improving calibration against TP concentrations (Table 6.19) we have also explored calibration against TP loads and against TSS (Table 6.20) as discussed below.

Lake modelling. Calibration of the lake model has been performed by Couture et al. (2014), and the performance for Lake Vansjø, westernmost basin (Figure 6.54) is reported on Table 6.21. We refer to the earlier publication for details on the model performance during calibration. Briefly, MyLake simulations captured the seasonal minima in PO_4 and maxima in both PP and Chl. The seasonal trends in Chl, a measure of the abundance of

phytoplankton, are also well captured by the model, with the exception of an algal bloom in the summer of 2006, whose magnitude was not fully captured (Figure 6.57). The algal bloom in the summer of 2008 is reproduced by the model, despite the high magnitude rain events that occurred throughout the catchment during that year.

Table 6.21. Outcome of MyLake calibration targeting best performance against total phosphorus (TP), phosphates (PO₄), chlorophyll-a (Chl) and particulate P (PP).

Parameter	R ²	RMSE	NS
TP	0.94	7.76 µg L ⁻¹	-0.23
PO ₄	0.72	2.54 µg L ⁻¹	-0.96
Chl	0.82	8.11 µg L ⁻¹	0.21
PP	0.85	8.16 µg L ⁻¹	-0.50

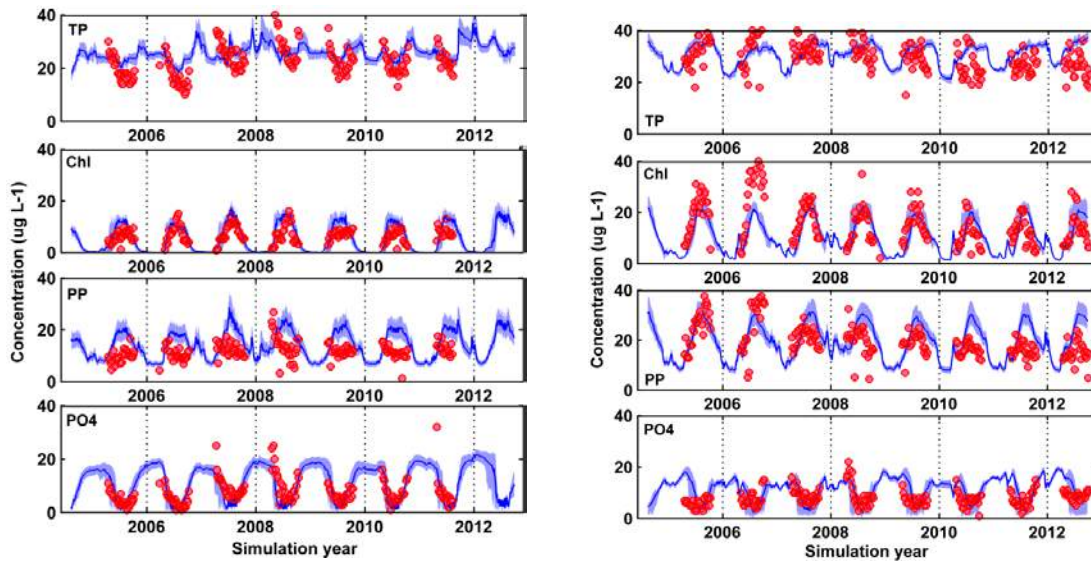


Figure 6.58 MyLake calibration in basin L1 and L2. Calibration performance of MyLake at Storefjorden (L1, left panels) and Vanemfjorden (L2, right panels) for total phosphorus (TP), chlorophyll (Chl), particulate phosphorus (PP) and phosphate (PO₄) over the calibration period of 2005-2012. The results are reported as the median (solid line), daily quartile statistics sampled from the parameter sets of equal likelihood (continuous area) together with the observations (circles).

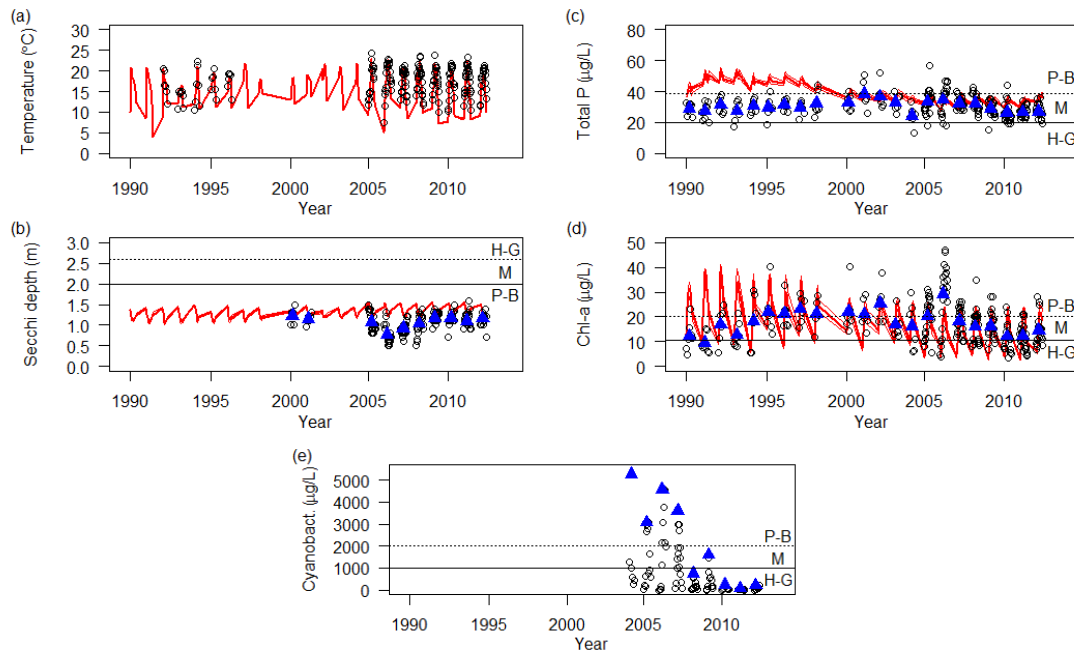


Figure 6.59 MyLake extension with Bayesian Network in basin L2. Observed (open black circles) and predicted (red curves) values of (a) temperature, (b) Secchi depth, (c) total P, (d) chl-a and (e) cyanobacteria. Predicted values are median values (with 25 and 75 percentiles) of 60 runs of the process model MyLake with different parameter combinations (see section 2.1.1). (Predicted values for cyanobacteria are not available from this model). Blue triangles represent seasonal mean values for Secchi depth, total P and chl-a, and seasonal maximum value for cyanobacteria (corresponding to the node CyanoMax). Horizontal lines indicate the boundaries between ecological status classes: High-Good (H-G), Moderate (M) and Poor-Bad (P-B). From Moe et al. (2016).

Empirical modelling results

Regression trees. Regression tree analyses were performed to explore which parent nodes had significant effect on the child nodes in Module 2, and to indicate break points for discretisation of the variables for the BN model. All indicator nodes varied with year and with month. The node Management had significant effects on all indicator nodes predicted by MyLake (Secchi, TP and Chl-a). Water temperature affected Chl-a, but not Total P. The node Irradiance was included as a parent for Chl-a, because of the particular importance for phytoplankton growth. The purpose was to distinguish between effects of Irradiance and Temperature; both variables varied during the year, but only Temperature was affected by Climate. TP and Chl-a were strongly correlated, as is commonly observed in lakes (Phillips et al., 2008), and therefore both variables could have been a suitable parent node for Cyanobacteria. We chose Chl-a as the parent node, because this variable has lately been reported to be a better predictor of cyanobacteria biomass than the more

commonly used TP (Ptacnik et al., 2008). The regression tree model for Cyanobacteria indicated breakpoints at water temperatures 18.9 and 20.2 °C, above which there were higher probabilities of high cyanobacteria concentrations (Figure 6.60).

The purpose of these exploratory analyses was to help construct generate conditional probability tables (CPTs); see Table 6.24 for an example. The CPTs are the links between variables in the BN model (illustrated by arrows in Figure 6.56).

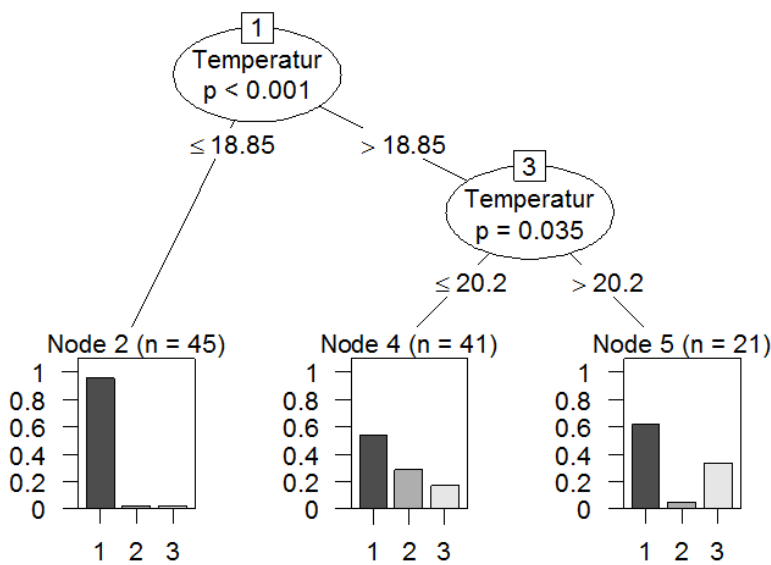


Figure 6.60 Boosted regression tree. Regression tree for effects of temperature on the variable CyanoMax (seasonal maximum of cyanobacteria biomass). The numbers on the branches (18.85 and 20.2) show the significant breakpoints along temperature gradient. The bar plots in each resulting node show the probability distribution of CyanoMax across the three status classes: 1: High-Good (<10.5 µg/L), 2: Moderate (10.5-20 µg/L), Poor-Bad (≥20 µg/L). n = number of observations in each node. From Moe et al. (2016).

Boosted regression trees. The BRT analysis indicates that for Chla, temperature is the most important predictor and TP the least important (Figure 6.61a). For Cyano and Microcystin, Secchi and Colour seem to be more important predictors than TP and temperature (Figures 6.57c, 6.57d). These results do not seem meaningful, since TP is normally considered the main stressor for chl-a, and temperature is considered a more important stressor for Cyano than for chl-a. Moreover, the partial responses plot for Cyano (Figure 6.62) indicates that the (weak) effect of TP is negative. However, TP is often negatively correlated with Secchi depth; the expected positive effect of TP might

therefore have been accounted for by the estimated negative effect of Secchi. Interestingly, there is a strong positive effect of temperature as well as a strong negative effect of colour. These effects are both consistent with the expected effects of climate change on cyanobacteria, which will be tested experimentally in MARS WP3. The strongest interaction was found for Temperature and Secchi (interaction size 0.36), followed by Temperature and Colour (interaction size 0.13). The interaction plot for Temperature and Secchi (Figure 6.63) indicates that the positive effect of temperature on cyanobacteria is slightly higher at lower Secchi. Lower Secchi depths is often correlated with higher concentrations of nutrients and phytoplankton, therefore this results may represent a positive interaction between nutrient and temperature stress.

Considerations of uncertainty / confidence. For some of these predictor variables it is not straight-forward to interpret the effect. Secchi depth is both affected by and affecting chl-a concentration. It may therefore be better to exclude this variable from the model. Temperature has strong seasonal component and co-varies with light, nutrients and other variables. Yearly average could be used instead of the biweekly data, to get remove the seasonal effect. However, the number of data points would then be reduced to 9, which is probably too low for this kind of analysis. In conclusion, the BRT approach may not be suitable for the current dataset.

Random Forest. In the Random Forest analysis we selected only Cyanobacteria and Microcystin as response variables and TP, temperature and colour as predictor variables.

For Cyanobacteria (n=78), the model explained 67% of the variance. The partial dependence plot (Figure 6.64) indicates that colour has the strongest influence, and that the Cyano concentrations decreases rapidly with colour in the range 0-50 mg Pt/L. Moreover, it shows a positive effect of temperature increase in the range 17-21°C, which is consistent with the results from the simpler regression tree analysis for the BN model (Figure 6.56). The estimated pairwise interaction is strongest for colour and TP, followed by colour and temperature (Table 6.60). The corresponding model for Microcystin (n=67) explains 70% of the variance, and yields qualitatively similar results as for Cyanobacteria (Figure 6.65, Table 6.23). The lack of a strong effect of TP is surprising. Nevertheless, these results supports the view that colour may be an important limiting factor for

cyanobacteria, especially in Nordic lakes (Moe et al. 2014, Chapter 2). This factor has so far received much less attention than TP and temperature.

Table 6.22. Paired interactions for Cyanobacteria, estimated by Random Forest.

Interaction	Var 1	Var 2	Paired	Additive	Difference
Color:Temperature	1247202	140115	1391375	1387317	4057
Color:TP	1247202	-21231	1265189	1225970	39215
Temperature:TP	141281	-21231	122882	120049	2831

Table 6.23. Paired interactions for Microcystin, estimated by Random Forest.

Interaction	Var 1	Var 2	Paired	Additive	Difference
Color:Temperature	3.5089	0.1027	3.6344	3.6117	0.0326
Color:TP	3.5098	0.0059	3.5809	3.5148	0.0660
Temperature:TP	0.9864	0.0059	0.1036	0.1016	0.0020

Table 6.24. CPT for Cyanobacteria conditional on Chl-a (observed) and water temperature (observed). Each column contains the probability distribution of a child node for a given combination of states of the parent nodes. The bottom row ("Experience") contains the total count of observations for each combination of parent nodes. From Moe et al. 2016.

Chl-a (obs.)	0 - 10.5		10.5 - 20		20 - 60	
	0 - 19	19 - 25	0 - 19	19 - 25	0 - 19	19 - 25
Cyano						
0 - 1000	1	1	1	0.923	0.333	0.323
1000 - 2000	0	0	0	0.077	0.333	0.290
2000 - 6000	0	0	0	0	0.333	0.387
Experience	20	1	22	13	3	31

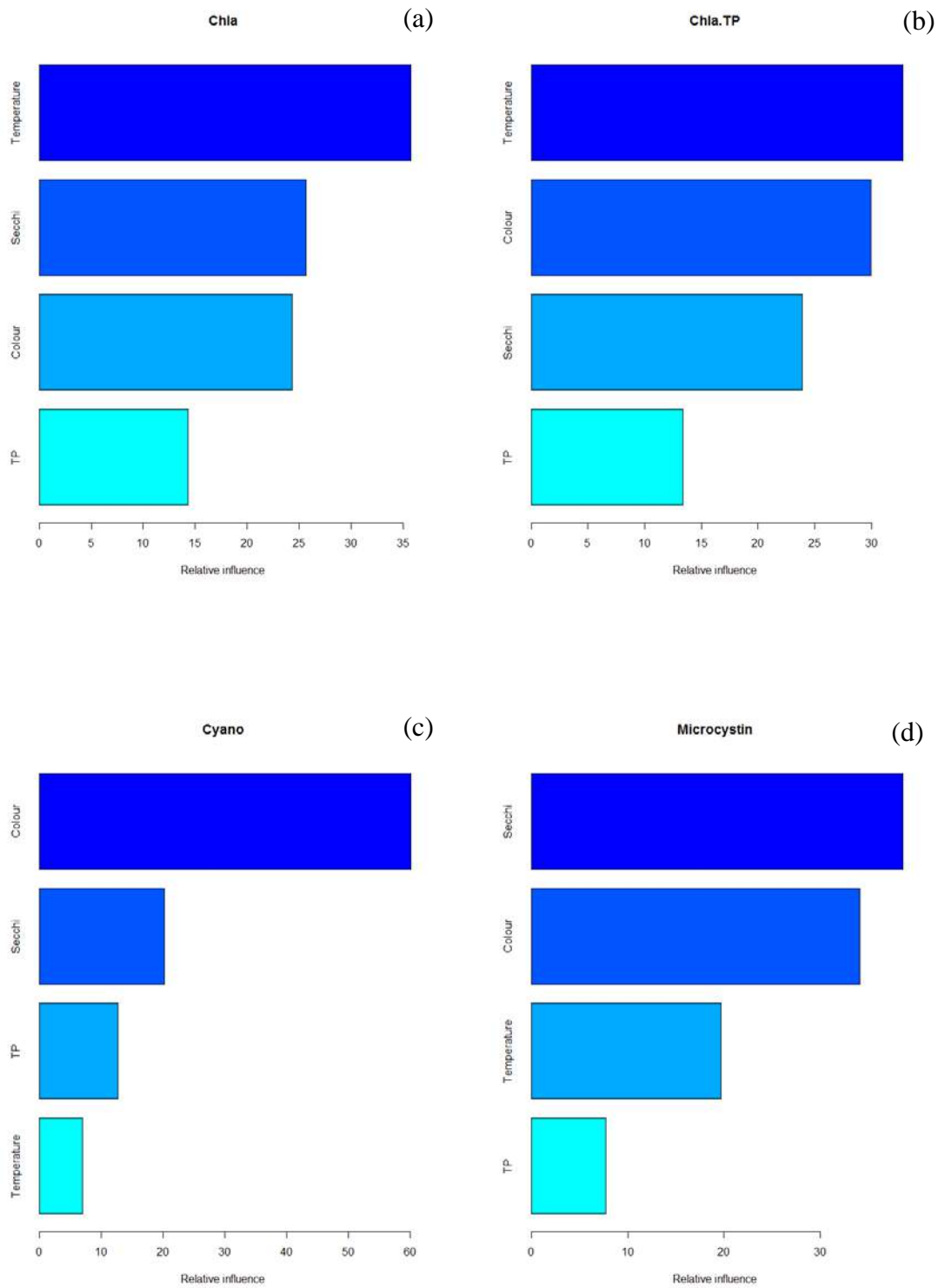


Figure 6.61 Boosted Regression Tree results. Relative influence of the four predictor variables (Temperature, Colour, Secchi and TP) on (a) Chl-a, (b) Chl-a:TP, (c) Cyano and (d) Microcystin, estimated by Boosted Regression Tree.

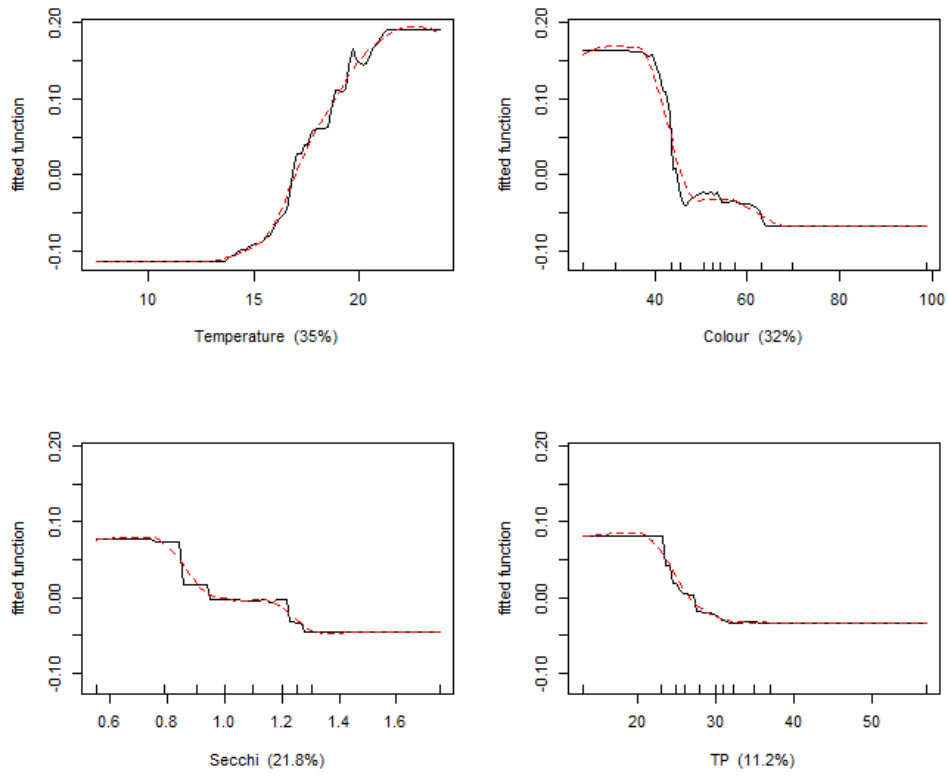


Figure 6.62 Partial responses estimated by BRT. Partial responses of Cyanobacteria to the four predictor variables (Temperature, Colour, Secchi and TP), estimated by Boosted Regression Tree.

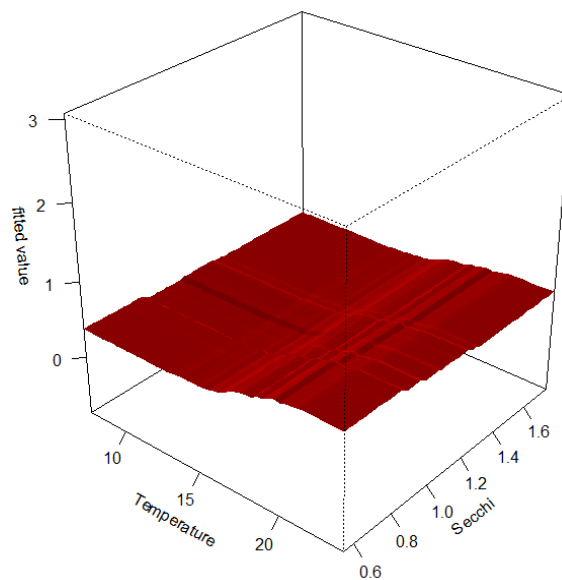


Figure 6.63 Interaction plot estimated by BRT. Interaction plot for combined effects of Temperature and Secchi on Cyano, estimated by Boosted Regression Tree.

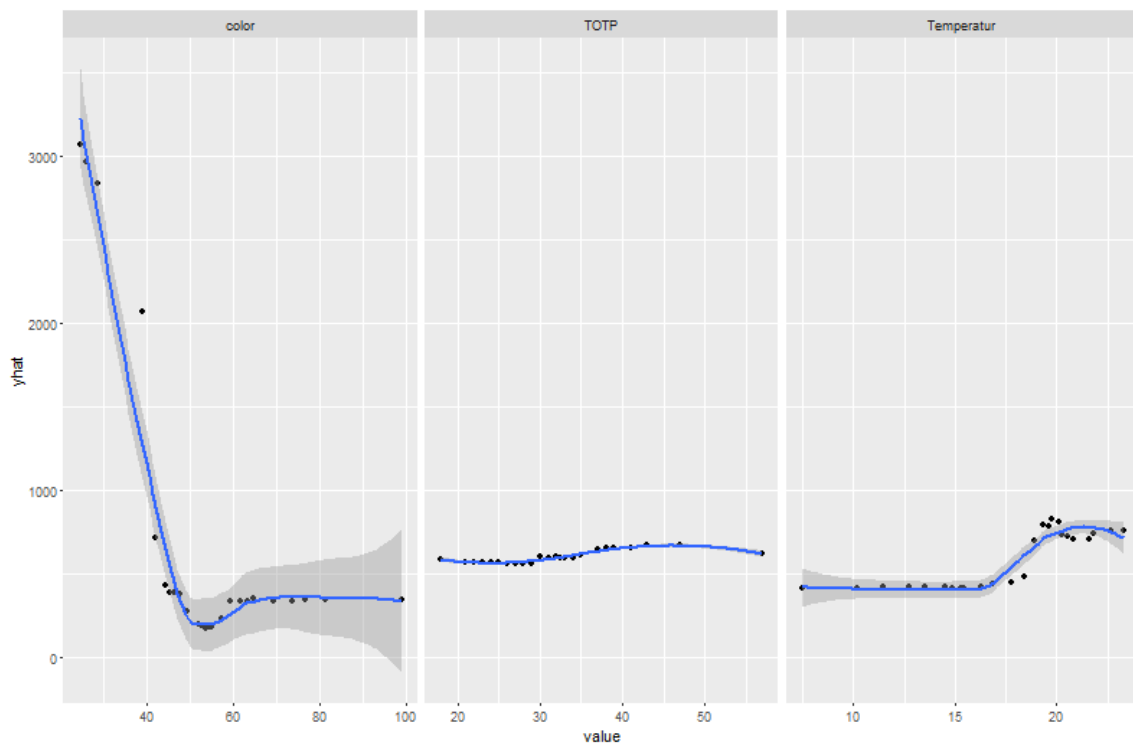
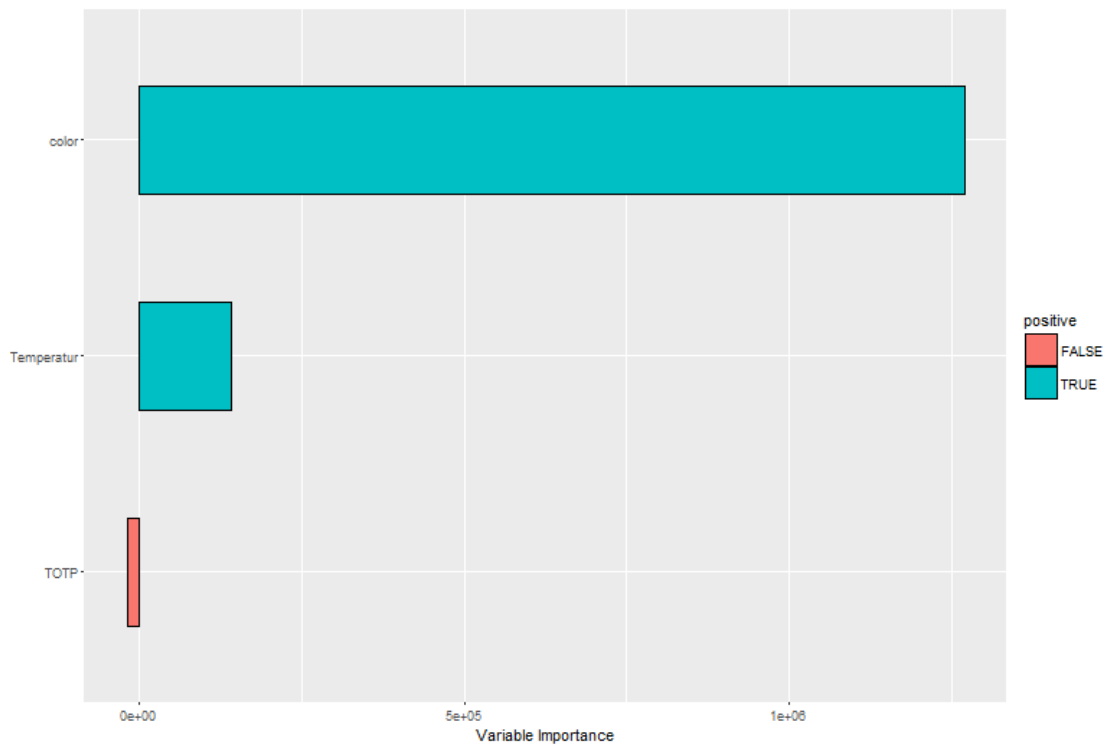


Figure 6.64 Random Forest results. Partial dependence plot for combined effects of Colour, Temperature and TP on Cyanobacteria, estimated by Random Forest.

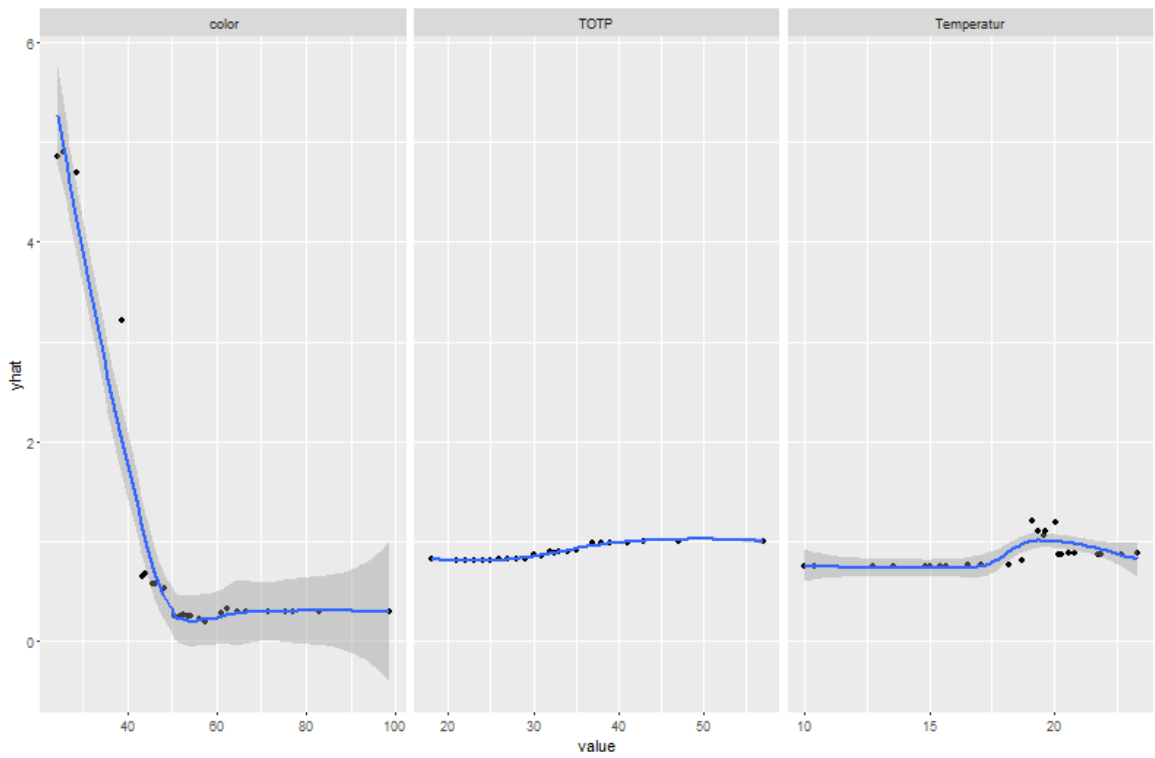
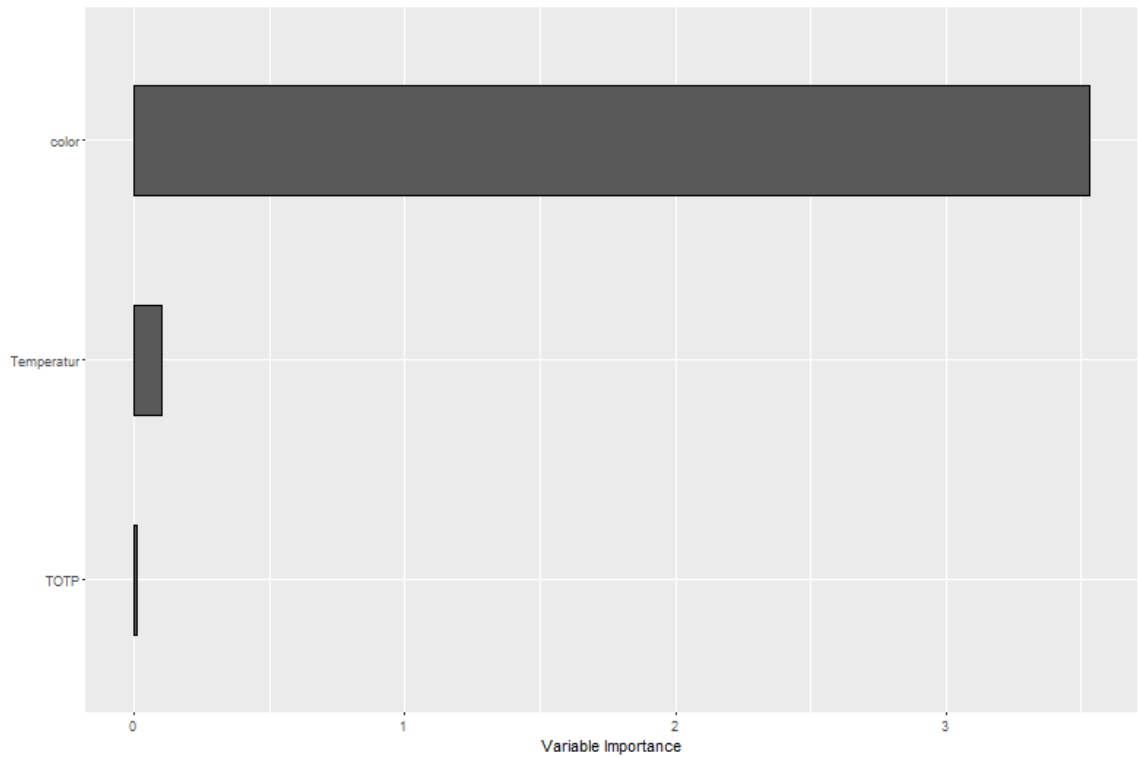


Figure 6.65 Random Forest results. Partial dependence plot for combined effects of Colour, Temperature and TP on Microcystin, estimated by Random Forest.

6.5.4 Discussion

Notes on river basin modelling. The INCA model has been recalibrated within the MARS project to improve on previously published calibration (Couture et al. 2014). In general, this new calibration performs better, and this under a longer calibration period of 30 yrs. Performance metrics for Q and TSS are shown on Tables 6.19 and 6.20. Nonetheless, achieving satisfactory performance at the daily time-scale remains a challenge outside the scope of this work. Here, we instead focus on relevant P loads – rather than instantaneous concentrations – to the lake basins, as those have the controlling influence on algal blooms. We thus present here a calibration against TP loads (Figure 6.57) , as recommended by Farkas et al. (2013)) for the Skuterud catchment (Norway), which is a small (4.5 km²) catchment located a few kilometres north-west of Vansjø-Hobøl. Tables 6.19 and 6.20 show that targeting TP loads during calibration allows to reach satisfactory performance against TP loads while decreasing performance against TP concentrations. While shortcomings in the INCA model are likely responsible for some of the calibration challenges (Jackson-Blake et al., 2015), it is also likely that the nature of the sampling program does not lend itself to accurate calculation of loads. This is because sampling occurs manually mostly during calm weather, therefore outside of high storm/flow events that carry the highest particulate and thus TP concentrations. This uncertainty, combined with greater uncertainty in runoff measurements at peak flow, also causes uncertainty in TP loads calculations at high loads. Nevertheless, we find that targeting TP loads as the calibration target yields the best model performance, while allowing to model the parameter that is most relevant for lake P dynamics.

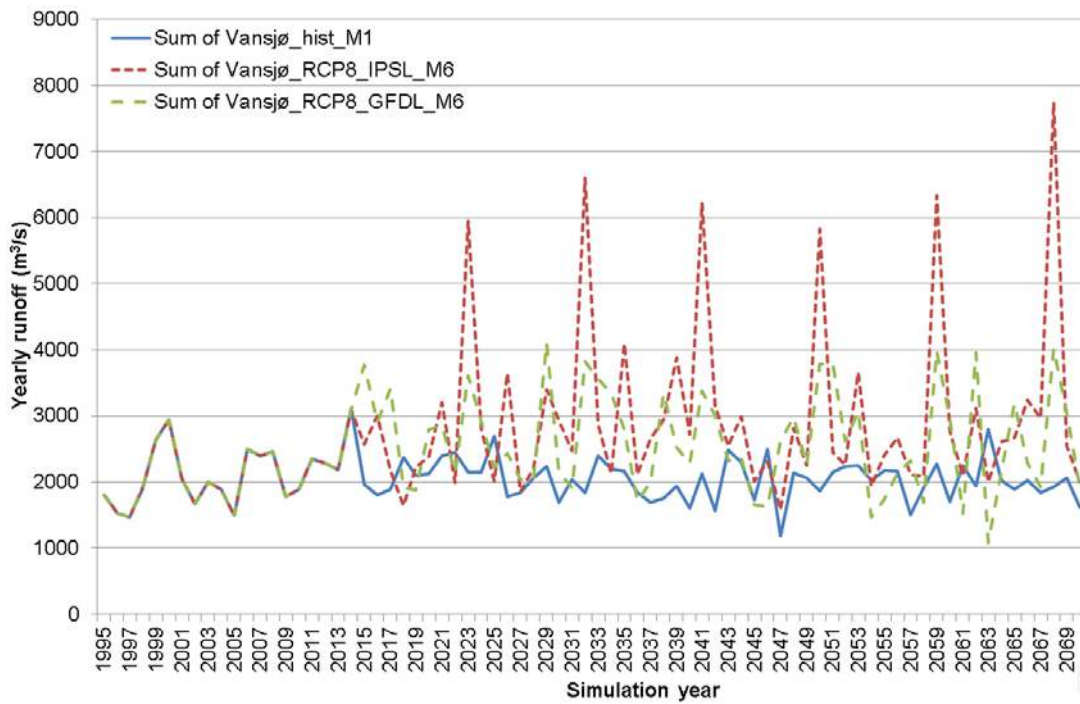


Figure 6.66 Simulated runoff. Simulated yearly runoff as a function of time loads at the outlet of the Hobøl river from 1995 to 2070 using the extended baseline climate (solid line), and the RCP8 climate scenario with either the IPSL (short dashed line) or the GFDL (long dashed line) model ensemble.

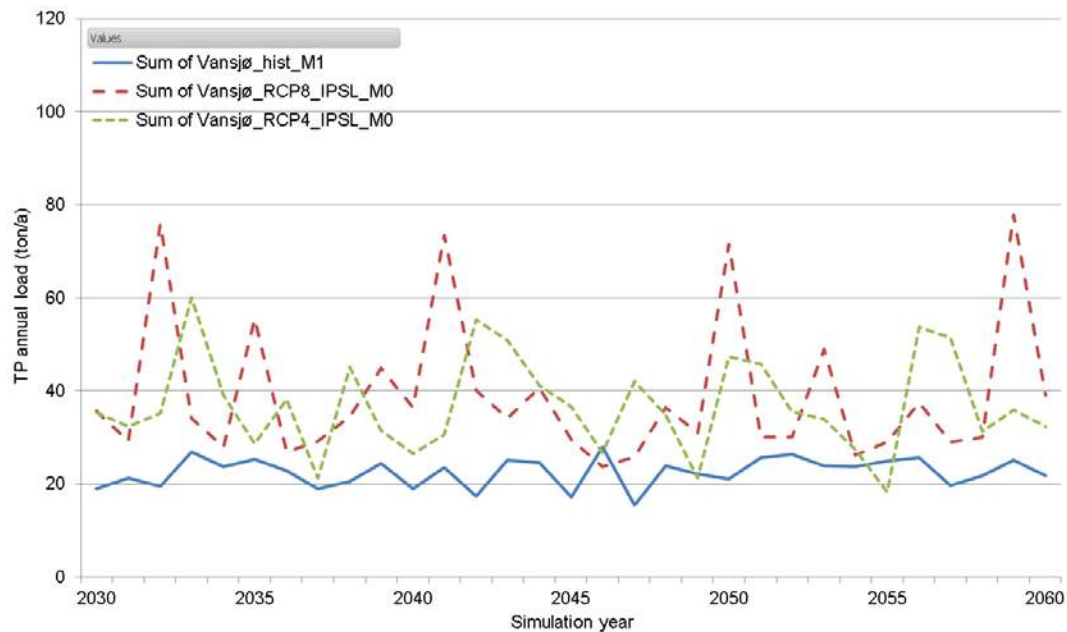


Figure 6.67 Effect of climate scenario. Simulated annual TP loads (ton/yr) as a function of time at the outlet of the Hobøl river from 2030 to 2060 using the extended baseline climate (solid line), the RCP4 climate scenario (short dashed line) or the RCP8 climate scenario (long dashed line) by the IPSL model ensemble.

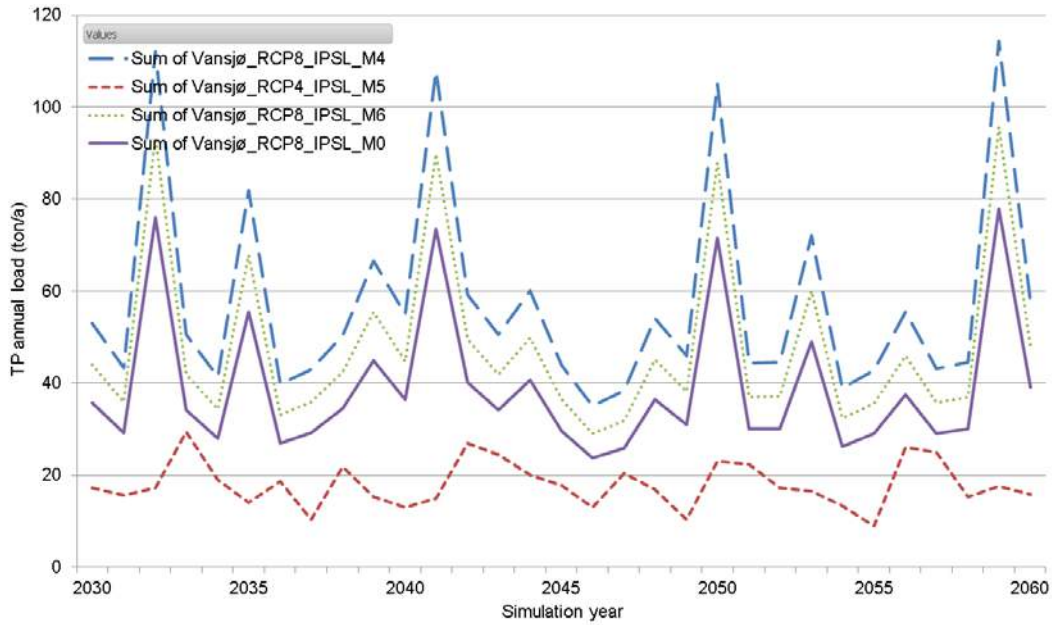


Figure 6.68 Effect of storylines. Simulated annual TP loads (ton/yr) as a function of time at the outlet of the Hobøl river from 2030 to 2060 during storylines M0 (extended, solid line), M4 (Techno, long dashed line), M5 (Consensus, short dashed line) and M6 (Fragmented, dotted line). Storylines are detailed on Tables 6.2 and 6.3.

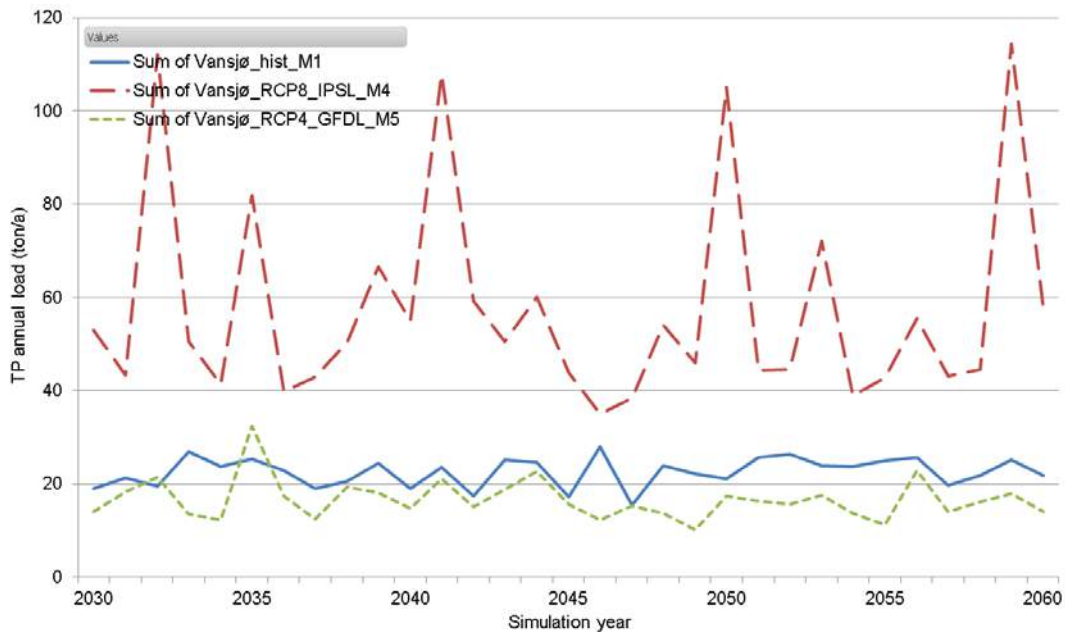


Figure 6.69 Best vs Worst cases. Simulated annual TP loads (ton/yr) as a function of time at the outlet of the Hobøl river from 2030 to 2070 during storylines M1 (extended baseline, solid line), best-case scenario (i.e., Consensus with GFDL, short long dashed line) and worst-case (i.e., Techno with IPSL long dashed line). Storylines are detailed on Tables 6.17 and 6.18.

Outcome of scenarios at the river basin scale. Result of hydrological modelling shows that the RCP 8 lead to more annual runoff, due to higher precipitation, than RCP 4. It should also be noted that there is differences between the outputs of the two climate model used, such that IPSL generally predict more extreme inter-annual variations (Figure 6.66).

INCA simulations suggest that TP concentrations are not directly affected by climate. TP loads, however, are affected by climates due to variations in runoff resulting from changing precipitations. Consequently, storylines relying on RCP8 (e.g., Techno & Fragmented, see Tables 6.17 and 6.18) produce higher annual TP loads (Figure 6.67). For those storylines, IPSL-based storylines yield higher TP loads to the river outlet, while for storyline based on RCP4 both IPSL and GFDL give similar outcome.

The effect of changing land-use according to the storylines (Table 6.18 is shown in Figure 6.68. As previously estimated (Couture et al. 2014) for different storylines, land-use is the chief driver of TP loads in the basin. Here, the Consensus scenario is worth highlighting as it predicts a sharp reduction of TP loads in the river (60% for GFDL ensemble and 80% for IPSL ensemble). To look at the spread of predicted TP loads found in all the simulations, we defined a worst and best-case outcome, and compare them to the historical extended baseline on Figure 6.69. The best-case becomes the Consensus storylines running the RCP4 scenario with the GFDL model, while the worst case becomes the Techno-world scenario running the RCP8 scenario with the IPSL model. All other simulations, including the baseline, are within those two extremes.

The great spread of predicted P loads associated with the worst case and best case scenario will imply widely different water qualities in receiving waters and potentially also significantly different responses within the biotic community (more about this in the coming section). It is worth noting here that the different storylines includes a mixture of different measures within both the agriculture and the wastewater sectors. A closer evaluation of the efficiency of each measure is therefore not possible without a more detailed analysis where the measures are simulated one by one and in various combinations. *Need for transient catchment modelling.* INCA does not allow parameters (e.g., % land-use -) do vary during the course of multi-year simulations. This is the case for many catchment models. As a result, storylines are implemented as a sudden event rather than as progressive changes. In reality, changes in the catchment land-use occur gradually.

Multi-stressor interactions identified. The most important stressor is the percentage of agricultural farmland and land management (fertilization rates, erosion control), followed by climate change, via precipitation.

Although the model do not include time-series of land-uses, we tested the effect of land-use change by implemented all the changes in one event, at the beginning of the simulation. This gives a strong signal that land-use is the chief stressor affecting TP loads in the basin. In the following section, the response of the lake to changes in the river basin TP loads along scenarios are shown and discussed.

Bayesian Network modelling done at this site with the dataset showcased here (Moe et al., 2016) shows interaction between temperature and chl-a as stressors for cyanobacteria; this interaction was included in the CPT for cyanobacteria in the BN model. The new additional analyses (BRT and RF) indicated the importance of colour (TOC). Colour was not included in the old analyses for BN because it was not an output from MyLake. But it's important in relation to climate change because of brownification. This relationship, identified with the help of empirical modelling, thus represents an avenue for improvements of the process-based model.

Outcome of scenarios at the lake scale

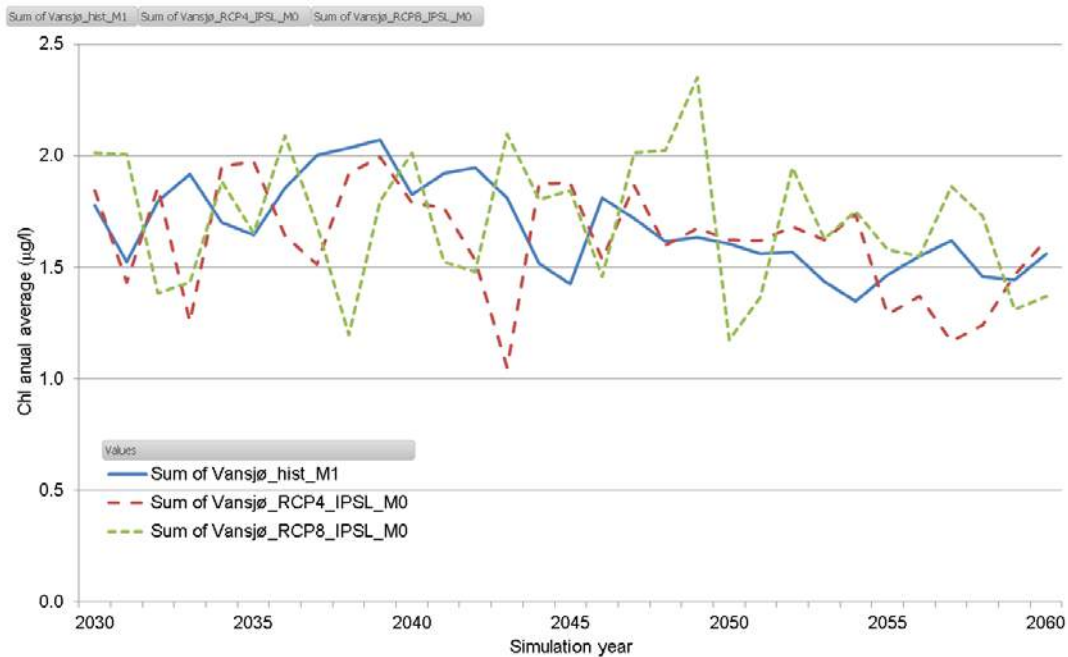


Figure 6.70 Effect of climate. Simulated annual average Chl (µg/L) at Storefjorden river from 2030 to during from 2030 to 2060 using the extended baseline climate (solid line), the RCP4 climate scenario (short dashed line) or the RCP8 climate scenario (long dashed line) by the IPSL model ensemble.

As with the catchment model, the linked catchment-lake model was tested under scenarios of climate change, keeping historical land-use throughout the simulations. The result (Figure 6.70) shows that climate change, regardless of its magnitude (e.g., RCP4 vs RCP8) does not cause a significant increase or decrease in the average phytoplankton biomass at Vansjø. In comparison, Couture et al. (2014) had found a significant, but small, positive relationship between climate changes (i.e., increasing temperature) on phytoplankton biomass. Here, in addition to testing different climate models, we also tested two climate scenarios during which climate change affects temperature to different extents (Table 6.16). The results show that the variance in the 2030-2060 mean annual phytoplankton biomass increase with the magnitude of the climate change, with variance of 4.1 , 6.6 , and 8.7×10^{-2} for historical, RCP4 and RCP8 climates, respectively.

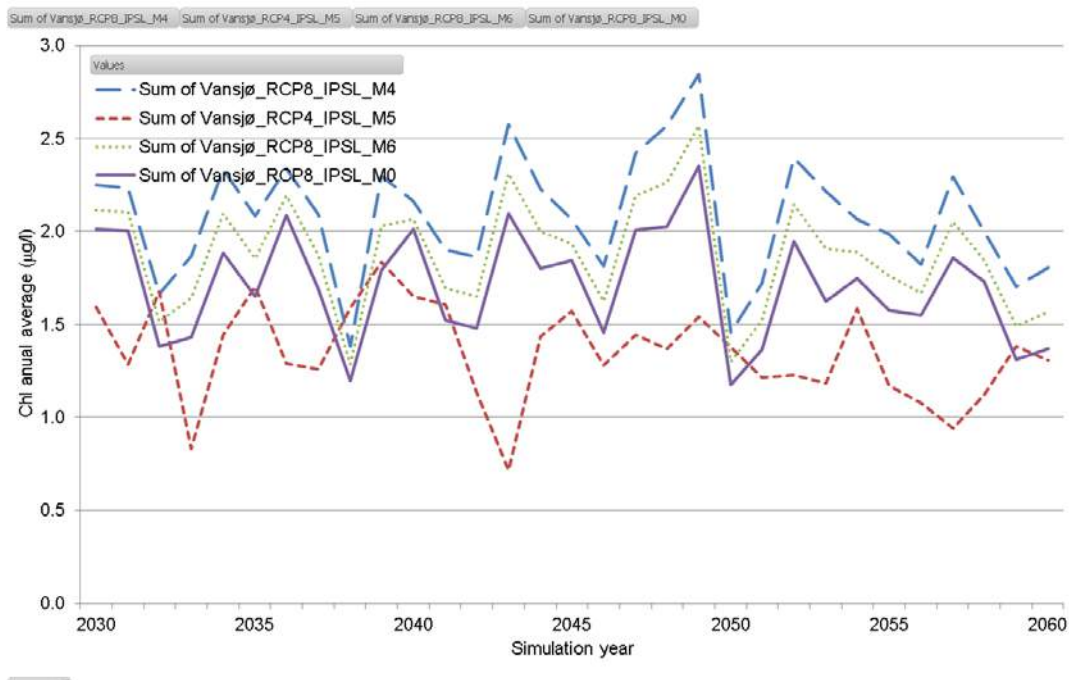


Figure 6.71 Effect of storylines. Simulated annual average Chl (µg/L) at Storefjorden river from 2030 to 2060 during storylines M0 (extended, solid line), M4 (Techno, long dashed line), M5 (Consensus, short dashed line) and M6 (Fragmented, dotted line). Storylines are detailed on Tables 6.2 and 6.3.

Figure 6.71 shows the simulated mean annual Chl through the 2030-2070 period. Here the effect of land-use and effluent loads change are clearly seen for each storylines. Mean annual Chl is highest for the Techo storylines and the Fragmented storylines, and lowest

for the Consensus storylines. These differences reflect the measures implemented for these scenarios.

The Techno and Fragmented storylines produce mean annual river TP (Figure 6.68) and lake Chl (Figure 6.71) that linearly correlated with each other, but not with the time-series simulated under the Consensus storyline. Higher erosion control measures in the Consensus storylines, combined with different variance induced by using RCP4 (for Consensus) or RCP8 (for Techno and Fragmented) are likely responsible for this outcome. This also explains why the Consensus storyline predicts mean annual Chl that is higher than the baseline simulation for 5 of the 40 simulated years (Figure 6.71).

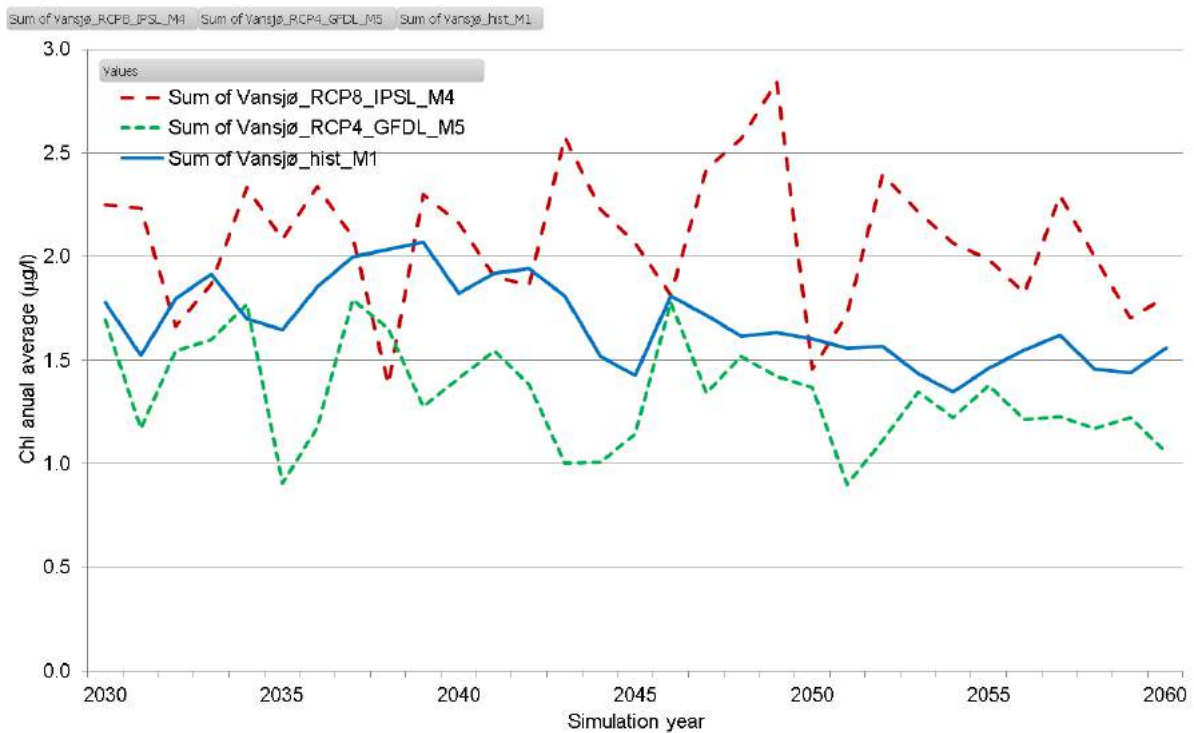


Figure 6.72 Best vs Worst cases. Simulated annual average Chl ($\mu\text{g/L}$) at Storefjorden river from 2030 to 2060 during storylines M1 (extended baseline, solid line), best-case scenario (i.e., Consensus with GFDL, short long dashed line) and worst-case (i.e., Techno with IPSL, long dashed line) Storylines are detailed on Tables 6.2 and 6.3.

The Techno storyline, which uses RCP8 (IPSL model), stands out as the worst-case scenario at Lake Vansjø, while the Consensus storyline, which uses RCP 4 (GFDL model), stands out as the best-case scenario (Figure 6.72). To gain insight on likelihood

of crossing the good to moderate water-quality threshold in the lake, the average of each simulation month over the 2030-2070 period was computed for the three simulations depicted above (Figure 6.73). Putting these results in the context of WFD water quality status, this results suggest that that summer blooms, under all but the most severe land-use change scenario, largely remain under the threshold of 7.5 $\mu\text{g/L}$ set for a lake type L-N3, relevant for Lake Vansjø.

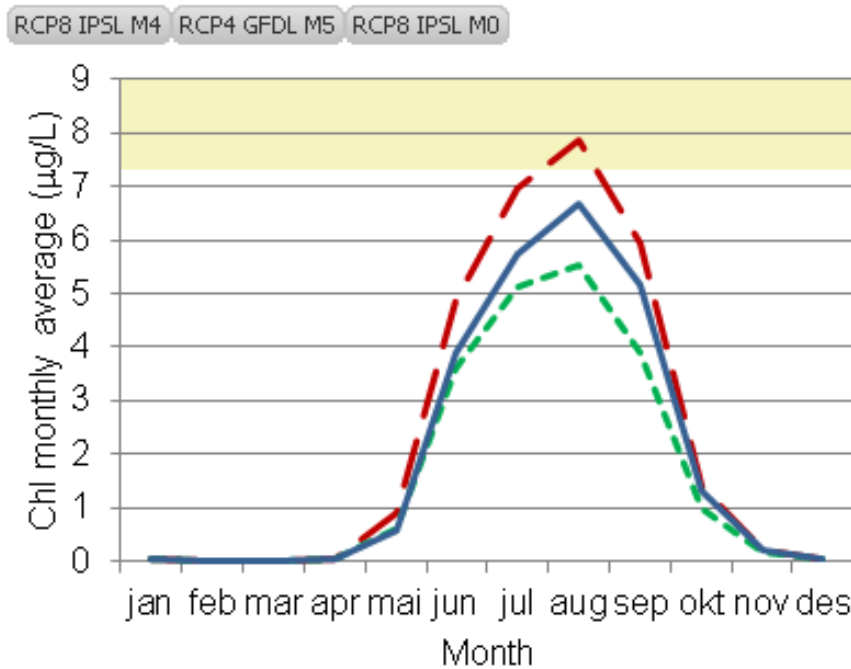


Figure 6.73 Monthly averages. Simulated monthly average Chl ($\mu\text{g/L}$) at Storefjorden during the entire simulation period during storylines M1 (extended baseline, solid line), best-case scenario (i.e., Consensus with GFDL, short long dashed line) and worst-case (i.e., Techno with IPSL, long dashed line). The shaded area indicates the Good/Moderate WFD status threshold.

6.5.5 Conclusion

- Apart from change in land-use devoted to agriculture, which are the main driver of total P in the river-basin, the modelling suggests that reducing fertilization rate and improved erosion control are the most effective measures of TP reduction.
- In the lake, climate change alone does not cause significant increase in algal biomass, but more severe climate change does increase the variance in the inter annual phytoplankton biomass.

- Higher inter-annual variation in water quality and algal biomass associated with future climate change implies that measure-oriented monitoring programmes should be run for several years to produce credible results. This might slow down decision processes related to River basin management plans and the Programme of measures.
- Cyanobacteria are predicted once the process-based model is augmented with an empirical model based on a Bayesian Network approach.
- Empirical modelling points to water temperature and Chl – thus TP – as the main stressors towards cyanobacterial blooms.
- Water color is identified as a stressor, although it was not handled by the process-based model. We identify this as an avenue for model development.
- The worst-case scenario, with respect to WFD water quality status, is represented by using the Techno storyline along with the climate scenario RCP8 as predicted by the ISPL climate model.

6.6 Wales

6.6.1 Introduction

Basin overview. The Welsh catchments (UK) are made up from the radial drainage system formed by river systems flowing from upland mid- and north- Wales toward the Irish Sea and Bristol Channel (Wye, Usk, Severn, Tywi, Dyfi, Teifi, Conwy, etc.). The study area covers around 4,000 km² of Wales, where a temperate oceanic climate prevails (locations' mean annual temperature: 7.2-9.5 °C and mean annual precipitation: 1,000-1,600 mm). Sampling sites were spread throughout upland areas (44-438 m a.s.l.), underlain by base-poor rocks and soils composed dominantly from Ordovician, Silurian and Devonian shales and mudstones, with some older igneous formations. The main land-uses include rough or improved pastures, remnants of broadleaf vegetation and conifer plantations above 250 m. Wales' major urban areas are in the southern coastal strip around Cardiff, Newport and Swansea, and the study area is dominantly rural.

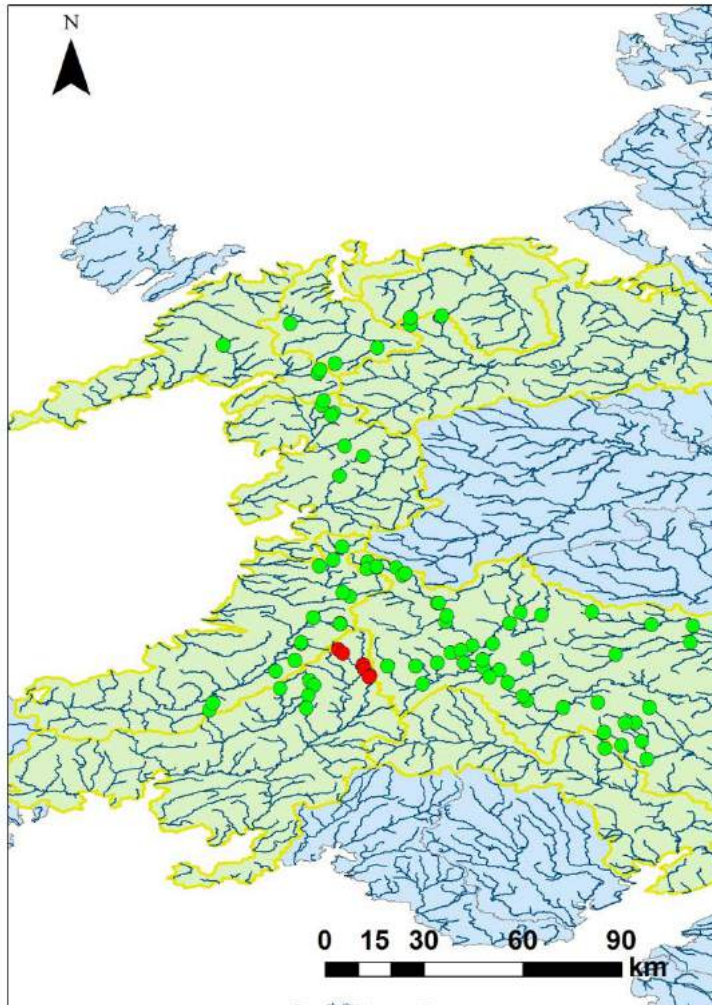


Figure 6.74 Map of the sampling sites of upland Wales. Green dots represent locations included in the spatially spread dataset, while the red dots indicate those sites used for the long-term dataset. See Data section for more info.

Summary of the River Basin Management Plans (RBMP). Nearly half (43%) of the surface waters of the study area show a good or high ecological status according to Water Framework Directive criteria (Figure 6.75). The main reasons of failing to achieve a good ecological status are physical modifications, pollution from abandoned mines, pollution from agriculture, pollution from waste-water, pollution from urban areas and changes in natural flow or water level (Figure 6.76: excluding acidification). The RBMP goal is increasing the number of water bodies showing a good or high status up to >70% in 2021 and >95% by 2027 (Figure 6.77). The likelihood of Brexit has not, so far, changed this goal.

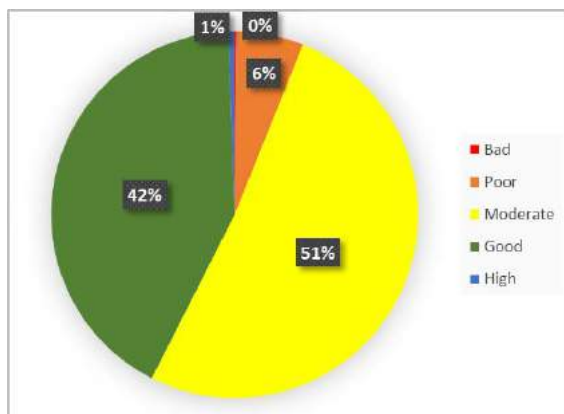


Figure 6.75 Ecological status of surface water bodies in Western Wales in 2015.

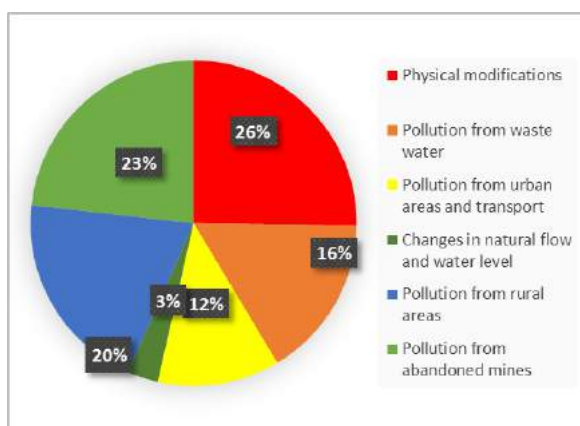


Figure 6.76 Reasons for not achieving a good ecological status in 2015 (acidification is not included).

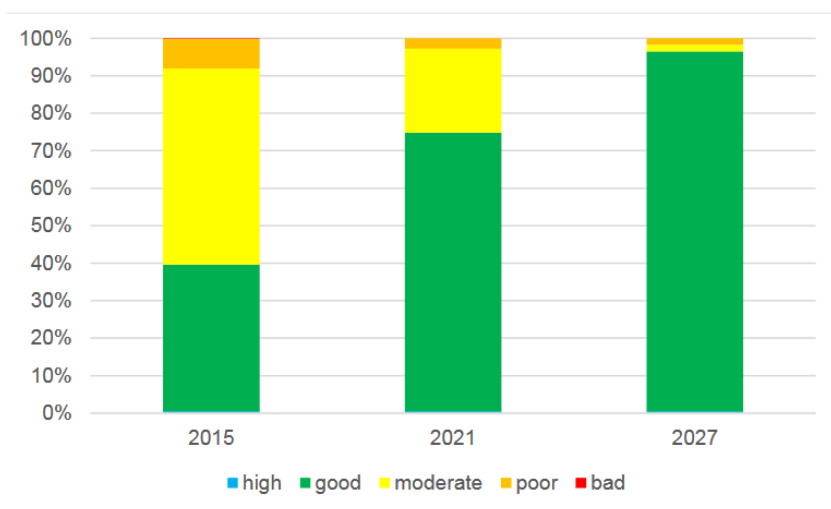


Figure 6.77 Percentage overall water body status and objectives for 2015, 2021 and 2027.

Main anthropogenic drivers in the basins

Drivers:

- past acidification
- land-use intensification (food and wood provision)
- climate change

Acid rain reached a peak in the UK during the 70s, contemporaneous with peak industrial activity across Europe. The effects were marked in areas with large rainfall and poor-base lithologies such as Wales, where half of the river network was severely affected by intermittent or chronic acidification (pH ranging 4.0 – 5.7) (Edwards et al., 1990). Acidification had detrimental effects on algae, macrophytes, invertebrates, salmonids, riverine birds and ecosystem functions in Wales and elsewhere (e.g., Rosemond and Reice, 1992; Buckton et al., 1998; Petrin et al., 2008). During the last 30 years, acid deposition has been reduced leading to a chemical recovery of Welsh running waters. However, despite the chemical improvement, the biological recovery is progressing at a slower pace, and depends on land-use settings (Ormerod and Durance, 2009). Streams draining conifer plantations have recovered most slowly.

Otherwise, pasture, agriculture and plantations are the most wide-spread land-uses in the study area. Many river sections are affected by diffuse pollutants, including nutrient enrichment, which may affect community structure and functioning. Climate change and variation is also affecting Welsh rivers reducing the invertebrate abundance and changing community composition (Durance and Ormerod, 2007).

Questions to be addressed by the modelling. Our main aim in this report was to quantify the individual and combined effects of past acidification, land-use intensification and climate change asking:

- Is land-use intensification affecting the recovery from past-acidification?
- Is climate change modifying rivers differentially if they are affected by past acidification or land-use intensification?

Ecosystem services quantified

- Occurrence of culturally-valued birds (Eurasian dipper) - ES Capacity
- Biomass of salmonid juveniles (brown trout and Atlantic salmon) - ES Capacity

General modelling strategy and DPSIR model. Two major datasets were available for the Welsh catchments:

- Spatially extensive data from 78 sites (green dots in Figure 6.74)
- Annual long-term data covering the period 1981-2014 for six sites (red dots in Figure 6.74)

The interlinks between anthropogenic drivers, pressures, abiotic states, biotic states, impact and response used in the models are shown in Figure 6.78.

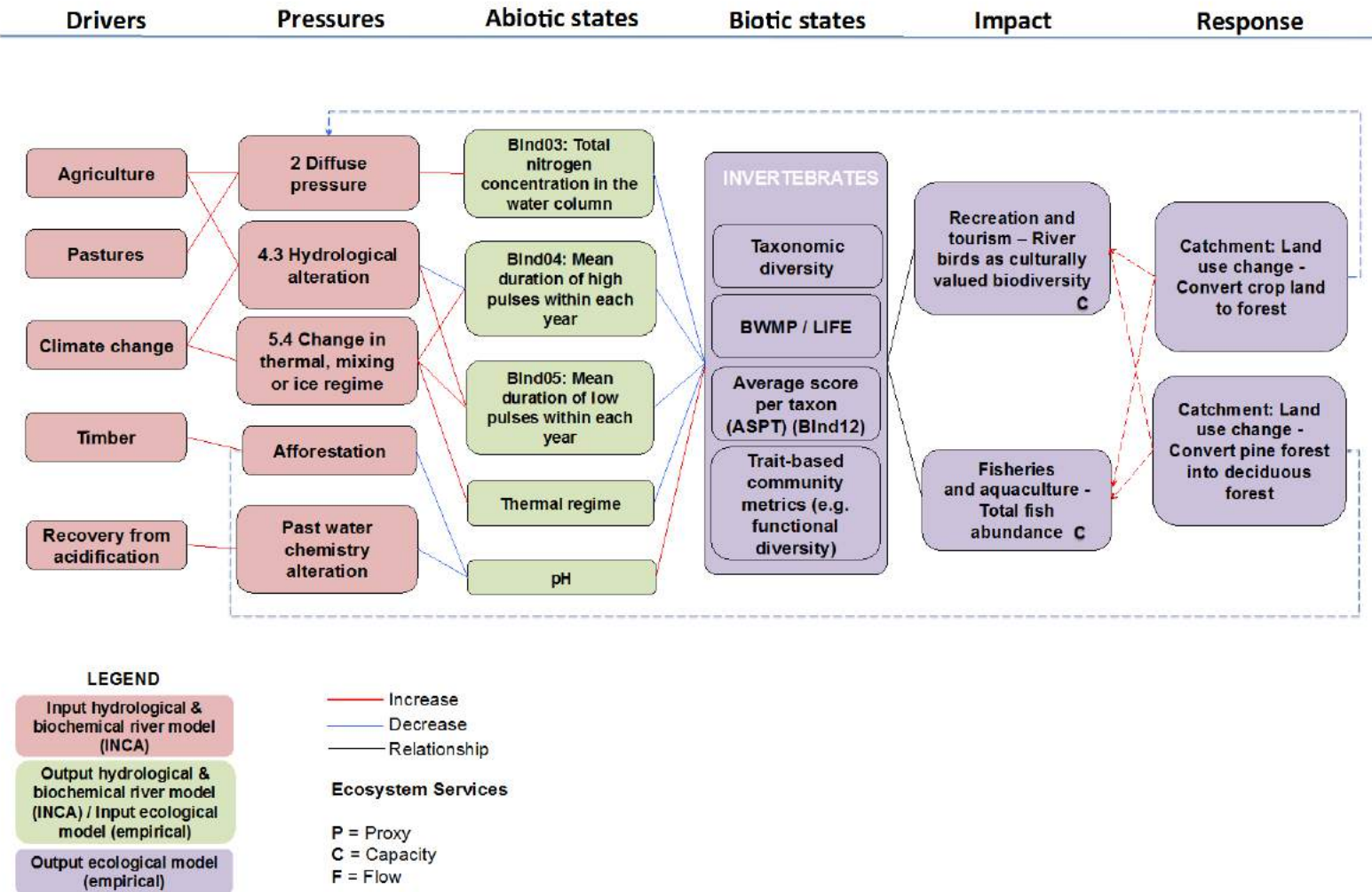


Figure 6.78 Drivers – Pressures – States – Impact – Response (DPSIR) model for the Welsh catchments. See legend for more info.

6.6.2 Data and Methods

Dataset description. Two datasets were compiled to assess the combined effects of the selected stressors in the Welsh catchments:

- *Long-term dataset*: six sites at the Llyn Brienne Stream Observatory (mid-West Wales) had data spanning over three decades (1981-2014). These sites represent three land-use types - acid forest (L1 / L2 – 31 years), acid moorland (C1 / C4 – 29 years), and circumneutral (L6 / L7 – 30 years), which modulate their response to climate change (Durance and Ormerod, 2007).

- *Spatial dataset*: **78 sites across Wales surveyed once in 2012-13.**

For both datasets, we gathered measures to describe natural environmental variation in the catchments, abiotic states, biotic states and ecosystem services (only for spatial dataset).

Environmental descriptors

Basin area: basins were delimited and the surface estimated in hectares.

Climatic data (Spatial dataset): to characterise static, current average climate, we estimated a range of descriptors of historical averaged annual and seasonal air temperature and rainfall patterns from worldclim.com database (Hijmans et al., 2005). Note that these variables were not used to assess the effect of climate change, but to use climate as a static feature of each site.

Coordinates: geographic latitude and longitude for each location.

Elevation of each sampling point: in m a.s.l.

Land-use: the percentage dedicated to arable land, improved grasslands was estimated. This pressure variable was used for informative purposes, but not in the analyses.

Lithology: the percentage of siliceous, calcareous and mixed surface was derived.

Abiotic states - stressors (water chemistry and climate)

Annual climate (long-term dataset): descriptors of long-term climate change as annual mean, maximum, minimum and seasonal air temperature and rainfall from British Meteorological Office (<http://www.metoffice.gov.uk/>).

Major ions and conductivity: for the spatially distributed data we gathered measures of mean conductivity and major ions (Aluminium, Calcium, Chloride, Iron, Magnesium, Manganese, Potassium, Sodium, Sulphur, Zinc).

Nutrients: the annual mean of total oxidised nitrogen was estimated for each of the locations, ranging 0.154 - 1.350 mg L⁻¹ in the acid forest, 0.085 – 0.240 mg L⁻¹ in the acid moorland and 0.005 - 0.210 mg L⁻¹ in the circumneutral type (long-term dataset), and 0.005 - 4.424 mg L⁻¹ in the spatial dataset.

pH: annual mean pH values were characterised for each sampling location. pH spans 4.6 – 6.0 in the acid forest type, 4.9 – 6.6 in the acid moorland type and 6.0 to 7.3 in the circumneutral moorland (long-term dataset), and 4.6 - 8.5 in the spatial dataset.

Biotic states - Invertebrate metrics

Invertebrates were collected in spring (March-April) using kick-sampling (3 minutes in riffles and riffles for the long-term dataset, and 2-minutes just in riffles for the spatial dataset). Individuals were counted and identified to species level when possible, except for small organisms or for taxonomically complex orders (e.g., Diptera, Hydracarina, Oligochaeta), which were identified at coarser levels. We used presence absence data in all analyses. We also compiled a table of response traits (i.e. attributes to cope with disturbance) and effect traits (i.e. biological features influencing ecosystem function). Response traits included fuzzy coded traits about number of generations per year, lifespan, reproduction mode, respiration type, resistance form and dispersal capacity (Tachet et al., 2002). As effect traits we gathered information about functional feeding preferences, i.e., shredders, grazers, predators, gathering-collectors and filterers, which was provided also as fuzzy coding traits (Moog, 2002; Schmidt-Kloiber and Hering, 2015). Trait information was available at the genus level.

We calculated a set of taxonomic and functional descriptors of the community (Table 6.25). Functional descriptors were estimated using different methods, which are fully detailed in literature (Villéger et al., 2008; Laliberté et al., 2010; Bruno et al., 2016b). In brief, we created a response functional multidimensional space deriving a Gower dissimilarity matrix based on the response trait table. In this space, we estimated the hypervolume enclosed by each community as a measure of the response diversity. In addition, we classified genera into effect groups based on their feeding preferences, using a Ward's cluster based on the Gower dissimilarity matrix derived from effect trait table. Functional redundancy was estimated as the ratio between genus richness and the number of effect groups at each community. We also quantified the number of genera representing shredding and grazing strategies.

Measures of ecosystem services. Ecosystem services were only available for a subset of the spatial dataset:

- *Culturally-valued birds*: **The occurrence of the Eurasian dipper (*Cinclus cinclus*) was characterised once in 61 sites in 2013 as the number of territories present at each sampling point (ranging 0-5).**
- *Commercial fish biomass*: **We quantified the sum of juvenile biomass of Brown trout (*Salmo trutta*) and Atlantic salmon (*Salmo salar*) in 23 locations. Up to four samples for location were collected during summer and autumn of 2012 and 2013, resulting in 87 observations.**

Water chemistry for the spatial data set was incomplete for major ions. After preliminary analysis, we used pH and TON to characterise the pressures of past acidity and diffuse pollution, respectively.

We rearranged the long-term dataset to reduce the number of missing values for water chemistry. We averaged biotic, environmental and stressor values for each pair of sites described above, when values for the two sites were available. Otherwise, we just used the value available. The final subset included aggregated data for acid forest (n=31 years), acid moorland (n=29 years), and circumneutral moorland types (n=30 years).

Table 6.25. Biotic states used to characterise invertebrate biodiversity.

Acronym	Biotic state	Description	Reference
<i>abun</i>	Abundance	Number of individuals (only in long-term dataset)	
<i>fam.ric</i>	Family richness	Number of families	
<i>gen.ric</i>	Genus richness	Number of genera	
<i>spp.ric</i>	Species richness	Number of species	
<i>ept</i>	EPT	Number of Ephemeroptera, Plecoptera and Trichoptera species	
<i>bmwp</i>	BMWP	Biological Monitoring Working Party, sum of family scores relative to their tolerance to organic pollution. Revised version.	(Armitage et al., 1983; Walley and Hawkes, 1996)
<i>life</i>	LIFE	Lotic-invertebrate Index for Flow Evaluation, in which lower values indicate preference for faster flows	(Extence et al., 1999)
<i>aspt</i>	ASPT	Averaged Score Per Taxon. BMWP / family richness	Armitage et al., 1983
<i>RD</i>	Response diversity	Diversity of response traits as functional richness (hypervolume enclosed by each community within functional space)	(Villéger et al., 2008)
<i>FR</i>	Functional Redundancy	Number of functional feeding groups / number of genera	(Laliberté et al., 2010)
<i>shr</i>	Shredder richness	Number of shredding genera	(Laliberté et al., 2010)
<i>gra</i>	Grazer richness	Number of grazing genera	(Laliberté et al., 2010)

6.6.3 Methods

Process-based modelling. The variables used in the empirical modelling were obtained from surveys. We used process-based models to predict future values for stressors under each scenario (See section 2.2.3. Scenarios implementation for more details).

Empirical modelling. The empirical modelling followed Feld *et al.* (in press). This method consists of a previous data screening, exploratory modelling using flexible, non-parametric Classification and Regression Trees to rank environmental descriptors and single stressors, along with their pairwise interactions. Multi-stressor effects are finally quantified using Generalised Linear Models or Linear Mixed Models and multi-inference modelling. For each of these steps, we ran a separate model for each biotic state in response to multi-stressors for both spatial and long-term datasets.

Data screening included checking for outliers and transforming response variables and predictors to reduce distribution skewness for each of the subsets used. Then, all the continuous predictors were standardised to mean=0 and SD=1 to allow for within-model coefficient comparison in form of Standardised Effect Sizes (SES). As exploratory

analysis, we used Random Forest (RF, Cutler et al., 2007; Ishwaran et al., 2014) regression to rank environmental descriptors, single stressors and the interaction between stressors, and stressors and environmental descriptors. The number of trees (ntree) was set to 2000 and the number of variables used in each split (mtry) was set to one third of the number of predictors. For the long-term dataset, we run RF for each of the three sites (acid forest, acid moorland, circumneutral moorland). As a result of the exploratory analysis we selected a different set of stressors and environmental descriptors (single and interaction terms) for each dataset. The full list of predictors used is shown in Table 6.26

Table 6.26. Final set of predictors used in the global models. ¹For the spatial dataset, these variables are the average of historical series of climatic data from worldclim.com. ²For the long-term dataset, we calculated the climatic features of the precedent 12 months from Met Office UK (Aberporth, latitude=52.139, longitude=-4.570).

Variable	Description	Unit
pH	Mean annual pH (average of up to four measures of pH)	pH units
TON	Total Oxidised Nitrogen	mg/L
alt	Altitude	m a.s.l.
lat	Geographical latitude	degrees
lon	Geographical longitude	degrees
prec_max ¹	Precipitation of the wettest month	mm
prec_win ²	Precipitation of the wettest quarter (Oct-Dec)	mm / year
prec_sum ²	Precipitation of the summer (Jun-Aug)	mm / year
tmean ²	Mean annual temperature	°C
tmin ²	Annual minimum temperature	°C

To estimate predictor SES values and their significance, we adopted a multi-model inference approach following the protocol suggested in Feld *et al.* (2016) and Grueber *et al.* (2011). First, we built a global model for each biotic indicator and for each dataset, including stressors and, spatial and natural descriptors as predictors. The global model was different depending on the presence of repeated measures in the dataset (i.e., Generalised lineal model or lineal mixed model) and response variable nature (i.e., integer or continuous values).

For the long-term dataset, we fitted generalised linear models with a Gaussian or Poisson (fam.ric, gen.ric, spp.ric, ept, shr and gra) error distributions for each of the biotic indicators. We included pH, TON, climate and the interactions pH : TON and pH : climate

as stressors. Climate was characterised as the summer precipitation (prec_sum) for acid forest and acid moorland sites, whereas minimum temperature (tmin) was used for circumneutral moorlands.

Acid forest long-term model:

$$\text{biotic} = \text{pH} + \text{TON} + \text{prec_sum} + \text{pH} : \text{TON} + \text{pH} : \text{prec_sum}$$

Acid moorland long-term model:

$$\text{biotic} = \text{pH} + \text{TON} + \text{prec_sum} + \text{pH} : \text{TON} + \text{pH} : \text{prec_sum}$$

Circumneutral moorland long-term model:

$$\text{biotic} = \text{pH} + \text{TON} + \text{tmin} + \text{pH} : \text{TON} + \text{pH} : \text{tmin}$$

For the spatial dataset, we fitted generalised linear models with a Gaussian (bmwp, life, RD, FR) or Poisson / Quasipoisson (fam.ric, gen.ric, spp.ric, ept, shr, gra) error distributions for each of the biotic indicators.

We included pH, TON and the interaction pH : TON as stressors, and elevation (alt), precipitation of the wettest month (prec_max), latitude, longitude, and the interaction pH : latitude as descriptors of natural variability:

$$\text{biotic} = \text{pH} + \text{TON} + \text{pH} : \text{TON} + \text{alt} + \text{prec_max} + \text{lat} + \text{lon} + \text{pH} : \text{lat}$$

For the ecosystem services, we fitted generalised linear models with a Quasipoisson error distribution for birds (to account for overdispersed data) and a linear mixed model with a Gaussian error distribution for juvenile fish biomass. The later model also included “Site” as random intercept to account for the repeated measures at each location for different seasons and years. For the dipper model, we included pH, TON (linear and quadratic terms) and the interaction pH : TON as stressors, and elevation as descriptor of natural variability. For the fish model, we included pH, TON and the interaction pH : TON as stressors, and elevation as descriptor of natural variability:

$$\text{dipper} = \text{pH} + \text{TON} + \text{TON}^2 + \text{pH} : \text{TON} + \text{alt}$$

$$\text{salmonids} = \text{pH} + \text{TON} + \text{pH} : \text{TON} + \text{alt}$$

For each global model and biotic indicator / ecosystem service, we produced a set of candidate models with all the possible predictor combinations, using the package ‘MuMin’ (Bartoń, 2014). These models were ranked and weighted based on Akaike Information Criterion (AIC) values. Then, when no single model had an AIC weight > 0.90, we selected the top models for which AIC value differed no more than 2 units from the top model ($\Delta\text{AIC} \leq 2$). In these cases, we derived a weighted mean of the coefficients from the top models where each predictor appeared, using model weights (‘natural average’, Burnham and Anderson, 2002). For each of the top models, we estimated goodness-of-fit and checked residuals to assess the normality, homoscedasticity and absence of spatial autocorrelation assumptions. For linear mixed models, two measures of goodness-of-fit were estimated (Nakagawa and Schielzeth, 2013). Marginal goodness-of-fit (r^2_m) indicates the variance explained just by the fixed factors, while conditional goodness-of-fit (r^2_c) shows the combined variance accounted by fixed and random terms.

Scenario implementation. We created future scenarios with different degree of anthropogenic impact for river ecosystems in Wales. These scenarios were projected to two 10 year periods of time, named as 2030 (2025-2034) and 2060 (2055-2064). The results of the future scenarios were compared to a baseline situation, whose exact temporal definition is specified differently for the long-term and spatial datasets.

For the long-term dataset, we simulated future changes in climate and nitrogen concentration in water. We considered each of the three river types as a different land-use management scenario (acid conifer forest, acid moorland, circumneutral moorland). Thus, for all the simulations, pH was set for each site as their respective 2010-2014 pH baseline mean (after 2010 pH was relatively stable, and recovered after past acidification). We will predict the response of invertebrate abundance and species richness under baseline and future conditions. Climatic baseline was set as 2006-2015, while nitrogen baseline was defined for a different period (2011-2020).

For the spatial dataset, the focus was in changes in nitrogen concentration and pH under each of the MARS scenarios (consensus world, technoworld and fragmented world, see Report Task 2.6). We used baseline climate in all the simulations (rainfall of the wettest

month), although modelled climate was used for nitrogen estimations. Here, we used three sites of the Wye catchment (spatial dataset) representing the upper, middle and lower river section. We will predict the response of species richness and response diversity under baseline and future conditions. Baseline conditions were described for the period 2006-2015.

In order to model the impact of climate change, future scenarios of precipitation and temperature were needed. These were obtained using two different global circulation models (GCMs): the GFDL (Geophysical Fluid Dynamics Laboratory) model, developed by the National Oceanic and Atmospheric Administration (NOAA, US) (Donner et al., 2011), and the IPSL (Institut Pierre Simon Laplace) model, developed by the IPSL Climate Modelling Centre (France) (Dufresne et al., 2013). Daily precipitation and temperature for the Brianne and Wye catchment (spatially averaged) were obtained from these two models forced by two different Representative Concentration Pathways (RCPs), or greenhouse gas concentration trajectories (Moss et al., 2008), the RCP4.5 and the RCP8.5. RCP4.5 describes a mean global warming of 1.4 (0.9 to 2.0) °C for 2046-2065, while RCP8.5 presents a global warming of 2.0 (1.4 to 2.6) °C.

Details about bias correction of climatic data were indicated in Appendix 1.

To predict the flow and nitrogen concentration (total oxidised nitrogen) in the long-term and spatial dataset scenarios, we used INCA-N (Whitehead et al., 1998a) and PERSiST models (Futter et al., 2014a). The INCA model is a process-based model which simulates the main processes related with rainfall-runoff transformation and the cycle and fate of several compounds, such as nitrate, ammonium and phosphorus. PERSiST is a simple and flexible hydrological model especially created to produce input for the INCA family of models. Details about the application of INCA-N in the Welsh catchments are available in Appendices 2 (methodological details), 3 (long-term application) and 4 (spatial application).

These are the assumptions used to build MARS scenarios for the spatial dataset were:

- *Consensus world:*
 - 10% of the grassland was turned into forest land;
 - 30% of arable land was turned into grassland;
 - The nitrogen fertiliser application was decreased by 50%

- The growing season was extended two months due to climate change.
- The effluent flows were increased by 30% due to population growth.
- Baseline acid sulphur deposition, resulting in no changes in pH
- *Technoworld:*
 - 5% of the forest area was turned into grassland;
 - 15% of grassland was turned into arable land;
 - The nitrogen fertiliser application was increased by 15%
 - The growing season was extended two months due to climate change.
 - The effluent flows were increased by 30% due to population growth.
- *Fragmented world:*
 - 10% of the forest area was turned into arable land;
 - 30% of grassland was turned into arable land;
 - The nitrogen fertiliser application was increased by 30%
 - The growing season was extended two months due to climate change.
 - The effluent flows were increased by 30% due to population growth.

Very intense use of fossil energy (coal and unconventional sources) with absence of flue-gas desulphurisation technologies to reduce costs. This would lead to a pervasive and large acid sulphur deposition, which decreases pH (2030: -0.50 pH units / 2060: -0.75 pH units).

6.6.4 Results

Empirical modelling. The biological features of river types included in the long-term dataset responded differently to multi-stress.

Model results for the acid-forest type revealed that TON was the most important stressor, followed by climate, which was significant only in one case (Table 6.27). There was no significant evidence of stressor interactions (Table 6.27, Figure 6.79). However, biological responses to TON and summer rainfall at maximum pH values appeared to differ (violet fitted values in columns two and three in Figures 6.79b and 6.79c). Increased TON was associated with reductions in invertebrate abundance, richness (at all levels), EPT family richness, biotic indexes (BWMP and LIFE) and functional redundancy

(Figure 6.79b). In contrast, higher rainfall during precedent summer was linked only with reduced invertebrate abundance (Figure 6.79c). The most responsive biotic variables for the acid forest type were invertebrate abundance and species richness.

For the acid-moorland, model results displayed significant effects of pH, and climate only on few biotic indicators (Table 6.28). Response diversity decreased with higher summer rainfall. Grazer richness increased at circumneutral pH (Figure 6.80a). The combined opposing effects between pH and precedent summer temperature only affected shredder richness. As Figure 6.80c shows, precipitation had detrimental effects under more acidic conditions (red, yellow and green fitted lines, representing minimum, Q10 and Q50 pH values). However, for circumneutral values precipitation had a positive effect on shredder richness (blue and violet fitted lines, representing Q90 and maximum pH values). There was no evidence of combined effects between pH and TON (Figure 6.80a). The most responsive variables for this river type were grazer richness and shredder richness.

The model results for circumneutral streams showed significant effects of pH and climate on invertebrates (Table 6.29). Surprisingly, pH related negatively with genus and species richness, functional redundancy, shredder richness and grazer richness (Figure 6.81a). More interestingly, increased annual minimum temperature of related with a reduced invertebrate abundance (Figure 6.81c). Increased TON was also related with higher functional richness. There was no evidence of interactions between abiotic states (Figure 6.81). The most responsive variables were species richness, functional redundancy, genus richness and grazer richness.

The results of the spatial modelling showed that pH was the most important spatial stressor, with a strong latitudinal interaction (Table 6.30, Figure 6.82c). pH was positively related with biotic indicators (taxonomic richness, EPT families, BMWP, LIFE, RD and FR), with no evident interaction with TON (Figures 6.82a and 6.82b). At lower latitudes (red: minimum latitude, yellow: latitude Q10 and green: latitude Q50) acidity had a much lower effect on biotic metrics, compared to higher latitudes in North Wales (blue: latitude Q90, violet: maximum latitude). Increased TON values reduced only response diversity (Figure 6.82b), which was the most responsive variable. Spatial and environmental descriptors were also generally important. In particular, rainfall (prec_max) and elevation, in a lesser extent, had a general negative influence in biotic variables. Biotic indicators showed contrasting capacity to detect stressors. Thus, ASPT, shredder richness

and grazer richness were not able to detect either acid or nutrient stress. Response diversity, functional redundancy, species richness, BMWP, EPT family richness, LIFE and genus richness were the most responsive biological variables.

The model results for the ecosystem services reflected different responses for the culturally valued bird, dipper and salmonid juvenile biomass (Table 6.31, Figure 6.83). The bird model showed a significant interaction between pH and TON (Figure 6.83a), with opposing effects. The number of dipper territories tended to increase at circumneutral pH values only at intermediate and high TON levels (green line: TON Q50, blue: Q90, violet: maximum value). Otherwise, pH had a negative influence on bird presence. The model also reflected a non-linear effect of TON, modulated by pH (Figure 6.83b). At acidic and moderate pH values (red: minimum pH value, yellow: pH Q10, green: pH Q50), low TON levels had a positive effect on dipper territories, which turned soon into a detrimental effect at higher TON values. At high pH values (blue line: Q90, violet: maximum pH), the effect on TON on birds was generally positive with a saturation effect at high nutrient levels. Additionally, elevation had a negative effect on dipper presence.

On the other hand, salmonid fish biomass clearly increased at circumneutral pH values (Figure 6.83c), with no evidence of interaction with TON. In addition, elevation had a negative effect on fish biomass.

Scenarios' forecast. The forecasted nitrogen, flow and climate values for each of the land-use types used in the long-term dataset are shown in Appendix (Figures A.8-A.10). Nitrogen is expected to fluctuate around 0.2 mg L^{-1} in upland Welsh streams during simulated future years, showing a slight increasing trend (Figure A.9). Winter and summer rainfall are expected to change little in general (Figure A.10). However, the model GFDL using RCP 8.5 shows that winter rainfall might decrease considerably during the periods 2030 and 2060. Both climatic models show a clear increase of minimum temperature for 2060, except for the GFDL model based on RCP 4.5. The future simulated nitrogen and flow values for the three sites included in the spatial dataset are presented in the Appendix (Figures A.16 and A.17). Nitrogen prediction reveals clear increments under technoworld and fragmented world for the upper and middle Wye

(Figure A.16). Nitrogen concentration is expected to decrease in the consensus world for the middle and low Wye.

Table 6.27 Results of the multi-model inference for acid forest long-term dataset, showing the averaged SES and significance of abiotic states. Goodness-of-fit (r^2) is also shown. See Tables 7.1 and 7.2 to see biotic and abiotic state descriptions. * $p < 0.05$, ** $p < 0.01$, *** $p < 0.001$. Abiotic states with $p < 0.05$ are in bold.

Biotic state	Intercept	pH	TON	prec_sum	pH : TON	pH : prec_sum	r^2
<i>abun</i>	20.47***	-2.60	-3.39**	-2.30*	3.00	0.84	0.56
<i>fam.ric</i>	10.77***	0.21	-1.06*	-0.52			0.21
<i>gen.ric</i>	13.52***	0.31	-1.45**	-0.79			0.27
<i>spp.ric</i>	14.80***	0.33	-1.58**	-1.05	1.03		0.31
<i>ept</i>	6.39***	0.28	-0.39*	-0.15	-0.02		0.18
<i>bmwp</i>	63.19***	0.99	-5.11*	-2.57			0.21
<i>life</i>	27.66***	-0.17	-2.89*	-0.79			0.18
<i>aspt</i>	5.97***	0.00	0.09	0.09			0.02
<i>RD</i>	0.31***	0.01	-0.01	-0.02			0.01
<i>FR</i>	3.29***	0.01	-0.23*	-0.06			0.17
<i>shr</i>	6.24***	-0.20	-0.42	-0.15			0.09
<i>gra</i>	0.35***	0.00	-0.06	-0.08			0.01

Table 6.28. Results of the multi-model inference for acid moorland long-term dataset, showing the averaged SES and significance of abiotic states. Goodness-of-fit (r^2) is also shown. See Table 7.1 and 7.2 to see biotic and abiotic state descriptions. * $p < 0.05$, ** $p < 0.01$, *** $p < 0.001$. Abiotic states with $p < 0.05$ are in bold.

Biotic states	Intercept	pH	TON	prec_sum	pH : TON	pH : prec_sum	r^2
<i>abun</i>	16.43***	-1.10	0.46	-1.27	-2.79	1.20	0.17
<i>fam.ric</i>	15.24***	0.08	0.68	-0.65			0.09
<i>gen.ric</i>	17.11***	-0.40	0.95	-0.8		0.71	0.10
<i>spp.ric</i>	18.31***	-0.38	1.02	-0.72		0.91	0.08
<i>ept</i>	8.81***	0.07	0.02	-0.10			0.00
<i>bmwp</i>	85.29***	1.55	2.06	-1.66			0.01
<i>life</i>	35.78***	-0.53	2.04	-1.38			0.08
<i>aspt</i>	5.6***	0.10	-0.13	0.12			0.10
<i>RD</i>	0.5***	0.01	0.03	-0.05*			0.18
<i>FR</i>	3.55***	-0.21	0.21	-0.12	0.02	0.13	0.13
<i>shr</i>	4.84***	-0.53**	0.09	-0.28		0.40**	0.48
<i>gra</i>	1.7***	0.64***	0.22	-0.04	0.31	0.22	0.55

Table 6.29 Results of the multi-model inference for circumneutral moorland long-term dataset, showing the averaged SES and significance of abiotic states. Goodness-of-fit (r^2) is also shown. See Table 7.1 and 7.2 to see biotic and abiotic state descriptions. * $p < 0.05$, ** $p < 0.01$, *** $p < 0.001$. Abiotic states with $p < 0.05$ are in bold. We removed outlier data from year 1992.

Biotic states	Intercept	pH	TON	tmin	pH : TON	pH : tmin	r^2
<i>abun</i>	27.81***	-1.39	-0.13	-2.40*			0.20
<i>fam.ric</i>	21.88***	-1.21	0.28	-0.67	-0.98	-0.50	0.21
<i>gen.ric</i>	27.75***	-3.00**	0.27	-0.92		-0.20	0.32
<i>spp.ric</i>	31.20***	-3.57**	0.64	-1.15		-0.37	0.35
<i>ept</i>	3.66***	-0.09	0.01	-0.02		-0.06	0.11
<i>bmwp</i>	123.37***	-7.01	-0.74	-2.08			0.15
<i>life</i>	47.38***	-2.49	0.77	-2.19		1.10	0.17
<i>aspt</i>	5.66***	0.04	-0.13	0.04			0.15
<i>RD</i>	0.61***	-0.04	0.04*	-0.001	-0.01		0.22
<i>FR</i>	5.61***	-0.59***	0.01	-0.15			0.34
<i>shr</i>	2.54***	-0.10*	-0.01	-0.06		-0.03	0.22
<i>gra</i>	7.92***	-1.09**	0.23	-0.11			0.26

Table 6.30 Results of the multi-model inference for the spatial dataset (2012-13), showing the averaged SES and significance of abiotic states. Goodness-of-fit (r^2) is also shown. See Tables 7.1 and 7.2 to see biotic and abiotic state descriptions. * $p < 0.05$, ** $p < 0.01$, *** $p < 0.001$. Abiotic states with $p < 0.05$ are in bold.

Biotic states	Intercept	pH	TON	pH : TON	alt	prec_max	lat	lon	pH : lat	r^2
<i>fam.ric</i>	3.34***	0.13	-0.02		-0.09		-0.11*	-0.16**	0.08*	0.51
<i>gen.ric</i>	3.25***	0.13	-0.05		-0.09	-0.17***	-0.10*	-0.15**	0.10**	0.50
<i>spp.ric</i>	3.34***	0.13	-0.02		-0.10	-0.18***	-0.10*	-0.16**	0.09*	0.51
<i>ept</i>	2.08***	0.04	-0.02		0.05	-0.17***	-0.12**	-0.16**	0.07*	0.51
<i>bmwp</i>	114.71***	6.25	3.27		-6.68	-21.74***	-14.11**	-14.97**	7.37*	0.53
<i>life</i>	40.03***	1.91	-1.46		-0.43	-7.59***	-3.53*	-3.10	3.24*	0.49
<i>aspt</i>	5.68***	-0.14	0.12		-0.15	-0.09	-0.11	-0.07		0.06
<i>RD</i>	0.51***	0.03	-0.05*	0.0001	-0.04	-0.10***	-0.05*	-0.01	0.03*	0.60
<i>FR</i>	2.29***	0.13*	0.01		-0.04	-0.16***	-0.09*	-0.15**	0.08*	0.55
<i>shr</i>	2.91***	0.61	0.34		-0.21	-0.62*	-0.42	-0.42	-0.02	0.55
<i>gra</i>	13.30***	1.01	0.59		-	-1.34*	-0.50	-1.96**	0.79	0.55
						2.33***				

Table 6.31 Results of the multi-model inference for the ecosystem service dataset, showing the averaged SES and significance of abiotic states. Goodness-of-fit of the fixed (r^2_m) and fixed and random (r^2_m) terms are also shown. See Tables 7.1 and 7.2 to see biotic and abiotic state descriptions. * $p < 0.05$, ** $p < 0.01$, *** $p < 0.001$. Abiotic states with $p < 0.05$ are in bold.

Ecosystem services	Intercept	pH	TON	TON ²	pH : TON	alt	r^2_m	r^2_c
Dipper	-1.56	0.90*	-2.70	-0.22*	0.39*	-0.01**	0.19	
salmonid biomass	6.16***	0.62***	-0.32		0.02	-0.31*	0.36	0.66

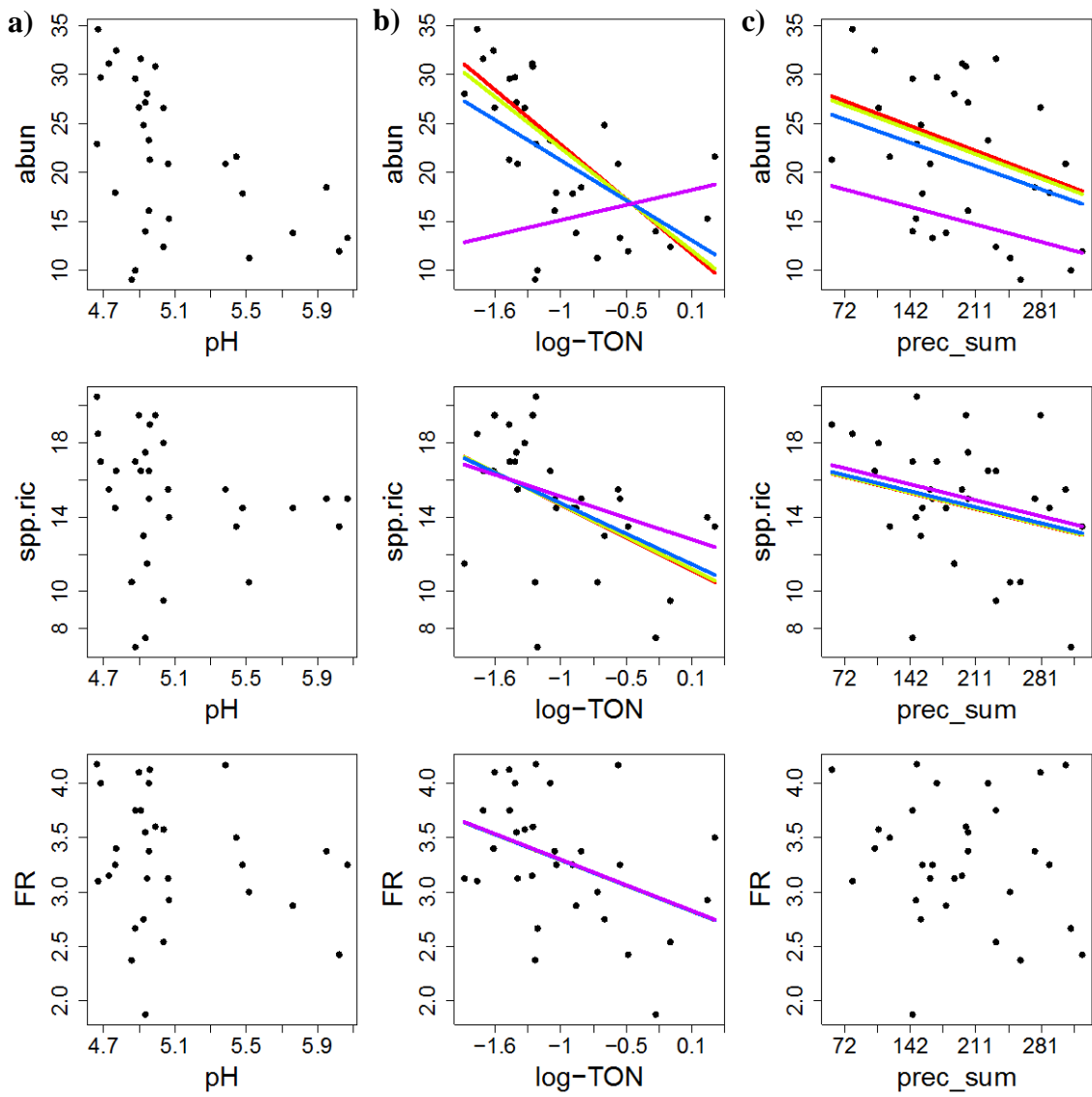


Figure 6.79 Plots showing biological responses to multi-stress at acid forest river type. The interaction between pH and TON (a), TON and pH (b) and precipitation and pH (c) are shown. Lines represent fitted values at different levels of the interacting stressor non-shown in the abscise axis (red: minimum value, yellow: Q10, green: Q50, blue: Q90 and violet: maximum value). See Table 7.3 for more info.

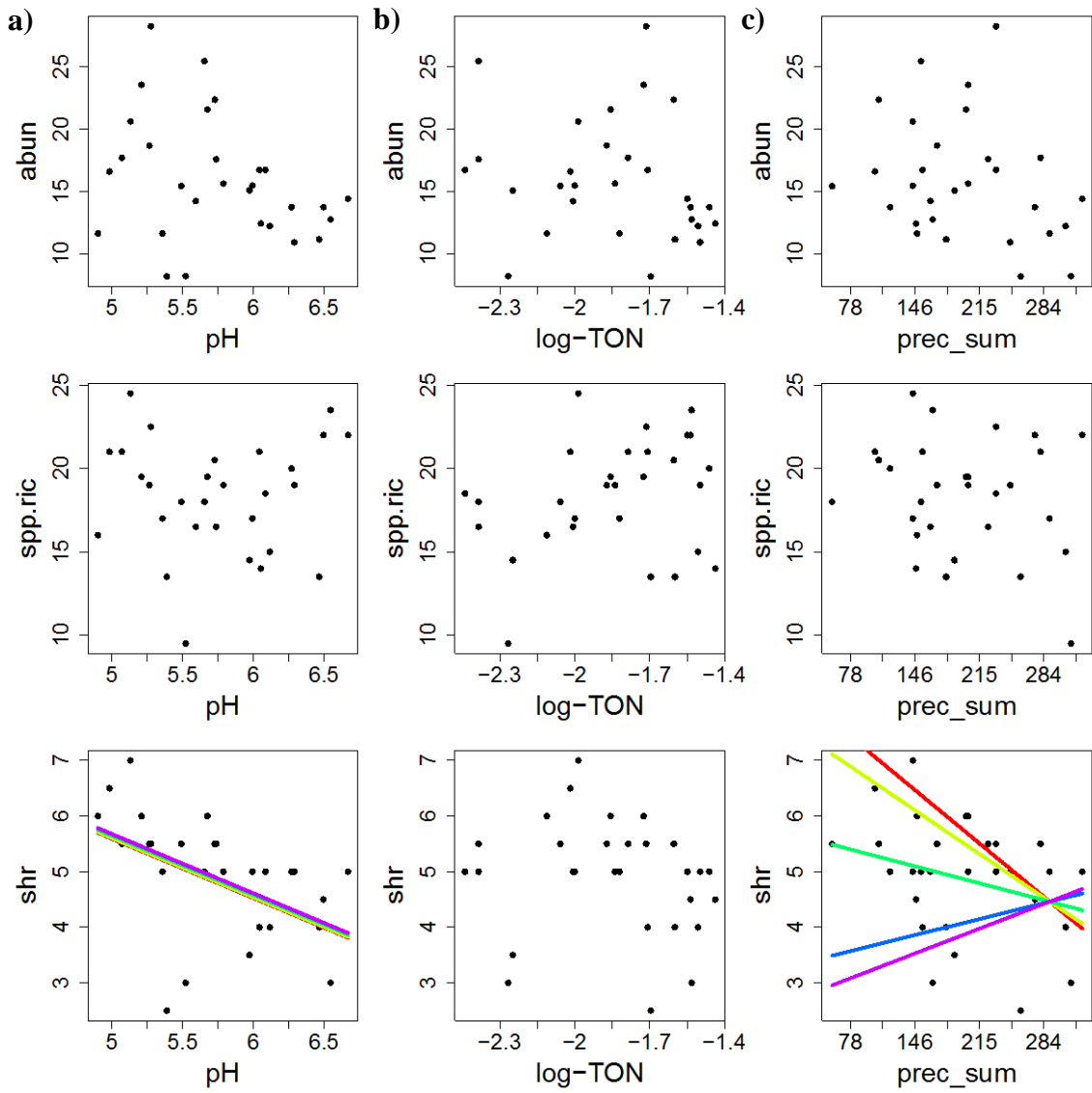


Figure 6.80 Plots showing biological responses to multi-stress at acid moorland river type. The interaction between pH and TON (a), TON and pH (b) and precipitation and pH (c) are shown. Lines represent fitted values at different levels of the interacting stressor non-showed in the abscise axis (red: minimum value, yellow: Q10, green: Q50, blue: Q90 and violet: maximum value). See Table 7.4 for more info.

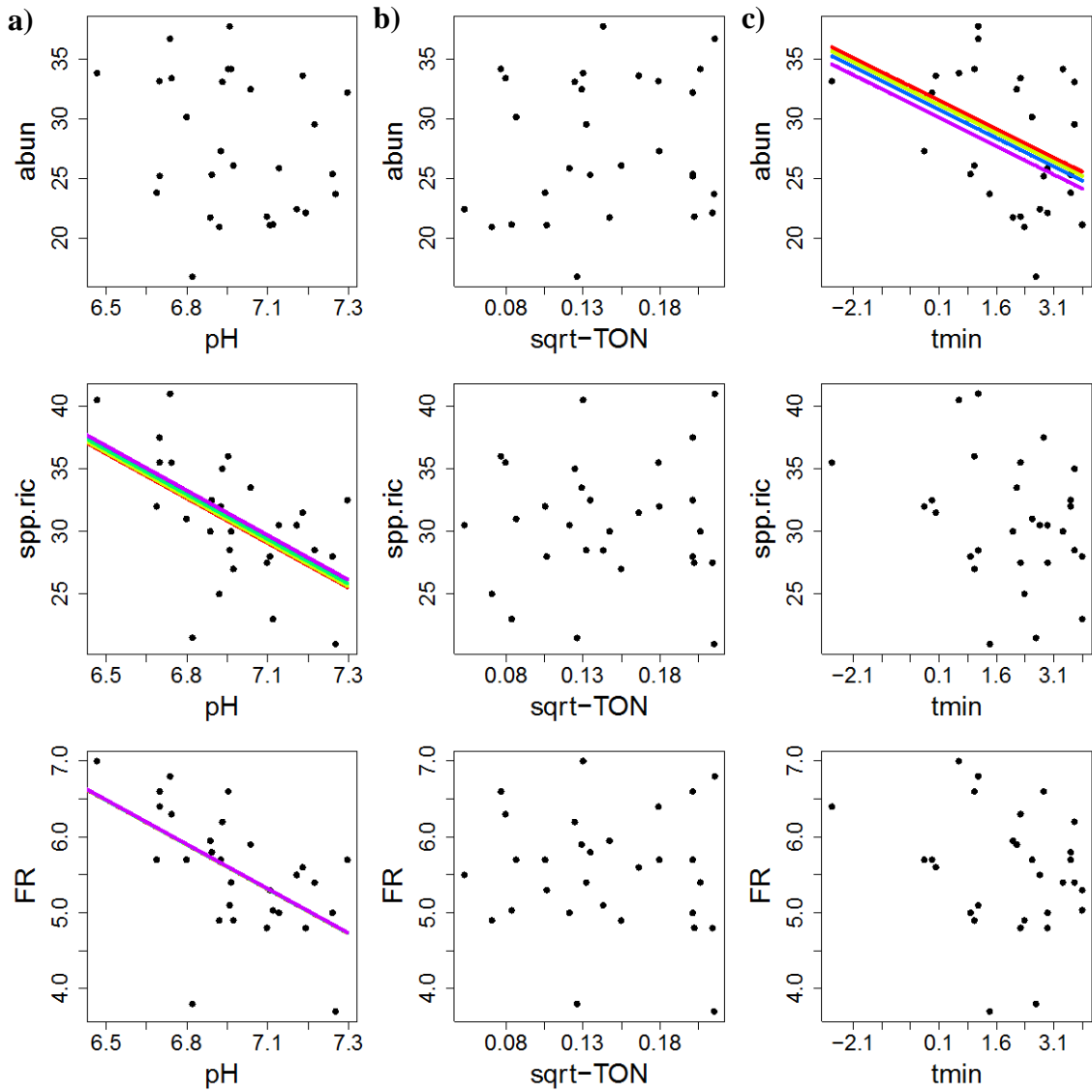


Figure 6.81 Plots showing biological responses to multi-stress at circumneutral moorland river type. The interaction between pH and TON (a), TON and pH (b) and minimum temperature and pH (c) are shown. Lines represent fitted values at different levels of the interacting stressor non-showed in the abscise axis (red: minimum value, yellow: Q10, green: Q50, blue: Q90 and violet: maximum value). See Table 7.5 for more info. We removed outlier data from year 1992.

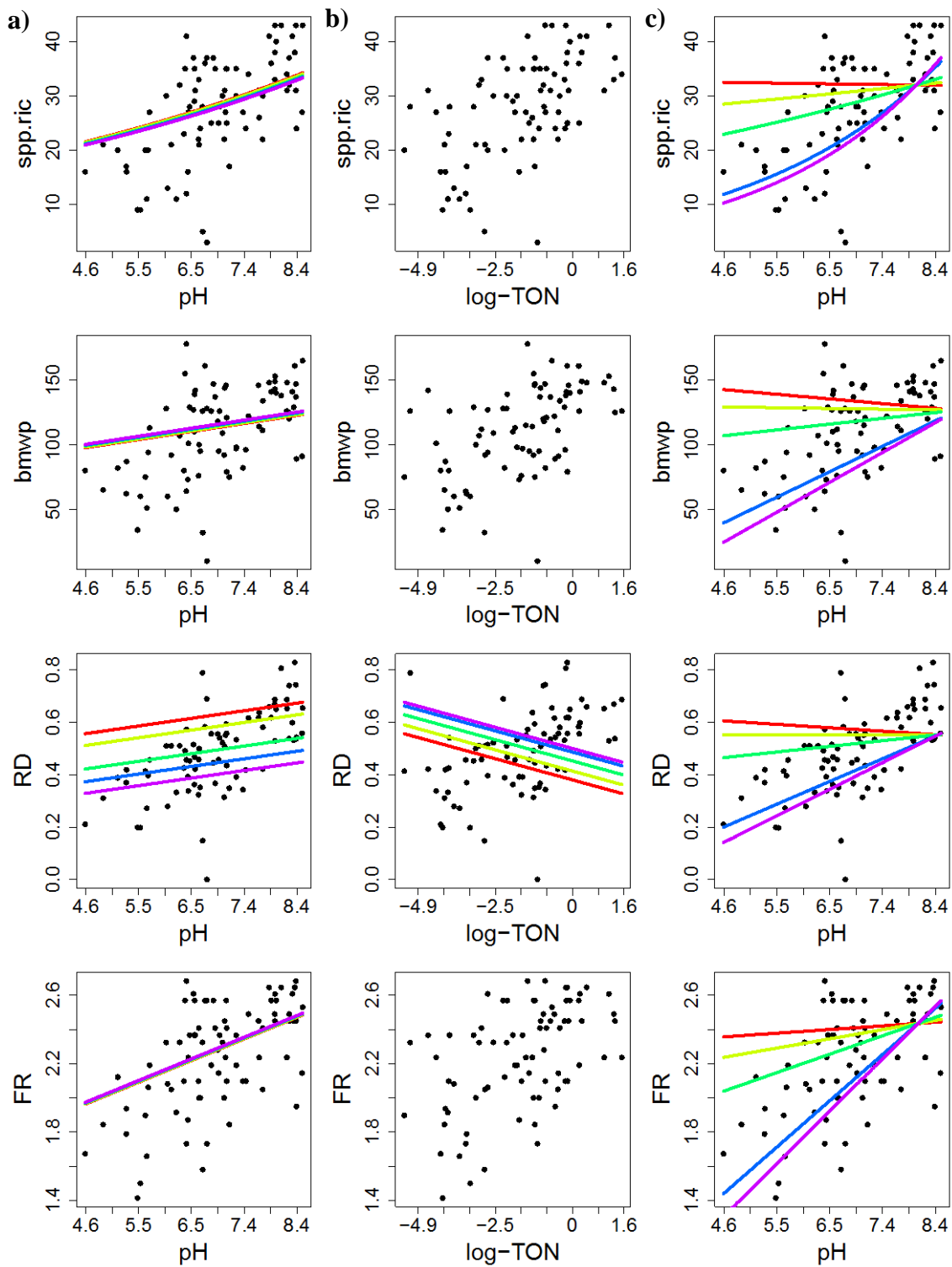


Figure 6.82 Plots showing biological responses to multi-stress in the spatial dataset. The interaction between pH and TON (a), TON and pH (b) and pH and latitude (c) are shown. Lines represent fitted values at different levels of the interacting stressor non-showed in the abscise axis (red: minimum value, yellow: Q10, green: Q50, blue: Q90 and violet: maximum value). See Table 6 for more info.

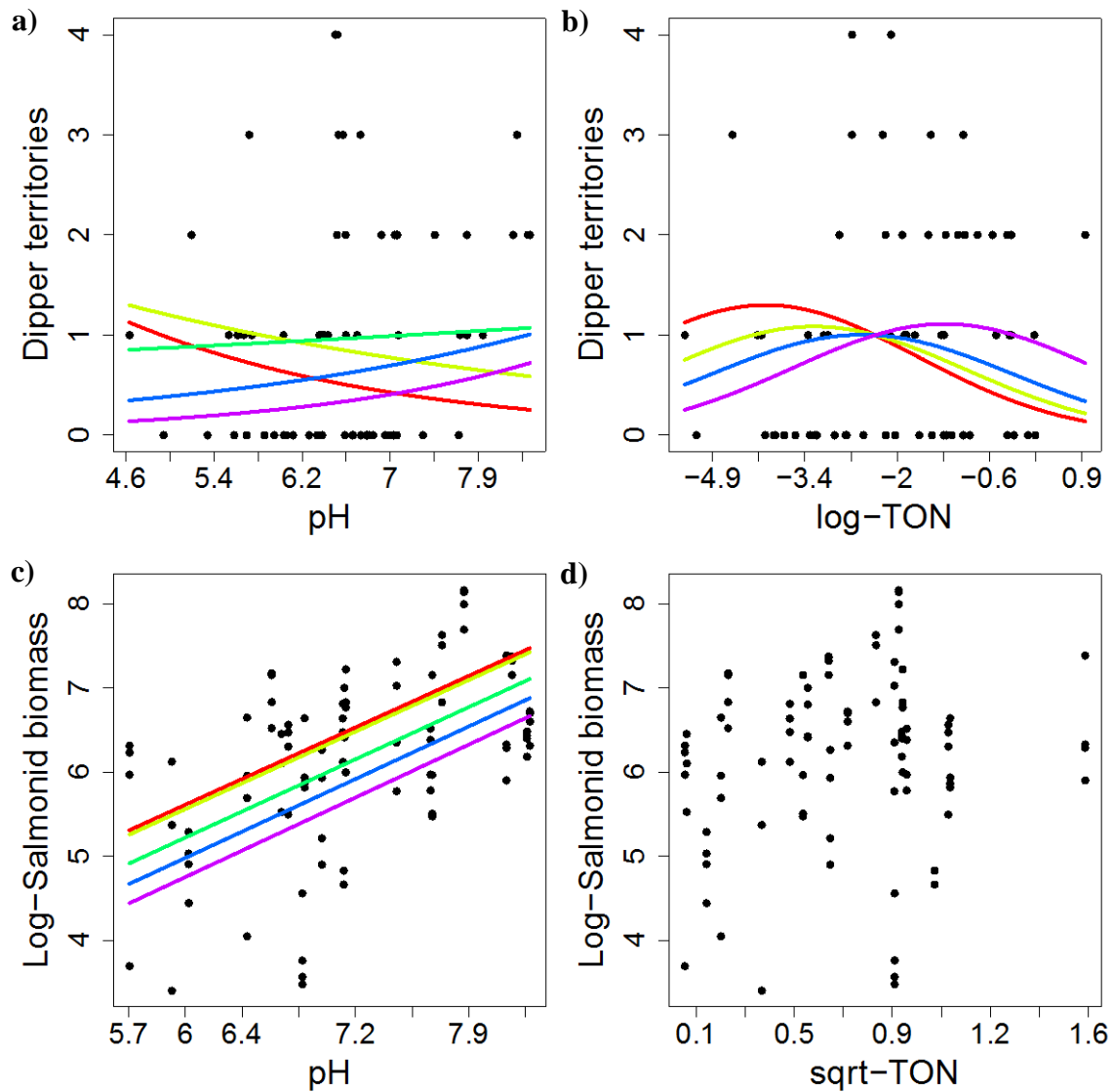


Figure 6.83 Plots showing ecosystem services' responses to multi-stress in the spatial dataset. The interaction between pH and TON (a, c) and TON and pH (b, d) are shown. Lines represent fitted values at different levels of the interacting stressor non-shown in the abscise axis (red: minimum value, yellow: Q10, green: Q50, blue: Q90 and violet: maximum value). See Table 7.7 for more info.

For the long-term dataset, invertebrate abundance seems to change little in the future scenarios, especially during the 2030 period (Figure 6.84). It shows an evident decrease only in the circumneutral moorland land-use type during the 2060 period. In this case, the GFDL climatic model shows that any of the scenarios would lead to a decreased abundance of invertebrates, whilst the IPSL climatic model points to abundance reduction only under technoworld and fragmented world scenarios. The results for species richness are shown in Appendix (Figure A.11), revealing just small changes.

The future predictions for the spatial dataset reflected clear patterns in relation with the longitudinal position in the river and future scenario considered (Figure 6.85). The prediction results for species richness are shown in Appendix (Figure A.18). The upper Wye site seems to reflect a substantial reduction in response diversity under technoworld and fragmented world scenarios for both 2030 and 2060 periods, which is greater in the latter scenario. However, the middle site shows a similar but less pronounced pattern of response diversity decline under technoworld and fragmented world scenarios, and an increase under the consensus world scenario for both periods. The lower Wye is expected to change little respect to current conditions under any of the scenarios considered. Despite the low magnitude of the changes in the lower Wye section, it is remarkable that it is expected an increase in response diversity under any of the scenarios considered. Species richness declined only in the fragmented world scenario in the three Wye sections.

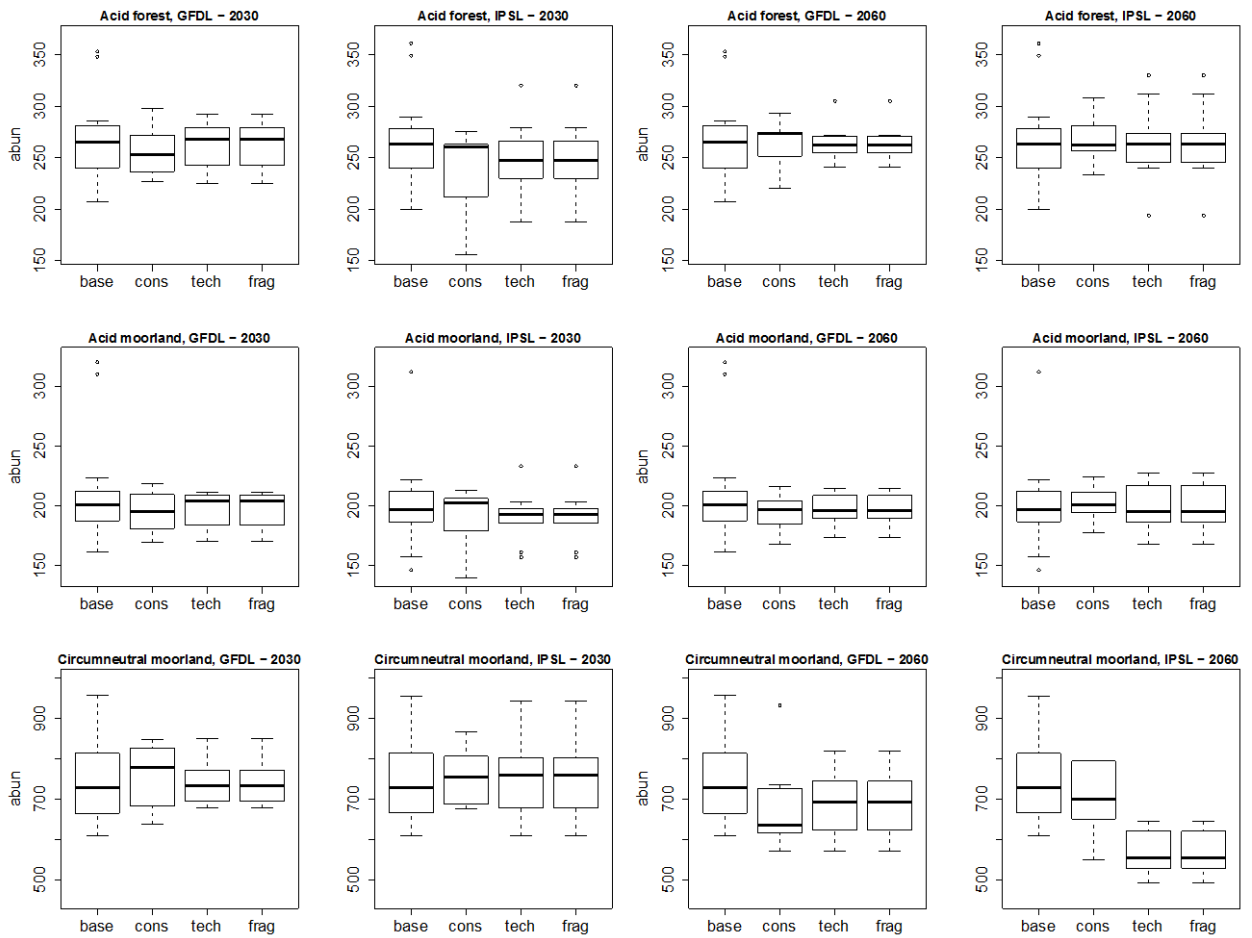


Figure 6.84 Projected changes for invertebrate abundance (abun) in the acid forest, acid moorland and circumneutral moorland river types (long-term dataset) for the baseline period (base), 2030 and 2060, and for each of the climatic models (GFDL, IPSL) and scenarios (cons: consensus world, tech: technoworld and frag: fragmented world).

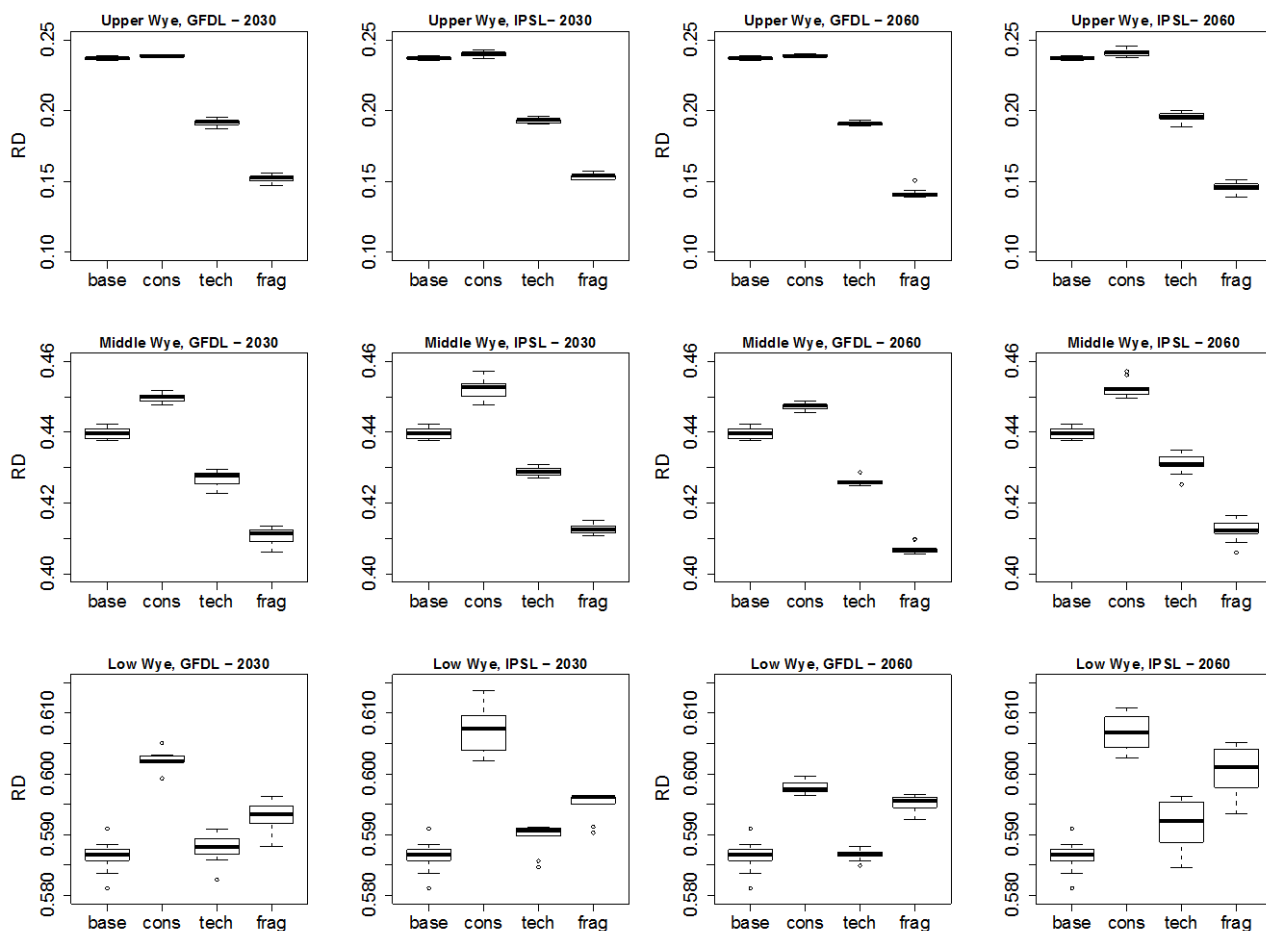


Figure 6.85 Projected changes for invertebrate response diversity (RD) in the upper, middle and low Wye catchment for the baseline period (base), 2030 and 2060, and for each of the climatic models (GFDL, IPSL) and scenarios (cons: consensus world, tech: technoworld and frag: fragmented world).

6.6.5 Discussion

Empirical Modelling. Our results suggest that past acidification has not generally interacted with nutrient enrichment or climate change in the Welsh uplands. Rather, these three stressors may display isolated or additive effects depending on the spatial and temporal scale studied.

For several post-industrial decades, acidification affected water bodies in regions with base-poor lithology, such as those in Northern Europe. In Wales, half of the river network was severely affected by intermittent or chronic acidification (pH ranging 4.0 – 5.7) (Edwards et al., 1990). Currently, and despite a great chemical improvement after severe reductions in non-marine acid deposition, the biological response is slow and incomplete.

Previous studies pointed to episodic acidification (Kowalik et al., 2007), land-use (Ormerod and Durance, 2009) or climate (Durance and Ormerod, 2007; Ormerod and Durance, 2009) as potential forces delaying the biological recovery. Here, we found that the three river types experiencing pH recovery in the long-term dataset responded differently over time. In the acid forest type, declines in abundance, taxonomic richness and functional redundancy were attributed apparently to nutrient enrichment, which seemed to offset the effects of pH increase - from 4.6-5.0 during the 80s to 5.4-6.0 since 2010. Also, summer precipitation seemed to delay biological recovery. For the acid moorland type, few biological metrics responded to the increase from pH values of 5.0-5.3 to pH>6.0 since 2010. This lack of response could be caused by the contrasting trends between functional groups of invertebrates. For example, grazer richness increased following the pH recovery but shredders showed a more complex pattern. The interaction between pH and summer rainfall, led to decreased shredder richness under acidic conditions and large rainfall, and increased number of shredding species when pH was higher. Finally, in the circumneutral moorland we found two type of responses. Increased minimum temperature seems to be associated with a reduction in invertebrate abundance. However, and surprisingly, increased pH was related with decreased taxonomic richness, functional redundancy, shredder and grazer richness. Apparently, there is no biological basis to support this result considering the maximum pH values observed (pH 7.3), pointing to a spurious relationship. A potential hypothesis might be that the temporal co-variation between pH and temperature, both increasing during last three-decades at the same time that abundance and other biodiversity features declined.

Spatial modelling revealed that pH is the most relevant variable explaining biological differences among locations in upland Wales, as reflected previously for acid sensitive regions in UK (Buckton et al., 1998; Monteith et al., 2005) and other northern areas (e.g., Rosemond and Reice, 1992; Petrin et al., 2008). Nonetheless, we detected that the way in which acidity affects biological communities seems to be different in Mid and North Wales, as reflected by the interaction between pH and latitude, i.e. sites placed in Mid Wales tend to be less affected by acidic pH. A potential explanation for this pattern could be the differences in lithology between the igneous north and the sedimentary rocks of mid Wales. The fact that most of the sites exhibiting nitrogen enrichment were confined to the lower Wye (South East Wales), could have limited our analysis. First, the waters of the lower part of the Wye generally show pH >7.5, while acidic waters in other parts

of Wales are usually nutrient poor. For this reason, it is unlikely to find interactions between pH and nutrients in this dataset. Furthermore, the fact that nutrient enrichment were restricted to lowland, circumneutral sites in the Wye system might also affect to our capacity to distinguish between anthropogenic and natural variation, which could mask the effect of nutrients on invertebrates. Most of the biotic features studied responded negatively to increased winter rainfall, probably reflecting higher peaks of flow during winter in those sites with larger rainfall.

Future scenarios. The results from the simulated future scenarios suggest that land-use and longitudinal position seem to be critical in mediating the response to future increase in anthropogenic pressures. Thus, only circumneutral moorlands could be significantly affected by climate change or nutrient enrichment. Sites affected by past acidification (acid forests and moorlands) seem to be less affected by climate change as detected previously (Durance and Ormerod, 2007). One potential explanation might relate with the capacity of acidification to filter community toward a more tolerant and resilient assemblage able to cope with novel stressors (Buchwalter et al., 2008). The slight increase in nitrogen predicted for the three upland types seems to not be substantially damaging compared to the effect of climate change.

On the other hand, uplands could be more sensitive to nutrient enrichment or potential acidification, compared to lowlands as reflected in the scenarios modelled for the Wye system. In fact, for the upper part of the Wye, our models predicted a 4-fold or 8-fold increase in nitrogen concentration under the technoworld or fragmented world scenarios. The middle section could be also severely affected. The combination of increased nutrients and reduced pH (fragmented world) seems to affect more dramatically to the diversity of response traits of the invertebrates, than their taxonomic diversity. A reduced diversity of response traits could result in a less stable and resilient community (Hooper et al., 2005). On the other hand, the restorative land-use changes simulated for the consensus world seems to have little impact respect to the biological baseline conditions, despite the projected reductions in nitrogen. These results might advocate for more ambitious measures if we aim to produce a real recovery of the sites severely impacted by nutrient enrichment.

Implications for MARS project. The combined use of long-term and spatially extended data resulted in a powerful strategy to analyse multiple stressors. Otherwise, the use of temporal or spatial data in isolation might yield site-specific responses or too static pictures. Fortunately, the increased effort in biomonitoring across Europe during the last two decades have resulted in robust databases covering both time and space. However, biomonitoring data are still fragmented and unavailable for systematic analysis in most cases, despite being funded with public national or EU money. Therefore, it is necessary to request a public effort to make them ready and available for further and refined analysis to provide a more comprehensive picture of multi-stressor situation globally.

Another limitation for multi-stressor analysis is the current co-occurrence of anthropogenic and natural impacts, compared to which is expected to happen in the future. For example, we found in Wales that catchments exposed to past and current acidification are usually nutrient poor, probably as a result of being less exposed to agriculture or pastures. However, land-use intensification to secure food provision might be a plausible scenario as a result of oil shortages or political changes, which increase food importation costs. Then, acid sensitive sites might be exposed nutrient enrichment in a near future as revealed by the most intensive scenarios (technoworld and fragmented world). To address this challenge, the use of experimental mesocosms is becoming a successful strategy, especially when they are guided by biomonitoring program experiences (e.g., Matthaei et al., 2010).

Overall, among the biotic indicators used in both modelling exercises, species richness, genus richness, response diversity and functional redundancy were generally the best indicators. In particular, response diversity and functional redundancy were the most responsive variable in terms of goodness-of-fit in the spatial dataset. Also, the use of functional groups helped to disentangle some complex recovery patterns in the long-term dataset. Functional indicators has been regarded as promising tools in biomonitoring compared with traditional taxonomic approaches (Bruno et al., 2016a). In addition, these measures can reduce identification effort (genus level) and provide predictive capacity respect to changes in ecosystem function (e.g., an increase in shredder richness can increase litter decomposition). Our results support the use of a combination of taxonomic and functional measures for a better bioassessment of water bodies.

6.6.6 Conclusion

- The outcomes of the long-term analysis point to land use exerting a strong influence in the response of biological communities to multiple stressors in the long-term
- Acid forest streams were impacted by nutrients and summer rainfall, which offset pH recovery since the 80s
- pH recovery in acid moorland streams had contrasting effects, resulting in increased grazers and a complex response of shredders
- Circumneutral moorland streams were affected by the increase in minimum temperatures, which reduced invertebrate abundance
- pH is the main anthropogenic driver explaining spatial differences in invertebrate communities and ecosystem services (bird occurrence and salmonid biomass) across upland Wales
- The results of the spatial analysis suggest that past acidification and land-use do not have combined effects. Instead, they showed additive effects on invertebrates and the ecosystem services considered
- Trait-based invertebrate metrics seem to provide novel and complementary information about multi-stressor responses
- The projection of the future scenarios showed that circumneutral moorlands are sensitive to climate change, while acid sensitive uplands may experience biological impairment due to nutrient enrichment and future re-acidification.

7 Overall

7.1 Multiple stressors at the basin scale

The modelling undertaken across the study basins allow us to have an understanding of the trends displayed by the data gathered at the various case-studies, encompassing a global view of European riverscapes. Overall, the studies highlight a general difficulty to identify significant pair-wise multi-stressor interactions, even if considering that suitable data is not always available.

The significance and strength of the interactions revealed by empirical data treatments also depend on the length of the environmental and disturbance gradients displayed by

the data, in fact, enough gradient is needed to obtain good responses, as was shown in the Elbe basin case, or a proper scale of disturbance to fit the time scale of the biotic response, as was shown in the Thames basin study. Therefore, some guidance and basic requirements are needed to detect multi-stressor trends and treat the data, for each basin, in order to account for the multiple stressor interactions. In other words, it is not easy to post hoc detect interactions based on prior monitoring schemes.

The multi-stressor interactions were addressed using a common methodology of a set of empirical models including correlation analysis, general linear models, random forest and boosted regression trees allowing for interpretable common outputs. Abiotic states showed a moderate to high capacity to explain changes in biotic indicators and similarly predict changes in ecosystem services indicators. In Otra case study, SO_4 concentration (the main driver of pH) was found to be the single most important predictor of salmon abundance. At Vansjø case study, on the other hand, temperature and total phosphorus were found to have a synergistic influence on phytoplankton biomass. Nevertheless, few significant multiple-stressor interactions were found, in spite of all biological elements and metrics being investigated (26 significant interactions in all basins: 11 antagonistic positive or negative, 14 synergistic and 1 additive). Indices/combined and trait based metrics were generally more responsive to multi-stressor combinations than sensitivity or tolerance metrics.

In some case studies it could be clearly demonstrated multi-stressor interactions, e.g. temperature and nutrient stress for fish abundance in Regge and Dinkel; however, in other cases, pair-wise interactions could be identified as significant but the interaction type could not be defined, e.g. water residence time ratio x total phosphorus for Lower Danube. In many cases, however, no interactions could be identified, e.g. in Beysehir and Pinios case studies. It is clear that interaction signaling (type and direction) vary a lot across basins, even for similar biological indicators or stressor combinations. In Welsh uplands case study, acidification has not generally interacting with nutrient enrichment or climate change. Rather, these three stressors may display isolated or additive effects depending on the spatial and temporal scale studied.

Interactions were searched for, in each case study, using unique combinations of indicators, sole process-based or empirical based modeling, or both, in a search for best predictive results. The Welsh uplands case study used combined long-term and spatially

extended data, which resulted in a powerful strategy to analyse multiple stressors. This seems to indicate that for each basin, a combination of ecological expertise and modeling skills are needed, in order to obtain the trends of ecological status' response that have to be delivered to the water administration in order to guide the PoM. Multi-pressure interactions also seem to be indicator-specific and therefore, the parameters that better illustrate or predict multi-stressor processes should be prioritized in the monitoring.

An increase in the number of significant interactions seem to depend also on the existence of large empirical biological data sets, e.g. 7 significant interactions in the Ruhr basin. Although responses and interactions were found for all WFD biological elements, many come from macroinvertebrate traits; nonetheless, this trend may simply reflect the available data for empirical models' use.

A large number of these significant interactions detected by the empirical data treatments were strongly affected by natural variables such as basin size, fish zonation, or the natural vegetation cover of the basin. For example, in Welsh uplands, catchments exposed to acidification are usually nutrient poor, probably as a result of being less exposed to agriculture or pastures, however, land-use intensification to secure food provision may result in acid sensitive sites exposed to nutrient enrichment in a near future as revealed by the most intensive scenarios (Techno world and Fragmented world). In Sorraia, the strongest relationship with biological indicators was natural environmental variability, followed by land use variables, and then hydrological and nutrient variables. In fact, frequently in river case studies, land use variables/stressors (likely as proxies of multiple stressors in their own), have stronger relationships with biological indicators than single hydrological and nutrient stressors.

No multi-stressor interactions were found for indicators of ecosystem services, in the case studies where these were studied.

7.2 Scenarios of change

Scenario changes were studied using either empirical or process based modeling, or a combination. Though the three scenarios were pre-defined (see this Deliverable, chapter 3), many storylines were applied essentially using land use changes, with or without temperature increases. For example, in Lake Vörtsjärvi case study, a predicted decrease

in flow caused an increase in cyanobacteria biomass and a probable decline in rotifer biomass. Conversely, both Vansjø and Mustajoki case studies point to increasing dissolved organic carbon, and its effect on water colour, as a feature with possible effects on algal biomass or macrophyte growth. Both Vansjø and Lepsämänjoki case studies point to the dominant effect of land-used change on phytoplankton biomass, overriding the effect of climate.

In most case studies, storylines were downscaled to include different suites of parameters, therefore basin specificities, such as altered shade or increased water abstraction in Thames basin. This downscaling is interesting from the basin management point of view and was frequently done following stakeholder's interests and comments. As a result, a possibility of a joint comparison between basins is limited.

Some interesting conclusions arose at the local level, for example, in Regge and Dinkel basins a synergistic effect was detected when water temperature was predicted to be higher when combining climate change and storylines than the sum of the single effects of climate change and storyline scenarios. In some cases, it was possible to show how measures acting at the landscape level such as natural forestation, would mitigate global changes (Ruhr basin). However, in Welsh catchments, the results from the simulated future scenarios suggest that land-use and longitudinal position are critical in mediating the response to future increase in anthropogenic pressures, and only circum-neutral moorlands could be significantly affected by climate change or nutrient enrichment. Also, interactions between water compartments could be pointed, such as the relative dominance of groundwater components in certain scenarios (Odense case study). Scenarios projection combined with storylines and indicators' response enabled to see the possibility of extreme events of deterioration, for example the water quality in Thames.

Scenario and storyline modelling, and in a sense also the related variations in land and water uses, was shown as very interactive. Taken separately, it is impossible and even nonsensical to model all stressors, in fact, the analysis of combinations of measures profits the understanding of multi-stressor gradients. Empirical modelling suffers from some limitations in the projections for the future, when all relevant variables in need are considered (e.g. the Drava case study), however not all major processes of interest are necessarily covered by the process-based modeling (e.g. lack of precise flow routing for Regge and Dinkel or lack of silica dynamics for Elbe case studies). Clearly,

comprehensive and robust modeling is needed to decrease the uncertainty in the results and prospect new responses.

In many aspects, the storylines used to project future responses already trace what will happen under certain scenarios of change, either negative evolution or improvement through land use or other changes. In some cases, more pessimistic scenarios show drops in water resources below minimum management level, e.g. Beysehir case study, profoundly affecting the ecosystem and the services it provides. Similarly, in other case studies, it was shown the unsustainability of the present land use; in the Sorraia case study, the implementation of the measures in the storyline of the strictest climate scenario shows that irrigation activities can only continue by adopting optimum farming practices, with the application of a right/less amount of fertilizer and water to irrigate.

Climate-mediated changes, especially in flow and runoff, were shown to be major drivers of pollutants in Mediterranean rivers, notably N, e.g. Pinios case study, however in this case the result is decreasing N concentrations in the river through runoff. Both the Techno and the Fragmented Worlds generally yielded decreases in the quality displayed by biological indicators, especially for the farthest away period, but in general the Consensus World indicates a slight improvement in biological metrics (e.g. ASPT in Pinios case study). The Sorraia case study also showed a clear decrease in water availability through climate change, resulting in alterations in sediment and nutrient loads, but only a mild impact in the ecological status, or no impact at all considering the Consensus World storyline. Similar results were obtained in other Mediterranean river basins.

For most case studies, the spatial indicators for ecosystem services represent only a first spatially explicit attempt to assess how global changes affects them. In the Sorraia basin case-study, the annual average water provision, nutrient purification capacity, ecological status classification and quality of freshwater for angling were used as proxy services indicators. However, the ecological status presented an opposing interaction term (altitude X % urban upstream), which resulted in a mild future reduction of the number of Good and Very Good sites; and the quality of freshwaters for angling presented an interaction effect where the % of agriculture area in the upstream catchment is dependent of the distance to source.

7.3 Last notes

This report includes an enormous amount of data analyses directed towards river basin management and ways to understand the effects of multiple stressors. Each basin addressed this issue according to its specific conditions prevailing, either environmental or as possibilities of data treatment, extensively and singularly described at the core of this report (section 4, 5, and 6). Additionally, basin leads have made thorough synthesis and pointed out key-results (see Mars Regional Reports D4.1-1, D4.1-2 and D4.1-3 available at the Mars site). However, the sensitivity of a specific biotic or service response variables to particular stress combinations, across groups of basins and case studies, has not been attempted yet and will be the focus of the forthcoming WP4 actions and Deliverables. This Deliverable reports the raw material, single basin case-studies, that will be the building blocks of Deliverables to come.

All case-studies, one way or the other, elaborated over the implications of the results to river basin management and the delineation of the programs of Measures. Therefore, the contents of the individual case study reports represent an important contribution for water management and stakeholders, in the line of improving WFD goals. Working at the larger scale of the regions may also allow finding consistent patterns that can help target relevant restoration measures. In this context, it is very important to describe and explain the implications of these results at the river basin level and to water management people involved. For example, it was demonstrated that basins from the Northern region with agricultural activities, have the potential to improve water quality and overcome the detrimental effect of climate change by implementing a judicious basket of measures, notably reverse land use toward an overall reduction of agricultural surfaces, or by implementing “smarter” agricultural activities. For Southern basins, the variations in water availability will determine the biological responses, and determine the programs of measures needed for ecological status improvement, under different climate change scenarios.

Overall, multi-pressure interactions found, seem to be indicator-specific, water-body specific and regional-specific. Yet, the large amount of data and data treatments gathered in Mars case studies will now be used to appraise cross-case commonalities and trends, to be consequently used in water management and ecological status improvement.

Overall, multi-pressure interactions found, seem to be indicator-specific, water-body specific and regional-specific. Yet, the large amount of data and data treatments gathered in Mars case studies will now be used to appraise cross-case commonalities and trends, to be consequently used in water management and ecological status improvement.

8 References

Aas, W., Solberg, S., Manø, S., Yttri, K.E., 2013. Overvåking av langtransportert forurenset luft og nedbør. Atmosfæriske tilførsler 2012. Statlig program for forurensningsovervåking. Rapport 1148/2013. M-3/2013.(14/2013).

Adrian, R., Walz, N., Hintze, T., Hoeg, S. and Rusche, R., 1999. Effects of ice duration on plankton succession during spring in a shallow polymictic lake. *Freshwater Biology* 41(3) 621-634.

Agder, V. 2014. Vannområdet Otra. Lokal tiltaksanalyse.

Allen, R.G., Pereira, L.S., Raes, D. and Smith, M., 1998. Crop evapotranspiration: Guidelines for computing crop requirements. Irrigation and Drainage Paper No. 56, FAO, Rome, Italy 300 p.

Amt der Kärntner Landesregierung, 2014. Gewässerentwicklungskonzept Obere Drau II. Oberdrauburg - Mauthbrücke. Amt der Kärntner Landesregierung Abteilung 8 – Unterabteilung Wasserwirtschaft.

Arabi, M., Frankenberger, J.R., Engel, B.A., Arnold, J.G., 2008. Representation of agricultural conservation practices with SWAT. *Hydrological processes* 22, 3042-3055.

Argillier, C., Teichert, N., Sagouis, A., Lepage, M., Schinegger, R., Palt, M., Schmutz, S., Segurado, P., Ferreira, T., Chust, G., Uriarte, A., Borja, A., 2014. Deliverable 5.A: Report on the comparison of the sensitivity of fish metrics to multi-stressors in rivers, lakes and transitional waters. MARS project: Managing Aquatic ecosystems and water Resources under multiple Stress.

Arlinghaus, R., 2006. On the apparently striking disconnect between motivation and satisfaction in recreational fishing: the case of catch orientation of German anglers. *North American Journal of Fisheries Management* 26:592–605.

- Armitage, P.D., Moss, D., Wright, J.F., Furse, M.T. ,1983. The performance of a new water quality score system based on macroinvertebrates over a wide range of unpolluted running- water sites. *Water Research* 17, 333-347.
- Arnold, J. G., Srinivasan, R., Muttiah, R. S., & Williams, J. R., 1998. Large area hydrologic modeling and assessment part i: Model development1. *JAWRA Journal of the American Water Resources Association*, 34(1), 73-89. doi:10.1111/j.1752-1688.1998.tb05961.x
- Arvola, L., Hakala, I., Järvinen, M., Huitu, E. and Mäkelä, S., 2002. Effect of weather conditions on water quality in two small boreal rivers. *Large Rivers* 13 195-208.
- Ayllón, D., Almodóvar, A., Nicola, G.G., Elvira, B., 2009. Interactive effects of cover and hydraulics on brown trout habitat selection patterns. *River Res. Appl.* 25, 1051–1065. doi:10.1002/rra.1215
- Barnes, R.T. , Raymond, P.A., 2009. The contribution of agricultural and urban activities to inorganic carbon fluxes within temperate watersheds. *Chemical Geology* 266(3) 318-327.
- Bartoń K., 2016. MuMIn: Multi-Model Inference. R package version 1.15.6. <https://cran.r-project.org/web/packages/MuMIn/index.html> (accessed June 2016).
- Bartoń, K., 2014. MuMIn: Multi-model inference. R package version 1.10.5., R Package.
- Basheer, A.K., Lu, H., Omer, A., Ali, A.B., Abdelgader, A.M.S., 2016. Impacts of climate change under CMIP5 RCP scenarios on the streamflow in the Dinder River and ecosystem habitats in Dinder National Park, Sudan. *Hydrol. Earth Syst. Sci.* 20, 1331-1353.
- Baulch, H.M., Futter, M.N., Jin, L., Whitehead, P.G., Woods, D.T., Dillon, P.J., Butterfield, D.A., Oni, S.K., Aspden, L.P., O'Connor, E.M. and Crossman, J., 2013. Phosphorus dynamics across intensively monitored subcatchments in the Beaver River. *Inland Waters* 3(2) 187-206.
- BAW IGF, 2015. Leitbildkatalog [WWW Document]. URL <http://www.baw.at/index.php/igf-download/1693-leitbildkatalog.html> (accessed 5.23.15).

- Baxter, R.M., 1977. Environmental Effects of Dams and Impoundments. *Annu. Rev. Ecol. Syst.* 8, 255–283. doi:10.1146/annurev.es.08.110177.001351
- Bechmann, M.E., Deelstra, J., 2006. Source areas of phosphorus transfer in an agricultural catchment, south-eastern Norway. *Acta Agriculturae Scandinavica Section B-Soil and Plant Science* 56(4) 292-306.
- Becker A. , Venohr M., 2015. Anwendung des Nährstoffbilanzierungsmodells MONERIS – final report – on behalf of Flussgebietsgemeinschaft Elbe (FGG Elbe) - Geschäftsstelle Magdeburg. DHI WASY & IGB.
- Behrendt, H., Huber,P., Kornmilch, M., Opitz, D., Schmoll, O.,Scholz , G., Uebe, R., 2000. Nutrient emissions into river basins of Germany. – UBA-Texte 23/00, 266 pp.
- Beklioğlu, M., Romo, S., Kagalou, I., Quintana, X., Bécares, E., 2007. State of the art in the functioning of shallow Mediterranean lakes: workshop conclusions. *Hydrobiologia.* 584, 317–326. <http://dx.doi.org/10.1007/s10750-007-0577-x>
- BirdLife International, 2015. Important Bird Areas factsheet: Downloaded from <http://www.birdlife.org> on 28/08/2015.
- Bivand, R., 2011. Spatial dependence: weighting schemes, statistics and models. R Package Version 0.5-33. Available at: <http://www.R-project.org> (accessed June 2016).
- BMLFUW, 2013. EU Wasserrahmenrichtlinie 2000/60/EG - Methodik der Istbestandsanalyse 2013. Sektion IV Wasserwirtschaft.
- BMLFUW, 2015. Nationaler Gewässerbewirtschaftungsplan 2015 - Entwurf. Sektion IV Wasserwirtschaft.
- Breiman, L., 2001. Random forests. *Machine Learning* 45:5–32.
- Bruce, L. C., Hamilton, D., Imberger, J., Gal, G., Gophen, M., Zohary, T., Hambright, K. D., 2006. A numerical simulation of the role of zooplankton in C, N and P cycling in Lake Kinneret, Israel. *Ecological Modelling*, 193(3), 412-436.
- Bruno, D., Gutiérrez-Cánovas, C., Sánchez-Fernández, D., Velasco, J., Nilsson, C., 2016b. Impacts of environmental filters on functional redundancy in riparian vegetation. *Journal of Applied Ecology* 53 846-855.

- Bruno, D., Gutiérrez-Cánovas, C., Velasco, J. and Sánchez-Fernández, D., 2016a. Functional redundancy as a tool for bioassessment: A test using riparian vegetation. *Science of The Total Environment* 566 1268-1276.
- Bucak, T., Saraoğlu, E., Levi, E. E., Tavşanoğlu, Ü. N., Çakiroğlu, A.İ., Jeppesen, E., Beklioğlu, M., 2012. The influence of water level on macrophyte growth and trophic interactions in eutrophic Mediterranean shallow lakes: a mesocosm experiment with and without fish. *Freshw. Biol.* 57, 1631–1642. <http://dx.doi.org/10.1111/j.1365-2427.2012.02825.x>
- Buchwalter, D.B., Cain, D.J., Martin, C.A., Xie, L., Luoma, S.N. and Garland, T., 2008. Aquatic insect ecophysiological traits reveal phylogenetically based differences in dissolved cadmium susceptibility. *Proceedings of the National Academy of Sciences of the United States of America* 105 8321-8326.
- Buckton, S.T., Brewin, P.A., Lewis, A., Stevens, P. and Ormerod, S.J., 1998. The distribution of dippers, *Cinclus cinclus* (L.), in the acid-sensitive region of Wales, 1984-95. *Freshwater Biology* 39 387-396.
- Buijse, A. D., H. Coops, M. Staras, L. H. Jans, G. J. Van Geest, R. E. Grift, B. W. Ibelings, W. Oosterberg And F. C. J. M. Roozen.,2002. Restoration strategies for river floodplains along large lowland rivers in Europe. *Freshwater Biology* (2002) 47, 889–907.
- Bunn, S.E., Arthington, A.H., 2002., Basic principles and ecological consequences of altered flow regimes for aquatic biodiversity. *Environ. Manage.* 30, 492-507.
- Burnham, K. P. , Anderson, D. R., 2002. Model selection and multimodel inference: a practical information-theoretic approach. 2nd ed. New York, Springer-Verlag.
- Calbó, J., 2010. Possible climate change scenarios with specific reference to Mediterranean regions, in Sabater, S., Barceló, D. (Eds.), *Water Scarcity in the Mediterranean*. Springer, Berlin, Heidelberg, pp. 1–13.
- Carvalho, L., Spears, B., Dudley, B., Gunn, I., Zimmermann, S., Defew, L., May, L., 2008. *Loch Leven 2007: trends in water quality and biological communities*.
- Chatzinikolaou, Y., 2007. Effect of management practices on the water quality and ecology of rivers in Greece. Pinios River as a study case, 2007 Doctorate thesis.

Department of Biology, Aristotle University of Thessaloniki, Volume A: pp. 229 and volume B, p. 470 <http://dx.doi.org/10.12681/eadd/20876>.

Chatzinikolaou, Y., Ioannou, A., Lazaridou, M., 2010. Intra-basin spatial approach on pollution load estimation in a large Mediterranean river. *Desalination* 250, 118-129.

Chen, C., Ji, R., Schwab, D. J., Beletsky, D., Fahnenstiel, G. L., Jiang, M., Bundy, M. H., 2002. A model study of the coupled biological and physical dynamics in Lake Michigan. *Ecological Modelling*, 152(2), 145-168.

Christensen, R.H.B., 2015. A Tutorial on fitting Cumulative Link Mixed Models with `clmm2` from the `ordinal` Package. https://cran.r-project.org/web/packages/ordinal/vignettes/clmm2_tutorial.pdf (accessed June 2016).

Clapcott, J.E., Collier, K.J., Death, R.G., Goodwin, E.O., Harding, J.S., Kelly, D., Leathwick, J.R., Young, R.G., 2012. Quantifying relationships between land-use gradients and structural and functional indicators of stream ecological integrity. *Freshw. Biol.* 57, 74–90. doi:10.1111/j.1365-2427.2011.02696.x

Cosby, B.J., Ferrier, R.C., Jenkins, A., Wright, R.F., 2001. Modelling the effects of acid deposition: refinements, adjustments and inclusion of nitrogen dynamics in the MAGIC model. *Hydrology and Earth System Sciences* 5 499-518.

Cosby, B.J., Wright, R.F., Hornberger, G.M., Galloway, J.N., 1985. Modelling the effects of acid deposition: estimation of long term water quality responses in a small forested catchment. *Water Resources Research* 21 1591-1601.

Couture, R.-M., Tominaga, K., Starrfelt, J., Moe, S.J., Kaste, O., Wright, R.F., 2014. Modelling phosphorus loading and algal blooms in a Nordic agricultural catchment-lake system under changing land-use and climate. *Environ. Sci.: Processes Impacts* 16(7) 1588-1599.

Couture, R.-M., Tominaga, K., Starrfelt, J., Moe, S.J., Kaste, Ø., Wright, R.F., Farkas, C., Engebretsen, A., 2013. Report on the catchment-scale modelling of the Vansjø-Hobøl and Skuterud catchments, Norway (Strategies to Mitigate the Impacts of Climate Change on European Freshwater Ecosystems: Work package 5 – Integrated Biophysical Modelling; (EU FP7 no. 244121) <http://www.refresh.ucl.ac.uk/Deliverable+5.10+abstract>

- Crawley, M.J., 2007. *The R Book*. John Wiley & Sons, Ltd., Chichester.
- Cremona, F., Kõiv, T., Kisand, V., Laas, A., Zingel, P., Agasild, H., Feldmann, T., Järvalt, A., Nõges, P., Nõges T., 2014a. From Bacteria to Piscivorous Fish: Estimates of Whole-Lake and Component-Specific Metabolism with an Ecosystem Approach. *PloS One* 9. e101845.
- Cremona, F., Kõiv, T., Nõges, P., Pall, P., Rõõm, E.-I., Feldmann, T., Viik, M., Nõges, T., 2014b. Dynamic carbon budget of a large shallow lake assessed by a mass balance approach. *Hydrobiologia* 731 109–123.
- Crossman, J., Futter, M.N., Oni, S.K., Whitehead, P.G., Jin, L., Butterfield, D., Baulch, H.M., Dillon, P.J., 2013. Impacts of climate change on hydrology and water quality: Future proofing management strategies in the Lake Simcoe watershed, Canada. *Journal of Great Lakes Research* 39(1) 19-32.
- Cunjak, R.A., Linnansaari, T., Caissie, D., 2013. The complex interaction of ecology and hydrology in a small catchment: a salmon's perspective. *Hydrol. Process.* 27, 741–749. doi:10.1002/hyp.9640
- Cutler, D.R., Edwards, T.C., Beard, K.H., Cutler, A., Hess, K.T., Gibson, J., Lawler, J.J., 2007. Random forests for classification in ecology. *Ecology* 88 2783-2792.
- D.B., Xie, S.-P., Zhou, T., 2013. Climate Phenomena and their Relevance for Future Regional Climate Change, in Stocker, T.F., Qin, D., Plattner, G.-K., Tignor, M., Allen, S.K., Boschung, J.,
- De Zwart, D., Dyer, S.D., Posthuma, L., Hawkins, C.P., 2006. Predictive models attribute effects on fish assemblages to toxicity and habitat alteration. *Ecol. Appl.* 16, 1295–1310. doi:10.1890/1051-0761(2006)016[1295:PMAEOF]2.0.CO;2
- Dean, S., Freer, J., Beven, K., Wade, A.J., Butterfield, D., 2009. Uncertainty assessment of a process-based integrated catchment model of phosphorus. *Stochastic Environmental Research and Risk Assessment* 23(7) 991-1010.
- Deltares Systems, 2014. *SOBEK User Manual*. Delft, the Netherlands. http://content.oss.deltares.nl/delft3d/manuals/SOBEK_User_Manual.pdf.

- Devia, G. K., Ganasri, B. P., Dwarakish, G. S., 2015. A review on hydrological models. *Aquatic Procedia*, 4(0), 1001-1007. doi:<http://dx.doi.org/10.1016/j.aqpro.2015.02.126>
- Dibike, Y., Prowse, T., Bonsal, B., Rham, L.d., Saloranta, T., 2012. Simulation of North American lake-ice cover characteristics under contemporary and future climate conditions. *Int. J. Climatol.* 32(5) 695-709.
- Directive 2000/60/EC of the European Parliament and of the council of 23 October 2000 establishing a framework for Community action in the field of water policy. *Official Journal of the European Communities* L327/1.
- Duarte, G., Oliveira, T. Segurado, P., Branco, P., Haidvogel, G., Pont, D., Ferreira, M.T., 2016. River Network Toolkit (RivTool) – A new software for river networks. 19th Agile Conference on Geographic Information Science, At Helsinki, Finland, Volume: CCM2 River and Catchment Database for Europe - Applications Workshop.
- Durance, I., Ormerod, S.J., 2007. Climate change effects on upland stream macroinvertebrates over a 25-year period. *Global Change Biology* 13 942-957.
- Edwards, R.W., Stoner, J.H., Gee, A.S., 1990. *Acid Waters in Wales*. Kluwer Academic Publishers, Dordrecht, The Netherlands.
- Elith, J., Leathwick, J.R., Hastie, T., 2008. A working guide to boosted regression trees. *Journal of Animal Ecology* 77:802–813.
- Elith, J., Leathwick, J.R., Hastie, T., 2008. A working guide to boosted regression trees. *J. Anim. Ecol.* 77, 802–13. doi:10.1111/j.1365-2656.2008.01390.x
- Elliott, A.J., May, L., 2008. The sensitivity of phytoplankton in Loch Leven (UK) to changes in nutrient load and water temperature. *Freshwater Biology*, 53(1), 32-41.
- Elliott, J. A., Defew, L., 2012. Modelling the response of phytoplankton in a shallow lake (Loch Leven, UK) to changes in lake retention time and water temperature. *Hydrobiologia*, 681(1), 105-116.
- Elliott, J. A., Irish, A. E., Reynolds, C. S., Tett, P., 2000. Modelling freshwater phytoplankton communities: an exercise in validation. *Ecological Modelling*, 128(1), 19-26.

Eloranta, P., Marja-aho, J., 1982. Transect studies on the aquatic macrophyte vegetation of Lake Saimaa in 1980. *Biol. Res. Rep. Univ. Jyväskylä* 9 35-65.

Eloranta, P., 1978. Light penetration in different types of lakes in Central Finland. *Holarct. Ecol* 1 362-366.

Erol, A., Randhir, T.O., 2012. Climatic change impacts on the ecohydrology of Mediterranean watersheds. *Clim. Change.* 114, 319–341.
<http://dx.doi.org/10.1007/s10584-012-0406-8>

Ertürk, A., Ekdal, A., Gürel, M., Karakaya, N., Guzel, C., Gönenç, E., 2014. Evaluating the impact of climate change on groundwater resources in a small Mediterranean watershed. *Sci. of Total Env.* 499, 437–447.
<http://dx.doi.org/10.1016/j.scitotenv.2014.07.001>

ESRI, 2011. ArcGIS Desktop: Release 10. Redlands, CA: Environmental Systems Research Institute.

European Commission, 2000. Directive 2000/60/ EC of the European Parliament and the Council of 23 October 2000 Establishing A Framework for Community Action in the Field of Water Policy. *OJEC, L 327*, 1–73.

Extence, C.A., Balbi, D.M. , Chadd, R.P., 1999. River flow indexing using British benthic macroinvertebrates: A framework for setting hydroecological objectives. *Regulated Rivers-Research & Management* 15 543-574.

Faneca Sanchez, M., Duel, H., Alejos Sampedro, A., Rankinen, K., Holmberg, M., Prudhomme, C., Birk, S., 2015. Deliverable 2.1 four manuscripts on the multiple stressor framework: Report on the MARS scenarios of future changes in drivers and pressures with respect to europe's water resources (4/4). ().

Farkas, C., Beldring, S., Bechmann, M., Deelstra, J., 2013. Soil erosion and phosphorus losses under variable land use as simulated by the INCA-P model. *Soil Use Manag.* 29(Suppl. 1) 124-137.

Fauth J.E., Bernadro J., Camara M., Resetarits Jr. W.J., Van Buskrik J., McCollum S.A., 1996. Simplifying the jargon of community ecology: a conceptual approach. *American Naturalist* 147(2):282-286.

FDDB, 2015. Datenbankauszug der Fischdatenbank Österreich. Stand: September 2015. Bundesamt für Wasserwirtschaft; Institut für Gewässerökologie, Fischereibiologie und Seenkunde.

Feld, C.K., Birk, S., Eme, D., Gerisch, M., Hering, D., Kernan, M., Maileht, K., Mischke, U., Ott, I., Pletterbauer, F., Poikane, S., Salgado, J., Sayer, C.D., van Wichelen, J., Malard, F., 2016. Disentangling the effects of land use and geo-climatic factors on diversity in European freshwater ecosystems. *Ecol. Indic.* 60, 71–83. doi:10.1016/j.ecolind.2015.06.024

Feld, C.K., Segurado, P., Gutiérrez-Cánovas, C., 2016. Analysing the impact of multiple stressors in aquatic biomonitoring data: A ‘cookbook’ with applications in R. *Science of The Total Environment*. <http://dx.doi.org/10.1016/j.scitotenv.2016.06.243>

FGGE 2009: Bewirtschaftungsplan nach Artikel 13 der Richtlinie 2000/60/EG für den deutschen Teil der Flussgebietseinheit Elbe. 11.11.2009. <http://www.fgg-elbe.de/berichte.html>

FGGE 2015a: Aktualisierung des Maßnahmenprogramms nach § 82 WHG bzw. Artikel 11 der Richtlinie 2000/60/EG für den deutschen Teil der Flussgebietseinheit Elbe für den Zeitraum von 2016 bis 2021. 12.11.2015. <http://www.fgg-elbe.de/berichte.html>

FGGE 2015b: Aktualisierung des Bewirtschaftungsplans nach § 83 WHG bzw. Artikel 13 der Richtlinie 2000/60/EG für den deutschen Teil der Flussgebietseinheit Elbe für den Zeitraum von 2016 bis 2021. The second River Basin Management Plans 2015 of River Basin District Labe according to EU Directive 2000/60/EG, WFD) 12.11.2015. Publisher: Flussgebietsgemeinschaft Elbe. <http://www.fgg-elbe.de/berichte.html>

Fink, M., Moog, O., Wimmer, R., 2000. Fließgewässer-Naturräume Österreichs; Monographien Band 128.

Fowler, H.J., Blenkinsop, S., Tebaldi, C., 2007. Linking climate change modelling to impacts studies: recent advances in downscaling techniques for hydrological modelling. *International journal of climatology* 27(12) 1547-1578.

Futter, M.N., Butterfield, D., Cosby, B.J., Dillon, P.J., Wade, A., Whitehead, P.G., 2007. Modeling the mechanisms that control in-stream dissolved organic carbon dynamics in upland and forested catchments. *Water Resour. Res.* 43 1-16.

Futter, M.N., Erlandsson, M.A., Butterfield, D., Whitehead, P.G., Oni, S.K., Wade, A.J., 2013. PERSiST: the precipitation, evapotranspiration and runoff simulator for solute transport. *Hydrol. Earth Syst. Sci. Discuss.* 10(7) 8635-8681.

Futter, M.N., Erlandsson, M.A., Butterfield, D., Whitehead, P.G., Oni, S.K., Wade, A.J., 2014a. PERSiST: A flexible rainfall-runoff modelling toolkit for use with the INCA family of models. *Hydrology and Earth System Sciences* 18 855-873.

Futter, M.N., Erlandsson, M.A., Butterfield, D., Whitehead, P.G., Oni, S.K., Wade, A.J., 2014c. PERSiST: the precipitation, evapotranspiration and runoff simulator for solute transport. *Hydrol. Earth Syst. Sci.* 18 855–873.

Gal, G., Hipsey, M. R., Parparov, A., Wagner, U., Makler, V., Zohary, T., 2009. Implementation of ecological modeling as an effective management and investigation tool: Lake Kinneret as a case study. *Ecological Modelling*,220(13), 1697-1718.

Gal, G., Imberger, J., Zohary, T., Antenucci, J., Anis, A., Rosenberg, T., 2003. Simulating the thermal dynamics of Lake Kinneret. *Ecological Modelling*, 162(1), 69-86.

García-Ruiz, J. M., López-Moreno, J. I., Vicente-Serrano, S. M., Lasanta-Martínez, T., Beguería, S., 2011. Mediterranean water resources in a global change scenario. *Earth-Science Reviews*, 105(3), 121-139.

Gassman, P.W., Reyes, M. R., Green, C.H., Arnold, J.G., 2007. The soil and water assessment tool: historical development, applications and future research directions. *Trans. Am. Soc. Agric. Biol. Eng.* 50, 1211–1250.

Gebre, S., Boissy, T., Alfredsen, K., 2013. Sensitivity of lake ice regimes to climate change in the nordic region. *The Cryosphere Discuss.* 7(2) 743-788.

Gierk M., de Roo A., 2008. The impact of retention polders, dyke-shifts and reservoirs on discharge in the Elbe river. Hydrological modelling study in the framework of the Action Plan for the Flood Protection in the Elbe River Basin of the International Commission for the Protection of the Elbe River (ICPER). JRC Scientific and Technical Reports. JRC49172, OPOCE, Luxembourg

- Gophen, M., Smith, V. H., Nishri, A., Threlkeld, S. T., 1999. Nitrogen deficiency, phosphorus sufficiency, and the invasion of Lake Kinneret, Israel, by the N₂-fixing cyanobacterium *Aphanizomenon ovalisporum*. *Aquatic sciences*, 61(4), 293-306.
- Griffith, D.A., Peres-Neto, P.R., 2006. Spatial modeling on ecology: the flexibility of eigenfunction spatial analysis. *Ecology*, 87:2603–2613.
- Grimm V., 1994. Mathematical models and understanding in ecology. *Ecological Modelling*, 75, 641–651.
- Grizzetti B., Lanzasova D., Liqueste C., Reynaud A., Cardoso A.C., 2016. Assessing water ecosystem services for water resource management. *Environmental Science and Policy* 61:194-203
- Grizzetti B., Lanzasova D., Liqueste C., Reynaud A., 2015. Cook-book for water ecosystem service assessment and valuation. European Commission, Joint Research Centre, Institute for Environment and Sustainability, doi:10.2788/67661
- Grueber, C.E., Nakagawa, S., Laws, R.J., Jamieson, I.G., 2011. Multimodel inference in ecology and evolution: Challenges and solutions, *Journal of Evolutionary Biology*, pp. 699-711.
- Gyllström, M., Hansson, L.A., Jeppesen, E., Criado, F.G., Gross, E., Irvine, K., Kairesalo, T., Kornijow, R., Miracle M.R., Nykänen, M., Nöges, T., 2005. The role of climate in shaping zooplankton communities of shallow lakes. *Limnology and Oceanography* 50(6) 2008-2021.
- Haakana, M., Ollila, P., Regina, K., Riihimäki, H., Tuomainen, T. , 2015. Menetelmä maankäytön muutosten ennustamiseen. Pinta-alan muutos ja kasvihuonekaasupäästöjen ennustaminen vuoteen 2040. (Luonnonvara- ja biotalouden tutkimus 51/2015.
- Haberman, J., Virro, T., 2004. Zooplankton. In: Haberman, J., Pihu, E., Raukas, A. (Eds.) *Lake Võrtsjärv*. Estonian Encyclopedia Publishers, Tallinn.
- Haines-Young R., Potschin M., 2014. CICES V4.3 - Report prepared following consultation on CICES Version 4, August-December 2012. EEA Framework Contract No EEA/IEA/09/003

- Han, B. P., Armengol, J., Garcia, J. C., Comerma, M., Roura, M., Dolz, J., Straskraba, M., 2000. The thermal structure of Sau Reservoir (NE: Spain): a simulation approach. *Ecological Modelling*, 125(2), 109-122.
- Hanssen-Bauer, I., Førland, E.J., Haddeland, I., Hisdal, H., Mayer, S., Nesje, A., Nilsen, J.E.Ø., Sandven, S., Sandø, A.B., Sorteberg, A., Ådlandsvik, B. 2015. Klima i Norge 2100. NCCS report no. 2/2015.
- Hargreaves, G.L., Hargreaves G.H., Riley J.P., 1985. Agricultural benefits for Senegal River Basin. *Journal of Irrigation and Drainage Engineering* 111(2):113-124.
- Hattermann F.F., Huang S., Koch H., 2015. Climate change impacts on hydrology and water resources. *Meteorologische Zeitschrift*, Vol. 24, 2, 201–211
- Hattermann, F., Wattenbach M., Krysanova V., Wechsung F., 2005. Runoff simulations on the macroscale with the ecohydrological model swim in the Elbe catchment-validation and uncertainty analysis. – *Hydrol. Proc.* 19, 693–714.
- Haunschmid, R., Schotzko, N., Petz-Glechner, R., Honsig-Erlenburg, W., Schmutz, S., Spindler, T., Unfer, G., Wolfram, G., Bammer, V., Hundritsch, L., Prinz, H., Sasano, B., 2010. Leitfaden zur Erhebung der biologischen Qualitätselemente Teil a1 - Fische. BMLFUW, Umwelt und Wasserwirtschaft, Sektion VII.
- Haunschmid, R., Wolfram, G., Spindler, T., Honsig-Erlenburg, W., Wimmer, R., Jagsch, A., Kainz, E., Hehenwarter, K., Wagner, B., Konecny, R., Riedmüller, R., Ibel, G., Sasano, B., Schotzko, N., 2006. Erstellung einer fischbasierenden Typologie Österreichischer Fließgewässer sowie einer Bewertungsmethode des fischökologischen Zustandes gemäß EU-Wasserrahmenrichtlinie. Schriftenreihe des Bundesamtes für Wasserwirtschaft Band 23, Wien.
- HELCOM., 2007. Baltic sea action plan. (). Krakow, Poland: HELCOM Ministerial Meeting.
- Hellsten, S., 1997. Environmental factors related to water level fluctuation - a comparative study in northern Finland. *Boreal Environmental Research* 2 345-367.

Henshilwood C. S., D'errico F., Marean C. W., Milo R. G., Yates R., 2001. An early bone tool industry from the Middle Stone Age at Blombos Cave, South Africa: implications for the origins of modern human behavior, symbolism and language. *Journal of Human Evolution* 41:6, 631-678

Hering D., Borja A., Carstensen J., Carvalho L., Elliott M., Feld C.K., Heiskanen A.S., Johnson R.K., Moe J., Pont D., Lyche-Solheim A., van de Bund W., 2010. The European Water Framework Directive at the age of 10: A critical review of the achievements with recommendations for the future. *Science of the Total Environment* 408:4007-4019.

Hering D., Carvalho L., Argillier C., Beklioglu M., Borja A., Cardoso A. C., Duel H., Ferreira T., Globevnik L., Hanganu J., Hellsten S., Jeppesen E., Kodeš V., Lyche Solheim A., Nõges T., Ormerod S., Panagopoulos Y., Schmutz S., Venohr M., Birk S., 2015. Managing aquatic ecosystems and water resources under multiple stress - an introduction to the MARS project. *Science of The Total Environment*, 503-504, 10-21.

Hering, D., Borja, A., Carvalho, L., Feld, C.K., 2013. Assessment and recovery of European water bodies: Key messages from the WISER project. *Hydrobiologia* 704, 1–9.

Hering, D., Carvalho, L., Argillier, C., Beklioglu, M., Borja, A., Cardoso, A. C., Birk, S. , 2015. Managing aquatic ecosystems and water resources under multiple stress — an introduction to the MARS project. *Science of the Total Environment*, 503–504, 10-21. doi:<http://dx.doi.org/10.1016/j.scitotenv.2014.06.106>

Hernández-Morcillo M., Plieninger T., Bieling C., 2011. Review: An empirical review of cultural ecosystem service indicators. *Ecological Indicators* 29, 434–444.

Hessen, D., 2013. Inorganic nitrogen deposition and its impacts on N:P-ratios and lake productivity. *Water*, 5(2), 327.

Hijmans, R.J., Cameron, S.E., Parra, J.L., Jones, P.G., Jarvis, A., 2005. Very high resolution interpolated climate surfaces for global land areas. *International Journal of Climatology* 25 1965-1978.

Hijmans, R.J., Phillips, S., Leathwick, J., Elith, J., 2013. Species distribution modelling. Package “dismo”. – Available at: <http://cran.r-project.org/web/packages/dismo/dismo.pdf>.

Hipsey, M.R., Bruce, L.C., Hamilton, D.P., 2013. Aquatic Ecodynamics (AED) Model Library: Science Manual Draft V4.

Hipsey, M.R., Bruce, L.C., Hamilton, D.P., 2014. General Lake Model: Model Overview and User Information v2.0

Holmlund C., Hammer M., 1999. Ecosystem services generated by fish populations, *Ecological Economics*, 29, 253–26

Holst H., Zimmermann-Timm H., Kausch H., 2002. Longitudinal and transverse distribution of plankton rotifers in the potamal of the river Elbe (Germany) during late summer. *Int Rev Hydrobiol* 87:267–280

Holzappel, P., Wagner, B., Zeiringer, B., Graf, W., Leitner, P., Habersack, H., Hauer, C., 2014. Anwendung der Habitatmodellierung zur integrativen Bewertung von Schwall und Restwasser im Bereich der Wasserkraftnutzung. *Österreichische Wasser- und Abfallwirtschaft* 66, 179–189. doi:10.1007/s00506-014-0154-2

Hooper, D.U., Chapin III, F.S., Ewel, J.J., 2005. Effects of biodiversity on ecosystem functioning: a consensus of current knowledge. *Ecological Monographs* 75 3-35.

Hopkinson, C.S., Vallino, J.J., Nolin, A., 2002. Decomposition of dissolved organic matter from the continental margin. *Deep-Sea Research II* 49 4461-4478.

Horbat A., Remy C., Mutz D., Meyerhoff J., Kruse N., Matranga M., Venohr M., Rouault P., 2016. Kosten und Nutzen einer verbesserten Gewässergüte am Beispiel der Berliner Unterhavel. NITROLIMIT Diskussionspapier Band 4, Juni 2016 <http://www.nitrolimit.de/index.php/Aktuelles.html>

Huang S., Krysanova, V., Hattermann F., 2015. Projections of climate change impacts on floods and droughts in Germany using an ensemble of climate change scenarios. *Reg Environ Change* 15: 461-473

Huang, S., Hattermann F.F., Krysanova V., Bronstert A., 2013. Projections of climate change impacts on river flood conditions in Germany by combining three different RCMs with a regional eco-hydrological model. *Climatic Change* 116: 631 –663

Huet, M., 1959. Profiles and biology of western European streams as related to fish management. *Trans. Am. Fish. Soc.* 88, 155–163.

Humpel, M., 2011. Metaanalyse von eingriffen und deren Restaurationsmaßnahmen an der österreichischen Drau. University of Natural Resources and Applied Life Sciences Vienna.

Hunt, K.M., Hutt, C.P., 2010. Characteristics of Texas Catfish Anglers and their Catch and Management Preferences. Texas Parks & Wildlife Department Inland Fisheries Division.

Hutchins, M.G.; Johnson, A.C.; Deflandre-Vlandas, A.; Comber, S.; Posen, P.; Boorman, D., 2010. Which offers more scope to suppress river phytoplankton blooms: Reducing nutrient pollution or riparian shading? *The Science of the Total Environment*, 408 (21). 5065-5077.

Illies, J., 1978. *Limnofauna Europaea. A checklist of the Animals inhabiting European Inland Waters, with Account of their Distribution and Ecology*, Second rev. ed. Gustav Fischer Verlag, Stuttgart and Swets & Zeitlinger, Amsterdam.

INE, 2011, Censos (2011) - XV Recenseamento Geral da população e V Recenseamento Geral da Habitação.

Ishwaran H., Kogalur U.B., 2016. Random Forests for Survival, Regression and Classification (RF-SRC), R package version 2.2.0.

Ishwaran, H., 2007. Variable importance in binary regression trees and forests. *Electronic Journal of Statistics* 1: 519-537.

Ishwaran, H., Gerds, T.a., Kogalur, U.B., Moore, R.D., Gange, S.J., Lau, B.M., 2014. Random survival forests for competing risks. *Biostatistics (Oxford, England)* 1-17. 10.1093/biostatistics/kxu010.

Ishwaran, H., Kogalur, U.B., 2014. Random Forests for Survival, Regression and Classification (RF-SRC), R package version 1.5.

Jackson-Blake, L.A., Dunn, S.M., Helliwell, R.C., Skeffington, R.A., Stutter, M.I., Wade, A.J., 2015. How well can we model stream phosphorus concentrations in agricultural catchments? *Environmental Modelling & Software* 64(0) 31-46. <http://dx.doi.org/10.1016/j.envsoft.2014.11.002>

Jackson-Blake, L.A., Wade, A.J., Futter, M.N., Butterfield, D., Couture, R.M., Cox, B., Crossman, J., Ekholm, P., Halliday, S.J., Jin, L., Lawrence, D.S.L., Lepistö, A., Lin, Y., Rankinen, K., Whitehead, P.G., 2016a. The INtegrated CATCHment model of phosphorus dynamics (INCA-P): Description and demonstration of new model structure and equations. *Environmental Modelling & Software* 83 1-31.

Janse, J. H., 2005. Model studies on the eutrophication of shallow lakes and ditches. PhD Thesis. Wageningen

Janssen, A. B., Arhonditsis, G. B., Beusen, A., Bolding, K., Bruce, L., Bruggeman, J., Gal, G., 2015. Exploring, exploiting and evolving diversity of aquatic ecosystem models: a community perspective. *Aquatic Ecology*, 49(4), 513-548.

Jayakrishnan, R.; Srinivasan, R.; Santhi, C., Arnold, J.G., 2005. Advances in the application of the SWAT model for water resources management. *Hydrol. Process.*, 19:749-762.

Jeppesen, E., Brucet, S., Naselli-Flores, L., Papastergiadou, E., Stefanidis, K., Noges, T., Bucak, T., 2015. Ecological impacts of global warming and water abstraction on lakes and reservoirs due to changes in water level and related changes in salinity. *Hydrobiologia*, 750(1), 201-227.

Jeppesen, E., Kronvang, B., Meerhoff, M., Søndergaard, M., Hansen, K. M., Andersen, E., Olesen, J., 2009. Climate change effects on runoff, catchment phosphorus loading and lake ecological state, and potential adaptations

Jeppesen, E., Kronvang, B., Olesen, J. E., Audet, J., Søndergaard, M., Hoffmann, C. C., Özkan, K., 2011. Climate change effects on nitrogen loading from cultivated catchments in Europe: Implications for nitrogen retention, ecological state of lakes and adaptation. *Hydrobiologia*, 663(1), 1-21; 21. doi:10.1007/s10750-010-0547-6

Jeppesen, E., Meerhoff, M., Davidson, T.A., Trolle, D., Søndergaard, M., Lauridsen, T.L., Beklioglu, M., Brucet, S., Volta, P., Gonzalez-Bergonzoni, I., Nielsen A., 2014. Climate change impacts on lakes: an integrated ecological perspective based on a multi-faceted approach, with special focus on shallow lakes. *J Limnol.* 73 88-111.

Jin, L., Whitehead, P.G., Baulch, H.M., Dillon, P.J., Butterfield, D., Oni, S.K., Futter, M.N., Crossman, J., O'Connor, E.M., 2013. Modelling phosphorus in Lake Simcoe and

its subcatchments: scenario analysis to assess alternative management strategies. *Inland Waters* 3(2) 207-220.

Jin, L., Whitehead, P.G., Sarkar, S., Sinha, R., Futter, M.N., Butterfield, D., Singh, R., 2015. Assessing the impacts of climate change and socio-economic changes on flow and phosphorus flux in the Ganga river system. *Environ. Sci.: Processes Impacts* 17 1098-1110.

Joensuu, I., Karonen, M., Kinnunen, T., Mäntykoski, A., Nylander, E., Teräsvuori, E., 2010. Uudenmaan vesienhoidon toimenpideohjelma. (Uudenmaan Elinkeino-, liikenne- ja ympäristökeskus. 192 p.

Johnson, A.C., Acreman, M.C., Dunbar, M.J., Feist, S.W., Giacomello, A.M., Gozlan, R.E., Hinsley, S.A., Ibbotson, A.T., Jarvie, H.P., Jones, J.I., Longshaw, M., Maberly, S.C., Marsh, T.J., Neal, C., Newman, J.R., Nunn, M.A., Pickup, R.W., Reynard, N.S., Sullivan, C.A., Sumpter, J.P., Williams, R.J., 2009. The British river of the future: How climate change and human activity might affect two contrasting river ecosystems in England. *Sci. Total Environ.* 407, 4787–4798. doi:10.1016/j.scitotenv.2009.05.018

Jones, I. D., Elliott, J. A., 2007. Modelling the effects of changing retention time on abundance and composition of phytoplankton species in a small lake. *Freshwater Biology*, 52(6), 988-997.

Karr, J.R., 1991. Biological integrity: a long-neglected aspect of water resource management. *Ecol. Appl.* doi:10.2307/1941848

Kaspersen, B. S., Jacobsen, T. V., Butts, M. B., Boegh, E., Müller, H. G., Stutter, M., Kjaer, T., 2016. Integrating climate change mitigation into river basin management planning for the water framework directive – A danish case. *Environmental Science & Policy*, 55, Part 1, 141-150. doi:http://dx.doi.org/10.1016/j.envsci.2015.10.002

Kogler, O., 2008. Übersicht von Gewässerbetreuungskonzepten in Österreich. Universität für Bodenkultur Wien.

Kohl, F., 2000. Soziale und ökonomische Bedeutung der Angelfischerei in Österreich. Diplomarbeit, Universität für Bodenkultur, Wien.

Korhonen, J., Haavanlammi, E. , 2012. Hydrologinen vuosikirja 2006-2012. (Hydrological Yearbook 2006-2010.). (Suomen ympäristö 8/2012, Luonnonvarat. URN:ISBN 978-952-11-3988-8, ISBN 978-952-11-3988-8 (pbk.).

Kortelainen, P., 1993. Content of Total organic Carbon in Finnish Lakes and Its Relationship to Catchment Characteristics. *Can. J. Fish. Aquat. Sci.* 50 1477-1483.

Kosten, S., Huszar, V. L., Bécares, E., Costa, L. S., Donk, E., Hansson, L. A., Kosten, S., Huszar, V.L.M., Beares, E., Costa, L.S., Van Donk, E., Hansson, L.-A., Jeppesen, E., Kruk, C., Ell Lacerot, G.S.S., Mazzeo, N., De Meester, L., Moss, B., Lurling, M., Noges, T., Romokk, S., Meester, L., 2012. Warmer climates boost cyanobacterial dominance in shallow lakes. *Global Change Biology* 18(1) 118-126.

Kottek, M., Grieser, J., Beck, C., Rudolf, B., Rubel, F., 2006. World map of the köppen-geiger climate classification updated. *Meteorologische Zeitschrift*, 15(3), 259-263. doi:doi:10.1127/0941-2948/2006/0130"

Kovats, R. S., Valentini, R., Bouwer, L. M., Georgopoulou, E., Jacob, D., Martin, E., Soussana, J. F. ,2014. Europe. In V. R. Barros, C. B. Field, D. J. Dokken, M. D. Mastrandrea, K. J. Mach, T. E. Bilir, L. L. White (Eds.), *Climate change 2014: Impacts, adaptation, and vulnerability. part B: Regional aspects. contribution of working group II to the fifth assessment report of the intergovernmental panel on climate change* (pp. 1267-1326). Cambridge, United Kingdom and New York, USA: Cambridge University Press.

Kowalik, R.A., Cooper, D.M., Evans, C.D., Ormerod, S.J., 2007. Acidic episodes retard the biological recovery of upland British streams from chronic acidification. *Global Change Biology* 13 2439-2452.

Kriegler, E., O'Neill, B.C., Hallegatte, S., Kram, T., Lempert, R., Moss, R., Wilbanks, T. 2012. The need for and use of socio-economic scenarios for climate change analysis: a new approach based on shared socioeconomic pathways. *Glob Environ Chang.* 22, 807-822.

Kristensen, P., 2012. European waters: Assessment of status and pressures.

Kroglund, F., Høgberget, R., Hindar, K., Østborg, G., Balstad, T., 2008a. Salmon and water quality in the Otra River, 1990-2006. NIVA Report 5531-2008.

Kroglund, F., Rosseland, B.O., Teien, H.C., Salbu, B., Kristensen, T., Finstad, B., 2008b. Water quality limits for Atlantic salmon (*Salmo salar* L.) exposed to short term reductions in pH and increased aluminum simulating episodes. *Hydrology and Earth System Sciences* 12(2) 491-507.

Kronvang B., Jeppesen E., Conley D.J., Sondergaard M., Larsen S.E., Ovesen N.B., Carstensen J., 2005. Nutrient pressures and ecological responses to nutrient loading reductions in Danish streams, lakes and coastal waters. *J Hydrol* 304, 274–288

Kronvang, B., Andersen, H. E., Børgesen, C., Dalgaard, T., Larsen, S. E., Bøgestrand, J., Blicher-Mathiasen, G., 2008. Effects of policy measures implemented in denmark on nitrogen pollution of the aquatic environment. *Environmental Science & Policy*, 11(2), 144-152. doi:<http://dx.doi.org/10.1016/j.envsci.2007.10.007>

Kronvang, B., Behrendt, H., Andersen, H. E., Arheimer, B., Barr, A., Borgvang, S. A., Bouraoui, F., Granlund, K., Grizetti, B., Groenendijk, P., Schwaiger, E., Hejzlar, J., Hoffmann, L., Johnsson, H., Panagopoulos, Y., Lo Porto, A., Reisser, H., Schoumans, O., Anthony, Silgram, S. M., Venohr, M. S., Larsen, E., 2009. Ensemble modelling of nutrient loads and nutrient load portioning in 17 European catchements. – *J. Environ. Monit.* 11: 572–583.

Krysanova, V, Vetter, T., Hattermann, F.F., 2008. Detection of change in drought frequency in the Elbe basin: comparison of three methods, *Hydrological Sciences Journal*, 53:3, 519-537

Krysanova, V., D. Müller-Wohlfeil, A. Becker, 1998. Development and test of a spatially distributed hydrological water quality model for mesoscale watersheds. – *Ecol. Model.* 106, 261–289.

Laliberté, E., Wells, J.A., Declerck, F., Metcalfe, D.J., Catterall, C.P., Queiroz, C., Aubin, I., Bonser, S.P., Ding, Y., Fraterrigo, J.M., McNamara, S., Morgan, J.W., Sánchez Merlos, D., Vesk, P.A., Mayfield, M.M., 2010. Land-use intensification reduces functional redundancy and response diversity in plant communities. *Ecology Letters* 13 76-86.

- Lange, K., Townsend, C.R., Gabrielsson, R., Chanut, P.C.M., Matthaei, C.D., 2014. Responses of stream fish populations to farming intensity and water abstraction in an agricultural catchment. *Freshw. Biol.* 59, 286–299. doi:10.1111/fwb.12264
- Larssen, T., Clarke, N., Tørseth, K., Skjelkvåle, B.L., 2002. Prognoses for future acidification recovery of water, soils and forests: dynamic modeling of Norwegian data from ICP Forests, ICP IM and ICP Waters.
- Lazar, A.N., Butterfield, D., Futter, M.N., Rankinen, K., Thouvenot-Korppoo, M., Jarritt, N., Lawrence, D.S.L., Wade, A.J., Whitehead, P.G., 2010. An assessment of the fine sediment dynamics in an upland river system: INCA-Sed modifications and implications for fisheries. *Science of the Total Environment* 408(12) 2555-2566.
- Ledesma, J.L.J., Köhler, S.J., Futter, M.N., 2012. Long-term dynamics of dissolved organic carbon: implications for drinking water supply. *Science of the Total Environment* 432:1-11.
- Lilja, H., Uusitalo, R., Yli-Halla, M., Nevalainen, R., Väänänen, T., Tamminen, P., 2006. Suomen maannostietokanta. Maannoskartta 1:250 000 ja maaperän ominaisuuksia. (MTT:n selvityksiä 114.
- Liu, X., Zhang, Y., Shi, K., Lin, J., Zhou, Y., 2016. Determining critical light and hydrological conditions for macrophyte presence in a large shallow lake: The ratio of euphotic depth to water depth. *Ecological Indicators* 71 317-326.
- Lorenzen, C.J., 1967. Determination of chlorophyll and phaeopigments: spectrophotometric equations. *Limnol Oceanogr* 12: 343-346.
- Makropoulos, C., Mimikou, M., 2012. “i-adapt”: Innovative approaches to halt desertification in Pinios: Piloting emerging technologies - A monograph. School of Civil Engineering, National Technical Univ. of Athens, Athens, Greece.
- Malagó M.A., Venohr M., Gericke A., Vigiak O., Bouraoui F., Grizzetti B., Kovacs A., 2015. Modelling nutrient pollution in the Danube River Basin: a comparative study of SWAT, MONERIS and GREEN models. JRC Technical Reports. EUR 27676 EN, doi:10.2788/156278.

Malmaeus, J.M., Blenckner, T., Markensten, H., Persson, I., 2006. Lake phosphorus dynamics and climate warming: A mechanistic model approach. *Ecological Modelling* 190(1) 1-14.

Mantyka-Pringle, C.S., Martin, T.G., Moffatt, D.B., Linke, S., Rhodes, J.R., 2014. Understanding and predicting the combined effects of climate change and land-use change on freshwater macroinvertebrates and fish. *J. Appl. Ecol.* 51, 572–581. doi:10.1111/1365-2664.12236

MARS project, 2015. Report task 2.6: definition of future scenarios. 77 pp.

Marzin, A., Verdonschot, P.F.M., Pont, D., 2013. The relative influence of catchment, riparian corridor, and reach-scale anthropogenic pressures on fish and macroinvertebrate assemblages in French rivers. *Hydrobiologia* 704, 375–388. doi:10.1007/s10750-012-1254-2

Matthaei, C.D., Piggott, J.J., Townsend, C.R., 2010. Multiple stressors in agricultural streams: Interactions among sediment addition, nutrient enrichment and water abstraction. *Journal of Applied Ecology* 47 639-649.

Mattila, P., Rankinen, K., Grönroos, J., Siimes, K., Karhu, E., Laitinen, P., Granlund, K., Ekholm, P., Antikainen, R., 2007. Viljelytoimenpiteet ja vesistökuormitus ympäristötukitiloilla vuosina 2003-2005 (Changes in cultivation practices and nutrient loading to the waters due to the agri-environmental support scheme in 2003-2005, in Finnish with English abstract). *Suomen ympäristö* 40.

McCullagh P., Nelder J.A., 1989. *Generalized linear models*. Chapman and Hall, London.

Meinshausen, M., Smith, S.J., Calvin, K., Daniel, J.S., Kainuma, M.L.T., Lamarque, J.F., Matsumoto, K., Montzka, S.A., Raper, S.C.B., Riahi, K., Thomson, A., Velders, G.J.M., van Vuuren, D.P.P., 2011. The RCP greenhouse gas concentrations and their extensions from 1765 to 2300. *Climatic Change* 109(1-2) 213-241.

Meldgaard, T., Nielsen, E.E., Loeschcke, V., 2003. Fragmentation by weirs in a riverine system: A study of genetic variation in time and space among populations of European grayling (*Thymallus thymallus*) in a Danish river system. *Conserv. Genet.* 4, 735–747.

- Mercier, L., Darnaude, A.M., Bruguier, O., Vasconcelos, R.P., Cabral, H.N., Costa, M.J., Lara, M., Jones, D.L., Mouillot, D., 2011. Selecting statistical models and variable combinations for optimal classification using otolith microchemistry. *Ecol. Appl.* 21, 1352–1364. doi:10.1890/09-1887.1
- Mielach, C., 2010. GIS-based Analyses of Pressure-Fish Relationships in Austrian Rivers on Different Spatial Scales. University of Natural Resources and Applied Life Sciences Vienna.
- Millenium Ecosystem Assessment, 2005. *Ecosystems and Human Wellbeing: Current State and Trends*, Volume 1, Island Press, Washington D.C.
- Ministry of Environment and Climate Change, 2013. Romania's Sixth National Communication on Climate Change and First Biennial Report.
- Mischke U., Venohr M., Behrendt H., 2011. Using Phytoplankton to Assess the Trophic Status of German Rivers. *International Revue of Hydrobiology* 96 (5), 578-598
- Moe, S.J., Haande, S., Couture, R.-M., 2016. Climate change, cyanobacteria blooms and ecological status of lakes: A Bayesian network approach. *Ecological Modelling* 337 330-347. <http://dx.doi.org/10.1016/j.ecolmodel.2016.07.004>
- Molina-Navarro, E., Trolle, D., Martínez-Pérez, S., Sastre-Merlín, A., Jeppesen, E., 2014. Hydrological and water quality impact assessment of a Mediterranean limno-reservoir under climate change and land use management scenarios. *J. Hydrol.* 509, 354–366. <http://dx.doi.org/10.1016/j.jhydrol.2013.11.053>
- Monteith, D.T., Hildrew, A.G., Flower, R.J., Raven, P.J., Beaumont, W.R.B., Collen, P., Kreiser, A.M., Shilland, E.M., Winterbottom, J.H., 2005. Biological responses to the chemical recovery of acidified fresh waters in the UK. *Environmental Pollution* 137 83-101.
- Monteith, J.L., 1965. Evaporation and the environment. p. 205-234. In *The state and movement of water in living organisms*. Proceedings of the 19th Symposia of the Society for Experimental Biology. Cambridge Univ. Press, London, U.K.
- Moog, O., 2002. *Fauna Aquatica Austriaca - Catalogue for autecological classification of Austrian aquatic organisms*.

Mooij, W. M., Hülsmann, S., Domis, L. N. D. S., Nolet, B. A., Bodelier, P. L., Boers, P. C., Portielje, R., 2005. The impact of climate change on lakes in the Netherlands: a review. *Aquatic Ecology*, 39(4), 381-400.

Mooney, H., Larigauderie, A., Cesario, M., Elmquist, T., Hoegh-Guldberg, O., Lavorel, S., Yahara, T., 2009. Biodiversity, climate change, and ecosystem services. *Current Opinion in Environmental Sustainability*, 1(1), 46-54.

Morón - Tejeda, E., Zabalza, J., Rahman, K., Gago - Silva, A., López - Moreno, J. I., Vicente - Serrano, S., Lehmann, A., Tague, C.L., Beniston, M., 2014. Hydrological impacts of climate and land - use changes in a mountain watershed: uncertainty estimation based on model comparison. *Ecohydrology*. <http://dx.doi.org/10.1002/eco.1590>

Moriasi, D. N., Arnold, J. G., Van Liew, M. W., Bingner, R. L., Harmel, R. D., Veith, T. L., 2007. Model evaluation guidelines for systematic quantification of accuracy in watershed simulations. *Transactions of the ASABE*, 50(3), 885-900. doi:10.13031/2013.23153

Moss R. H., Edmonds J. A., Hibbard K. A., Manning M. R., Rose S. K., van Vuuren D. P., Carter T. R., Emori S., Kainuma M., Kram T., Meehl G. A., Mitchell J. F. B., Nakicenovic N., Riahi K., Smith S. J., Stouffer R. J., Thomson A. M., Weyant J. P., Wilbanks T. J., 2010. The next generation of scenarios for climate change research and assessment. *Nature* 463:747-56.

Moss, B., Kosten, S., Meerhof, M., Battarbee, R., Jeppesen, E., Mazzeo, N., Paerl, H., 2011. Allied attack: climate change and eutrophication. *Inland waters*, 1(2), 101-105.

Moss, R., Babiker, M., Brinkman, S., et.al., 2008. *Towards New Scenarios for Analysis of Emissions, Climate Change, Impacts, and Response Strategies*.

Muhar, S., 2013. Fließgewässer, Ökologie. *Österreichische Wasser-und Abfallwirtschaft*, 65(11-12), 385-385.

Nakagawa, S, Schielzeth, H., 2013. A general and simple method for obtaining R^2 from Generalized Linear Mixed-effects Models. *Methods in Ecology and Evolution* 4:133–142.

Nash, J. E., Sutcliffe, J. V., 1970. River flow forecasting through conceptual models part I — A discussion of principles. *Journal of Hydrology*, 10(3), 282-290. doi:[http://dx.doi.org/10.1016/0022-1694\(70\)90255-6](http://dx.doi.org/10.1016/0022-1694(70)90255-6)

Natho S., Venohr M., Henle K., Schulz-Zunkel K., 2013. Modelling nitrogen retention in floodplains with different degrees of degradation for three large rivers in Germany. *Journal of Environmental Management* 122:47-55

Nauels, A., Xia, Y., Bex, V., Midgley, P.M. (Eds.), *Climate Change 2013: The Physical Science Basis. Contribution of Working Group I to the Fifth Assessment Report of the Intergovernmental Panel on Climate Change*. Cambridge University Press, Cambridge, United Kingdom and New York, NY, USA.

Năvodaru I., Năstase A., 2011. What fish and how many there are in Danube delta lakes? *Sc. Annals I.D.D.*, vol. 17, Tulcea (Romania), p. 71-82.

Neitsch, S.L., Arnold J.G., Kiniry J.R., Williams J.R., 2009. *Soil and Water Assessment Tool (SWAT) Theoretical Documentation*. Blackland Research Center, Texas. Agricultural Experiment Station, Temple, Texas (BRC Report 02-05). Available online at <http://swatmodel.tamu.edu/documentation>.

Neitsch, S.L., Arnold, J.G., Kiniry, J.R., Williams, J.R., 2005. *Soil and Water Assessment Tool, Theoretical Documentation, Version 2005*. Blackland Research Center/Soil and Water Research Laboratory, Agricultural Research Service, Grassland/Temple, TX.

Nelson, K.C., Palmer, M.A., Pizzuto, J.E., Moglen, G.E., Angermeier, P.L., Hilderbrand, R.H., Dettinger, M., Hayhoe, K., 2009. Forecasting the combined effects of urbanization and climate change on stream ecosystems: from impacts to management options. *J. Appl. Ecol.* 46, 154–163. doi:10.1111/j.1365-2664.2008.01599.x

Nõges, P., Argillier, C., Borja, Á., Garmendia, J.M., Hanganu, J.J., Kodeš, V., Pletterbauer, F., Sagouis, A., Birk, S., 2015. Quantified biotic and abiotic responses to multiple stress in freshwater, marine and ground waters. *Sci. Total Environ.* 540, 43–52. doi:10.1016/j.scitotenv.2015.06.045

Nõges, P., Nõges, T., Laas, A., 2010. Climate-related changes of phytoplankton seasonality in large shallow Lake Võrtsjärv, Estonia. *Aquatic Ecosystem Health & Management* 13(2) 154-163.

- Nõges, T., Nõges, P., Laugaste, R., 2003. Water level as the mediator between climate change and phytoplankton composition in a large shallow temperate lake. *Hydrobiologia* 506 257–263.
- Nohara, D., Kitoh, A., Hosaka, M., Oki, T., 2006. Impact of Climate Change on River Discharge Projected by Multimodel Ensemble, *Journal of Hydrometeorology*, volume 7.
- O’Neill, B.C et al., 2014. A new scenario framework for climate change research: the concept of shared socioeconomic reference pathways. *Clim Chang.* 112, 387-400.
- O’Reilly, C.M., Sharma, S., Gray, D.K., Hampton, S.E., Read, J.S., Rowley, R.J., Zhang, G., 2015. Rapid and highly variable warming of lake surface waters around the globe. *Geophysical Research Letters* 42.
- Ogura, N., 1972. Rate and extent of decomposition of dissolved organic matter in surface seawater. *Marine Biology* 13 89-93.
- Oğuzkurt, D., 2001. Limnology of Lake Beyşehir. Hacettepe University. PhD Thesis
- Olesen, J. E., Jeppesen, E., Porter, J. R., Børgesen, C. D., Trolle, D., Refsgaard, J. C., Karlsson, I. B., 2014. Scenarier for fremtidens arealanvendelse i danmark. *Vand Og Jord*, 21(3), 126-129.
- Oliveira, J.M., Ferreira, M.T., Morgado, P., Hughes, R.M., Teixeira, A., Cortes, R.M., Bochechas, J.H., 2009. A Preliminary Fishery Quality Index for Portuguese Streams, *North American Journal of Fisheries Management* 29:1466-1478.
- Ormerod, S.J., Durance, I., 2009. Restoration and recovery from acidification in upland Welsh streams over 25 years. *Journal of Applied Ecology* 46 164-174.
- Øygarden, L., Deelstra, J., Lagzdins, A., Bechmann, M., Greipsland, I., Kyllmar, K., Iital, A., 2014. Climate change and the potential effects on runoff and nitrogen losses in the Nordic–Baltic region. *Agriculture, Ecosystems & Environment*, 198, 114-126. doi:<http://dx.doi.org/10.1016/j.agee.2014.06.025>
- Özen, A., Karapınar, B., Kucuk, I., Jeppesen, E., Beklioğlu, M., 2010. Drought-induced changes in nutrient concentrations and retention in two shallow Mediterranean lakes subjected to different degrees of management. *Hydrobiologia.* 646, 61–72. <http://dx.doi.org/10.1007/s10750-010-0179-x>

Paerl, H. W., Huisman, J., 2008. Blooms like it hot. *SCIENCE-NEW YORK THEN WASHINGTON-*, 320(5872), 57.

Pall, P., Vilbaste, S., Kõiv, T., Kõrs, A., Käiro, K., Laas, A., Nõges, P., Nõges, T., Piirsoo, K., Toomsalu, L., Viik, M., 2011. Fluxes of carbon and nutrients through the inflows and outflow of Lake Võrtsjärv, Estonia. *Estonian Journal of Ecology* 60 39–53.

Panagopoulos, et al., 2015. *Cook-Book on Scenarios Implementation for MARS*.

Panagopoulos, Y., Makropoulos, C., Gkiokas, A., Kossida, M., Evangelou, E., Lourmas, G., Michas, S., Tsadilas, C., Papageorgiou, S., Perleros, V., Drakopoulou, S. Mimikou, M., 2014. Assessing the cost-effectiveness of irrigation water management practices in water stressed agricultural catchments: the case of Pinios . *Agr. Water. Manage.* 139, 31-42.

Panagopoulos, Y., Makropoulos, C., Kossida, M., Mimikou, M., 2013. Optimal implementation of irrigation practices: a cost effective desertification action plan for Pinios. *J. Water Res. Pl-Asce*140, 05014005.

Panagopoulos, Y., Makropoulos, C., Mimikou, M., 2012. A multi-Objective Decision Support Tool for Rural Basin Management. *International Environmental Modelling and Software Society (iEMSs). International Congress on Environmental Modelling and Software, Managing Resources of a Limited Planet: Pathways and Visions under Uncertainty (2012) Leipzig, Germany (1–5 July 2012)*.

Papadaki C., Soulis K., Muñoz-Mas R., Martinez-Capel F., Zogaris S., Ntoanidis L., Dimitriou E., 2016. Potential impacts of climate change on flow regime and fish habitat in mountain rivers of the south-western Balkans. *Sci. Total. Environ.* 540, 418-428.

Paparrizos S., Maris F., Matzarakis A., 2016. Integrated analysis of present and future responses of precipitation over selected Greek areas with different climatic conditions. *Atmos. Res.* 169, 199-208.

Park A. R., Clough S. J., Wellman C. M., 2008. AQUATOX: Modeling environmental fate and ecological effects in aquatic ecosystems *Ecological Modelling*, Vol. 213, No. 1. (24 April 2008), pp. 1-15, doi:10.1016/j.ecolmodel.2008.01.015

Peltonen-Sainio, P., Jauhiainen, L., Hakala, K., Ojanen, H., 2009. Climate change and prolongation of growing season: changes in regional potential for field crop production in Finland. *Agricultural and Food Science* 18 171-190.

Peltonen-Sainio, P., Jauhiainen, L., Trnka, M., Olesen, J.E., Calanca, P., Eckersten, H., Eitzinger, J., Gobin, A., Kersebaum, K.C., Kozyra, J., Kumar, S., Dalla Marta, A., Micale, F., Schaap, B., Seguin, B., Skjelvag, A.O., Orlandini, S., 2010. Coincidence of variation in yield and climate in Europe. *Agriculture Ecosystems & Environment* 139(4) 483-489.

Petrin, Z., Englund, G., Malmqvist, B., 2008. Contrasting effects of anthropogenic and natural acidity in streams: a meta-analysis. *Proceedings of the Royal Society B-Biological Sciences* 275(1639) 1143-1148.

Philips, G., Free, G., Karottki, I., Laplace-Treyture, C., Maileht, K., Mischke, U., Ott, Ingmar, Pasztaleniec, A., Portielje, R., Søndergaard, M., Trodd, W., Van Wichelen, J., 2014. Water Framework Directive Intercalibration Technical Report: Central Baltic Lake Phytoplankton Ecological Assessment Methods

PlantLife International, 2015. Important Plant Areas factsheet: Beyşehir Lake. Downloaded from <http://www.plantlife.org.uk/international> on 28/08/2015

Poff, N.L., Olden, J.D., Merritt, D.M., Pepin, D.M., 2007. Homogenization of regional river dynamics by dams and global biodiversity implications. *Proc. Natl. Acad. Sci. U. S. A.* 104, 5732-5737.

Priestley, C.H.B., Taylor R.J., 1972. On the assessment of surface heat flux and evaporation using large-scale parameters. *Monthly Weather Review* 100:81- 92.

Ptacnik, R., Lepisto, L., Willen, E., Brettum, P., Andersen, T., Rekolainen, S., Solheim, A.L., Carvalho, L., 2008. Quantitative responses of lake phytoplankton to eutrophication in Northern Europe. *Aquatic Ecology* 42(2) 227-236.

Pusch, M., Andersen, H.E., Bäche J., Behrendt, H., Fischer, H. et al., 2009. Rivers of the Central European Highlands and plains - Chapter 14. In: Tockner K., Robinson C.T. & Uehlinger U., 2009: Rivers of Europe. Elsevier.p. 525-576.

Quiel, K., Becker A., Kirchesch V., Schöl A., Fischer H., 2011. Influence of global change on phytoplankton and nutrient cycling in the Elbe River. *Reg Environ Change* 11:405–421

QZV Ökologie, 2010. 99. Verordnung des Bundesministers für Land- und Forstwirtschaft, Umwelt und Wasserwirtschaft über die Festlegung des ökologischen Zustandes für Oberflächengewässer (Qualitätszielverordnung Ökologie Oberflächengewässer), ausgegeben am 29. März 2010.

R Core Team, 2015. R: A language and environment for statistical computing. R Foundation for Statistical Computing, Vienna, Austria. URL <https://www.R-project.org/>.

Rankinen, K., Gao, G., Granlund, K., Grönroos, J., Vesikko, L., 2015. Comparison of impacts of human activities and climate change on water quantity and quality in Finnish agricultural catchments. *Landscape Ecology*.

Rankinen, K., Karvonen, T., Butterfield, D., 2004. A simple model for predicting soil temperature in snow covered and seasonally frozen soil: Model description and testing. *Hydrol. Earth. Syst. Sci.* 8 706-716.

Rankinen, K., Peltonen-Sainio, P., Granlund, K., Ojanen, H., Laapas, M., Hakala, K., Sippel, K., Helenius, J., Forsius, M., 2013. Climate change adaptation in arable land use, and impact on nitrogen load at catchment scale in northern agriculture. *Agricultural and Food Science* 22 342-355.

RBMP-DB, 2015. Database extract of the Austrian River Basin Management Plan 2015. Status: Mai 2015.

Reynolds C.S., Descy, J.P., 1996. The production, biomass and structure of phytoplankton in large rivers. *Ach. Hydrobiol. Suppl.* 113 (1-4): 161-187.

Reynolds, C.S., Irish, A.E., Elliott, J.A., 2001. The ecological basis for simulating phytoplankton responses to environmental change (PROTECH). *Ecological Modelling* 140(3) 271-291. [http://dx.doi.org/10.1016/S0304-3800\(01\)00330-1](http://dx.doi.org/10.1016/S0304-3800(01)00330-1)

Ridgeway, G., 2013. gbm: Generalized Boosted Regression Models R Package Version 2.0-8 [WWW Document]. URL Available at: <http://CRAN.Rproject.org/package=gbm>

- Rinke, K., Yeates, P., ROTHHAUPT, K. O., 2010. A simulation study of the feedback of phytoplankton on thermal structure via light extinction. *Freshwater Biology*, 55(8), 1674-1693.
- Roberts, J.J., Fausch, K.D., Peterson, D.P., Hooten, M.B., 2013. Fragmentation and thermal risks from climate change interact to affect persistence of native trout in the Colorado River basin. *Glob. Chang. Biol.* 19, 1383–1398. doi:10.1111/gcb.12136
- Roers, M., Venohr M., Wechsung F., Paton E.N., 2016. Effekte des Klimawandels und von Reduktionsmaßnahmen auf die Nährstoffeinträge und –frachten im Elbegebiet bis zur Jahrhundertmitte. *Hydrologie und Wasserbewirtschaftung* 60: 196–212
- Rosemond, A., Reice, S., 1992. The effects of stream acidity on benthic invertebrate communities in the south - eastern United States. *Freshwater Biology* 27 193-209.
- Saaty, T.L., 2008. Decision making with the analytic hierarchy process', *Int. J. Services Sciences*, Vol. 1, No. 1, pp.83–98.
- Sælthun, N.R. 1996. The“Nordic”HBV model. Description and documentation of the model version developed for the project Climate Change and Energy Production. (82-410-0273-4).
- Saloranta, T.M., Andersen, T., 2007a. MyLake - A multi-year lake simulation model code suitable for uncertainty and sensitivity analysis simulations. *Ecological Modelling* 207(1) 45-60.
- Saltveit, S.J., Halleraker, J.H., Arnekleiv, J. V., Harby, A., 2001. Field experiments on stranding in juvenile atlantic salmon (*Salmo Salar*) and brown trout (*Salmo Trutta*) during rapid flow decreases caused by hydropeaking. *River Res. Appl.* 17, 609–622.
- Sanchez, M.F., Deltares), Duel, H., Sampedro A.A., Rankinen K., Holmberg M., Prudhomme C., Bloomfield J., Couture R.M., Panagopoulos Y., Ferreira R., Venohr M., Birk S., 2015. Deliverable 2.1 - Four manuscripts on the multiple stressor framework. Part 4: Report on the MARS scenarios of future changes in drivers and pressures with respect to Europe’s water resources

Sanchez, M.F., Duel, H., Sampedro, A.A., Rankinen, K., Holmberg, M., Prudhomme, C., Bloomfield, J., Couture, R.M., Panagopoulos, Y., Ferreira, T., Venohr, M., Birk, S., 2015. Report task 2.6 Definition of future scenarios. MARS project.

Santucci, V.J., Gephard, S.R., Pescitelli, S.M., 2005. Effects of Multiple Low-Head Dams on Fish, Macroinvertebrates, Habitat, and Water Quality in the Fox River, Illinois. *North Am. J. Fish. Manag.* 25, 975–992. doi:10.1577/M03-216.1

Schiemer F., Guti, G., Keckeis, H., Staras, M., 2004. Ecological status and problems of the Danube River and its fish fauna: a review. In: Proceedings of the second symposium on the management of large rivers for fisheries, Vol I, Welcomme R. and T. Petr, Eds., FAO Regional Office for Asia and the Pacific, Bangkok, Thailand. RAP Publication 2004/16, pp. 273-279.

Schinegger, R., Trautwein, C., Schmutz, S., 2013. Pressure-specific and multiple pressure response of fish assemblages in European running waters. *Limnol. - Ecol. Manag. Int. Waters* null, 348–361. doi:10.1016/j.limno.2013.05.008

Schmidt-Kloiber, A., Hering, D., 2015. www.freshwaterecology.info - An online tool that unifies, standardises and codifies more than 20,000 European freshwater organisms and their ecological preferences. *Ecological Indicators* 53 271-282.

Schmutz, S., Bakken, T.H., Friedrich, T., Greimel, F., Harby, A., Jungwirth, M., Melcher, A., Unfer, G., Zeiringer, B., 2014. Response of fish communities to hydrological and morphological alterations in hydropeaking rivers of Austria. *River Res. Appl.* 7, 919–930. doi:10.1002/rra.2795

Schmutz, S., Cowx, I.G., Haidvogel, G., Pont, D., 2007a. Fish-based methods for assessing European running waters: A synthesis. *Fish. Manag. Ecol.* 14, 369–380. doi:10.1111/j.1365-2400.2007.00585.x

Schmutz, S., Melcher, A., Muhar, S., Zitek, A., Poppe, M., Trautwein, C., Jungwirth, M., 2007b. MIRR-Model-based instrument for River Restoration. Entwicklung eines strategischen Instruments zur integrativen Bewertung ökologischer Restaurationsmaßnahmen an Fließgewässern. Studie im Auftrag von Lebensministerium und Land Niederösterreich, Wien.

Schmutz, S., Melcher, A., Muhar, S., Zitek, A., Poppe, M., Trautwein, C., Jungwirth, M., 2008. MIRR-Model-based Instrument for River Restoration. Entwicklung eines strategischen Instruments zur integrativen Bewertung ökologischer Restaurationsmaßnahmen an Fließgewässern. Österreichische Wasser- und Abfallwirtschaft 60, 95–103.

Schmutz, S., Schinegger, R., Muhar, S., Preis, S., Jungwirth, M., 2010. Ökologischer Zustand der Fließgewässer Österreichs - Perspektiven bei unterschiedlichen Nutzungsszenarien der Wasserkraft. Osterr. Wasser- und Abfallwirtschaft 62, 162–167. doi:10.1007/s00506-010-0221-2

Schoumans, O. F., Silgram, M., Walvoort, D. J. J., Groenendijk, P., Bouraoui, F., Andersen, H. E., Barr, A., 2009. Evaluation of the difference of eight model applications to assess diffuse annual nutrient losses from agricultural land. Journal of Environmental Monitoring, 11(3), 540-553. doi:10.1039/B823240G

Scoccimarro E., Gualdi S., Bellucci A., Zampieri M., Navarra A., 2016. Heavy precipitation events over the Euro-Mediterranean region in a warmer climate: results from CMIP5 models. Reg Environ Change 16, 595-602.

Scruton, D.A., Pennell, C., Ollerhead, L.M.N., Alfredsen, K., Stickler, M., Harby, A., Robertson, M., Clarke, K.D., LeDrew, L.J., 2008. A synopsis of “hydropeaking” studies on the response of juvenile Atlantic salmon to experimental flow alteration. Hydrobiologia 609, 263–275. doi:10.1007/s10750-008-9409-x

Segurado P., Almeida C., Santos J. M., Neves R., Ferreira M. T., 2015. Biological and environmental database of Sorraia catchment (Portugal). Freshwater Metadata Journal 5: 1-10. <http://dx.doi.org/10.15504/fmj.2015.5>

Segurado P., Feld C., Gutierrez-Canovas C., Banin L., 2015a. Preparation for the WP4 data analysis workshop in Tulcea, Romania: a cookbook for data handling and screening (including R script).

Segurado P., Feld C., Gutierrez-Canovas C., Banin L., 2015b. Preparation for the WP4 data analysis workshop in Tulcea, Romania: a cookbook for analysing the response of benchmark indicators to multiple stressors

Shrestha M., 2015. Data analysis relied on Linear Scaling bias correction (V.1.0) Microsoft Excel file.

Skarbøvik, E., Bechmann, M.E., 2010. Some Characteristics of the Vansjø-Hobøl (Morsa) Catchment. 5)(128).

Skarbøvik, E., Haande, S., Bechmann, M., 2013. Overvåking Vansjø/Morsa 2011-2012. Resultater fra overvåkingen i perioden oktober 2011 til oktober 2012.

Smed, P., 1982. Landskabskort over Danmark [Geomorphological map of Denmark]. Copenhagen, Denmark: Geografforlaget.

Smol, J.P., Wolfe, A.P., Birks, H.J.B., Douglas, M.S., Jones, V.J., Korhola, A., Brooks, S.J., 2005. Climate-driven regime shifts in the biological communities of arctic lakes. *Proceedings of the National Academy of Sciences of the United States of America* 102(12) 4397-4402.

Sorvari, S., Korhola, A., Thompson, R., 2002. Lake diatom response to recent Arctic warming in Finnish Lapland. *Global Change Biology* 8(2) 171-181.

Staraş M., Năvodaru I., 1995. Changing fish communities as a result of biotope features change. In: *Scientific Annals of Danube Delta Institute*. Vol. 4, pp. 233-239 (in Romanian with English abstract).

Statistics Denmark, 2014. Retrieved from <http://www.dst.dk/en>

Stocker, T.F., 2014. *Climate Change 2013: The Physical Science Basis*. Working Group 1 (WG1) Contribution to the Intergovernmental Panel on Climate Change (IPCC) 5th Assessment Report (AR5). Cambridge University Press: Cambridge UK.

Stockwell, D.R., Peterson, A.T., 2002. Effects of sample size on accuracy of species distribution models. *Ecol. Modell.* 148, 1–13. doi:10.1016/S0304-3800(01)00388-X

SWAT , 2013. ArcSWAT: ArcGIS-ArcView extension and graphical user input interface for SWAT. U.S. Department of Agriculture, Agricultural Research Service, Grassland, Soil & Water Research Laboratory, Temple, TX. <http://swat.tamu.edu/software/arcswat/>.

Tachet, H., Richoux, P., Bournaud, M., Usseglio-Polatera, P., 2002. Invertébrés d'eau douce. Systematique, biologie, écologie (2nd corrected impression). CNRS éditions, Paris.

Thodsen, H., Andersen, H. E., Blicher-Mathiesen, G., Trolle, D., 2015. The combined effects of fertilizer reduction on high risk areas and increased fertilization on low risk areas, investigated using the SWAT model for a danish catchment. *Acta Agriculturae Scandinavica, Section B — Soil & Plant Science*, 65, 217-227. doi:10.1080/09064710.2015.1010564

Tiemann, J.S., Gillette, D.P., Wildhaber, M.L., Edds, D.R., 2004. Effects of lowhead dams on riffle-dwelling fishes and macroinvertebrates in a midwestern river. *Trans. Am. Fish. Soc.* 133.

Tikkanen, M., Seppälä, M., Heikkinen, O., 1985. Environmental properties and material transport of two rivulets in Lammi, southern Finland. *Fennia* 163(2) 217-282.

Tolika, C.K., Zanis, P., Anagnostopoulou, C., 2012. Regional climate change scenarios for Greece: future temperature and precipitation projections from ensembles of RCMs. *Glob. Nest J.* 14, 407-421.

Tranvik, L.J., 1988. Availability of dissolved organic carbon for planktonic bacteria in oligotrophic lakes of differing humic content. *Microbial Ecology* 16(3) 11-22.

Trautwein, C., Schinegger, R., Schmutz, S., 2011. Cumulative effects of land use on fish metrics in different types of running waters in Austria. *Aquat. Sci.* 74, 329–341. doi:10.1007/s00027-011-0224-5

Trolle, D., Hamilton, D. P., Pilditch, C. A., Duggan, I. C., Jeppesen, E., 2011. Predicting the effects of climate change on trophic status of three morphologically varying lakes: Implications for lake restoration and management. *Environmental Modelling & Software*, 26(4), 354-370. doi:10.1016/j.envsoft.2010.08.009

Trolle, D., Hamilton, D., Hipsey, M., Bolding, K., Bruggeman, J., Mooij, W., Hanson, P., 2012. A community-based framework for aquatic ecosystem models. *Hydrobiologia*, 683(1), 25-34. doi:10.1007/s10750-011-0957-0

Trolle, D., Jørgensen, T. B., Jeppesen, E., 2008. Predicting the effects of reduced external nitrogen loading on the nitrogen dynamics and ecological state of deep Lake Ravn, Denmark, using the DYRESM–CAEDYM model. *Limnologica-Ecology and Management of Inland Waters*, 38(3), 220-232.

Turkish Statistical Institute (TUIK), 2013. Database for agricultural statistics. <http://tuikapp.tuik.gov.tr/> Accessed June 2012.

Underwood A.J., 1989. The analysis of stress in natural populations. *Biological Journal of the Linnean Society* 37:51–78.

UNECE, 2014. Convention on Long-range Transboundary Air Pollution http://www.unece.org/env/lrtap/lrtap_h1.html

Unterberger, A., 2014. Habitat and population status assessment of European Grayling (*Thymallus thymallus* L.) in Tyrol and South Tirol. University of Natural Resources and Life sciences Vienna.

USDA-Soil Conservation Service, 1972. Soil Series of the United States, Puerto Rico and the Virgin Islands: Their taxonomic classification. Supplement to Agricultural Handbook No. 436. US Government Printing Office, Washington, DC, pp. 363.

Van Looy, K., Tormos, T., Souchon, Y., 2014. Disentangling dam impacts in river networks. *Ecol. Indic.* 37, 10–20. doi:10.1016/j.ecolind.2013.10.006

Van Vuuren, D.P., Edmonds, J., Kainuma, M., Riahi, K., Thomson, A., Hibbard, K., Hurtt, G.C., Kram, T., Krey, V., Lamarque, J.F., Masui, T., Meinshausen, M., Nakicenovic, N., Smith, S.J., Rose, S.K., 2011. The representative concentration pathways: an overview. *Climatic Change* 109(1-2) 5-31.

Van Vuuren, D.P., Kriegler, E., O'Neill, B.C., Ebi, K.L., Riahi, K., Carter, T.R., Edmonds, J., Hallegatte, S., Kram, T., Mathur, R., Winkler, H., 2014. A new scenario framework for climate change research: scenario matrix architecture. *Clim Chang.* 122 373-386.

Vasiliades, L., Loukas, A., Liberis, N., 2011. A Water Balance Derived Drought Index for Pinios River Basin, Greece, *Water Resources Management* 25, 1087-1101.

Venohr, M., Hirt, U., Hofmann, J., Opitz, D., Gericke, A., Wetzig, A., Ortelbach, S., Natho, S., Neumann, F., Hürdler, J., 2009. The model system MONERIS: Version 2.14.1vba – Manual. – Leibniz-Institute for Freshwater Ecology and Inland Fisheries Berlin, 116 pp.

Venohr, M., Hirt, U., Hofmann, J., Opitz, D., Gericke, A., Wetzig, A., Natho, S., Neumann, F., Hürdler, J., Matranga, M., Mahnkopf, J., Gadegast, M., Behrendt, H., 2011. Modelling of nutrient emissions in river systems – MONERIS – methods and background. *International Review of Hydrobiology* 96 (5), 435–483.

Venohr, M., Donohue, I., Fogelberg, S., Arheimer, B., Behrendt, H., 2005. Modelling nitrogen transfer in river systems: The importance river morphology and the occurrence of lakes. – *Water Sci. Technol.* 54: 19–29.

Villamagna AM., Mogollóna B., Angermeier P.L., 2014. A multi-indicator framework for mapping cultural ecosystem services: The case of freshwater recreational fishing, *Ecological Indicators*, 45, 255–265

Villéger, S., Mason, N.W.H., Mouillot, D., 2008. New multidimensional functional diversity indices for a multifaceted framework in functional ecology. *Ecology* 89 2290–2301.

Vinebrooke R., Cottingham K., Norberg M., 2004. Impacts of multiple stressors on biodiversity and ecosystem functioning: the role of species co-tolerance. *Oikos* 104:451–457.

Visser, P. M., Ibelings, B. W., Bormans, M., Huisman, J., 2015. Artificial mixing to control cyanobacterial blooms: a review. *Aquatic Ecology*, 1-19.

Vogt J., Soille P., de Jager A., Rimaviciutè E., Mehl W., Foisneau S., Bodis K., Dusart J., Paracchini M.L., Haastrup P., Bamps C., 2007. A pan-European river and catchment database. European Commission–JRC, EUR 22920 EN, Luxembourg.

Wade, A., Durand, P., Beaujoan, V., Wessels, W., Raat, K., Whitehead, P.G., Butterfield, D., Rankinen, K., Lepistö, A., 2002a. Towards a generic nitrogen model of European ecosystems: New model structure and equations. *Hydrology and Earth System Sciences* 6(3) 559-582.

Wade, A.J., 2004. Errata in INCA-N equations to simulate nitrogen storage and transport in river systems [Hydrol. Earth Sys. Sci., 6, 559-582]. *Hydrology and Earth System Sciences* 8 858-859.

Wade, A.J., Whitehead, P.G., Butterfield, D., 2002c. The Integrated Catchments model of Phosphorus dynamics (INCA-P), a new approach for multiple source assessment in heterogeneous river systems: model structure and equations. *Hydrology and Earth System Sciences* 6 583-606.

Walley, W.J., Hawkes, H.A., 1996. A computer-based reappraisal of the biological monitoring working party scores using data from the 1990 river quality survey of England and Wales. *Water Research* 30 2086-2094.

Walters, A.W., BARTZ, K.K., McClure, M.M., 2013. Interactive Effects of Water Diversion and Climate Change for Juvenile Chinook Salmon in the Lemhi River Basin (U.S.A.). *Conserv. Biol.* 27, 1179–1189. doi:10.1111/cobi.12170

Wechsung, F., Hartje V., Kaden S., Venohr M., Hansjürgens B., Grafe P., 2013. Die Elbe im globalen Wandel – Eine integrative Betrachtung. Series band 9: Konzepte für die nachhaltige Entwicklung einer Flusslandschaft- WeissenseeVerlag, Berlin, pp 613

Wenger, S.J., Isaak, D.J., Luce, C.H., Neville, H.M., Fausch, K.D., Dunham, J.B., Dauwalter, D.C., Young, M.K., Elsner, M.M., Rieman, B.E., Hamlet, A.F., Williams, J.E., et. al., 2011. Flow regime, temperature, and biotic interactions drive differential declines of trout species under climate change. *Proc. Natl. Acad. Sci. U. S. A.* 108, 14175–14180. doi:10.1073/pnas.1103097108

Wetzel, R.G., 2001. *Limnology. Lake and River Ecosystems*. Third Edition. Academic Press, San Diego, 1006p.

Whitehead, P.G., Barbour, E., Futter, M.N., Sarkar, S., Rodda, H., Caesar, J., Butterfield, D., Jin, L., Sinha, R., Nicholls, R., Salehin, M., 2015. Impacts of climate change and socio-economic scenarios on flow and water quality of the Ganges, Brahmaputra and Meghna (GBM) river systems: low flow and flood statistics. *Environmental science. Processes & impacts* 17 1057-1069.

Whitehead, P.G., Hill, T.J., Neal, C., 2004. Impacts of forestry on nitrogen in upland and lowland catchments: a comparison of the River Severn at Plynlimon in mid-Wales and

the Bedford Ouse in south-east England using the INCA Model. *Hydrology and Earth System Sciences Discussions* 8 533-544.

Whitehead, P.G., Jin, L., Baulch, H.M., Butterfield, D.A., Oni, S.K., Dillon, P.J., Futter, M., Wade, A.J., North, R., O'Connor, E.M., Jarvie, H.P., 2011. Modelling phosphorus dynamics in multi-branch river systems: A study of the Black River, Lake Simcoe, Ontario, Canada. *Sci. Tot. Environ.* 412 315-323.

Whitehead, P.G., Wilson, E.J., Butterfield, D., 1998a. A semi-distributed Integrated Nitrogen model for multiple source assessment in Catchments (INCA): Part I - Model structure and process equations. *Science of the Total Environment* 210-211 547-558.

Whitehead, P.G., Wilson, E.J., Butterfield, D., Seed, K., 1998c. A semi-distributed integrated flow and nitrogen model for multiple source assessment in catchments (INCA): Part II - Application to large river basins in south Wales and eastern England. *Science of the Total Environment* 210-211 559-583.

Wickham, H., 2009. *ggplot2: Elegant Graphics for Data Analysis*. Springer-Verlag New York.

Wright, R.F., Helliwell, R., Hruska, J., Larssen, T., Rogora, M., Rzychoń, D., Skjelkvåle, B.L., Worsztynowicz, A., 2011. Impacts of Air Pollution on Freshwater Acidification under Future Emission Reduction Scenarios; ICP Waters contribution to WGE report. NIVA-report 6243-2011.

Yeğen, V., Balik, S., Bostan, H., Uysal, R., Bilçen, E., 2006. Göller Bölgesindeki Bazı Göl ve Baraj Göllerinin Balık Faunalarının Son Durumu. In: 1. Balıklandırma ve Rezervuar Yönetimi Sempozyumu, Antalya. 07-09 February 2006 (in Turkish).

Zingel, P., Haberman, J., 2008. A comparison of zooplankton densities and biomass in Lakes Peipsi and Võrtsjärv (Estonia): rotifers and crustaceans versus ciliates. *Hydrobiologia* 599(1) 153-159.

Zitek, A., Schmutz, S., Jungwirth, M., 2008. Assessing the efficiency of connectivity measures with regard to the EU-Water Framework Directive in a Danube-tributary system. *Hydrobiologia* 609, 139–161. doi:10.1007/s10750-008-9394-0

Zuur A.F., Ieno E.N., Walker N., Saveliev A.A., Smith G.M., 2009. *Mixed Effects Models and Extensions in Ecology with R (Statistics for Biology and Health)*. Springer, New York.

Zuur, A.F., Ieno, I.N., Smith, G.M., 2007. *Analysing ecological data*, 672 pp. ed. Springer, New York.